Advances in Experimental Medicine and Biology 979

Steven D. Schwartzbach
Shigeru Shigeoka *Editors*

Euglena: Biochemistry, Cell and Molecular Biology

Springer

Advances in Experimental Medicine and Biology

Volume 979

More information about this series at http://www.springer.com/series/5584

Steven D. Schwartzbach
Shigeru Shigeoka
Editors

Euglena: Biochemistry, Cell and Molecular Biology

Springer

Editors
Steven D. Schwartzbach
Department of Biological Sciences
University of Memphis
Memphis, TN, USA

Shigeru Shigeoka
Faculty of Agriculture
Kindai University
Nara, Japan

ISSN 0065-2598 ISSN 2214-8019 (electronic)
Advances in Experimental Medicine and Biology
ISBN 978-3-319-54908-8 ISBN 978-3-319-54910-1 (eBook)
DOI 10.1007/978-3-319-54910-1

Library of Congress Control Number: 2017936664

Printed on acid-free paper

This Springer imprint is published by Springer Nature
The registered company is Springer International Publishing AG
The registered company address is: Gewerbestrasse 11, 6330 Cham, Switzerland

This volume is dedicated to the trailblazers, the late Shozaburo Kitaoka and the late Jerome A. Schiff, who recognized the potential of Euglena and over the years provided training, encouragement, and guidance as we endeavored to shed light on its fascinating and novel biology.

Preface

For over 50 years, *Euglena* has been an organism of choice for addressing fundamental questions in eukaryotic biochemistry and cellular and molecular biology. *Euglena* grows rapidly in the dark to high cell densities using a diverse array of organic compounds and industrial waste streams. Rapid growth is also achieved in the light using photosynthesis as the sole source of carbon and energy for growth or using both photosynthesis and organic carbon. Grown in the dark, *Euglena* has a poorly developed plastid which upon light exposure develops into a photosynthetically competent chloroplast. Unique among photosynthetic organisms, the chloroplast is totally gratuitous to growth. Permanently white relatives of photosynthetic euglenoids are found in nature, and chloroplast loss is readily induced by a variety of treatments in the laboratory. Due to a rapid growth rate combined with simple nutritional requirements, the large number of cells required for isolation of subcellular organelles can easily be obtained in less than a week allowing both in vivo and in vitro studies of organelle biochemistry and molecular biology.

The availability of large quantities of permanently white and green *Euglena* resulted in the *Euglena* chloroplast being among the first photosynthetic organelles whose genome was physically characterized and sequenced. The undeveloped plastids in dark-grown *Euglena*, the facile induction by light exposure of the enzymatic machinery required to transform the plastid into a photosynthetically competent chloroplast, and the subcellular organelle which allows CO_2 to be used as the sole source of carbon and energy for growth made *Euglena* a model system for studies of organelle biogenesis. Studies of *Euglena* were instrumental in establishing the contribution of the nuclear and chloroplast genome to the development of chloroplasts. As additional information became available from studies of higher plants and other algae, it became apparent that *Euglena* was an atypical organism; it had its own way of doing things. The focus of *Euglena* research shifted from being a model organism to being an organism that could be used to elucidate novel patterns of genome organization, transcript processing, gene expression, and transport of proteins to chloroplasts providing insights into the evolutionary origin of eukaryotic cellular processes.

The diverse nature of organic carbon compounds and industrial waste streams supporting growth, the ability to grow photosynthetically, and the evolutionary relationship to the parasitic trypanosomes make *Euglena* an organism of choice for investigations of diverse and in some cases unique

biochemical pathways. *Euglena* mitochondria are the site of a classical respiratory pathway, an alternative respiratory pathway, and an anaerobic fermentation pathway producing wax esters. The photorespiratory pathway and glyoxylate pathway for ethanol assimilation are localized in most organisms to specialized organelles called microbodies, but these metabolic pathways appear to be localized to *Euglena* mitochondria. During photosynthetic and aerobic growth, *Euglena* produces a β-1,3-glucan, paramylum, as the major storage product, while wax esters are accumulated during mitochondrial anaerobic fermentation. A number of uses for paramylum have been found, and the *Euglena* wax ester has potential as a biofuel. *Euglena* accumulates nutraceuticals and cosmeceuticals, and its biomass has a large nutritional value. The novel nature of the biochemical pathways found in *Euglena* makes it a source of genes for genetic engineering of other organisms for production of high-value compounds.

The facile large-scale cultivation of *Euglena* on a wide array of organic compounds and industrial waste streams over a pH range of approximately 3.5–9 taken together with its metabolic diversity suggests a multitude of potential biotechnology applications. To make this potential a reality requires an in-depth understanding of the biochemistry and cellular and molecular biology of *Euglena*. Our current knowledge regarding these topics is plentiful, but it is scattered throughout the plant, protist, biochemical cell biology, and evolutionary biology literature of the past 50 years. It is over 25 years since the final volume of the four-volume compilation of *Euglena* biochemical and molecular biology research, *The Biology of Euglena*, appeared. The 14 chapters of this volume are contributed by well-known experts who in many cases played a major role in elucidating the phenomena discussed. The content is divided into three sections. The first section describes novel biochemical pathways which in some cases have an atypical subcellular localization. The next section details atypical cellular mechanisms of organelle protein import, organelle nuclear genome interdependence, and gene regulation and expression providing insights into the evolutionary origins of eukaryotic cells. The final section discusses how biotechnologists have capitalized on the novel cellular and biochemical features of *Euglena* to produce value-added products. The reader will come away from this volume with an understanding of the atypical biochemistry and cellular and molecular biology of one organism, *Euglena*, and realize the diversity of cellular processes yet to be discovered on the different branches of the tree of life.

Memphis, TN, USA — Steven D. Schwartzbach
Nara, Japan — Shigeru Shigeoka

Contents

Contributors

Mark Carrington Department of Biochemistry, University of Cambridge, Cambridge, UK

Dion G. Durnford Department of Biology, University of New Brunswick, Fredericton, NB, Canada

ThankGod Echezona Ebenezer Department of Biochemistry, University of Cambridge, Cambridge, UK

School of Life Sciences, University of Dundee, Dundee, UK

Mark C. Field School of Life Sciences, University of Dundee, Dundee, UK

Jorge D. García-García Departamento de Bioquímica, Instituto Nacional de Cardiología Ignacio Chávez, Ciudad de México, Mexico

Donat-P. Häder Department of Biology, Friedrich-Alexander Universität, Erlangen-Nürnberg, Möhrendorf, Germany

Ruth Hemmersbach Gravitational Biology, Institute of Aerospace Medicine, German Aerospace Center (DLR), Cologne, Germany

Hiroshi Inui Department of Nutrition, Osaka Prefecture University, Osaka, Japan

Mineo Iseki Faculty of Pharmaceutical Sciences, Toho University, Funabashi, Chiba, Japan

Takahiro Ishikawa Faculty of Life and Environmental Science, Shimane University, Matsue, Shimane, Japan

Ricardo Jasso-Chávez Departamento de Bioquímica, Instituto Nacional de Cardiología Ignacio Chávez, Ciudad de México, Mexico

Anna Karnkowska Department of Molecular Phylogenetics and Evolution, Faculty of Biology, Biological and Chemical Research Centre, University of Warsaw, Warsaw, Poland

Steven Kelly Department of Plant Sciences, University of Oxford, Oxford, UK

Michael Lebert Cell Biology Division, Department of Biology, University of Erlangen-Nuremberg, Erlangen, Germany

William F. Martin Institute of Molecular Evolution, Heinrich-Heine-Universität Düsseldorf, Düsseldorf, Germany

Takanori Maruta Faculty of Life and Environmental Science, Shimane University, Matsue, Shimane, Japan

David C. McWatters Department of Biological Sciences, University of Lethbridge, Lethbridge, AB, Canada

Alberta RNA Research and Training Institute, University of Lethbridge, Lethbridge, AB, Canada

Rafał Milanowski Department of Molecular Phylogenetics and Evolution, Faculty of Biology, Biological and Chemical Research Centre, University of Warsaw, Warsaw, Poland

Rafael Moreno-Sánchez Departamento de Bioquímica, Instituto Nacional de Cardiología Ignacio Chávez, Ciudad de México, Mexico

Masami Nakazawa Faculty of Life and Environmental Sciences, Osaka Prefecture University, Sakai, Osaka, Japan

Cessa Rauch Institute of Molecular Evolution, Heinrich-Heine-Universität Düsseldorf, Düsseldorf, Germany

Sara Rodríguez-Enríquez Departamento de Bioquímica, Instituto Nacional de Cardiología Ignacio Chávez, Ciudad de México, Mexico

Anthony G. Russell Department of Biological Sciences, University of Lethbridge, Lethbridge, AB, Canada

Alberta RNA Research and Training Institute, University of Lethbridge, Lethbridge, AB, Canada

Emma Saavedra Departamento de Bioquímica, Instituto Nacional de Cardiología Ignacio Chávez, Ciudad de México, Mexico

Steven D. Schwartzbach Department of Biological Sciences, University of Memphis, Memphis, TN, USA

Shigeru Shigeoka Faculty of Agriculture, Kindai University, Nara, Japan

Kengo Suzuki Department of Research and Development, euglena Co., Ltd., Tokyo, Japan

Shun Tamaki Faculty of Life and Environmental Science, Shimane University, Matsue, Shimane, Japan

Masahiro Tamoi Faculty of Agriculture, Kindai University, Nara, Japan

Aloysius G.M. Tielens Department of Medical Microbiology and Infectious Diseases, Erasmus University Medical Center, Rotterdam, The Netherlands

Department of Biochemistry and Cell Biology, Faculty of Veterinary Medicine, Utrecht University, Utrecht, The Netherlands

Jaap J. van Hellemond Department of Medical Microbiology and Infectious Diseases, Erasmus University Medical Center, Rotterdam, The Netherlands

Fumio Watanabe Faculty of Agriculture, School of Agricultural, Biological and Environmental Sciences, Tottori University, Tottori, Japan

Kazuya Yoshimura Department of Food and Nutritional Sciences, College of Bioscience and Biotechnology, Chubu University, Kasugai, Aichi, Japan

Bożena Zakryś Department of Molecular Phylogenetics and Evolution, Faculty of Biology, Biological and Chemical Research Centre, University of Warsaw, Warsaw, Poland

Verena Zimorski Institute of Molecular Evolution, Heinrich-Heine-Universität Düsseldorf, Düsseldorf, Germany

Part I

Biochemistry and Physiology

Evolutionary Origin of *Euglena*

1

Bożena Zakryś, Rafał Milanowski,
and Anna Karnkowska

Abstract

Euglenids (Excavata, Discoba, Euglenozoa, Euglenida) is a group of free-living, single-celled flagellates living in the aquatic environments. The uniting and unique morphological feature of euglenids is the presence of a cell covering called the pellicle. The morphology and organization of the pellicle correlate well with the mode of nutrition and cell movement. Euglenids exhibit diverse modes of nutrition, including phagotrophy and photosynthesis. Photosynthetic species (Euglenophyceae) constitute a single subclade within euglenids. Their plastids embedded by three membranes arose as the result of a secondary endosymbiosis between phagotrophic eukaryovorous euglenid and the *Pyramimonas*-related green alga. Within photosynthetic euglenids three evolutionary lineages can be distinguished. The most basal lineage is formed by one mixotrophic species, *Rapaza viridis*. Other photosynthetic euglenids are split into two groups: predominantly marine Eutreptiales and freshwater Euglenales. Euglenales are divided into two families: Phacaceae, comprising three monophyletic genera (*Discoplastis*, *Lepocinclis*, *Phacus*) and Euglenaceae with seven monophyletic genera (*Euglenaformis*, *Euglenaria, Colacium*, *Cryptoglena*, *Strombomonas*, *Trachelomonas*, *Monomorphina*) and polyphyletic genus *Euglena*. For 150 years researchers have been studying *Euglena* based solely on morphological features what resulted in hundreds of descriptions of new taxa and many artificial intra-generic classification systems. In spite of the progress towards defining *Euglena,* it still remains polyphyletic and morphologically almost undistinguishable from members of the recently described genus *Euglenaria*; members of both genera

B. Zakryś (✉) • R. Milanowski • A. Karnkowska
Department of Molecular Phylogenetics and Evolution, Faculty of Biology, Biological and Chemical Research Centre, University of Warsaw, Żwirki i Wigury 101, 02-089 Warsaw, Poland
e-mail: zakrys@biol.uw.edu.pl

S.D. Schwartzbach, S. Shigeoka (eds.), *Euglena: Biochemistry, Cell and Molecular Biology*, Advances in Experimental Medicine and Biology 979, DOI 10.1007/978-3-319-54910-1_1

have cells undergoing metaboly (dynamic changes in cell shape), large chloroplasts with pyrenoids and monomorphic paramylon grains. Model organisms *Euglena gracilis* Klebs, the species of choice for addressing fundamental questions in eukaryotic biochemistry, cell and molecular biology, is a representative of the genus *Euglena*.

Keywords

Euglena • euglenids • Euglenales • Euglenophyceae • evolution • Excavata • phylogeny • taxonomy

Abbreviations

cpSSU	Cytoplasmic small subunit
EGT	Endosymbiotic gene transfer
hsp90	Heat shock protein 90
ITS	Internal transcribed spacer
LGT	Laterar gene transfer
nLSU	Nuclear large subunit
nSSU	Nuclear small subunit
psbO	Photosystem II manganese-stabilizing polypeptide
RuBisCO	Ribulose-1,5-bisphosphate carboxylase oxygenase

1.1 The Phylogeny of Euglenids

Most of the knowledge about the group of protists called euglenids (Euglenida) comes from extensive studies of the photosynthetic model species *Euglena gracilis*. However, there are thousands of other euglenid species, which differ substantially from *E. gracilis* in morphology or mode of nutrition. Euglenids are a monophyletic group of free-living, single-celled flagellates (in most cases with two flagella) living predominantly in aquatic environments. Their common feature is a unique cell covering called the pellicle, a complex structure consisting of proteinaceous strips which are covered by a cell membrane and underlain by the microtubule system and the cisternae of the endoplasmic reticulum. The pellicle strips extend along the entire length of the cell. The adjacent strips are connected to each other and a sliding movement of one strip relative to another is possible. Cells with helically arranged strips and without fusions of adjacent strips can dynamically change their shape, a process called metaboly, euglenoid motion or euglenoid movement (Leander et al. 2007; Farmer 2011).

Euglenids are closely related to heterotrophic flagellates Symbiontida (free-living flagellates living in low-oxygen marine sediments), Diplonemea (free-living marine flagellates) and Kinetoplastea (free-living and parasitic flagellates, e.g. *Trypanosoma*) (Fig. 1.1). Euglenids, symbiontids, diplonemids and kinetoplastids form a monophyletic group Euglenozoa (Cavalier-Smith 1981; Breglia et al. 2010; Burki 2014). There are three main synapomorphies shared by all members of Euglenozoa: (a) a unique pattern of flagellar root with two basal bodies and three asymmetrically arranged microtubular roots, (b) the presence of a paraxial rod in one or both flagella, (c) the presence of tubular extrusomes (e.g. trichocysts, mucocysts) (Cavalier-Smith 1981; Simpson 1997; Farmer 2011). Molecular and morphological analyses also indicate that Euglenozoans are members of a larger group known as Excavata – one of the five supegroups of Eukayotes – where they form a sister clade to Hetrolobosea (e.g. parasitic species *Naegleria fowleri*) (Hampl et al. 2009; Yabuki et al. 2011; Adl et al. 2012; Burki 2014). However, there are also some reports indicating that the root of Eukayotes should be placed within excavates and that Euglenozoa is the first group which branched off from the main evolutionary lineage of eukaryotes (Cavalier-Smith 2010; Burki 2014). Whereas the monophyly of the Euglenozoa is indisputable, the internal relationships among kinetoplastids, diplonemids, symbiontids

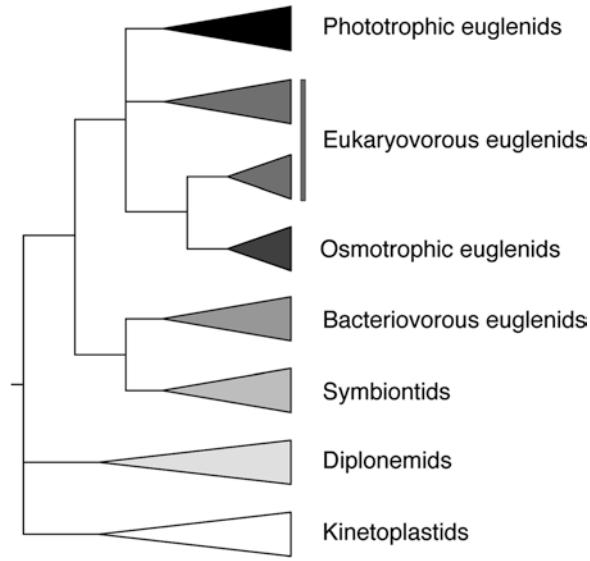

Fig. 1.1. The schematic phylogenetic tree of Euglenozoa according to Breglia et al. 2013

and euglenids are less clear. The most controversial is the phylogenetic position of symbiontids, which group together with bacteriovorus euglenids – in effect the Euglenida seems to be paraphyletic (Yamaguchi et al. 2012; Breglia et al. 2013). Symbiontids are a small group of microaerophilic or anaerobic euglenozoans enveloped by episymbiotic bacteria. In contrast to euglenids, their cells are not covered by a pellicle. So far only three species were classified as symbiontids and further analysis is obviously needed to resolve their relationships with euglenids (Yubuki et al. 2009, 2013; Breglia et al. 2010).

Several different modes of nutrition are observed within euglenids. Most species are heterotrophs (bacteriotrophs, eukaryotrophs or osmotrophs), but there is also one lineage of plastid-bearing photoautotrophs and mixotrophs (Fig. 1.1). The changes of nutritional mode can be tracked on phylogenetic trees (Leander et al. 2007). The basal lineages of euglenids contain phagotrophic species with rigid cell covering; they feed on small prey cells like bacteria. Later more flexible and larger species evolved which feed on larger cells such as other protists. A more elastic cell covering of eukaryovores is the effect of a higher number of helically arranged pellicle strips. Two monophyletic groups of euglenids evolved independently from eukaryovorous ancestors: osmotrophs and photoautotrophs. This indicates that changes in the mode of nutrition, from phagotrophy to osmotrophy as well as from phagotrophy to phototrophy, took place once in the evolution of the group (Linton et al. 1999; Preisfeld et al. 2000, 2001; Müllner et al. 2001; Marin et al. 2003). The rise of phototrophic euglenids (ophyceae) was the result of an unprecedented evolutionary event: a secondary endosymbiosis between a phagotrophic eukaryovorous euglenid and a green alga closely related to extant members of the *Pyramimonas* genus (Gibbs 1978; Turmel et al. 2009; Hrdá et al. 2012). In the most likely scenario, the alga was engulfed and enslaved by the host cell, resulting in chloroplasts surrounded initially by four membranes, two membranes of the primary plastid, the plasma membrane of the green alga and the food vacuole membrane of the euglenid. Subsequently, one of the membranes has been lost, since plastids in all known phototrophic euglenids are surrounded by three membranes. The alternative scenario assumes that chloroplasts of euglenids have never been surrounded by four membranes because the endosymbiont was not acquired by phagocytosis but rather by myzocytosis so that only the cellular contents of the green alga including the chloroplasts were sucked into the food vacuole of a heterotrophic species (Delwiche 1999; Farmer 2011). Apart from the number of membranes, euglenid chloroplasts are

very similar to chloroplasts found in green algae. They contain chlorophyll *a* and *b* and their tylakoids are arranged in groups of three. However, their storage carbohydrate is different. While green algae synthesize starch in the plastids, phototrophic as well as heterotrophic euglenids synthesize a β-1,3-glucan, paramylon, in the cytoplasm. (Kiss et al. 1987). This suggests that the ability to synthesize paramylon must have been present before acquisition of the chloroplasts. Chloroplasts have so far been shown to be present among all genera of Euglenophyceae. There are however known secondary heterotrophic species, which have lost photosynthetic ability. The best known example of such an euglenid is *Euglena longa*, a close relative of *E. gracilis*. This species contains photosynthetically inactive plastids with a reduced plastid genome (Gockel and Hachtel 2000). It is worth mentioning that phototrophic euglenids are not the only eukaryotic group with secondary plastids acquired from green algae. Chlorarachniophytes and dinoflagellates from the genus *Lepidodinium* have chloroplasts acquired from green algae but this does not reflect a close evolutionary relationship. The chloroplasts of euglenids (Excavata), chlorarachniophytes (Rhizaria) and *Lepidodinium* dinoflagellates (Alveolata) were acquired in independent endosymbiotic events from different groups of green algae: prasinophytes, core chlorophytes (Rogers et al. 2007; Turmel et al. 2009) and peridinophytes (Kamikawa et al. 2015), respectively.

The acquisition of chloroplasts by the ancestor of green euglenids was accompanied by endosymbiotic gene transfer (EGT) from the plastid and nuclear genomes of the endosymbiont to the nuclear genome of the host. This process not only integrated the new organelle into the euglenid cell but it also allowed new metabolic pathways to emerge. Surprisingly, it was revealed that the *E. gracilis* nuclear genome contains not only genes of green algal origin but also genes of red algal origin. Genes of red algal origin have also been found in the primary heterotrophic euglenid *Peranema trichophorum* (Maruyama et al. 2011). It is uncertain whether red algal genes were acquired by lateral gene transfer (LGT) or whether they are evidence of a past endosymbiosis with a red alga. Nonetheless, the observed mosaicism of euglenid genome is a result of acquisition of genes derived from not only a distant ancestor and a green algal endosymbiont but also from other evolutionary lineages (Maruyama et al. 2011). For example, several genes encoding enzymes of the Calvin-Benson cycle share an ancestry with red algae and/or chromophytes (organisms with secondary plastids derived from red-algae) (Markunas and Triemer 2016). It seems that some of these genes were already present in the cell of the phagotrophic euglenid which enslaved the green algal endosymbiont and their presence would have facilitated the transition from an endosymbiont to a chloroplast (Maruyama et al. 2011; Markunas and Triemer 2016). Such examples show the impact of lateral/endosymbiotic gene transfers (LGT/EGT) on the evolutionary history of euglenids, the structure of their genomes and the position they hold in ecological niches.

Within the group of Euglenophyceae, three evolutionary lineages can be distinguished (Adl et al. 2012) (Fig. 1.2). The most basal lineage is formed by the genus *Rapaza* with one known marine mixotrophic species, *Rapaza viridis*. This species contains functional chloroplasts but its photosynthetic capacity is probably not sufficient to support growth. The crucial component of the *R. viridis* diet is a green alga prey *Tetraselmis* sp., which is engulfed by phago- or myzocytosis (Yamaguchi et al. 2012). Other green euglenids are split into two groups: Eutreptiales, which comprises species living in marine and brackish environment and Euglenales (=Euglenea) containing species living mostly in small, astatic freshwater reservoirs. The cells of Eutreptiales (two genera: *Eutreptia* and *Eutreptiella*) have 2–4 emergent flagella of equal or unequal length. Because of the presence of helically arranged pellicle strips without fusions they undergo dynamic metaboly. The members of Euglenales have a single emergent flagellum, whereas the second one is hidden within a reservoir – an invagination at the anterior end of the cell (Adl et al. 2012). The Euglenales group is divided into two families: (a) Phacaceae, comprising three monophyletic genera (*Discoplastis*, *Lepocinclis*,

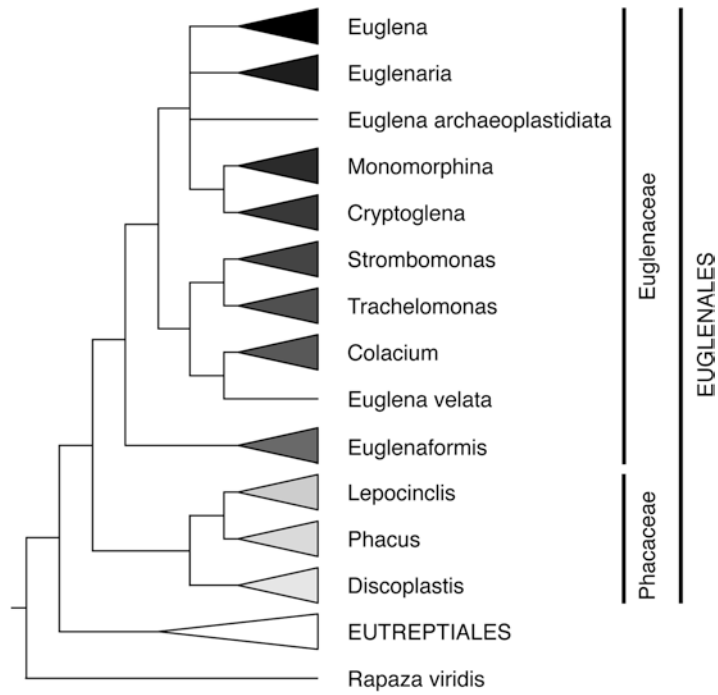

Fig. 1.2. The schematic phylogenetic tree of phototrophic euglenids (Euglenea) according to Karnkowska et al. 2015 and Kim et al. 2015

Phacus) and (b) Euglenaceae with seven monophyletic genera (*Euglenaformis*, *Colacium*, *Strombomonas*, *Trachelomonas*, *Monomorphina*, *Cryptoglena*, *Euglenaria*) (Kim et al. 2010). *Euglena*, the eighth genus of the Euglenaceae family, seems to be polyphyletic and needs reclassification (Karnkowska et al. 2015; Kim et al. 2015). Two species, *Euglena archaeoplastidiata* and *Euglena velata* always remain outside of the main *Euglena* clade and their phylogenetic position is uncertain (Fig. 1.2).

1.2 The Taxonomy of *Euglena*: Nineteenth and Twentieth century

Taxonomic research on phototrophic euglenids dates back to 1830 when Ehrenberg established the genus *Euglena* by grouping together four already described taxa: *Euglena viridis* (= *Cercaria viridis* Müller), *E. sanguinea* (= *Enchelys sanguinea* Ness and Golgfufs), *E. acus* (= *Vibrio acus* Müller), *E. pleuronectes* (= *Cercaria pleuronectes* Müller) with two new species he discovered (*E. pyrum* and *E. longicauda*) (Ehrenberg 1830). During his lifetime Ehrenberg described many new taxa in the genus *Euglena* and established three new genera: *Cryptoglena* Ehrenberg (1831), *Colacium* Ehrenberg (1833) and *Trachelomonas* Ehrenberg (1833); Ehrenberg's original drawings are now available online at the Museum in Berlin (http://download.naturkunde-museum-berlin.de/Ehrenberg/Ec%20Drawings/).

For the next 150 years many researchers have been studying the diversity of euglenids and many new species have been described based solely on their morphological features. This resulted in descriptions of thousands of new taxa (3200 validly published names listed in AlgaeBase: http://www.algaebase.org) and new genera (*Phacus* Dujardin 1841, *Lepocinclis* Perty 1849, *Eutreptia* Perty 1852, *Monomorphina* Mereschkowsky 1877, *Eutreptiella* Da Cunha 1913, *Strombomonas* Deflandre 1930). Many species from the genus *Euglena* were successively transferred to other genera but at the same time, the genus *Euglena* served as kind of a "bag" into which all newly described species that "do not fit" morphologically to other genera were "thrown". That resulted in a morphologically heterogeneous group and correct identification of its

representatives was very difficult. To facilitate the recognition of *Euglena* members, subsequent investigators proposed various intra-generic classification systems. Unfortunately, they were based only on morphological features that different researchers considered as diagnostic in an arbitrary manner. For example, Gojdics (1953) distinguished eight "groups" (A-E) based on chloroplast organization. Pringsheim (1956) distinguished five "tentative Groups (Taxa) or subgenera" (Rigidae, Lentiferae, Catilliferae, Radiatae, Serpentes) based on cell shape and chloroplast morphology. Zakryś (1986) distinguished three subgenera (Euglena, Calliglena and Discoglena) taking into account the number, morphology and position of the chloroplasts in the cells, the number and morphology of paramylon grains and presence or absence of pyrenoids. As mentioned before, our understanding of morphological features was changing substantially over the time and more recently it started to be interpreted in the context of the evolution of autotrophic euglenids.

1.3 The Main Morphological Diagnostic Features

Detailed studies on morphological plasticity and tracing morphological characters on the reliable phylogenetic tree were unable to decipher the evolution of the characters and define diagnostic features for individual clades. Two characters, the presence of lorica and mucilaginous stalks, are synapomorphic (lorica for the clade grouping *Strombomonas* and *Trachelomonas* and mucilaginous stalks for *Colacium*). Evolution of other characters, cell metaboly, morphology of chloroplasts, presence of pyrenoids, morphology of paramylon grains and the presence and shape of mucocysts, was more complicated but they also can serve as useful diagnostic features.

Metaboly: The morphology and organization of the pellicular strips correlates well with the cell plasticity. Cells with fewer strips tend to be rigid while those with many strips often exhibit euglenoid movement called also metaboly (Leander et al. 2007; Farmer 2011). The ancestral state reconstruction suggested that the ancestor of the freshwater photosynthetic euglenids was characterized by cell undergoing dynamic metaboly and that is the predominant character observed among extant photosynthetic euglenids, including *Euglena*. Rigid cells among Euglenophyceae arose twice. Once in the common ancestor of *Phacus* and *Lepocinclis* and once in the common ancestor of *Monomorphina* and *Cryptoglena* (Karnkowska et al. 2015).

Chloroplasts: Chloroplasts of euglenids exhibit great morphological diversity. The ancestor of freshwater autotrophic euglenids probably had numerous small discoid plastids (a few micrometers in diameter) without a pyrenoid. This type of chloroplast is characteristic for representatives of the family Phacaceae and the genus *Euglenaformis,* the most basal clade of the family Euglenaceae (Karnkowska et al. 2015). Other Euglenaceae are characterized by larger chloroplasts but they vary in shape (stellate, lobed or spherical), size, number per cell (from one to numerous) and location (parietal, partly parietal or axial). Typically, they possess pyrenoids.

Pyrenoid: One of the structural features associated with many euglenoid chloroplasts is the pyrenoid, an area in which ribulose-1,5-bisphosphate carboxylase oxygenase (RuBisCO) tends to be concentrated (Osafune et al. 1990). Pyrenoids are not visible under the light microscope but often the pyrenoids are accompanied by a bilateral paramylon cap, "diplopyrenoid", a single paramylon cap "haplopyrenoid" or a cluster of small paramylon grains, "paramylon center"; in some species pyrenoid is "naked". Often the presence of the pramylon cap indicates the presence of the pyrenoid. The common ancestor of the freshwater photosynthetic euglenids most probably had pyrenoids as supported by the presence of pyrenoids in the green algae related to the possible donor of the *Euglena* chloroplast. However, not all autotrophic euglenids possess pyrenoids and it was proposed that they were lost independently twice, in the common ancestor of

the family Phacaceae, and in the genus *Euglenaformis* (Karnkowska et al. 2015).

Paramylon: The storage material paramylon, a β-1, 3 glucan, can be found free in the cytoplasm or may be associated with the chloroplasts forming "caps" or "paramylon centers" over the pyrenoids. Small paramylon grains are observed in all euglenoid cells. In addition to these ubiquitous small grains, many phototrophic species produce a larger type of paramylon grains (Monfils et al. 2011). The presence of small and large grains is referred to as "dimorphic" in contrast to "monomorphic" when only small grains are present in the cell. An ancestral state reconstruction suggested that dimorphic paramylon grains evolved twice, once in the common ancestor of the family Phacaceae, and once in the common ancestor of *Monomorphina* and *Cryptoglena*, members of the family Euglenaceae (Karnkowska et al. 2015).

Mucocysts: Mucocysts are membrane bound small bodies with openings, positioned under the pellicle, which contain mucilaginous threads. Mucocysts are always uniform in size and shape, either spherical or spindle-shaped, arranged in parallel rows which follow the spiral alignment of the pellicle strips. In some taxa, the mucocysts are readily visible but in most cases they are visible only after staining with neutral red. Mucocysts are only characteristic for some representatives of *Euglena*. Ancestral state reconstruction indicated that the common ancestor of *Euglena* lacked mucocysts so they probably appeared independently at least two times in the genus *Euglena* (Karnkowska et al. 2015).

1.4 The Current View on the Taxonomy and Phylogeny of *Euglena*

The advent of molecular phylogenetics and combination of molecular and morphological data has had a huge impact on our understanding of the relationships within the genus *Euglena* and in the whole group of euglenids. The first phylogenetic tree was based on nuclear small subunit (nSSU) rDNA sequences including only four species of euglenids (Montegut-Felkner and Triemer 1997). Later, the number of species used for phylogenetic analyses increased (Linton et al. 1999, 2010; Moreira et al. 2001; Müllner et al. 2001; Marin et al. 2003; Nudelman et al. 2003; Shin and Triemer 2004; Kosmala et al. 2007a, b; Karnkowska-Ishikawa et al. 2010, 2011, 2012, 2013; Łukomska-Kowalczyk et al. 2015) and other molecular markers were employed: internal transcribed spacer (ITS) (Zakryś et al. 2004), nuclear large subunit (nLSU) rDNA (Brosnan et al. 2003; Ciugulea et al. 2008; Linton et al. 2010; Kim et al. 2012, 2013; Kim and Shin 2014), cytoplasmic small subunit (cpSSU rDNA) (Zakryś et al. 2002; Milanowski et al. 2001, 2006; Linton et al. 2010), chloroplast LSU rDNA (Kim and Shin 2008; Kim et al. 2015) and nuclear encoded protein coding sequences of *hsp*90 and *psb*O genes (Karnkowska et al. 2015).

The molecular phylogenetic trees clearly demonstrated that the "bag all-catch" genus *Euglena* was indeed paraphyletic and/or polyphyletic (Linton et al. 1999, 2010) and required the transfer of several of the more rigid "*Euglena*" species with numerous small discoid plastids without pyrenoids (classified into subgenus *Discoglena sensu* Zakryś 1986, e.g. *Euglena acus* (O.F. Müller) Ehrenberg, *E. oxyuris* Schmarda, *E. tripteris* (Dujardin) Klebs, *E. spirogyra* Ehrenberg, *E. fusca* (Klebs) Lemmermann) to the genus *Lepocinclis* (Marin et al. 2003; Kosmala et al. 2005). That was the first step in a major reorganization of the genus *Euglena*. The new genus *Discoplastis* was created for two taxa, *E. spathirhyncha* Skuja and *E. adunca* Schiller, both having highly metabolic cells and numerous small discoid plastids without pyrenoids, and formed a well suported clade near the base of the euglenoid lineage independent of the *Euglena* clade (Triemer et al. 2006). Similar plastids were also observed in *E. proxima*, but the species formed an independent lineage from *Discoplastis* and *Euglena* (Milanowski et al. 2006), and was finally described as a new genus *Euglenaformis* based on phylogenomic analyses (Bennett et al. 2014). After this change,

all taxa with small numerous discoid chloroplasts without pyrenoids were moved from the genus *Euglena*, which now contains only species with large stellate or lobed chloroplasts with pyrenoids. Surprisingly, phylogenetic analyses revealed that three more species, *Euglena anabaena* Mainx, *E. caudata* Hübner and *E. clavata* Skuja, formed well-supported clade outside of the *Euglena* despite having morphology that fit well into the genus *Euglena*. This group of cryptic species was transferred into a new genus *Euglenaria* (Linton et al. 2010). Currently the genus *Euglenaria* contains four species after including *Eu. clepsydroides* Zakryś, a newly discovered species recently found in Poland (Zakryś et al. 2013). Nevertheless, the genus *Euglena* still remains paraphyletic/polyphyletic with two species branching out of the main *Euglena* trunk, *Euglena archaeoplastidiata* and *Euglena velata*. On phylogenetic trees, *E. archaeoplastidiata* diverges prior to the *Monomorphina/Cryptoglena* or the *Euglenaria* clade (Karnkowska et al. 2015; Kim et al. 2015) while the *E. velata* strain complex is sister to the genus *Colacium* (Kim et al. 2015) (Fig. 1.2). *Euglena archaeoplastidiata* has a single, parietal chloroplast similar to those observed in *Monomorphina* and *Cryptoglena* but some characters like the presence of only small paramylon grains (monomorphic), diplopyrenoids (pyrenoid with two paramylon caps) and metaboly are more similar to the characters of *Euglena* or *Euglenaria*. *Euglena velata* shares morphological features with representatives of the genus *Euglena* (or *Euglenaria*).

Comparative morphological and molecular studies have revealed that many taxa from the genus *Euglena* described in the literature are taxonomically not justified. For many species, diagnostic descriptions were emended, epitypes established, keys to correct identification were created and complicated nomenclature issues were sorted out (Zakryś et al. 2002; Shin and Triemer 2004; Kosmala et al. 2009; Karnkowska-Ishikawa et al. 2012, 2013), and two new species were described (*E. pseudostellata* Zakryś and Kosmala and *E. pseudochadefaudii* Zakryś and Kosmala) (Kosmala et al. 2009). In summary, to-date about 150 taxa have been verified taxonomically representing almost one third of all the taxa described in the genus *Euglena* (AlgaeBase: http://www.algaebase.org provides 560 validly published names of species, varieties and forms).

1.5 The Taxonomic Future of the Genus *Euglena*

Recent advances in the taxonomy of the genus *Euglena* are the result of the increased taxon sampling in phylogenetic analyses. New lineages, not related with *Euglena*, but previously classified in this genus based on their morphology (Marin et al. 2003; Triemer et al. 2006; Linton et al. 2010) have been revealed. In spite of the progress in the taxonomy of *Euglena*, it still remains polyphyletic. Moreover, many more taxa resembling *Euglena* have been described but not studied at the molecular level so far.

The most commonly used molecular marker for autotrophic euglenids is nuclear SSU rDNA, with available sequences representing 148 taxonomically verified taxa. That is less than 5% of all described taxa and as a consequence, most genera are poorly represented on the phylogenetic trees (Fig. 1.2). Those sequences mainly represent most common species deposited in culture collections and do not reflect the large morphological diversity of phototrophic euglenids. Only 20% of the sequences are from taxa recently isolated from the environment.

Almost all of the strains from the culture collections have been already sequenced, therefore more strains need to be isolated from the environment. However, establishing new cultures is a very labour-intensive and time-consuming process with a very low efficiency because many of species do not survive in the laboratory conditions (Bennett and Triemer 2012; Lax and Simpson 2013). New approaches such as multiple displacement amplification using just a few cells (Bennett and Triemer 2012) or the single-cell approach (Lax and Simpson 2013) have recently been shown to be a valuable tool to overcome those limitations and have been employed to study the biodiversity and phylogeny of both

phototrophic (Bennett and Triemer 2012; Łukomska-Kowalczyk et al. 2015) and phagotrophic euglenids (Lax and Simpson 2013).

1.6 The Molecular Identification of Photosynthetic Euglenids

Knowledge about the biodiversity of euglenids is limited mainly due to difficulties with species identification based on morphological characters and species definition in an asexual group. Nowadays, molecular techniques of identification are an increasingly valuable tool for studying the diversity of this group. One of the most widely used methods for molecular identification is DNA barcoding. This technique is based on the assumption that the diversity of short DNA fragments reflects the diversity of the organisms themselves (Hebert et al. 2003). This is true for many groups of organisms and valuable barcodes have been assigned and successfully used in animals, fungi and plants. The species assignment is based on a comparison of the sequence of interest with the reference database. Once a good barcode and reference database are established, the method is fast and accurate (Blaxter 2004). It is a valuable tool for biodiversity research (Hajibabaei et al. 2007), detection of a particular species in the environment (Hajibabaei et al. 2011), detection of new species (Hajibabaei et al. 2007) and ecological studies (Joly et al. 2014). A database of nSSU rDNA sequences of taxonomically validated species (reference sequences) was recently established for autoptrophic euglenids and the variable regions, V2-V3 and V4, of nuclear rDNA were recommend as DNA barcodes (Łukomska-Kowalczyk et al. 2016). Using DNA barcoding will facilitate research on biodiversity of autotrophic euglenids and will enable research on species other than *Euglena gracilis.* The majority of applied and basic research utilize *E. gracilis* Klebs 1883 mainly because it is easy to isolate, maintain in the laboratory, and there are many strains of *E. gracilis* in the culture collections of algae including the best-known strain "Z". It is not a species commonly found in a typical for euglenids eutrophic habitats that have a high content of organic compounds and it does not create blooms as seen for many other representatives of the autotrophic euglenids e.g. *Euglena stellata*, *Euglena sanguinea*, *Euglenaria anabaena*, *Lepocinclis oxyuris* or *Phacus salina* (long-term observations of the authors). For these reasons, *E. gracilis* is not a typical representative inhabitant of the eutrophic and hyper eutrophic environment where euglenids are very common. Molecular identification methods (e.g. barcodes) can change the status quo by allowing isolation of new species (characteristic for some environments, toxic or rare) from natural populations for many kinds of basic and applied research such as industrial wastewater purification, the production of biofuels or the development of new monitoring methods which could predict the mass appearance of toxic species (like *Euglena sanguinea*) in fish breeding ponds, recreational places or drinking water reservoirs.

1.7 The Current Classification of Euglenids

Taking into account the recent changes in the taxonomy of euglenids, the current classification is as follows:

EXCAVATA Cavalier-Smith 2002, *emended* by Simpson 2003

Euglenozoa Cavalier-Smith 1981, *emended* by Simpson 1997

- Euglenida Bütschli 1884, *emended* by Simpson 1997
- Euglenophyceae Schoenichen 1925 (in Eyferth and Schoenichen 1925), *emended* by Marin and Melkonian 2003 (in Marin et al. 2003)
- Euglenales Leedale 1967, emended by Marin and Melkonian 2003 (in Marin et al. 2003) (= Euglenea Bütschli 1884, emended by Busse and Preisfeld 2003)
- Euglenaceae Dujardin 1841, emended by Kim, Triemer and W. Shin 2010 (in Kim et al. 2010)
- *Euglena* Ehrenberg 1830, emended by Marin and Melkonian 2003 (in Marin et al. 2003)
- *Cryptoglena* Ehrenberg 1831, emended by Kosmala and Zakryś 2007 (in Kosmala et al. 2007a)
- *Colacium* Ehrenberg 1833

- *Trachelomonas* Ehrenberg 1833
- *Monomorphina* Mereschkowsky 1877, *emended* by Kosmala and Zakryś 2007 (in Kosmala et al. 2007a)
- *Strombomonas* Deflandre 1930
- *Euglenaria* Karnkowska, Linton and Kwiatowski 2010 (in Linton et al. 2010)
- *Euglenaformis* M. S. Bennett and Triemer 2014 (in Bennett et al. 2014)
- Phacaceae Kim, Triemer and W. Shin 2010 (in Kim et al. 2010)
- *Phacus* Dujardin 1841, *emended* by Linton and Karnkowska 2010 (in Linton et al. 2010)
- *Lepocinclis* Perty 1849, *emended* by Marin and Melkonian 2003 (in Marin et al. 2003)
- *Discoplastis* Triemer 2006 (in Triemer et al. 2006)
- Eutreptiales Leedale 1967, *emended* by Marin and Melkonian 2003 (in Marin et al. 2003)
- Eutreptiaceae Hollande 1942
- *Eutreptia* Perty 1852
- *Eutreptiella* Da Cunha 1913, *emended* by Marin and Melkonian 2003 (in Marin et al. 2003)
- *Rapaza* Yamaguchi, Yubuki and Leander 2012 (in Yamaguchi et al. 2012)

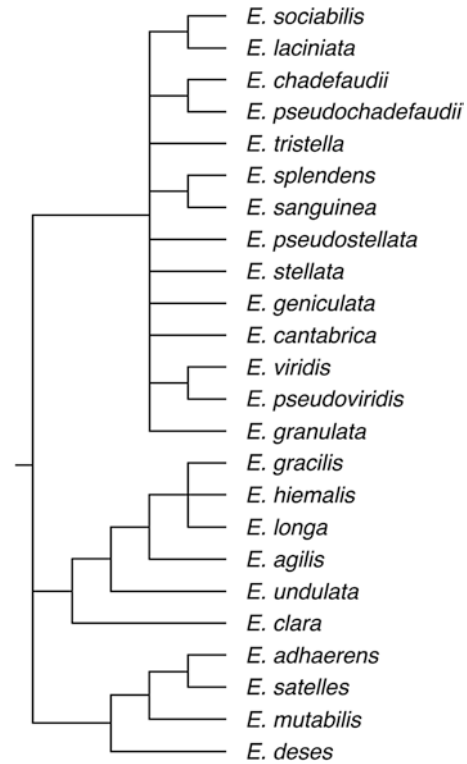

Fig. 1.3. The schematic phylogenetic tree of the genus *Euglena* according to Karnkowska et al. 2015 and Kim et al. 2015

1.8 Short Descriptions of the Families and Genera Classified in the Euglenales

The family Euglenaceae Dujardin 1841, *emended* by Kim et al. 2010

Comprise eight genera whose members have one emergent flagella and large chloroplasts with pyrenoids. The exception to this is the genus *Euglenaformis* with chloroplasts without pyrenoids.

Euglena Ehrenberg 1830, *emended* by Marin and Melkonian 2003

After all the recent reclassifications the genus *Euglena* includes only species with not flattened cells undergoing dynamic metaboly, characterized also by monomorphic paramylon grains (except some physiological forms of *E. deses*) and large chloroplasts with pyrenoids. Based on the number and shape of the chloroplasts, their location in the cell, parietal, partly parietal, axial, and the form of paramylon accompanying the pyrenoids, diplopyrenoids, haplopyrenoids, paramylon centers, naked pyrenoids, all species can be divided into four morphological groups (Triemer and Zakryś 2015).

1. Species with a single, parietal, spherical chloroplast and two diplopyrenoids. Only one species (*E. archaeoplastidiata*) represents this morphogroup but its position on the phylogenetic tree is unstable (Fig. 1.2).
2. Species with axial, stellate chloroplasts (1, 2 or 3) with each chloroplast having a paramylon center. There are nine species in this group which are accepted after the latest taxonomic revision: five taxa with one chloroplast: *E. cantabrica, E. stellata, E. pseudostellata, E. viridis E. pseudoviridis*; three taxa with two chloroplasts: *E. geniculata, E. chadefaudii, E. pseudochadefaudii,* and one species with three chloroplasts; *E. tristella* (Kosmala et al. 2009). Most species are common and cosmopolitan

in bodies of water rich in organic compounds. Fusiform or spherical mucocysts are present in most species which is a very useful diagnostic feature. Members of this group do not form a monophyletic clade on the phylogenetic tree (Fig. 1.3).

3. Species with parietal, lobed chloroplasts. Each chloroplast has a single pyrenoid (naked, diplo- or haplopyrenoid). *Euglena gracilis* belongs to this morphogroup and is closely related to *E. hiemalis*, a species hardly distinguishable morphologically from *E. gracilis,* and *E. longa*, a colourless species. Although *Euglena gracilis* is a model species for studies on phototrophic euglenids, its taxonomy and taxonomy of closely related species has not been emended so far based on molecular phylogenetic analyses. Some species are very common and cosmopolitan, *E. agilis, E. deses* or *E. granulata.* They can be identified based only on morphological diagnostic features but in the case of most species it is much easier to distinguish them at the molecular level and sometimes this is the only way to separate them (Karnkowska et al. 2012) (Figs. 1.2 and 1.3).
4. Species with plate-like, partially parietal chloroplasts where the centers of the chloroplasts are located deep within the cytoplasm while the rest of the chloroplast surface, which is radially cut into long bands, reaches the pellicle. Each chloroplast has a diplopyrenoid. Fusiform mucocysts are present in cells of all species. There are four currently accepted species in this group, *E. laciniata*; *E. sanguinea, E. sociabilis* and *E. splendens* (Karnkowska-Ishikawa et al. 2013). All of them are common and cosmopolitan. Toxic blooms of *E. sanguinea* were recently observed (Zimba et al. 2004). Ichthyotoxins produced by this species cause important economic losses in commercial agriculture ponds in the United States (Zimba et al. 2004, 2010). Members of this group do not form a monophyletic clade on the phylogenetic tree (Fig. 1.3).

- ***Euglenaria*** Karnkowska, Linton and Kwiatowski 2010

Species of the genus *Euglenaria* are morphologically indistinguishable from the members of the genus *Euglena* that have plate-like chloroplasts with diplopyrenoids. Instead, the molecular nSSU characters are the diagnostic characters that separate *Euglenaria* from *Euglena* (Linton et al. 2010). There are four species in this genus: *E. anabaena, E. clavata, E. caudata* and *E. clepsydroides*. Most of them are common and cosmopolitan in eutrophic environments rich in organic material, where they very often form blooms.

- ***Euglenaformis*** M.S. Bennett and Triemer 2014

This genus contains only one species *Euf. proxima* which differs from the members of *Euglena* by having chloroplasts without pyrenoids.

- ***Colacium*** Ehrenberg 1833

Members of this genus have *Euglena*-like cells that attach to a substratum (mostly planktonic animals - copepods, rotifers) by production of mucilaginous stalks.

- ***Monomorphina*** Mereschkowsky 1877, *emended* by Kosmala and Zakryś 2007

The presence of a single spherical chloroplast with haplopyrenoids in rigid pear-shaped cells and large parietal paramylon plates, located between the pellicle and the chloroplast are diagnostic features of eight species classified in this genus after recent taxonomical verification. Only one, *M. aenigmatica*, is morphologically identifiable. The remaining seven species can only be identified at the molecular level (Kim et al. 2012).

- ***Cryptoglena*** Ehrenberg 1831, *emended* by Kosmala and Zakryś 2007

This genus contains five species taxonomically verified and all of them can be identified only at

the molecular level. Cells of the members of this genus resemble a coffee bean in shape. The single, parietal, large chloroplast forms an open cylinder in the shape of the letter "C" and contains two haplopyrenoids whose presence is not sufficiently described. Two large paramylon plates are located laterally between the chloroplast and the pellicle.

- ***Trachelomonas*** Ehrenberg 1833, ***Strombomonas*** Deflandre 1913

In both genera, cells undergoing metaboly (*Euglena*-like) are enclosed in a mineralized envelope, the lorica, with an apical pore through which the locomotory flagellum emerges. Shape and ornamentation of the lorica are used as classical diagnostic features for distinguishing both genera.

The family Phacaceae Kim, Triemer and Shin 2010

Contains three genera whose members have one emergent flagella and numerous, parietal, small, disc-shaped chloroplasts that lack pyrenoids.

- ***Phacus*** Dujardin 1841, *emended* by Linton and Karnkowska 2010

All members of this genus have dimorphic paramylon grains and rigid, flattened, leaf-shaped, sometimes twisted cells. There are only two exceptions from this characteristic; *P. limnophila* and *P. salina* recently moved into *Phacus*. Cells of both species are not flattened and *P. salina* has monomorphic paramylon grains. Colorless forms are known [e.g. *Phacus ocellatus* (Pringsheim) Marin and Melkonian].

- ***Lepocinclis*** Perty1849, *emended* by Marin and Melkonian 2003

Cells are not flattened, only rarely compressed or triangular in apical view, rigid or semi rigid and sometimes twisted. Paramylon grains are dimorphic in size. Colorless forms are known (*L. cyclidiopsis* M. S. Bennett and Triemer).

- ***Discoplastis*** Triemer 2006

This genus currently contains two species, *D. adunca* and *D. spathirhyncha,* reclassified from the genus *Euglena*. Morphologically these species are very similar to *Lepocinclis* and *Phacus* because of the presence of small, parietal, discoid chloroplasts lacking pyrenoids but they are distinguishable from the other two genera by having cells undergoing dynamic metaboly.

References

Adl SM, Simpson AGB, Lane CE et al (2012) The revised classification of eukaryotes. J Eukaryot Microbiol 59:429–493

Bennett MS, Triemer RE (2012) A new method for obtaining nuclear gene sequences field samples and taxonomic revisions of the photosynthetic euglenoids *Lepocinclis* (*Euglena*) *helicoideus* and *Lepocinclis* (*Phacus*) *horridus* (Euglenophyta). J Phycol 48: 254–260

Bennett M, Wiegert KE, Triemer RE (2014) Characterization of new genus *Euglenaformis* and the chloroplast genome of *Euglenaformis* [*Euglena*] *proxima* (Euglenophyta). Phycologia 53:66–73

Blaxter ML (2004) The promise of a DNA taxonomy. Philos Trans R Soc Lond Ser B Biol Sci 359:669–679

Breglia SA, Yubuki N, Hoppenrath M, Leander BS (2010) Ultrastructure and molecular phylogenetic position of a novel euglenozoan with extrusive episymbiotic bacteria: *Bihospitebacati* n.gen. et n.sp.(Symbiontida). BMC Microbiol 10:145

Breglia SA, Yubuki N, Leander BS (2013) Ultrastructure and Molecular Phylogenetic Position of Heteronema scaphurum: A Eukaryovorous Euglenid with a Cytoproct. J Eukaryot Microbiol 60:107–120

Brosnan S, Shin W, Kjer KM, Triemer RE (2003) Phylogeny of the photosynthetic euglenophytes inferred from the nuclear SSU and partial LSU rDNA. Int J Syst Evol Microbiol 53:1175–1186

Burki F (2014) The eukaryotic tree of life from a global phylogenomic perspective. Cold Spring Harb Perspect Biol 6:a016147

Busse I, Preisfeld A (2003) Systematics of primary osmotrophic euglenids: a molecular approach to the

phylogeny of *Distigma* and *Astasia* (Euglenozoa). Int J Syst Evol Microbiol 53:617–624
Bütschli O (1884) Mastigophora in Bronn's Klassen u. Ordnungen des Thierreichs, vol 1. Winter's Verlag, Leipzig, pp 617–1097
Cavalier-Smith T (1981) Eukaryote kingdoms: seven or nine? Biosystems 14:461–481
Cavalier-Smith T (2002) The phagotrophic origin of eukaryotes and phylogenetic classification of Protozoa. Int J Syst Evol Microbiol 52:297–354
Cavalier-Smith T (2010) Kingdoms Protozoa and Chromista and the eozoan root of the eukaryotic tree. Biol Lett 6:342–345
Ciugulea I, Nudelman MA, Brosnan S, Triemer RE (2008) Phylogeny of the euglenoid loricate genera *Trachelomonas* and *Strombomonas* (Euglenophyta) inferred from nuclear SSU and LSU rDNA. J Phycol 44: 406–418
Da Cunha AM (1913) Contribuicao para o conhecimento da fauna de Protozoarios do Brasil. Mem Inst Oswaldo Cruz 5:101–122
Deflandre G (1930) *Strombomonas*, nouveau genre d'Euglénacées (Trachelomonas EHR. pro parte). Arch Protistenkd 69:551–614
Delwiche CF (1999) Tracing the thread of plastid diversity through the tapestry of life. Am Nat 154:S164–S177
Dujardin F (1841) Historie naturelle des zoophytes infusoires: comprenant la physiologie et la classification de ces animaux et la maniere de les etudier a l'aide du microscope. Libraire encyclopedique de Roret, Paris, p 684
Ehrenberg GC (1830) Beiträge zur Kenntnß der Organisation der Infusorien und ihrer geographischen Verbreitung, brsonders in Sibirien. Abhandlungen der Königlichen Akademie der Wissenschaften zu Berlin, pp 1–88
Ehrenberg CG (1831) Über die Entwickelung und Lebensdauer der Infusionsthiere; nebst ferneren Beiträgen zu einer Vergleichung ihrer organischen Systeme. Abhandlungen der Königlichen Akademie der Wissenschaften Berlin (1832)
Ehrenberg CG (1833) Dritter Beitrag zur Erkenntniß großer Organisation in der Richtung des kleinstes Raumes. Physikalishe Abhandlungen Königlichen Akademie der Wissenschaften zu Berlin (1835), pp 145–336
Eyferth B and Schoenichen W (1925) Einfachste Lebensformen des Tier- und Pflanzenreiches. 5. Aufl. Band I. Spaltpflanzen, Geissellinge, Algen, Pilze. Berlin: Lichterfelde, pp vii + 519
Farmer MA (2011) Euglenozoa. Eucaryotic Microbes: 311–321
Gibbs SP (1978) The chloroplast of Euglena may have evolved from symbiotic green algae. Can J Bot 56:2883–2889
Gockel G, Hachtel W (2000) Complete Gene Map of the Plastid Genome of the Nonphotosynthetic Euglenoid Flagellate *Astasia longa*. Protist 151:347–351
Gojdics M (1953) The Genus Euglena. The University of Wisconsin Press, Madison, p 253
Hajibabaei M, Singer GAC, Hebert PDN, Hickey DA (2007) DNA barcoding: how it complements taxonomy, molecular phylogenetics and population genetics. Trends Genet 23:167–172
Hajibabaei M, Shokralla S, Zhou X, Singer GAC, Baird DJ (2011) Environmental barcoding: A next-generation sequencing approach for biomonitoring applications using river benthos. PLoS One 6(4)
Hampl V, Hug L, Leigh JW, Dacks JB, Lang BF, Simpson AGB, Roger AJ (2009) Phylogenomic analyses support the monophyly of Excavata and resolve relationships among eukaryotic "supergroups". Proc Natl Acad Sci U S A 106:3859–3864
Hebert PDN, Cywinska A, Ball SL, deWaard JR (2003) Biological identifications through DNA barcodes. Proc Biol Sci 270:313–321
Hollande A (1942) Étude cytologique et biologique de quelques flagellés libres. Arch Zool exp et gén 83: 1–268
Hrdá Š, Fousek J, Szabová J, Hampl V, Vlček Č (2012) The plastid genome of *Eutreptiella* provides a window into the process of secondary endosymbiosis of plastid in euglenids. PLoS One 7:e33746
Joly S, Davies TJ, Archambault A, Bruneau A, Derry A, Kembel SW, Peres-Neto P, Vamosi J, Wheeler T (2014) Ecology in the age of DNA barcoding: The resource, the promise and the challenges ahead. Mol Ecol Resour 14:221–232
Kamikawa R, Tanifuji G, Kawachi M, Miyashita H, Hashimoto T, Inagaki Y (2015) Plastid genome-based phylogeny pinpointed the origin of the green-colored plastid in the dinoflagellate *Lepidodinium chlorophorum*. Genome Biol Evol 7:1133–1140
Karnkowska A, Bennett MS, Watza D, Kim JI, Zakryś B, Triemer RE (2015) Phylogenetic relationships and morphological character evolution of photosynthetic euglenids (Excavata) inferred from taxon-rich analyses of five genes. J Eukaryot Microbiol 62:362–373
Karnkowska-Ishikawa A, Milanowski R, Kwiatowski J, Zakryś B (2010) Taxonomy of the *Phacus oscillans* (Euglenaceae) and its close relatives – balancing morphological and molecular features. J Phycol 46: 172–182
Karnkowska-Ishikawa A, Milanowski R, Zakryś B (2011) The species *Euglena deses* (Euglenaceae) revisited: new morphological and molecular data. J Phycol 47:653–661
Karnkowska-Ishikawa A, Milanowski R, Triemer RE, Zakryś B (2012) Taxonomic revisions of morphologically similar species from two genera: *Euglena* (*E. granulata* and *E. velata*) and *Euglenaria* (*Eu. anabaena, Eu. caudata, Eu. clavata*). J Phycol 48: 729–739
Karnkowska-Ishikawa A, Milanowski R, Triemer RE, Zakryś B (2013) A redescription of morphologically similar species from the genus *Euglena*: *E. laciniata*,

E. sanguinea, *E. sociabilis*, and *E. splendens*. J Phycol 49:616–626

Kim JI, Shin W (2008) Phylogeny of the Euglenales inferred from plastid LSU rDNA sequences. J Phycol 44:994–1000

Kim JI, Shin W (2014) Molecular phylogeny and cryptic diversity of the genus *Phacus* (Phacaceae, Euglenophyceae) and the descriptions of seven new species. J Phycol 50:948–959

Kim JI, Shin W, Triemer RE (2010) Multigene analyses of photosynthetic euglenoids and new family Phacaceae (Euglenales). J Phycol 46:1278–1287

Kim IJ, Shin W, Triemer RE (2012) Phylogenetic reappraisal of the genus *Monomorphina* (Euglenophyceae) based on molecular and morphological data. J Phycol 49:82–91

Kim IJ, Shin W, Triemer RE (2013) Cryptic speciation in the genus *Cryptoglena* (Euglenaceae) revealed by nuclear and plastid SSU and LSU rDNA gene. J Phycol 49:92–102

Kim JI, Linton EW, Shin W (2015) Taxon-rich multigene phylogenty of photosynthetic euglenoids (Euglenohpyceae). Front Ecol Evol 3:98

Kiss JZ, Vasconcelos AC, Triemer RE (1987) Structure of the euglenoid storage carbohydrate, Paramylon. Am J Bot 74:877–882

Klebs G (1883) Über die Organisation einiger Flagellaten-Gruppen und ihre Beziehungen zu Algen und Infusorien. Unters Bot Inst Tübingen 1:233–262

Kosmala S, Karnkowska A, Milanowski R, Kwiatowski J, Zakryś B (2005) Phylogenetic and taxonomic position of *Lepocinclis fusca* comb. nov. (= *Euglena fusca*) (Euglenaceae): Morphological and molecular justification. J Phycol 41:1258–1267

Kosmala S, Milanowski R, Brzóska K, Pękala M, Kwiatowski J, Zakryś B (2007a) Phylogeny and systematics of the genus *Monomorpina* (Euglenaceae) based on morphological and molecular data. J Phycol 43:171–185

Kosmala S, Bereza M, Milanowski R, Kwiatowski J, Zakryś B (2007b) Morphological and molecular examination of relationships and epitype establishment of *Phacus pleuronectes, Phacus orbicularis* and *Phacus hamelii*. J Phycol 43:1071–1082

Kosmala S, Karnkowska-Ishikawa A, Milanowski R, Kwiatowski J, Zakryś B (2009) Phylogeny and systematics of species from the genus *Euglena* (Euglenaceae) with axial, stellate chloroplasts based on morphological and molecular data - new taxa, emended diagnoses and epitypifications. J Phycol 45:464–481

Lax G, Simpson AGB (2013) Combining molecular data with classical morphology for uncultured phagotrophic Euglenids (Excavata): a single-cell approach. J Eukaryot Microbiol 60(6):615–625

Leander BS, Esson HJ, Breglia SA (2007) Macroevolution of complex cytoskeletal systems in euglenids. BioEssays 29:987–1000

Leedale GF (1967) *Euglenoid flagellates*. Prentice-Hall, Englewood Cliffs, N. J. p. 242

Linton EW, Hittner D, Lewandowski C, Auld T, Triemer RE (1999) A molecular study of euglenoid phylogeny using small subunit rDNA. J Eukaryot Microbiol 46:217–223

Linton EW, Karnkowska-Ishikawa A, Kim JI, Shin W, Bennett MS, Kwiatowski J, Zakryś B, Triemer RE (2010) Reconstructing Euglenoid Evolutionary Relationships using Three Genes: Nuclear SSU and LSU, and Chloroplast SSU rDNA Sequences and the Description of *Euglenaria* gen. nov. (Euglenophyta). Protist 161:603–619

Łukomska-Kowalczyk M, Karnkowska A, Milanowski R, Łach Ł, Zakryś B (2015) Delimiting species in the *Phacus longicauda* complex (Euglenida) through morphological and molecular analyses. J Phycol 51:1147–1157

Łukomska-Kowalczyk M, Karnkowska A, Krupska M, Milanowski R, Zakryś B (2016) DNA barcoding in autotrophic euglenids: evaluation of COI and 18S rDNA. J Phycol 52:951–960

Marin B, Palm A, Klingberg MM (2003) Phylogeny and taxonomic revision of plastid-containing Euglenophytes based on SSU rDNA sequence comparisons and synapomorphic signatures in the SSU rRNA secondary structure. Protist 154:99–145

Markunas CM, Triemer RE (2016) Evolutionary history of the enzymes involved in the Calvin–Benson cycle in euglenids. J Eukaryot Microbiol 63:326–339

Maruyama S, Suzaki T, Weber APM, Archibald JM, Nozaki H (2011) Eukaryote-to-eukaryote gene transfer gives rise to genome mosaicism in euglenids. BMC Evol Biol 11:105

Mereschkowsky KS (1877) Etjudy nad prostejsimi zivotnymi severa Rossii. Trudy S-Peterburgsk Obshch Estestvoisp 8:1–299

Milanowski R, Zakryś B, Kwiatowski J (2001) Phylogenetic analysis of chloroplast small-subunit rRNA genes of the genus *Euglena* Ehrenberg. Int J Syst Evol Microbiol 51:773–781

Milanowski R, Kosmala S, Zakryś B, Kwiatowski J (2006) Phylogeny of photosynthetic euglenophytes based on combined chloroplast and cytoplasmic SSU rDNA sequence analysis. J Phycol 42:721–730

Monfils AK, Triemer RE, Bellairs EF (2011) Characterization of paramylon morphological diversity in photosynthetic euglenoids (Euglenales, Euglenophyta). Phycologia 50:156–169

Montegut-Felkner AE, Triemer RE (1997) Phylogenetic relationships of selected euglenoid genera based on morphological and molecular data. J Phycol 33: 512–519

Moreira D, López-García P, Rodriguez-Valera F (2001) New insights into the phylogenetic position of diplonemids: G+C content bias, differences of evolutionary rate and a new environmental sequence. Int J Syst Evol Microbiol 51:2211–2219

Müllner AN, Angeler DG, Samuel R, Linton EW, Triemer RE (2001) Phylogenetic analysis of phagotrophic, phototrophic and osmotrophic euglenoids by using the

nuclear 18S rDNA sequence. Int J Syst Evol Microbiol 51:783–791

Nudelman MA, Rossi MS, Conforti V, Triemer RE (2003) Phylogeny of Euglenophyceae based on small subunit rDNA sequences: taxonomic implications. J Phycol 39:226–235

Osafune T, Yokota A, Sumida,S, Hase E (1990) Immunogold Localization of Ribulose-1,5-Bisphosphate Carboxylase with Reference to Pyrenoid Morphology in Chloroplasts of Synchronized *Euglena gracilis* Cells. Plant Physiol 92(3):802–808

Perty M (1849) Über vertikale Verbreitung mikroskopischer Lebensformen. *Lepocinclis* n. gen. Mitth Naturforsh Ges Bern 28:17–45

Perty M (1852) Zur Kenntniss kleinster Lebensformen nach Bau, Funktionen. Systematik mit Specialverzeichniss der in der Schweiz beobachteten. Verlag von Jent und Reinert, Bern, p 228

Preisfeld A, Berger S, Busse I, Liller S, Ruppel HG (2000) Phylogenetic analyses of various euglenoid taxa (Euglenozoa) based on 18S rDNA sequence data. J Phycol 36:220–226

Preisfeld A, Busse I, Klingberg M, Talke S, Ruppel HG (2001) Phylogenetic position and inter-relationships of the osmotrophic euglenids based on SSU rDNA data, with emphasison the Rhabdomonadales (Euglenozoa). Int J Syst Evol Microbiol 51:751–758

Pringsheim EG (1956) Contributions towards a monograph of the genus Euglena. Nova Acta Leopoldina 18:1–168

Rogers MB, Gilson PR, Su V, McFadden GI, Keeling PJ (2007) The complete chloroplast genome of the chlorarachniophyte *Bigelowiella natans*: evidence for independent origins of chlorarachniophyte and euglenid secondary endosymbionts. Mol Biol Evol 24:54–62

Shin W, Triemer RE (2004) Phylogenetic analysis of the genus Euglena (Euglenophyceae) with particular reference to the species *Euglena viridis*. J Phycol 40:759–771

Simpson AGB (1997) The identity and composition of the Euglenozoa. Archiv Protistenk 148:318–328

Simpson AGB (2003) Cytoskeletal organization, phylogenetic affinities and systematics in the contentious taxon Excavata (Eukaryota). Int J Syst Evol Microbiol 53:1759–1779

Triemer RE and Zakryś B (2015) Photosynthetic euglenoids In: Wehr JD, Sheath RG, Kociolek JP (eds) Freshwater algae of North America: ecology and classification, 2nd edition. Academic Press, Amsterdam, pp. 457–482

Triemer RE, Linton E, Shin W, Nudelman A, Monfils A, Bennett M, Brosnan S (2006) Phylogeny of the Euglenales based upon combined SSU and LSU rDNA sequence comparisons and description of *Discoplastis* gen. nov. (Euglenophyta). J Phycol 42:731–740

Turmel M, Gagnon M-C, O'Kelly CJ, Otis C, Lemieux C (2009) The chloroplast genomes of the green algae Pyramimonas, Monomastix, and Pycnococcus shed new light on the evolutionary history of prasinophytes and the origin of the secondary chloroplasts of euglenids. Mol Biol Evol 26:631–648

Yabuki A, Nakayama T, Yubuki N, Hashimoto T, Ishida KI, Inagaki Y (2011) *Tsukubamonas globosa* n. gen., n. sp., a novel excavate flagellate possibly holding a key for the early evolution in "Discoba". J Eukaryot Microbiol 58:319–331

Yamaguchi A, Yubuki N, Leander BS (2012) Morphostasis in a novel eukaryote illuminates the evolutionary transition from phagotrophy to phototrophy: description of *Rapaza viridis* n. gen. et sp. (Euglenozoa, Euglenida). BMC Evol Biol 12:29

Yubuki N, Edgcomb VP, Bernhardt JM, Leander BS (2009) Ultrastructure and molecular phylogeny of *Calkinsia aureus*: cellular identity of a novel clade of deep-sea euglenozoans with epibiotic bacteria. BMC Microbiol 9:16

Yubuki N, Simpson AGB, Leander BS (2013) Reconstruction of the feeding apparatus in *Postgaardi mariagerensis* provides evidence for character evolution within the Symbiontida (Euglenozoa). Eur J Protistol 49:32–39

Zakryś B (1986) Contribution to the monograph of Polish members of the genus *Euglena* Ehr. 1830. Nova Hedwigia 42:491–540

Zakryś B, Milanowski R, Empel J, Borsuk P, Gromadka R, Kwiatowski J (2002) Two different species of *Euglena*, *E. geniculata* and *E. myxocylindracea* (Euglenophyceae), are virtually genetically and morphologically identical. J Phycol 38:1190–1199

Zakryś B, Empel J, Milanowski R, Gromadka R, Borsuk P, Kędzior M, Kwiatowski J (2004) Genetic variability of *Euglena agilis* (Euglenophyceae). Acta Soc Bot Pol 73(4):305–309

Zakryś B, Karnkowska-Ishikawa A, Łukomska-Kowalczyk M, Milanowski R (2013) New photosynthetic euglenoid isolated in Poland*: Euglenaria clepsydroides* sp. nova (Euglenea). Eur J Phycol 48(3):260–269

Zimba PV, Rowan M, Triemer R (2004) Identification of euglenoid algae that produce ichthyotoxin (s). J Fish Dis 27:115–117

Zimba PV, Moeller PD, Beauchesne K, Lane HE, Triemer RE (2010) Identification of euglenophycin – A toxin found in certain euglenoids. Toxicon 55:100–104

The Mitochondrion of *Euglena gracilis*

2

Verena Zimorski, Cessa Rauch, Jaap J. van Hellemond, Aloysius G.M. Tielens, and William F. Martin

Abstract

In the presence of oxygen, *Euglena gracilis* mitochondria function much like mammalian mitochondria. Under anaerobiosis, *E. gracilis* mitochondria perform a malonyl-CoA independent synthesis of fatty acids leading to accumulation of wax esters, which serve as the sink for electrons stemming from glycolytic ATP synthesis and pyruvate oxidation. Some components (enzymes and cofactors) of *Euglena's* anaerobic energy metabolism are found among the anaerobic mitochondria of invertebrates, others are found among hydrogenosomes, the H_2-producing anaerobic mitochondria of protists.

Keywords

Euglena gracilis • Mitochondrion • Anaerobiosis • Wax ester fermentation • Mitochondrial genome

V. Zimorski • C. Rauch • W.F. Martin (✉)
Institute of Molecular Evolution, Heinrich-Heine-Universität Düsseldorf, Düsseldorf, Germany
e-mail: bill@hhu.de

J.J. van Hellemond
Department of Medical Microbiology and Infectious Diseases, Erasmus University Medical Center, Rotterdam, The Netherlands

A.G.M. Tielens
Department of Medical Microbiology and Infectious Diseases, Erasmus University Medical Center, Rotterdam, The Netherlands

Department of Biochemistry and Cell Biology, Faculty of Veterinary Medicine, Utrecht University, Utrecht, The Netherlands

Abbreviations

ADH	Alcohol dehydrogenase
ALDH	Aldehyde dehydrogenase
AOX	Alternative oxidase
APX	Ascorbate peroxidase
ATP	Adenosine triphosphate
CCR	Crotonyl-CoA reductase
CoA	Coenzyme A
FAD	Flavin adenine dinucleotide
FAS	Fatty acid synthase
FMN	Flavin mononucleotide
FRD	Fumarate reductase

S.D. Schwartzbach, S. Shigeoka (eds.), *Euglena: Biochemistry, Cell and Molecular Biology*, Advances in Experimental Medicine and Biology 979, DOI 10.1007/978-3-319-54910-1_2

ICL	Isocitrate lyase
MS	Malate synthase
NAD^+	Nicotinamide adenine dinucleotide (oxidized form)
NADH	Nicotinamide adenine dinucleotide (reduced form)
$NADP^+$	Nicotinamide adenine dinucleotide phosphate (oxidized form)
NADPH	Nicotinamide adenine dinucleotide phosphate (reduced form)
PDH	Pyruvate dehydrogenase
PFO	Pyruvate:ferredoxin oxidoreductase
PKS	Polyketide synthase
PNO	Pyruvate:$NADP^+$ oxidoreductase
Prx	Peroxiredoxin
ROS	Reactive oxygen species
RQ	Rhodoquinone
TER	*trans*-2-enoyl-CoA reductase

2.1 Introduction

Mitochondria are essential components of eukaryotic cells. In eukaryotes that spend all of their life cycle in oxic environments, the inner mitochondrial membrane is the site of chemiosmotic ATP synthesis. Eukaryotes that spend all or part of their life cycle in anoxic environments harbor anaerobic forms of mitochondria. Some forms of anaerobically functioning mitochondria possess cytochromes and quinones, generating proton gradients through an electron transport chain using terminal acceptors other than oxygen, while others generate ATP through fermentative substrate level phosphorylation, and still others have no role in ATP synthesis at all (Müller et al. 2012). The mitochondrion of *Euglena gracilis* generates ATP with and without the help of oxygen as a terminal acceptor. The organelle was last reviewed in the classical chapter by Buetow (1989). The purpose of the current chapter is to cover more recent progress in understanding the *Euglena* mitochondrion.

Euglenids are a broad and diverse group of unicellular eukaryotes that typically inhabit shallow aquatic environments. In the region around the northern Rhine river, springtime rains can lead to small puddles alongside bicycle paths and forest trails. If the puddles remain for a couple of weeks or so, they tend to turn green, as a rule due to growth of euglenids. Though typically encountered in oxic freshwater systems, euglenids also occur in anoxic freshwater ecosystems (Simpson et al. 1997; Klaveness and Løvhøiden 2007) and in anoxic marine sediments (Bernhard et al. 2000; Edgcomb et al. 2011). Some euglenids possess organelles ultrastructurally similar to hydrogenosomes (Simpson et al. 1997; Edgcomb et al. 2011), the hydrogen-producing forms of mitochondria found in diverse anaerobic protists (Müller et al. 2012). From the standpoint of core carbon and energy metabolism, only one member of the euglenids has been extensively studied: the photosynthetic flagellate *Euglena gracilis*.

2.2 The Morphology of Mitochondria

The mitochondrion of *Euglena* is a single, large and reticulated organelle, a trait that is by no means unique among algae (Leedale et al. 1965; Wolken 1967; Buetow 1989; Hayashi and Ueda 1989). As with many other protists (Bereiter-Hahn and Vöth 2005), the mitochondria of *Euglena* have been reported to change shape in response to different conditions of growth, in response to different modes of nutrition (Brönstrup and Hachtel 1986) or when exposed to a variety of inhibitors (Calvayrac and Butow 1971; Calvayrac et al. 1971; Nass and Ben-Shaul 1972; Michaels and Gibor 1973; Neumann and Parthier 1973). In dark-adapted *Euglena*, the network of mitochondria is located close to the cell surface and is adjacent to other organelles (Pellegrini 1980; Hayashi and Ueda 1989). In light-adapted cells, the mitochondrial reticulum is more randomly distributed throughout the cytoplasm, but still tends to localize adjacent to the plastids, which might relate to local oxygen production of the latter (Fig. 2.1) (Wolken 1967). Like mitochondria of higher animals and plants, *Euglena* mitochondria have flat cristae (Stewart and Mattox 1980). The main contents of *Euglena* mitochondria (apart from water and protein) are lipids, amino acids (with a

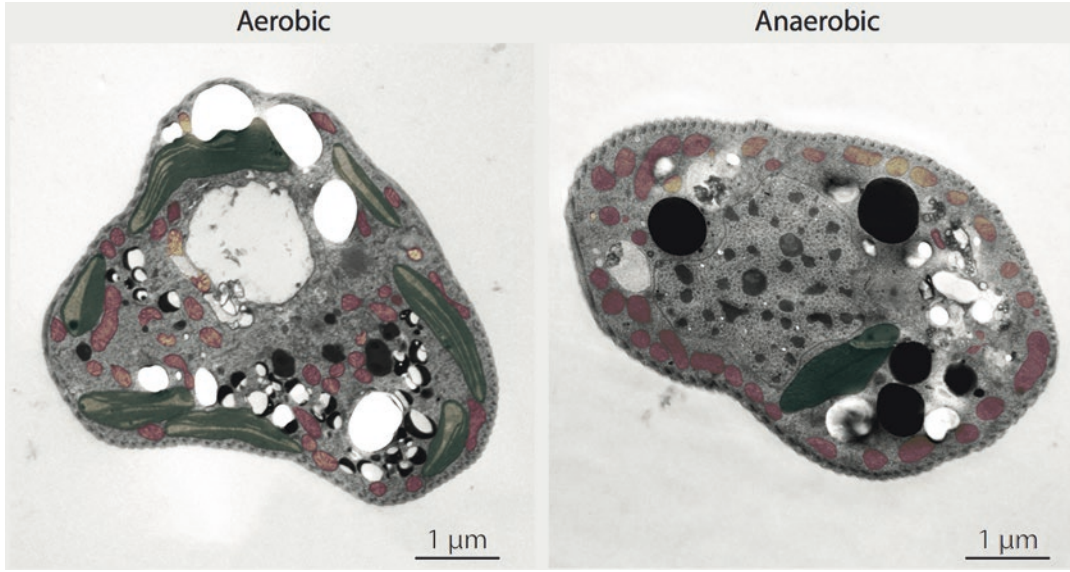

Fig. 2.1 Transmission electron microscopy (TEM) images taken from aerobic and anaerobic grown *E. gracilis* cultures. Mitochondria are highlighted by false colouring in *red*, plastids are shaded in *green*. In anaerobic cultures of *E. gracilis*, the network of mitochondria is located closer to the cell surface and adjacent to other organelles. In comparison to the aerobic cultures the mitochondria are more randomly distributed throughout the cell, but still tend to localize adjacent to the plastids. *White* parts (*holes*) are preparation artefacts

large amount of proline), thiamine, cobalamins, quinones, tocopherols (vitamin E) and cytochromes, which *Euglena* loses during prolonged anoxia (Buetow 1989).

2.3 Aerobic and Anaerobic Metabolic Pathways

Organisms that can grow either with or without oxygen are called facultative anaerobes. Many eukaryotes can use their mitochondria for ATP synthesis and growth under aerobic or anaerobic conditions (Tielens et al. 2002; Tielens and van Hellemond 2007; Müller et al. 2012). Such organisms can be said to possess facultatively anaerobic mitochondria, which is the case for *E. gracilis*. It can grow autotrophically in the light, producing oxygen through photosynthesis and consuming oxygen via mitochondrial respiration, but many strains can also grow as anaerobic heterotrophs in the dark. Importantly, there are distinct differences among *E. gracilis* strains when it comes to the issue of being able to simply survive anoxic conditions versus being able to actively grow under anoxic conditions. Most *E. gracilis* strains have no problem surviving anoxia, but only some strains have the ability to actively grow heterotrophically under anoxia in the dark (Tucci et al. 2010). In our experience each new strain has to be tested, and recent work shows that anoxic cultivation on plates tends to deliver faster growth rates than anoxic liquid culture (C. Rauch, unpublished). Because *Euglena*'s anaerobic energy metabolism entails many components, as we will elaborate in subsequent sections, it is safe to assume that those strains that do not grow anaerobically have lost the ability to do so during the prolonged laboratory culture.

Some eukaryotes with oxygen respiring mitochondria can survive anoxia for prolonged periods using cytosolic fermentations. Goldfish (*Carassius auratus*) and crucian carp (*Carassius carassius*) provide such an example, being able to survive complete anoxia for several weeks via cytosolic ethanol fermentation (van Waarde et al. 1993). *Euglena* belongs to the eukaryotes with facultatively anaerobic mitochondria, that is, it

synthesizes ATP anaerobically in mitochondria. The biochemistry and physiology of anaerobic mitochondria and facultatively anaerobic mitochondria has been studied in only a few model systems (Tielens et al. 2002; Mentel and Martin 2008; Müller et al. 2012).

2.3.1 Aerobic Metabolic Pathway

In *Euglena*, pyruvate from the glycolysis pathway enters the mitochondrion and in the presence of oxygen undergoes oxidative decarboxylation via pyruvate dehydrogenase (PDH) (Tielens et al. 2002; Hoffmeister et al. 2004; Müller et al. 2012). *Euglena* PDH was shown to be active under aerobic conditions (Krnáčová et al. 2015), but the question remains open whether the *Euglena* mitochondrion imports pyruvate or malate, which in many eukaryotes with anaerobic mitochondria is converted into pyruvate in the organelle by malic enzyme (Tielens et al. 2002; Müller et al. 2012). Oxidative decarboxylation yields acetyl-CoA that enters a modified Krebs cycle in which alpha-ketoglutarate decarboxylase and succinate semialdehyde dehydrogenase (Buetow 1989) replace the alpha-ketoglutarate dehydrogenase of the classical Krebs cycle. This modification of the Krebs cycle is also found among some alphaproteobacteria, like *Bradyrhizobium* (Green et al. 2000), and among cyanobacteria (Zhang and Bryant 2011).

During aerobic ATP synthesis, electrons from glucose breakdown are transferred via a branched respiratory chain to oxygen as the terminal electron acceptor (Fig. 2.2) (Buetow 1989; Kitaoka et al. 1989). The *E. gracilis* respiratory chain consists of the multi-subunit complexes I, II, III and IV of canonical mitochondrial electron-transport chains, plus a plant-like alternative oxidase, as explained later in this section. The respiratory chain complexes of *E. gracilis* harbor in total at least 48 subunits that *Euglena* shares with various eukaryotes and 41 subunits that they share exclusively with trypanosomatids (Duarte and Tomas 2014; Perez et al. 2014). Characterization of enzymes involved in *E. gracilis* oxidative phosphorylation revealed the presence of two catalytically active forms of complex I, but only a single active form of complex II (Krnáčová et al. 2015). Isolated complex III (cytochrome c reductase) from *E. gracilis* contained cytochrome c_1 and b. It contained 10 subunits, showed only a low activity, was not sensitive to antimycin A and the cytochrome c_1 had an atypical heme-binding structure (Mukai et al. 1989; Braun and Schmitz 1995). The presence of two complexes III in *E. gracilis* was suggested by Moreno-Sánchez et al. (2000); one sensitive to antimycin A and resistant to myxothiazol and *vice versa* for the other one, while complexes III from other organisms are sensitive to both inhibitors. Complex IV (cytochrome *c* oxidase) was also purified from *E. gracilis* mitochondria. It contains 15 subunits and showed a high activity in the presence of '*Euglena* cytochrome c', however it had a very low activity in the presence of horse cytochrome c (Brönstrup and Hachtel 1989; Mukai et al. 1989). For the ATP synthase, two main active forms were detected in *Euglena* (Krnáčová et al. 2015).

The activity of enzymes involved in *Euglena* oxidative phosphorylation did not show any effects in comparisons of light vs. dark or functionality vs. nonfunctionality of plastids (Krnáčová et al. 2015). Isolated mitochondria of *E. gracilis* used NADH as an external substrate for oxygen consumption (Uribe et al. 1994; Jasso-Chávez and Moreno-Sánchez 2003; Krnáčová et al. 2015). This seems surprising at first sight, because NADH is generally thought not to be transported across the mitochondrial inner membrane, and the enzyme or enzymes responsible for the use of NADH as an exogenous substrate during oxygen consumption in *E. gracilis* mitochondria have not been identified (Krnáčová et al. 2015).

There is evidence for alternative respiratory pathways in *E. gracilis*: an alternative oxidase (AOX) transfers electrons directly from ubiquinol to oxygen (Devars et al. 1992). The presence of AOX was confirmed *in silico* (Perez et al. 2014) and *in vivo* (Krnáčová et al. 2015). Another pathway includes lactate dehydrogenase, which transfers electrons from lactate directly to ubiquinone (Moreno-Sánchez et al. 2000) and is part of the lactate/pyruvate shuttle (Jasso-Chávez et al.

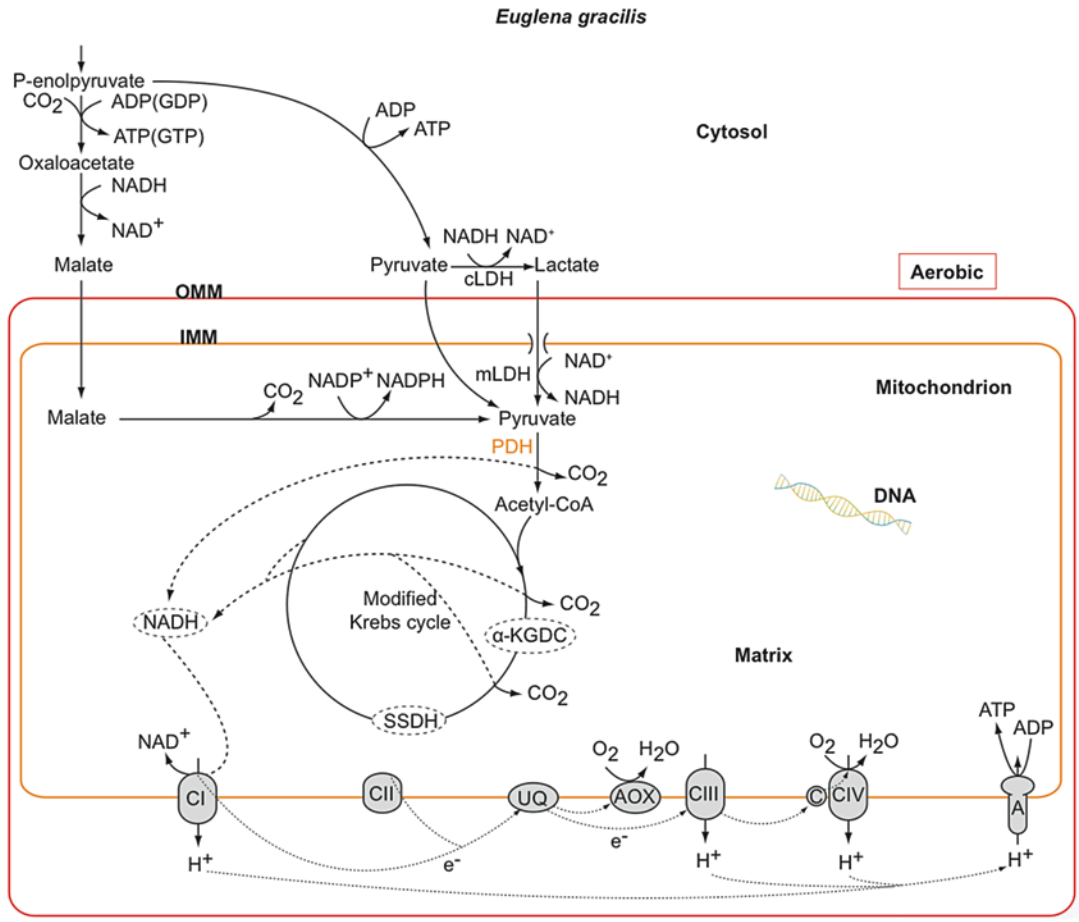

Fig. 2.2 Metabolic pathways in mitochondria of the facultatively anaerobic photosynthetic flagellate *Euglena gracilis*. The map is redrawn based on Müller et al. (2012). Under aerobic conditions (shown in the upper part in *red*) either pyruvate from the glycolytic pathway enters the mitochondrion or malate or lactate via the lactate shuttle enter the mitochondrion, where they are converted to pyruvate. Pyruvate undergoes oxidative decarboxylation via pyruvate dehydrogenase (PDH) yielding acetyl-CoA that enters a modified Krebs cycle in which alpha-ketoglutarate decarboxylase and succinate semialdehyde dehydrogenase replace the alpha-ketoglutarate dehydrogenase and succinate thiokinase (STK) of the classical Krebs cycle. Electrons are transferred via a branched respiratory chain to oxygen as the terminal electron acceptor generating the proton gradient for ATP synthesis. *A* ATPase, *AOX* alternative oxidase, *C* cytochrome c, *CI to CIV* respiratory complexes I to IV, *FRD* fumarate reductase, *IMM* inner mitochondrial membrane, *LDH* lactate dehydrogenase, *OMM* outer mitochondrial membrane, *RQ* rhodoquinone

2001, 2005; Jasso-Chávez and Moreno-Sánchez 2003). Alternative respiratory pathways are likely involved in cellular responses to oxidative stress (Castro-Guerrero et al. 2004, 2008), since *E. gracilis* lacks catalase, but contains ascorbate peroxidase (APX), which localizes exclusively to the cytosol (Shigeoka et al. 2002). Other enzymes involved in detoxification of reactive oxygen species (ROS) have not been found yet, thus little is known about ROS metabolism in *Euglena* (Tamaki et al. 2014). *Euglena* was shown to contain 2-CysPrxs in the mitochondria (Castro and Tomás 2008). Tamaki et al. (2014) examined four peroxiredoxins (Prx), two localized in the cytosol and the others in the plastids and the mitochondria, respectively. All could reduce both H_2O_2 and alkyl hydroperoxide and might contribute to ROS metabolism – also in mitochondria

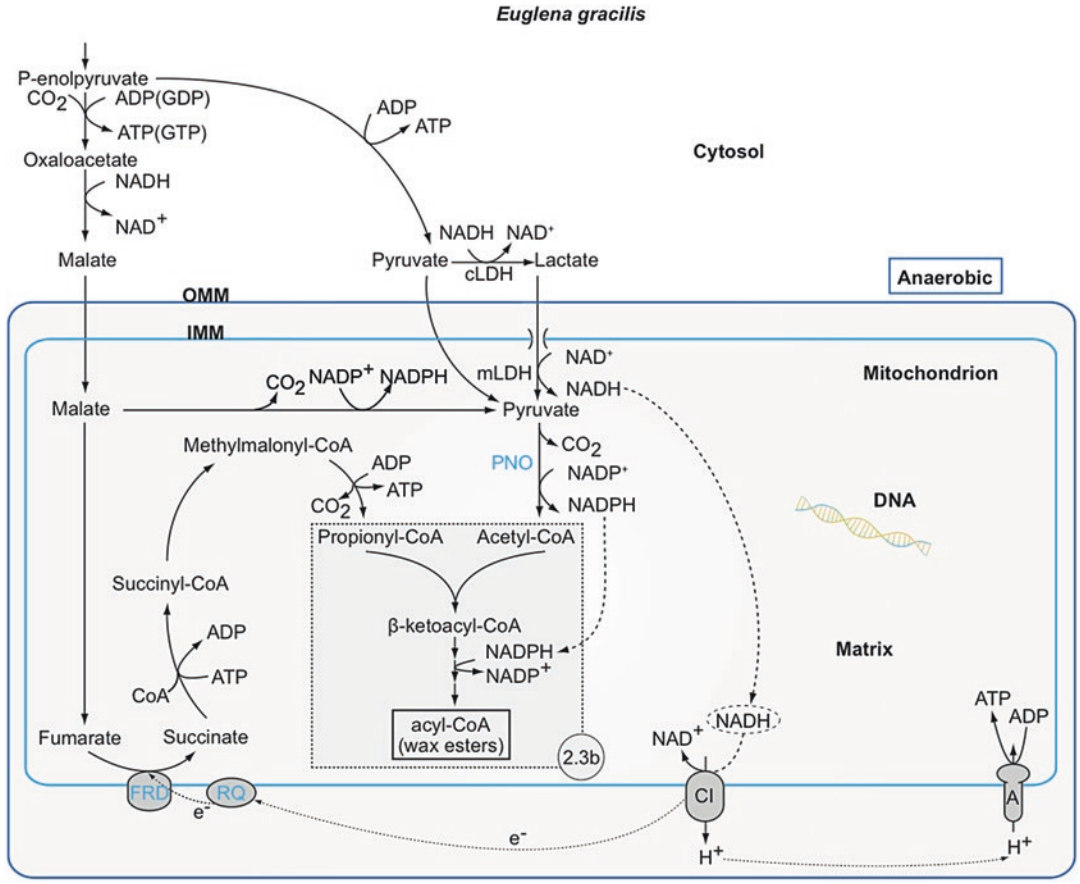

Fig. 2.3 Metabolic pathways in mitochondria of the facultatively anaerobic photosynthetic flagellate *Euglena gracilis*. The map is redrawn based on Müller et al. (2012). Under anaerobic conditions (shown at the bottom in blue) *E. gracilis* uses acetyl-CoA produced by pyruvate:NADP oxidoreductase as the terminal electron acceptor, leading to the formation of an unusual end product among eukaryotes: wax esters. Mitochondrial wax ester fermentation includes anaerobic fumarate respiration and the same propionyl-CoA formation pathway as the one found in mitochondria of facultative anaerobic animals excreting propionate. Note however that succinate thiokinase participates in the propionyl-CoA generating pathway under anaerobic conditions and that STK homologues are present in *Euglena* EST libraries (Müller et al. 2012). *A* ATPase, *AOX* alternative oxidase, *C* cytochrome c, *CI to CIV* respiratory complexes I to IV, *FRD* fumarate reductase, *IMM* inner mitochondrial membrane, *LDH* lactate dehydrogenase, *OMM* outer mitochondrial membrane, *RQ* rhodoquinone

(Tamaki et al. 2014). But H_2O_2 can also diffuse from the mitochondria into the cytosol, where it is then detoxified by APX (Ishikawa et al. 1993).

2.3.2 Anaerobic Metabolic Pathway

When oxygen is absent, *E. gracilis* uses acetyl-CoA as the terminal electron acceptor of glucose oxidation and produces wax esters as end products of its metabolism (Figs. 2.3 and 2.4) (Buetow 1989; Inui et al. 1982, 1983, 1984; Tucci et al. 2010; Ogawa et al. 2015). When shifted from aerobic to anaerobic conditions, PDH protein levels decrease in *Euglena* (Hoffmeister et al. 2004). The shift to anaerobic conditions leads to the malonyl-CoA independent synthesis of wax esters, levels of which can reach up to 40 µg per 10^6 *Euglena* cells (Inui et al. 1982). The wax esters are not excreted but accumulate in the cytosol instead (Tucci et al. 2010; Ogawa et al. 2015). Some *E. gracilis* strains accumulate wax

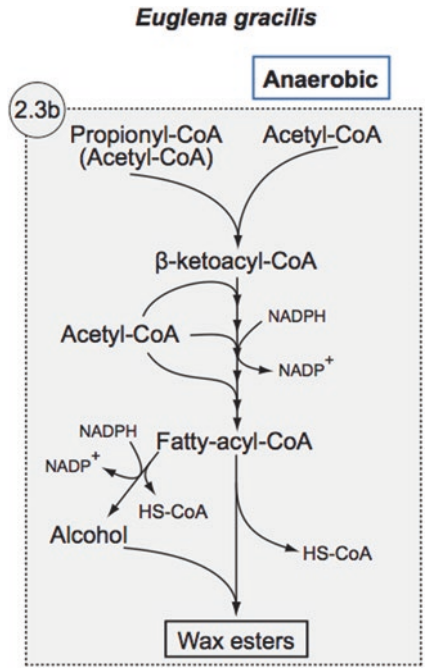

Fig. 2.4 Expanded view of the pathway leading to formation of wax-esters shown in Fig. 2.3a. The fatty acid CoA-ester is elongated by starting again at ß-ketoacyl-CoA. A part of the final fatty acid product is reduced to the alcohol which is then esterified with other fatty acids and deposited in the cytosol as wax-esters. Fatty acid synthesis is mitochondrial, wax ester synthesis is cytosolic. Odd chain fatty acids (roughly 40% of the total, see text) start from propionyl-CoA

esters at levels of up to 65% total dry weight (Tucci et al. 2010) and acid mine drainage biofilms mainly constituted by *Euglena mutabilis* contain large amounts of wax esters (Dasgupta et al. 2012). Because of this high wax ester production there is a general interest in selective breeding of *E. gracilis* for biofuel, nutritional foods and cosmetic purposes (Yamada et al. 2016) (see Chaps. 13 and 14 of this volume). Under aerobic conditions, the wax esters can be converted back to acetyl-CoA, which can be oxidized to CO_2 in the mitochondria or used to form paramylon (β-1,3-glucan) reserves (Inui et al. 1992; Ono et al. 1995b; Atteia et al. 2013). This metabolism probably involves β-oxidation, the glyoxylate cycle and conversion of acetyl-CoA, which either enters the glyoxylate cycle to be converted to succinate which can be used for gluconeogenesis, or the acetyl-CoA enters the modified Krebs cycle to be oxidized to CO_2 (Ono et al. 2003; Hoffmeister et al. 2005).

2.3.3 Five Different Systems for Fatty Acid Synthesis

Five different systems of fatty acid synthesis have been reported for *E. gracilis* (Kitaoka et al. 1989). The first two systems, localized in the chloroplasts, are acyl-carrier protein dependent systems (FAS II), which synthesize products with chain lengths of C16 and C18 that can be further elongated to C20–C24 (Ernst-Fonberg and Bloch 1971; Hendren and Bloch 1980). The third, a multifunctional fatty acid synthase (FAS I) located in the cytosol of *Euglena*, has as main products C16 fatty acids with C14 and as minor products C18 chain lengths (Goldberg and Bloch 1972; Walker et al. 1981). The fourth is a microsomal fatty acid synthase activity (Khan and Kolattukudy 1973). The fifth is involved in anaerobic wax ester fermentation and part of the mitochondrial system. It uses acetyl-CoA as a primer and C2-donor, a portion of the fatty acids is reduced to alcohols, esterified with another fatty acid and deposited in the cytosol as waxes (Inui et al. 1982, 1984; Buetow 1989). The mitochondrial system synthesizes products of chain length C8–18 with a majority of C14 (mainly myristyl myristate) (Inui et al. 1983, 1984). Synthesis of odd numbered fatty acids starts from propionyl-CoA, which is synthesized via the methylmalonyl-CoA pathway (Nagai et al. 1971; Schneider and Betz 1985; Pönsgen-Schmidt et al. 1988) and requires the participation of rhodoquinones (Hoffmeister et al. 2004; Castro-Guerrero et al. 2005). Labeling experiments indicate the involvement of Krebs cycle intermediates leading to propionyl-CoA in the synthesis of odd numbered chains during anaerobic wax ester fermentation (Padermshoke et al. 2016).

The mitochondrial wax ester fermentation by *Euglena* is similar in general principle to the synthesis of branched short-chain fatty acids in *Ascaris* or butyrate in *Dasytricha*. The adult parasitic nematode *Ascaris suum* is known to be

adapted to anaerobic conditions in that they possess anaerobically functioning mitochondria (Kita et al. 2002). Early larval stages of *Ascaris* are aerobic and their mitochondria possess a functional Krebs cycle and cytochrome *c* oxidase (Komuniecki and Vanover 1987; Takamiya et al. 1993) whereas adults use organic acids instead of oxygen as terminal electron acceptors (Komuniecki et al. 1981; Mei et al. 1997). Main end products of the anaerobic energy metabolism of *Ascaris* mitochondria are the methyl-branched fatty acids 2-methylbutyrate and 2-methylvalerate (Komuniecki and Tielens 2003). These reactions of anaerobic mitochondrial metabolism resemble *Euglena* mitochondrial fatty acid synthesis in that acetyl-CoA and propionyl-CoA condensations are involved and the final reduction is catalyzed by a 2-methyl branched chain enoyl-CoA reductase (Komuniecki and Tielens 2003; Komuniecki et al. 1987). However, the *Ascaris* 2-methyl branched chain enoyl-CoA reductase does not accept NADH as an electron donor, in contrast to *trans*-2-enoyl-CoA reductase (TER) in *Euglena* (Hoffmeister et al. 2005), but accepts electrons from an electron transporting flavoprotein and shows sequence similarities to acyl-CoA dehydrogenases (Komuniecki et al. 1985; Duran et al. 1993, 1998). This indicates that *Euglena* TER is clearly distinct from the *Ascaris* enzyme.

In *Euglena*, fatty acids for wax esters are synthesized via condensation of acetyl-CoA with an acyl-CoA (starting with acetyl-CoA or propionyl-CoA), a reduction of the resulting 3-oxoacid to 3-hydroxy acid, dehydration thereof, and a reduction of the resulting trans-enoyl-CoA to the elongated acyl-CoA. The acetyl-CoA stems from pyruvate via the oxygen-sensitive enzyme; pyruvate:$NADP^+$ oxidoreductase (PNO) (Inui et al. 1987; Nakazawa et al. 2000), the core catalytic component of which is pyruvate:ferredoxin oxidoreductase, a typical enzyme of hydrogenosomes (Rotte et al. 2001). In contrast to malonyl-CoA-dependent fatty acid synthesis, the acetyl-CoA-dependent *Euglena* route allows net fermentative ATP synthesis from glucose, because acetyl-CoA is condensed without prior ATP-dependent carboxylation to malonyl-CoA (Inui et al. 1982, 1984; Schneider and Betz 1985).

The condensing enzyme 3-ketoacyl-CoA thiolase (EC 2.3.1.9 and 2.3.1.16) catalyzes the condensation of propionyl-CoA and acetyl-CoA in the mitochondrial fatty acid synthesis in *E. gracilis*. A recent study showed that gene silencing of this enzyme altered both the wax ester content and the wax ester composition in *E. gracilis*, inducing a significant compositional shift to shorter carbon chain lengths in wax esters (Nakazawa et al. 2015). Six putative 3-ketoacyl-CoA thiolase isoenzymes were found in an *E. gracilis* EST database (O'Brien et al. 2007), but only the gene silencing of three of them had an effect on wax esters. For two isoforms (3 and 1) the total wax ester production was lowered to approximately 25% and 85% of the control level, when cells were exposed to hypoxic conditions for 48 h. Gene silencing of isoforms 1 and 2 also induced different acyl chain length distributions of wax esters compared to those in control cells. C28 wax esters were dominant in the control cells and in thiolase-silenced cells C26 (isoform 1) and C27 (isoform 2). Gene silencing of these two isoforms significantly increased the amount and the ratio of wax esters with an acyl chain length shorter than C26 (Nakazawa et al. 2015). The study suggests different roles for each isoenzyme in hypoxic wax ester production (Nakazawa et al. 2015). Isoenzyme 3 might be a short- and medium-chain-specific enzyme important for the hypoxic synthesis of wax esters from paramylon, while isoforms 1 and 2 might be medium- and long-chain-specific in the acyl-CoA production in mitochondrial fatty acid synthesis (Nakazawa et al. 2015).

Euglena's mitochondrial fatty acid synthesis has been formally described as a reversal of β-oxidation (Inui et al. 1984; Buetow 1989) because it proceeds via CoA rather than acyl carrier protein (ACP) bound intermediates. However, the key difference relative to β-oxidation is that *trans*-2-enoyl-CoA reductase (TER; EC 1.3.1.44) reduces the double bond in enoyl-CoA to produce acyl-CoA (Inui et al. 1984). In β-oxidation this step is oxidative and irreversible under physiological conditions because acyl-CoA dehydrogenase (mitochondrial β-oxidation) and acyl-CoA oxidase (peroxisomal β-oxidation) are both linked to

O_2-reduction (Kunau et al. 1995; Graham and Eastmond 2002). A portion of the fatty acids is reduced to alcohols, esterified with another fatty acid, and deposited into the cytosol as wax (wax ester fermentation). The fatty acyl-CoA reductase and the wax synthase involved in the synthesis of the medium-chain wax aliphatic side chains of *Euglena* were recently characterized (Teerawanichpan and Qiu 2010); the gene is ubiquitous among eukaryotes. Upon a return to an oxic environment, the stored waxes are degraded via aerobic dissimilation in the mitochondrion (Inui et al. 1982).

An NADPH-specific crotonyl-CoA reductase (CCR) from *Streptomyces collinus* catalyzes the synthesis of butyryl-CoA from crotonyl-CoA (Wallace et al. 1995), a reaction very similar to that catalyzed by *Euglena* TER. However, no detectable sequence similarity exists between TER and CCR (Hoffmeister et al. 2005). Furthermore, *S. collinus* CCR shows no activity with NADH in contrast to *Euglena* TER (Wallace et al. 1995; Liu and Reynolds 1999). CRR provides butyryl-CoA units for synthesis of polyketides (Reynolds et al. 1992), but is again distinct from *Euglena* TER.

A variety of enoyl reductases (ER) and ER-modules are known among polyketide synthases (Metz et al. 2001; Wallis et al. 2002), but none characterized so far has sequence similarity with *Euglena* TER. TER is expressed both under aerobic and anaerobic conditions, in line with findings from other anaerobic mitochondria, which seem to have adopted a strategy of being prepared for anaerobiosis without the need for specific enzyme induction (Hoffmeister et al. 2004; Tielens 1994). *Euglena* TER has strong sequence similarity to proteins annotated as hypothetical reading frames in several dozen prokaryotes, most conspicuously among gamma-proteobacteria. The operon context of TER homologues from sequenced genomes revealed that TER homologues (annotated so far as hypothetical reading frames) most commonly occur next to other hypothetical reading frames, but sometimes occur downstream of enzymes associated with fatty acid biosynthetic pathways and in one case downstream of a polyketide synthase in the *S. avermitilis* genome (Hoffmeister et al. 2005). This raises the possibility that TER homologues (and *Euglena* TER itself) could operate in fatty acid biosynthesis, polyketide biosynthesis, or conceivably both, since both pathways involve thioester-bound enoyl reduction. TER is active as a monomer, suggesting that catalysis of the NADH- and NADPH-dependent reduction of the double bond in crotonyl-CoA does not require interactions with other proteins (Hoffmeister et al. 2005).

2.4 The Biosynthetic Route to Wax Esters in *Euglena*

Under anaerobic conditions *Euglena gracilis* produces wax esters as end products of its metabolism (Fig. 2.4) (Buetow 1989; Inui et al. 1982, 1983, 1984; Tucci et al. 2010; Ogawa et al. 2015). The key enzyme is pyruvate:$NADP^+$ oxidoreductase, which decarboxylates pyruvate to acetyl-CoA. Acetyl-CoA serves as the terminal electron acceptor from glucose oxidation whereby fatty acids are synthesized. The fatty acids contain 8 to 18 carbon atoms and consist mainly of myristic acid and myristic alcohol (C14) (Inui et al. 1983). Sixty percent of the produced fatty acids are even number carbon chains (Tucci et al. 2010). Acetyl-CoA is used both as a primer and a C2 donor during even-numbered fatty acid synthesis in mitochondria. In addition to these even-numbered wax esters, also odd-numbered wax esters are synthesized. The synthesis of odd numbered wax esters start from propionyl-CoA instead of acetyl-CoA, stemming from the methyl-malonyl-CoA pathway (Nagai et al. 1971; Schneider and Betz 1985; Pönsgen-Schmidt et al. 1988).

The fatty acids are subsequently transported into the cytosol, where a portion of the fatty acids is reduced to alcohol, esterified with another fatty acid in the microsomes (Kolattukudy 1970; Khan and Kolattukudy 1973) and accumulate in the cytosol in an insoluble, crystalline form: waxes, hence this biochemical pathway is called wax ester fermentation. An unusual phenomenon, because fermentations usually generate soluble substances like alcohols or organic acids as end products. *Euglena* cells are able to produce 40 µg

of wax per 10^6 cells in the first 24 h of anaerobic incubation (Tucci et al. 2010).

Fatty acid biosynthesis catalyzed by fatty acid synthase (FAS) complexes and polyketide biosynthesis catalyzed by polyketide synthases (PKS) involve four fundamentally similar steps: (i) the condensation of an acetyl moiety onto an acyl thioester to form a β-ketoacyl thioester, (ii) reduction of the keto group to a β-hydroxyacyl thioester, (iii) dehydration to form the double bond in the resulting enoyl thioester, and (iv) reduction of the double bond to form an acyl thioester two carbons longer than the first one. The thiol moiety of the thioester is pantothenate, which is covalently bound to acyl carrier protein (ACP) in PKS and FAS complexes (Hopwood and Sherman 1990; Bentley and Bennett 1999; Hoffmeister et al. 2005). Fatty acid elongases, which extend C18 fatty acids to C20 and longer, generally operate with CoA esters (Trenkamp et al. 2004). In mitochondria and peroxisomes, β-oxidation operates through steps (iv) to (i) with the CoA esters, whereby the oxidative step (iv) is physiologically irreversible, since it is finally linked to oxygen reduction (Reddy and Hashimoto 2001).

TER catalyzes the step corresponding to (iv) above with the CoA ester, reducing crotonyl-CoA to butyryl-CoA (Hoffmeister et al. 2005; Tucci et al. 2010). No TER activity was found in the reverse reaction using butyryl-CoA as substrate with either NAD^+ or $NADP^+$ (Hoffmeister et al. 2005). The recombinant TER enzyme showed highest activity with crotonyl-CoA but also reduces C6 enoyl-CoAs and thus relates in terms of substrate preference to enoyl-CoA reductase previously described by Inui et al. (1984). Under anaerobiosis, active photosynthesis and consumption of external carbon sources, activities of glutamate dehydrogenase and $NADP^+$-dependent malic enzyme were enhanced, and malate dehydrogenase activity was reduced (Santiago-Martínez et al. 2015).

The synthesis of fatty acids, in particular long-chain polyunsaturated fatty acids (PUFAs), via polyketide synthesis has been shown both for the prokaryote *Shewanella* and the eukaryote *Schizochytrium* (Metz et al. 2001; Napier 2002). TER homologues are found within many sequenced prokaryotic genomes, however no true homologues for TER have so far been identified from any eukaryote other than *Euglena.* We must however qualify the foregoing statement as being only conditionally true, because several sequences in the 2016 release of GenBank have highly significant sequence identity to *Euglena* TER and are currently annotated as existing in eukaryotic genomes (*Nematostella* for example), but these are prokaryotic contaminations in the eukaryote assembly; such cases are fairly common and are often mistaken for lateral gene transfer (Ku and Martin 2016). Comprehensive analyses indicate that eukaryotes have rarely, if ever, acquired genes outside the context of the endosymbiotic origins of chloroplast and mitochondria (Ku et al. 2015; Ku and Martin 2016).

The apicomplexan protist *Cryptosporidium parvum*, which possesses the same unusual pyruvate:$NADP^+$-oxidoreductase as *Euglena* (Rotte et al. 2001), was found to encode a polyketide synthase (Zhu et al. 2002), and various groups of dinoflagellates synthesize large and complex polyketides (Rein and Borrone 1999). However, polyketides are not specific to eukaryotic groups that possess plastids (or, in the case of *Cryptospridium*, have secondarily lost plastids), since fungi also synthesize polyketides and possess PKS genes (Bohnert et al. 2004).

2.5 Rhodoquinone

Similar to the situation for anaerobic mitochondria of metazoa (Tielens et al. 2002; van Hellemond et al. 2003), wax ester fermentation of *Euglena* involves malate dismutation and mitochondrial fumarate reduction, and thus entails rhodoquinone (RQ) (Hoffmeister et al. 2004) for the synthesis of propionyl-CoA. In its physiological role, RQ is reduced by complex I and oxidized by fumarate reductase (FRD) (van Hellemond et al. 2003), but it can also donate electrons to other components of the *Euglena* mitochondrial respiratory chain (Castro-Guerrero et al. 2005), including the cytochrome bc_1 complex and the alternative oxidase (Castro-Guerrero et al. 2004).

Propionyl-CoA is used as the starter for the synthesis of fatty acids with odd-number chain lengths, which comprise about 50% (by weight) of hydrocarbon chains in accumulated wax esters under various conditions (Kawabata and Kaneyama 1989) and in different *Euglena* strains (Tucci et al. 2010). Propionyl-CoA is produced via the same short methylmalonyl-CoA-dependent route as that found in animal mitochondria (Schneider and Betz 1985), and homologs of the underlying enzymes, methylmalonyl-CoA mutase and propionyl-CoA carboxylase (which provides ATP via substrate-level phosphorylation), are abundantly expressed in euglenoid EST data (Ahmadinejad et al. 2007). Methylmalonyl-CoA mutase from *Euglena* has been characterized (Miyamoto et al. 2010); the enzyme is also present in humans, where it is one of our only two vitamin B_{12} (cobalamin)-dependent enzymes (Roth et al. 1996). *Euglena* growth was once the standard assay for serum B_{12} levels, because of its B_{12}-dependent ribonucleotide reductase (Torrents et al. 2006).

When grown under anaerobic conditions, *Euglena* expresses PNO (Inui et al. 1985, 1987, 1991), which performs the oxidative decarboxylation of pyruvate and is a fusion protein, with an N-terminal PFO (pyruvate:ferredoxin oxidoreductase) domain fused to a C-terminal flavoprotein domain with NAD-, FMN-, and FAD-binding modules (Nakazawa et al. 2003; Rotte et al. 2001). The flavoprotein domain is found in many other proteins, sometimes alone as NADPH:cytochrome P450 reductase and sometimes fused to other domains, such as in nitric oxide synthases of metazoans. The flavoprotein domain is best understood as a transducer of one-electron transport (from the FeS clusters of the PFO domain) to two-electron transport (NADPH). PNO supplies acetyl-CoA and NADPH for the production of wax esters. PNO was first described for *Euglena* and was long considered an enzyme unique to the *Euglena* lineage, but the same PNO (PFO fusion) is found in the apicomplexan *Cryptosporidium* (Rotte et al. 2001) as well as in *Blastocystis* (Lantsman et al. 2008). PNO homologs from many disparate eukaryotic lineages have been turning up in EST sequencing projects (Hug et al. 2010), indicating that the enzyme is far more widespread among eukaryotes than previously thought. Sequences clearly homologous to PFO occur in "typical" eukaryotes as well but in the guise of sulfite oxidases among fungi (Horner et al. 1999; Rotte et al. 2001), which exhibit fusions similar to those of *Euglena* mitochondrial PNO.

2.6 The Mitochondrial Genome

It is known that mitochondrial genomes of excavates are complicated to sequence, however in 2015 the mitochondrial genome and transcriptome of *E. gracilis* was described by Dobáková et al. (NCBI BioProject PRJNA294935). The mitochondrial DNA of *E. gracilis* appears to be combined with proteins to form nucleoids in the organelles. Most nucleoids in the mitochondria are spherical or ovoid and are, with a diameter of 70–130 nm, smaller than those in plastids (Hayashi-Isimaru et al. 1993). Many attempts to analyze the mitochondrial genome of *E. gracilis* failed and led only to the detection of a single cox1-bearing fragment (Tessier et al. 1997; Yasuhira and Simpson 1997), so mtDNA structure and size remained elusive (Roy et al. 2007), until Spencer and Gray (2011) established the general architecture of *E. gracilis* mtDNA. They isolated mtDNA comprising a heterodisperse collection of short linear fragments of heterogeneous size (modal size 4 kbp) bearing terminal repeats and many small, likely nonfunctional protein and rRNA gene fragments and showed that the mitochondrial large and small subunit rRNA are each split into two pieces (Spencer and Gray 2011). The mitochondrial genome of *E. gracilis* is fragmented, like Flegontov et al. (2011) suggested. Dobáková et al. (2015) analysed the mitochondrial genome in detail and reported that it encodes only a very limited set of seven protein-coding genes (three subunits of respiratory complex I, one subunit of complex III, and three subunits of complex IV) and a single SSU rRNA gene fragment. Surprisingly not a single subunit of the ATP synthase is encoded in the mitochondrial genome. The transcriptomic data

revealed that the transcripts of the mitochondrial genes are not post-translationally modified. RNA editing seems not to operate in the mitochondrion of *E. gracilis* as it does in diplonemids and kinetoplastids, the sister groups of euglenids. These findings suggest that mitochondrial panediting and processing machineries in diplonemids and kinetoplastids evolved late in evolution from the genome and transcriptome of the common ancestor of the Euglenozoa (Dobáková et al. 2015).

2.7 Mitochondrial Targeting

The majority of mitochondrial proteins in *E. gracilis* (and all eukaryotes) is encoded in the nucleus and imported into the organelles after translation in the cytosol. The mitochondrial import apparatus of Euglenozoa is supposed to be primitive; most components of the canonical mitochondrial import machinery could not be identified in euglenozoan sequences – including Tom40 (Schneider et al. 2008). Recently a protein assumed to have the same function as Tom40 in eukaryotes (Zársky et al. 2012) was found in trypanosomes: ATOM (Pusnik et al. 2011), but it was not found in the transcriptomes of euglenids (Krnáčová et al. 2012).

The mitochondrial proteins of *Euglena* possess presequences with a common (M/L)RR motif at the N-terminus or within the presequence for the organellar targeting (Krnáčová et al. 2012), as in some trypanosomatid mitochondrial proteins (Häusler et al. 1997). The presequences seem to be highly variable in sequence length (5–118 amino acids) with an average size of 31–41 amino acids, but apparently share statistically significant similarities. In most presequences the (M/L)RR motif is followed by a positively charged, hydrophobic region rich in alanine, leucine, and valine (Krnáčová et al. 2012). The presequences in *E. gracilis* can be divided into two types: i) short (up to 10 amino acids long) and ii) long (10–30 amino acids) – although some presequences can be longer (up to 118 amino acids). It was not possible to find predicted cleaved presequences in all analyzed mitochondrial proteins of *E. gracilis*, although they were predicted to be targeted to mitochondria (Krnáčová et al. 2012), similar to hydrogenosomes of *Trichomonas vaginalis*, where the majority of hydrogenosomal proteins do not harbor an N-terminal targeting sequence (Garg et al. 2015).

2.8 Alcohol Metabolizing Enzymes

An investigation of alcohol metabolizing enzymes in *E. gracilis* revealed their presence in the cytosol and the mitochondria (Yoval-Sánchez et al. 2011). Several alcohol dehydrogenases (ADHs) have been reported to localize to the cytosol (Munir et al. 2002; Palma-Gutiérrez et al. 2008), whereas prior work had identified ADHs only in *Euglena* mitochondria (Ono et al. 1995a). Furthermore, one aldehyde dehydrogenase (ALDH) (Ono et al. 1995b; Rodríguez-Zavala et al. 2006) and one acetyl-CoA synthase (Ono et al. 1995a) were found in the mitochondria. Ethanol is converted in the mitochondria to acetaldehyde by alcohol dehydrogenase and the produced acetaldehyde is converted to acetate by aldehyde dehydrogenase. Acetate is converted to acetyl-CoA by acetyl-CoA synthetase and can enter the modified Krebs cycle and after two reactions isocitrate is formed which can then either be further oxidized to carbon dioxide, or be converted by the bifunctional glyoxylate cycle enzyme to malate and succinate. Although significant fractions of ADH activity (26%), and ALDH activity (24%) were found in the cytosol, 68% of the ADH and 67% of the ALDH activities were measured in the mitochondria (Yoval-Sánchez et al. 2011). Most of the mitochondrial ADH activity was found in the mitochondrial matrix (60%), while 27% was detected in the inner membrane fraction. For ALDH activity it was *vice versa*: 20% in the mitochondrial matrix and 60% in the mitochondrial membrane fraction. Nevertheless, the active sites of both enzymes were not exposed to the cytosolic compartment. Furthermore, both enzymes were able to use aliphatic substrates of different chain

length, so they might be active in the metabolism of fatty alcohols released from wax esters (Yoval-Sánchez et al. 2011).

2.9 Glyoxylate Cycle

In 2003, a glyoxylate cycle to synthesize four-carbon compounds from two-carbon compounds, such as acetate and ethanol, was shown to be present only in mitochondria of *E. gracilis* (Ono et al. 2003). The glyoxylate cycle is important in gluconeogenesis and connects the conversion of fat to carbohydrate with some enzymes for β-oxidation of fatty acids. In those eukaryotes that possess a glyoxylate cycle, it is usually present in specialized peroxisomes known as glyoxysomes. Isocitrate lyase (ICL) and malate synthase (MS) are the main enzymes of the glyoxylate cycle. Isocitrate is reversibly cleaved by isocitrate lyase to succinate and glyoxylate, and the latter condenses with acetyl-CoA to malate catalyzed by malate synthase (Nakazawa et al. 2011). The bifunctional protein, called glyoxylate cycle enzyme (also known as the bifunctional glyoxylate cycle enzyme, malate synthase/isocitrate lyase) (Liu et al. 1995, 1997), is a fusion protein with ICL and MS domains. The N-terminal domain (amino acids 1–519) of *Euglena* glyoxylate cycle enzyme has high sequence similarity to other MS enzymes and the C-terminal domain (amino acids 597–1165) is related to ICL family proteins (Nakazawa et al. 2005). Despite the resemblance of the C-terminal domain to ICLs it was not possible to yield ICL activity by expression of the domain in *E. coli*. Instead the N-terminal domain was sufficient to provide MS and ICL activities. The ICL activity might be regulated by acetyl-CoA, binding to a site other than the catalytic center, for the MS reaction (Nakazawa et al. 2011).

The detection of the *Euglena* glyoxylate cycle enzyme in the mitochondria shows that these organelles play an important role in providing carbon sources for gluconeogenesis during wax ester and ethanol utilization. The isocitrate is metabolized in the mitochondria via two cycles, the glyoxylate cycle and the Krebs cycle (Ono et al. 2003).

2.10 A multifunctional β-oxidation Enzyme

Winkler et al. purified a novel multifunctional β-oxidation complex composed of 3-hydroxyacyl-CoA dehydrogenase, 2-enoyl-CoA hydratase, thiolase, and epimerase activities from *E. gracilis* mitochondria (Winkler et al. 2003). The novel β-oxidation complex resembles the composition of monofunctional β-oxidation enzymes and consists of 45.5-, 44.5-, 34- and 32-kD subunits. On the large subunits hydratase and thiolase functions were located and on the two smaller subunits two different 3-hydroxyacyl-CoA dehydrogenase functions were found, whereas epimerase activity was found in the complete enzyme. The 3-hydroxyacyl-CoA dehydrogenases were specific to L-isomers, the 2-enoyl-CoA hydratase catalyzed the formation of 1-hydroxyacyl-CoA isomers. This indicates that the multifunctional *Euglena* enzyme might belong to the family of β-oxidation enzymes that degrade acyl-CoAs via L-isomers (Winkler et al. 2003).

2.11 Evolutionary Considerations

Metabolic maps summarizing the main contours of energy metabolism in the mitochondria of *Euglena* grown under aerobic (Fig. 2.2) and anaerobic conditions (Figs. 2.3 and 2.4) are presented. Currently, the main interest in *Euglena* mitochondria focuses on the application of the enzymes of wax ester fermentation to biofuel production. The energetic finesse behind wax ester fermentation in *Euglena* resides in the condensing enzyme of mitochondrial fatty acid biosynthesis; it can condense acetyl-CoA to 2-oxoacyl-CoA moieties (Inui et al. 1984), in contrast to standard fatty acid biosynthesis, which condenses malonyl-CoA units. The malonyl-CoA independence means that the one ATP per pyruvate obtained from glycolysis need not be spent on synthesis of malonyl-CoA for fatty acid synthesis (conversion of acetyl-CoA to malonyl-CoA requires one ATP), allowing net gain of one ATP per pyruvate during wax ester accumulation.

The ability of *Euglena* mitochondria to function in ATP synthesis with or without oxygen raises a number of interesting evolutionary questions, and there has been considerable interest in the evolutionary origin of anaerobic energy metabolism in *Euglena* mitochondria (Rotte et al. 2001; Hoffmeister et al. 2005; Müller et al. 2012). When the cells are grown aerobically, *Euglena* mitochondria appear to function much like a normal textbook rat liver mitochondrion, except for the modified Krebs cycle. When the cells are cultured anaerobically, *Euglena* mitochondria share properties both with hydrogenosomes and with the anaerobic mitochondria characterized from several metazoans. Shared with hydrogenosomes is, for example, the use of PFO in the PNO fusion protein for oxidative decarboxylation of pyruvate. Shared with anaerobic mitochondria of animals is, for example, the use of RQ and the propionate cycle involving methylmalonyl-CoA mutase, a cobalamin dependent enzyme. With one exception, none of the proteins involved in anaerobic energy metabolism of eukaryotes investigated so far are lineage specific, they all trace to the eukaryote common ancestor (Müller et al. 2012). The single exception is currently the TER enzyme of *Euglena*, which is still unique among eukaryotes studied to date.

2.12 Future Directions

Recent studies have investigated transcriptomic comparisons of anaerobically versus aerobically treated *E. gracilis* cultures (Yoshida et al. 2016). But the anaerobic treatments were restricted to 24 h and no data were reported about growth of the cultures under anaerobic conditions. Additional transcriptomic studies comparing suitable *Euglena* strains that grow and divide under a variety of aerobic and anaerobic conditions are needed in order to better understand the corresponding differences in mitochondrial energy metabolism. An earlier proteomic study of short-term treated aerobic and anaerobic cultures revealed that the transition to anaerobic conditions did not result in an induction of enzymes specific for anaerobic function, but that enzymes and cofactors (RQ) required for anaerobiosis were already present before anaerobic treatment, with proteins for aerobic ATP synthesis being lost during anaerobic adaptation (Hoffmeister et al. 2004). This indicates that *Euglena* is prepared for anaerobic conditions before they are encountered, a strategy often encountered among eukaryotes. The biosynthesis of RQ has still not been elucidated in any eukaryote, this is an important topic for future work on *Euglena*.

References

Ahmadinejad N, Dagan T, Martin W (2007) Genome history in the symbiotic hybrid *Euglena gracilis*. Gene 402:35–39

Atteia A, van Lis R, Tielens AG, Martin WF (2013) Anaerobic energy metabolism in unicellular photosynthetic eukaryotes. Biochim Biophys Acta 1827:210–223

Bentley R, Bennett JW (1999) Constructing polyketides: from collie to combinatorial biosynthesis. Annu Rev Microbiol 53:411–446

Bereiter-Hahn J, Vöth M (2005) Dynamics of mitochondria in living cells: shape changes, dislocations, fusion and fission of mitochondria. Microsc Res Tech 27:198–219

Bernhard JM, Buck KR, Farmer MA, Bowser SS (2000) The Santa Barbara Basin is a symbiosis oasis. Nature 403:77–80

Bohnert HU, Fudal I, Dioh W, Tharreau D, Notteghem JL, Lebrun MH (2004) A putative polyketide synthase/peptide synthetase from *Magnaporthe grisea* signals pathogen attack to resistant rice. Plant Cell 16:2499–2513

Braun HP, Schmitz UK (1995) Molecular structure of the 8.0 kDa subunit of cytochrome *c* reductase from potato and its $\Delta\Psi$-dependent import into isolated-mitochondria. Biochim Biophys Acta 1229:181–186

Brönstrup U, Hachtel W (1986) Protein synthesis in isolated mitochondria from a streptomycin-bleached mutant of *Euglena gracilis* Klebs. J Plant Physiol 124:45–53

Brönstrup U, Hachtel W (1989) Cytochrome *c* oxidase of *Euglena gracilis*: purification, characterization, and identification of mitochondrially synthesized subunits. J Bioenerg Biomembr 21:359–373

Buetow DE (1989) The mitochondrion. In: Buetow DE (ed) The biology of *Euglena*, vol 4. Academic Press, San Diego, pp 247–314

Calvayrac R, Butow RA (1971) Action de l'antimycine A sur la respiration et la structure des mitochondries d'*Euglena gracilis*. Arch Microbiol 80:62–69

Calvayrac R, van Lente F, Butow RA (1971) *Euglena gracilis*: formation of giant mitochondria. Science 173:252–254

Castro H, Tomás AM (2008) Peroxidases of trypanosomatids. Antioxid Redox Signal 10:1593–1606

Castro-Guerrero NA, Krab K, Moreno-Sanchez R (2004) The alternative respiratory pathway of *Euglena* mitochondria. J Bioenerg Biomembr 36:459–469

Castro-Guerrero NA, Jasso-Chavez R, Moreno-Sanchez R (2005) Physiological role of rhodoquinone in *Euglena gracilis* mitochondria. Biochim Biophys Acta 1710:113–121

Castro-Guerrero NA, Rodríguez-Zavala JS, Marín-Hernández A, Rodríguez-Enríquez S, Moreno-Sánchez R (2008) Enhanced alternative oxidase and antioxidant enzymes under Cd(2+) stress in *Euglena*. J Bioenerg Biomembr 40:227–235

Dasgupta S, Fang J, Brake SS, Hasiotis ST, Zhang L (2012) Biosynthesis of sterols and wax esters by *Euglena* of acid mine drainage biofilms: implications for eukaryotic evolution and the early Earth. Chem Geol 306:139–145

Devars S, Torres-Márquez ME, González-Halphen D, Uribe A, Moreno-Sánchez R (1992) Cyanide-sensitive and cyanide-resistant respiration of dark-grown *Euglena gracilis*. Plant Sci 82:37–46

Dobáková E, Flegontov P, Skalicky T, Lukeš J (2015) Unexpectedly streamlined mitochondrial genome of the euglenozoan *Euglena gracilis*. Genome Biol Evol 7:3358–3367

Duarte M, Tomas AMJ (2014) The mitochondrial complex I of trypanosomatids – an overview of current knowledge. Bioenerg Biomembr 46:299–311

Duran E, Komuniecki RW, Komuniecki PR, Wheelock MJ, Klingbeil MM, Ma YC, Johnson KR (1993) Characterization of cDNA clones for the 2-methyl branched-chain enoyl-CoA reductase. An enzyme involved in branched-chain fatty acid synthesis in anaerobic mitochondria of the parasitic nematode Ascaris suum. J Biol Chem 268:22391–22396

Duran E, Walker DJ, Johnson KR, Komuniecki PR, Komuniecki RW (1998) Developmental and tissue-specific expression of 2-methyl branched-chain enoyl CoA reductase isoforms in the parasitic nematode, *Ascaris suum*. Mol Biochem Parasitol 91:307–318

Edgcomb VP, Breglia SA, Yubuki N, Beaudoin D, Patterson DJ, Leander BS, Bernhard JM (2011) Identity of epibiotic bacteria on symbiontid euglenozoans in O_2-depleted marine sediments: evidence for symbiont and host co-evolution. ISME J 5:231–243

Ernst-Fonberg ML, Bloch K (1971) A chloroplast-associated fatty acid synthetase system in *Euglena*. Arch Biochem Biophys 143:392–400

Flegontov P, Gray MW, Burger G, Lukeš J (2011) Gene fragmentation: a key to mitochondrial genome evolution in Euglenozoa? Curr Genet 57:225–232

Garg S, Stölting J, Zimorski V, Rada P, Tachezy J, Martin WF, Gould SB (2015) Conservation of transit peptide-independent protein import into the mitochondrial and hydrogenosomal matrix. Genome Biol Evol 7:2716–2726

Goldberg I, Bloch K (1972) Fatty acid synthetases in *Euglena gracilis*. J Biol Chem 247:7349–7357

Graham IA, Eastmond PJ (2002) Pathways of straight and branched chain fatty acid catabolism in higher plants. Prog Lipid Res 41:156–181

Green LS, Li Y, Emerich DW, Bergersen FJ, Day DA (2000) Catabolism of α-ketoglutarate by a *sucA* mutant of *Bradyrhizobium japonicum*: evidence for an alternative tricarboxylic acid cycle. J Bacteriol 182:2838–2844

Häusler T, Stierhof YD, Blattner J, Clayton C (1997) Conservation of mitochondrial targeting sequence function in mitochondrial and hydrogenosomal proteins from the early-branching eukaryotes *Crithidia*, *Trypanosoma* and *Trichomonas*. Eur J Cell Biol 73:240–251

Hayashi Y, Ueda K (1989) The shape of mitochondria and the number of mitochondrial nucleoids during the cell cycle of *Euglena gracilis*. J Cell Sci 93:565–570

Hayashi-Isimaru Y, Ueda K, Nonaka M (1993) Detection of DNA in the nucleoids of chloroplasts and mitochondria in *Euglena gracilis* by immunoelectron microscopy. J Cell Sci 105:1159–1164

Hendren RW, Bloch K (1980) Fatty acid synthetases from *Euglena gracilis*. Separation of component activities of the ACP-dependent fatty acid synthetase and partial purification of the beta-ketoacyl-ACP synthetase. J Biol Chem 255:1504–1508

Hoffmeister M, van der Klei A, Rotte C, van Grinsven KW, van Hellemond JJ, Henze K, Tielens AG, Martin W (2004) *Euglena gracilis* rhodoquinone:ubiquinone ratio and mitochondrial proteome differ under aerobic and anaerobic conditions. J Biol Chem 279: 22422–22429

Hoffmeister M, Piotrowski M, Nowitzki U, Martin W (2005) Mitochondrial trans-2-enoyl-CoA reductase of wax ester fermentation from *Euglena gracilis* defines a new family of enzymes involved in lipid synthesis. J Biol Chem 280:4329–4338

Hopwood DA, Sherman DH (1990) Molecular genetics of polyketides and its comparison to fatty acid biosynthesis. Annu Rev Genet 24:37–66

Horner DS, Hirt RP, Embley TM (1999) A single eubacterial origin of eukaryotic pyruvate:ferredoxin oxidoreductase genes: implications for the evolution of anaerobic eukaryotes. Mol Biol Evol 16:1280–1291

Hug LA, Stechmann A, Roger AJ (2010) Phylogenetic distributions and histories of proteins involved in anaerobic pyruvate metabolism in eukaryotes. Mol Biol Evol 27:311–324

Inui H, Miyatake K, Nakano Y, Kitaoka S (1982) Wax ester fermentation in *Euglena gracilis*. FEBS Lett 150:89–93

Inui H, Miyatake K, Nakano Y, Kitaoka S (1983) Production and composition of wax esters by fermentation of *Euglena gracilis*. Agric Biol Chem 47:2669–2671

Inui H, Miyatake K, Nakano Y, Kitaoka S (1984) Fatty acid synthesis in mitochondria of *Euglena gracilis*. Eur J Biochem 142:121–126

Inui H, Miyatake K, Nakano Y, Kitaoka S (1985) The physiological role of oxygen-sensitive pyruvate

dehydrogenase in mitochondrial fatty acid synthesis in *Euglena gracilis*. Arch Biochem Biophys 237:423–429

Inui H, Ono K, Miyatake K, Nakano Y, Kitaoka S (1987) Purification and characterization of pyruvate:NADP+ oxidoreductase in *Euglena gracilis*. J Biol Chem 262:9130–9135

Inui H, Yamaji R, Saidoh H, Miyatake K, Kitaoka S (1991) Pyruvate:$NADP^+$ oxidoreductase from *Euglena gracilis*: limited proteolysis of the enzyme with trypsin. Arch Biochem Biophys 286:270–276

Inui H, Miyatake K, Nakano Y, Kitaoka S (1992) Synthesis of reserved polysaccharide from wax esters accumulated as the result of anaerobic energy generation in *Euglena gracilis* returned from anaerobic to aerobic conditions. Int J Biochem 24:799–803

Ishikawa T, Takeda T, Shigeoka S, Hirayama O, Mitsunaga T (1993) Hydrogen peroxide generation in organelles of *Euglena gracilis*. Phytochemistry 33:1297–1299

Jasso-Chávez R, Moreno-Sánchez R (2003) Cytosol-mitochondria transfer of reducing equivalents by a lactate shuttle in heterotrophic *Euglena*. Eur J Biochem 270:4942–4951

Jasso-Chávez R, Torres-Márquez ME, Moreno-Sánchez R (2001) The membrane-bound L- and D-lactate dehydrogenase activities in mitochondria from *Euglena gracilis*. Arch Biochem Biophys 390:295–303

Jasso-Chávez R, García-Cano I, Marín-Hernández A, Mendoza-Cózatl D, Rendón JL, Moreno-Sánchez R (2005) The bacterial-like lactate shuttle components from the heterotrophic *Euglena gracilis*. Biochim Biophys Acta 1709:181–190

Kawabata A, Kaneyama M (1989) The effect of growth temperature on wax ester content and composition of *Euglena gracilis*. J Gen Microbiol 135:1461–1467

Khan AA, Kolattukudy PE (1973) A microsomal fatty acid synthtase coupled to acyl-CoA reductase in *Euglena gracilis*. Arch Biochem Biophys 158:411–420

Kita K, Hirawake H, Miyadera H, Amino H, Takeo S (2002) Role of complex II in anaerobic respiration of the parasite mitochondria from *Ascaris suum* and *Plasmodium falciparum*. Biochim Biophys Acta 1553:123–139

Kitaoka S, Nakano Y, Miyatake K, Yokota A (1989) Enzymes and their functional localization. In: Buetow DE (ed) The biology of Euglena, vol 4. Academic Press, San Diego, pp 2–135

Klaveness D, Løvhøiden F (2007) Meromictic lakes as habitats for protists: life in the chemocline and below? In: Seckbach J (ed) Algae and cyanobacteria in extreme environments. Springer, Dordrecht, pp 59–78

Kolattukudy PE (1970) Reduction of fatty acids to alcohols by cell-free preparations of *Euglena gracilis*. Biochemist 9:1095–1102

Komuniecki R, Tielens AGM (2003) Carbohydrate and energy metabolism in parasitic helminths. In: Marr JJ, Nilsen TW, Komuniecki RW (eds) Molecular medical parasitology. Academic press, San Diego, pp 339–358

Komuniecki PR, Vanover L (1987) Biochemical changes during the aerobic-anaerobic transition in Ascaris suum larvae. Mol Biochem Parasitol 22:241–248

Komuniecki R, Komuniecki PR, Saz HJ (1981) Relationships between pyruvate decarboxylation and branched-chain volatile acid synthesis in *Ascaris* mitochondria. J Parasitol 67:601–608

Komuniecki R, Fekee S, Thissen-Parra J (1985) Purification and characterization of the 2-methyl branched-chain Acyl-CoA dehydrogenase, an enzyme involved in NADH-dependent enoyl-CoA reduction in anaerobic mitochondria of the nematode, *Ascaris suum*. J Biol Chem 260:4770–4777

Komuniecki R, Campbell T, Rubin N (1987) Anaerobic metabolism in *Ascaris suum*: Acyl CoA intermediates in isolated mitochondria synthesizing 2-methyl branched-chain fatty acids. Mol Biochem Parasitol 24:147–154

Krnáčová K, Vesteg M, Hampl V, Vlček Č, Horváth A (2012) *Euglena gracilis* and Trypanosomatids possess common patterns in predicted mitochondrial targeting presequences. J Mol Evol 75:119–129

Krnáčová K, Rýdlová I, Vinarčíková M, Krajčovič J, Vesteg M, Horváth A (2015) Characterization of oxidative phosphorylation enzymes in *Euglena gracilis* and its white mutant strain W(gm)ZOflL. FEBS Lett 589:687–694

Ku C, Martin WF (2016) A natural barrier to lateral gene transfer from prokaryotes to eukaryotes revealed from genomes: the 70% rule. BMC Biol 14:89

Ku C, Nelson-Sathi S, Roettger M, Sousa FL, Lockhart PJ, Bryant D, Hazkani-Covo E, McInerney JO, Landan G, Martin WF (2015) Endosymbiotic origin and differential loss of eukaryotic genes. Nature 524:427–432

Kunau WH, Dommes V, Schulz H (1995) β-oxidation of fatty acids in mitochondria, peroxisomes, and bacteria: a century of continued progress. Prog Lipid Res 34:264–342

Lantsman Y, Tan KSW, Morada M, Yarlett N (2008) Biochemical characterization of a mitochondrial-like organelle from *Blastocystis* sp. subtype 7. Microbiology 154:2757–2766

Leedale GF, Meeuse BJD, Pringsheim EG (1965) Structure and physiology of *Euglena spirogyra* I and II. Arch Microbiol 50:68–102

Liu H, Reynolds KA (1999) Role of crotonyl coenzyme A reductase in determining the ratio of polyketides monensin A and monensin B produced by *Streptomyces cinnamonensis*. J Bacteriol 181:6806–6813

Liu F, Thatcher JD, Barral JM, Epstein HF (1995) Bifunctional glyoxylate cycle protein of *Caenorhabditis elegans*: a developmentally regulated protein of intestine and muscle. Dev Biol 169:399–414

Liu F, Thatcher JD, Epstein HF (1997) Induction of glyoxylate cycle expression in *Caenorhabditis elegans*: a fasting response throughout larval development. Biochemistry 36:255–260

Mei B, Komuniecki R, Komuniecki PR (1997) Localization of cytochrome oxidase and the 2-methyl branched-chain enoyl CoA reductase in muscle and hypodermis of *Ascaris suum* larvae and adults. J Parasitol 83:760–763

Mentel M, Martin W (2008) Energy metabolism among eukaryotic anaerobes in light of Proterozoic ocean

chemistry. Philos Trans R Soc Lond B 363: 2717–2729

Metz JG, Roessler P, Facciotti D, Levering C, Dittrich F, Lassner M, Valentine R, Lardizabal K, Domergue F, Yamada A, Yazawa K, Knauf V, Browse J (2001) Production of polyunsaturated fatty acids by polyketide synthases in both prokaryotes and eukaryotes. Science 293:290–293

Michaels A, Gibor A (1973) Ultrastructural changes in *Euglena* after ultraviolet irradiation. J Cell Sci 13:779–809

Miyamoto E, Tanioka Y, Nishizawa-Yokoi A, Yabuta Y, Ohnishi K, Misono H, Shigeika S, Nakano Y, Watanabe F (2010) Characterization of methylmalonyl-CoA mutase involved in the propionate photoassimilation of *Euglena gracilis* Z. Arch Microbiol 192:437–446

Moreno-Sánchez R, Covián R, Jasso-Chávez R, Rodríguez-Enríquez S, Pacheco-Moisés E, Torres-Márquez ME (2000) Oxidative phosphorylation supported by an alternative respiratory pathway in mitochondria from *Euglena*. Biochim Biophys Acta 1457:200–210

Mukai K, Yoshida M, Toyosaki H, Yao Y, Wakabayashi S, Matsubara H (1989) An atypical heme-binding structure of cytochrome *c*1 of *Euglena gracilis* mitochondrial complex III. Eur J Biochem 178:649–656

Müller M, Mentel M, van Hellemond JJ, Henze K, Woehle C, Gould SB, Yu R-Y, van der Giezen M, Tielens AGM, Martin WF (2012) Biochemistry and evolution of anaerobic energy metabolism in eukaryotes. Microbiol Mol Biol Rev 76:444–495

Munir I, Nakazawa M, Harano K, Yamaji R, Inui H, Miyatake K, Nakano Y (2002) Occurrence of a novel $NADP^+$ –linked alcohol dehydrogenase in *Euglena gracilis*. Comp Biochem Physiol B Biochem Mol Biol 132:535–540

Nagai J, Otha T, Saito E (1971) Incorporation of propionate into wax esters by etiolated *Euglena*. Biochem Biophys Res Commun 42:523–529

Nakazawa M, Inui H, Yamaji R, Yamamoto T, Takenaka S, Ueda M, Nakano Y, Miyatake K (2000) The origin of pyruvate:$NADP^+$ oxidoreductase in mitochondria of *Euglena gracilis*. FEBS Lett 479:155–156

Nakazawa M, Takenaka S, Ueda M, Inui H, Nakano Y, Miyatake K (2003) Pyruvate:$NADP^+$ oxidoreductase is stabilized by its cofactor, thiamin pyrophosphate, in mitochondria of *Euglena gracilis*. Arch Biochem Biophys 411:183–188

Nakazawa M, Minami T, Teramura K, Kumamoto S, Hanato S, Takenaka S, Ueda M, Inui H, Nakano Y, Miyatake K (2005) Molecular characterization of a bifunctional glyoxylate cycle enzyme, malate synthase/isocitrate lyase, in *Euglena gracilis*. Comp Biochem Physiol B Biochem Mol Biol 141:445–452

Nakazawa M, Nishimura M, Inoue K, Ueda M, Inui H, Nakano Y, Miyatake K (2011) Characterization of a bifunctional glyoxylate cycle enzyme, malate synthase/isocitrate lyase, of *Euglena gracilis*. J Eukaryot Microbiol 58:128–133

Nakazawa M, Andoh H, Koyama K, Watanabe Y, Nakai T, Ueda M, Sakamoto T, Inui H, Nakano Y, Miyatake K (2015) Alteration of wax ester content and composition in *Euglena gracilis* with gene silencing of 3-ketoacyl-CoA thiolase isozymes. Lipids 50:483–492

Napier JA (2002) Plumbing the depths of PUFA biosynthesis: a novel polyketide synthase-like pathway from marine organisms. Trends Plant Sci 7:51–54

Nass MMK, Ben-Shaul Y (1972) A novel closed circular duplex DNA in bleached mutant and green strains of *Euglena gracilis*. Biochim Biophys Acta 272:130–136

Neumann D, Parthier B (1973) Effects of nalidixic acid, chloramphenicol, cycloheximide, and anisomycin on structure and development of plastids and mitochondria in greening *Euglena gracilis*. Exp Cell Res 81:255–268

O'Brien EA, Koski LB, Zhang Y, Yang L, Wang E, Gray MW, Burger G, Lang BF (2007) TBestDB: a taxonomically broad database of expressed sequence tags (ESTs). Nucleic Acids Res 35:D445–D451

Ogawa T, Kimura A, Sakuyama H, Tamoi M, Ishikawa T, Shigeoka S (2015) Identification and characterization of cytosolic fructose-1,6-bisphosphatase in *Euglena gracilis*. Biosci Biotechnol Biochem 79:1957–1964

Ono K, Kawanaka Y, Izumi Y, Inui H, Miyatake K, Kitaoka S, Nakano Y (1995a) Mitochondrial alcohol dehydrogenase from ethanol-grown *Euglena gracilis*. J Biochem 117:1178–1182

Ono K, Miyatake K, Inui H, Kitaoka S, Nakano Y (1995b) Wax ester production by anaerobic *Euglena gracilis*. J Mar Biotechnol 2:157–161

Ono K, Kondo M, Osafune T, Miyatake K, Inui H, Kitaoka S, Nishimura M, Nakano Y (2003) Presence of glyoxylate cycle enzymes in the mitochondria of *Euglena gracilis*. J Eukaryot Microbiol 50:92–96

Padermshoke A, Ogawa T, Nishio K, Nakazawa M, Nakamoto M, Okazawa A, Kanaya S, Arita M, Ohta D (2016) Critical involvement of environmental carbon dioxide fixation to drive wax ester fermentation in *Euglena*. PLoS One 11:e0162827

Palma-Gutiérrez HN, Rodríguez-Zavala JS, Jasso-Chávez R, Moreno-Sánchez R, Saavedra E (2008) Gene cloning and biochemical characterization of an alcohol dehydrogenase from *Euglena gracilis*. J Eukaryot Microbiol 55:554–561

Pellegrini M (1980) Three-dimensional reconstruction of organelles in *Euglena gracilis* Z. II. Qualitative and quantitative changes of chloroplasts and mitochondrial reticulum in synchronous cultures during bleaching. J Cell Sci 46:313–340

Perez E, Lapaille M, Degand H, Cilibrasi L, Villavicencio-Queijeiro A, Morsomme P, González-Halphen D, Field MC, Remacle C, Baurain D, Cardol P (2014) The mitochondrial respiratory chain of the secondary green alga *Euglena gracilis* shares many additional subunits with parasitic Trypanosomatidae. Mitochondrion 19:338–349

Pönsgen-Schmidt E, Schneider T, Hammer U, Betz A (1988) Comparison of phosphoenolpyruvate-carboxykinase from autotrophically and heterotrophi-

cally grown *Euglena* and its role during dark anaerobiosis. Plant Physiol 86:456–462

Pusnik M, Schmidt O, Perry AJ, Oeljeklaus S, Niemann M, Warcheid B, Lithgow T, Meisinger C, Schneider A (2011) Mitochondrial preprotein translocase of trypanosomatids has a bacterial origin. Curr Biol 21:1738–1743

Reddy JK, Hashimoto T (2001) Peroxisomal beta-oxidation and peroxisome proliferator-activated receptor alpha: an adaptive metabolic system. Annu Rev Nutr 21:193–230

Rein KS, Borrone J (1999) Polyketides from dinoflagellates: origins, pharmacology and biosynthesis. Comp Biochem Physiol B Biochem Mol Biol 124:117–131

Reynolds KA, Wang P, Fox KM, Speedie MK, Lam Y, Floss HG (1992) Purification and characterization of a novel enoyl coenzyme A reductase from *Streptomyces collinus*. J Bacteriol 174:3850–3854

Rodríguez-Zavala JS, Ortiz-Cruz MA, Moreno-Sánchez R (2006) Characterization of an aldehyde dehydrogenase from *Euglena gracilis*. J Eukaryot Microbiol 53:36–42

Roth JR, Lawrence JG, Bobik TA (1996) Cobalamin (coenzyme B_{12}): synthesis and biological significance. Annu Rev Microbiol 50:137–181

Rotte C, Stejskal F, Zhu G, Keithly JS, Martin W (2001) Pyruvate:NADP$^+$ oxidoreductase from the mitochondrion of *Euglena gracilis* and from the apicomplexan *Cryptosporidium parvum*: a biochemical relic linking pyruvate metabolism in mitochondriate and amitochondriate protists. Mol Biol Evol 18:710–720

Roy J, Faktorov D, Lukeš J, Burger G (2007) Unusual mitochondrial genome structures throughout the Euglenozoa. Protist 158:385–396

Santiago-Martínez MG, Lira-Silva E, Encalada R, Pineda E, Gallardo-Pérez JC, Zepeda-Rodriguez A, Moreno-Sánchez R, Saavedra E, Jasso-Chávez R (2015) Cadmium removal by *Euglena gracilis* is enhanced under anaerobic growth conditions. J Hazard Mater 288:104–112

Schneider T, Betz A (1985) Wax ester fermentation in *Euglena gracilis* T. Factors favouring the synthesis of odd-numbered fatty acids and alcohols. Planta 166:67–73

Schneider A, Bursa D, Lithgow T (2008) The direct route: a simplified pathway for protein import into the mitochondrion of trypanosomes. Trends Cell Biol 18:12–18

Shigeoka S, Ishikawa T, Tamoi M, Miyagawa Y, Takeda T, Yabuta Y, Yoshimura K (2002) Regulation and function of ascorbate peroxidase isoenzymes. J Exp Bot 53:1305–1319

Simpson AGB, van den Hoff J, Bernard C, Burton HR, Patterson DJ (1997) The ultrastructure and systematic position of the Euglenozoon *Postgaardi mariagerensis*, Fenchel et al. Arch Protistenkd 147:213–225

Spencer DF, Gray MW (2011) Ribosomal RNA genes in *Euglena gracilis* mitochondrial DNA: fragmented genes in a seemingly fragmented genome. Mol Gen Genomics 285:19–31

Stewart KD, Mattox K (1980) Phylogeny of phytoflagellates. In: Cox ER (ed) Phytoflagellates. Elsevier, North Holland, pp 433–462

Takamiya S, Kita K, Wang PP, Weinstein A, Hiraishi H, Oya H, Aoki T (1993) Developmental changes in the respiratory chain of *Ascaris* mitochondria. Biochim Biophys Acta 1141:65–74

Tamaki S, Maruta T, Sawa Y, Shigeoka S, Ishikawa T (2014) Identification and functional analysis of peroxiredoxin isoforms in *Euglena gracilis*. Biosci Biotechnol Biochem 78:593–601

Teerawanichpan P, Qiu X (2010) Fatty acyl-CoA reductase and wax synthase from *Euglena gracilis* in the biosynthesis of medium-chain wax esters. Lipids 45:263–273

Tessier LH, van der Speck H, Gualberto JM, Grienenberger JM (1997) The *cox1* gene from *Euglena gracilis*: a protist mitochondrial gene without introns and genetic code modifications. Curr Genet 31:208–213

Tielens AGM (1994) Energy generation in parasitic helminths. Parasitol Today 10:346–352

Tielens AGM, van Hellemond JJ (2007) Anaerobic mitochondria: properties and origin. In: Martin W, Müller M (eds) Origin of mitochondria and hydrogenosomes. Springer, Berlin, Heidelberg, pp 85–103

Tielens AGM, Rotte C, van Hellemond JJ, Martin W (2002) Mitochondria as we don't know them. Trends Biochem Sci 27:564–572

Torrents E, Trevisiol C, Rotte C, Hellman U, Martin W, Reichard P (2006) *Euglena gracilis* ribonucleotide reductase: the eukaryotic class II enzyme and the antiquity of eukaryotic B_{12}-dependence. J Biol Chem 281:5604–5611

Trenkamp S, Martin W, Tietjen K (2004) Specific and differential inhibition of very-long-chain fatty acid elongases from *Arabidopsis thaliana* by different herbicides. Proc Natl Acad Sci U S A 101:11903–11908

Tucci S, Vacula R, Krajcovic J, Proksch P, Martin W (2010) Variability of wax ester fermentation in natural and bleached *Euglena gracilis* strains in response to oxygen and the elongase inhibitor flufenacet. J Eukaryot Microbiol 57:63–69

Uribe A, Cávez E, Jiménez M, Zazueta C, Moreno-Sánchez R (1994) Characterization of Ca^{2+}-transport in *Euglena gracilis* mitochondria. Biochim Biophys Acta 1186:107–116

Van Hellemond JJ, van der Klei A, van Weelden SWH, Tielens AGM (2003) Biochemical and evolutionary aspects of anaerobically functioning mitochondria. Philos Trans R Soc Lond Ser B Biol Sci 358:205–213

van Waarde A, Van den Thillart G, Verhagen M (1993) Ethanol formation and pH regulation in fish. In: Hochachka PW et al (eds) Surviving hypoxia. CRC Press, Boca Raton, pp 157–170

Walker TA, Jonak ZL, Worsham LM, Ernst-Fonberg ML (1981) Kinetic studies oft he fatty acid synthetase multienzyme complex from *Euglena gracilis* variety *bacillaris*. Biochem J 199:383–392

Wallace KK, Bao ZY, Dai H, Digate R, Schuler G, Speedie MK, Reynolds KA (1995) Purification of crotonyl-CoA

reductase from *Streptomyces collinus* and cloning, sequencing and expression of the corresponding gene in *Escherichia coli*. Eur J Biochem 233:954–962

Wallis JG, Watts JL, Browse J (2002) Polyunsaturated fatty acid synthesis: what will they think of next? Trends Biochem Sci 27:467–473

Winkler U, Säftel W, Stabenau H (2003) A new type of a multifunctional β-oxidation enzyme in *Euglena*. Plant Physiol 131:753–762

Wolken JJ (1967) *Euglena*—an experimental organism for biochemical and biophysical studies, 2nd edn. Springer, New York

Yamada K, Suzuki H, Takeuchi T, Kazama Y, Mitra S, Abe T, Goda K, Suzuki K, Iwata O (2016) Efficient selective breeding of live oil-rich *Euglena gracilis* with fluorescence-activated cell sorting. Sci Rep 6:26327

Yasuhira S, Simpson L (1997) Phylogenetic affinity of mitochondria of *Euglena gracilis* and kinetoplastids using cytochrome oxidase I and hsp60. J Mol Evol 44:341–347

Yoshida Y, Tomiyama T, Maruta T, Tomita M, Ishikawa T, Arakawa K (2016) De novo assembly and comparative transcriptome analysis of *Euglena gracilis* in response to anaerobic conditions. BMC Genomics 17:182

Yoval-Sánchez B, Jasso-Chávez R, Lira-Silva E, Moreno-Sánchez R, Rodríguez-Zavala JS (2011) Novel mitochondrial alcohol metabolizing enzymes of *Euglena gracilis*. J Bioenerg Biomembr 43:519–530

Zársky V, Tachezy J, Dolezal P (2012) Tom40 is likely common to all mitochondria. Curr Biol 22:R479–R481

Zhang SY, Bryant D (2011) The tricarboxylic acid cycle in cyanobacteria. Science 334:1551–1553

Zhu G, LaGier MJ, Stejskal F, Millership JJ, Cai X, Keithly JS (2002) *Cryptosporidium parvum*: the first protist known to encode a putative polyketide synthase. Gene 298:79–89

C2 metabolism in *Euglena*

3

Masami Nakazawa

Abstract

Euglenoids are able to assimilate fatty acids and alcohols with various carbon-chain lengths, and ethanol is known to be one of the best carbon sources to support the growth of *Euglena gracilis*. Ethanol is first oxidized to acetate by the sequential reactions of alcohol dehydrogenase and acetaldehyde dehydrogenase in the mitochondria, and then converted to acetyl coenzyme A (acetyl-CoA). Acetyl-CoA is metabolized through the glyoxylate cycle which is a modified tricarboxylic acid (TCA) cycle in which isocitrate lyase (ICL) and malate synthase (MS) function to bypass the two decarboxylation steps of the TCA cycle, enabling the net synthesis of carbohydrates from C2 compounds. ICL and MS form a unique bifunctional enzyme localized in *Euglena* mitochondria, not in glyoxysome as in other eukaryotes. The unique glyoxylate and glycolate metabolism during photorespiration is also discussed in this chapter.

Keywords

Glyoxylate cycle • Alcohol dehydrogenase • Aldehyde dehydrogenase • Gluconeogenesis • Bifunctional enzyme • *Euglena gracilis* glyoxylate cycle enzyme (EgGCE)

Abbreviations

ACS	Acetyl-coenzyme A synthetase
ADH	Alcohol dehydrogenase
ALDH	Acetaldehyde dehydrogenase
CeGCE	*Caenorhabditis elegans* bifunctional glyoxylate cycle enzyme
CoA	Coenzyme A
EgGCE	*Euglena gracilis* bifunctional glyoxylate cycle enzyme

M. Nakazawa (✉)
Faculty of Life and Environmental Sciences, Osaka Prefecture University, Sakai, Osaka, Japan
e-mail: mami@biochem.osakafu-u.ac.jp

S.D. Schwartzbach, S. Shigeoka (eds.), *Euglena: Biochemistry, Cell and Molecular Biology*, Advances in Experimental Medicine and Biology 979, DOI 10.1007/978-3-319-54910-1_3

FBPase	Fructose-1,6-bisphosphatase
G6P	Glucose-6-phosphate
GGT	Glutamate:glyoxylate aminotransferase
ICL	Isocitrate lyase
MDH	Malate dehydrogenase
MS	Malate synthase
PEPCK	Phosphoenolpyruvate carboxykinase
PFK	Phosphofructokinase
PPi	Pyrophosphate
TCA	Tricarboxylic acid

3.1 Introduction

When an organism assimilates C2 compounds, the glyoxylate pathway which bypasses the tricarboxylic acid (TCA) cycle is needed. The glyoxylate pathway is found in bacteria, fungi, algae and plants. In general, the glyoxylate pathway is localized to specialized microbodies called glyoxysomes or to the cytosol in eukaryotes (Kunze et al. 2006). *Euglena* can use ethanol and acetate as the sole source of carbon and energy for growth. In contrast to most eukaryotes, the metabolic pathway and enzymes required for assimilation of ethanol and acetate are mainly localized in the mitochondria of *Euglena*. One topic of this chapter will be a detailed discussion of the properties of the mitochondrial glyoxylate cycle enzymes found in *Euglena* and their role in ethanol and acetate assimilation.

C2 compounds must also be metabolized during photorespiration. The CO_2 fixation enzyme Ribulose bisphosphate carboxylase-oxygenase (Rubisco) can react with CO_2 to form 3-phosphoglycerate or with O_2 forming 2-phosphoglycolate. Because of the much higher concentration of O_2 compared to CO_2 in the present air, a significant amount of 2-phosphoglycolate is formed during photosynthesis. The 2-phosphoglycolate produced by photorespiration is converted back to the Calvin cycle intermediate 3-phosphoglycerate using the enzymes of the photorespiratory pathway. In higher plants, some of these enzymes are localized in specialized microbodies called peroxisomes. *Euglena* metabolizes photorespiratory glycolate in the mitocohondria, not in the microbodies. The unique role of mitochondria in *Euglena* photorespiratory metabolism is the second topic of this chapter.

3.2 C2-metabolism in *Euglena*

Euglenoids have been shown to use non-carbohydrate carbon sources including fatty acids and alcohols with varying carbon chain lengths as a sole carbon and energy for growth (Buetow 1968; Wilson and Danforth 1958; Hosotani et al. 1988). Ethanol is a very good non-carbohydrate carbon source just as glucose is a good carbohydrate carbon source. Ethanol taken up by *Euglena* is converted to acetate by the sequential reactions of alcohol dehydrogenase (ADH) and acetaldehyde dehydrogenase (ALDH). These activities are greatly induced after ethanol is added to the *Euglena* culture (Ono et al. 1995; Rodríguez-Zavala et al. 2006).

ADH and ALDH are localized in the mitochondria (Ono et al. 1995; Rodríguez-Zavala et al. 2006). Mitochondrial ADH purified by Ono et al. (1995) was NAD^+-dependent and used ethanol, 1-butanol, 1-heptanol, cinnamyl alcohol and myristyl alcohol as substrates. Yoval-Sánchez et al. (2011) revealed that NAD^+-dependent ADHs and ALDHs localized not only to the mitochondrial matrix but also to the mitochondrial inner membrane. The preferred substrate of the NAD^+-dependent ADH in the mitochondrial matrix was ethanol rather than longer chain alcohols in contrast to the NAD^+-dependent ADH in the inner mitochondrial membrane which preferred myristyl alcohol (C14) to ethanol. The presence of ADH and ALDH in the inner mitochondrial membrane might favor the use of ethanol and acetaldehyde in the vicinity of the internal mitochondrial membrane, thus preventing the toxic effects of these compounds on the respiratory chain and mitochondrial matrix enzymes. In fact, intact mitochondria isolated from *E. gracilis* can use ethanol as a respiratory substrate (Ono et al. 1995). As well as metabolizing ethanol, ADHs and ALDHs which react with various aliphatic compounds are thought to have an

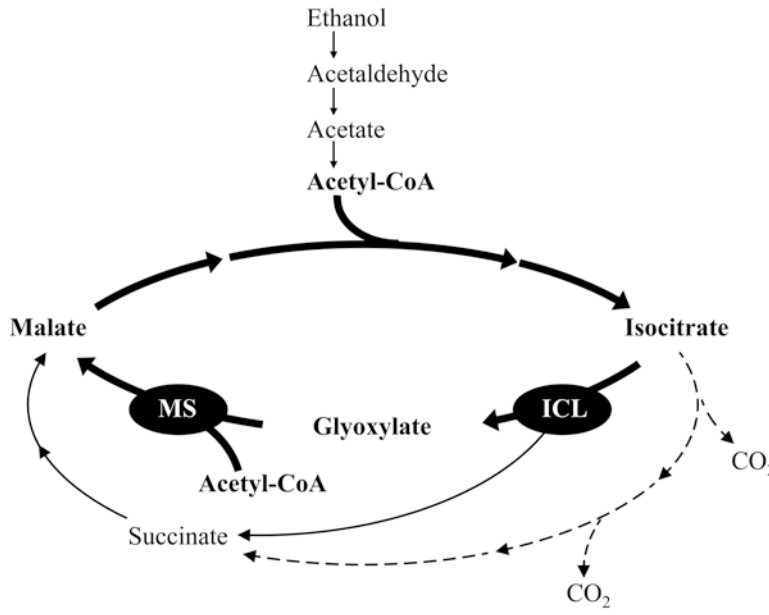

Fig. 3.1 Schematic diagram of the assimilation of ethanol in *Euglena gracilis* (modified scheme inferred from Nakazawa et al. 2011). MS, malate synthase; ICL, isocitrate lyase

important role in the assimilation of various chain length fatty alcohols and in the metabolism of wax ester-derived medium chain length fatty alcohols (see Chap. 13). Anaerobically produced wax esters (main component is C14:0-C14:0Alc) are degraded under aerobic conditions in the cytosol, and aliphatic alcohols are produced. Medium and long chain fatty alcohols are poorly soluble in water therefore they are thought to preferentially interact with the membrane (Yoval-Sánchez et al. 2011). Munir et al. (2002) identified a *Euglena* $NADP^+$-dependent ADH (whose localization is unknown) showing broad substrate specificity (C2 to C14). ADHs and ALDHs that react with various chain length substrates could play an important role in supplying medium and long chain fatty acids to the mitochondrial fatty acid beta-oxidation system.

The acetate synthesized from ethanol by the combined action of ADH and ALDH and the acetate taken up from the growth media are converted to acetyl coenzyme A (acetyl-CoA) by the ATP-dependent reaction of acetyl-CoA synthetase (ACS) (Ohmann 1964). The acetyl-CoA enters the glyoxylate cycle (Kornberg and Krebs 1957), a modified TCA cycle where the decarboxylation steps catalyzed by isocitrate dehydrogenase and 2-oxoglutarate decarboxylase for the synthesis of succinate from isocitrate are bypassed (Fig. 3.1). The TCA cycle decarboxylation steps are bypassed by the action of isocitrate lyase (ICL) which catalyzes the cleavage of D-isocitrate to glyoxylate and succinate. The glyoxylate formed by the ICL reaction is condensed with acetyl-CoA to produce L-malate by the action of malate synthase (MS). The glyoxylate cycle is essential for growth on C2 compounds because by bypassing the two decarboxylation steps of the TCA cycle it converts two molecules of acetyl-CoA formed by the ACS reaction to malate resulting in a net gain of 4 carbon atoms. Eukaryotes transport malate across the mitochondrial membrane using the mitochondrial inner membrane 2-oxoglutarate/malate carrier protein and the dicarboxylate carrier protein which catalyzes the electroneutral exchange of malate and 2-oxoglutarate, and then across the outer membrane porin channels. The malate in the cytoplasm is reduced by malate dehydrogenase (MDH) to oxaloacetate which can then be converted to phosphoenolpyruvate by cytosolic phosphoenolpyruvate carboxykinase (PEPCK) and ultimately to carbohydrates via gluconeogenesis.

Ethanol and acetate appear to induce an increase in the activity of the enzymes, including the glyoxylate cycle enzymes, required to form

carbohydrates from ethanol and acetate. ADH, MS and ICL activities are induced by ethanol (Cook and Carver 1966; Woodward and Merrett 1975; Collins and Merrett 1975a; Horrum and Schwartzbach 1981; Ono et al. 1994, 1995). Both the mitochondrial and cytosolic MDH had higher activity in ethanol-grown than in glucose-grown *Euglena* (Peak et al. 1972). Miyatake et al. (1984a) reported that cytosolic PEPCK showed three times higher activity in ethanol-grown than in glucose-grown *Euglena*. These results suggest that MDH and PEPCK play important roles in gluconeogenesis in ethanol-grown *E. gracilis*.

The phosphoenolpyruvate in the cytosol is metabolized to glucose-6-phosphate (G6P) via a reversal of glycolysis with fructose-1,6-bisphosphatase (FBPase) instead of the irreversible reaction with phosphofructokinase in general animals. In *E. gracilis*, pyrophosphate-dependent phosphofructokinase (PPi-PFK), which catalyzes a reversible reaction from fructose 6-phosphate and pyrophosphate (PPi) to fructose 1,6-bisphosphate and orthophosphate (Pi), was found in addition to ATP-PFK in the cytosol, and the activity of PPi-PFK was 10–30 times higher than that of ATP-PFK and FBPase throughout cell growth (Miyatake et al. 1984b; Enomoto et al. 1988). PPi-PEPCK catalyzes an easily reversible reaction, so it may play a dual role in gluconeogenesis as well as in glycolysis. Excess amounts of G6P are converted to UDP-glucose by the action of phosphoglucomutase (producing glucose-1-phosphate, G1P) and UTP:G1P uridylyltransferase, and then synthesized to storage sugar paramylon.

The glyoxylate cycle and gluconeogenesis also play an important role in the conversion of wax ester to paramylon when cells are moved from anaerobic to aerobic conditions (Inui et al. 1992) (see Chap. 13). Fatty acids derived from wax esters are degraded into acetyl-CoA and propionyl-CoA by the action of fatty acid beta-oxidation, and then the acetyl-CoA is converted to malate via the glyoxylate cycle. The unique features of the glyoxylate pathway in *E. gracilis* will be described in detail in the following section.

3.3 Novel Features of the Glyoxylate Pathway in *E. gracilis*

ICL and MS are usually localized in glyoxysomes (Breidenbach and Beevers 1967), which is a specialized form of peroxisome containing glyoxylate cycle enzymes in higher plants and algae. Peroxisomes are defined as organelles that contain catalase and a H_2O_2-producing oxidase, such as acyl-CoA oxidase, which is the initial enzyme of the peroxisomal fatty acid beta-oxidation. In early studies, *Euglena* ICL and MS were believed to be localized in glyoxysomes as in higher plants and other algae (Graves et al. 1972; Collins and Merrett 1975a). In an immunohistochemical analysis by Ono et al. (2003), MS localized to *E. gracilis* mitochondria. Mitochondrial localization of glyoxylate pathway enzymes is rare; two examples are the larvae of the nematodes *Turbatrix aceti* (McKinley and Trelease 1978) and *Ascaris suum* (Rubin and Trelease 1976).

Nakazawa et al. (2005) demonstrated that purified MS from *E. gracilis* also catalyzed the ICL reaction. Molecular cloning of the enzyme (Nakazawa et al. 2005) revealed that *E. gracilis* has a bifunctional glyoxylate cycle enzyme having both ICL and MS domains on a single polypeptide. The *E. gracilis* bifunctional MS/ICL glyoxylate cycle enzyme (EgGCE) consists of four identical 110 kDa subunits. The nematode *Caenorhabditis elegans* (Liu et al. 1995) also has a bifunctional glyoxylate cycle enzyme having both the ICL and MS domains on a single polypeptide. Interestingly, EgGCE has an amino-terminal MS domain and a carboxy-terminal ICL domain, while in the nematode *C. elegans* GCE (CeGCE), the ICL domain is amino-terminal and the ICL domain is carboxy-terminal (Liu et al. 1995). Homology analysis of the *Euglena* and nematode enzymes suggests their different ancestral origin (Nakazawa et al. 2005). EgGCE showed low homology to other glyoxylate cycle enzymes; the MS domain showed 35–40% identity to MS from γ-proteobacterium and the ICL domain showed 20–25% identity to the ICL from proteobacterium

and nematodes. In contrast, CeGCE showed very high amino acid homology to bacterial glyoxylate cycle enzymes; the MS domain showed about 60% identity to α- and γ-proteobacterial MS and the ICL domain showed about 70% identity to α-proteobacterial ICL. These different domain organizations might represent evolution from unrelated ancestral genes with different operon structures. Immunofluorescent microscopy localized the CeGCE to the *C. elegans* glyoxysomes (Liu et al. 1995), while EgGCE was localized by immunoelectron microscopy to *Euglena* mitochondria (Ono et al. 2003).

The *Euglena* bifunctional glyoxylate cycle enzyme may reduce the inhibitory effects of glyoxylate on mitochondrial TCA cycle enzymes (Yokota and Kitaoka 1979, 1981) by channeling the glyoxylate produced by the ICL domain to the MS domain *in vivo*. A unique catalytic feature of EgGCE is the activation of the ICL reaction by acetyl-CoA which is one of the substrates of the following MS reaction. The K_m value for isocitrate in the ICL reaction is considerably higher in EgGCE (6.7 mM, Nakazawa et al. 2005) than in other ICL family enzymes (less than 2 mM in the BRENDA database, Chang et al. 2009). When acetyl-CoA was added to the EgGCE reaction mixture at concentrations higher than 5 μM, the K_m value for isocitrate decreased by about one-third, while the V_{max} value increased about twofold. Thus, EgGCE is activated only when a sufficient amount of acetyl-CoA is available avoiding the accumulation of toxic glyoxylate in mitochondria. Heterologous expression of a mutated EgGCE in which acetyl-CoA cannot bind to the catalytic site of the MS domain showed that acetyl-CoA still activated the ICL reaction (Nakazawa et al. 2011). This suggests that acetyl-CoA regulates ICL activity in EgGCE by binding to a site other than the catalytic center for the MS reaction. Unfortunately, the enzymatic properties of the CeGCE are presently unknown so we can not compare the enzymatic properties of the bifunctional glyoxylate cycle enzymes.

3.4 Glycolate and Glyoxylate Metabolism Related to Photorespiration in *E. gracilis*

Metabolism of the C2 compounds glycolate and glyoxylate is important during photorespiration in *Euglena*. Photorespiration is the light-dependent release of CO_2 by photosynthetic organisms and results from the ability of the CO_2 fixing enzyme Rubisco to react with O_2 as well as CO_2. As a result of the Rubisco oxygenase reaction, 3-phosphoglycerate and 2-phosphoglycolate are produced in the chloroplast. Chloroplast phosphoglycolate phosphatase converts 2-phosphoglycolate to glycolate (James and Schwartzbach 1982). The compartmentation of the enzymes for glycolate metabolism differs significantly between *Euglena* and higher plants. Glycolate is transported from the chloroplast to the mitochondria in *Euglena* while in higher plants glycolate is transported to the peroxisome. The *Euglena* mitochondrial glycolate dehydrogenase converts glycolate to glyoxylate using NAD^+ as an electron acceptor. The NADH formed by the glycolate dehydrogenase reaction can then donate electrons to the respiratory electron transport chain for ATP synthesis (Collins et al. 1975b; Yokota et al. 1978). This is in contrast to higher plants where the microbody, peroxisomal localized enzyme glycolate oxidase converts glycolate to glyoxylate using O_2 as an electron acceptor forming the toxic compound H_2O_2 which must be detoxified by catalase within the peroxisome.

There are three metabolic fates of glyoxylate produced by photorespiration in *Euglena*. Glyoxylate can be converted to glycine by mitochondrial glutamate:glyoxylate aminotransferase (GGT) and the glycine converted to serine within the mitochondria by serine hydroxymethyl transferase. The serine formed from glycine is further converted first to hydroxypyruvate, then to glycerate, and finally to 3-phosphoglycerate which is used for carbohydrate synthesis (Merrett and Lord 1973). The efficiency of the GGT mediated

reaction is low, and only a quarter to one-third of the glyoxylate formed in mitochondria is converted to glycine (Yokota et al. 1985a).

Increased mitochondrial glyoxylate levels could inhibit the TCA cycle enzymes. The mitochondrial glycolate-glyoxylate cycle consisting of glycolate dehydrogenase and glyoxylate reductase provides a second mechanism to avoid an increase in mitochondrial glyoxylate levels which would be inhibitory to the TCA cycle. Glyoxylate in mitochondria is re-reduced to glycolate by NADPH:glyoxylate reductase (Yokota and Kitaoka 1979; Yokota et al. 1985b). The third metabolic fate of glyoxylate is to return it to the chloroplast where it is oxidatively converted to formate and CO_2 by H_2O_2 produced by the chloroplast Mn^{2+}-dependent NADPH oxidase (Yokota et al. 1983, 1985c). The formate is then used for serine synthesis (Yokota et al. 1985d) and the CO_2 is photosynthetically refixed by Rubisco (Yokota et al. 1985e).

Resent genomic database searches revealed that both mitochondrial glycolate dehydrogenase and peroxisomal glycolate oxidase are present in *Arabidopsis* and *Chlamydomonas* (Bari et al. 2004; Chauvin et al. 2008). Biochemical and functional analysis showed that the mitochondrial glycolate dehydrogenase contributes to photorespiration in *Arabidopsis* (Niessen et al. 2007). In contrast, our EST database search (unpublished data) found that only a glycolate dehydrogenase gene is present in *E. gracilis*.

Acknowledgement The author thanks Dr. Hiroshi Inui and Dr. Akiho Yokota for their critical reading of the manuscript.

References

Bari R, Kebeish R, Kalamajka R, Rademacher T, Peterhhänsel C (2004) A glycolate dehydrogenase in the mitochondria of *Arabidopsis thaliana*. J Exp Bot 55:623–630

Breidenbach RW, Beevers H (1967) Association of the glyoxylate cycle enzymes in a novel subcellular particle from castor bean endosperm. Biochem Biophys Res Commun 27:462–469

Buetow DE (1968) The Biology of Euglena (vol 2). Academic Press, New York

Chang A, Scheer M, Grote A, Schomburg I, Schomburg D (2009) BRENDA, AMENDA and FRENDA the enzyme information system: new content and tools in 2009. Nucleic Acids Res 37:D588–D592

Chauvin LS, Tural B Moroney JV (2008) *Chlamydomonas reinhardtii* has genes for both glycolate oxidase and glycolate dehydrogenase. In: Allen J, Osmond B, Golbeck JK, Gantt E (eds), Photosynthesis: energy from the sun. Proceedings of the 14th International Congress on Photosynthesis. Springer, pp 823–827

Collins N, Merrett MJ (1975a) Microbody-marker enzymes during transition from phototropic to organotropic growth in Euglena. Plant Physiol 55:1018–1022

Collins N, Brown RH, Merrett MJ (1975b) Oxidative phosphorylation during glycollate metabolism in mitochondria from phototrophic Euglena gracilis. Biochem J 150:373–377

Cook JR, Carver M (1966) Partial photo-repression of the glyoxylate by-pass in Euglena. Plant Cell Physiol 7:377–383

Enomoto T, Miyatake K, Kitaoka S (1988) Purification and immunological properties of fructose 2,6-bisphosphate-sensitive pyrophosphate: D-fructose 6-phosphate 1-phosphotransferase from the protist Euglena gracilis. Comp Biochem Physiol Part B Comp Biochem 90:897–902

Graves LB, Trelease RN, Grill A, Becker WM (1972) Localization of glyoxylate cycle enzymes in glyoxysomes in Euglena. J Protozool 19:527–532

Horrum MA, Schwartzbach SD (1981) Nutritional regulation of organelle biogenesis in Euglena. Plant Physiol 68:430–434

Hosotani K, Ohkochi T, Inui H, Yokota A, Nakano Y, Kitaoka S (1988) Photoassimilation of fatty acids, fatty alcohols and sugars by Euglena gracilis Z. J Gen Microbiol 134:61–66

Inui H, Miyatake K, Nakano Y, Kitaoka S (1992) Synthesis of reserved polysaccharide from wax esters accumulated as the result of anaerobic energy generation in Euglena gracilis returned from anaerobic to aerobic conditions. Int J Biochem 24:799–803

James L, Schwartzbach S (1982) Differential regulation of phosphoglycolate and phosphoglycerate phosphatases in Euglena. Plant Sci Lett 27:223–232

Kornberg HL, Krebs HA (1957) Synthesis of cell constituents from C2-units by a modified tricarboxylic acid cycle. Nature 179:988–991

Kunze M, Pracharoenwattana I, Smith SM, Hartig A (2006) A central role for the peroxisomal membrane in glyoxylate cycle function. Biochim Biophys Acta 1763:1441–1452

Liu F, Thatcher JD, Barral JM, Epstein HF (1995) Bifunctional glyoxylate cycle protein of Caenorhabditis elegans: a developmentally regulated protein of intestine and muscle. Dev Biol 169:399–414

McKinley MP, Trelease RN (1978) Coexistence of isocitrate lyase and NADP-isocitrate dehydrogenase in Turbatrix aceti mitochondria. Biochem Biophys Res Commun 81:434–438

Merrett MJ, Lord JM (1973) Glycollate formation and metabolism by algae. New Phytol 72:751–767

Miyatake K, Ito T, Kitaoka S (1984a) Subcellular location and some properties of phosphoenolpyruvate carboxykinase (PEPCK) in Euglena gracilis. Agric Biol Chem 48:2139–2141

Miyatake K, Enomoto T, Kitaoka S (1984b) Detection and subcellular distribution of pyrophosphate:D-fructose 6-phosphate phosphotransferase (PFP) in Euglena gracilis. Agric Biol Chem 48:2857–2859

Munir I, Nakazawa M, Harano K, Yamaji R, Inui H, Miyatake K, Nakano Y (2002) Occurrence of a novel $NADP^+$-linked alcohol dehydrogenase in Euglena gracilis. Comp Biochem Physiol B Biochem Mol Biol 132:535–540

Nakazawa M, Minami T, Teramura K, Kumamoto S, Hanato S, Takenaka S, Ueda M, Inui H, Nakano Y, Miyatake K (2005) Molecular characterization of a bifunctional glyoxylate cycle enzyme, malate synthase/isocitrate lyase, in Euglena gracilis. Comp Biochem Physiol B Biochem Mol Biol 141:445–452

Nakazawa M, Nishimura M, Inoue K, Ueda M, Inui H, Nakano Y, Miyatake K (2011) Characterization of a bifunctional glyoxylate cycle enzyme, malate synthase/isocitrate lyase, of Euglena gracilis. J Eukaryot Microbiol 58:128–133

Niessen M, Thiruveedhi K, Rosenkranz R, Kebeish R, Hirsch HJ, Kreuzaler F, Peterhänsel C (2007) Mitochondrial glycolate oxidation contributes to photorespiration in higher plants. J Exp Bot 58:2709–2715

Ohmann E (1964) Acetataktivierung in grünalgen. I. Oxidation und Aktivierung des Acetats in Euglena gracilis. Biochim Biophys Acta 82:325–335

Ono K, Miyatake K, Inui H, Kitaoka S, Nakano Y (1994) Induction of glyoxylate cycle-key enzymes, malate synthase, and isocitrate lyase in ethanol-grown Euglena gracilis. Biosci Biotechnol Biochem 58:582–583

Ono K, Kawanaka Y, Izumi Y, Inui H, Miyatake K, Kitaoka S, Nakano Y (1995) Mitochondrial alcohol dehydrogenase from ethanol-grown Euglena gracilis. J Biochem 117:1178–1182

Ono K, Kondo M, Osafune T, Miyatake K, Inui H, Kitaoka S, Nishimura M, Nakano Y (2003) Presence of glyoxylate cycle enzymes in the mitochondria of Euglena gracilis. J Eukaryot Microbiol 50:92–96

Peak M, Peak J, Ting I (1972) Isoenzymes of malate dehydrogenase and their regulation in Euglena gracilis Z. Biochim Biophys Acta 284:1–15

Rodríguez-Zavala JS, Ortiz-Cruz MA, Moreno-Sanchez R (2006) Characterization of an aldehyde dehydrogenase from Euglena gracilis. J Eukaryot Microbiol 53:36–42

Rubin H, Trelease RN (1976) Subcellular localization of glyoxylate cycle enzymes in Ascaris suum larvae. J Cell Biol 70:374–383

Wilson B, Danforth W (1958) The extent of acetate and ethanol oxidation by Euglena gracilis. J Gen Microbiol 18:535–542

Woodward J, Merrett MJ (1975) Induction potential for glyoxylate cycle enzymes during the cell cycle of Euglena gracilis. Eur J Biochem 55:555–559

Yokota A, Kitaoka S (1979) Occurrence and operation of the glycollate-glyoxylate shuttle in mitochondria of Euglena gracilis Z. Biochem J 184:189–192

Yokota A, Kitaoka S (1981) Occurrence and subcellular distribution of enzymes involved in the glycolate pathway and their physiological function in a bleached mutant of Euglena gracilis z. Agric Biol Chem 45:15–22

Yokota A, Nakano Y, Kitaoka S (1978) Metabolism of glycolate in mitochondria of Euglena gracilis. Agric Biol Chem 42:121–129

Yokota A, Kawabata A, Kitaoka S (1983) Mechanism of glyoxylate decarboxylation in the glycolate pathway in Euglena gracilis Z. Plant Physiol 71:772–776

Yokota A, Suehiro S, Kitaoka S (1985a) Purification and some properties of mitochondrial glutamate:glyoxylate aminotransferase and mechanism of its involvement in glycolate pathway in Euglena gracilis z. Arch Biochem Biophys 242:507–514

Yokota A, Komura H, Kitaoka S (1985b) Different metabolic fate of two carbons of glycolate in its conversion to serine in Euglena gracilis z. Arch Biochem Biophys 242:498–506

Yokota A, Komura H, Kitaoka S (1985c) Refixation of photorespired CO_2 during photosynthesis in Euglena gracilis z. Agric Biol Chem 49:3309–3310

Yokota A, Haga S, Kitaoka S (1985d) Purification and some properties of glyoxylate reductase ($NADP^+$) and its functional location in mitochondria in Euglena gracilis z. Biochem J 227:211–216

Yokota A, Kitaoka S, Miura K, Wadano A (1985e) Reactivity of glyoxylate with hydrogen perioxide and simulation of the glycolate pathway of C3 plants and Euglena. Planta 165:59–67

Yoval-Sánchez B, Jasso-Chávez R, Lira-Silva E, Moreno-Sánchez R, Rodríguez-Zavala JS (2011) Novel mitochondrial alcohol metabolizing enzymes of Euglena gracilis. J Bioenerg Biomembr 43:519–530

4 Biochemistry and Physiology of Reactive Oxygen Species in *Euglena*

Takahiro Ishikawa, Shun Tamaki, Takanori Maruta, and Shigeru Shigeoka

Abstract

Reactive oxygen species (ROS) such as superoxide and hydrogen peroxide are by-products of various metabolic processes in aerobic organisms including *Euglena*. Chloroplasts and mitochondria are the main sites of ROS generation by photosynthesis and respiration, respectively, through the active electron transport chain. An efficient antioxidant network is required to maintain intracellular ROS pools at optimal conditions for redox homeostasis. A comparison with the networks of plants and animals revealed that *Euglena* has acquired some aspects of ROS metabolic process. *Euglena* lacks catalase and a typical selenocysteine containing animal-type glutathione peroxidase for hydrogen peroxide scavenging, but contains enzymes involved in ascorbate-glutathione cycle solely in the cytosol. Ascorbate peroxidase in *Euglena*, which plays a central role in the ascorbate-glutathione cycle, forms a unique intra-molecular dimer structure that is related to the recognition of peroxides. We recently identified peroxiredoxin and NADPH-dependent thioredoxin reductase isoforms in cellular compartments including chloroplasts and mitochondria, indicating the physiological significance of the thioredoxin system in metabolism of ROS. Besides glutathione, *Euglena* contains the unusual thiol compound trypanothione, an unusual form of glutathione involving two molecules of glutathione joined by a spermidine linker, which has been identified in pathogenic protists such as Trypanosomatida and Schizopyrenida. Furthermore, in contrast to plants, photosynthesis by *Euglena* is not susceptible to hydrogen peroxide because of resistance of the Calvin cycle enzymes fructose-1,6-bisphosphatse, $NADP^+$-glyceraldehyde-3-phosphatase, sedoheptulose-1,7-bisphosphatase, and phosphoribulokinase

T. Ishikawa (✉) • S. Tamaki • T. Maruta
Faculty of Life and Environmental Science, Shimane University, 1060 Nishikawatsu, Matsue, Shimane 690-8504, Japan
e-mail: ishikawa@life.shimane-u.ac.jp

S. Shigeoka
Faculty of Agriculture, Kindai University, 3327-204 Nakamachi, Nara 631-8505, Japan

S.D. Schwartzbach, S. Shigeoka (eds.), *Euglena: Biochemistry, Cell and Molecular Biology*, Advances in Experimental Medicine and Biology 979, DOI 10.1007/978-3-319-54910-1_4

to hydrogen peroxide. Consequently, these characteristics of *Euglena* appear to exemplify a strategy for survival and adaptation to various environmental conditions during the evolutionary process of euglenoids.

Keywords
Ascorbate-glutathione cycle • Ascorbate peroxidase • NADPH-dependent thioredoxin reductase • Peroxiredoxin • Redox • Reactive oxygen species • Trypanothione

Abbreviations

AOX	Alternative oxidase
APX	Ascorbate peroxidase
AsA	L-ascorbic acid
DHA	Dehydroascorbate
DHAR	Dehydroascorbate reductase
FBPase	Fructose-1,6-bisphosphatse
FTR	Ferredoxin-dependent Trx reductase
GAPDH	Glyceraldehyde-3-phosphate dehydrogenase
GPX	Glutathione peroxidase
GR	Glutathione reductase
GSH	Reduced glutathione
GSH1	γ-glutamylcysteine synthetase
GSH2	Glutathione synthetase
GSP	Glutathionylspermidine
GSPS	Glutathionylspermidine synthetase
GSSG	Oxidized glutathione
MDA	Monodehydroascorbate
MDAR	Monodehydroascorbate reductase
NTR	NADPH-dependent Trx reductase
OvoA	5-histidylcysteine sulfoxide synthase
Prx	Peroxiredoxin
PSI	Photosystem I
PSII	Photosystem II
ROS	Reactive oxygen species
RuPK	Ribulose-5-phosphate kinase
SBPase	Sedoheptulose-1,7-bisphosphatase
SOD	Super oxide dismutase
Srx	Sulfiredoxin
$T(SH)_2$	Trypanothione
Trx	Thioredoxin
TRYR	Trypanothione reductase
γ-EC	γ-Glu-Cys

4.1 General Aspects of ROS Metabolism

Oxygen is a double-edged sword for all aerobes; it is an essential molecule for normal cell growth but unavoidably leads to formation of reactive oxygen species (ROS) as a by-product of aerobic metabolic processes including respiration and photosynthesis. The superoxide anion (O_2^-) is produced by the transfer of one electron to molecular O_2. It is subsequently converted to hydrogen peroxide (H_2O_2) and the strongest oxidant, the hydroxyl radical. Singlet oxygen ($^1O_2$) is produced in energy transfer reactions from the excited triplet status of chlorophyll molecules. These ROS molecules induce oxidative damage to every biomolecule such as proteins, DNA, lipids and pigments. On the other hand, increasing evidence supports the indispensable physiological roles of ROS as signaling molecules in stress responses (Mittler et al. 2011; Sies 2014; Shigeoka and Maruta 2014). Thus, aerobic organisms have developed various ROS-metabolic systems from low-molecular-weight chemical compounds to enzymes. Cellular levels of ROS are highly variable due to an imbalance between the production and scavenging capacity of ROS under changeable conditions. In addition, severe stress conditions disrupt the metabolic balance of ROS resulting in oxidative stress. L-Ascorbic acid (AsA) and the tripeptide thiol glutathione (γ-glutamyl-cysteinyl-glycine; GSH) are representative water-soluble antioxidants in *Euglena*. In addition to GSH, *Euglena* also contains the unusual thiol compound trypanothione, an

unusual form of GSH composed of two molecules of GSH joined by a spermidine linker. Trypanothione has only been found in Kinetoplastida such as *Leishmania* and *Trypanosomes*, which are evolutionarily related to *Euglena*. Furthermore, carotenoids and tocopherols play important roles in ROS scavenging as representative hydrophobic antioxidants in photosynthetic organisms including *Euglena*. Peroxidases effectively scavenge H_2O_2 by reducing it to H_2O using electron donors. The function of peroxidases is of importance in *Euglena* because it lacks catalase (Lord and Merrett 1971; Miyake et al. 1991). Electron donors for H_2O_2-scavenging peroxidase have diverged among organisms as follows: animal, GSH; yeast, cytochrome *c*; and protozoa, eukaryotic algae, and plants, AsA. Thioredoxin is a ubiquitous and common electron donor for thioredoxin peroxidase which is also called peroxiredoxin in all aerobes. This chapter discusses the basic aspects of ROS metabolism in *Euglena* together with recent topics on how *Euglena* has developed a number of unique mechanisms to cope with the over-accumulation of toxic levels of ROS.

4.2 Generation, Toxicity, and Function of ROS in *Euglena*

4.2.1 Photosynthesis

The production of ROS is an unavoidable consequence of oxygenic photosynthesis and thus, chloroplasts are a dominant well-established source of ROS generation in photosynthetic organisms. The principal ROS generated in chloroplasts under a light environment are $^1O_2$ by photosystem II (PSII) and O_2^- by photosystem I (PSI). Singlet oxygen is continuously produced by a photosensitization reaction of chlorophylls during photosynthesis. When the redox state of the plastoquinone pool in photosynthetic electron transport is over-reduced by excess light energy, charge separation cannot be completed and oxidized chlorophyll P680, the reaction center of PSII, recombines with reduced pheophytin, which is located upstream of the planstquinone pool. These conditions result in the formation of the triplet state of P680, and excitation energy is then transferred to the ground state triplet O_2 molecules, converting them to the singlet state. There has been no direct experimental evidence to date for $^1O_2$ generation in *Euglena* species however, *Euglena* contains significant amounts of carotenoids and tocopherols, effective quenchers of $^1O_2$, indicating the development of a defense mechanisms against $^1O_2$ generation under severe environmental conditions similar to other photosynthetic organisms (Ruggeri et al. 1985; Shigeoka et al. 1992; Ogbonna 2009; Takaichi 2011; Kato et al. 2016). A previous study reported that the content of α-tocopherol in *E.gracilis* increased 6- to 7-fold under high light and low temperature conditions which promot the production of $^1O_2$ (Ruggeri et al. 1985). Singlet oxygen is now recognized as a signaling molecule that evokes nuclear gene expression in response to high light stress in photosynthetic organisms. EXEXUTER1 and 2 are plastid proteins that function in $^1O_2$-mediated signaling in plants (Kim and Apel 2013). In the case of microalgae, singlet oxygen-mediated signal transduction has been studied in detail in *Chlamydomonas*. The putative bZIP transcription factor SOR1 and phosphoprotein SAK1 have been identified as causal genes for *singlet oxygen resistant 1* (*sor1*) and *singlet oxygen acclimation knocked-out 1* (*sak1*) mutants, respectively and they are involved in signal transduction and activation of $^1O_2$-mediated responses (Fischer et al. 2012; Wakao et al. 2014). A BLASTX search against a database of *Euglena* transcripts constructed by RNA-Seq analysis showed no significant orthologous genes to these known proteins (Yoshida et al. 2016) indicating that *Euglena* may have developed different mechanisms for $^1O_2$-mediated signaling.

The site of generation of O_2^- in chloroplasts is the reducing side of PSI. Among four intrinsic redox proteins in the reaction center of PSI, Fe-S centers X and A/B residues mainly reduce molecular O_2 to O_2^- because of their low redox potential and prompt reactions to the center X from P700 (Asada 1992a). Superoxide radical generated

within PSI reaction center then diffuses to the surface of thylakoid membrane and disproportionates to H_2O_2 and O_2 catalyzed by SOD, which is attached to the membrane periphery. In plants, the production rate of O_2^- under saturated light is approximately 30 μmol mg chlorophyll^{-1} h^{-1} (Asada and Badger 1984), and based on this value, the production rates of O_2^- and H_2O_2 diffusing into stroma have been calculated as approximately 240 μM s^{-1} and 120 μM s^{-1}, respectively, assuming a chloroplast volume of 35 μL mg chlorophyll^{-1} (Asada 1992a). Photosynthesis in higher plants is very sensitive to low concentrations of H_2O_2; photosynthetic CO_2 fixation was previously reported to be inhibited by 50% following the exogenous application of 10 μM H_2O_2 (Kaiser 1979). This is because thiol-modulated enzymes participating in the Calvin cycle, such as fructose-1,6-bisphosphatse (FBPase), glyceralgehyde-3-phosphate dehydrogenase (GAPDH), ribulose-5-phosphate kinase (RuPK), and sedoheptulose-1,7-bisphosphatase (SBPase), are readily oxidized by H_2O_2 through the formation of disulfide bridge, resulting in the critical impairment of photosynthetic activity. Therefore, these enzymes are regarded some of the primary targets of photo-oxidative stress in plants, and photosynthesis may rapidly cease if no ROS scavenging system operates. A previous study reported that the H_2O_2 generation rate from isolated chloroplasts from *Euglena* was calculated to be 5 μmol mg chlorophyll^{-1} h^{-1}, which is similar to that of chloroplasts from higher plants (Ishikawa et al. 1993a). However, unlike higher plants, the corresponding thiol enzymes in the Calvin cycle in algae including *Euglena* exhibit strong resistance to H_2O_2 (Takeda et al. 1995; Ogawa et al. 2015). This finding indicates the existence of selective pressure for acquiring different ROS metabolic systems in chloroplasts between land plants and aquatic algae. Hydrogen peroxide is one of the representative redox signaling molecules because it is permeable cell membrane (Mittler et al. 2011; Shigeoka and Maruta 2014). However, the function of H_2O_2 as a redox signal in *Euglena* remains largely unknown as does its role in $^1O_2$-mediated signaling described above.

4.2.2 Respiration

In mammalian cells, the mitochondrion is the main production site of ROS during respiration. The main production sites of O_2^- are complex III (cytochrome bc_1 complex; ubiquinol:cytochrome *c* oxidoreductase) and complex I (NADH: ubiquinone oxidoreductase) of the respiratory electron transport chain (Murphy 2009; Bleier and Dröse 2013). Although the production of ROS also occurs in photosynthetic organisms, the relative contribution of mitochondria to ROS production in whole cells may be limited by the presence of alternative oxidase (AOX), which is lacked in animals. This enzyme catalyzes the tetravalent reduction of molecular O_2 by ubiquinone and competes with cytochrome bc_1 complex for electrons, thereby suppressing the generation of ROS in mitochondria (Purvis 1997; Vanlerberghe 2013). This may also be the case in *Euglena* because it possesses AOX orthologue of higher plants and some algae, fungi, and protists; however, its physiological function has not yet been analyzed. A previous study reported that isolated *Euglena* mitochondria produced H_2O_2 following the exogenous addition of various respiratory substrates, and the maximum production rate was 9.5 nmol min^{-1} mg protein^{-1} when 5 mM lactate, the most effective substrate, was added (Ishikawa et al. 1993a).

4.2.3 Photorespiration

In higher plants, during photorespiration, the oxygenation reaction of ribulose-1,5-bisphospate carboxylase/oxygenase yields 2-glycolate phosphate, which is then dephosphorylated to glycolate. This compound is translocated from chloroplasts to peroxisomes, which are the sites of H_2O_2 production as a result of the glycolate oxidase reaction. Thus, catalase in plant peroxisomes plays an important role in the maintenance of H_2O_2 levels during photorespiration (Vandenabeele et al. 2004). In contrast, *Euglena* possesses glycolate dehydrogenase in mitochondria instead of glycolate oxidase, and the process of photorespiration differs from that of higher

plants (Yokota et al. 1978). Glyoxylate, the resultant oxidized metabolite by mitochondrial glycolate dehydrogenase, is mainly decarboxylated in chloroplasts by the action of H_2O_2 produced by an Mn^{2+}-dependent NADPH oxidase (Yokota et al. 1983). A recent comprehensive gene expression analysis of *Euglena* (Yoshida et al. 2016) indicated the presence of at least four probable NADPH oxidase genes, which had particular transit signals for *Euglena* plastid localization (Durnford and Gray 2006). Acquiring this photorespiration process may be one of the reasons why *Euglena* genetically lacks catalase.

4.2.4 Environmental Conditions and Oxidative Stress in *Euglena*

Various environmental factors, such as high light, UV, heavy metals, low and high temperature promote the excess production of ROS which causes oxidative stress in photosynthetic organisms. This is also the case in *Euglena*. We herein describe some examples to show the relationship between environmental factors and oxidative stress in *Euglena*.

Exposure to UV-A or UV-B was found to inhibit cell growth and decrease cell viability (Palmer et al. 2002; Kottuparambil et al. 2012). The effects of UV exposure on cell growth and viability were enhanced by a co-treatment with methyl viologen, an O_2^- generator, through coupling with electron transport chains in chloroplasts and mitochondria (Palmer et al. 2002). These oxidative stress conditions induced abnormal cell morphologies in *Euglena*, indicating DNA damage caused by over-accumulation of ROS.

Environmental pollution including heavy metals has been attracting increased attention due to serious concerns regarding toxicity in living organisms. For example, cadmium is a serious environmental contaminant that is highly toxic to living organisms even at low concentrations because it is a non-essential ion. *Euglena* has the ability to accumulate not only Cd^{2+}, but also other heavy metals such as Hg^{2+}, Cu^{2+}, Zn^{2+}, Pb^{2+}, Tc^{7+} and Cr^{6+}, and thus, may contribute to the remediation of waste and polluted water (Rodríguez-Zavala et al. 2007). This hyper-accumulation of heavy metals partially depends on formation of high-molecular-weight complexes with cysteine, GSH, and phytochelatins, as chelating effectors for inactivation of free metal ions. The content of GSH was found to markedly increase 12 fold following exposure to Cd^{2+} and two fold following exposure to Cr^{6+} (Mendoza-Cozatl et al. 2002; Jasso-Chávez et al. 2010). In other words, the accumulation and production of these thiol compounds may be an antioxidative strategy against heavy metal stress in *Euglena*. However, excess amounts of these heavy metals cause severe oxidative damage through the generation of ROS. Watanabe and Suzuki (2002) have previously reported that exposure of cells to a high dose of Cd^{2+} resulted in the marked accumulation of ROS and 2-thiobarbituric acid reactive substances as well as abnormal cell morphologies presumably caused by DNA strand breaks. The primary target of heavy metals is suggested to be the PSII reaction center in chloroplasts and malfunctioning photosynthesis may be a source of increased ROS production (Rocchetta and Küpper 2009). Rocchetta et al. (2012) showed that *Euglena* cells isolated from a polluted river had higher IC50 values for Cr^{6+}, together with a higher GSH content and SOD activity than cells obtained from public culture collection indicating that the up-regulation of antioxidative components is important for acclimation to harsh environments.

4.3 Superoxide Dismutase, Ascorbate Peroxidase and the Ascorbate Redox Cycle

4.3.1 Superoxide Dismutase

Superoxide dismutase catalyzes the disproportionation of O_2^- to H_2O_2 and O_2 in order to eliminate toxic levels of O_2^- generated in cells. Based on the prosthetic metal co-factor, SOD

isoenzymes are generally classified into three members: Fe-SOD, Mn-SOD and Cu/ZnSOD. These SOD isoenzymes are distributed differentially among photosynthetic organisms and are located in different subcellular compartments (Asada et al. 1977; Grace 1990). Most eukaryotic algae lack Cu/Zn-SOD, and possess Fe-SOD and Mn-SOD in the chloroplast stroma and thylakoid membranes respectively. In contrast, most land plants contain Cu/Zn-SOD in the cytosol and chloroplasts and similarly to eukaryotic algae, Fe-SOD and Mn-SOD have also been found in chloroplasts and mitochondria, respectively. In the case of SOD isoforms in *Euglena*, similar to other green algae, Fe-SOD and Mn-SOD have been detected in the soluble fraction including stroma and thylakoid membrane, respectively, while Cu/Zn-SOD is absent (Kanematsu and Asada 1979). A recent transcriptome analysis showed several contigs for Fe-SOD and Mn-SOD, but no contigs for Cu/Zn-SOD clearly supporting the absence of Cu/Zn-SOD in *Euglena* (Table 4.1) (Yoshida et al. 2016). Purified *Euglena* Fe-SOD formed a dimeric structure with a subunit molecular weight of 22,000 and was easily lost its activity by H_2O_2 treatment (Kanematsu and Asada 1979). The half-life of Fe-SOD activity in the presence of 0.5 mM H_2O_2 was 6.5 min. In contrast, thylakoid-membrane-associated Mn-SOD was stable in the presence of H_2O_2. Enzyme activity was not lost for at least 2 h after treatment with 0.5 mM H_2O_2. Thus, it is reasonable to conclude that Mn-SOD functions effectively at the site at which O_2^- is generated during photosynthesis in *Euglena* chloroplasts. It is important to note that the level of SOD activity in *E.gracilis* is significantly affected by growth conditions (Asada et al. 1977). Total SOD activity in *E.gracilis* grown under photoautotrophic conditions was markedly higher than that in cells grown under photoheterotrophic and heterotrophic conditions strongly indicating that active photosynthesis induces the production of ROS in *Euglena* resulting in the adaptive induction of SOD (Asada et al. 1977).

4.3.2 Ascorbate Peroxidase and Ascorbate-Regenerating System

Euglena accumulates millimolar concentrations of AsA and GSH as water-soluble redox compounds (Shigeoka et al. 1979, 1987a; Ishikawa et al. 2008). In addition to their own ROS-scavenging abilities, these compounds constitute an effective H_2O_2 metabolic system by coupling with their redox enzymes. The enzyme ascorbate peroxidase (APX) was initially identified in *E.gracilis*, and given the EC number 1.11.1.11 on the basis of the detailed enzymological properties of this organism (Shigeoka et al. 1980a, b). Thereafter, APX was found to be widely distributed in plants, eukaryotic algae, and protozoa that have acquired the ability to synthesize AsA (Asada 1992b; Shigeoka et al. 2002; Ishikawa and Shigeoka 2008; Wheeler et al. 2015). As shown in Fig. 4.1, APX utilizes AsA as its specific electron donor to reduce H_2O_2 to water with the concomitant generation of monodehydroascorbate (MDA), a univalent oxidant of AsA. MDA is a radical molecule, but has a sufficiently long life allowing its quantitation by electron paramagnetic resonance. MDA is spontaneously disproportionated to AsA and dehydroascorbate (DHA), a divalent oxidant of AsA, and also enzymatically reduced back to AsA by the action of NAD(P)H-dependent MDA reductase (MDAR) (Fig. 4.1). DHA reductase (DHAR) functions to regenerate DHA to AsA by GSH as the electron donor. The resultant oxidized GSH is then regenerated by GSH reductase (GR) through the use of NAD(P)H. This series of metabolic processes are termed the so-called 'AsA-GSH cycle', and APX plays a central role in maintaining optimum H_2O_2 levels in combination with this cycle at all times.

Genome-wide analyses have indicated that plant APXs belong to a multigene family because there are nine genes in *Arabidopsis*, eight in rice and seven in tomato (Chew et al. 2003; Teixeira et al. 2004; Najami et al. 2008). It should be noted that among Arabidopsis isoforms, AtAPX6

Table 4.1 List of genes related to ROS metabolism in *Euglena* cells

	Enzyme	Gene	Length (aa)	Predicted localization	Active site Cys	Subclass	Accession number
AsA-GSH cycle	SOD	comp8199	197	Cyto	–	Fe-SOD	–
		comp8207	207	Cyto	–	Fe-SOD	–
		comp8231	248	Chl	–	Mn-SOD	–
		comp22672	236	Mito	–	Fe-SOD	–
		comp32447	207	Cyto	–	Fe-SOD	–
		comp34078	604	Chl	–	Fe-SOD	–
		comp34216	559	Mito	–	Fe-SOD	–
		comp34603	384	Chl	–	Fe-SOD	–
	APX	EgAPX	649	Cyto	–	–	AB077953
	MDAR	unidentified	–	–	–	–	–
	DHAR	comp32977	602		–	–	–
	GR	comp32835	485	Cyto	CVNVGC	–	–
Thiol peroxidase	Prx	EgPrx1	195	Cyto	C_{48}, C_{169}	2-CysPrx	AB853312
		EgPrx2	330	Chl	C_{184}, C_{305}	2-CysPrx	AB853313
		EgPrx3	269	Mito	C_{120}, C_{241}	2-CysPrx	AB853314
		EgPrx4	188	Cyto	C_{55}, C_{80}	Type II Prx	AB853315
	GPX	comp13015	247	Mito	C_{124}, C_{152}, C_{167}	Plant type	–
		comp16152	173	Cyto	C_{45}, C_{74}	Animal type	–
		comp26099	not FL	unknown	C_X, C_X, C_X	Plant type	–
		comp39029	159	Cyto	C_{36}, C_{64}, C_{79}	Plant type	–
Redoxin family	Trx	comp11711	109	Mito	WCGPC	–	–
		comp12684	105	Cyto	WCGPC	–	–
		comp14773	108	Cyto	WCGPC	–	–
		comp16690	136	Cyto	WCGPC	–	–
		comp20673	155	Mito	WCGPC	–	–
		comp21428	229	Cyto	WCGPC	–	–
		comp22562	234	Cyto	WCGPC	–	–
		comp27028	100	Cyto	WCGPC	–	–
		comp27088	286	Chl	WCGPC	–	–
		comp29308	200	Chl	WCGPC	–	–
		comp34856	228	Cyto	WCGPC	–	–
	Grx	comp12990	164	Mito	CGFS	Monothiol	–
		comp18579	86	Cyto	CGYS	Monothiol	–
		comp29620	261	Chl	CAFS	Monothiol	–
		comp33950	212	Cyto	CGFS	Monothiol	–
		comp18481	180	Mito	CPYC	Dithiol	–
		comp19991	203	Cyto	CPFC	Dithiol	–
		comp22855	156	Cyto	CPYC	Dithiol	–
		comp23337	134	Cyto	CPAC	Dithiol	–
		comp23427	465	Chl	CPYC	Dithiol	–
		comp26916	353	Chl	CPYC	Dithiol	–
		comp28072	307	Chl	CPYC	Dithiol	–
		comp32593	417	Chl	CPYC	Dithiol	–
	Srx	comp24332	293	Chl	GCHR	–	–
	TXN	comp17763	240	Mito	WCPPC	–	–
		comp18063	185	Cyto	WCPPC	–	–
		comp18661	146	Cyto	WCPPC	–	–
		comp20833	165	Cyto	WCPPC	–	–
	NRX	comp23816	463	Nuc	WCPPC, WCGPC	–	–

(continued)

Table 4.1 (continued)

	Enzyme	Gene	Length (aa)	Predicted localization	Active site Cys	Subclass	Accession number
Thiol biosynthesis	GSH1	comp36329	1074	Cyto	–	–	–
	GSH2	comp27362	1093	Cyto	–	–	–
	TRYS	comp28519	640	Cyto	–	–	–
		comp25796	461	Cyto	–	–	–
	OvoA	comp32656	824	Cyto	–	–	–
Thiol recycling	NTR	EgNTR1	319	Mito	CAVC	Small type	AB853316
		EgNTR2	500	Cyto	CVNVGC, CGGGKCG	Large type	AB853317
		EgNTRC	645	Chl	CAIC, CGPC	NTRC type	AB853318
	FTR	comp20454	276	Chl	$(CXC)_3$	–	–
	GR	comp32835	485	Cyto	CVNVGC	–	–
	TRYR	comp31534	501	Cyto	CVNVGC	–	–

The data is based on biological analyses and homology search by BLASTX program for the selected components related to ROS metabolism in E.gracilis. The sequencing data sets are available at the DDBJ Sequence Read Archive (DRA) with accession number SRP060591 and GDJR00000000.1(GenBank), respectively. FL, full-length, Cyto, cytosol; Chl, chloroplast; Mito, mitochondrion. Putative localization is based on the previous findings and results of TMHMM (http://www.cbs.dtu.dk/services/TMHMM/) and TargetP (http://www.cbs.dtu.dk/services/TargetP/). Note that a part of 5′ end of GPX sequence (comp26099) is lack and thus its length, localization, and positions of active site residues are unknown

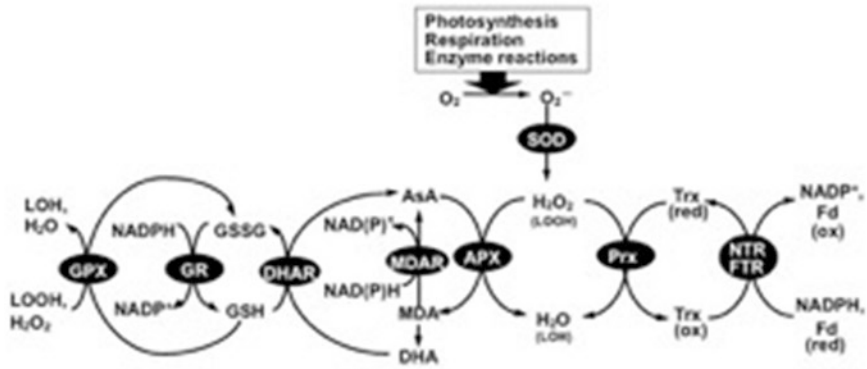

Fig. 4.1 Overview of representative ROS metabolic pathways. Abbreviations are the following; APX; ascorbate peroxidase, AsA; ascorbate, DHA; dehydroascorbate, DHAR; dehydroascorbate reductase, Fd; ferredoxin, FTR; ferredoxin-dependent thioredoxin reductase, GPX; glutathione peroxidase, GR; glutathione reductase, GSH; reduced glutathione, GSSG; oxidized glutathione, LOOH; lipid hydroperoxide, MDA; monodehydroascorbate, MDAR; monodehydroascorbate reductase, NTR; NADPH-dependent thioredoxin reductase, Prx; peroxiredoxin, Trx; thioredoxin

and AtAPX7 are not functional (Maruta et al. 2016). APX isoenzymes have been further classified into four subfamilies according to their subcellular localization in the cytosol, peroxisomes, mitochondria, and the stroma and thylakoid membranes of chloroplasts (Shigeoka et al. 2002; Ishikawa and Shigeoka 2008; Maruta et al. 2016). Thus, plants have evolved the strategy of scavenging H_2O_2 at the sites where it is generated. The primary structure of the membrane-binding types of APX, the peroxisome- and thylakoid membrane-bound forms, is very similar to the primary structure of soluble APX, the cytosolic and stromal forms respectively, but

they also have a C-terminal extension with a hydrophobic anchor region for associating with membranes. The native cytosolic APX is typically a homodimer consisting of a 28 kDa subunit whereas the stromal APX is monomeric with a size of 34 kDa. The catalytic properties of cytosolic APX are similar to those of stromal APX with respect to specificity for H_2O_2 with similar *K*m values (up to 50 μM) and a failure to reduce alkyl hydroperoxides such as *t*-butyl hydroperoxide and cumene hydroperoxide (Shigeoka et al. 2002; Ishikawa and Shigeoka 2008; Mittler and Poulos 2005). In contrast to the APX proteins of higher plants, the number and distribution of *Euglena* APXs (EgAPX) are limited; APX in *E.gracilis* is restricted to the cytosol with no isoform existing in chloroplasts or other organelles (Shigeoka et al. 1980a). Furthermore, the AsA–GSH cycle involving MDAR, DHAR, and GR was exclusively found to reside in the cytosol (Shigeoka et al. 1987b, c). In contrast to known APXs from plants, EgAPX has several unique characteristics. It has a calculated molecular mass of approximately 70 kDa and consists of two catalytic domains entirely homologous with the catalytic domain of plant cytosolic APX. EgAPX is predicted to form a novel intramolecular dimeric protein structure (Ishikawa et al. 1996, 2010). The benefit of this unique structure has not yet been clarified but may affect substrate recognition because the entire enzyme has the ability to catalyze a reaction with alkyl hydroperoxides while the truncated individual domains do not (Ishikawa et al. 2010). The expression of *EgAPX* is post-transcriptionally regulated in response to light, and the induction of *de novo* synthesis of the EgAPX protein is coupled with the development of chloroplasts (Madhusudhan et al. 2003). These findings indicate that a retrograde signal from chloroplasts contributes to the light dependent translation of EgAPX. In terms of this retrograde signal, H_2O_2 may be removed from consideration because APX activity was not induced in dark grown *Euglena* cells treated with H_2O_2 (Madhusudhan et al. 2003). After synthesis of EgAPX, incorporation of heme into the apo-EgAPX protein is an important step for forming the mature active enzyme (Ishikawa et al. 1993b, 2003).

Euglena lacks APX isoenzymes in its chloroplasts raising the significant question of how *Euglena* metabolizes H_2O_2 generated in these organelles. Tamaki et al. (2014) reported that *Euglena* possesses peroxiredoxin (EgPrx2), also called thioredoxin peroxidase, in chloroplasts as well as NADPH-dependent thioredoxin reductase (type NTRC) indicating that a thiol-redox system functions to metabolize ROS in chloroplasts replacing the AsA-GSH cycle (Fig. 4.2). A detailed description of Prx and NTR has been provided in Sect. 4.4. However, *Euglena* cell lines in which EgPrx2 and NTRC gene expression were individually silenced did not show any critical cell damages by oxidative stress under illumination suggesting that the thiol-redox system is not a decisive factor for ROS metabolism in *Euglena* chloroplasts (Tamaki et al. 2014, 2015). As described in Sect. 4.2.1, photosynthesis by *Euglena* is not susceptible to H_2O_2 at concentrations up to 1 mM because the thiol Calvin cycle enzymes such as GAPDH, FBPase, SBPase, and RuPK are resistant to H_2O_2 (Takeda et al. 1995; Ogawa et al. 2015). Aquaporins are probably utilized for transport of H_2O_2 generated in *Euglena* chloroplasts through the chloroplast envelop and cell plasma membrane (Ishikawa et al. 1993a; Mubarakshina et al. 2010). Consequently, the balance between the individual functions among H_2O_2-scavenging, −tolerance, and -diffusion may provide an insight into ROS metabolism in *Euglena* chloroplasts. Roach et al. (2015) recently reported that environmental H_2O_2 concentrations in fresh water algal communities including *Euglena* species increased in the daytime in a light intensity-dependent manner indicating the presence of an active excretion system for H_2O_2 generated in chloroplasts. Increases in environmental H_2O_2 may be used as a signal molecule for algae communication. In support of this view, *Chlamydomonas reinhardtii* exhibits positive phototaxis when treated with exogenous H_2O_2 because of cellular redox changes (Wakabayashi et al. 2011).

4.4 The Thiol Redox System

The thiol redox system is an important ROS metabolic pathway and cellular redox regulator, in addition to the AsA-GSH system described above. In this section, a detailed description including recent advances of the thiol redox system of *Euglena* is presented.

4.4.1 The Thiol Peroxidases

Peroxiredoxins (Prxs) constitute a family of thiol-based peroxidases in all kingdoms of life (Dietz 2003; Rouhier and Jacquot 2005). Prxs have been classified into four types based on their structural and catalytic properties: 1-CysPrx, 2-CysPrx, type II Prx (PrxII), and PrxQ (Wood et al. 2003). Prxs reduce peroxides by dithiol/disulfide exchange reactions of active site Cys residues and are then commonly regenerated by thioredoxin (Trx) for subsequent catalytic cycles (Fig. 4.1). Prxs are physiologically important proteins because of their roles as not only peroxidases, but also molecular chaperones and regulators of various cellular processes.

Four Prx genes (*EgPrx1 ~ 4*) have been identified in *Euglena* based on transcriptome data (Tamaki et al. 2014). EgPrx1 ~ 3 have been classified as 2-CysPrx, and EgPrx4 as PrxII. A phylogenetic analysis showed that EgPrx1 and -3 were close to the clade of trypanosomatids, and EgPrx2 and -4 to the clade of photosynthetic organisms such as *Synechocystis* sp. PCC6803 (Tamaki et al. 2014). The subcellular localization prediction program (TargetP 1.1; http://www.cbs.dtu.dk/services/TargetP/) and the reported properties of plastid-targeting sequences in *Euglena* (Durnford and Gray 2006) suggest that EgPrx1 and -4 are localized in the cytosol, EgPrx2 in chloroplasts, and EgPrx3 in mitochondria (Fig. 4.2). All recombinant *Euglena* Prxs can reduce H_2O_2 and alkyl hydroperoxides indicating their broad substrate specificities (Tamaki et al. 2014). The catalytic efficiencies (k_{cat}/K_m) of *Euglena* Prxs (2.3 ~ 6.6 × 10^4 M^{-1} s^{-1}) for H_2O_2 were previously shown to be similar to those of plant Prx, but were markedly lower than that of *Euglena* APX (1.7 × 10^7 M^{-1} s^{-1}) (Ishikawa et al. 2010). While difficulties are associated with accurately comparing the activity of Prx with that of APX because of electron donor differences, APX may be an efficient peroxidase for cytosolic H_2O_2 metabolism in *Euglena* cells. In contrast to enzymatic properties, the transcript levels of *EgPrx1*, *-2*, and *-3* were approx. 20 ~ 160-fold higher than those of EgAPX suggesting that the lower catalytic efficiencies of EgPrxs relative to EgAPX were compensated for by a greater enzyme abundance (Tamaki et al. 2014). The simultaneous knockdown of EgPrx1 and -4, negatively affected the growth of *Euglena* cells while knockdown of only one of these genes did not suggesting that EgPrxs and EgAPX are also

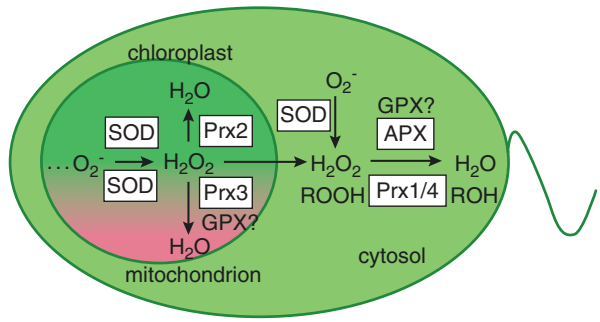

Fig. 4.2 Distribution of ROS metabolic enzymes in *Euglena*. Abbreviations are the same with those in Fig. 4.1. Superoxide radicals generated in chloroplast, mitochondrion, and cytosol are disproportionated O_2^- to H_2O_2 by individual SOD isozymes located in each compartment. The resultant H_2O_2 in chloroplast and mitochondrion is catalyzed by peroxiredoxin isozymes (Prx2 and Prx3), and/or diffused into cytosol. APX and Prx1/4 function as efficient H_2O_2-metabolic enzymes in cytosol

important enzymes for cytosolic ROS metabolism and redox regulation in *Euglena* (Tamaki et al. 2014). In the presence of H_2O_2, the active site Cys of Prx may become overoxidized to sulfinic or sulfonic acid leading to the inactivation of the enzyme and conversion to a molecular chaperone. The sulfinic form of 2-CysPrxs may be regenerated in an ATP-dependent reaction catalyzed by sulfiredoxin (Srx, Sevilla et al. 2015). *Arabidopsis* contains one Srx enzyme dual-targeted to plastids and mitochondria which plays a role in controlling ROS production and scavenging (Iglesias-Baena et al. 2011). It has been suggested that *Euglena* contains a single gene encoding a putative Srx that may be localized in chloroplasts (Table 4.1). This enzyme may contribute to modulate the redox status of chloroplastic EgPrx2.

SeCys-containing glutathione peroxidases (GPXs) are efficient antioxidant enzymes in animal cells. The GPX-like enzymes found in plants have been classified as an additional Prx subclass due to utilization of Trx, but not GSH as an electron donor (Navrot et al. 2006). Animal and plant GPXs are distinguished by conserved active site sequences: SeCys and Cys residues in animal GPXs, and three Cys residues in plant GPXs. On the other hand, *Chlamydomonas* has GPXs with and without SeCys, which use GSH and Trx as electron donors, respectively (Shigeoka et al. 1991; Fischer et al. 2009). Interestingly, GPX isolated from *Euglena* was found to be a cytosol localized SeCys-independent enzyme that uses GSH as an electron donor(Overbaugh and Fall 1985). *Euglena* transcriptome data suggest the existence of four GPX homologous genes (Table 4.1) three of which have three conserved Cys residues similar to plant enzymes. Since the remaining GPX has two conserved Cys residues and is phylogenetically related to the animal enzymes, it may correspond to the previously isolated GPX. (Overbaugh and Fall 1985).

4.4.2 The Thioredoxin Superfamily Proteins

The Trx superfamily proteins, including the Prxs, are critical for redox regulation of protein function in all living organisms. The Trxs are small proteins (~12 kDa) with the catalytic site motif, WCGPC, and they act as redox regulators in numerous cellular processes including DNA synthesis and photosynthesis (Arnér and Holmgren 2000). Eleven Trx homologous genes appear to exist in *Euglena* based on the findings of a recent transcriptome analysis (Table 4.1, Yoshida et al. 2016). These *Euglena* Trxs have the conserved catalytic motif, WCGPC, and are predicted to be localized in the cytosol, chloroplasts, and mitochondria suggesting a role as the reductant for EgPrx1 ~ 4 in each intracellular location. In addition to ROS metabolism, *Euglena* Trxs are also believed to function as redox regulators of enzymes on diverse metabolic pathways such as the cytosolic enzyme, ribonucleotide reductase, RNR, involved in DNA metabolism, the Calvin cycle enzymes, GAPDH, FBPase, SBPase, and RuPK in the chloroplast, and the TCA cycle enzyme, citrate synthase, in mitochondria (Holmgren and Sengupta 2010; Michelet et al. 2013; Schmidtmann et al. 2014). *Euglena* Trxs may also be involved in the redox regulation of flagella movement as reported in *Chlamydomonas* (Wakabayashi 2009).

Trxs use NADPH as the electron donor for reduction in a reaction catalyzed by NADPH-dependent Trx reductase (NTR). NTR is an FAD-binding disulfide oxidoreductase which has the ability to transfer the reducing electrons of NADPH to FAD and then use these electrons to reduce disulfides at the active site Cys residues of oxidized Trx. This two-component redox system formed by Trx and NTR is the so-called 'Trx system' (Schürmann and Jacquot 2000). Based on their structural and catalytic properties, NTRs have been further divided into two major subclasses: a low molecular mass (~35 kDa) form found in diverse organisms including prokaryotes, fungi, plants, and algae, and a high molecular mass (~55 kDa) form found in some eukaryotes including animals and protists (Jacquot et al. 2009). Plants and some algae possess an additional NTR enzyme, called NTRC, which contains a small-type NTR domain at the N-terminus and a Trx domain at the C-terminus (Serrato et al. 2004). Previous studies demonstrated that NTRs play an essential role in various biological processes such as stress tolerance,

development, and metabolism including the biosynthesis of starch and chlorophyll (Cha et al. 2014; Reichheld et al. 2007; Cejudo et al. 2012).

Three NTR enzymes, EgNTR1, -NTR2, and -NTRC have been identified and characterized in *Euglena* (Tamaki et al. 2015). A phylogenetic analysis revealed that EgNTR1, -NTR2, and -NTRC are classified as the small, the large, and the NTRC type respectively. EgNTR2, in particular was closely related to the Cys-type enzymes found in malaria parasites, but not the SeCys-type enzymes found in eukaryotic algae and mammals. EgNTR1, -NTR2, and -NTRC are predicted to be localized in mitochondria, the cytosol, and chloroplasts, respectively, suggesting that a complete Trx-mediated ROS metabolic pathway is found in in each subcellular compartment. A biochemical analysis using recombinant enzymes showed that the catalytic efficiency of EgNTR2 for NADPH (1.22×10^6 M^{-1} s^{-1}) was markedly higher than those of EgNTR1 and -NTRC ($2.65 \sim 3.95 \times 10^4$ M^{-1} s^{-1}, Tamaki et al. 2015). This was attributed to structural and catalytic differences between the large and small types of the NTR family members. The silencing of *EgNTR1* and *EgNTR2* gene expression disturbed cell growth in *Euglena* cells. Moreover, the silencing of *EgNTR2* gene expression impaired cell division (Tamaki et al. 2014). *Euglena* has the class II RNR found in prokaryotes which was activated by *E. coli* Trx as a reductant (Torrents et al. 2006). Thus, it is possible that the phenotype of EgNTR2 knockdown cells may be caused by inhibition of RNR activity.

Chloroplasts contain a ferredoxin-dependent Trx reductase (FTR) which is a heterodimer consisting of one variable and one catalytic subunit with an iron-sulfur cluster. Since reduced ferredoxin is provided by the photosynthetic electron transport chain, the ferredoxin-dependent Trx system plays an important role in the light-dependent redox regulation of chloroplast proteins, while NTRC functions at night when the level of reduced ferredoxin is low (Schürmann and Buchanan 2008). A previous study suggested that *Euglena* possessed a ferredoxin-dependent Trx system due to the identification of a FTR catalytic subunit homolog in the *Euglena* transcriptome (Table 4.1). Unlike the FTR catalytic subunit, the variable subunit has <15% identity within photosynthetic organisms (Jacquot et al. 2009) explaining why the *Euglena* FTR variable subunit gene was not identified by the homology search. Silencing *EgNTRC* gene expression resulted in no obvious phenotypic change in *Euglena* (Tamaki et al. 2015). This may result from the ability of the ferredoxin-dependent Trx system to mimic the functions of NTRC.

Glutaredoxins (Grxs) are ubiquitous Trx superfamily proteins that use GSH as an electron donor. Under oxidative conditions, a number of proteins undergo a post-translational modification termed glutathionylation involving the formation of a mixed disulfide bound between GSH and a protein cysteine residue. In contrast, the reverse reaction, named deglutathionylation, is catalyzed by Grxs (Fernandes and Holmgren 2004). Grxs are divided into two major subgroups based on their active sites: monothiols (CXXS) and dithiols (CXXC). The CC-type Grxs that contain the active site CCXX are specific to plant species (Ziemann et al. 2009). Dithiol-type Grxs exhibit disulfide reductase, DHAR, and protein deglutathionylation activity and are reduced by GSH. Monothiol Grxs catalyze the deglutathionylation of proteins and are reduced by NTR or FTR but not by GSH (Zaffagnini et al. 2008). In yeast, monothiol Grxs regulate the nuclear localization of transcription factors (Pujol-Carrion et al. 2006). Importantly, Grxs play an essential role in iron-sulphur cluster assembly (Rouhier et al. 2010). *Euglena* has been suggested to contain 12 Grx homologous genes, and four isoforms have been classified into monothiols and eight into dithiols (Table 4.1). They were predicted to localize to the cytosol, chloroplasts, and mitochondria, and may be involved in the regulation of protein functions and metabolism in each subcellular compartment (Fig. 4.2). CC-type Grxs are absent in *Euglena* and other eukaryotic algae and trypanosomatids.

The Trx superfamily proteins tryparedoxins (TXNs) are found in trypanosomatids instead of Trx. TXNs have a different active site motif,

WCPPC, and are approximately 5 kDa larger than the Trxs due to several insertions (Hofmann et al. 2001). While TXNs and Trxs have the same core structure, their sequence similarity is restricted to the active site and adjacent regions. Trypanosomatids contain cytoplasmic and mitochondrial TXN isoforms (Castro et al. 2004) and a specific ROS metabolic system consisting of Prx, trypanothione ($T(SH)_2$), and trypanothione reductase (TRYR) (see Sect. 4.4.3 for $T(SH)_2$ and TRYR). Previous studies have demonstrated that TXNs function as electron donors for the Prxs required for ROS metabolism, DNA and protein synthesis through protein-protein interactions, thus making them essential for parasite survival (Piñeyro et al. 2011; Flohé 2012). Four TXN homologous genes have been found in *Euglena*, with three isoforms being predicted to be localized in the cytosol and the other in mitochondria (Table 4.1, Fig. 4.2). Thus, *Euglena* may be an evolutionarily unique organism with respect to co-existence of Trx and TXN enzymes. Since cytosolic EgPrx1 and mitochondrial EgPrx3 were phylogenetically related to the Prxs from *Trypanosoma brucei* and *Leishmania major* (Tamaki et al. 2014), *Euglena* TXNs may function as more efficient electron donors of EgPrx isoforms.

Nucleoredoxin (NRX) is a Trx family protein that is localized in the cytosol and nucleus of most organisms. Its catalytic site motif closely resembles that of TXN. *Arabidopsis* NRX1 is reduced by cytosolic NTR (Marchal et al. 2014). NRX is essential for the redox regulation of development such as ROS-mediated Wnt signaling in mammals and pollen tube growth in plants (Funato and Miki 2010; Marchal et al. 2014). There is no evidence to support a physiological role for NRXs in eukaryotic algae. *Euglena* contains a single NRX homologous gene (Table 4.1), and functional characterization of algal NRXs is required to understand their function.

4.4.3 Low-Molecular-Weight Thiols

Glutathione is an important component of the AsA-GSH cycle, as discussed in Sect. 4.3.2 and it also functions in the direct scavenging of hydroxyl radicals, the direct scavenging of singlet oxygen, in protection of enzyme thiol groups, and in signal transduction (Foyer and Noctor 2005). GSH is synthesized in two steps catalyzed by γ-glutamylcysteine synthetase (GSH1) and glutathione synthetase (GSH2). In the first step, GSH1 ligates Cys with Glu to produce γ-Glu-Cys (γ-EC). In the second step, Gly is ligated to γ-EC by GSH2 to yield GSH (Gill et al. 2013). The content of GSH in *Euglena* grown with illumination was previously shown to be 4-fold higher than in cells grown without illumination. A parallel change in the content of AsA occurs suggesting the importance of the AsA-GSH cycle in scavenging ROS generated by photosynthesis (Shigeoka et al. 1987a). A transcriptomic homology search suggested the presence of GSH1 and GSH2 genes in *Euglena* (Table 4.1). The Pfam program (http://pfam.xfam.org/) found that the proteins encoded by these genes contain additional domains such as a DEAD/DEAH box helicase and a DUF4243 domain. While plants contain GSH1 solely in plastids and GSH2 in both the plastids and the cytosol (Gill et al. 2013), *Euglena* GSH1 and GSH2 appear to be localized in the cytosol (Fig. 4.1) because no plastid targeting signal has been found. The silencing of *GSH2* gene expression in *Euglena* cells markedly inhibited cell growth and decreased the content of GSH suggesting its prominent contribution to the biosynthesis and physiological importance of GSH in *Euglena*.

On the other hand, trypanosomatids use a unique thiol, $T(SH)_2$ (N^1,N^8-bis(glutathionyl) spermidine), as a redox buffer instead of GSH (Müller et al. 2003). $T(SH)_2$ is an essential thiol compound involved in various processes including ROS metabolism, DNA replication, and iron-sulphur cluster assembly as electron donors of TXN and Grx in trypanosomatids (Manta et al. 2013). The biosynthesis of $T(SH)_2$ was originally considered to be catalyzed by two distinct enzymes. Glutathionylspermidine (GSP) synthetase (GSPS) conjugates the first GSH molecule to spermidine, and trypanothione synthetase (TRYS) adds the second GSH molecule to GSP. Some parasites (e.g. in *Crithidia*

fasciculata) possess two distinct enzymes for the biosynthesis of $T(SH)_2$ (Tetaud et al. 1998). However, TRYS by itself was able to catalyze $T(SH)_2$ biosynthesis in some parasites (e.g. in *T. cruzi*) (Oza et al. 2002). O'Neill et al. (O'Neill et al. 2015) clearly demonstrated the existence of $T(SH)_2$ and its 14-Da lower molecular weight compound, nor-$T(SH)_2$ in *Euglena* by an LC-MS analysis. Moreover, two TRYS homologes were identified in the *Euglena* transcriptome (Table 4.1). These findings suggest that *Euglena* can synthesize not only GSH but also $T(SH)_2$. *Euglena* TRYS enzymes were more similar to TRYS (25%) than GSPS (21%) from *C. fasciculata*, but shared greater similarities with bacterial GSPS (31% to *E. coli* GSPS). Further studies are needed determine whether these enzymes exhibit GSPS activity, TRYS activity or both activities.

Ovothiol is a histidine-derived thiol with antioxidant properties that has been identified in trypanosomatids and some marine organisms (Ariyanayagam and Fairlamb 2001). The first ovothiol biosynthetic enzyme, 5-histidylcysteine sulfoxide synthase (OvoA), was identified in *T. cruzi* (Braunshausen and Seebeck 2011). OvoA encodes a non-heme iron dioxygenase at the N-terminus and an *N*-methyl transferase at the C-terminus. A single OvoA homologous gene was identified in the *Euglena* transcriptome (Table 4.1). Moreover, an LC-MS analysis demonstrated that *Euglena* contains an ovothiol molecule (O'Neill et al. 2015).

GSH and $T(SH)_2$ are continuously oxidized to disulfide forms, GSSG and TS_2, respectively, which are recycled to their reduced forms by GR and TRYR, respectively. Reverse genetic approaches using *Arabidopsis* plants demonstrated that GR was involved in development, pathogen responses, and hormone signaling as well as ROS metabolism. A gene encoding GR was identified in *Chlamydomonas* sp. ICE-L (Ding et al. 2012). Its physiological roles in eukaryotic algae are poorly understood. In a previous study, a *Euglena* GR enzyme was isolated and functionally characterized (Shigeoka et al. 1987c). Almost all GR activity was detected in the *Euglena* cytosolic fraction indicating that *Euglena* GR is localized in the cytosol as are other enzymes of the AsA-GSH cycle including APX, DHAR, and MDAR (Shigeoka et al. 1980a, b). The K_m values of *Euglena* GR for NADPH and GSSG were 14 and 50 μM, respectively which are similar to those of other GRs. The sequence of this enzyme was obtained from the *Euglena* transcriptome (Table 4.1). The silencing of *GR* gene expression in *Euglena* induced a marked decrease in total GR activity and the accumulation of GSSG strongly supporting the role of GR in GSH/GSSG redox homeostasis in *Euglena*.

TRYRs have been found in trypanosomatids that lack GR enzyme. TRYR-deficient parasites showed growth retardation, increased sensitivity to oxidative stress and they were avirulent in an animal infection model. Thus, trypanosomatid-specific TRYR enzymes have been characterized in detail as potential drug targets (Flohé 2012). However, *Euglena* was shown to be a unique organism with not only GR, but also TRYRs (Montrichard et al. 1999). The kinetic parameters of TRYR isolated from *Euglena* were similar to those of TRYRs from organisms such as *T. cruzi* and *L. donovani*, and they did not reduce GSSG. A partial peptide sequence of this enzyme was determined and the gene encoding TRYR containing the peptide sequences was identified in the *Euglena* transcriptome (Table 4.1). The predicted subcellular localization of *Euglena* TRYR is the cytosol (Fig. 4.2) corresponding to the reported localization of TRYRs in trypanosomatids (Smith et al. 1991). *Euglena* TRYR was found to be very similar to *Euglena* GR (50%), whereas their substrate specificities differed markedly. This may be explained by most residues involved in interactions with TS_2 being conserved in *Euglena* TRYR, but not GR (Zhang et al. 1996; Jones et al. 2010). Unlike in trypanosomatids, even though Trx system and AsA-GSH cycle are operating in *Euglena*, silencing of the *TRYR* gene results in an obvious inhibition of cell growth, raising the possibility that these redox systems, GSH and $T(SH)_2$, are not redundant but are functionally differentiated.

References

Arnér ES, Holmgren A (2000) Physiological functions of thioredoxin and thioredoxin reductase. Eur J Biochem 267:6102–6109

Ariyanayagam MR, Fairlamb AH (2001) Ovothiol and trypanothione as antioxidants in trypanosomatids. Mol Biochem Parasitol 115:189–198

Asada K, Kanematsu S, Uchida K (1977) Superoxide dismutases in photosynthetic organisms: absence of the cuprozinc enzyme in eukaryotic algae. Arch Biochem Biophys 179:243–256

Asada K, Badger MR (1984) Photoreduction of $^{18}O_2$ and $H_2{}^{18}O_2$ with concomitant evolution of $^{16}O_2$ in intact spinach chloroplasts: evidence for scavenging of hydrogen peroxide by peroxidase. Plant Cell Physiol 25:1169–1179

Asada K (1992a) Production and scavenging of active oxygen species in chloroplasts. In: Scandalios JG (ed) Molecular Biology of Free Radical Scavenging Systems: Current Communications in Cell and Molecular Biology, vol 5. CSHL Press, New York, pp 173–192

Asada K (1992b) Ascorbate peroxidase – a hydrogen peroxide-scavenging enzyme in plants. Physiol Plant 85:235–241

Bleier L, Dröse S (2013) Superoxide generation by complex III: From mechanistic rationales to functional consequences. Biochim Biophys Act 1827:1320–1331

Braunshausen A, Seebeck FP (2011) Identification and characterization of the first ovothiol biosynthetic enzyme. J Am Chem Soc 133:1757–1759

Castro H, Sousa C, Novais M, Santos M, Budde H, Cordeiro-da-Silva A, Flohé L, Tomás AM (2004) Two linked genes of *Leishmania infantum* encode tryparedoxins localised to cytosol and mitochondrion. Mol Biochem Parasitol 136:137–147

Cejudo FJ, Ferrández J, Cano B, Puerto-Galán L, Guinea M (2012) The function of the NADPH thioredoxin reductase C-2-Cys peroxiredoxin system in plastid redox regulation and signaling. FEBS Lett 586:2974–2980

Cha JY, Kim JY, Jung IJ, Kim MR, Melencion A, Alam SS, Yun DJ, Lee SY, Kim MG, Kim WY (2014) NADPH-dependent thioredoxin reductase A (NTRA) confers elevated tolerance to oxidative stress and drought. Plant Physiol Biochem 80:184–191

Chew O, Whelan J, Millar AH (2003) Molecular definition of the ascorbate-glutathione cycle in Arabidopsis mitochondria reveals dual targeting of antioxidant defenses in plants. J Biol Chem 278:46869–46877

Dietz KJ (2003) Plant peroxiredoxins. Annu Rev Plant Biol 54:93–107

Ding Y, Liu Y, Jian JC, Wu ZH, Miao JL (2012) Molecular cloning and expression analysis of glutathione reductase gene in *Chlamydomonas* sp. ICE-L from Antarctica. Mar Genomics 5:59–64

Durnford DG, Gray MW (2006) Analysis of *Euglena gracilis* plastid-targeted proteins reveals different classes of transit sequences. Eukaryot Cell 5:2079–2091

Fernandes AP, Holmgren A (2004) Glutaredoxins: glutathione-dependent redox enzymes with functions far beyond a simple thioredoxin backup system. Antioxid Redox Signal 6:63–74

Fischer BB, Dayer R, Schwarzenbach Y, Lemaire SD, Behra R, Liedtke A, Eggen RI (2009) Function and regulation of the glutathione peroxidase homologous gene GPXH/GPX5 in *Chlamydomonas reinhardtii*. Plant Mol Biol 71:569–583

Fischer BB, Ledford HK, Wakao S, Huang SG, Casero D, Pellegrini M, Merchant SS, Koller A, Eggen RI, Niyogi KK (2012) SINGLET OXYGEN RESISTANT 1 links reactive electrophile signaling to singlet oxygen acclimation in *Chlamydomonas reinhardtii*. Proc Natl Acad Sci U S A 109:E1302–E1311

Flohé L (2012) The trypanothione system and the opportunities it offers to create drugs for the neglected kinetoplast diseases. Biotechnol Adv 30:294–301

Foyer CH, Noctor G (2005) Redox homeostasis and antioxidant signaling: a metabolic interface between stress perception and physiological responses. Plant Cell 17:1866–1875

Funato Y, Miki H (2010) Redox regulation of Wnt signalling via nucleoredoxin. Free Radic Res 44:379–388

Gill SS, Anjum NA, Hasanuzzaman M, Gill R, Trivedi DK, Ahmad I, Pereira E, Tuteja N (2013) Glutathione and glutathione reductase: a boon in disguise for plant abiotic stress defense operations. Plant Physiol Biochem 70:204–212

Grace SC (1990) Phylogenetic distribution of superoxide dismutase supports an endosymbiotic origin for chloroplasts and mitochondria. Life Sci 47:1875–1886

Hofmann B, Budde H, Bruns K, Guerrero SA, Kalisz HM, Menge U, Montemartini M, Nogoceke E, Steinert P, Wissing JB, Flohé L, Hecht HJ (2001) Structures of tryparedoxins revealing interaction with trypanothione. Biol Chem 382:459–471

Holmgren A, Sengupta R (2010) The use of thiols by ribonucleotide reductase. Free Radic Biol Med 49:1617–1628

Iglesias-Baena I, Barranco-Medina S, Sevilla F, Lázaro JJ (2011) The dual-targeted plant sulfiredoxin retroreduces the sulfinic form of atypical mitochondrial peroxiredoxin. Plant Physiol 155:944–955

Ishikawa T, Takeda T, Shigeoka S, Hirayama O, Mitsunaga T (1993a) Hydrogen peroxide generation in organelles of *Euglena gracilis*. Phytochemistry 33:1297–1299

Ishikawa T, Takeda T, Shigeoka S, Hirayama O, Mitsunaga T (1993b) Requirement for iron and its effect on ascorbate peroxidase in *Euglena gracilis*. Plant Sci 93:25–29

Ishikawa T, Takeda T, Kohno H, Shigeoka S (1996) Molecular characterization of *Euglena* ascorbate peroxidase using monoclonal antibody. Biochim Biophys Acta 1290:69–75

Ishikawa T, Madhusudhan R, Shigeoka S (2003) Effect of iron on the expression of ascorbate peroxidase in *Euglena gracilis*. Plant Sci 165:1363–1376

Ishikawa T, Shigeoka S (2008) Recent advances in ascorbate biosynthesis and the physiological significance of ascorbate peroxidase in photosynthesizing organisms. Biosci Biotechnol Biochem 72:1143–1154

Ishikawa T, Nishikawa H, Gao Y, Sawa Y, Shibata H, Yabuta Y, Maruta T, Shigeoka S (2008) The pathway *via* D-galacturonate/L-galactonate is significant for ascorbate biosynthesis in *Euglena gracilis*: identification and functional characterization of aldonolactonase. J Biol Chem 283:31133–31141

Ishikawa T, Tajima N, Nishikawa H, Gao Y, Rapolu M, Shibata H, Sawa Y, Shigeoka S (2010) *Euglena gracilis* ascorbate peroxidase forms an intramolecular dimeric structure: its unique molecular characterization. Biochem J 426:125–134

Jacquot JP, Eklund H, Rouhier N, Schürmann P (2009) Structural and evolutionary aspects of thioredoxin reductases in photosynthetic organisms. Trends Plant Sci 14:336–343

Jasso-Chávez R, Pacheco-Rosales A, Lira-Silva E, Gallardo-Pérez JC, García N, Moreno-Sánchez R (2010) Toxic effects of Cr(VI) and Cr(III) on energy metabolism of heterotrophic *Euglena gracilis*. Aquat Toxicol 100:329–338

Jones DC, Ariza A, Chow WH, Oza SL, Fairlamb AH (2010) Comparative structural, kinetic and inhibitor studies of *Trypanosoma brucei* trypanothione reductase with *T. cruzi*. Mol Biochem Parasitol 169:12–19

Kaiser WM (1979) Reversible inhibition of the Calvin cycle and activation of the oxidative pentose phosphate cycle in isolated intact chloroplasts by hydrogen peroxide. Planta 145:377–382

Kanematsu S, Asada K (1979) Ferric and manganic superoxide dismutases in *Euglena gracilis*. Arch Biochem Biophys 195:535–545

Kato S, Takaichi S, Ishikawa T, Asahina M, Takahashi S, Shinomura T (2016) Identification and functional analysis of the geranylgeranyl pyrophosphate synthase gene (*crtE*) and phytoene synthase gene (*crtB*) for carotenoid biosynthesis in *Euglena gracilis*. BMC Plant Biol 16:4

Kim C, Apel K (2013) Singlet oxygen-mediated signaling in plants: moving from flu to wild type reveals an increasing complexity. Photosynth Res 116:455–464

Kottuparambil S, Shin W, Brown MT, Han T (2012) UV-B affects photosynthesis, ROS production and motility of the freshwater flagellate, *Euglena agilis* Carter. Aquat Toxicol 122-123:206–213

Lord JM, Merrett MJ (1971) The intracellular localization of glycollate oxidoreductase in *Euglena gracilis*. Biochem J 124:275–281

Madhusudhan R, Ishikawa T, Sawa Y, Shigeoka S, Shibata H (2003) Post-transcriptional regulation of ascorbate peroxidase during light adaptation of *Euglena gracilis*. Plant Sci 165:233–238

Manta B, Comini M, Medeiros A, Hugo M, Trujillo M, Radi R (2013) Trypanothione: a unique bis-glutathionyl derivative in trypanosomatids. Biochim Biophys Acta 1830:3199–3216

Marchal C, Delorme-Hinoux V, Bariat L, Siala W, Belin C, Saez-Vasquez J, Riondet C, Reichheld JP (2014) NTR/NRX define a new thioredoxin system in the nucleus of *Arabidopsis thaliana* cells. Mol Plant 7:30–44

Maruta T, Sawa Y, Shigeoka S, Ishikawa T (2016) Diversity and evolution of ascorbate peroxidase functions in chloroplasts: more than just a classical antioxidant enzyme? Plant Cell Physiol 57:1377–1386

Mendoza-Cozatl D, Devars S, Loza-Tavera H, Moreno-Sánchez R (2002) Cadmium accumulation in the chloroplast of *Euglena gracilis*. Physiol Plant 115:276–283

Michelet L, Zaffagnini M, Morisse S, Sparla F, Pérez-Pérez ME, Francia F, Danon A, Marchand CH, Fermani S, Trost P, Lemaire SD (2013) Redox regulation of the Calvin-Benson cycle: something old, something new. Front Plant Sci 4:470

Mittler R, Poulos TL (2005) Ascorbate peroxidase. In: Smirnoff N (ed) Antioxidants and Reactive Oxygen Species in Plants. Blackwell, Oxford, pp 87–100

Mittler R, Vanderauwera S, Suzuki N, Miller G, Tognetti VB, Vandepoele K et al (2011) ROS signaling: the new wave? Trends Plant Sci 16:300–309

Miyake C, Michihata F, Asada K (1991) Scavenging of hydrogen peroxide in prokaryotic and eukaryotic algae: acquisition of ascorbate peroxidase during the evolution of Cyanobacteria. Plant Cell Physiol 32:33–43

Montrichard F, Le Guen F, Laval-Martin DL, Davioud-Charvet E (1999) Evidence for the co-existence of glutathione reductase and trypanothione reductase in the non-trypanosomatid Euglenozoa: *Euglena gracilis* Z. FEBS Lett 442:29–33

Mubarakshina MM, Ivanov BN, Naydov IA, Hillier W, Badger MR, Krieger-Liszkay A (2010) Production and diffusion of chloroplastic H_2O_2 and its implication to signalling. J Exp Bot 61:3577–3587

Müller S, Liebau E, Walter RD, Krauth-Siegel RL (2003) Thiol-based redox metabolism of protozoan parasites. Trends Parasitol 19:320–328

Murphy MP (2009) How mitochondria produce reactive oxygen species. Biochem J 417:1–13

Najami N, Janda T, Barriah W, Kayam G, Tal M, Guy M, Volokita M (2008) Ascorbate peroxidase gene family in tomato: its identification and characterization. Mol Gen Genomics 279:171–182

Navrot N, Collin V, Gualberto J, Gelhaye E, Hirasawa M, Rey P, Knaff DB, Issakidis E, Jacquot JP, Rouhier N (2006) Plant glutathione peroxidases are functional peroxiredoxins distributed in several subcellular compartments and regulated during biotic and abiotic stresses. Plant Physiol 142:1364–1379

Ogawa T, Kimura A, Sakuyama H, Tamoi M, Ishikawa T, Shigeoka S (2015) Characterization and physiological role of two types of chloroplastic fructose-1,6-bisphosphatases in *Euglena gracilis*. Arch Biochem Biophys 575:61–68

Ogbonna JC (2009) Microbiological production of tocopherols: current state and prospects. Appl Microbiol Biotechnol 84:217–225

O'Neill EC, Trick M, Hill L, Rejzek M, Dusi RG, Hamilton CJ, Zimba PV, Henrissat B, Field RA (2015) The transcriptome of *Euglena gracilis* reveals unexpected metabolic capabilities for carbohydrate and natural product biochemistry. Mol BioSyst 11:2808–2820

Overbaugh JM, Fall R (1985) Characterization of a selenium-independent glutathione peroxidase from *Euglena gracilis*. Plant Physiol 77:437–442

Oza SL, Tetaud E, Ariyanayagam MR, Warnon SS, Fairlamb AH (2002) A single enzyme catalyses formation of Trypanothione from glutathione and spermidine in *Trypanosoma cruzi*. J Biol Chem 277:35853–35861

Palmer H, Ohta M, Watanabe M, Suzuki T (2002) Oxidative stress-induced cellular damage caused by UV and methyl viologen in *Euglena gracilis* and its suppression with rutin. J Photochem Photobiol B 67:116–129

Piñeyro MD, Parodi-Talice A, Portela M, Arias DG, Guerrero SA, Robello C (2011) Molecular characterization and interactome analysis of *Trypanosoma cruzi* tryparedoxin 1. J Proteome 74:1683–16892

Pujol-Carrion N, Belli G, Herrero E, Nogues A, de la Torre-Ruiz MA (2006) Glutaredoxins Grx3 and Grx4 regulate nuclear localisation of Aft1 and the oxidative stress response in *Saccharomyces cerevisiae*. J Cell Sci 119:4554–4564

Purvis AC (1997) Role of the alternative oxidase in limiting superoxide production by plant mitochondria. Physiol Plant 100:165–170

Reichheld JP, Khafif M, Riondet C, Droux M, Bonnard G, Meyer Y (2007) Inactivation of thioredoxin reductases reveals a complex interplay between thioredoxin and glutathione pathways in *Arabidopsis* development. Plant Cell 19:1851–1865

Roach T, Miller R, Aigner S, Kranner I (2015) Diurnal changes in the xanthophyll cycle pigments of freshwater algae correlate with the environmental hydrogen peroxide concentration rather than non-photochemical quenching. Ann Bot 116:519–527

Rocchetta I, Küpper H (2009) Chromium- and copper-induced inhibition of photosynthesis in *Euglena gracilis* analysed on the single-cell level by fluorescence kinetic microscopy. New Phytol 182:405–420

Rocchetta I, Mazzuca M, Conforti V, Balzaretti V, del Carmen Ríos de Molina M. (2012) Chromium induced stress conditions in heterotrophic and auxotrophic strains of *Euglena gracilis*. Ecotoxicol Environ Saf 84: 147–154

Rodríguez-Zavala JS, García-García JD, Ortiz-Cruz MA, Moreno-Sánchez R (2007) Molecular mechanisms of resistance to heavy metals in the protist *Euglena gracilis*. J Environ Sci Health A Tox Hazard Subst Environ Eng 42:1365–1378

Rouhier N, Jacquot JP (2005) The plant multigenic family of thiol peroxidases. Free Radic Biol Med 38:1413–1421

Rouhier N, Couturier J, Johnson MK, Jacquot JP (2010) Glutaredoxins: roles in iron homeostasis. Trends Biochem Sci 35:43–52

Ruggeri BA, Gray RJ, Watkins TR, Tomlins RI (1985) Effects of low-temperature acclimation and oxygen stress on tocopheron production in *Euglena gracilis* Z. Appl Environ Microbiol 50:1404–1408

Schürmann P, Jacquot JP (2000) Plant thioredoxin systems revisited. Annu Rev Plant Physiol Plant Mol Biol 51:371–400

Schürmann P, Buchanan BB (2008) The ferredoxin/thioredoxin system of oxygenic photosynthesis. Antioxid Redox Signal 10:1235–1274

Schmidtmann E, König AC, Orwat A, Leister D, Hartl M, Finkemeier I (2014) Redox regulation of Arabidopsis mitochondrial citrate synthase. Mol Plant 7:156–169

Serrato AJ, Pérez-Ruiz JM, Spínola MC, Cejudo FJ (2004) A novel NADPH thioredoxin reductase, localized in the chloroplast, which deficiency causes hypersensitivity to abiotic stress in *Arabidopsis thaliana*. J Biol Chem 279:43821–43827

Sevilla F, Camejo D, Ortiz-Espín A, Calderón A, Lázaro JJ, Jiménez A (2015) The thioredoxin/peroxiredoxin/sulfiredoxin system: current overview on its redox function in plants and regulation by reactive oxygen and nitrogen species. J Exp Bot 66:2945–2955

Shigeoka S, Yokota A, Nakano Y, Kitaoka S (1979) The effect of illumination on the L-ascorbic acid content in *Euglena gracilis* Z. Agric Biol Chem 43:2053–2058

Shigeoka S, Nakano Y, Kitaoka S (1980a) Purification and some properties of L-ascorbic-acid-specific peroxidase in *Euglena gracilis* Z. Arch Biochem Biophys 201:121–127

Shigeoka S, Nakano Y, Kitaoka S (1980b) Metabolism of hydrogen peroxide in *Euglena gracilis* Z by L-ascorbic acid peroxidase. Biochem J 186:377–380

Shigeoka S, Onishi T, Nakano Y, Kitaoka S (1987a) Photoinduced biosynthesis of glutathione in *Euglena gracilis*. Agric Biol Chem 51:2257–2258

Shigeoka S, Yasumoto R, Onishi T, Nakano Y, Kitaoka S (1987b) Properties of monodehydroascirbate reductase and dehydroascorbate reductase and their participation in the regeneration of ascorbate in *Euglena gracilis*. J Gen Microbiol 133:227–232

Shigeoka S, Onishi T, Nakano Y, Kitaoka S (1987c) Characterization and physiological function of glutathione reductase in *Euglena gracilis* Z. Biochem J 242:511–515

Shigeoka S, Takeda T, Hanaoka T (1991) Characterization and immunological properties of selenium-containing glutathione peroxidase induced by selenite in *Chlamydomonas reinhardtii*. Biochem J 275:623–627

Shigeoka S, Ishiko H, Nakano Y, Mitsunaga T (1992) Isolation and properties of gamma-tocopherol methyltransferase in *Euglena gracilis*. Biochim Biophys Acta 1128:220–226

Shigeoka S, Ishikawa T, Tamoi M, Miyagawa Y, Takeda T, Yabuta Y, Yoshimura K (2002) Regulation and function of ascorbate peroxidase isoenzymes. J Exp Bot 53:1305–1319

Shigeoka S, Maruta T (2014) Cellular redox regulation, signaling, and stress response in plants. Biosci Biotechnol Biochem 78:1457–1470

Sies H (2014) Role of metabolic H_2O_2 generation: redox signaling and oxidative stress. J Biol Chem 289:8735–8741

Smith K, Opperdoes FR, Fairlamb AH (1991) Subcellular distribution of trypanothione reductase in bloodstream and procyclic forms of *Trypanosoma brucei*. Mol Biochem Parasitol 48:109–112

Takaichi S (2011) Carotenoids in algae: distributions, biosyntheses and functions. Mar Drugs 9:1101–1118

Takeda T, Yokota A, Shigeoka S (1995) Resistance of photosynthesis to hydrogen peroxide in algae. Plant Cell Physiol 36:1089–1095

Tamaki S, Maruta T, Sawa Y, Shigeoka S, Ishikawa T (2014) Identification and functional analysis of peroxiredoxin isoforms in *Euglena gracilis*. Biosci Biotechnol Biochem 78:593–601

Tamaki S, Maruta T, Sawa Y, Shigeoka S, Ishikawa T (2015) Biochemical and physiological analyses of NADPH-dependent thioredoxin reductase isozymes in *Euglena gracilis*. Plant Sci 236:29–36

Teixeira FK, Menezes-Benavente L, Margis R, Margis-Pinheiro M (2004) Analysis of the molecular evolutionary history of the ascorbate peroxidase gene family: inferences from the rice genome. J Mol Evol 59:761–770

Tetaud E, Manai F, Barrett MP, Nadeau K, Walsh CT, Fairlamb AH (1998) Cloning and characterization of the two enzymes responsible for trypanothione biosynthesis in *Crithidia fasciculata*. J Biol Chem 273:19383–19390

Torrents E, Trevisiol C, Rotte C, Hellman U, Martin W, Reichard P (2006) *Euglena gracilis* ribonucleotide reductase: the eukaryote class II enzyme and the possible antiquity of eukaryote B12 dependence. J Biol Chem 281:5604–5611

Vandenabeele S, Vanderauwera S, Vuylsteke M, Rombauts S, Langebartels C, Seidlitz HK, Zabeau M, Van Montagu M, Inzé D, Van Breusegem F (2004) Catalase deficiency drastically affects gene expression induced by high light in *Arabidopsis thaliana*. Plant J 39:45–58

Vanlerberghe GC (2013) Alternative oxidase: a mitochondrial respiratory pathway to maintain metabolic and signaling homeostasis during abiotic and biotic stress in plants. Int J Mol Sci 14:6805–6847

Wakabayashi K (2009) Analysis of redox-sensitive dynein components. Methods Cell Biol 92:153–161

Wakabayashi K, Misawa Y, Mochiji S, Kamiya R (2011) Reduction-oxidation poise regulates the sign of phototaxis in *Chlamydomonas reinhardtii*. Proc Natl Acad Sci U S A 108:11280–11284

Wakao S, Chin BL, Ledford HK, Dent RM, Casero D, Pellegrini M, Merchant SS, Niyogi KK (2014) Phosphoprotein SAK1 is a regulator of acclimation to singlet oxygen in *Chlamydomonas reinhardtii*. elife 3:e02286

Watanabe M, Suzuki T (2002) Involvement of reactive oxygen stress in cadmium-induced cellular damage in *Euglena gracilis*. Comp Biochem Physiol C Toxicol Pharmacol 131:491–500

Wheeler G, Ishikawa T, Pornsaksit V, Smirnoff N (2015) Evolution of alternative biosynthetic pathways for vitamin C following plastid acquisition in photosynthetic eukaryotes. elife 4:e06369

Wood ZA, Schröder E, Robin Harris J, Poole LB (2003) Structure, mechanism and regulation of peroxiredoxins. Trends Biochem Sci 28:32–40

Yokota Y, Nakano Y, Kitaoka S (1978) Metabolism of glycolate in mitochondria of *Euglena gracilis*. Agric Biol Chem 42:121–129

Yokota A, Kawabata A, Kitaoka S (1983) Mechanism of glyoxylate decarboxylation in the glycolate pathway in *Euglena gracilis* Z: participation of Mn^{2+}-dependent NADPH oxidase in chloroplasts. Plant Physiol 71:772–776

Yoshida Y, Tomiyama T, Maruta T, Tomita M, Ishikawa T, Arakawa K (2016) *De novo* assembly and comparative transcriptome analysis of *Euglena gracilis* in response to anaerobic conditions. BMC Genomics 17:182

Zaffagnini M, Michelet L, Massot V, Trost P, Lemaire SD (2008) Biochemical characterization of glutaredoxins from *Chlamydomonas reinhardtii* reveals the unique properties of a chloroplastic CGFS-type glutaredoxin. J Biol Chem 283:8868–8876

Zhang Y, Bond CS, Bailey S, Cunningham ML, Fairlamb AH, Hunter WN (1996) The crystal structure of trypanothione reductase from the human pathogen *Trypanosoma cruzi* at 2.3 Å resolution. Protein Sci 5:52–61

Ziemann M, Bhave M, Zachgo S (2009) Origin and diversification of land plant CC-type glutaredoxins. Genome Biol Evol 1:265–277

Biochemistry and Physiology of Vitamins in *Euglena*

5

Fumio Watanabe, Kazuya Yoshimura, and Shigeru Shigeoka

Abstract

Euglena gracilis Z requires vitamins B1 and B12 for growth. It takes up and accumulates large amounts of these exogenous vitamins through energy-dependent active transport systems. Except for these essential vitamins, *E. gracilis* Z has the ability to synthesize all human vitamins. *Euglena* synthesizes high levels of antioxidant vitamins such as vitamins C and E, and, thus, are used as nutritional supplements for humans and domestic animals. Methods to effectively produce vitamins in *Euglena* have been investigated.

Previous biochemical studies indicated that *E. gracilis* Z contains several vitamin-related novel synthetic enzymes and metabolic pathways which suggests that it is a highly suitable organism for elucidating the physiological functions of vitamins in comparative biochemistry and biological evolution. *E. gracilis* Z has an unusual biosynthetic pathway for vitamin C, a hybrid of the pathways found in animals and plants. This chapter presents up-to-date information on the biochemistry and physiological functions of vitamins in this organism.

Keywords

Biosynthetic pathway • Essential nutrients • *Euglena gracilis* Z • Fat-soluble vitamins • Nutritional supplements • Water-soluble vitamins

F. Watanabe (✉)
Faculty of Agriculture, School of Agricultural, Biological and Environmental Sciences, Tottori University, Tottori 680-8553, Japan
e-mail: watanabe@muses.tottori-u.ac.jp

K. Yoshimura
Department of Food and Nutritional Sciences, College of Bioscience and Biotechnology, Chubu University, Kasugai, Aichi 487-8501, Japan

S. Shigeoka
Faculty of Agriculture, Kindai University,
3327-204 Nakamachi, Nara 631-8505, Japan

S.D. Schwartzbach, S. Shigeoka (eds.), *Euglena: Biochemistry, Cell and Molecular Biology*,
Advances in Experimental Medicine and Biology 979, DOI 10.1007/978-3-319-54910-1_5

Abbreviations

ACP	Acyl-carrier protein
AdoB12	Adenosylcobalamin
ALase	Aldonolactonase
AsA	L-ascorbic acid
B12	Vitamin B12
cADPR	Cyclic ADP-ribose
cAMP	Cyclic AMP
CN-B12	Cyanocobalamin
CoA	co-enzyme A
DAsA	Dehydroascorbate
D-GalUA	D-galacturonate
D-GlcUA	D-glucuronate
D-Man	D-mannose
DXP	1-deoxy-D-xylulose-5-phosphate
IF	Intrinsic factor
L-Gal	L-galactose
L-GalA	L-galactonate
L-GalL	L-galactono-1,4-lactone
L-GulA	L-gulonate
L-GulL	L-gulono-1,4-lactone
MCM	Methylmalonyl-CoA mutase
MDAsA	Monodehydroascorbate
MeB12	Methylcobalamin
MetH	Methionine synthase
MMAA	Methylmalonic aciduria type A protein
MVA	Mevalonate
NAADP	Nicotinic acid adenine dinucleotide phosphate
NADK	NAD^+ kinase
OH-B12	Hydroxocobalamin
PABA	*p*-aminobenzoate
PL	Pyridoxal
PLP	Pyridoxal-5′-phosphate
PM	Pyridoxamine
PMP	Pyridoxamine-5′-phospahte
PN	Pyridoxine
PNP	Pyridoxine-5′-phoshate
RNR	Ribonucleotide reductase
SHMT	Serine hydroxymethyltransferase
TC	Transcobalamin II
TDP	Thiamine diphosphate
TMP	Thiamine monophosphate
TTP	Thiamine triphosphate

5.1 Introduction

Humans require essential and trace nutriments, vitamins, which consist of 13 organic compounds. Vitamins have been classified into two groups: water-soluble vitamins, B1, B2, B6, B12, C, niacin, pantothenic acid, folic acid, and biotin, and fat-soluble vitamins, A, D, E, and K. Microalgae are diverse photosynthetic eukaryotes in which vitamin auxotrophy is prevalent with 22% of surveyed species requiring vitamin B1, approximately 5% requiring biotin, and more than 50% requiring vitamin B12 (Croft et al. 2006). Cook (1968) reported that *E. gracilis* Z requires vitamin B1 and vitamin B12 for growth. Vitamin B12 is universally required among *Euglena* species, whereas vitamin B1 is not (Leedale et al. 1965). Except for these essential vitamins, *E. gracilis* Z has the ability to synthesize all of the vitamins described above. Furthermore, *Euglena* synthesizes high levels of antioxidant vitamins and related compounds (Takeyama et al. 1997), the levels of which are significantly affected during growth and/or by growth conditions. Methods to effectively produce vitamins and optimum biomass yield in *Euglena* have been investigated because these cells are used as nutritional supplements for humans and domestic animals.

Previous biochemical studies reported that *E. gracilis* Z contains various vitamin-related novel enzymes and metabolic pathways. The findings obtained using *E. gracilis* Z have been beneficial for obtaining a clearer understanding of the physiological functions of vitamins in other organisms, higher plants, algae, and even mammals. Therefore, *E. gracilis* Z appears to be a highly suitable organism for elucidating the physiological functions of vitamins from the viewpoint of comparative biochemistry and biological evolution. In this chapter, we discuss up-to-date information on the physiological functions of vitamins in this organism, in addition to fundamental knowledge on vitamins.

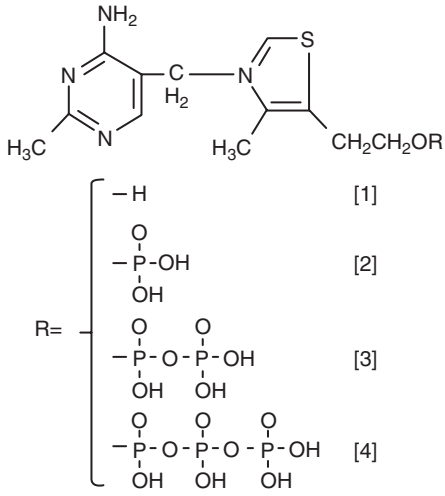

Fig. 5.1 Structures of thiamine and its related compounds. 1, Thiamine; 2, thiamine monophosphate (TMP); 3, thiamine diphosphate or thiamine pyrophosphate (TDP); and 4, thiamine triphosphate (TTP)

5.2 Water-soluble Vitamins

5.2.1 Vitamin B1

Vitamin B1 (or thiamine) not only plays a fundamental role as the active enzymatic co-factor in universal metabolic pathways in all living organisms (Roje 2007; Goyer 2010; Begley et al. 2012), but it is also crucially involved in resistance to abiotic and biotic stresses in plants (Ahn et al. 2005; Sayed and Gadallah 2002; Tunc-Ozdemir et al. 2009; Rapala-Kozik et al. 2008). Thiamine is composed of a pyrimidine (4-amino-2-methyl-5-pyrimidyl) ring linked to a thiazole (4-methyl-5-β-hydroxyethylthiazolium) ring by a methylene bridge (Fig. 5.1). It is phosphorylated on its hydroxyl group to form monophosphate (TMP), diphosphate (TDP), or triphosphate (TTP) esters. Although thiamine is not universally required among all *Euglena* species, *E. gracilis* var. *bacillaris* requires this vitamin for its growth (Cramer and Myers 1952; Leedale et al. 1965). *E. gracilis* Z showed an absolute thiamine requirement for growth with the addition of approximately 30 nM thiamine to medium being required for maximum growth (Cook 1968; Shigeoka et al. 1987a). *E. gracilis* Z has an alternative route in the TCA cycle that is distinct from other living organisms. *Euglena* mitochondria lack the 2-oxoglutarate dehydrogenase complex and, instead, contain a novel TDP-dependent 2-oxoglutarate decarboxylase coupled to $NAD(P)^+$-dependent succinate semialdehyde dehydrogenase, by which 2-oxoglutarate is converted into succinate (Shigeoka et al. 1986a; Shigeoka and Nakano 1991, 1993). In addition, the oxidative decarboxylation of pyruvate was found to be catalyzed in a CoA-dependent reaction to form acetyl-CoA and CO_2 by the action of a TDP-dependent pyruvate : $NADP^+$ oxidoreductase (Kitaoka et al. 1989; Inui et al. 1987, 1991). This enzyme has not yet been detected in any other organism. One of its two domains, the N-terminal domain, has three [4Fe–4S] clusters and one TDP as its prosthetic groups, and the other domain contains one FAD and one FMN per subunit (Nakazawa et al. 2000). TDP was previously reported to be required for the stabilization and/or activation of these enzymes (Shigeoka and Nakano 1991; Nakazawa et al. 2003).

The biosynthetic pathway of thiamine differs slightly depending on the species (Begley et al. 1999; Nosaka 2006; Roje 2007). In plants, yeast, and bacteria, TMP is similarly synthesized by condensation of the thiazole and pyrimidine rings, while the biosynthetic pathway for each ring is different (Roje 2007; Goyer 2010; Begley et al. 2012). The addition of 4-amino-2-methyl-5-pyrimidine, but not 4-methyl-5-β-hydroxyethylthiazole, to thiamine-deficient *Euglena* has been shown to enhance the cell number to the same extent as the addition of thiamine, indicating that *Euglena* is unable to synthesize the pyrimidine ring of thiamine (Shigeoka et al. 1987a). A previous study reported that thiamine-sufficient cells grown in thiamine (100 μg/150 ml medium) containing medium under photoheterotrophic conditions accumulated intracellular thiamine, TMP, and TDP at concentrations of 74.5 (70.0%), 2.9 (2.7%), and 29.1 (27.3%) pmol 10^6 cells^{-1}, respectively (Shigeoka et al. 1987a).

In plants, the synthesis of thiazole and pyrimidine rings takes place in plastids, while the phosphorylation of thiamine, which produces TDP, occurs exclusively in the cytosol (Julliard and Douce 1991). *E. gracilis* Z has three different types of thiamine pyrophosphokinase which catalyzes the pyrophosphorylation of free thiamine, in chloroplasts, mitochondria, and the cytosol (Shigeoka et al. 1987b). The cellular distribution of this enzyme activity was 9.2% in chloroplasts, 15.7% in mitochondria, and 65.7% in the cytosol. In agreement with this finding, chloroplasts had 4.3% of the total TDP, mitochondria 35.2%, and the cytosol 60.4%, while the amount of total cellular thiamine accumulated in chloroplasts was 12.1%, 25.4% in mitochondria, and 60.6% in the cytoplasm.

Information on the transport of thiamine is very limited. Only the yeast TDP carrier Tpc1p (thiamine pyrophosphate carrier protein), human Tpc, and *Drosophila melanogaster* DmTpc1p have been shown to be involved in the mitochondrial transport of TDP (Iacopetta et al. 2010; Lindhurst et al. 2006; Marobbio et al. 2002). Although thiamine-deficient *Euglena* have been shown to grow with the addition of TMP and TDP, the requirement for optimal growth was approximately 12- and 39-fold higher, respectively, than that for thiamine (Shigeoka et al. 1987a). Similar to yeast cells, as much as 96% of the total amount of thiamine taken up by thiamine-deficient *Euglena* was found to exist in the free form irrespective of the forms added, thiamine, TMP, or TDP, suggesting that the phosphate moiety is hydrolyzed prior to its incorporation into cells. *E. gracilis* Z appears to possess an active transport system for thiamine with a K_m value of 17 nM and V_{max} value of 7.8 pmol 10^6 cells^{-1} min^{-1} (Shigeoka et al. 1987c). The uptake of thiamine continued until the cellular thiamine concentration reached approximately 1 mM, which was 1000-fold higher than in medium. This activity was competitively inhibited by TMP, TDP, or TTP, suggesting that the hydrolysis of bound phosphate was closely associated with the transport system. Inhibitors of the respiratory chain and anaerobic conditions have been shown to inhibit thiamine uptake in *Euglena* suggesting the involvement of energy sources generated by respiration and glycolysis in the transport system (Shigeoka et al. 1987c).

5.2.2 Vitamin B2

Vitamin B2 (or riboflavin) is the precursor of FMN and FAD which are co-factors for various enzymes involved in vital processes in all organisms such as mitochondrial electron transport, photosynthesis, fatty acid oxidation, and the metabolism of vitamins B6, B12, and folates (Bacher et al. 2000; Roje 2007; Haase et al. 2014). In *E. gracilis* Z, short chain length-specific *trans*-2-enoyl-CoA reductase, which is involved in mitochondrial fatty acid synthesis, contains loosely bound FAD as a co-enzyme that may cause the enzyme to change its conformation, thereby decreasing its affinity for substrates (Inui et al. 1986). The *Euglena* long chain fatty-acid synthetase (type-I FAS) is a flavoprotein; the flavin co-factor, in contrast to yeast, appears to be covalently attached to the enzyme. NADPH-dependent glyoxylate reductase, which is involved in the glycollate-glyoxylate cycle in *E. gracilis* Z, and ferredoxin-NADP$^+$ reductase from *E. gracilis* Klebs var. *Bacillaris* Cori have also been identified as flavoproteins (Yokota et al. 1985; Spano and Schiff 1987). Details of the flavoproteins in *Euglena* have been described (Kitaoka et al. 1989). The blue-light receptor, photoactivated adenylyl cyclase, which functions as a photoreceptor for the photoavoidance of *Euglena*, was found to non-covalently bind FAD at two FAD-binding sites on each subunit of the heterotetrameric enzyme (Iseki et al. 2002).

The riboflavin biosynthetic pathway appears to proceed through the same steps in plants, yeast, and bacteria, although the enzymes in plants remain to be identified (Fischer et al. 2004, 2005; Sandoval and Roje 2005; Sandoval et al. 2008; Giancaspero et al. 2009; Rawat et al. 2011; Maruta et al. 2012). *E. gracilis* Z has been shown to synthesize, store (39.0 ng mg^{-1} dry weight), and excrete (39 ng ml^{-1} medium) riboflavin (Baker et al. 1981). Intracellular riboflavin, FMN, and FAD showed constant levels during growth

of light- and dark-adapted *E. gracilis* Z, but decreased temporarily in the logarithmic growth phase in light- and dark-adapted bleached mutant cells (Ochi et al. 1988a, b). All *Euglena* contain riboflavin and its co-enzyme forms at a constant ratio (riboflavin: FMN: FAD =4: 25: 70) during their growth (Ochi et al. 1988a). However, the molecular and enzymatic characteristics of the factors involved in the biosynthetic pathway and transport system are not yet known.

5.2.3 Vitamin B6

Vitamin B6 compounds are known as pyridoxine (PN), pyridoxal (PL), and pyridoxamine (PM). The 5′-phosphate ester of pyridoxal, pyridoxal-5′-phosphate (PLP), is the co-enzyme form of vitamin B6 (Hellmann and Mooney 2010). Vitamin B6 enzymes synthesize, degrade, and interconvert amino acids and, thus, link nitrogen and carbon metabolism, replenish the pool of C1 units, and produce polyamines as well as important signaling molecules (Wu et al. 2011). Pyridoxamine-5′-phospahte (PMP) and pyridoxine-5′-phoshate (PNP) are widely distributed in animal and plant cells (Sang et al. 2007).

The intracellular content of vitamin B6 has been shown to change during growth of *E. gracilis* Z (Ochi et al. 1988a, b). PLP was identified as the predominant vitamin B6 compound throughout cell growth, while small amounts of PN, PL, PM, PNP, and PMP were also detected (Ochi et al. 1988a). PLP levels significantly increased in the logarithmic phase and were then maintained at constant levels in light- and dark-adapted cells. The maximum amount of PLP in dark-adapted cells was half the amount detected in light-adapted cells (Ochi et al. 1988a). These findings suggest that *E. gracilis* Z contains a PLP biosynthesis pathway that is significantly stimulated under illumination. However, there is currently no detailed information available on the enzymatic systems for vitamin B6 biosynthesis in this organism. Details of the PLP-dependent enzymes involved in *Euglena* amino acid metabolism are given in the cited reference (Kitaoka et al. 1989).

5.2.4 Niacin

Niacin (or nicotinic acid and nicotinamide) is the moiety for the co-factor NAD^+ and its derivative $NADP^+$ which are essential metabolites for numerous redox reactions in living organisms. In some plants, this compound is also a precursor of pyridine alkaloids (Noctor et al. 2006; Roje 2007). NAD^+ also acts as a substrate for (cyclic) ADP-ribose generation, poly(ADP-ribos)ylation, and protein deacetylation, during which NAD^+ is broken down to nicotinamide.

E. gracilis Z has the ability to synthesize and store 29.7 ng mg^{-1} dry weight of nicotinate, and excrete large amounts (580 ng mg^{-1} dry weight) of the vitamin into the surrounding medium (Baker et al. 1981). The *de novo* pathway and salvage (recycling) pathway (Ying 2008; Hashida et al. 2009) are two known NAD^+ biosynthetic pathways in living organisms. Mammals have only one NAD^+ kinase (NADK), which is involved in the *de novo* generation of $NADP^+$ from NAD^+ in the cytosol, while yeast and plants have three NADK isoenzymes, two of which are located in the cytosol and the other in mitochondria or chloroplasts (Pollak et al. 2007; Turner et al. 2004; Berrin et al. 2005; Chai et al. 2005, 2006). NADK and NAD^+ phosphatase activities have both been detected in the soluble and membrane-bound fractions of the achlorophyllous ZC mutant of *E. gracilis* Z. The levels and affinities of these activities change depending on circadian rhythms and cell division cycles suggesting a relationship between NAD^+/$NADP^+$ metabolism and the circadian oscillating loop (Laval-Martin et al. 1990a, 1990b). Pou de Crescenzo et al. (1997) proposed three possibilities for the regulation of these activities: (1) structural changes in NAD^+ binding sites depending on NAD^+ concentrations; (2) the possible binding of Mg-ATP^{2-} (or Ca-ATP^{2-}) on NAD^+ sites, and (3) different and specific modulations of the kinetic parameters of the two types of NAD^+ binding sites by the calmodulin complex. Stephan et al. (2000) demonstrated that *E. gracilis* Z has two soluble NADK isoenzymes (isoenzymes 1 and 2), which display similar molecular weights (68 kDa), but differ in their substrate

specificities toward triphosphate nucleotides and their catalytic mechanisms. Similar to the enzyme previously described in bacteria, isoenzyme 1 was found to be as active in the presence of ATP as GTP, functioned using a ping-pong mechanism with K_m values of 0.26 mM for NAD^+ and 0.03 mM for ATP. Isoenzyme 2 was 3-fold more active in the presence of GTP than ATP which is a unique feature among the other NADKs and operates by a sequential mechanism with K_m values of 1.03 and 0.20 mM for NAD^+ and GTP, respectively.

ADP-ribosyl cyclase, which catalyzes the conversion of NAD^+ to cyclic ADP-ribose (cADPR) in *E. gracilis* Z, was identified as a monomeric membrane-bound protein with a molecular weight of 40 kDa (Masuda et al. 1999). Its K_m value for NAD^+ was 0.4 mM, and cADPR, a product of the enzyme, competitively inhibited its activity, whereas another product, nicotinamide, showed non-competitive inhibition. Unlike the mammalian enzyme, *Euglena* ADP-ribosyl cyclase did not exhibit cADPR hydrolase activity. Masuda et al. (1997a) demonstrated that the activity of *Euglena* ADP-ribosyl cyclase oscillated during the cell cycle in a synchronous culture induced by the light-dark cycle, with the activity increasing immediately before the start of cell division. In addition, cADPR was shown to act as an inducer of Ca^{2+} release from the microsomal fraction, presumably by activating the Ca^{2+}-induced Ca^{2+}-releasing mechanism through the ryanodine receptor (Masuda et al. 1997b). These findings suggest that ADP-ribosyl cyclase and cADPR participate in cell cycle regulation from the G2 phase to the M phase through Ca^{2+}-dependent mechanisms in *Euglena*. Nicotinic acid adenine dinucleotide phosphate (NAADP) was also reported to be a Ca^{2+} messenger derived from $NADP^+$ (Lee 2001). Although NAADP is a linear molecule structurally distinct from the cyclic cADPR, they both are synthesized by the same enzymes, ADP-ribosyl cyclase and its homolog, CD38 in mammals. NAADP has been shown to be involved in a wide range of cellular functions including cell cycle regulation in *Euglena*.

Ferredoxin-$NADP^+$ reductase, which catalyzes the synthesis in *E. gracilis* Klebs var. *Bacillaris* Cori of NADPH by the reduction of $NADP^+$ using ferredoxin as an electron donor, was purified and characterized (Kitaoka et al. 1989; Spano and Schiff 1987). *Euglena* ferredoxin-$NADP^+$ reductase was unusual in that it had two subunits (typical 36-kDa and unusual 15-kDa polypeptides) that were tightly associated. This enzyme activity in greening illuminated cells was 4-fold higher than the activity in dark-grown cells. Half of the enzyme activity in dark-grown cells was soluble, whereas nearly all of the activity in illuminated cells was found to be membrane-bound correlating with the extent of thylakoid membrane formation. These findings suggest that this enzyme is involved in the light reactions of photosynthesis.

5.2.5 Pantothenic Acid

Pantothenic acid is synthesized in plants and some microorganisms from pantoic acid and β-alanine through the actions of several enzymes (Velisek and Davidek 2000). However, there is currently no information available on the enzymatic systems of pantothenic acid biosynthesis in *Euglena* . The biologically active forms of pantothenic acid are coenzyme A (CoA) and the acyl-carrier protein (ACP). CoA forms high-energy bonds with acetic acid *via* its sulfhydryl group to yield acetyl-CoA, which is formed from lipid, amino acid, and carbohydrate metabolism. CoA may also be converted to a number of other acyl-CoA derivatives. Acetyl-CoA and short-chain acyl-CoA esters have been shown to enter various biochemical reactions for numerous cellular components (Velisek and Davidek 2000).

The biosynthesis of long-chain fatty acids takes place on the fatty acid synthase complex. The growing fatty acid chain is covalently bound to ACP during the entire synthesis of the fatty acid. *E. gracilis* Z has an ACP with a molecular mass of 10.4 kDa and an amino acid composition that is similar to those of proteins from other sources (Di Nello and Ernst-Fonberg 1973; Simoni et al. 1967). Dark-grown *Euglena* were

previously shown to contain type I and type III fatty acid synthase complexes (Goldberg and Bloch 1972), while an ACP-dependent type II enzyme was induced in light-grown *Euglena* (Delo et al. 1971). Type I fatty acid synthase contained an ACP as an integral component of the multienzyme complex (Delo et al. 1971) and was similar to the yeast and animal enzymes (Willecke et al. 1969; Londesborough and Webster 1974). The type II fatty acid synthase resembles the plant and bacterial enzymes (Vagelos 1973). *Euglena* has both the plant-type and animal-type systems for fatty acid synthesis which is highly interesting from an evolutionary point of view. Details on the synthesis of these ACP-dependent fatty acids and also on the CoA-dependent enzymes involved in lipid metabolism are described in the cited reference (Kitaoka et al. 1989) and in Chapter 13.

5.2.6 Biotin

Biotin serves as a covalently bound co-enzyme in five human carboxylases. Although it is also attached to the histones H2A, H3, and H4, the abundance of biotinylated histones is low (Zempleni et al. 2012). Biotin is required by all living cells, but is only biosynthesized by plants, fungi, and microorganisms (Maruyama et al. 2012). The biotin content and biotin biosynthetic pathway have not yet been examined in *Euglena*. Biotin-dependent enzymes include three classes of enzymes: carboxylases, transcarboxylases, and decarboxylases (Waldrop et al. 2012).

In *Euglena* as well as other organisms, fatty acid synthesis starts with malonyl-CoA, which is formed by acetyl-CoA carboxylase (Evers and Ernst-Fongerg 1974). This enzyme, together with phosphenolpyruvate carboxylase and malate dehydrogenase, forms a multienzyme complex, which is located in the cytosol (Wolpert and Ernst-Fonberg 1975). *Euglena* acetyl-CoA carboxylase was found to be active with propionyl-CoA at a rate of 11% of that with acetyl-CoA, whereas *Euglena* propionyl-CoA carboxylase was only located in the mitochondria (Inui et al. 1984; Watanabe et al. 1988a). Other *Euglena* biotin-dependent enzymes are summarized in the cited reference (Kitaoka et al. 1989).

5.2.7 Folic Acid

Folic acid (or pteroyl-L-glutamic acid) is a tripartite molecule composed of pterin, *p*-aminobenzoate (PABA), and glutamate moieties (Fig. 5.2). Folic acid does not occur naturally but is used for food fortification and nutritional supplements because it is more stable than naturally occurring folates (Shane 2011). The natural forms are tetrahydrofolates (reduced forms), which exist in the polyglutamate form with 2–8 molecules of glutamic acid (McGuire and Bertino 1981). Folates are co-enzymes that are required in many metabolic pathways including purine and pyrimidine biosynthesis and amino acid interconversion (Choi et al. 2014).

Euglena growth was previously shown to be inhibited by the addition of sulfanilamide (Crosti et al. 1984) which inhibits the bacterial synthesis of dihydrofolic acid, the immediate precursor of folic acid, by competing with PABA at dihydropteroate synthase (Brown 1962). The inhibition of growth was fully reversed by the addition of folic acid (Crosti et al. 1984). The enzymatic systems involved in the biosynthetic pathway of folate have been characterized in plants, and the pathway involved is essentially the same as that in bacteria (Basset et al. 2005). However, the pathway of folate biosynthesis has not yet been investigated in *Euglena*.

E. gracilis Z was found to contain approximately 60 μg of folic acid per g of dry weight using a *Lactobacillus casei* bioassay (Crosti and Bianchetti 1983). No folates with an oxidized pteridine ring were detected in *Euglena*. The reduced folates found in *Euglena* were formyl-monoglutamate (1%), formyl di- and triglutamate (8.6%), formyl-polyglutamate (25.9%), methyl-monoglutamate (1.5%), methyl di- and triglutamate (10.4%), and methyl-polyglutamate (52.4%). The polyglutamate forms found in *Euglena* were previously shown to be mostly derived from the hexaglutamate forms (Crosti and Bianchetti 1983).

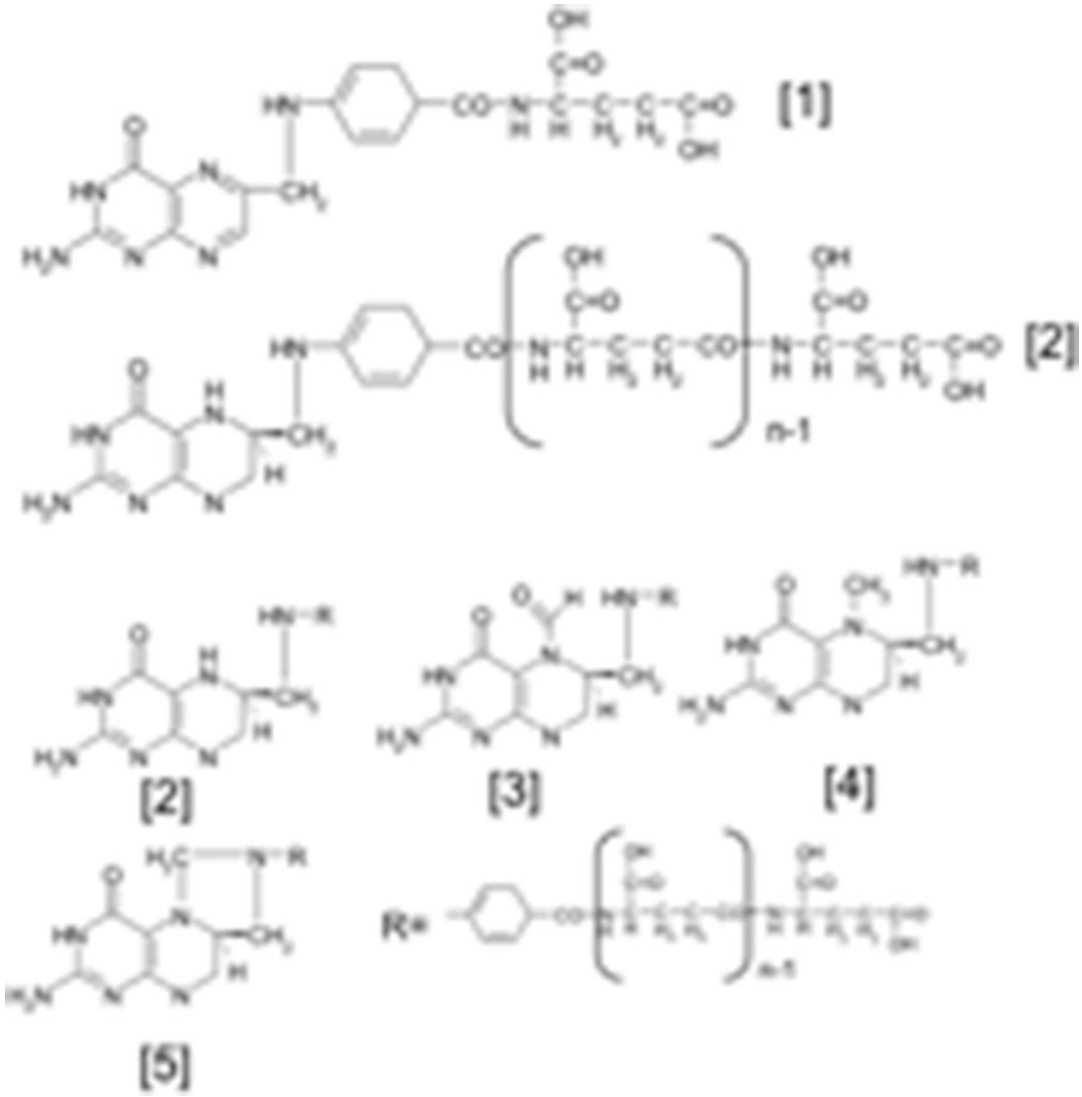

Fig. 5.2 Structures of folic acid and its related compounds. 1, Folic acid or pteroyl-L-glutamic acid; 2, tetrahydrofolate (n ≥ 2, polyglutamate form); 3, 5-formyl-tetrahydrofolate; 4, 5-methyl-tetrahydrofolate; and 5, 5,10-methlene-tetrahydrofolate

The content of folate in *Euglena* changes significantly during growth. Cellular folate levels were found to rapidly increase before entry into the logarithmic growth phase and then continuously decrease to 1/5 of the highest value (Crosti et al. 1984). The biosynthesis of folate reached a maximum (86 ng folic acid 10^6 cells^{-1} h^{-1}) when the culture entered the logarithmic growth phase and thereafter rapidly decreased to approximately 1/20 of the highest value (Crosti et al. 1987) indicating that the biosynthesis of folate is strongly repressed in the logarithmic growth phase.

A PLP-dependent enzyme involved in C1 transfer, serine hydroxymethyltransferase (L-serine: tetrahydrofolate 5,10-hydroxymethyltransferase, SHMT) simultaneously catalyzes mutual transfer between L-serine and glycine and the conversion of tetrahydrofolate to 5,10-methylenetetrahydrofolate. SHMT is located in the cytosol, mitochondria, and chloroplasts of *E. gracilis* Z (Sakamoto et al. 1996). The

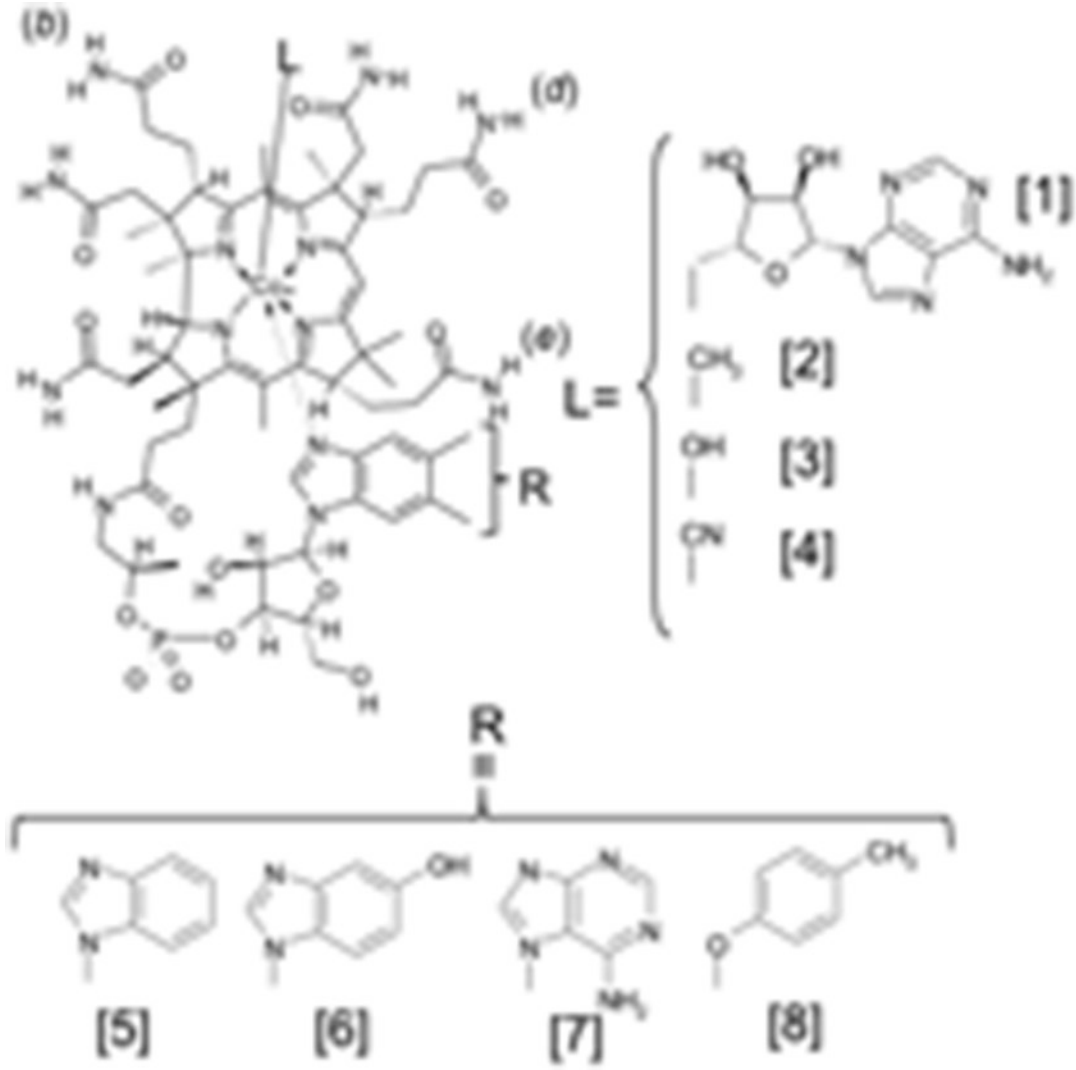

Fig. 5.3 Structures of vitamin B12 (cobalamin) and its related compounds. 1, Adenosylcobalamin (AdoB12); 2, methylcobalamin (MeB12); 3, hydroxocobalamin (OH-B12); 4, cyanocobalamin (CN-B12); 5, benzimidazolyl cobamide; 6, 5-hydroxylbenzimidazolyl cobamide; 7, adenylyl cobamide (or pseudovitamin B12); and 8, *p*-cresolyl cobamide

cytosolic and mitochondrial enzymes have been highly purified and characterized (Sakamoto et al. 1991, 1996). *Euglena* cytosolic and mitochondrial SHMT catalyzed the conversion of L-threonine to glycine and acetaldehyde (L-threonine aldolase reaction) as well as the conversion of L-serine and tetrahydrofolate to glycine and 5,10-methylenetetrahydrofolate. Animal (Masuda et al. 1987) and plant (Masuda et al. 1980) SHMTs do not react with L-threonine. Therefore the *Euglena* enzymes appears to play important physiological roles in the metabolism of L-serine, glycine, and L-threonine in each organelle.

5.2.8 Vitamin B12

Vitamin B12 belongs to corrinoids, a group of compounds having a corrin macrocycle (Fig. 5.3). The term "vitamin B12" is generally restricted to

cyanocobalamin, which is the most chemically stable and unnatural form of cobalamin (Watanabe 2007). However in this chapter, vitamin B12 (B12) refers to all biologically active cobalamins. Cyanocobalamin (CN-B12) is readily converted into the co-enzyme forms of cobalamin in living cells (Watanabe et al. 2013). B12 is only synthesized by certain bacteria, and not by plants or animals. Corrinods carrying a base other than 5,6-dimethylbenzimidazole as the lower ligands are also found in nature (Watanabe et al. 2013).

E. gracilis Z shows an absolute requirement of B12 for growth and at least 22,000 molecules of B12 per cell are necessary for normal growth (Carell 1969). *Euglena* has the ability to take up and accumulate exogenous B12 (Varma et al. 1961). The kinetics of CN-B12 uptake in *Euglena* are biphasic (Sarhan et al. 1980) as in *E. coli* and *Ochromonas malhamensis* (Bradbeer 1971; Bradbeer and Woodrow 1976). The B12 structural specificities for cell growth and the B12 uptake system of *Euglena* were studied using a number of B12 analogues (Watanabe et al. 1992). *Euglena* did not have the ability to utilize most of the B12 analogues for cell growth, whereas benzimidazolyl cyanocobamide and CN-B12 (*b*)-, (*d*)-, and (*e*)-monocarboxylates exerted similar effects on cell growth to that of authentic CN-B12. The inhibition of radiolabeled CN-B12 uptake caused by the addition of various B12 analogues indicates that the lower ligand (the cobalt-coordinated nucleotide) and (*b*)-propionamide side chain of the molecule are essential for the B12 uptake system.

E. gracilis Z has been widely used as one of the organisms employed in microbiological assays of B12 in food and biological samples (Ross 1952). Thus the B12 structural specificity of *Euglena* cell growth is critical information when assaying B12. *Euglena* pellicle (a cell membrane complex) fragments prepared by stepwise sucrose density gradient centrifugation were found to exhibit B12-binding activity (Watanabe et al. 1988b) because the B12-binding protein involved in B12 uptake was embedded in the pellicle fragments. A radioisotope dilution assay method was devised for the quantitation of B12 using isolated pellicle fragments as a solid-phase B12-binding material (Watanabe et al. 1993a).

E. gracilis Z contains numerous non-enzymatic B12-binding proteins, which are distributed in the cytosolic, mitochondrial, chloroplastic, and microsomal fractions (Isegawa et al. 1984). Some of these B12-binding proteins have been purified and characterized (Watanabe et al. 1987a, b, 1988b, c). Thus, *Euglena* has intracellular B12 transfer and/or accumulation systems (Watanabe et al. 1989) which differ from the mammalian and bacterial systems (Watanabe and Nakano 1991).

The *Euglena* cytosolic B12-binding protein showed an absolute requirement for the lower ligand in B12 binding but was not able to recognize differences in the base or ribose moiety (Watanabe et al. 1993b). Regarding the contributions of the (*b*)-, (*d*)-, and (*e*)-propionamide side chains in the binding of B12 to the cytosolic protein, the order of the contributions was found to be $b > d > e$; the (*b*)-propionamide side chain was essential for the formation of the protein-B12 complex. The upper ligand was not involved in the binding of B12 to the protein. Mammalian intrinsic factor (IF) and transcobalamin II (TC), which are B12-binding proteins for the gastrointestinal absorption and blood circulation of B12, respectively, have an absolute requirement for the lower ligand in B12 binding (Kolhouse and Allen 1977; Stupperich and Nexo 1991) similar to the *Euglena* cytosolic protein whereas the *E. coli* outer membrane receptor (Kenley et al. 1978) and mammalian haptocorrin (a B12-binding protein located widely in tissues) (Kolhouse and Allen 1977; Stupperich and Nexo 1991) do not.

B12 uptake by *Euglena* mitochondria is a biphasic process consisting of the energy-independent binding of B12 to mitochondrial membranes and energy-dependent active transport (Watanabe et al. 1993c). The energy-dependent phase of B12 uptake was previously shown to be dependent upon the presence of ATP within the mitochondrial matrix but not mitochondrial respiration. The inhibition of mitochondrial B12 uptake by various B12 analogues indicates that *Euglena* mitochondria have an

absolute requirement for the complete structure of the B12 molecule (Watanabe et al. 1993c). Rat liver mitochondria take up B12 by the diffusion of free B12, a process that is dependent on mitochondrial swelling rather than on ionic fluxes or the mitochondrial metabolic state (Fenton et al. 1976). Rat liver mitochondrial B12 uptake selects natural upper ligands rather than CN-B12.

A previous study demonstrated that CN-B12 is promptly converted into the co-enzyme forms of B12, methylcobalamin (MeB12) and adenosylcobalamin (AdoB12), after feeding CN-B12 to B12-limited *Euglena* (Isegawa et al. 1984). MeB12 was detected in chloroplasts, mitochondria, microsomes, and the cytosol and AdoB12 in the mitochondria and the cytosol 2 h after feeding radiolabeled CN-B12 to *Euglena* . The conversion of hydroxocobalamin (OH-B12) to AdoB12 in bacteria has been suggested to involve three enzymatic steps (Watanabe and Nakano 1991); 1) the reduction of Co^{3+} in OH-B12 to Co^{2+} by aquacobalamin reductase, 2) the reduction of Co^{2+} to Co^{+} by cob(II)alamin reductase, and 3) the adenosylating reaction of Co^{+} to AdoB12 by cob(I)alamin adenosyltransferase. *Euglena* aquacobalamin reductase has been purified and characterized (Watanabe et al. 1987c, d, 1993d). This enzyme was found in the mitochondria and it is a flavoprotein with an apparent molecular mass of 65–66 kDa by SDS-PAGE and Sephadex G-100 gel filtration. CN-B12 reductase, which catalyzes the conversion of CN-B12 to OH-B12, has been detected in *Euglena* (Watanabe et al. 1988d) whereas the other enzymatic systems involved in the synthesis of AdoB12 and MeB12 have not yet been characterized in mitochondria. Although no information is currently available on the chloroplastic system for co-enzyme B12 synthesis, Isegawa et al. (1987) reported that MeB12 functioned as a co-enzyme of methionine synthase in chloroplasts and photosynthetic activity was decreased during B12 deficiency due to the loss of photosystem I.

Euglena contains three B12-dependent enzymes (methionine synthase, methylmalonyl-CoA mutase, and ribonucleotide reductase), which are involved in various cellular metabolic pathways. Methionine synthase catalyzes the conversion of homocysteine to methionine using a methyl group donated by N^5-methyltetrahydrofolate in the *de novo* biosynthesis of methionine. Two types of methionine synthase, B12-dependent and -independent, have been identified in organisms and catalyze the same overall reaction (Banerjee and Matthews 1990). The B12-dependent methionine synthase (MetH) has been detected in bacteria and animals (Banerjee and Matthews 1990; Leclerc et al. 1996). The B12-independent methionine synthase (MetE) showed no sequence similarity with MetH and catalyzes methyl transfer to L-homocyteine directly from N^5-mentyltetrahydrofote (polyglutamate forms, n > 3) (Ravanel et al. 1998). MetE and MetH have both been detected in bacteria (Banerjee and Matthews 1990) whereas fungi and plants only possess MetE (Ravanel et al. 1998; Saint-Macary et al. 2015). Although the green alga *Chlamydomonas reinhardtii* and the diatom *Phaeodactylum tricornutum* do not require B12 for their growth, they both possess MetE and MetH (Helliwell et al. 2011).

E. gracilis Z contains B12-dependent methionine synthase, the activity of which is distributed in the cytosol (68.9%), the chloroplast (18.4%), and mitochondria (9.5%), suggesting that it is a distinct protein that functions to supply methionine for protein synthesis in the individual organelles (Isegawa et al. 1994). B12-independent methionine synthase activity has only been observed in the *Euglena* cytosolic fraction (Isegawa et al. 1994).

E. gracilis Z has the ability to utilize propionate for growth as a sole carbon source only under illumination and is converted into cellular components through the methylmalonyl-CoA pathway (Yokota et al. 1982). This pathway metabolizes odd-chain fatty acids and branched-chain amino acids to *R*-methylmalonyl-CoA which is converted to the Krebs cycle intermediate succinyl-CoA by methylmalonyl-CoA mutase (MCM). Thus, MCM is the key enzyme for the photoassimilation of propionate in this organism. *Euglena* MCM activity is significantly higher in propionate-adapted cells than in photoautotrophic cells (Watanabe et al. 1996). The *Euglena*

MCM apoenzyme accumulated significantly at the end of the logarithmic growth phase (Miyamoto et al. 2010). The apparent molecular mass of *Euglena* MCM was found to be 149.0 kDa and 75.0 kDa using Superdex 200 gel filtration and SDS-PAGE, respectively, indicating that the *Euglena* enzyme is composed of two identical subunits (Miyamoto et al. 2010). The enzyme contained one mole of prosthetic AdoB12 per mole of the enzyme subunit similar to AdoB12 content of the human liver (Fenton et al. 1982), intestinal worm (Han et al. 1984), and other algal (Miyamoto et al. 2004, 2007) MCMs. *Euglena* MCM encodes a putative mitochondrial targeting signal consisting of nine amino acids. Most *Euglena* MCM activity is recovered only in mitochondria (Miyamoto et al. 2010).

Human methylmalonic aciduria type A protein (MMAA) plays an important role in the protection and reactivation of MCM *in vitro* (Takahashi-Iniguez et al. 2011). The cDNA encoding MMAA was isolated from *E. gracilis* Z and the deduced amino acid sequence of the cDNA showed approximately 80% similarity to MMAAs of mammals and bacteria (Yabuta et al. 2013). The *Euglena* MCM transcript level was increased significantly during B12 deficiency whereas the MMAA transcript level was unchanged. No significant differences in MCM activity were observed between *E. coli* expressing either MCM together with MMAA or MCM alone (Yabuta et al. 2013). Thus, the physiological function of the MMAA protein remains unknown in *E. gracilis* Z.

Ribonucleotide reductases (RNRs) provide all cells with the deoxyribonucleoside triphosphates required for DNA replication and repair (Jordan and Reichard 1998). They catalyze the replacement of an OH group in the ribose moiety of a ribonucleoside di- or triphosphate by a hydrogen atom. Three classes of enzymes have been identified and differ widely in their amino acid sequences but have similar structural motifs and allosteric sites (Jordan and Reichard 1998). Class I enzymes occur in eukaryotes and aerobic prokaryotes and consist of two homodimeric proteins (Reichard 1993). Class II enzymes occur in aerobic and anaerobic prokaryotes and consist of a single polypeptide chain, the cysteine radical of which is generated by AdoB12 (Lawrence and Stubbe 1998). Class III enzymes occur in anaerobic prokaryotes (Stubbe 2003). *E. gracilis* Z contains a class II enzyme and represents an exception from the general rule that eukaryotes contain class I enzymes (Gleason and Hogenkamp 1970; Hamilton 1974; Torrents et al. 2006). The amino acid sequence and general properties (including allosteric behavior) of the *Euglena* enzyme are similar to the class II reductase from *Lactobacillus leichimannii* (Torrents et al. 2006). Both enzymes belong to a distinct small group of reductases that unlike all other homodimeric reductases are monomeric. Database searches and sequence comparisons identified a homolog from the eukaryote *Dictyostelium discoideum* as the closest relative to the *Euglena* RNR (Torrents et al. 2006). A recombinant enzyme showed an apparent molecular mass of 82 kDa on SDS-PAGE and Superdex-200 chromatography and the protein peak was eluted with a calculated molecular mass of 470 kDa (Torrents et al. 2006). Similar values have been reported in RNR purified from a *Euglena* cell homogenate (Hamilton 1974). In B12-sufficient medium, enzyme activity was shown to be approximately 20 nmol h^{-1} mg $protein^{-1}$ in the exponential stage and very low in the plateau stage. As cells progress into B12 deficiency, enzyme activity increases reaching maximum values that are approximately 20-fold higher than those found in the exponential stage of B12-sufficient cells (Carell and Seeger 1980).

Euglena cells deprived of B12 were found to have a longer generation time accompanied by an increase in cell volume until division was completely arrested at which time the volume was 10-fold greater than that of control cells (Bre et al. 1975). During the course of B12 starvation, total cellular RNA and protein levels were 400–500% higher than those in control cells (Carell et al. 1970). Lefort-Tran et al. (1987) reported that B12 starvation in *Euglena* led to defective DNA synthesis. Blocked cells had different DNA contents corresponding to the blockade of DNA replication during the S phase. A second block prevented the onset of mitosis even for 4C cells.

B12 starvation for short periods made it possible to induce synchronous growth by the addition of the vitamin. Culture conditions were established to optimize replenishment synchrony (Shehata and Kempner 1979).

A B12 deficiency has also been shown to affect phospholipid levels in *Euglena* (Inui et al. 1996). Although phosphatidylcholine synthesis was significantly decreased, large amounts of triglycerides and wax esters accumulated in B12-deficient cells. The depletion of B12 altered the fatty acid composition notably due to increases in the proportion of odd-numbered fatty acids. However, no net difference was observed in overall O_2 uptake in B12-deficient and B12-replenished cells indicating that a B12 deficiency does not significantly affect respiration in *Euglena* (Seeger and Carell 1991). Isolated mitochondrial preparations from B12-deficient and -sufficient *Euglena* showed no significant differences in their respiratory control or P/O ratio or in cellular ultrastructure as seen in the electron microscope (Tokunaga et al. 1976). This contrasts with mammalian liver mitochondria that exhibited morphological and/or functional changes during B12 deficiency (Frenkel et al. 1976).

Tokunaga et al. (1976) employed a bleached mutant of *E. gracilis* Z that had swollen due to growth under B12-limited conditions in order to increase the digestibility of the tough pellicle with a protease in the fractionation of subcellular organelles. This method has been applied successfully to wild-type cells for use in determinations of the subcellular locations of enzymes.

5.2.9 Vitamin C

Vitamin C (or L-ascorbic acid, AsA) is a hydrophilic antioxidant synthesized by all animals except for primates and photosynthetic organisms including plants and algae. AsA plays a pivotal role as an antioxidant and enzyme co-factor in animals. In plants, AsA has been documented to play multiple roles in the control of photosynthesis, cell expansion and growth, and transmembrane electron transport in addition to its indispensable role as an antioxidant (Smirnoff 2000, 2001; Valpuesta and Botella 2004; Ishikawa et al. 2006, Ishikawa and Shigeoka 2008). In *Euglena*, AsA constitutes the AsA-GSH cycle as a cardinal antioxidative mechanism (Kitaoka et al. 1989) as described in Chapter 4. AsA levels in *Euglena* have been shown to synchronize well with circadian rhythms (Kiyota et al. 2006). Periodic variations in cyclic AMP (cAMP) levels play a major signaling role in the progression of the *Euglena* cell cycle (Carré and Edmunds 1992) and AsA augments the levels of cGMP which serves as an upstream effector that mediates cAMP oscillations by regulating metabolic enzymes, in human lymphocytes (Atkinson et al. 1979) suggesting a positive relationship between the biosynthesis of AsA and regulation of the cell cycle.

The biosynthetic pathway for AsA differs between animals and plants and possibly certain species of algae. In animals, the committed step in the biosynthesis of AsA consists of a branch of the D-glucuronate (D-GlcUA) pathway *via* the pentose phosphate pathway in which uronic acid, D-GlcUA, L-gulonate (L-GulA) and L-gulono-1,4-lactone (L-GulL) are precursors involving inversion of the carbon chain for AsA (Nishikimi and Yagi 1996). In this pathway, the microsome-localized enzyme, L-GulL oxidase, catalyzes the final step to produce AsA. In plants the D-Man/L-Gal pathway is the primary AsA biosynthetic pathway utilizing D-mannose (D-Man), L-galactose (L-Gal), and L-galactono-1,4-lactone (L-GalL) as intermediates without inversion of the carbon chain (Smirnoff 2000, 2001; Valpuesta and Botella 2004; Ishikawa and Shigeoka 2008). L-GalL is finally oxidized to produce AsA by the action of L-GalL dehydrogenase located in the mitochondrial inner membrane (Bartoli et al. 2000; Yabuta et al. 2000). Possible alternative biosynthetic pathways have been proposed for AsA. AsA is produced *via* uronic acid and D-galacturonate (D-GalUA) in ripening strawberry fruits (Agius et al. 2003) although the aldonolactonase (ALase) required to catalyze the conversion of L-galactonate (L-GalA), the product derived from the reduction of D-GalUA, to L-GalL has not been found.

Some eukaryotic microorganisms contain significant concentrations of cellular AsA however, details of the biosynthetic pathway remain unclear. *Chlorella* and *Prototheca* contain appreciable amounts of AsA and the addition of D-Man, L-GalA, or L-GalL to *Prototheca* medium resulted in a significant increase in the level of AsA suggesting the presence of a pathway similar to the plant pathway (Running et al. 2002, 2003). The protozoan parasite, *Trypanosoma brucei*, was found to possess a functional gene encoding D-arabinono-1,4-lactone oxidase which also oxidizes L-GalL however, the exact pathway arriving at the final precursor has not yet been determined (Wilkinson et al. 2005).

E. gracilis Z accumulates high concentration of AsA and excretes 3000 ng mg^{-1} D.W. of the vitamin into the surrounding medium (Shigeoka et al. 1979b, c; Baker et al. 1981). Cellular AsA levels in wild type green and bleached *Euglena* were previously reported to be rapidly and markedly increased by light exposure. Only blue light, but not red or green light, induced an increase in AsA levels (Shigeoka et al. 1979b; Ishikawa et al. personal communication). Since treatment with inhibitors of chloroplast development and photosynthesis had little or no effect on the blue light-dependent AsA increase, the regulation of AsA biosynthesis in *Euglena* is suggested to be independent of photosynthesis.

The AsA biosynthetic pathway in *E. gracilis* Z was proposed by Shigeoka et al. (1979c). Some uronic acids, UDP-D-GlcUA, UDP-D-GalUA, and D-GalUA, in addition to L-GalA and L-GalL were detected as intermediates in the production of AsA (Fig. 5.4). A similar pathway appears to be functional in some stramenopile algae (Helsper et al. 1982; Grün and Loewus 1984). D-GalUA reductase was recently purified and characterized from *Euglena* (Ishikawa et al. 2006). This enzyme utilized NADPH (K_m value =62.5 μM) as an electron donor, and the uronic acids, D-GalUA (3.79 μM) and D-GlcUA (4.67 μM), to irreversibly produce L-GalA and L-GulA, respectively. More recently Ishikawa et al. (2008) identified ALase in *Euglena* cells which showed significant sequence identity with rat gluconolactonase, a key enzyme for the production of AsA *via* D-GlcUA in animals. This enzyme catalyzed the reversible reaction of L-GalA and L-GalL with K_m values of 1.55 mM and 1.67 mM, respectively. Silencing the expression of ALase in *Euglena* cells caused the arrest of cell growth which was restored to the normal state by supplementation with L-GalL indicating that ALase plays a significant role in the biosynthesis of AsA in *Euglena* (Ishikawa et al. 2008). D-GalUA reductase and ALase have almost the same catalytic efficiency with the uronic acids, D-GalUA and D-GlcUA, making it difficult to determine which is the more effective route to produce AsA in *Euglena*. Wild-type *Euglena* accumulated more than 2-fold higher amounts of AsA on supplementation with D-GalUA than with D-GlcUA (Ishikawa et al. 2008). Furthermore, *Euglena* L-GalL dehydrogenase had higher activity with L-GalL than L-GulL as a substrate while no oxidase activity was detected with either lactone (Shigeoka et al. 1979a, c; Ishikawa et al. 2008). These findings indicate that the pathway *via* D-GalUA/L-GalA, which is analogous to the animal pathway and an alternative pathway in plants, is predominantly utilized to produce AsA in *Euglena* cells.

A gene encoding a protein with significant homology to *Euglena* ALase has been found in a limited number of eukaryotic algae, including *Ostreococcus lucimarinus*, *Thalassiosira pseudonana*, and *P. tricornutum* (Ishikawa et al. 2008). On the other hand, *Cyanidioschyzon merolae*, *C. reinhardtii*, *Volvox carteri*, and *O. tauri* have no ALase homologue, while these algae had predicted orthologs encoding L-GalL dehydrogenase. Therefore, algae are assumed to have developed diverse pathways for the biosynthesis of AsA including the pathway *via* D-GalUA/L-GalA found in *Euglena* and the D-Man/L-Gal pathway found in higher plants.

The AsA biosynthetic pathway in *Euglena* involves the inversion of the carbon chain of precursor sugar and uses L-GalL dehydrogenase. Thus the AsA biosynthetic pathway in *Euglena* is a hybrid of the animal and plant pathways. The generation of photosynthetic eukaryotes arose following the endosymbiotic acquisition of a

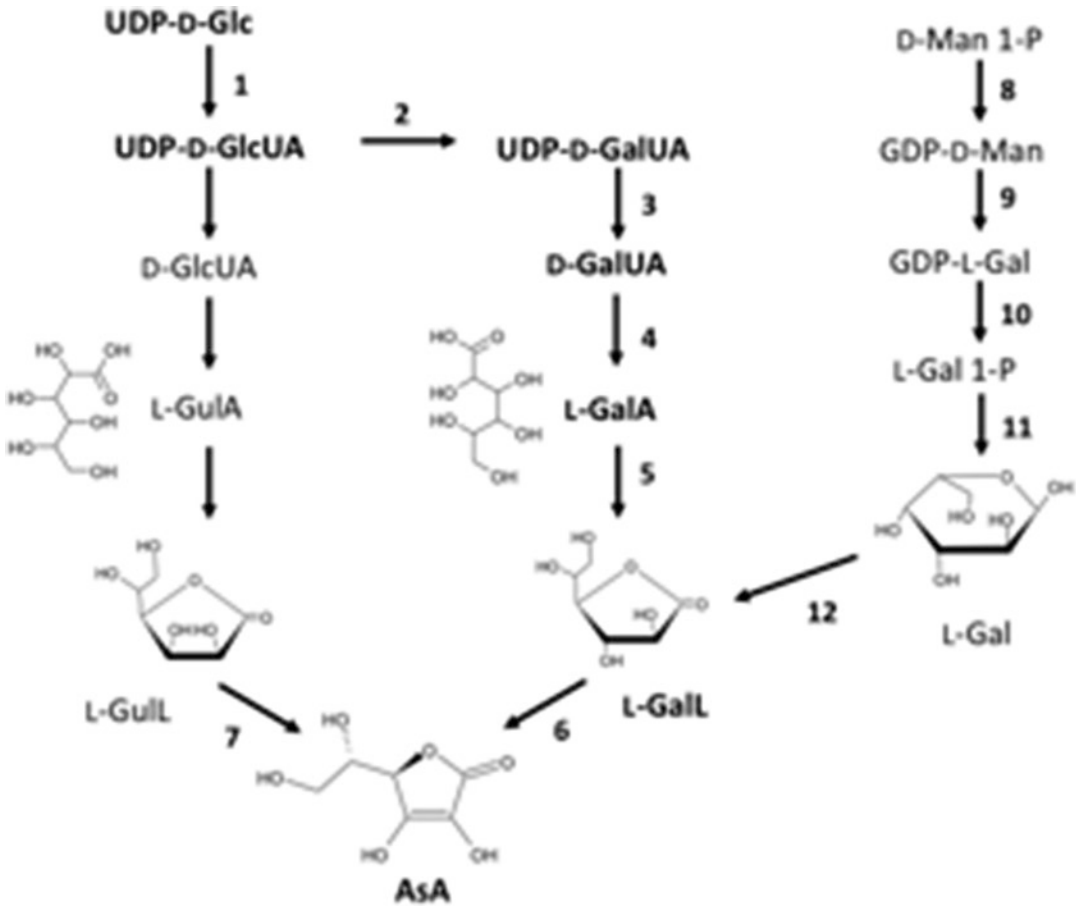

Fig. 5.4 AsA biosynthesis pathway in *Euglena* and plants (Ishikawa et al. 2008). AsA is produced through the pathway *via* D-GalUA/L-GalA in *Euglena* . The pathway from D-Man 1-phosphate (D-Man 1-P) to L-GalL (D-Man/L-Gal pathway) mainly operates in higher plants. The unnumbered reactions are uncertain. Enzymes catalyzing the numbered reactions are: 1, UDP-Glc dehydrogenase; 2, UDP-Glc-4-epimerase; 3, UDP-D-GalUA pyrophosphatase/phosphorylase; 4, D-GalUA reductase; 5, ALase; 6, L-GalL dehydrogenase; 7, L-GulL oxidase/dehydrogenase; 8, GDP-D-Man pyrophosphorylase; 9, GDP-Man-3′,5′-epimerase; 10, GDP-L-Gal phosphorylase; 11, L-Gal 1-P phosphatase; 12, L-Gal dehydrogenase. This research was originally published in The Journal of Biological Chemistry. Ishikawa T, Nishikawa H, Gao Y, Sawa Y, Shibata H, Yabuta Y, Maruta T, Shigeoka S. The pathway *via* D-galacturonate/L-galactonate is significant for ascorbate biosynthesis in *Euglena gracilis*: identification and functional characterization of aldonolactonase. The Journal of Biological Chemistry. 2008; 283: 31,133–31,141. © the American Society for Biochemistry and Molecular Biology

cyanobacterial ancestor by a non-photosynthetic eukaryote in the Archaeplastida (Plantae) lineage (Keeling 2010). Several other eukaryote lineages, including the diatoms, haptophytes and euglenids, subsequently gained plastids through secondary endosymbiosis with either a red or green alga. Wheeler et al. (2015) proposed that the host initially synthesized AsA *via* an animal-type pathway (involving inversion of the chain and L-GulL oxidase) and that the red or green algal symbiont used a plant-type pathway (involving non-inversion of the carbon chain and L-GalL dehydrogenase). However, neither pathway appears to operate in photosynthetic eukaryotes with secondary plastids, including *Euglena*, which instead uses a euglenid-type pathway. In such organisms, the endosymbiotic gene transfer of L-GalL dehydrogenase from the symbiont may have resulted in the functional replacement of L-GulL oxidase in the animal-type pathway of

the host leading to a hybrid biosynthetic pathway involving inversion of the carbon chain that employed D-GalUA rather than D-GlcUA as the intermediate in order to provide L-GalL as a substrate for L-GalL dehydrogenase.

The oxidation of AsA in cell metabolism gives monodehydroascorbate (MDAsA) as the primary product and dehydroascorbate (DAsA) as the final product (Smirnoff 2000, 2001; Valpuesta and Botella 2004; Ishikawa and Shigeoka 2008). Cytosolic enzymes involved in the reduction of MDAsA and DAsA, MDAsA reductase and DAsA reductase, were partially purified from *E. gracilis* Z (Shigeoka et al. 1987d). The activity of *Euglena* MDAsA reductase was 3-fold higher with NADPH (K_m value =7 μM) than with NADH (210 μM). The *Euglena* DAsA reductase specifically requires reduced glutathione (K_m value =0.85 mM) as an electron donor and dehydroascorbate (0.26 mM).

5.3 Fat-soluble Vitamins

5.3.1 Vitamin A

Vitamin A is found in animal-based foods as retinyl esters (mainly retinyl palmitate). In fruits and vegetables, it occurs as the provitamin A carotenoids (mainly β-carotene, α-carotene, and β-cryptoxanthin), which are cleaved and metabolized into retinol after absorption by intestinal cells (Rebou 2013). Vitamin A is essential for normal cell growth, cell differentiation, immunological functions, and vision (Gerster 1997).

Carotenogenesis pathways and the enzymes involved have been mainly investigated among oxygenic phototrophs in cyanobacteria and land plants. Isopentenyl pyrophosphate is the source of isoprenoids, terpenes, quinones, sterols, the phytol of chlorophylls, and of carotenoids. Two independent pathways of isopentenyl pyrophosphate synthesis have been identified to date; 1) the classical mevalonate (MVA) pathway and 2) the alternative, nonmevalonate, 1-deoxy-D-xylulose-5-phosphate (DXP) pathway. The DXP pathway is found in cyanobacteria, the plastids of algae and land plants, and in some bacteria. Carotenoids are synthesized in plastids. Exceptionally among oxygenic phototrophs, Euglenophyceae only have the MVA pathway, while Chlorophyceae only have the DXP pathway (Lange et al. 2000). Takaichi (2011) reported that the major carotenoids are alloxanthin (Cryptophyta), fucoxanthin (Chrysophyceae, Raphidophyceae, Bacillariophyceae, Phaeophyceae and Haptophyta), diadinoxanthin and vaucheriaxanthin (Xanthophyceae), violaxanthin and vaucheriaxanthin (Eustigmatophyceae), peridinin (Dinophyta), diadinoxanthin (Euglenophyta), siphonaxanthin (Chlorophyceae and Ulvophyceae), and lutein, violaxanthin, and 9-*cis* neoxanthin (land plants). In photosynthesis, carotenoids and chlorophylls both bind peptides in order to form the pigment-protein complexes in the thylakoid membrane. β-Carotene is present in most divisions of the reaction-center complexes and light-harvesting complexes of photosystem I as well as photosystem II (Takaichi 2011).

Kinsky and Goldsmith (1960) previously reported that the principal carotenoid of *E. gracilis* was antheraxanthin accounting for more than 80% of the carotenoids present, followed by β-carotene at approximately 11% and neoxanthin at 7%, with astaxanthin, astacene, vitamin A, and retinene being undetectable.

When the provitamin A content of *E. gracilis* Z grown under various conditions was determined using HPLC, β-carotene was the predominant provitamin A compound in these cells (Hosotani and Kitaoka 1984). The contents of β-carotene in light- and dark-grown wild-type cells at the stationary phase in heterotrophic medium were 577.8 μg 10^9 cells^{-1} (706.2 μg g^{-1} wet weight) and 47.3 μg 10^9 cells^{-1}, respectively. Bleached mutant cells grown under the same conditions contained less β-carotene (169.9 μg 10^9 cells^{-1} and 58.4 μg 10^9 cells^{-1}, respectively) than the wild-type cells. Dolphin (1970) previously reported that light induced the synthesis of β-carotene in *E. gracilis*. Carotenoids appear to protect normal *Euglena* cells from the photosensitizing effects of chlorophyll by quenching triplet oxygen formed in the light.

5.3.2 Vitamin E

Tocopherols and tocotrienols, collectively known as tocochromanols, are fat-soluble molecules that belong to the group of vitamin E compounds. These tocochromanols consist of α-, β-, δ-, and γ-isoforms. Among them, α-tocopherol is the most predominant and active form of vitamin E and thus, is essential in the human diet (Ogbonna 2009; Falk and Munné-Bosch 2010). These fat-soluble vitamins are antioxidants and free radical scavengers that act together with other antioxidants, such as AsA, in cells (Ogbonna 2009). Although most of the physiological roles of vitamin E are due to their antioxidant properties, some functions such as the inhibition of platelet aggregation and monocyte adhesion, antiproliferative and neuroprotective effects, and regulation of cell signaling are not directly linked to their antioxidant activities. Tocopherols are more active than their corresponding tocotrienols and α-tocopherol is the most predominant and active form of vitamin E in most human and animal tissues (Ogbonna 2009).

Tocopherols are synthesized by plants and photosynthetic microorganisms but not by animals. Although it is difficult to compare intracellular tocopherol levels among algal species because of differences in culture conditions, *Euglena* cells appear to accumulate relatively higher levels of tocopherols than other algae. *E. gracilis Z* was identified as the highest tocopherol producer among 285 strains in the 56 genera of microorganisms tested (Tani and Tsumura 1989). A large number of studies have measured intracellular tocopherol levels in *Euglena* cells (Ogbonna 2009). More than 97% of the tocopherols produced by *Euglena* cells were the α-isoform (Tani and Tsumura 1989; Shigeoka et al. 1986b). Heterotrophically grown *Euglena* cells accumulated 5.3 mg L medium^{-1} of α-tocopherol and photoautotrophic growth conditions were found to increase these levels to 8.6 mg L^{-1} (Grimm et al. 2015).

There are conflicting findings on the distribution of tocopherols and the subcellular localization of the enzymes involved in the biosynthesis of tocopherols in *Euglena*. This may be due to the methods employed for organelle isolation and the separation/detection of tocopherols. Threlfall and Goodwin (1967) reported that more than 95% of α-tocopherol was located in the chloroplasts of *E. gracilis Z*. On the other hand, Shigeoka et al. (1986b) showed that, in the same *Euglena* cells, 23.5% of α-tocopherol accumulated in chloroplasts, while 46.8% and 13.2% were in mitochondria and microsomes, respectively. Mitocondria contained 78.2% of β- and 62.5% of γ-tocopherols in the crude homogenate. Mitochondria of bleached cells showed a similar distribution of tocopherols. On the other hand, as described below, γ-tocopherol methyltransferase, which converts γ-tocopherol to α-tocopherol, was found in chloroplasts (Shigeoka et al. 1992). A relationship has been shown to exist between tocopherol levels and chloroplast development. Light-adapted bleached mutants of *Euglena* without chloroplasts produced even higher levels of tocopherols than the photosynthetic strain while these levels were markedly reduced in dark-adapted cells (Shigeoka et al. 1986b). Simultaneous increases in chlorophyll and α-tocopherol have been reported for *Euglena* cells (Takeyama et al. 1997) while Carballo-Cardenas et al. (2003) demonstrated that α-tocopherol levels did not change correlating with chlorophyll levels. A relationship has also been observed between tocopherol levels and oxidative stress treatments. Low temperature stress was previously reported to cause a 6- to 7-fold enhancements in α-tocopherol production in photoheterotrophically cultured *Euglena* (Ruggeri et al. 1985). On the other hand, oxygen stress caused a decline in α-tocopherol with a concomitant increase in α-tocopherylquinone, the natural oxidation product of α-tocopherol (Whistance and Threlfall 1970).

Tocotrienols differ from their corresponding tocopherols by the presence of three isolated double bonds in their prenyl side chains. The unsaturated side chain in tocotrienols allows them to penetrate tissues with saturated fatty layers such as the brain and liver more efficiently (Ogbonna 2009). They are very effective oxygen radical scavengers in lipophilic environments such as oils and the lipid layer of biological

membranes. All four derivatives (α, β, γ, and δ) occur in plant tissue and photosynthetic microbial cells; however, their concentrations and relative proportions depend on the plant species, tissues, microalgae species, and culture conditions (Ogbonna 2009; Dörmann 2007). α-tocotrienol levels of photoheterotrophically cultured *Euglena* gradually decreased with the age of the culture (Ruggeri et al. 1985). Low temperature and oxygen stresses also caused declines in α-tocotrienol levels.

2-Methyl-6-phytylplastoquinol and 2,3-dimethyl-5-phytyl-1,4-benzoquinone, tocopherols intermediates, have been detected in *E. gracilis Z* (Thomas and Threlfall 1975). *Euglena* γ-tocopherol methyltransferase, catalyzes the final step of α-tocopherol biosynthesis, and it has been partially purified and characterized (Shigeoka et al. 1992). This enzyme loosely binds to the outer membrane of chloroplasts. Its activity was shown to be higher with γ-tocopherol than with β- and δ-tocopherols as a substrate. It was specific for *S*-adenosylmethionine as a methyl donor with a K_m value of 50 μM. The addition of homogentisic acid, L-tyrosine, or L-phenylalanine into the *Euglena* growth medium increased the pool size of α- and γ-tocopherols but not that of β- and δ-tocopherols (Shigeoka et al. 1992). Tocopherol levels in the chloroplasts of *Euglena* were found to be higher than those in any other fraction after the addition of all of the above precursors suggesting that α-tocopherol is produced in chloroplasts of *Euglena*. It has not yet been determined whether tocopherols are synthesized in other organelles or are transported from the chloroplast to other organelles.

5.3.3 Vitamin D

Vitamin D has two main forms, D2 and D3. Vitamin D3 is the endogenous form produced by humans. Biosynthesis begins with the photoisomerization of provitamin D3 (7-dehydrocholesterol) by ultraviolet (UV) radiation to form vitamin D3 (cholecalciferol) in cutaneous tissue. Most foods contain small amounts of vitamin D, except for fatty fish which contain D3 (Mabey and Honsawek 2015).

Vitamin D2 (ergocalciferol) is sourced from the UV irradiation of ergosterol, which is a steroid found in some plants, but largely in fungi (Tripkovic et al. 2012). The conversion of vitamin D2 and D3 into active compounds requires a 2-step enzymatic hydroxylation process (Tripkovic et al. 2012). At the first site of synthesis, the liver, vitamins D2 and D3 are converted to 25-hydroxyvitamin D *via* the action of 25-hydroxylase. The kidney is the site of the second step of synthesis in which 1α-hydroxylase converts 25-hydroxyvitamin D to 1,25-dihydroxy-vitamin D2 or D3.

Ergosterol has become so established as the sole fungal sterol that it is used as a marker to estimate fungal biomass in plants and soil (Weete et al. 2010). Ergosterol is a sterol that is found in the cell membranes of fungi and protozoa serving many of the same functions as cholesterol in animal cells. *Leishmania* and *Trypanosoma* parasites have been shown to produce ergosterol-related sterols by a biosynthetic pathway similar to that operating in pathogenic fungi (Roberts et al. 2003). Stern et al. (1960) isolated ergosterol as the main sterol from *Euglena* cells grown under various conditions. Brandt et al. (1970) reported that *E. gracilis* contained various sterol compounds including ergosterol. A previous study demonstrated that ergosterol accounted for 30% and 73% of all sterols in light-grown and dark-grown cells, respectively (Anding and Ourisson 1973).

5.3.4 Vitamin K

Vitamin K is an essential fat-soluble vitamin existing in multiple dietary forms. Vitamin K1 (phylloquinone) is the predominant dietary form and is primarily found in green leafy vegetables and their oils. Vitamin K2 (menaquinone) is primarily synthesized by bacteria and is found at markedly lower amounts in meat, dairy, and fermented food products. It plays an important role as a co-factor for the post-translational γ-carboxylation of glutamic acid residues in a

number of proteins however new roles for vitamin K in bone, cardiovascular, and metabolic health are emerging (Walther et al. 2013; Margueritta et al. 2014). The physiological role of phylloquinone is as an electron transfer cofactor in photosystem I (Nowicka and Kruk 2010).

The classical menaquinone biosynthetic pathway includes the following steps; chorismate derived from the shikimate pathway is initially converted into isochorismate by isochorismate synthase, and then into 2-succinyl-6-hydroxy-2,4-cyclohexadiene-1-carboxylate, which is dehydrated to give *o*-succinylbenzoate, followed by the attachment of CoA to yield *o*-succinylbenzoyl-CoA. *o*-Succinylbenzoyl-CoA is then converted into 1,4-dihydroxy-2-naphthoate. In the last two steps of the pathway, menaquinone is synthesized by catalyzing prenylation and *S*-adenosylmethionine-dependent methylation, respectively (Hiratsuka et al. 2008). The biosynthetic pathway of phylloquinone is analogous to that of menaquinones. The principle reactions involved in phylloquinone biosynthesis in plants occur in the inner chloroplast envelope membrane. The isoprenoid chain can be synthesized by two distinct and independent biosynthetic pathways; the MVA and the DXP pathway. Higher plants use both pathways. The DXP pathway proceeds in plastids while enzymes in the MVA pathway are found in the cytosolic compartment (Nowicka and Kruk 2010). Among photosynthetic eukaryotes, the chlorophytes *Scenedesmus obliquus*, *C. reinhardtii*, and *Chlorella fusca* use the DXP pathway exclusively while the rhodophyte *Cyanidium caldarum* and the heterokontophyte *Ochromonas danica* possess both the DXP pathway and MVA pathway. *E. gracilis* uses the MVA pathway for the synthesis of all isoprenoids (Lange et al. 2000).

The synthesis of the phylloquinone precursors, o-succinylbenzoate and 1,4-dihydroxy-2-naphthoate was previously determined using *E. gracilis* Z and the derived aplastidic mutant PR-4 (Seeger and Bentley 1991). The enzymes involved in the synthesis of *o*-succinylbenzoate from isochorismate and 2-ketogluarate are located in the cytosol and linked to the presence and development of the photosynthetic apparatus. Evidence for the synthesis of 1,4-dihydroxy-2-naphthoate from *o*-succinylbenzoate suggests that these enzymes are associated with chloroplasts and synthesis occurs at the chloroplast envelope membrane.

5.3.5 Production of Vitamins by *Euglena* Cells

E. gracilis Z is one of the few microorganisms that simultaneously produce antioxidant vitamins such as β-carotene and vitamins C and E. In order to efficiently produce these vitamins, cells have been grown photoheterotrophically and transferred to photoautotrophic conditions (Takeyama et al. 1997). When *E. gracilis* Z cells were grown in fed-batch culture under photoheterotrophic conditions, their density reached 19 g L medium^{-1} after 145 h. The subsequent transfer of these cells to photoautotrophic conditions increased the vitamin content to 71.0 mg L^{-1} of β-carotene, 30.1 mg L^{-1} of vitamin E (α-tocopherol), and 86.5 mg L^{-1} of vitamin C.

When *Euglena* was grown at 27 °C for 6 days in the illumination in heterotrophic medium supplemented with an excess of each of the following water-soluble vitamins and related compounds (vitamin B1, vitamin B2, vitamin B6, vitamin B12, vitamin C, biotin, folic acid, pantothenic acid, nicotinic acid, and *p*-aminobenzoic acid), none of the added vitamins affected cell growth and *Euglena* cells took up and accumulated nicotinic acid and vitamins B1 and B12, but not the other vitamins (Ochi et al. 1988b). The maximum intracellular content of the vitamins in cells grown at 27 °C for 6 days in the light were: vitamin B1, 7.9 ± 0.3 (mg; 100 g dry basis); vitamin B2, 3.5 ± 0.2; vitamin B6, 7.5 ± 0.6; vitamin B12, 1.4 ± 0.2; vitamin C, 27.2 ± 0.4; folic acid, 1.7 ± 0.5; pantothenic acid, 12.9 ± 0.1; nicotinic acid, 41.0 ± 0.2; biotin, 4.6 ± 0.3.

When the effect of mixed carbon sources (glucose and ethanol) on the growth and production of vitamin E and β-carotene by *Euglena* was investigated in batch culture, the mixed carbon sources enhanced cell growth but the cellular content of

the antioxidant vitamins was low (Afiukwa and Ogbonna 2007). On the other hand, vitamin E levels in photoheterotrophically grown *E. gracilis* Z were increased more by ethanol addition than addition of various sugars (Fujita et al. 2008). In chloroplast-deficient mutants, the addition of ethanol also resulted in increased vitamin E levels and membrane-electric potential reflecting mitochondrial activity. When a mixture of glucose and ethanol was added to photoheterotrophically grown wild *E. gracilis* Z, vitamin E productivity was 38.9 μg L^{-1} h^{-1}, which was higher than the value obtained without the addition of an organic carbon source (9.2 μg L^{-1} h^{-1}). Furthermore, under fed-batch cultivation in the presence of glucose and ethanol using an internally illuminated photobioreactor, vitamin E productivity reached 162.7 μg L^{-1} h^{-1}. Similar increase in vitamin E productivity by the addition of ethanol to bleached *Euglena* cells were also reported by Rodríguez-Zavala et al. (2010). Although antioxidant content of cells grown under photoautotrophic conditions was higher than in cells grown photoheterotrophically or heterotrophically (Shigeoka et al. 1980; Hosotani and Kitaoka 1984), biomass production under photoautotrophic conditions was low. Ogbonna et al. (1999) previously reported that vitamin E levels in *Euglena* cells sequentially grown under heterotrophic conditions using ethanol and then under photoautotrophic conditions using corn steep liquor as a nitrogen source reached 1.7 mg g^{-1} D.W. Cells continuously cultivated heterotrophically in a mini-jar fermenter in which the effluent was continuously passed through the photobioreactor, produced 7 g L^{-1} (1.1 mg g^{-1} D.W.) of α-tocopherol after more than 420 h, resulting in productivity of 100 μg L^{-1} h^{-1}.

Notes The authors declare no competing financial interest.

References

Afiukwa CA, Ogbonna JC (2007) Effects of mixed substrates on growth and vitamin production by *Euglena gracilis*. African J Biotechnol 6:2612–2615

Agius F, González-Lamothe R, Caballero JL, Muñoz-Blanco J, Botella MA, Valpuesta V (2003) Engineering increased vitamin C levels in plants by overexpression of a D-galacturonic acid reductase. Nat Biotechnol 21:177–181

Ahn IP, Kim S, Lee YH (2005) Vitamin B1 functions as an activator of plant disease resistance. Plant Physiol 138:1505–1515

Anding C, Ourisson G (1973) Presence of ergosterol in light-grown and dark-grown *Euglena gracilis* Z. Eur J Biochem 34:345–346

Atkinson JP, Weiss A, Ito M, Kelly J, Parker CW (1979) Effects of ascorbic acid and sodium ascorbate on cyclic nucleotide metabolism in human lymphocytes. J Cyclic Nucleotide Res 5:107–123

Bacher A, Eberhardt S, Fischer M, Kis K, Richter G (2000) Biosynthesis of vitamin B_2 (riboflavin). Annu Rev Nutr 20:153–167

Baker RB, McLaughlin JJA, Hutner SH, DeAngelis B, Feingold S, Frank O, Baker H (1981) Water-soluble vitamins in cells and spent culture supernatants of *Poteriochromonas stipitata*, *Euglena gracilis*, and *Tetrahymena thermophila*. Arch Microbiol 129:310–313

Banerjee RV, Matthews RG (1990) Cobalamin-dependent methionine synthase. FASEB J 4:1450–1459

Bartoli CG, Pastori GM, Foyer CH (2000) Ascorbate biosynthesis in mitochondria is linked to the electron transport chain between complexes III and IV. Plant Physiol 123:335–344

Basset GJC, Quinlivan EP, Gregory JF III, Hanson AD (2005) Folate synthesis and metabolism in plants and prospects For biofortification. Crop Sci 45:449–453

Begley TP, Downs DM, Ealick SE, McLafferty FW, Van Loon AP, Taylor S, Campobasso N, Chiu HJ, Kinsland C, Reddick JJ, Xi J (1999) Thiamin biosynthesis in prokaryotes. Arch Microbiol 171:293–300

Begley TP, Ealick SE, McLafferty FW (2012) Thiamin Biosynthesis - still yielding fascinating biological chemistry. Biochem Soc Trans 40:555–560

Berrin JG, Pierrugues O, Brutesco C, Alonso B, Montillet JL, Roby D, Kazmaier M (2005) Stress induces the expression of AtNADK-1, a gene encoding a NAD(H) kinase in *Arabidopsis thaliana*. Mol Gen Genomics 273:10–19

Bradbeer C (1971) Transport of vitamin B12 in *Ochromonas malhamensis*. Arch Biochem Biophys 144:184–192

Bradbeer C, Woodrow ML (1976) Transport of vitamin B12 in *Escherichia coli*: energy-dependence. J Bacteriol 128:99–104

Brandt RD, Pryce RJ, Anding C, Ourisson G (1970) Sterol biosynthesis in *Euglena gracilis* Z. Comparative study of free and bound sterols in light and dark grown *Euglena gracilis* Z. Eur J Biochem 17:344–349

Bre MH, Diamond J, Jacques R (1975) Factors mediating the vitamin B12 requirement of *Euglena*. J Protozool 22:432–434

Brown GM (1962) The biosynthesis of folic acid II. Inhibition by sulfonamides. J Biol Chem 237:536–540

Carballo-Cardenas EC, Tuan PM, Janssen M, Wijffels RH (2003) Vitamin E (α-tocopherol) production by the marine microalgae *Dunaliella tertiolecta* and

Tetraselmis suecica in batch cultivation. Biomolecular Eng 20:139–147
Carell EF (1969) Studies on chloroplast development and replication in *Euglena*. I. Vitamin B12 and chloroplast replication. J Cell Biol 41:431–440
Carell EF, Seeger JW Jr (1980) Ribonucleotide reductase activity in vitamin B12-deficient *Euglena gracilis*. Biochem J 188:573–576
Carell EF, Johnston PL, Christopher AR (1970) Vitamin B12 and the macromolecular composition of *Euglena*. J Cell Biol 47:525–530
Carré IA, Edmunds LN Jr (1992) Oscillator control of cell division in *Euglena*: cyclic AMP oscillations mediate the phasing of the cell division cycle by the circadian clock. J Cell Sci 104:1163–1173
Chai MF, Chen QJ, An R, Chen YM, Chen J, Wang XC (2005) NADK2, an Arabidopsis chloroplastic NAD kinase, plays a vital role in both chlorophyll synthesis and chloroplast protection. Plant Mol Biol 59:553–564
Chai MF, Wei PC, Chen QJ, An R, Chen J, Yang S, Wang XC (2006) NADK3, a novel cytoplasmic source of NADPH, is required under conditions of oxidative stress and modulates abscisic acid responses in Arabidopsis. Plant J 47:665–674
Choi JH, Yates Z, Veysey M, Heo YR, Lucock M (2014) Contemporary Issues Surrounding Folic Acid Fortification Initiatives. Prev Nutr Food Sci 19:247–260
Cook JR (1968) The cultivation and growth of Euglena. In: Buetow DE (ed) The biology of *Euglena*, vol 1. Academic Press, New York, pp 243–314
Cramer M, Myers J (1952) Growth and photosynthetic characteristics of *Euglena gracilis*. Arch Microbiol 17:384–402
Croft MT, Warren MJ, Smith AG (2006) Algae need their vitamins. Eukaryot Cell 5:1175–1183
Crosti P, Bianchetti R (1983) Identification and cell level of folate derivatives from growing cultures of streptomycin-bleached *Euglena gracilis*. Plant Sci Lett 31:205–214
Crosti P, Lorusso V, Bianchetti R (1984) Folate cell content and distribution during the culture cycle of *Euglena gracilis*. Plant Sci Lett 34:363–368
Crosti P, Gambini A, Bianchetti R (1987) Repression of folate synthesis in the logarithmic phase of *Euglena gracilis* growth. Plant Sci 50:91–86
Delo J, Ernst-Fonberg ML, Bloch K (1971) Fatty acid synthases from *Euglena gracilis*. Arch Biochem Biophys 143:384–391
Di Nello RK, Ernst-Fonberg ML (1973) Purification and partial characterization of an acyl carrier protein from *Euglena gracilis*. J Biol Chem 248:1707–1711
Dolphin WD (1970) Photoinduced carotenogenesis in chlorotic *Euglena gracilis*. Plant Physiol 46:685–691
Dörmann P (2007) Functional diversity of tocochromanols in plants. Planta 225:269–276
Evers A, Ernst-Fongerg ML (1974) Differential responses of two carboxylases from *Euglena* to the state of chloroplast development. FEBS Lett 46:234–235
Falk J, Munné-Bosch S (2010) Tocochromanol functions in plants: antioxidation and beyond. J Exp Bot 61:1549–1566
Fenton WA, Ambani LM, Rosenberg LE (1976) Uptake of hydroxocobalamin by rat liver mitochondria. Binding to a mitochondrial protein. J Biol Chem 251:6616–6623
Fenton WA, Hack AM, Willard HF, Gertler A, Rosenberg LE (1982) Purification and properties of methylmalonyl coenzyme a mutase from human liver. Arch Biochem Biophys 214:815–826
Fischer M, Schott AK, Römisch W, Ramsperger A, Augustin M, Fidler A, Bacher A, Richter G, Huber R, Eisenreich W (2004) Evolution of vitamin B2 biosynthesis. A novel class of riboflavin synthase in Archaea. J Mol Biol 343:267–278
Fischer M, Haase I, Feicht R, Schramek N, Köhler P, Schieberle P, Bacher A (2005) Evolution of vitamin B2 biosynthesis: riboflavin synthase of *Arabidopsis thaliana* and its inhibition by riboflavin. Biol Chem 386:417–428
Frenkel EP, Mukherjee A, Hackenbrock CR, Srere PA (1976) Biochemical and ultrastructural hepatic changes during vitamin B12 deficiency in animals and man. J Biol Chem 251:2147–2154
Fujita T, Aoyagi H, Ogbonna JC, Tanaka H (2008) Effect of mixed organic substrate on α-tocopherol production by *Euglena gracilis* in photoheterotrophic culture. Appl Microbiol Biotechnol 79:371–378
Gerster H (1997) Vitamin A-functions, dietary requirements and safety in humans. Int J Vit Nutr Res 67:71–90
Giancaspero TA, Locato V, de Pinto MC, De Gara L, Barile M (2009) The occurrence of riboflavin kinase and FAD synthetase ensures FAD synthesis in tobacco mitochondria and maintenance of cellular redox status. FEBS J 276:219–231
Gleason FK, Hogenkamp HPC (1970) Ribonucleotide reductase from *Euglena gracilis*, a deoxyadenosylcobalamin-dependent enzyme. J Biol Chem 245:4894–4899
Goldberg I, Bloch K (1972) Fatty acid synthetases in *Euglena gracilis*. J Biol Chem 247:7349–7357
Goyer A (2010) Thiamine in plants: Aspects of its metabolism and functions. Phytochemistry 71:1615–1624
Grimm P, Risse JM, Cholewa D, Müller JM, Beshay U, Friehs K, Flaschel E (2015) Applicability of *Euglena gracilis* for biorefineries demonstrated by theproduction of α-tocopherol and paramylon followed by anaerobicdigestion. J Biotechnol 215:72–79
Grün M, Loewus FA (1984) L-Ascorbic-acid biosynthesis in the euryhaline diatom *Cyclotella cryptica*. Planta 160:6–11
Haase I, Gräwert T, Illarionov B, Bacher A, Fisher M (2014) Recent advantage in riboflavin biosynthesis. Methods Mol Biol 1146:15–40
Hamilton FD (1974) Ribonucleotide reductase from *Euglena gracilis*. A 5′-deoxyadenosylcobalamin-dependent enzyme. J Biol Chem 249:4428–4434
Han YS, Bratt JM, Hogenkamp HPC (1984) Purification and characterization of methylmalonyl-CoA mutase

from *Ascaris lumbricodes*. Comp Biochem Physiol 78B:41–45

Hashida S, Takahashi H, Uchimiya H (2009) The role of NAD biosynthesis in plant development and stress responses. Ann Bot 103:819–824

Helliwell KE, Wheeler GL, Leptos KC, Goldstein RE, Smith AG (2011) Insights into the evolution of vitamin B12 auxotrophy from sequenced algal genomes. Mol Biol Evol 28:2921–2933

Hellmann H, Mooney S (2010) Vitamin B6: A Molecule for Human Health? Molecules 15:442–459

Helsper JP, Kagan L, Hilby CL, Maynard TM, Loewus FA (1982) L-Ascorbic acid biosynthesis in *Ochromonas danica*. Plant Physiol 69:465–468

Hiratsuka T, Furihata K, Ishikawa J, Yamashita H, Itoh N, Seto H, Dairi T (2008) An alternative menaquinone biosynthetic pathway operating in microorganisms. Science 321:1670–1673

Hosotani K, Kitaoka S (1984) Determination of provitamin A in *Euglena gracilis* Z by high performance liquid chromatography and changes of the contents under various culture conditions. J Jpn Soc Nutr Food Sci 37:519–524

Iacopetta D, Carrisi C, De Filippis G, Calcagnile VM, Cappello AR, Chimento A, Curcio R, Santoro A, Vozza A, Dolce V, Palmieri F, Capobianco L (2010) The biochemical properties of the mitochondrial thiamine pyrophosphate carrier from *Drosophila melanogaster*. FEBS J 277:1172–1181

Inui H, Miyatake K, Nakano Y, Kitaoka S (1984) Fatty acid synthesis in mitochondria of *Euglena gracilis*. Eur J Biochem 142:121–126

Inui H, Miyatake K, Nakano Y (1986) Kitaoka S (1986) Purification and some properties of short chain-length specific *trans*-2-enoyl-CoA reductase in mitochondria of *Euglena gracilis*. J Biochem 100:995–1000

Inui H, Ono K, Miyatake K, Nakano Y, Kitaoka S (1987) Purification and characterization of pyruvate:NADP$^+$ oxidoreductase in *Euglena gracilis*. J Biol Chem 262:9130–9135

Inui H, Yamaji R, Saidoh H, Miyatake K, Nakano Y, Kitaoka S (1991) Pyruvate:NADP$^+$ oxidoreductase from *Euglena gracilis*: limited proteolysis of the enzyme with trypsin. Arch Biochem Biophys 286:270–276

Inui H, Ohya O, Isegawa Y, Kitaoka S, Miyatake K, Nakano Y (1996) Effect of cobalamin deficiency on the biosynthesis of phosphatidylcholine in *Euglena gracilis*. J Euk Microbiol 43:177–180

Isegawa Y, Nakano Y, Kitaoka S (1984) Conversion and distribution of cobalamin in *Euglena gracilis* Z, with special reference to its location and probable function within chloroplasts. Plant Physiol 76:814–818

Isegawa Y, Nakano Y, Kitaoka S (1987) Photosynthesis of *Euglena gracilis* under cobalamin-sufficient and -limited growing conditions. Plant Physiol 84:609–612

Isegawa Y, Watanabe F, Kitaoka S, Nakano Y (1994) Subcellular distribution of cobalamin-dependent methionine synthase in *Euglena gracilis* Z. Phytochemistry 35:59–61

Iseki M, Matsunaga S, Murakami A, Ohno K, Shiga K, Yoshida K, Sugai M, Takahashi T, Hori T, Watanabe M (2002) A blue-light activated adenylyl cyclase mediates photoavoidance in *Euglena gracilis*. Nature 415:1047–1051

Ishikawa T, Shigeoka S (2008) Recent advances in ascorbate biosynthesis and the physiological significance of ascorbate peroxidase in photosynthesizing organisms. Biosci Biotechnol Biochem 72:1143–1154

Ishikawa T, Masumoto I, Iwasa N, Nishikawa H, Sawa Y, Shibata H, Nakamura A, Yabuta Y, Shigeoka S (2006) Functional characterization of D-galacturonic acid reductase, a key enzyme of the ascorbate biosynthesis pathway, from *Euglena gracilis*. Biosci Biotechnol Biochem 70:2720–2726

Ishikawa T, Nishikawa H, Gao Y, Sawa Y, Shibata H, Yabuta Y, Maruta T, Shigeoka S (2008) The pathway via D-galacturonate/L-galactonate is significant for ascorbate biosynthesis in *Euglena gracilis*: identification and functional characterization of aldonolactonase. J Biol Chem 283:31133–31141

Jordan A, Reichard P (1998) Ribonucleotide reductases. Annu Rev Biochem 67:71–98

Julliard JH, Douce R (1991) Biosynthesis of the thiazole moiety of thiamin (vitamin B1) in higher plant chloroplasts. Proc Natl Acad Sci U S A 88:2042–2045

Keeling PJ (2010) The endosymbiotic origin, diversification and fate of plastids. Philos Trans R Soc Lond Ser B Biol Sci 365:729–748

Kenley JS, Leighton M, Bradbeer C (1978) Transport of vitamin B12 in *Escherichia coli.* Corrinoid specificity of the outer membrane receptor. J Biol Chem 253:1341–1346

Kitaoka S, Nakano Y, Miyatake K, Yokota A (1989) Enzymes and their functional location. In: Buetow DE (ed) Biology of Euglena, vol 4. Academic Press, New York, pp 1–135

Kiyota M, Numayama N, Goto K (2006) Circadian rhythms of the L-ascorbic acid level in *Euglena* and spinach. J Photochem Photobiol B 84:197–203

Kolhouse JF, Allen RH (1977) Absorption, plasma transport, and cellular retention of cobalamin analogues in the rabbit. Evidence for the existence of multiple mechanisms that prevent the absorption and tissue dissemination of naturally occurring cobalamin analogues. J Clin Invest 60:1381–1392

Kinsky NI, Goldsmith TH (1960) The carotenoids of the flagellated alga, *Euglena gracilis*. Arch Biochem Biophys 91:271–279

Lange BM, Rujan T, Martin W, Croteau R (2000) Isoprenoid biosynthesis: The evolution of two ancient and distinct pathways across genomes. Proc Natl Acad Sci U S A 97:13172–13177

Laval-Martin DL, Carré IA, Barbera SJ, Edmunds LN Jr (1990a) Circadian variations in the affinities of NAD kinase and NADP phosphatase for their substrates, NAD$^+$ and NADP$^+$, in dividing and nondividing cells of the achlorophyllous ZC mutant of *Euglena gracilis* Klebs (strain Z). Chronobiol Int 7:99–105

Laval-Martin DL, Carré IA, Barbera SJ, Edmunds LN Jr (1990b) Rhythmic changes in the activities of NAD

kinase and NADP phosphatase in the Achlorophyllous ZC mutant of *Euglena gracilis* Klebs (Strain Z). Arch Biochem Biophys 276:433–441

Lawrence CC, Stubbe J (1998) The function of adenosylcobalamin in the mechanism of ribonucleotide triphosphate reductase from *Lactobacillus leichimannii*. Curr Opin Chem Biol 2:650–655

Leclerc D, Campeau E, Goyette P, Adjalla CE, Christensen B, Ross M, Eydoux P, Rosenblatt DS, Rozen R, Gravel RA (1996) Human methionine synthase: cDNA cloning and identification of mutations in patients of the cblG complementation group of folate/cobalamin disorders. Human Mol Genet 5:1867–1874

Lee HC (2001) Physiological functions of cyclic ADP-ribose and NAADP as calcium messengers. Annu Rev Pharmacol Toxicol 41:317–345

Leedale GF, Messue BJD, Pringsheim EG (1965) Structure and physiology of *Euglena spirogyra*. Arch Mikrobiol 50:133–155

Lefort-Tran M, Bre MH, Pouphile M, Manigault P (1987) DNA flow cytometery of control *Euglena* and cell cycle blockage of vitamin B12-starved cells. Cytometry 8:46–54

Lindhurst MJ, Fiermonte G, Song S, Struys E, De Leonardis F, Schwartzberg PL, Chen A, Castegna A, Verhoeven N, Mathews CK, Palmieri F, Biesecker LG (2006) Knockout of Slc25a19 causes mitochondrial thiamine pyrophosphate depletion, embryonic lethality, CNS malformations, and anemia. Proc Natl Acad Sci U S A 103:15927–15932

Londesborough JC, Webster Jr LT (1974) Fatty acyl-CoA syntetases. In The enzymes (Boyer PD), vol. 10, Academic Press, New York, pp. 469–488.

Mabey T, Honsawek S (2015) Role of vitamin D in osteoarthritis: molecular, cellular, and clinical perspectives. Int J Endocrinol 3839

Margueritta S, El Asmar MS, Naoum JN, Arbid EJ (2014) Vitamin K dependent proteins and the role of vitamin K2 in the modulation of vascular calcification: A review. Oman Med J 29:172–177

Marobbio CM, Vozza A, Harding M, Bisaccia F, Palmieri F, Walker JE (2002) Identification and reconstitution of the yeast mitochondrial transporter for thiamine pyrophosphate. EMBO J 21:5653–5661

Maruta T, Yoshimoto T, Ito D, Ogawa T, Tamoi M, Yoshimura K, Shigeoka S (2012) An Arabidopsis FAD pyrophosphohydrolase, AtNUDX23, is involved in flavin homeostasis. Plant Cell Physiol 53:1106–1116

Maruyama J, Yamaoka S, Matsuo I, Tsutsumi N, Kitamoto K (2012) A newly discovered function of peroxisomes: involvement in biotin biosynthesis. Plant Signal Behav 7: 1589–1593

Masuda T, Yoshino M, Nishizaki I, Tai A, Osaki H (1980) Purification and properties of allothreonine aldolase from maise seedlings. Agric Biol Chem 44:2199–2201

Masuda T, Sakamoto M, Nishizaki I, Hayashi H, Yamamoto M, Wada H (1987) Affinity purification and characterization of serine hydroxymethyltransferase from rat liver. J Biochem 101:643–652

Masuda W, Takenaka S, Inageda K, Nishina H, Takahashi K, Katada T, Tsuyama S, Inui H, Miyatake K, Nakano Y (1997a) Oscillation of ADP-ribosyl cyclase activity during the cell cycle and function of cyclic ADP-ribose in a unicellular organism, *Euglena gracilis*. FEBS Lett 405:104–106

Masuda W, Takenaka S, Tsuyama S, Tokunaga M, Yamaji R, Inui H, Miyatake K, Nakano Y (1997b) Inositol 1,4,5-trisphosphate and cyclic ADP-ribose mobilize Ca^{2+} in a protest, *Euglena gracilis*. Comp Biochem Physiol C Pharmacol Toxicol Endocrinol 118:279–283

Masuda W, Takenaka S, Tsuyama S, Inui H, Miyatake K, Nakano Y (1999) Purification and characterization of ADP-ribosul cyclase from *Euglena gralisis*. J Biochem 125:449–453

McGuire JJ, Bertino JR (1981) Enzymatic synthesis and function of folylpolyglutamates. Mol Cell Biochem 38:19–48

Miyamoto E, Watanabe F, Yamaguchi Y, Takenaka H, Nakano Y (2004) Purification and characterization of methyl malonyl-CoA mutase from a photosynthetic coccolithophorid alga, Pleurochrysis carterae. Comp Biochem Physiol B 138:163–167

Miyamoto E, Tanioka Y, Yukino Y, Hayashi M, Watanabe F, Nakano Y (2007) Occurrence of 5′-deoxyadenosylcobalamin and its physiological function as the coenzyme of methyl malonyl-CoA mutase in a marine eukaryotic microorganism, *Schizochytrium limacinum* SR21. J Nutr Sci Vitaminol 53:471–475

Miyamoto E, Tanioka Y, Nishizawa-Yokoi A, Yabuta Y, Ohnishi K, Misono H, Shigeoka S, Nakano Y, Watanabe F (2010) Characterization of methylmalonyl-CoA mutase involved in the propionate photoassimilation of *Euglena gracilis* Z. Arch Microbiol 192:437–446

Nakazawa M, Inui H, Yamaji R, Yamamoto T, Takenaka S, Ueda M, Nakano Y, Miyatake K (2000) The origin of pyruvate:$NADP^+$ oxidoreductase in mitochondria of *Euglena gracilis*. FEBS Lett 479:155–157

Nakazawa M, Takenaka S, Ueda M, Inui H, Nakano Y, Miyatake K (2003) Pyruvate:$NADP^+$ oxidoreductase is stabilized by its cofactor, thiamin pyrophosphate, in mitochondria of *Euglena gracilis*. Arch Biochem Biophys 411:183–188

Nishikimi M, Yagi K (1996) Biochemistry and molecular biology of ascorbic acid biosynthesis. Subcell Biochem 25:17–39

Noctor G, Queval G, Gakiere B (2006) NAD(P) synthesis and pyridine nucleotide cycling in plants and their potential importance in stress conditions. J Exp Bot 57:1603–1620

Nosaka K (2006) Recent progress in understanding thiamin biosynthesis and its genetic regulation in *Saccharomyces cerevisiae*. Appl Microbiol Biotechnol 72:30–40

Nowicka B, Kruk J (2010) Occurrence, biosynthesis and function of isoprenoid quinones. Biochim Biophys Acta 1797:1587–1605

Ochi H, Shigeoka S, Watanabe F, Nakano Y, Kitaoka S (1988a) Changes of vitamin B2 and B6 contents dur-

ing growth of *Euglena gracilis*. Vitamins (Japan) 62:515–518

Ochi H, Watanabe F, Shigeoka S, Nakano Y, Kitaoka S (1988b) Water-soluble vitamin contents of *Euglena gracilis* Z. J Jpn Soc Nutr Food Sci 41:495–500

Ogbonna JC (2009) Microbiological production of tocopherols: current state and prospects. Appl Microbiol Biotechnol 84:217–225

Ogbonna JC, Tomiyama S, Tanaka H (1999) Production of α-tocopherol by sequential heterotrophic–photoautotrophic cultivation of *Euglena gracilis*. J Biotechnol 70:213–221

Pollak N, Niere M, Ziegler M (2007) NAD kinase levels control the NADPH concentration in human cells. J Biol Chem 282:33562–33571

Pou de Crescenzo MA, Goto K, Carré IA, Laval-Martin DL (1997) Regulation of a NAD^+ kinase activity isolated from asynchronous cultures of the achlorophyllous ZC mutant of *Euglena gracilis*. Z Naturforsch C 52:623–635

Rapala-Kozik M, Kowalska E, Ostrowska K (2008) Modulation of thiamine metabolism in *Zea mays* seedlings under conditions of abiotic stress. J Exp Bot 59:4133–4143

Ravanel S, Gakiere B, Job D, Douce R (1998) The specific features of methionine biosynthesis and metabolism in plants. Proc Natl Acad Sci U S A 95:7805–7812

Rawat R, Sandoval FJ, Wei Z, Winkler R, Roje S (2011) An FMN hydrolase of the haloacid dehalogenase superfamily is active in plant chloroplasts. J Biol Chem 286:42091–42098

Rebou E (2013) Absorption of vitamin A and carotenoids by the enterocyte: Focus on transport proteins. Nutrients 5:3563–3581

Reichard P (1993) The anaerobic ribonucleotide reductase from *Escherichia coli*. J Biol Chem 268:8383–8386

Roberts CW, McLeod R, Rice DW, Ginger M, Chance ML, Goad LJ (2003) Fatty acid and sterol metabolism: potential antimicrobial targets in apicomplexan and trypanosomatid parasitic protozoa. Mol Biochem Parasitol 126:129–142

Rodríguez-Zavala JS, Ortiz-Cruz MA, Mendoza-Hernández G, Moreno-Sánchez R (2010) Increased synthesis of α-tocopherol, paramylon and tyrosine by *Euglena gracilis* under conditions of high biomass production. J Appl Microbiol 109:2160–2172

Roje S (2007) Vitamin B biosynthesis in plants. Phytochemistry 68:1904–1921

Ross GIM (1952) Vitamin B12 assay in body fluids using *Euglena gracilis*. J Clin Pathol 5:250–256

Ruggeri BA, Gray RJH, Watkins TR, Tomlins RI (1985) Effect of low-temperature acclimation and oxygen stress on tocopherol production in *Euglena gracilis* Z. Appl Environ Microbiol 50:1404–1408

Running JA, Severson DK, Schneider KJ (2002) Extracellular production of L-ascorbic acid by *Chlorella protothecoides*, *Prototheca* species, and mutants of *P. moriformis* during aerobic culturing at low pH. J Ind Microbiol Biotechnol 29:93–98

Running JA, Burlingame RP, Berry A (2003) The pathway of L-ascorbic acid biosynthesis in the colourless microalga *Prototheca moriformis*. J Exp Bot 54:1841–1849

Saint-Macary ME, Barbisan C, Gagey MJ, Frelin O, Beffa R, Lebrun MH, Droux M (2015) Methionine biosynthesis is essential for infection in the rice blast fungus *Magnaporthe oryzae.* PLos One: pone.0111108.

Sakamoto M, Masuda T, Yanagimoto Y, Nakano Y, Kitaoka S (1991) Purification and characterization of cytosolic serine hydroxylmethyltransferase from *Euglena gracilis* Z. Agric Biol Chem 55:2243–2249

Sakamoto M, Masuda T, Yanagimoto Y, Nakano Y, Kitaoka S, Tanigawa Y (1996) Purification and characterization of serine hydroxylmethyltransferase from mitochondria of *Euglena gracilis* Z. Biosci Biotechnol Biolchem 60:1941–1944

Sandoval FJ, Roje S (2005) An FMN hydrolase is fused to a riboflavin kinase homolog in plants. J Biol Chem 280:38337–38345

Sandoval FJ, Zhang Y, Roje S (2008) Flavin nucleotide metabolism in plants: monofunctional enzymes synthesize fad in plastids. J Biol Chem 283:30890–30900

Sang Y, Barbosa JM, Wu H, Locy RD, Singh NK (2007) Identification of a pyridoxine (pyridoxamine) 5'-phosphate oxidase from *Arabidopsis thaliana*. FEBS Lett 581:344–348

Sarhan F, Houde M, Cheneval JP (1980) The role of vitamin B12 binding in the uptake of the vitamin by *Euglena gracilis*. J Protozool 27:235–238

Sayed SA, Gadallah MAA (2002) Effects of shoot and root application of thiamin on salt-stressed sunflower plants. Plant Growth Regul 36:71–80

Seeger JW, Bentley R (1991) Phylloquinone (vitamin K1) biosynthesis in *Euglena gracilis* strain Z. Pytochemistry 30:3585–3589

Seeger JW Jr, Carell EF (1991) Respiration of *Euglena gracilis* grown under conditions of vitamin B12-sufficiency,—deficiency, and -replenishment. Plant Sci 79:143–148

Shane B (2011) Folate status assessment history: implications for measurement of biomarkers in NHANES. Am J Clin Nutr 94:337S–342S

Shehata TE, Kempner ES (1979) Synchronization of division in vitamin B12-starved *Euglena gracilis*. J Protozool 26:626–630

Shigeoka S, Nakano Y (1991) Characterization and molecular properties of 2-oxoglutarate decarboxylase from *Euglena gracilis*. Arch Biochem Biophys 288:22–28

Shigeoka S, Nakano Y (1993) The effect of thiamin on the activation of thiamin pyrophosphate-dependent 2-oxoglutarate decarboxylase in *Euglena gracilis*. Biochem J 292:463–467

Shigeoka S, Yokota A, Nakano Y, Kitaoka S (1979a) The effect of illumination on the L-ascorbic acid content in *Euglena gracilis z.* Agric Biol Chem 43: 2053–2058

Shigeoka S, Nakano Y, Kitaoka S (1979b) The biosynthetic pathway of L-ascorbic acid in *Euglena gracilis z.* J Nutr Sci Vitaminol 25: 299–307

Shigeoka S, Nakano Y, Kitaoka S (1979c) Some properties and subcellular localization of L-gulono-γ-lactone dehydrogenase in *Euglena gracilis z*. Agric Biol Chem 43: 2187–2188

Shigeoka S, Nakano Y, Kitaoka S (1980) Occurrence of L-ascorbic acid in *Euglena gracilis* Z. Bull Univ Osaka Pref ser B 32:43–48

Shigeoka S, Onishi T, Maeda K, Nakano Y, Kitaoka S (1986a) Occurrence of thiamine pyrophosphate-dependent 2-oxoglutarate dehydrogenase in mitochondria of *Euglena gracilis*. FEBS Lett 195:43–47

Shigeoka S, Onishi T, Nakano Y, Kitaoka S (1986b) The contents and subcellular distribution of tocopherols in *Euglena gracilis*. Agric Biol Chem 50:1063–1065

Shigeoka S, Onishi T, Nakano Y, Kitaoka S (1987a) Requirement for Vitamin B_1 for growth of *Euglena gracilis*. J Gen Microbiol 133:25–30

Shigeoka S, Onishi T, Kishi N, Maeda K, Ochi H, Nakano Y, Kitaoka S (1987b) Occurrence and subcellular distribution of thiamine pyrophosphokinase isozyme in *Euglena gracilis*. Agric Biol Chem 51:2811–2813

Shigeoka S, Onishi T, Maeda K, Nakano Y, Kitaoka S (1987c) Thiamin uptake in *Euglena gracilis*. Biochim Biophys Acta 929:247–252

Shigeoka S, Yasumoto R, Onishi T, Nakano Y, Kitaoka S (1987d) Properties of monodehydroascorbate reductase and dehydroascorbate reductase and their participation in the regeneration of ascorbate in *Euglena gracilis*. J Gen Microbiol 133:227–232

Shigeoka S, Ishiko H, Nakano Y, Mitsunaga T (1992) Isolation and properties of γ-tocopherol methyltransferase in *Euglena gracilis*. Biochim Biophys Acta 1128:220–226

Simoni RD, Criddle RS, Stumpf PK (1967) Fat metabolism in higher plants XXXI. Purification and properties of plant and bacterial acyl carrier proteins. J Biol Chem 242:573–581

Smirnoff N (2000) Ascorbic acid: metabolism and functions of a multi-facetted molecule. Curr Opin Plant Biol 3:229–235

Smirnoff N (2001) L-ascorbic acid biosynthesis. Vitam Horm 61:241–266

Spano AJ, Schiff JA (1987) Purification, properties, and cellular localization of *Euglena* ferredoxin-NADP reductase. Biochim Biophys Acta 894:484–498

Stephan C, Renard M, Montrichard F (2000) Evidence for the existence of two soluble NAD^+ kinase isoenzymes in *Euglena gracilis* Z. Int J Biochem Cell Biol 32:855–863

Stern AI, Schiff JA, Klein HP (1960) Isolation of Ergosterol from *Euglena gracilis*; Distribution Among Mutant Strains. J Protozool 7:52–55

Stubbe J (2003) Di-iron-tyrosyl radical ribonucleotide reductases. Curr Opin Chem Biol 7:183–188

Stupperich E, Nexo E (1991) Effect of the cobalt-N coordination on the cobamide recognition by the human vitamin B12 binding proteins intrinsic factor, transcobalanin and haptocorrin. Eur J Biochem 199: 299–303

Takahashi-Iniguez T, Garcia-Arellano H, Trujillo-Roldan MA, Flores ME (2011) Protection and reactivation of human methylmalonyl-CoA mutase by MMAA protein. Biochem Biophys Res Commun 2011(404):443–447

Takaichi S (2011) Carotenoids in algae: Distributions, biosyntheses and functions. Mar Drugs 9:1101–1118

Takeyama H, Kanamaru A, Yoshino Y, Kakuta H, Kawamura Y, Matsunaga T (1997) Production of antioxidant vitamins, beta-carotene, vitamin C, and vitamin E, by two-step culture of *Euglena gracilis* Z. Biotechnol Bioeng 53:185–190

Tani Y, Tsumura H (1989) Screening for tocopherol-producing microorganisms and α-tocopherol production by *Euglena gracilis* Z. Agric Biol Chem 53:305–312

Thomas G, Threlfall DR (1975) Synthesis of 3-polyprenyltoluquinols and 4-carboxy-2-polyprenylphenols by cell-free preparations of *Euglena gracilis*. Phytochemistry 14:2607–2615

Threlfall DR, Goodwin TW (1967) Nature, intracellular distribution and formation of terpenoid quinines in *Euglena gracilis*. Biochem J 103:573–588

Tokunaga M, Nakano Y, Kitaoka S (1976) Preparation of physiological intact mitochondria from *Euglena gracilis* Z. Agric Biol Chem 40:1439–1440

Torrents E, Trevisiol C, Rotte C, Hellman U, Martin W, Reichard P (2006) *Euglena gracilis* ribonucleotide reductase. The eukaryote class II enzyme and the possible antiquity of eukaryote B12 dependence. J Biol Chem 281:5604–5611

Tripkovic L, Lambert H, Hart K, Smith CP, Bucca G, Penson S, Chope G, Hypponen E, Berry J, Vieth R, Lanham-New S (2012) Comparison of vitamin D2 and vitamin D3 supplementation in raising serum 25-hydroxyvitamin D status: a systematic review and meta-analysis. Am J Clin Nutr 95:1357–1364

Tunc-Ozdemir M, Miller G, Song L, Kim J, Sodek A, Koussevitzky S, Misra AN, Mittler R, Shintani D (2009) Thiamin confers enhanced tolerance to oxidative stress in Arabidopsis. Plant Physiol 151: 421–432

Turner WL, Waller JC, Vanderbeld B, Snedden WA (2004) Cloning and characterization of two NAD kinases from Arabidopsis. identification of a calmodulin binding isoform. Plant Physiol 135:1243–1255

Vagelos PR (1973) Acyl group transfer (acyl carrier protein). In: Boyer PD (ed) The Enzymes, vol 8. Academic Press, New York, pp 155–199

Valpuesta V, Botella MA (2004) Biosynthesis of L-ascorbic acid in plants: new pathway for an old antioxidant. Trends Plant Sci 9:573–577

Varma TNS, Abraham A, Hansen IA (1961) Accumulation of 58Co vitamin B12 by *Euglena gracilis*. J Protozool 8:212–216

Velisek J, Davidek J (2000) Pantothenic acid. In: De Leenheer AP, Lambert WE, Van Bocxlaer JF (eds) Modern chromatographic analysis of vitamins. Marcel Dekker, Inc., New York, pp 555–600

Waldrop GL, Holden HM, St Maurice M (2012) The enzymes of biotin dependent CO_2 metabolism: What structures reveal about their reaction mechanisms. Protein Sci 21:1597–1619

Walther B, Karl JP, Booth SL, Boyaval P (2013) Menaquinones, bacteria, and the food supply: The relevance of dairy and fermented food products to vitamin K requirements. Adv Nutr 4:463–473

Watanabe F (2007) Vitamin B12 sources and bioavailability. Exp Biol Med 232:1266–1274

Watanabe F, Nakano Y (1991) Comparative biochemistry of vitamin B12 (cobalamin) metabolism: biochemical diversity in the systems for intercellular cobalamin transfer and synthesis of the coenzymes. Int J Biochem 23:1353–1359

Watanabe F, Nakano Y, Kitaoka S (1987a) Purification and some properties of cytosolic cobalamin binding protein in *Euglena gracilis*. Biochem J 247:679–685

Watanabe F, Nakano Y, Kitaoka S (1987b) Isolation and some properties of soluble and membrane-bound cobalamin-binding proteins of *Euglena* mitochondria. Arch Microbiol 149:30–35

Watanabe F, Oki Y, Nakano Y, Kitaoka S (1987c) Occurrence and subcellular location of aquacobalamin reductase in *Euglena gracilis*. Agric Biol Chem 51:273–274

Watanabe F, Oki Y, Nakano Y, Kitaoka S (1987d) Purification and characterization of aquacobalamin reductase (NADPH) from *Euglena gracilis*. J Biol Chem 262:11514–11518

Watanabe F, Nakano Y, Kitaoka S (1988a) Subcellular location and some properties of propionyl-Coenzyme A carboxylase in *Euglena gracilis* Z. Comp Biochem Physiol 89B:565–568

Watanabe F, Ito T, Tabuchi T, Nakano Y, Kitaoka S (1988b) Isolation of pellicular cobalamin-binding proteins of the cobalamin uptake system of *Euglena gracilis*. J Gen Microbiol 134:67–74

Watanabe F, Nakano Y, Ochi H, Kitaoka S (1988c) Purification, some properties and possible physiological role of an extracellular cobalamin binding protein from *Euglena gracilis*. J Gen Microbiol 134:1385–1389

Watanabe F, Oki Y, Nakano Y, Kitaoka S (1988d) Occurrence and characterization of cyanocobalamin reductase (NADPH; CN-eliminating) involved in decyanation of cyanocobalamin in *Euglena gracilis*. J Nutr Sci Vitaminol 34:1–10

Watanabe F, Nakano Y, Tamura Y, Kitaoka S (1989) Transfer system of cobalamin from pellicle to cytosolic binding proteins in *Euglena gracilis*. Comp Biochem Physiol 94B:797–800

Watanabe F, Nakano Y, Stupperich E (1992) Different corrinoid specificities for cell growth and the cobalamin uptake system in *Euglena gracilis* Z. J Gen Microbiol 138:1807–1813

Watanabe F, Nakano Y, Stupperich E, Ushikoshi U, Ushikoshi S, Ushikoshi I, Kitaoka S (1993a) A radioisotope dilution method for quantitation of total vitamin B12 in biological samples using isolated *Euglena* pellicle fragments as a solid-phase vitamin B12-binding material. Anal Chem 65:657–659

Watanabe F, Nakano Y, Tamura Y, Stupperich E (1993b) Corrinoid specificity of cytosolic cobalamin binding protein of *Euglena gracilis*. J Biochem 113:97–100

Watanabe F, Tamura Y, Stupperich E, Nakano Y (1993c) Uptake of cobalamin by *Euglena* mitochondria. J Biochem 114:793–799

Watanabe F, Yamaji R, Isegawa Y, Yamamoto T, Tamura Y, Nakano Y (1993d) Characterization of aquacobalamin reductase (NADPH) from *Euglena gracilis*. Arch Biochem Biophys 305:421–427

Watanabe F, Abe K, Tamura Y, Nakano Y (1996) Adenosylcobalamin-dependent methylmalonyl-CoA mutase isozymes in the photosynthetic protozoon *Euglena gracilis* Z. Microbiology 142:2631–2634

Watanabe F, Yabuta Y, Tanioka Y, Bito T (2013) Biologically active vitamin B12 compounds in foods for preventing deficiency among vegetarians and elderly subjects. J Agric Food Chem 61:6769–6775

Weete JD, Abril M, Blackwell M (2010) Phylogenetic Distribution of Fungal Sterols. PLoS One 5:e10899

Wheeler G, Ishikawa T, Pornsaksit V, Smirnoff N (2015) Evolution of alternative biosynthetic pathways for vitamin C following plastid acquisition in photosynthetic eukaryotes. elife 4:e06369

Whistance GR, Threlfall DR (1970) Biosynthesis of phtoquinones. Biochem J 117:593–600

Wilkinson SR, Prathalingam SR, Taylor MC, Horn D, Kelly JM (2005) Vitamin C biosynthesis in trypanosomes: a role for the glycosome. Proc Natl Acad Sci U S A 102:11645–11650

Willecke K, Ritter E, Lynen F (1969) Isolation of an acyl carrier component from the multienzyme complex of yeast fatty acid synthetase. Eur J Biochem 8:503–509

Wolpert JS, Ernst-Fonberg ML (1975) Dissociation and characterization of enzymes from a multienzyme complex involved in carbon dioxide fixation. Biochemistry 14:1103–1107

Wu F, Christen P, Gehring H (2011) A novel approach to inhibit intracellular vitamin B6-dependent enzymes: proof of principle with human and plasmodium ornithine decarboxylase and human histidine decarboxylase. FASEB J 25:2109–2122

Yabuta Y, Yoshimura K, Takeda T, Shigeoka S (2000) Molecular characterization of tobacco mitochondrial L-galactono-γ-lactone dehydrogenase and its expression in *Escherichia coli*. Plant Cell Physiol 41:666–675

Yabuta Y, Takamatsu R, Kasagaki S, Watanabe F (2013) Isolation and expression of a cDNA encoding methylmalonic aciduria type A protein from *Euglena gracilis* Z. Metabolites 3:144–154

Ying W (2008) NAD^+/NADH and $NADP^+$/NADPH in cellular functions and cell death: regulation and biological consequences. Antioxid Redox Signal 10:179–206

Yokota A, Hosotani K, Kitaoka S (1982) Mechanism of metabolic regulation in photoassimilation of propionate in *Euglena gracilis* Z. Arch Biochem Biophys 249:530–537

Yokota A, Haga S, Kitaoka S (1985) Purification and some properties of glyoxylate resuctase ($NADP^+$) and its functional location in mitochondria in *Euglena gracilis* z. Biochem J 227:211–216

Zempleni J, Teixeira DC, Kuroishi T, Cordonier EL, Baier S (2012) Biotin requirements for DNA damage prevention. Mutat Res 733:58–60

Biochemistry and Physiology of Heavy Metal Resistance and Accumulation in *Euglena*

6

Rafael Moreno-Sánchez, Sara Rodríguez-Enríquez, Ricardo Jasso-Chávez, Emma Saavedra, and Jorge D. García-García

Abstract

Free-living microorganisms may become suitable models for removal of heavy metals from polluted water bodies, sediments, and soils by using and enhancing their metal accumulating abilities. The available research data indicate that protists of the genus *Euglena* are a highly promising group of microorganisms to be used in bio-remediation of heavy metal-polluted aerobic and anaerobic acidic aquatic environments. This chapter analyzes the variety of biochemical mechanisms evolved in *E. gracilis* to resist, accumulate and remove heavy metals from the environment, being the most relevant those involving (1) adsorption to the external cell pellicle; (2) intracellular binding by glutathione and glutathione polymers, and their further compartmentalization as heavy metal-complexes into chloroplasts and mitochondria; (3) polyphosphate biosynthesis; and (4) secretion of organic acids. The available data at the transcriptional, kinetic and metabolic levels on these metabolic/cellular processes are herein reviewed and analyzed to provide mechanistic basis for developing genetically engineered *Euglena* cells that may have a greater removal and accumulating capacity for bioremediation and recycling of heavy metals.

Keywords

Heavy metals accumulation • Bioremediation • Phytochelatins • Polyphosphates

Abbreviations

β-Ala	Beta-alanine
Cd-HMWC	High molecular weight complexes of thiol-molecules with Cd^{2+}
Cd-LMWC	Low molecular weight complexes of thiol-molecules with Cd^{2+}

R. Moreno-Sánchez, Ph.D. (✉)
S. Rodríguez-Enríquez • R. Jasso-Chávez
E. Saavedra • J.D. García-García
Departamento de Bioquímica, Instituto Nacional de Cardiología Ignacio Chávez, Tlalpan, Ciudad de México 14080, México
e-mail: rafael.moreno@cardiologia.org.mx; morenosanchez@hotmail.com

S.D. Schwartzbach, S. Shigeoka (eds.), *Euglena: Biochemistry, Cell and Molecular Biology*, Advances in Experimental Medicine and Biology 979, DOI 10.1007/978-3-319-54910-1_6

*Eg*PCS	Phytochelatin synthase from *E. gracilis*
ESTs	Expressed sequence tags
DW	Dry weight
PCs	Phytochelatins
PCS	Phytochelatin synthase
PolyP	Polyphosphates

6.1 Introduction

Pollution of aquatic systems by heavy metals has become a major environmental problem; once in the aquatic systems, contaminants accumulate in sediments. For instance, in coastal zones of the Gulf of Mexico and other seas and oceans around the world, cadmium levels in sediments have risen to as much as 400 mg/Kg (Simpson 1981). Increasing cadmium concentrations in sediments of fresh water bodies due to batteries and electronics waste have also been found in recent years with the concomitant perturbation of the inhabitant microorganisms (Huang et al. 2014; Jensen and Bro-Rasmunssen 1992). Heavy metal pollution by mining and industrial activities is another current environmental problem (Table 6.1). Exceedingly high amounts of cadmium (up to 7 mg/Kg) have been found in sediments of aquatic systems 500–1900 m away from mine sites in Spain and Portugal (Luís et al. 2011; Sarmiento et al. 2011). Pollution by cadmium and other heavy metals has also been detected up to 40 km from the mining regions in China (Wang et al. 2015). These mining contaminated areas become acidic (reaching pH values of 2–4) and with high sulfate contents (40–88 mM) depending on the proximity to the perturbed areas, the mixing with water from non-polluted rivers, and the weather season. By comparison, the non-polluted sites have rather neutral pHs and low sulfate concentrations of 0.1–0.5 mM (Luís et al. 2011; Sarmiento et al. 2011; Sun et al. 2010). It should also be emphasized that the polluted water bodies and sediments contain more than one heavy metal (Table 6.1), which must be kept in mind when designing and applying bioremediation strategies.

As heavy metal pollution is extremely toxic for humans, edible plants and cattle among other living organisms, effective strategies to decrease the heavy metal concentration in water bodies, sediments and soils are being currently developed. Furthermore, the deleterious effects of heavy metals on the methane-producing anaerobic archaea inhabiting bioreactor sludges have been also

Table 6.1 Heavy metal concentrations in water bodies and sediments close to mining or industrial areas

Site	Al	As	Cd	Cr	Cu	Ni	Pb	Zn	References
	Water bodies (mg/L)								
San Pedro River, México	–	0.16	0.01	0.2	–	0.3	–	–	Gutiérrez et al. (2008)
Tigre River-San Andrés Lagoon, México	–	–	0.45	–	–	–	4	–	Vázquez-Sauceda et al. (2012)
Iberian-Pyrite Belt, Spain	80	3.8	0.1	0.01	20	0.9	0.7	72	Sarmiento et al. (2011)
Lousal mine, Portugal	178	0.02	0.3	–	9.1	2.2	1	134	Luís et al. (2011)
	Sediments (mg/Kg)								
Lerma River, México	–	–	9.6	–	246	40	109	222	Brito et al. (2015)
Baluarte River, México	–	–	0.64	106	–	–	38.5	–	Ruelas-Inzunza et al. (2011)
Grand Bay Reserve-Gulf of México, USA	–	15	2.5	25	22	8	30	11	McComb et al. (2015)
Iberian-Pyrite Belt, Spain	8000	350	2	3	1800	3.7	120	900	Sarmiento et al. (2011)
Lousal mine, Portugal	–	817	7	–	1570	93	1060	4370	Luís et al. (2011)
Changjiang River, China	–	13.5	0.09	–	22	–	25	82	Hu et al. (2015)
Mawei River, China	–	1238	16	28	672	22	1188	2536	Wang et al. (2015)

documented (Altaş 2009). Removal of heavy metals from anaerobic sediments and sludges is also a relevant ecological and economical issue.

Bio-remediation of heavy metal-polluted ecosystems is a technology that involves the removal of toxic levels of non-essential and essential heavy metals from water bodies or soils by plants, fungi, algae and other microorganisms (Ali et al. 2013; García-García et al. 2016; Hashim et al. 2011; Paul et al. 2005; Watanabe 2001). In particular, phytoremediation has been considered as an ecologically friendly and commercially viable technology to clean soils and water systems and recycle valuable heavy metals (Bhargava et al. 2012). However, a number of factors severely limits the implementation of bio-remediation strategies with plants such as (1) the slow growth rates and low biomass yields (0.2–0.8 Kg/m^2 in 12 months) of heavy metal-hyperaccumulator plants such as *Thlaspi caerulescens* and *Alyssum bertolonii* (Robinson et al. 1998; Wójcik et al. 2005). (2) The lengthy processes for complete heavy metal removal and soil regeneration; it has been considered that *T. caerulescens* might clean 1 kg soil contaminated with 100 mg cadmium in 12 years (Robinson et al. 1998). (3) The low and slow metal ion bioavailability due to the tight binding of metal ions to soil components. And (4) biomagnification, *i.e.* risk of food chain contamination in case of mismanagement and lack of proper care (Ali et al. 2013).

6.2 Use of Microorganisms for Heavy Metal Bioremediation Processes

Microalgae and other free-living microorganisms such as *E. gracilis* have surged as promising models for efficient bio-remediation and bio-recovery processes of heavy metals because they show capacities of heavy metals removal by intracellular accumulation, of similar or greater magnitude than those of plants and macroalgae (García-García et al. 2016). In addition, the problematic step of metal desorption, when using biosorption (see Sect. 6.3.1), is avoided. Furthermore, microorganisms do not require complex and expensive infrastructure facilities for growth; in parallel they may use or bio-transform residual nutrients present in wastewater or sediments such as organic matter; and they could be used simultaneously for production of biofuel and other biotechnologically relevant secondary metabolites such as essential amino acids, vitamins and the immune-potentiator paramylum. To develop efficient treatments of wastewaters or polluted sediments by bioremediation, microorganisms able to grow in the presence and absence of O_2 and with a broad metabolic plasticity are required. In particular, the use of *E. gracilis* and other protists may have many advantages over plants and macroalgae for heavy metal removal.

6.2.1 Potential Advantages of *E. gracilis* for Remediation Purposes

6.2.1.1 The Flagellated Algae-Like *E. gracilis* Is a Unicellular Cosmopolitan Protist Able to Grow and Remove Heavy Metals Under Different Environmental Conditions

For heterotrophic growth, *E. gracilis* can use a wide variety of carbon sources such as organic acids (glutamate, malate, succinate, DL-lactate and acetate), glucose and ethanol, alone or their combinations (Jasso-Chávez and Moreno-Sánchez 2003; Moreno-Sánchez et al. 2000; Rodríguez-Zavala et al. 2006, 2010), and at acidic or neutral pH values (Jasso-Chávez et al. 2010; Rodríguez-Zavala et al. 2010). In addition, *E. gracilis* and other euglenophytes are able to inhabit and even grow in wastewater bodies, which have high concentrations of heavy metals, nutritional limitations, extreme pH and extreme temperatures. It has been documented that, under heterotrophic growth conditions, *E. gracilis* bleached cells (*i.e.*, cells unable to synthesize chlorophyll and hence with no functional chloroplasts) can remove Hg^{2+}, Cd^{2+}, Cr^{6+} and Cr^{3+} (Avilés et al. 2003; Jasso-Chávez et al. 2010; Lira-Silva et al. 2011). Under photo-heterotrophic conditions, *E. gracilis* removes Cu^{2+}, Hg^{2+}, Zn^{2+},

Cd^{2+}, Pb^{2+}, Tc^{7+} and Cr^{6+} (Albergoni et al. 1980; Devars et al. 2000; Einicker-Lamas et al. 2002; García-García et al. 2009; Ishii and Uchida 2006; Mendoza-Cózatl et al. 2002, 2006a). Cd^{2+}, Zn^{2+}, Cu^{2+} and Pb^{2+} as well as the metalloid arsenic are intracellularly accumulated at comparatively high levels (Einicker-Lamas et al. 2002; Halter et al. 2012a; Mendoza-Cózatl et al. 2006a), whereas Hg^{2+} and Cr^{6+} are reduced to volatile Hg^0 (Devars et al. 2000) and insoluble Cr^{3+} (García-García et al. 2009), respectively. Removal of other heavy metal ions by *E. gracilis* such as Co^{2+}, Ni^{2+}, Ag^{+}, Au^{3+}, Al^{3+}, Fe^{2+}, Fe^{3+} and U^{3+} has not been examined, although cell growth shows high sensitivity to Au^{3+}, with an IC_{50} value of 5 μM after 3 days culture (Nam et al. 2014) and moderate sensitivity to U^{3+} with an IC_{50} of 37 μM after 4 days of culture (Trenfield et al. 2012).

Aquatic acidic ecosystems (pH < 3) mainly derive from pollution by acid mine drainages and urban areas. In these perturbed habitats no vascular plants are usually found but extensive microbial diversity grows, and *Euglena* sp. may indeed be the most abundant eukaryotic microorganism (Brown et al. 2011; Nancucheo and Johnson 2012; Prasanna et al. 2011; Ruiz et al. 2004; Sittenfeld et al. 2002). In particular, *Euglena mutabilis* is able to endure, and become the dominant eukaryotic microorganism, in these highly stressful environmental conditions, which contain a variety of heavy metals present at toxic levels (Brake et al. 2001; Casiot et al. 2004; Hargreaves et al. 1975; Nancucheo and Johnson 2012; Sittenfeld et al. 2002). Comparatively, *E. gracilis* seems absent from highly heavy metal polluted acidic environments, although it grows better than *E. mutabilis* in culture media at pH values of 2.5–8 in the absence of heavy metals (Olaveson and Nalewajko 2000). Furthermore, *E. mutabilis* shows greater tolerance to Cd^{2+}, Al^{3+}, Fe^{3+} and Ni^{2+} (2–17 times) than *E. gracilis*, and similar to Cu^{2+} and Zn^{2+}, when cultured in an acidic (pH = 2.7) culture medium (Olaveson and Nalewajko 2000); *E. mutabilis* is also more tolerant to arsenite than *E. gracilis* but not to phenylarsine oxide (Halter et al. 2012a). In addition, *E. mutabilis* is thermo-tolerant since it has been found in water bodies at 40 °C (Sittenfeld et al. 2002) whereas *E. gracilis* growth decreases above 30–34 °C (Buetow 1962). Interestingly, mining and chemical weathering produce acidic, metal-rich hot fluids because oxidation reactions of the metal-sulfide-rich rocks are highly exothermic (Baker and Banfield 2003). Whether the greater heavy metal tolerance of *E. mutabilis* leads to increased metal accumulation or it is associated to other mechanisms such as external metal binding by the pellicle or secreted molecules, has not been studied but it is clear that this issue deserves further investigation.

6.2.1.2 High Biomass Is Needed to Increase the Efficiency of a Bioremediation Process

Under controlled optimal conditions, but also under stressful conditions, *Euglena* species grow at faster rates, generating much higher biomass yields, than plants or macro-algae. Taking advantage of its broad metabolic plasticity, cultures of these protists can yield high cell densities in as little as 4–13 days, which are compatible with biomass requirements for industrial use, by adjusting the growth conditions in particular pH, oxygen, light and carbon source availability (Table 6.2). For instance, fully aerated (~200 μM O_2 at 25 °C and initial pH of 3.5) heterotrophic bleached *E. gracilis* cultured with glutamate *plus* malate produces, in 5 days, much higher cell densities when ethanol is also added (Jasso-Chávez et al. 2010; Rodríguez-Zavala et al. 2010). Photoheterotrophic cells grown under anaerobiosis (<5 μM O_2) with a combination of glycolytic (glucose) and mitochondrial (glutamate *plus* malate) carbon sources yields, after 13 days, lower but still significant cell densities (Santiago-Martínez et al. 2015; Table 6.2). At acidic pHs, malate and glutamate are preferred over glucose (Santiago-Martínez et al. 2015) but at neutral pHs glucose is preferred over malate and glutamate by *E. gracilis* (unpublished data). Under anaerobiosis, ethanol consumption is strongly depressed, probably due to the marked diminution in the mitochondrial metabolism (unpublished data). On the other hand, *E. gracilis* growth in a bioreactor using as carbon and nitrogen sources (1) a waste stream product generated

Table 6.2 Biomass production under different growth conditions of *Euglena gracilis*

	Heterotrophic cells (bleached strains or culture in the dark)				Photosynthetic cells (growth under variable light/dark cycles)			
	Acidic pH of 3–5		*Neutral pH*		*Acidic pH of 3–4.5*		*Neutral pH*	
Oxygen condition	**Carbon source**	**Yield** Kg DW/m^3 (or millions cells/mL)	**Carbon source**	**Yield** Kg DW/m^3 (or millions cells/mL)	**Carbon source**	**Yield** Kg DW/m^3 (or millions cells/mL)	**Carbon source**	**Yield** Kg DW/m^3 (or millions cells/mL)
Fully aerated (200–250 µM O_2)	G + M	2.2 (6)[a]			G + M	1.9–3.1 (2.9–4.8)[a]	Glc (47 mM)	3 (4.6)[b]
	G + M + E	10.8 (29)[a]	G + M + E	13 (35)[c]			G + M + E	7.7 (12)[d]
	Lac	1.48 (4)[e]			Lac	2.2 (3.4)[b]		
	Glc (75 mM)	1.6 (4.3)[e]			Glc* (55 mM)	(2)[f]		
Micro-aerobiosis	G + M (60–90 µM O_2)	0.74 (2)[g]			Glc + G + M (<5 µM O_2)	5.5 (8.5)[h]	G + M + E (<5 µM O_2)	0.54 (0.83)[d]
	Potato liquor + Glc (0.37 M) (30% O_2)	20 (25)[i]						
	Corn steep solid + Fru (0.11 M) (30–40% O_2)	16 (35)[j]						

The equivalence of 1×10^7 cells = 6.5 mg DW was used for transformation of some values
G + M glutamate (34 mM) + malate (17 mM), *G + M + E* glutamate (34 mM) + malate (17 mM) + ethanol (170 mM), *Lac* DL-lactate (33 mM), *Glc* glucose, *Fru* fructose, *Glc + G + M* glucose (110 mM) + glutamate (34 mM) + malate (17 mM), *Fru* fructose
[a]Buetow (1962)
[b]Nicolas et al. (1980)
[c]Rodríguez-Zavala et al. (2010)
[d](unpublished data)
[e]Jasso-Chávez and Moreno-Sánchez (2003)
[f]Garlaschi et al. (1974)
[g]Baker and Banfield (2003)
[h]Santiago-Martínez et al. (2015)
[i]Šantek et al. (2012)
[j]Ivušić and Šantek (2015)
*Growth in darkness

during starch production from potatoes (+0.37 M glucose) (Šantek et al. 2012); or (2) corn steep solid (+0.11 M glucose or fructose) (Ivušić and Šantek 2015) produces as high a biomass yield as those obtained with a well-defined culture medium with glutamate + malate + ethanol (Table 6.2). Therefore, with the adequate supply of precursors for anabolic processes, *E. gracilis* may yield elevated biomass for its use in bioreactors.

Under aerobic conditions, *E. gracilis* synthesizes and accumulates paramylum (a glucose linear polymer with β1-3 glycosidic bonds) for energy and carbon storage. Under anaerobiosis, paramylum is metabolized through glycolysis and for wax ester synthesis (Matsuda et al. 2011; Schneider and Betz 1985). Studies of the anaerobic metabolism in *Euglena* have established that glucose and acetate are the preferred carbon sources (Inui et al. 1985, 1987, 1990; Matsuda et al. 2011; Teerawanichpan and Qiu 2010). However, the routes of degradation of the different carbon sources have not been completely elucidated. It has been determined, in *E. gracilis* cultured under acidic and anaerobic conditions with glutamate, malate and glucose as carbon sources (Santiago-Martínez et al. 2015), that (1) the cytosolic $NADP^+$-glutamate dehydrogenase is the main enzyme involved in glutamate oxidation; and (2) anaerobiosis induces an enhanced activity of the cytosolic $NADP^+$-malic enzyme for malate oxidation, together with a lower mitochondrial NAD^+-malate dehydrogenase activity. Clearly, more studies are required to elucidate the mechanisms involved in the metabolic shift (and transcriptional reprogramming) induced by the aerobiosis/anaerobiosis transition in *Euglena* species. This knowledge may be helpful for heavy metal bioremediation processes under anaerobiosis using *E. gracilis*.

6.2.1.3 Biomass Treatment and Disposal After Heavy Metal Removal and for Heavy Metal Recovery

With *Euglena* species and other unicellular microorganisms, the handling of great biomass volumes with unusable physiological structures, a common problem with plants and macroalgae, is avoided. The cell wall of macroalgae and plants is composed largely of complex sulfated polysaccharides and lipids (Mehta and Gaur 2005; Venkata Mohan et al. 2015). No commercial enzymes able to efficiently degrade these complex molecules are available. The established protocols for heavy metal recovery only include whole plant burning (Ali et al. 2013; Bhargava et al. 2012; Brooks et al. 1998). In addition, for the final recovery of heavy metals, trapped by biosorption in the extracellular cell layers or in the ashes derived from organic matter incineration, a desorption step to release the metal from the plant and algal cell wall is required, for which concentrated solutions of strong acids are commonly used. For biomass regeneration, strong alkalinization is then required. Therefore, the complete process of recovery of heavy metals by and from macroalgae generates wastewater with extreme pH values *plus* heavy metals. On the other hand, although the *E. gracilis* pellicle is also rigid, a mild acid treatment or mechanical rupture (*i.e.* sonication) is normally sufficient to disrupt the cells and release the accumulated heavy metals.

6.2.1.4 *Euglena* Species May Soon Become Suitable Models for Genetic Engineering

These microorganisms have naturally acquired all the genetic, cellular and metabolic features required to grow and flourish under stressful conditions with the additional advantage of being able to adsorb and accumulate heavy metals. However, the current main disadvantage for improving these properties is the limited knowledge regarding their genetic processes and hence the lack of molecular biology tools for genetic modification.

The genetic information codified in the *E. gracilis* chloroplastidic (Hallick et al. 1993) and mitochondrial (Dobáková et al. 2015) DNA has been of little applicability to understand the mechanisms of resistance and accumulation of heavy metals since most of the involved proteins in this process are encoded by nuclear genes. On the other hand, the use of *E. gracilis* Expressed Sequence Tags (ESTs) to analyze gene expres-

sion patterns in response to Cr^{6+} (Dos Santos Ferreira et al. 2007) may guide in the manipulation of key proteins involved in heavy-metal resistance and accumulation such as phytochelatin synthase (García-García et al. 2014). Furthermore, the recent annotation of putative functional transcripts (O'Neill et al. 2015; Yoshida et al. 2016) emphasizes the great metabolic plasticity of this microorganism and should provide a comprehensive gene sequence resource for *E. gracilis*.

6.3 Biological Mechanisms of Heavy Metal Management

6.3.1 Adsorption of Heavy Metal Ions to the External Cell Layers (Biosorption)

Biosorption is an unspecific resistance mechanism against heavy metal stress which depends on the chemical composition of the external cellular layer components. The cell walls of macroalgae have a surplus of electronegative groups in alginates, peptidoglycans, lipopolysaccharides and other insoluble carbohydrates, which enable them to establish strong bonds with heavy metals (García-García et al. 2016; Mehta and Gaur 2005) for their removal from the environment. In particular, the cell walls and dead biomass of several brown (*Fucus vesiculosus*, *Pachymeniopsis* sp.), red (*Palmaria palmata*), and green (*Ulva lactuca*, *Laminaria japonica*) algae can bind elevated amounts of Cd^{2+} (49–146 mg/g dry weight, DW, or 0.4–1.3 mmol/g DW), Cr^{3+} or Cr^{6+} (30–225 mg/g DW or 0.6–4.3 mmol/g DW), Pb^{2+} (15–349 mg/g DW or 0.07–1.7 mmol/g DW) and Au^{3+} (74 mg/g DW or 0.4 mmol/g DW) (Areco et al. 2012; Lee et al. 2000; Mata et al. 2009a, b; Mehta and Gaur 2005; Murphy et al. 2008).

Optimal adsorption of Cr^{3+} by macroalgal biomass has been observed at pH values greater than 4, which is linked to its interaction with carboxylate (negatively charged) groups (Murphy et al. 2008). A similar adsorption capacity for Cr^{6+} at pH < 2 after 3 h incubation was also reported (Murphy et al. 2008). However, the last data should be taken with caution because Cr^{6+} as CrO_4^{2-} is rapidly reduced to Cr^{3+} at pH below 6 (García-García et al. 2009); for instance, 10 and 50% of 1 mM CrO_4^{2-} is reduced to Cr^{3+} after 3 and 120 h, in a cell-free medium at pH 3.5 (García-García et al. 2009). Therefore, biosorption of chromium as Cr^{3+}, but not as Cr^{6+}, can be efficiently carried out under acidic conditions.

Regarding *E. gracilis*, the plasma membrane (pellicle) of cells grown aerobically and under continuous illumination is constituted of proteins (69%), lipids (18%) and carbohydrates (13%). Charged (15 mol%; Glu, Asp) and polar (14 mol%; Ser, Thr) amino acid residues; and sugar residues such as arabinose, fucose, xylose, and rhamnose (77 mol%) are present in high amounts in the protein and carbohydrate pellicle (Nakano et al. 1987). These polar components are very likely in higher proportion in the pellicle from cells cultured in anaerobiosis because Cd^{2+} removal by anaerobic *E. gracilis* exposed to 175 μM $CdCl_2$ was mainly by biosorption (90% total Cd^{2+} removed; 49 nmol cadmium/mg cellular protein) and was higher than that by aerobic cells (45%) (Santiago-Martínez et al. 2015). Interestingly, at 100 μM or lower $CdCl_2$ concentrations, Cd^{2+} biosorption was lower or negligible in both anaerobic and aerobic cells, and intracellular accumulation was the major contributor to Cd^{2+} removal. The *E. gracilis* Cd^{2+} biosorption values are much lower than those of macroalgae, even after correcting for dry weight instead of protein, suggesting that this mechanism of heavy metal removal may not be suitable for efficient bio-remediation using *Euglena* species and hence research in this direction seems unproductive.

6.3.2 Intracellular Mechanisms of Heavy Metal Resistance and Accumulation

6.3.2.1 Synthesis of Thiol-Metabolites in *E. gracilis*

The intracellular thiol-metabolites that bind and neutralize heavy metal ions are cysteine (Cys), gamma-glutamyl cysteine (γEC), glutathione (GSH), and phytochelatins. Aerobic photosynthetic

cells cultured with 50–200 μM cadmium accumulate 60–250 nmol cadmium/10^7 cells after 5–10 days (García-García et al. 2012; Mendoza-Cózatl et al. 2002, 2006a; Santiago-Martínez et al. 2015). The thiol-molecules (Cys + γEC + GSH + phytochelatins)/$cadmium_{accumulated}$ ratio is >2 for cultures with 25 μM $CdCl_2$, suggesting that the accumulated cadmium could be completely chelated by thiol-molecules and this correlates with the lack of cell toxicity (García-García et al. 2012; Mendoza-Cózatl et al. 2006a). However, at 100 μM or higher external $CdCl_2$ concentrations, the thiol-molecules/$cadmium_{accumulated}$ ratio is <2, indicating insufficient Cd^{2+} binding by thiol-molecules; since this is not accompanied by marked cell toxicity, it is expected that other chelating molecules and mechanisms are involved in Cd^{2+} neutralization.

The cadmium accumulation in *E. gracilis* is 33 times higher than in the green microalgae *Chlamydomonas acidophila* and *Chlamydomonas reinhardtii* (García-García et al. 2012; Mendoza-Cózatl et al. 2002, 2006a; Nishikawa et al. 2006; Santiago-Martínez et al. 2015). This ability makes *E. gracilis* a Cd-hyperaccumulator microorganism because its cadmium accumulation capacity (1.1–4.4 mg or 9.5–39 μmoles/g DW (García-García et al. 2012; Mendoza-Cózatl et al. 2002, 2006a; Santiago-Martínez et al. 2015)) exceeds the respective standard reference for cadmium in Cd-hyperaccumulator plants (0.1 mg/g DW) (Ali et al. 2013; Bhargava et al. 2012).

It is worth recalling that for binding and full inactivation of Cd^{2+}, four interacting electronegative groups are required (Belcastro et al. 2009). At physiological GSH concentrations and pH, Cd^{2+} spontaneously, rapidly and predominantly forms Cd-*bis*-glutathionate (GS-Cd-GS or Cd-GS_2; Fig. 6.1a), in which a tetrahedral coordination sphere with the two deprotonated thiol groups and two water molecules is established (Delalande et al. 2010). In turn, one molecule of phytochelatin-2 (PC_2) forms four bonds with Cd^{2+} at pH 7 (approximately 70% of total metal complexes) using its two thiol groups, and either (1) the C-terminal carboxylate group and the Cys_2 carbonyl group in the peptide bond (Fig. 6.1b); or (2) the N-terminal amine and carboxylic groups of Glu_1 (Dorčák and Krężel 2003), *i.e.* a thiol-molecule/Cd^{2+} ratio of 2 at physiological pH should suffice for complete metal ion inactivation. However, at neutral pH the Cd-$2PC_2$ is also formed (approximately 30% of total metal complexes), in which three (Fig. 6.1c) or four thiol groups (Fig. 6.1d) coordinate the metal ion; at pH higher than 7 this last complex prevails, and hence the thiol-molecule/cadmium ratio could also be 4 for reaching complete metal ion inactivation.

On the other hand, the intracellular zinc content reaches a maximum of approximately 240–320 nmol/10^7 cells in *E. gracilis* cultured with 300–1000 μM $ZnCl_2$ for at least ten cell generations (*i.e.*, two subcultures); higher external $ZnCl_2$ concentrations do not lead to greater intracellular zinc levels. At 300–400 μM $ZnCl_2$, the thiol-molecule/$zinc_{accumulated}$ ratio is 0.2, clearly indicating insufficient formation of thiol-molecules for handling Zn^{2+} stress. However, these elevated intracellular zinc levels do not affect cell functions (Sánchez-Thomas et al. 2016). *E. gracilis* can also be considered as a Zn-hyperaccumulator microorganism because its zinc accumulation capacity reaches 2.2–3 mg (34.7–46.1 μmoles) zinc/g DW (Sánchez-Thomas et al. 2016), which is close to the standard reference concentration for Zn^{2+} in Zn-hyperaccumulator plants (3.0 mg zinc/g DW; Ali et al. 2013).

Fig. 6.1 Molecular interactions of GSH and phytochelatin 2 (PC_2) with Cd^{2+}. (**a**) The predominant complex formed between GSH and Cd^{2+} is constituted by two GSH molecules and one Cd^{2+} ion. The two thiol groups and two water molecules establish the interaction with the divalent metal ion (Delalande et al. 2010). (**b**) At equimolar concentrations, and neutral pH, Cd^{2+} is bound by two thiol groups from Cys_1 and Cys_2, which upon binding release their hydrogens as H^+, and by two oxygens from the peptide bond between Cys_2 and Gly and the carboxylate group from Gly. (**c**) In the presence of higher amounts of PC_2, Cd^{2+} is bound by the two thiol groups from Cys_1 and Cys_2 and the carboxylate group of Gly of one PC_2 molecule, and one thiol group of a second PC_2. (**d**) Another stable structure is the interaction of Cd^{2+} with the four thiol groups of two PC_2 molecules at pH > 7. Structures were depicted using the physicochemical analysis described by Dorčák and Krężel (2003)

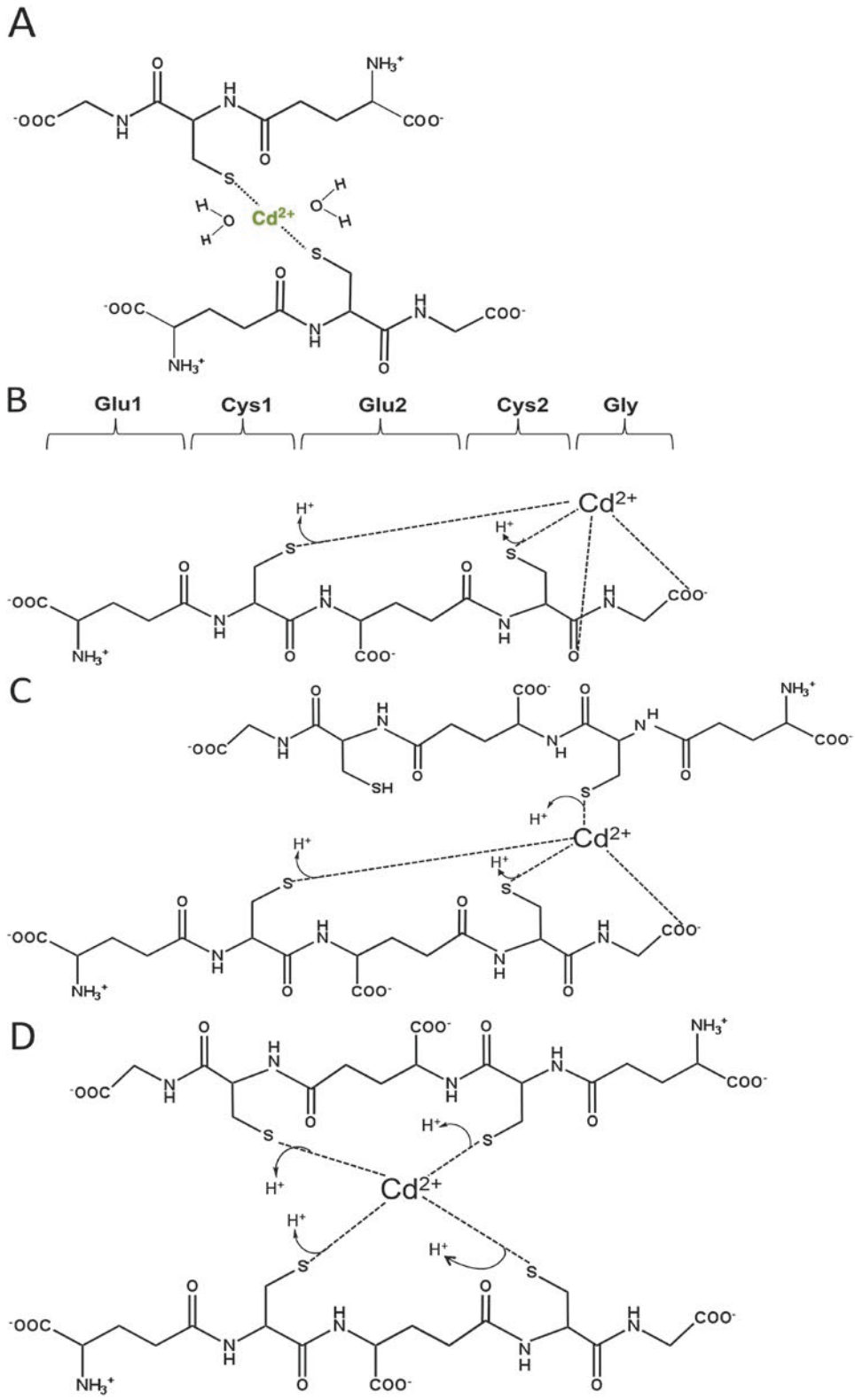
A
B
Glu1
Cys1
Glu2
Cys2
Gly
C
D

In summary, the ability of *E. gracilis* to accumulate heavy metals depends at least partially on the formation of complexes with Cys, GSH, and phytochelatins in a thiol-molecule/metal ratio of at least 2; and their subsequent compartmentalized into chloroplasts (Mendoza-Cózatl et al. 2006b) and probably mitochondria (Avilés et al. 2003), as *E. gracilis* lacks typical plant-like vacuoles (Rocchetta et al. 2006; Sittenfeld et al. 2002; Sommer and Blum 1965). The stoichiometry for heavy metal complexation with sulfide is one, resulting in the formation of insoluble salts (CdS and ZnS solubilities in water are 0.13 and 0.6 mg/100 mL, respectively). Sulfide can also be synthesized by *E. gracilis* (see Sect. 6.3.2.2). Therefore, these features place *E. gracilis* as one of the best candidates to be applied in the bioremediation of water bodies polluted with Cd^{2+} and Zn^{2+}. When the thiol-molecule/metal ratio cannot reach a value of 2 (*i.e.*, at high heavy metal concentrations), *E. gracilis* may still exhibit significant cell growth. Thus, other intracellular mechanisms of metal inactivation and accumulation most likely become involved such as the transcriptional and biochemical activation of the polyphosphates (PolyP) and organic acid biosyntheses (see Sects. 6.3.3 and 6.3.4).

6.3.2.2 Sulfur Assimilation Pathway

The backbone of the phytochelatins metabolism (Fig. 6.2) comprises the *sulfur assimilation pathway* (SAP; from extracellular sulfate to Cys), GSH biosynthesis, phytochelatins biosynthesis and Cd-phytochelatin complexes formation, transport and storage into vacuoles in plants and yeasts, and into chloroplasts and mitochondria in *E. gracilis* as this protist does not have typical vacuoles but it has minivacuoles (Rocchetta et al. 2006; Sittenfeld et al. 2002; Sommer and Blum 1965). Because phytochelatins metabolism consumes ATP and NADPH (eight high-energy bonds and eight NADPH molecules are used to synthesize one PC_2 molecule from sulfate, glutamate and glycine), there is a link with photophosphorylation, oxidative phosphorylation, and glycolysis as well as with the redox homeostasis pathways (thioredoxin, ferredoxin and NADPH redox reactions); and with serine, glutamate and glycine metabolism (Mendoza-Cózatl et al. 2005). The sulfur assimilation pathway synthesizes Cys, which is a precursor for methionine, GSH and protein syntheses (Koprivova and Kopriva 2014; Zheng et al. 2015). Plasma membrane sulfate transporters catalyze the first reaction in the sulfur assimilation pathway.

Sulfate transporters. The plasma membrane sulfate transporters are classified by their substrate affinity as high affinity sulfate transporters with K_m values for sulfate <100 μM, and low affinity sulfate transporters with K_m values >100 μM (García-García et al. 2016; Mendoza-Cózatl et al. 2005). The plasma membrane sulfate transporter activities are perturbed by ionophores in *E. gracilis, C. reinhardtii* and *Chlorella ellipsoidea* (García-García et al. 2012; Matsuda and Colman 1995; Yildiz et al. 1994), because the uptake reaction is an electrogenic process (co-transport of 3 H^+ and 1 sulfate molecule; Fig. 6.2) in which the H^+ gradient is generated by a plasma membrane H^+-ATPase activity. Oxidative phosphorylation seems the main contributor to ATP supply for sulfate uptake in *C. reinhardtii*, *C. ellipsoidea, E. gracilis* and *Rhodella maculata*; while the photosynthesis inhibitor 3-(3,4-dichlorophenyl)-1,1-dimethylurea partially disrupts the sulfate uptake in *E. gracilis* and *R. maculata* (García-García et al. 2012; Matsuda and Colman 1995; Millard and Evans 1982; Yildiz et al. 1994).

The plasma membrane sulfate transport has been considered a control step of Cys synthesis because the transporter activities are significantly lower than those of all other enzymes of the sulfur assimilation pathway, and GSH and phytochelatins syntheses (Table 6.3); thus, several groups have focused on studying their regulation mechanisms. For instance, under sulfate deficiency, the high-affinity plasma membrane sulfate transporters increase their activity in the green microalgae *C. reinhardtii* (Yildiz et al. 1994) and *C. ellipsoidea* (Matsuda and Colman 1995) as well as the mRNA content in *Triticum durum* (Ciaffi et al. 2013). In turn, the mRNA and protein contents of the low-affinity plasma membrane sulfate transporters in *Arabidopsis thaliana* xylem, shoots and roots are also increased under

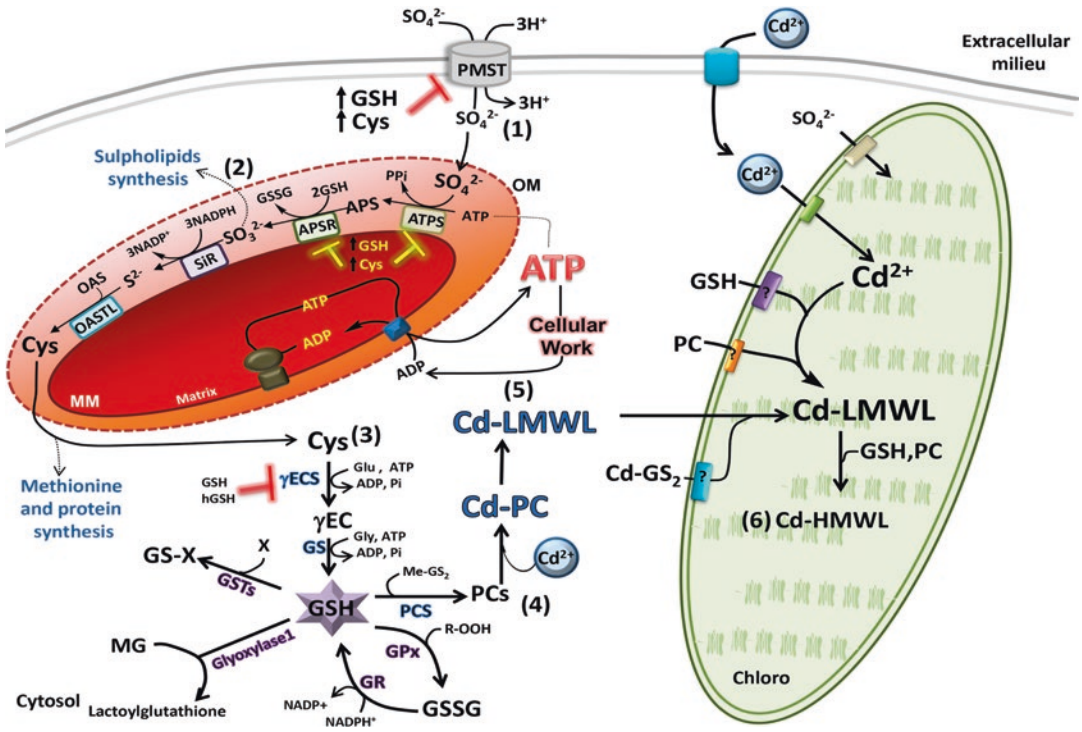

Fig. 6.2 Relationships of Cd^{2+} with the sulfur assimilation pathway and syntheses of Cys, GSH and phytochelatins in *Euglena gracilis*. (*1*) Sulfate (SO_4^{2-}) from the extracellular milieu is transported to the cytosol by PMSTs; (*2*) cytosolic SO_4^{2-} is reduced to sulfide (S^{2-}) which is used to synthesize Cys in the outer phase of the inner mitochondrial membrane; and cytosolic Cys (*3*) is one of the building blocks for GSH and phytochelatins (PCs) (*4*) syntheses. The thiol group of monothiols (Cys, γ-EC, GSH) and phytochelatins allows strong interactions with Cd^{2+} (and other heavy metal ions) in order to form Low Molecular Weight Complexes (Cd-LMWC) in the cytosol (*5*). This first inactivation mechanism is complemented by compartmentalization of Cd-LMWC into chloroplasts and perhaps mitochondria where further binding of Cd^{2+} by monothiols, phytochelatins, S^{2-} and some amino acids is undertaken, leading to the formation of High Molecular Weight Complexes (Cd-HMWC) (*6*). The origin of GSH and phytochelatins in mitochondria and chloroplasts is controversial because it is not clear whether they are also synthesized inside these organelles and/or they are transported from the cytosol. "?" symbol indicates reactions that are not completely characterized in *E. gracilis*. "X" symbol indicates a xenobiotic molecule. *APS* adenosine 5′-phosphosulfate, *APSR* APS reductase, *ATPS* ATP-Sulfurylase, *Cd-HMWC* Cd-High Molecular Weight Complexes, *Cd-LMWC* Cd-Low Molecular Weight Complexes, *GPX* GSH peroxidase, *GS* GSH synthetase, *GS-X* GSH conjugated with xenobiotic, *GSTS* GSH-S transferase, *MG* methylglyoxal, *Me-GS*$_2$ Metal-bis-glutathionate, *MM* mitochondrial inner membrane, *OAS* O-acetylserine, *OASTL* OAS-thiol lyase, *OM* mitochondrial outer membrane, *PCS* phytochelatin synthase, *PCs* phytochelatins, *PMST* plasma membrane sulfate transporter, *SiR* Sulfite reductase, *γECS* γ-glutamylcysteine synthetase. Inhibition is indicated with *red bars*; activation is indicated with *green arrows*

such conditions (Kataoka et al. 2004; Maruyama-Nakashita et al. 2015).

In addition to transcriptional regulation by the sulfur nutritional status, transcriptional and kinetic modulation of the plasma membrane sulfate transporters by some sulfur assimilation pathway metabolites and thiol metabolites has been described mainly in plants. High GSH or Cys seem to exert a dual effect on plasma membrane sulfate transporters, as well as on ATP sulfurylase and APS reductase, by decreasing their gene transcriptions and inhibiting their activities in *Zea mays*, *Brassica napus* and *A. thaliana* roots (Fig. 6.2; Bolchi et al. 1999; Lappartient and Touraine 1996; Lappartient et al. 1999). Heavy metal stress also affects plasma membrane sulfate transporters expression (Fig. 6.2); for instance, Cd^{2+} stress, which leads to GSH depletion, and

Table 6.3 Kinetic parameters of sulfate transporters (PMST) and enzymes of sulfur assimilation, GSH and phytochelatins biosynthetic pathways from protists, algae, and yeast

Enzyme	*Activity in cells*	K_m	Microorganism	References
PMST	0.004 (*Eg*HAST); 7.5 (*Sc*HAST)[a]	$K_{m\ \mathrm{SULFATE\ (LAST)}}$ = 0.06–3.3	*Saccharomyces cerevisiae*; *Chlamydomonas reinhardtii*; *Chlorella ellipsoidea*; *E. gracilis*	Breton and Surdin-Kerjan (1977); García-García et al. (2012); Yildiz et al. (1994); Matsuda and Colman (1995)
	0.009 (*Eg*LAST); 7 (*Sc*HAST)	$K_{m\ \mathrm{SULFATE\ (HAST)}}$ = 0.002–0.06		
ATPS	65–2300 (*Eg* mitos); 700 (*Eg* cytosol); 5 (*Sc*)	$K_{m\mathrm{SULFATE}}$ = 0.29 (*Pc*)	*E. gracilis* (mitochondria and citosol); *S. cerevisiae*; *Penicillium chrysogenum*	Hanna et al. (2004); Hawes and Nicholas (1973); Li et al. (1991); Saidha et al. (1988)
		$K_{m\mathrm{Mg\text{-}ATP}}$ = 0.07 (*Sc*); 0.21 (*Pc*)		
APSR	0.5–500	$K_{m\ \mathrm{APS}}$ = 0.0065 (*Ei*)	*Marine algae (Enteromorpha intestinalis*, *Tetraselmis* sp., *Dunaliella salina*, *Thalassiosira weissflogii*, *Thalassiosira oceanica*, *Isochrysis galbana*, *Emiliania huxleyi*, *Heterocapsa triquetra)*	Gao et al. (2000)
		$K_{m\ \mathrm{GSH}}$ = 1.4 (*Ei*)		
SiR	5 (*Sc*); 1850 (*Cm*)	$K_{m\ \mathrm{SULFITE}}$ = 0.0087 (*Cm*); 0.012–0.017 (*Sc*)	*S. cerevisiae*; *Cyanidioschyzon merolae*	Kobayashi and Yoshimoto (1982); Sekine et al. (2009); Yoshimoto and Sato (1968)
		$K_{m\ \mathrm{NADPH}}$ = 0.01–0.021 (*Sc*)		
OASTL	1640	$K_{m\mathrm{SULFIDE}}$ = 0.075	*C. reinhardtii*	León et al. (1987)
		$K_{m\mathrm{OAS}}$ = 2		
γECS	<2 (*Tc*); 2.6 (*Eg*)	$K_{m\ \mathrm{Cys}}$ = 2.9 (*Eg*); 0.21 (*Tc*)	*E. gracilis*; *T. cruzi*	García-García et al. (2012); Avilés et al. (2005); Olin-Sandoval et al. (2012)
		$K_{m\mathrm{Glu}}$ = 1.6 (*Eg*); 0.13 (*Tc*)		
		$K_{m\ \mathrm{Mg\text{-}ATP}}$ = 0.12 (*Eg*); 0.04 (*Tc*)		
		$K_{i\ \mathrm{GSH}}$ = 1.6 (*Tc*)		
GS	8.6 (*Tc*); 1.1 (*Eg*)	$K_{m}\gamma_{\mathrm{EC}}$ = 0.04 (*Tc*); 0.27 (*Sp*)	*E. gracilis*; *T. cruzi*; *Schizosaccharomyces pombe*	García-García et al. (2012); Olin-Sandoval et al. (2012); Nakagawa et al. (1993)
		$K_{m\mathrm{Gly}}$ = 1.2 (*Tc*); 0.67 (*Sp*)		
		$K_{m\ \mathrm{Mg\text{-}ATP}}$ = 0.03 (*Tc*); 0.45 (*Sp*)		
PCS	0.038 (cytosol)[b]	$K_{m\ \mathrm{GSH}}$ = 14–22	*E. gracilis*	García-García et al. (2014)
		$K_{m\ \mathrm{Cd\text{-}GS2}}$ = 0.0016		
		$K_{m\ \mathrm{Zn\text{-}GS2}}$ = 0.0025		
HMT1 *(vacuole)*	2.4	$K_{m\ \mathrm{Mg\text{-}ATP}}$ = 0.38	*S. pombe*	Ortiz et al. (1995)

Activities are in nmol (min × $mg_{protein}$)$^{-1}$ and K_m in mM

[a]Activity normalized by cellular protein, while all other activity values were normalized by cytosolic protein (which is enriched by 3–10 times *vs.* total cell protein); thus, values without asterisk will diminish when they are corrected by cellular protein

[b]Unpublished data

hence oxidative stress, induces in few hours significant increased plasma membrane sulfate transporter mRNA content and increased sulfate uptake in *Z. mays* (Nocito et al. 2006) and *Brassica juncea* roots (Lancilli et al. 2014), and *A. thaliana* seedlings (Liu et al. 2016). These data suggest that the sulfate transport reaction, together with ATP sulfurylase and APS reductase, are involved in the homeostasis of thiol-metabolites (Liu et al. 2016; Nocito et al. 2006). However, in other organisms of promising biotechnological relevance such as *Euglena* species, this knowledge is scarce.

In *E. gracilis*, activities of the high-affinity and low-affinity plasma membrane sulfate trans-

porters *Eg*PMST1 and *Eg*PMST2 increased 9 and 104 times under sulfur deficiency (60 μM sulfate in the culture medium); and 2.5 and 4 times, respectively, in cells exposed to 50 μM Cd^{2+} for 5 days (García-García et al. 2012). The enhanced expression of both plasma membrane sulfate transporters elevated the total cellular sulfate uptake capacity in order to counteract the sulfur deficiency or Cd^{2+}-induced GSH depletion, and thus be able to provide sulfate for SAP, GSH and phytochelatins synthesis reestablishing the Cys and GSH pools (García-García et al. 2012).

Sulfate transporters of vacuoles, chloroplasts and mitochondria have not been characterized in most microorganisms. Several isoforms of the low-affinity plasma membrane sulfate transporters catalyze the sulfate transference from the cytosol to the vacuole (SULTR4;1 and SULTR4;2) and chloroplasts (SULTR3;1) in *A. thaliana* (Cao et al. 2013; Zuber et al. 2010). A chloroplast isoform, called SulP, has been identified in *C. reinhardtii*, which has not yet been classified as low-affinity or high-affinity membrane sulfate transporter (Chen et al. 2005). *C. reinhardtii* SulP mutants anaerobically grown show decreased chloroplast sulfate uptake and photosynthesis activity because photosystem II is highly dependent on sulfate metabolites (as sulpholipids) (Chen et al. 2005). In chloroplasts isolated from photosynthetic *E. gracilis* (grown under 12 h light/12 h dark cycles at 25 °C for 4 days), the chromate (a sulfate structural analogue) uptake, determined at 15 °C, showed V_{max} of 37 nmol/min × $mg_{protein}$ and K_m of 1.2 mM. In mitochondria isolated from bleached *E. gracilis* (grown in the dark with lactate as carbon source at 25 °C for 4 days) the chromate uptake showed V_{max} of 1.2 nmol/min × $mg_{protein}$ and K_m of 0.76 mM whereas the sulfate uptake rate was also 1.2 nmol/min × $mg_{protein}$ at 10 mM sulfate. These chromate uptake values are higher (chloroplasts) or similar (mitochondria) to those determined for the plasma membrane sulfate transport (Table 6.3). As the sulfate assimilation pathway enzymes in *E. gracilis* are localized in the outer leaflet of the inner mitochondrial membrane (Fig. 6.2), both sulfate uptake reactions in chloroplasts and mitochondria are not essential for this pathway to proceed and hence they cannot be controlling steps in *E. gracilis*.

ATP sulfurylase and APS reductase. ATP sulfurylase transfers sulfate to ATP generating adenosine-5-phosphosulfate (APS) and PPi (Mendoza-Cózatl et al. 2005). Later, sulfate from APS is reduced to sulfite by APS reductase (also known as APS sulfotransferase) using GSH as cofactor (Suter et al. 2000). Atypically, the activities of ATP sulfurylase, APS reductase and APS kinase (an enzyme catalyzing the formation of adenosine-3-phosphate-5-phosphosulfate (PAPS), from which sulfite can also be formed by PAPS reductase or APS reductase; Fig. 6.2) are found in *E. gracilis* mitoplasts (mitochondria with no outer membrane), but not in chloroplasts (Saidha et al. 1985, 1988) like in plants. These activities co-localize with adenylate kinase (a mitochondrial intermembrane marker) and fumarase (a mitochondrial matrix marker), and inhibition of the adenine nucleotide translocator with carboxyatractyloside (to block any putative exit of intramitochondrial PAPS) does not impair PAPS formation (which is found outside mitochondria) in the presence of external ATP (Saidha et al. 1985). These observations led Schiff and coworkers (Li et al. 1991; Saidha et al. 1985, 1988) to propose that the *E. gracilis* sulfur assimilation pathway enzymes were ***all*** localized in the outer leaflet of the inner membrane (Fig. 6.2) instead of the mitochondrial matrix. The lack of significant APS reductase activity in the purified mitochondrial inner membrane fraction (Saidha et al. 1988) suggests that the sulfur assimilation pathway enzymes are loosely bound to the inner membrane, and this is probably why ATP sulfurylase, APS reductase and APS kinase are easily released by freezing and thawing of mitochondria or cells (Li et al. 1991; Saidha et al. 1988). Interestingly, these observations represent an evolutionary paradox because *E. gracilis* would be the sole photosynthetic organism that does not use the chloroplast to reduce sulfate (Kopriva 2006).

APS reductase and ATP sulfurylase have also been proposed as control steps of the sulfur assimilation pathway in plants because they are up-regulated by biotic (auxins, jasmonates, carbohydrates) and abiotic (sulfur limitation, oxidative and heavy metal stress) factors; and down-regulated by high GSH and nitrogen limitation (Koprivova and Kopriva 2014). Moreover,

some transcriptional and kinetic features indicate that the contribution of APS reductase to the control of the pathway is greater in plants because its activity is approximately 540 times lower (0.05–6.5 nmol/min × $mg_{protein}$; Phartiyal et al. 2008; Scheerer et al. 2010) than that of ATP sulfurylase (8–27 nmol/min × $mg_{protein}$; Phartiyal et al. 2006). However, such a difference in activities is not always observed (Table 6.3) and hence APS reductase may not be one of the controlling steps of the sulfur assimilation pathway in microorganisms. The GSH level seems to regulate the APS reductase activity in *A. thaliana* roots because incubations with external Cys or GSH (but not with Cys *plus* buthionine sulfoximine, a γ-glutamylcysteine synthetase inhibitor) inhibit this enzyme expression and activity, while ATP sulfurylase activity was not affected (Vauclare et al. 2002). Incubation with external *O*-acetyl-serine (OAS) increases APS reductase activity in poplar roots (*Populus tremula*x, *P. alba*) (Scheerer et al. 2010). Cd^{2+} stress also increases APS reductase activity (18 times) in poplar plants (Scheerer et al. 2010). The APS reductase regulation mechanisms under heavy metal stress have not been studied in *Euglena* species and microalgae.

Sulfite reductase and OAS-thiol lyase. Sulfite is reduced to sulfide by sulfite reductase using ferredoxin (in photosynthetic organisms) or NADPH (in prokaryotes and yeast) as electron donors (Mendoza-Cózatl et al. 2005; Park and Bakalinsky 2000). The subcellular localization and electron donor of sulfite reductase in *E. gracilis* are unknown but, as the sulfur assimilation pathway enzymes are apparently bound to the mitochondrial inner membrane, it seems possible that sulfite reductase may be a NAD(P)H-dependent mitochondrial enzyme (Fig. 6.2), although other electron donors and subcellular compartments cannot be ruled out. In photosynthetic *E. gracilis* cultured under anaerobiosis, the intracellular sulfide content is 2 times higher than in aerobic cells, and it is unaltered by the presence of 25 μM Cd^{2+} (Santiago-Martínez et al. 2015), suggesting that sulfite reductase activity is enhanced by anaerobiosis and unaltered by low Cd^{2+}.

The last reaction of the sulfur assimilation pathway is the incorporation of sulfide into *O*-acetylserine (OAS) to synthesize Cys and acetate by OAS-thiol lyase which requires pyridoxal-5′-phosphate as cofactor. In some fungi, sulfide is condensed with O-acetylhomoserine to form homocysteine (Patron et al. 2008). OAS-thiol lyase activity is structurally associated to serine-acetyltransferase, which acetylates Ser in an acetyl-CoA-dependent reaction to synthesize OAS. The association of these enzymes is called cysteine synthase complex (Romero et al. 2014). In *A. thaliana*, OAS-thiol lyase isoforms have been localized in the cytosol (*OAS-A1*), chloroplast (*OAS-B*) and mitochondria (*OAS-C*) (Romero et al. 2014). In *E. gracilis*, OAS-thiol lyase has been detected in mitoplasts (Saidha et al. 1988) probably associated to the outer phase of the inner membrane like the other sulfur assimilation pathway enzymes (Fig. 6.2).

6.3.2.3 GSH Biosynthesis

GSH synthesis is catalyzed by γ-glutamylcysteine synthetase (γECS) and GSH synthetase (Fig. 6.2). Increased biosynthesis of Cys, γEC, GSH and phytochelatins induced by Cd^{2+} stress has been widely documented for *E. gracilis* (Avilés et al. 2003; García-García et al. 2012; Mendoza-Cózatl et al. 2002, 2006a; Santiago-Martínez et al. 2015). The high cadmium accumulation capacity described for *E. gracilis* (1.1–4.4 mg or 9.5–39 μmoles/g DW) depends on an active phytochelatins synthesis, in which Cys and GSH are key precursors, and γECS and phytochelatin synthase are the main controlling steps (Mendoza-Cózatl and Moreno-Sánchez 2006) because these two enzymes exhibit the lower activities in the cells and GSH exerts a strong feed-back inhibition on γECS (Table 6.3).

γ-glutamyl cysteine synthetase (γECS). Also named glutamate-cysteine ligase, it is the first enzyme in GSH biosynthesis playing an important role in regulating the intracellular redox environment. This enzyme catalyzes the ATP-dependent formation of the dipeptide γEC from glutamate (Glu) and Cys (Fig. 6.2) and it is presumably the main controlling step of GSH synthe-

sis in bacteria, protists, algae, fungi, plants and animals because it has one of the lowest activities in cells (Table 6.3) and several regulation mechanisms. γECS expression is regulated by oxidative stress and lipid peroxidation products, through the action of the transcription factors AP-1 and Nrf2 in rats and humans (Lu 2013). Exposure to 25 μM Cu^{2+} (Schäfer et al. 1997) or Cd^{2+} (Schäfer et al. 1998) also increased the levels of γECS mRNA in *B. juncea,* although activity was not determined. In addition, phosphorylation of γECS by protein kinase A, protein kinase C or Ca^{2+}-calmodulin kinase, leading to a moderate loss of activity, has been observed in rat kidney and liver (Lu 2013). Transcriptional and covalent regulation of the γECS activity in *Euglena* species has not been elucidated.

The kinetic mechanism of γECS has been described as ping-pong (rat liver, *Xenopus laevis;* Davis et al. 1973), ordered with ATP as the obligatory first substrate (rat kidney; Yip and Rudolph 1976), random for the second and third (Glu/Cys) substrates (rat kidney; Schandle and Rudolph 1981), or random ter-reactant (*T. brucei*; Brekken and Phillips 1998). The competitive inhibition of γECS by GSH (*vs.* glutamate) is a widespread feed-back regulatory mechanism, from bacteria to humans including *E. gracilis* (García-García et al. 2012); the K_i value for GSH (Table 6.3) is close to the physiological intracellular concentration of this tripeptide (Lueder and Phillips 1996; Mendoza-Cózatl et al. 2005; Richman and Meister 1975). *In vivo*, higher γECS activity and GSH content has been found in *E. gracilis* under Cd^{2+} stress (Avilés et al. 2005; García-García et al. 2012), suggesting that by sequestering GSH the metal ion attenuates the feed-back inhibition on γECS and hence the metal ion-GSH complex is not a γECS inhibitor.

The *E. gracilis* γECS affinities for its three substrates are 4–10 times lower than those of the *T. cruzi* enzyme (Table 6.3). Considering the intracellular concentrations of GSH (0.8 mM in *T. cruzi* and 5–20 mM in *E. gracilis*; Avilés et al. 2003, 2005; García-García et al. 2012; Olin-Sandoval et al. 2012), and that the Glu concentration is usually saturating for γECS activity (8 mM in *T. cruzi* and 1 mM in *E. gracilis*; Olin-Sandoval et al. 2012; Santiago-Martínez et al. 2015), it may be predicted that under physiological conditions, the γECS activity in *E. gracilis*, but not in *T. cruzi*, is mainly regulated by the GSH level ($[Glu]/K_{m\ Glu} < [GSH]/K_{i\ GSH}$) in the short-term and by transcriptional mechanisms in the long-term.

Glutathione synthetase. This enzyme catalyzes the ATP-dependent condensation of γEC and Gly (Fig. 6.2). GSH is synthesized by glutathione synthetase in the cytosol in most organisms, but in plants it is also synthesized in chloroplasts (Clemente et al. 2012; Hell and Bergmann 1990; Preuss et al. 2014). Glutathione synthetase activity is usually higher than that of γECS, except in *E. gracilis* (Table 6.3). Glutathione synthetase expression is regulated by phytohormones in plants although this mechanism does not always lead to changes in the GSH pools (Clemente et al. 2012). Transcriptional regulation of the glutathione synthetase gene in mammalian cells is similar to that of the γECS gene, involving AP-1 and Nrf2 (Lu 2013). It has been described that all-trans retinoic acid selectively induces glutathione synthetase expression in tumor cells (Nefedova et al. 2007). The increased GSH contents induced by 0.4–2.4 μM Cu^{2+} in the brown algae *Ectocarpus siliculosus* have been attributed to increased glutathione synthetase expression, although this proposal was not confirmed by determinations of glutathione synthetase activity (Roncarati et al. 2015). In addition, enhanced γECS and phytochelatin synthase expression by Cu^{2+} was also observed (Roncarati et al. 2015). The GSH level increases 1.5 times in *E. gracilis* exposed to 50 μM Cd^{2+} although glutathione synthetase activity does not change, indicating no regulatory role for this enzyme (García-García et al. 2012).

HomoGSH (γGlu-Cys-β-Ala; Fig. 6.3a) is a GSH analogue more abundant than GSH in root nodules from the legumes *Glycine max*, *Phaseolus vulgaris* and *Vigna radiata*; this metabolite has been associated with root nodules development during the symbiotic interaction with *Rhizobium* bacteria (Frendo et al. 2005; Matamoros et al. 1999). HomoGSH is synthesized by homo-gluta-

thione synthetase (EC.6.3.2.23), which shares 77% identity with glutathione synthetase, and is up to 13-fold more active than glutathione synthetase in alfalfa leaves and roots (Clemente et al. 2012; Frendo et al. 2005; Matamoros et al. 1999). Also, it has been reported that the homoGSH concentration (0.7 mM) found in some *Rhizobium* infected areas of peas and beans suffices to inhibit γECS (Frendo et al. 2005; Hell and Bergmann 1990). Thus, it now appears necessary to consider that active non-canonical GSH metabolism does exist for some species and under still unknown conditions. The metabolism and regulatory interactions of these GSH analogues has not been analyzed in photosynthetic microorganisms. However, the existence of higher amounts of non-canonical GSH polymers in *E. gracilis* (Figs. 6.3 and 6.4; Sánchez-Thomas et al. 2016) and microalgae such as *C. reinhardtii*, *Chlorella fusca*, *Scenedesmus acutiformis*, *Navicula pelliculosa*, and *Monoraphidium minutum*, over canonical PC_2-PC_6 contents (Gekeler et al. 1988), suggests a more active biosynthesis of the precursors homoGSH (hGSH), hydroxymetylGSH (γGlu-Cys-Ser) and isoGSH (γGlu-Cys-Glu and γGlu-Cys-Gln) than of GSH.

GSH membrane transporters. Some cells have the ability to export GSH to other cells and organs. In cultures of mammalian cells as well as microorganisms, particularly in those subjected to oxidative stress, increased intracellular GSH levels are usually observed after its external addition. The molecular identity and kinetic properties of the GSH intake plasma membrane transporters have already been established for yeast and bacteria (Bachhawat et al. 2013). These proteins are members of the oligopeptide transporter family, which are present in plants, fungi, bacteria and archaea, but not in animals. They show high affinity for external GSH (K_m = 50–200 μM) and their expression is induced by sulfur limitation (Bachhawat et al. 2013).

The GSH mitochondrial pool accounts for 10–15% of the total cellular GSH pool which derives from transport of cytosolic GSH across the inner membrane to the mitochondrial matrix in a reaction catalyzed by either the dicarboxylate or 2-oxoglutarate carriers in exchange with Pi or 2-oxoglutarate, respectively. Uptake of GSH by rat kidney mitochondria shows hyperbolic kinetics with a K_m of 1.3 mM (Bachhawat et al. 2013). In bleached *E. gracilis* cells preconditioned to 1.5 μM $HgCl_2$, increased GSH contents in cells (2-times) and mitochondria (14-times) induced by 100 μM Cd^{2+} were attained, while Cys increased in cells (4-times) but did not vary in mitochondria (Avilés et al. 2003). Thus, it seems possible that free GSH, but not free Cys, can be transported by *E. gracilis* mitochondria. Although chloroplasts have their own GSH biosynthetic machinery, they are also able to take up cytosolic GSH. However, the molecular identity of the transporters involved is still unknown (Bachhawat et al. 2013). In this regard, elevated Cys and GSH contents have been observed in chloroplasts of photosynthetic *E. gracilis* stressed by 200 μM Cd^{2+}, suggesting active transport of these metabolites from the cytosol or active biosynthesis inside the organelle (Mendoza-Cózatl et al. 2002).

The multidrug resistance-associated proteins are plasma membrane H^+-ATPases in mammalian and plant cells able to use the ATP hydrolysis energy to expel a variety of hydrophobic molecules, including GSH-conjugates to a greater extent than GSH. None of these GSH membrane transporters have been identified at the genetic and kinetic levels in *Euglena* species*;* however, indirect experimental evidence suggests that they do exist (Fig. 6.2) because incubation of *E. gracilis* cells and isolated chloroplasts with GSH leads to increased internal levels of this metabolite.

Glutathione-S-Tranferases (GSTs). Besides phytochelatin synthase, the main GSH consumption reactions under heavy metal stress in plants, yeasts and algae are catalyzed by GSH-S-transferases (GSTs) and GSH peroxidases (GPx). These enzymes are the main competition of phytochelatin synthase for GSH and contribute to attenuate oxidative stress-induced damage. Some GSTs are transcriptionally activated by heavy metal stress. For instance, the GSTs (and GPx) activity increases in *Scenedesmus bijugatus* exposed to 200 μM Cu^{2+} (Nagalakshmi and Prasad 2001); in *C. reinhardtii* exposed to 115–150 μM

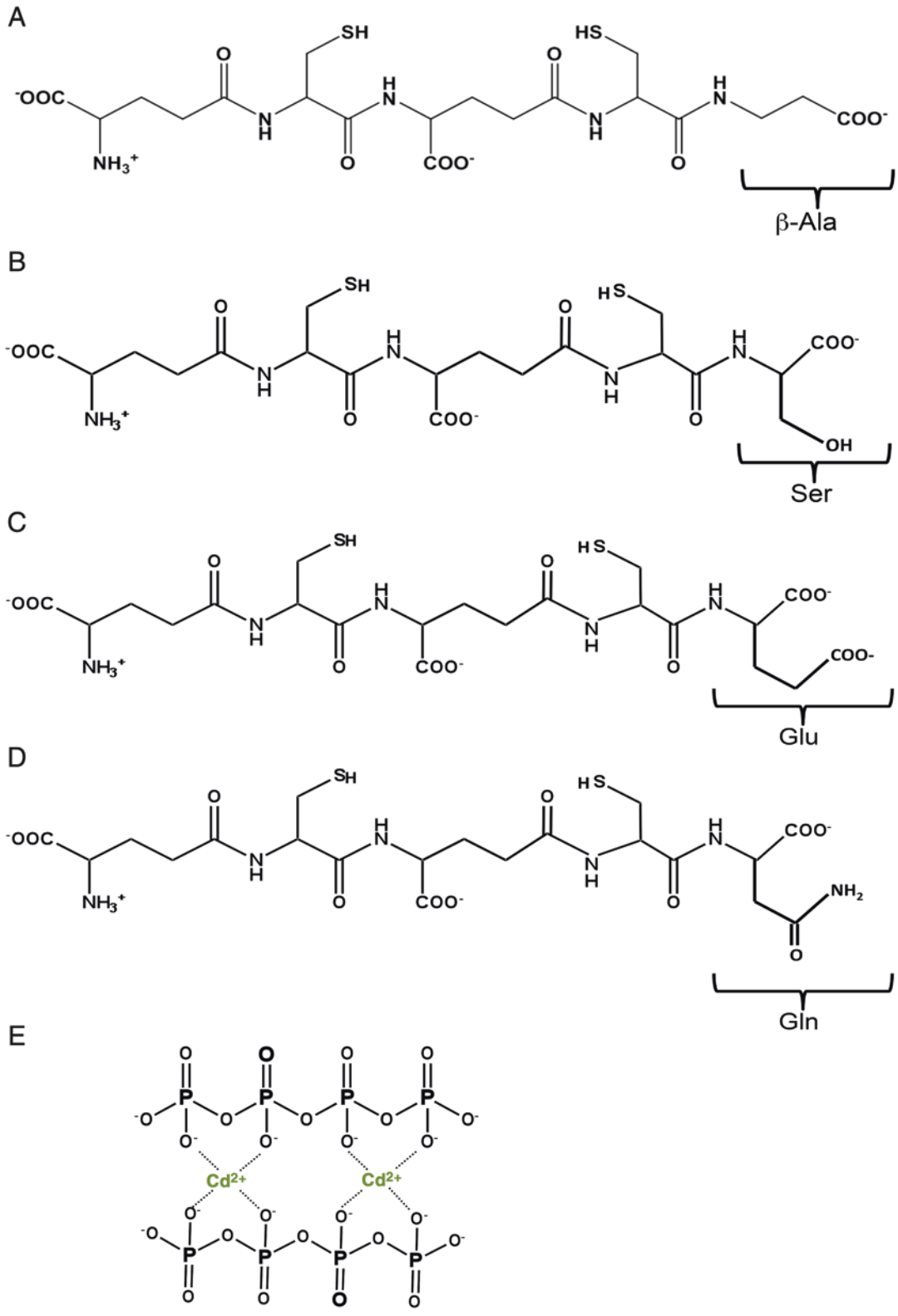

Fig. 6.3 Chemical structures of non-canonical phytochelatin 2 homologues and polyphosphates. Non-canonical PC_2 replace Gly by β-Alanine (β-Ala) in homo-PC_2 (**a**); serine in hydroxymetyl-PC_2 (**b**); and Glu (**c**) or Gln (**d**) in iso-PC_2. Polyphosphates-Cd^{2+} interaction (**e**)

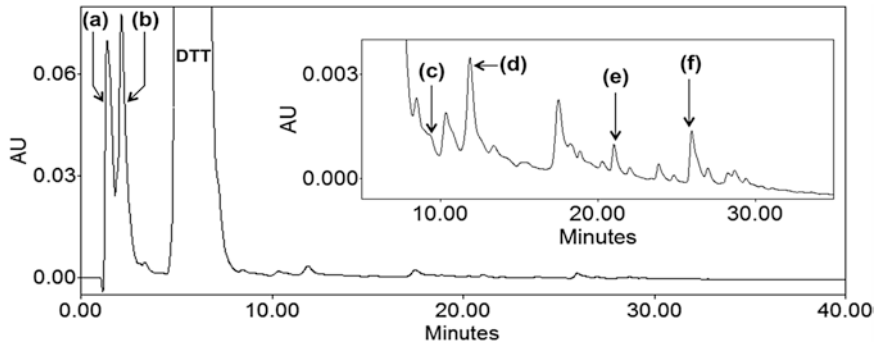

Fig. 6.4 HPLC profile of thiol-compounds in photosynthetic *E. gracilis* exposed to Cd^{2+}. Cells were grown for 8 days under 12 h light/12 h dark cycles in the presence of 200 μM $CdCl_2$. Acidic cell extracts were subjected to HPLC using a reverse phase C18 column and a discontinuous gradient of trifluoroacetic acid and acetonitrile. For detection, the separated thiol-compounds were post-column derivatized with DTNB (García-García et al. 2012, 2014). Cys (*a*), GSH+γEC (*b*), PC_2 (*c*), trypanothione (*d*), PC_3 (*e*), PC_4 (*f*). The content of canonical PC_2 + PC_3 + PC_4 and trypanothione accounted for 40.5% of the total GSH polymers. The identity of all other thiol-compounds shown in the inset is unknown but they are presumably non-canonical phytochelatins and account for the remaining 59.5% of total GSH polymers. *AU* arbitrary units

Cd^{2+} increased transcript and protein levels of GSTs (and GPx) have also been observed (Gillet et al. 2006; Jamers et al. 2013). However, these observations need to be complemented with determinations of GST (and GPx) activity to avoid over-interpretations as, due to regulation mechanisms at the different levels of biological complexity, variations in transcript and protein levels do not always lead to variations in activity (Moreno-Sánchez et al. 2016)

The GSTs constitute a diverse group of enzymes that catalyze the transfer of the entire glutathionyl-moiety (instead of a single functional group such as sulfide) to an electrophilic xenobiotic molecule (Fig. 6.2). Some GSTs catalyze GSH addition, redox or isomerization reactions. The canonical GSTs are cytosolic soluble enzymes, whereas some plant GST isoforms have mitochondrial, chloroplast or peroxisome targeting sequences or have been undoubtedly localized in these organelles (Deponte 2013). Genetic and kinetic characterizations of these GSH consuming enzymes have not been done in *E. gracilis*.

Glyoxylase I, which is a member of the methylglyoxal pathway from DHAP to D-lactate, uses GSH to inactivate methylglyoxal (and other toxic 2-oxoaldehydes) by forming lactoylglutathione (Fig. 6.2). Although glyoxylase I is classified as a lyase (EC 4.4.1.5), based on mechanistic studies glyoxylase I may also be considered a metal ion-dependent isomerase (EC 5; Deponte 2013). Glyoxylase I catalysis depends on heavy metal ions such as Zn^{2+} (or Fe^{2+}) or Ni^{2+} (or Co^{2+}) which are bound to a conserved domain within its active site.

6.3.2.4 Phytochelatin Metabolism

Phytochelatin Synthase. Phytochelatin synthase uses GSH and metal-*bis*-glutathionate (Me-GS_2; Fig. 6.1a) as co-substrates to synthesize phytochelatins (Fig. 6.2; García-García et al. 2014; Vatamaniuk et al. 2000). Phytochelatin synthase transcript or protein content are not modified by heavy metal stress, although a heavy metal ion is essential for activity.

Several heavy metal ions are able to induce phytochelatins synthesis in plants, worms, yeasts, algae and protists (Table 6.4; Bräutigam et al. 2011; Clemens et al. 1999; García-García et al. 2014; Grill et al. 1989; Hirata et al. 2001; Ramos et al. 2007; Ray and Williams 2011; Vatamaniuk et al. 2000). Phytochelatin synthases from *A. thaliana* and other plants, algae and yeast achieve their maximal activities with Cd^{2+}, while maximal activity by the purified recombinant *E. gracilis* enzyme and unpurified green alga *Dunaliella tertiolecta* native enzyme, is achieved with Zn^{2+}

Table 6.4 Preference sequence of metal and metalloids that stimulate the phytochelatin synthase activity from different organisms

Phytochelatin synthase source	Metal/metalloid	References
Recombinant A. thaliana	$Cd^{2+} > Hg^{2+} > As^{3+} > Cu^{2+} > Zn^{2+} > Pb^{2+} > Mg^{2+} > Ni^{2+} > Co^{2+}$	Vatamaniuk et al. (2000)
Native Silene cucubalus	$Cd^{2+} > Ag^{+} > Bi^{3+} > Pb^{2+} > Zn^{2+} > Cu^{2+} > Hg^{2+} > Au^{3+}$	Grill et al. (1989)
Native Lycopersicon esculentum	$Cd^{2+} > Ag^{+} > Cu^{2+} > Au^{+} > Zn^{2+} > Fe^{2+} > Hg^{2+} = Pb^{2+}$	Chen et al. (1997)
Recombinant Glycine max[a]	$Cd^{2+} > Hg^{2+} > Ga^{3+} > Ge^{2+} > Pb^{2+} > Sn^{2+} > Ag^{+}$	Oven et al. (2002)
Recombinant C. merolae (red algae)	$Cd^{2+} > Pb^{2+} > As^{5+} > As^{3+} > Ag^{+} > Cu^{2+} > Hg^{2+}$	Osaki et al. (2009)
D. tertiolecta cell extract (green algae)	$Zn^{2+} = Cd^{2+}$	Tsuji et al. (2003)
Recombinant E. gracilis	$Zn^{2+} > Cd^{2+} > Mn^{2+} = As^{5+} = As^{3+} > Cu^{2+} > Ag^{+}$	García-García et al. (2014)
S. pombe heterologous expressed in E. coli (cell extract)	$Cd^{2+} > Cu^{2+} > Pb^{2+} > Zn^{2+} > Ag^{+} > Hg^{2+}$	Ha et al. (1999)
Recombinant S. mansoni	$Zn^{2+} > Cd^{2+}$ [b]	Rigouin et al. (2013)
	$Cd^{2+} > Zn^{2+}$ [c]	

[a]This information corresponds to the activity of homo-phytochelatin synthase
[b]This preference order was observed when comparing the enzyme activity at 0.02 mM Zn^{2+} and 0.1 mM Cd^{2+}
[c]This preference order was observed when comparing the enzyme activity at 0.1 mM Zn^{2+} and 0.1–1 mM Cd^{2+}

(García-García et al. 2014; Grill et al. 1989; Hirata et al. 2001; Tsuji et al. 2003; Vatamaniuk et al. 2000). *Schistosoma mansoni* recombinant phytochelatin synthase achieves its maximal activity with 0.02 mM Zn^{2+} whereas at 0.1 mM Zn^{2+} its activity severely decreases, suggesting high affinity for Zn-GS_2 and also substrate inhibition at high Zn^{2+} (Rigouin et al. 2013). Thus, it remains unknown why some enzymes preferentially use Cd-GS_2 or Zn-GS_2. Such information may help to understand how to engineer enzymes with preference for GSH complexes with precious metal ions such as Au^{2+}, Ag^{+} and other economically interesting heavy metals.

Phytochelatin synthase is the slowest enzyme within the sulfur assimilation pathway and phytochelatins synthesis in plants (Grill et al. 1989; Mendoza-Cózatl et al. 2005; Table 6.3; Fig. 6.2). Phytochelatin synthase expression increases 50–180% in *C. reinhardtii*, the worm *S. mansoni*, as well as in *A. thaliana*, *Tricum aestivium* and *Lotus japonicus* plants, exposed acutely to 30–100 μM Cd^{2+} (Bräutigam et al. 2011; Brunetti et al. 2011; Clemens et al. 1999; Ramos et al. 2007; Ray and Williams 2011). However, it was not established in these studies whether the increased transcription in fact led to increased activity. The sole report describing phytochelatin synthase activity in cells under Cd^{2+} stress (100 μM) was determined in *S. cucubalus* plants, which was 0.17 nmol (min × $mg_{protein}$) (Grill et al. 1989). In contrast, phytochelatin synthase mRNA in *E. gracilis* (*Eg*PCS) remains constant during 5 days under 50 μM Cd^{2+} stress, although *Eg*PCS activity was not determined either (García-García et al. 2014). Nevertheless, it has been proposed that *Eg*PCS activity is mainly modulated by the co-substrate Zn-GS_2 or Cd-GS_2 availability in *E. gracilis* (García-García et al. 2014).

Phytochelatins. Phytochelatins (Figs. 6.1 and 6.3) are glutathione polymers initially described in 1983 for the yeast *Schizosaccharomyces pombe* and named cadystins (Kondo et al. 1983). Later, Grill et al. (1985) established the current nomenclature for phytochelatins after characterizing these thiol-metabolites in 13 plants from the *Angiospermae* division. Nowadays, phytochelatins have also been detected in protists, algae, yeast, fungi and nematodes (Avilés et al. 2003; Bräutigam et al. 2011; Mendoza-Cózatl et al. 2002; Osaki et al. 2009; Rigouin et al. 2013; Vatamaniuk et al. 2001), but not in humans and other mammals. The general formula of phytochelatins is $(\gamma Glu\text{-}Cys)_n$-Gly; where commonly n = 2–6. For instance, phytochelatin-2 or PC_2

(γGlu-Cys-γGlu-Cys-Gly; Fig. 6.1) is a phytochelatin synthesized from two GSH molecules, releasing one Gly. In nature, PC_2 to PC_4 have been detected in the red alga *Cyanidioschyzon merolae*, green algae *C. reinhardtii*, yeast *S. pombe,* and nematodes *S. mansoni* and *Caenorhabditis elegans* (Bräutigam et al. 2011; Osaki et al. 2009; Rigouin et al. 2013; Vatamaniuk et al. 2001); whereas plants mainly synthesize PC_2 to PC_6 (Vatamaniuk et al. 2000). It is worth emphasizing that no correlation has been found between phytochelatins length and the capacity to resist and/or accumulate heavy metals.

Phytochelatins accumulation has been observed in the green microalgae *Scenedesmus acutus* and *C. reinhardtii* exposed to Cd^{2+}, as well as in *D. tertiolecta* exposed to Zn^{2+}. The phytochelatins levels reached seemed sufficient to chelate most of accumulated cadmium in *C. reinhardtii* exposed to 70 μM $CdCl_2$ for 3 weeks, as the phytochelatins content/accumulated cadmium ratio was 4.8 (Bräutigam et al. 2011). In contrast, in *E. gracilis* exposed to Cd^{2+}, the phytochelatins content is usually a minor component (~10%) of the total thiol molecule (Cys + γEC + GSH + phytochelatins + non-canonical GSH polymers + trypanothione) content (García-García et al. 2012; Mendoza-Cózatl et al. 2002, 2006a; Sánchez-Thomas et al. 2016; Santiago-Martínez et al. 2015), indicating that other mechanisms besides phytochelatins synthesis are involved in the cadmium hyperaccumulation observed in this protist.

In contrast, over-expression of phytochelatin synthase in *A. thaliana* confers high-level of resistance to arsenate and, surprisingly, Cd^{2+} hypersensitivity (Li et al. 2004). In this regard, after 48 h exposure to arsenate the contents of at least three unknown thiol-rich peptides (presumably non-canonical PC_2 and PC_3), and γEC, increase whereas those of PC_2 and PC_3 slightly decrease, in comparison to the wild type strain. In contrast, Cd^{2+} induces increased levels of PC_2, PC_3 and PC_4, but not the unknown thiol-rich peptides, in both wild-type and phytochelatin synthase-overexpressing *A. thaliana* strains (Li et al. 2004). Specificity differences in phytochelatin synthase and phytochelatins storage into vacuoles might be involved in the cell response to arsenate and cadmium. No clear explanation for the Cd^{2+} hypersensitivity induced by phytochelatin synthase over-expression has been elaborated, although lower levels of essential heavy metals induced by the increased phytochelatins might be involved. However, this observation recalls the importance of gaining a full understanding of the regulation mechanisms of the biological functions studied, before faithfully (and blindly) embarking in the genetic transformation of plants and microorganisms.

In *G. max* and *L. japonicus* exposed to Cd^{2+}, homoPC_2 to homoPC_4 (Fig. 6.3) have been identified, besides canonical phytochelatins (Oven et al. 2002; Ramos et al. 2007). Accordingly, it has been reported that homo-phytochelatin synthase 1 from *G. max* and phytochelatin synthase 2–7 N and phytochelatin synthase 3–7 N from *L. japonicus* can use homoGSH to synthesize homophytochelatins in the presence of Cd^{2+} (Oven et al. 2002; Ramos et al. 2007). These alternative GSH enzymes and metabolites are not well characterized in other plants and organisms, although metabolite analysis in *A. thaliana* exposed to Cd^{2+} has identified homoPC_2 to homoP_4; hydroxymethylPC_3 $(\gamma Glu\text{-}Cys)_3$-Ser; hydroxymethyl$PC_4$ $(\gamma Glu\text{-}Cys)_4$-Ser; iso$PC_2$ $(\gamma Glu\text{-}Cys)_2$-Glu and iso$PC_3$ $(\gamma Glu\text{-}Cys)_3$-Gln (Fig. 6.3; Sarry et al. 2006). Phytochelatin synthase from *A. thaliana* is not active with homo-GSH (Oven et al. 2002), suggesting either that (1) the $K_{m\ \text{homo-GSH}}$ is much higher than 10 mM homoGSH (the assayed concentration); or (2) *A. thaliana* has homo-phytochelatin synthase isoforms that have not yet been identified.

Canonical phytochelatins (PC_2 to PC_4) represent only about 18% of total phytochelatins in *E. gracilis* exposed to Cd^{2+} (Figs. 6.3 and 6.4); thus, 82% of *E. gracilis* phytochelatins are non-canonical GSH polymers, including trypanothione which also increases in the presence of Cd^{2+} and Cr^{6+} or Cr^{3+} (Lira-Silva et al. 2011; Sánchez-Thomas et al. 2016). Indeed, homoPC_2, hydroxymethylPC_2 and isoPC_2 are detected in *E. gracilis* exposed to 50–200 μM Cd^{2+} for 8 days, along with many other longer non-canonical GSH polymers still not identified (*i.e.*, homoPC_3 and homoPC_4; hydroxymethylPC_3 and hydroxymethylPC_4;

isoPC$_3$ and isoPC$_4$). In this regard, enzymes with homo-glutathione synthetase activity that generates homo-GSH (or derivatives with Ser, Glu and Gln) and homo-phytochelatin synthase activity that generates homo-phytochelatins, have not yet been identified in *E. gracilis*.

Subcellular phytochelatins compartmentation. Heavy metal transporter 1 is an ABC type transporter (*i.e.* its reaction is driven by ATP hydrolysis) involved in compartmentalization of Cd-PC complexes into vacuoles, and which has been described in *S. pombe*, *C. elegans* and *Drosophila melanogaster* (Sooksa-Nguan et al. 2009; Vatamaniuk et al. 2005). Interestingly, *Drosophila* has no phytochelatin synthase gene and phytochelatins have not been detected, which suggests that the heavy metal transporter 1 could have another physiological function (Sooksa-Nguan et al. 2009). Other ABC type transporters implicated in the membrane transport of Cd-phytochelatins complexes from the cytosol into the vacuole are Abc2 in *S. pombe* and MRP1/ABCC1 and MRP2/ABCC2 in *A. thaliana* (Mendoza-Cózatl et al. 2011). The vacuolar PC transporters have not been characterized in algae and protists (Fig. 6.2); and their kinetic characterization (V_{max}, K_m, V_{max}/K_m and an appropriate rate equation) has not been performed in plants and yeast, which vey likely is linked to the difficulty to obtain suitable substrates.

In *E. gracilis*, which lacks typical plant vacuoles but seems to have minivacuoles (which are <10% cell volume) (Rocchetta et al. 2006; Sittenfeld et al. 2002; Sommer and Blum 1965), the phytochelatin transport studies need to be extended to chloroplasts and mitochondrion, organelles in which phytochelatins and Cd-phytochelatins complexes are stored (Fig. 6.2). Phytochelatins storage in chloroplasts has also been described for *C. reinhardtii* (Nagel et al. 1996). Nothing is known about these membrane transporters in *E. gracilis*; however, the uneven sub-cellular distribution of Cd-S, Cd-GSH, Cd-phytochelatins, and As-GSH suggests the presence of ABC type transporters to mobilize these complexes within the cell (Mendoza-Cózatl et al. 2006b; Miot et al. 2008; Weber et al. 1987).

The formation of Cd-PC complexes and their transport into vacuoles or other organelles are apparently only intermediate steps in the cellular detoxification process of heavy metals. The further generation of Low and High Molecular Weight Complexes (LMWC and HMWC) appears as the ultimate step (Fig. 6.2). In yeast (Ortiz et al. 1992) and plants (Marentes and Rauser 2007; Wu et al. 2008), LMWC are <5 kDa and HMWC are >5 kDa whereas in *E. gracilis* LMWC are <50 kDa and HMWC are >50 kDa (Mendoza-Cózatl et al. 2006b). The Cd-LMWC and Cd-HMWC have been characterized in the plants *Pistia stratiodes* and *Eichhornia crassipes* exposed to 1–10 μM Cd^{2+} (Marentes and Rauser 2007; Wu et al. 2008); and in *E. gracilis* and *S. pombe* exposed to 100–400 μM Cd^{2+} (Mendoza-Cózatl et al. 2006b; Ortiz et al. 1992, 1995). These Cd-complexes are constituted by not only phytochelatins, but also by other molecules such as homo-, iso- and hydroxymethyl-phytochelatins (Fig. 6.3), desglycyl-phytochelatins (γGlu-Cys)$_n$, sulfide, Cys, γEC, GSH, iso-GSH, Ser, and Asp (Marentes and Rauser 2007; Mendoza-Cózatl et al. 2006b; Wu et al. 2008). Due to the greater distance of the terminal carboxylate group in homo-PC$_2$ (Gly is replaced by β-Ala; Fig. 6.3a) or the presence of an extra terminal carboxylate group in iso-PC$_2$ (Gly is replaced by Glu; Fig. 6.3d), slightly weaker or stronger binding of Cd^{2+} (see Fig. 6.1b), respectively, by non-canonical phytochelatins *vs.* canonical phytochelatins may be expected.

Ortiz et al. (1995) determined that Cd-LMWC (3–4 kDa; mainly constituted by a few Cd-PC$_2$ and Cd-PC$_3$ molecules) were transported into *S. pombe* vacuoles while Cd-HMWC (6–9 kDa; constituted by more Cd-PC$_2$ and Cd-PC$_3$ molecules stabilized by sulfide) were transported at a slower rate (Ortiz et al. 1992, 1995). In addition, it has been suggested that Cd^{2+} is translocated from one tissue to another in plants as Cd-LMWC (Wu et al. 2008).

The *S. pombe* phytochelatin synthase (*pcs*) mutant, as well as the heavy metal tolerance factor-1 (*hmt1*) mutant, showed greater sensitivity to 5 μM Cd^{2+} than wild type cells; whereas the *S. pombe pcs hmt1* double mutant became

hypersensitive to Cd^{2+} (Mendoza-Cózatl et al. 2010). These results suggest that: (1) Cys, GSH, sulfide, polyphosphates and any other chelating molecule do not suffice to replace the Cd^{2+} inactivation provided by phytochelatins in *S. pombe*; and (2) heavy metal chelation by phytochelatins must be complemented by heavy metal tolerance factor-1 activity to fully inactivate toxic heavy metal ions.

6.3.3 Heavy Metal Binding by Poly-phosphates

Poly-phosphates (PolyP; Fig. 6.3e) or volutin granules are widespread in nature, since they have been detected in bacteria, archaea, protozoans, algae, plant and mammalian cells (Docampo and Moreno 2008; Lemercier et al. 2004; Ruiz et al. 2001). PolyP and its associated enzymes are essential for some structural functions, in bioenergetics and notably, stress responses (Pérez-Castiñeira et al. 2001). PolyP are involved in quorum sensing, biofilm formation, motility, virulence, sporulation, osmotic stress, oxidative stress, heat stress, and nutritional stress responses in bacteria. A close correlation between heavy metal resistance and polyP content has been observed in archaea (Lira-Silva et al. 2013; Orell et al. 2012). In plants, they appear involved in mycorrhizal colonization, symbiosis modulation, seed embryo development, germination, cytosolic pH regulation, Ca^{2+}-mediated cell signaling, osmotic stress response, photosynthesis regulation, Fe^{3+} storage and delivery, and heavy metal sequestration (Seufferheld and Curzi 2010).

PolyP metabolism is catalyzed by polyP kinase (PPK; EC 2.7.4.1), exopolyphosphatase (PPX; EC 3.6.1.11) and compartmentalization mechanisms (*i.e.*, acidocalcisome membrane transporters) (Seufferheld and Curzi 2010). PPKs are enzymes that synthesize polyP either by polymerization of orthophosphate molecules ($P_i \leftrightarrows$ polyP) or by transference of the phosphate residue from high-energy metabolites (ATP-Mg + (polyP)n $\leftrightarrows$ (polyP)n+1 + ADP-Mg). PPK has been well characterized in different bacterial species. The PPK affinities for P_i (K_m = 1.7 mM; Levinson et al. 1975), and ATP and GTP (K_m = 0.14–0.66 mM; Levinson et al. 1975; Linder et al. 2007; Shum et al. 2011) are within these metabolite physiological concentrations. The PPK reverse reaction, to produce Pi or ATP from polyP, is feasible. PPK can also use glucose-6-phosphate as a substrate (Keasling 1997). PPXs from bacteria, protists (*T. cruzi*), yeast (*S. cerevisiae*) and humans show K_m values for polyP (chain lengths of 3–208 units of P_i) of 0.001–0.6 mM and are strictly dependent on divalent essential metal ions (Andreeva et al. 2004; Fang et al. 2007; Keasling 1997; Proudfoot et al. 2004); the effect of non-essential metals has not been examined. ATP and GTP are not substrates for *S. cerevisiae* PPX (Andreeva et al. 2004).

Acidocalcisomes are acidic organelles with high concentrations of pyrophosphate (PPi), PolyP, and essential metal ions such as Ca^{2+}, Mg^{2+}, Fe^{3+}, and Zn^{2+} (Docampo and Moreno 2008; Seufferheld and Curzi 2010). Hence, acidocalcisomes have membrane cation transporters, amino acid transporters, aquaporin, a Ca^{2+}-ATPase, a Pi transporter, a PPi transporter, a H^+-Ca^{2+}-exchanger, a V-H^+-ATPase, a V-H^+-PPiase and a Cl^- channel (Docampo and Moreno 2008).

The essential role of polyP and acidocalcisomes for the cellular homeostasis of essential heavy metals supports the hypothesis that such a role might be extended to the regulation of the levels and subsequent accumulation of non-essential heavy metals by chelation and compartmentalization. This hypothesis is currently under experimental scrutiny. An *E. coli* strain that over-expresses both PPK and PPX becomes more resistant to Cd^{2+} than a strain over-expressing only PPK and with 23 times higher polyP levels (Keasling and Hupf 1996). Thus, it appears that the ability to hydrolyze polyP to maintain high Pi levels is more relevant for heavy metal resistance than the actual polyP content (Keasling and Hupf 1996). Similarly, tobacco plants genetically engineered to express bacterial PPK proved to be more resistant to Hg^{2+} and Cd^{2+}, correlating with an increase of 7 and 2.3 times in the heavy metal accumulation capacity in transgenic plants exposed to 10 μM Hg^{2+} and 0.5 μM Cd^{2+} for 1–2 weeks , respectively (Nagata et al. 2006, 2008).

Unfortunately, PPi and polyP content; and compartmentalization into acidocalcisomes of Hg- and Cd-complexes were not determined; nevertheless, these experiments suggest that manipulation of PolyP metabolism could be useful to increase the heavy metal accumulation capacity.

In photosynthetic *E. gracilis* under aerobiosis, the PolyP content doubles when cultured with 25 μM Cd^{2+} in comparison to control cultures (Santiago-Martínez et al. 2015). Furthermore, under anaerobiosis and in the presence of 2 mM Cr^{6+} + 1 mM Fe^{3+}, the polyP content increases by 17 times and, with 5 mM Zn^{2+}, 28 times (unpublished data), suggesting that indeed polyP may be an effective partner of thiol molecules for intracellular metal accumulation.

6.3.4 Secretion of Oxalate, Malate and Polysaccharydes (EPS) for Extracellular Heavy Metal Chelation

Extracellular chelation of Al^{3+} by secreted malate is a capture mechanism initially described in plants (Ma et al. 2001; Shen et al. 2005), and recently in *E. gracilis* exposed to Cr^{6+} (as CrO_4^{2-}) in order to chelate Cr^{3+} (Lira-Silva et al. 2011). In *P. fluorescens* and plants, extracellular Al^{3+} chelation by oxalate is the most well-described mechanism, although other metabolites such as citrate, oxaloacetate and phosphatidylethanolamine also contribute to alleviate Al^{3+} stress (Auger et al. 2013; Yang et al. 2005) as well as Cd^{2+}, Zn^{2+}, Mn^{2+} and Cu^{+} toxicities (Graz et al. 2009; Jarosz-Wilkołazka et al. 2006; Zhu et al. 2011). In *E. gracilis*, malate secretion is driven by an increased malate metabolism (Lira-Silva et al. 2011), and although the genes activated by heavy metal ions have not been identified, $NADP^{+}$-malic enzyme activity significantly increases when cells are cultured in the presence of Cr^{6+} (Lira-Silva et al. 2011). For *E. mutabilis*, putrescine appears to be the most specifically secreted metabolite, followed by monosaccharides such as mannitol, glucose, fructose and arabinose, and amino acids such as Gly, threonine and tyrosine. For these metabolites, a biological function remains to be identified, although a symbiotic role has been proposed in which the secreted metabolites promote the growth of iron- and sulfate-reducing acidophilic bacteria (Halter et al. 2012b; Nancucheo and Johnson 2012). However, *E. mutabilis* and anaerobically-grown *E. gracilis* are also able to secrete organic acids such as glycolate, *p*-hydroxybenzoate, succinate and lactate (Halter et al. 2012b; Nancucheo and Johnson 2012; Santiago-Martínez et al. 2015), which could bind heavy metal ions in the extracellular milieu.

Other metabolites extruded in response to heavy metal stress are extracellular polysaccharides. These molecules are constituted by glycoproteins, nucleic acids and lipids all which bind metal ions (Das et al. 2009; García-García et al. 2016). Extracellular polysaccharides are synthesized intracellularly and later extruded in *Chlorococcum* sp., *Phormidium* sp. and *Spirulina* sp. stressed by Cu^{2+} and Zn^{2+} (Das et al. 2009); the metal-extracellular polysaccharide complexes are insoluble, which is an advantage for metal recovery purposes (Das et al. 2009), because it avoids steps of metal desorption or release of metals from cells. The biosynthesis of extracellular polysaccharides such as alginates or celluloses is associated to the activity of plasma membrane glycosyltransferases, which transfer sugars from the cytosol to the extracellular polymer chains through a pore formed by their transmembrane region (Bi et al. 2015). Recent transcriptomic analysis of *E. gracilis* revealed 230 sequences for glycosyltransferases (O'Neill et al. 2015). Thus, extracellular polysaccharide biosynthesis and secretion in *E. gracilis* deserves further study to understand the contribution of this mechanism to heavy metal resistance.

6.4 Concluding Remarks

1. Intracellular internalization rather than biosorption is the main mechanism that *E. gracilis* uses to accumulate heavy metals.
2. Heavy metal binding by phytochelatins and other thiol-metabolites and their further compartmentalization into chloroplasts and

mitochondria are the best understood mechanisms for their accumulation in *E. gracilis*.
3. Non-canonical polymers of GSH are also involved in heavy-metal accumulation in *E. gracilis*.
4. Characterization of chloroplast and mitochondrial transporters of Cd-thiol metabolite complexes and sulfate is required to be able to improve the heavy metal accumulation capacity of *E. gracilis*.
5. PolyP metabolism has emerged as a mechanism that can help support the accumulation of high amounts of Cd^{2+}.
6. In-depth analysis of the biochemical mechanisms involved in the resistance and accumulation of heavy metals may allow the design of rational strategies for efficient improvement of genetically modified organisms.
7. *E. gracilis* is a suitable microorganism to be used in bioremediation processes of water wastes polluted with heavy metals.

Acknowledgements The present work was partially supported by grants from CONACyT-México (Nos. 107183, 239930, 178638 and 156969) and Instituto de Ciencia y Tecnología del Distrito Federal (No. PICS08-5) to SRE, RMS, ES and RJC.

References

Albergoni V, Piccinni E, Coppellotti O (1980) Response to heavy metals in organisms-I. Excretion and accumulation of physiological and non physiological metals in *Euglena gracilis*. Comp Biochem Physiol C 67C:121–127

Ali H, Khan E, Sajad MA (2013) Phytoremediation of heavy metals-concepts and applications. Chemosphere 91:869–881

Altaş L (2009) Inhibitory effect of heavy metals on methane-producing anaerobic granular sludge. J Hazard Mater 162:1551–1556

Andreeva NA, Kulakovskaya TV, KulaevI S (2004) Purification and properties of exopolyphosphatase from the cytosol of *Saccharomyces cerevisiae* not encoded by the PPX1 gene. Biochemistry (Mosc) 69:387–393

Areco MM, Hanela S, Duran J, Afonso Mdos S (2012) Biosorption of Cu(II), Zn(II), Cd(II) and Pb(II) by dead biomasses of green alga *Ulva lactuca* and the development of a sustainable matrix for adsorption implementation. J Hazard Mater 213–214:123–132

Auger C, Han S, Appanna VP, Thomas SC, Ulibarri G, Appanna VD (2013) Metabolic reengineering invoked by microbial systems to decontaminate aluminum: implications for bioremediation technologies. Biotechnol Adv 31:266–273

Avilés C, Loza-Tavera H, Terry N, Moreno-Sánchez R (2003) Mercury pretreatment selects an enhanced cadmium-accumulating phenotype in *Euglena gracilis*. Arch Microbiol 180:1–10

Avilés C, Torres-Márquez ME, Mendoza-Cózatl D, Moreno-Sánchez R (2005) Time-curse development of the Cd^{2+} hyper-accumulating phenotype in *Euglena gracilis*. Arch Microbiol 184:83–92

Bachhawat AK, Thakur A, Kaur J, Zulkifli M (2013) Glutathione transporters. Biochim Biophys Acta 1830:3154–3164

Baker BJ, Banfield JF (2003) Microbial communities in acid mine drainage. FEMS Microbiol Ecol 44: 139–152

Belcastro M, Marino T, Russo N, Toscano M (2009) The role of glutathione in cadmium ion detoxification: coordination modes and binding properties—a density functional study. J Inorg Biochem 103:50–57

Bhargava A, Carmona FF, Bhargava M, Srivastava S (2012) Approaches for enhanced phytoextraction of heavy metals. J Environ Manag 105:103–120

Bi Y, Hubbard C, Purushotham P, Zimmer J (2015) Insights into the structure and function of membrane-integrated processive glycosyltransferase. Curr Opin Struct Biol 34:78–86

Bolchi A, Petrucco S, Tenca PL, Foroni C, Ottonello S (1999) Coordinate modulation of maize sulfate permease and ATP sulfurylase mRNAs in response to variations in sulfur nutrition status: stereospecific down-regulation by L-cysteine. Plant Mol Biol 39:527–537

Brake SS, Dannelly HK, Connors KA, Hasiotis ST (2001) Influence of water chemistry on the distribution of an acidophilic protozoan in an acid mine drainage system at the abandoned Green Valley coal mine, Indiana, USA. Appl Geochem 16:1641–1652

Bräutigam A, Schaumlöffel D, Preud'homme H, Thondorf I, Wesenberg D (2011) Physiological characterization of cadmium-exposed *Chlamydomonas reinhardtii*. Plant Cell Environ 34:2071–2082

Brekken DL, Phillips MA (1998) *Trypanosoma brucei* gamma-glutamylcysteine synthetase. Characterization of the kinetic mechanism and the role of Cys-319 in cystamine inactivation. J Biol Chem 273:26317–26322

Breton A, Surdin-Kerjan Y (1977) Sulfate uptake in *Saccharomyces cerevisiae*: biochemical and genetic study. J Bacteriol 132:224–232

Brito EM, De la Cruz Barrón M, Caretta CA, Goñi-Urriza M, Andrade LH, Cuevas-Rodríguez G, Malm O, Torres JP, Simon M, Guyoneaud R (2015) Impact of hydrocarbons, PCBs and heavy metals on bacterial communities in Lerma River, Salamanca, Mexico: investigation of hydrocarbon degradation potential. Sci Total Environ 521–522:1–10

Brooks RR, Chambers MF, Nicks LJ, Robinson BH (1998) Phytomining. Trends Plant Sci 3:359–362

Brown JF, Jones DS, Mills DB, Macalady JL, Burgos WD (2011) Application of a depositional *Facies* model to an acid mine drainage site. Appl Environ Microbiol 77:545–554

Brunetti P, Zanella L, Proia A, De Paolis A, Falasca G, Altamura MM, Sanità di Toppi L, Costantino P, Cardarelli M (2011) Cadmium tolerance and phytochelatin content of *Arabidopsis* seedlings overexpressing the phytochelatin synthase gene *At*PCS1. J Exp Bot 62:5509–5519

Buetow DE (1962) Differential effects of temperature on the growth of *Euglena gracilis*. Exp Cell Res 27:137–142

Cao MJ, Wang Z, Wirtz M, Hell R, Oliver DJ, Xiang CB (2013) SULTR3;1 is a chloroplast-localized sulfate transporter in *Arabidopsis thaliana*. Plant J 73:607–616

Casiot C, Bruneel O, Personé JC, Leblanc M, Elbaz-Poulichet F (2004) Arsenic oxidation and bioaccumulation by the acidophilic protozoan *Euglena mutabilis*, in acidic mine drainage (Carnoulès, France). Sci Total Environ 320:259–267

Chen J, Zhou J, Goldsbrough PB (1997) Characterization of phytochelatin synthase from tomato. Physiol Plant 101:165–172

Chen HC, Newton AJ, Melis A (2005) Role of SulP, a nuclear-encoded chloroplast sulfate permease, in sulfate transport and H2 evolution in *Chlamydomonas reinhardtii*. Photosynth Res 84:289–296

Ciaffi M, Paolacci AR, Celletti S, Catarcione G, Kopriva S, Astolfi S (2013) Transcriptional and physiological changes in the S assimilation pathway due to single or combined S and Fe deprivation in durum wheat (*Tricum durum* L.) seedlings. J Exp Bot 64:1663–1675

Clemens S, Kim EJ, Neumann D, Schroeder JI (1999) Tolerance to toxic metals by a gene family of phytochelatin synthases from plants and yeast. EMBO J 18:3325–3333

Clemente MR, Bustos-Sanmamed P, Loscos J, James EK, Pérez-Rontomé C, Navascués J, Gay M, Becana M (2012) Thiol synthetases of legumes: immunogold localization and differential gene regulation by phytohormones. J Exp Bot 63:3923–3934

Das BK, Roy A, Koschorreck M, Mandal SM, Wendt-Potthoff K, Bhattacharya J (2009) Occurrence and role of algae and fungi in acid mine drainage environment with special reference to metals and sulfate immobilization. Water Res 43:883–894

Davis JS, Balinsky JB, Harington JS, Shepherd JB (1973) Assay, purification, properties and mechanism of action of gamma-glutamylcysteine synthetase from the liver of the rat and *Xenopus laevis*. Biochem J 133:667–678

Delalande O, Desvaux H, Godat E, Valleix A, Junot C, Labarre J, Boulard Y (2010) Cadmium-glutathione solution structures provide new insights into heavy metal detoxification. FEBS J 277:5086–5096

Deponte M (2013) Glutathione catalysis and the reaction mechanisms of glutathione-dependent enzymes. Biochim Biophys Acta 1830:3217–3266

Devars S, Avilés C, Cervantes C, Moreno-Sánchez R (2000) Mercury uptake and removal by *Euglena gracilis*. Arch Microbiol 174:175–180

Dobáková E, Flegontov P, Skalický T, Lukeš J (2015) Unexpectedly streamlined mitochondrial genome of the euglenozoan *Euglena gracilis*. Genome Biol Evol 7:3358–3367

Docampo R, Moreno SN (2008) The acidocalcisome as a target for chemotherapeutic agents in protozoan parasites. Curr Pharm Des 14:882–888

Dorčák V, Krężel A (2003) Correlation of acid-base chemistry of phytochelatin PC2 with its coordination properties towards the toxic metal ion Cd(II). Dalton Trans 11:2254–2259

Dos Santos Ferreira V, Rochetta I, Conforti V, Bench S, Feldman R, Levin MJ (2007) Gene expression patterns in *Euglena gracilis*: insights into the cellular response to environmental stress. Gene 389:136–145

Einicker-Lamas M, Mezian GA, Fernandes TB, Silva FL, Guerra F, Miranda K, Attias M, Oliveira MM (2002) *Euglena gracilis* as a model for the study of Cu^{2+} and Zn^{2+} toxicity and accumulation in eukaryotic cells. Environ Pollut 120:779–786

Fang J, Ruiz FA, Docampo M, Lou S, Rodrigues JC, Motta LS, Rohloff P, Docampo R (2007) Overexpression of the Zn^{2+}-sensitive soluble exopolyphosphatase from *Trypanosoma cruzi* depletes polyphosphates and affects osmoregulation. J Biol Chem 282:32501–32510

Frendo P, Harrison J, Norman C, Hernandez Jimenez MJ, Van de Sype G, Gilabert A, Puppo A (2005) Glutathione and homoglutathione play a critical role in the nodulation process of *Medicago truncatula*. Mol Plant-Microbe Interact 18:254–259

Gao Y, Schofield OM, Leustek T (2000) Characterization of sulfate assimilation in marine algae focusing on the enzyme 5′-adenylylsulfate reductase. Plant Physiol 123:1087–1096

García-García JD, Rodríguez-Zavala JS, Jasso-Chávez R, Mendoza-Cózatl D, Moreno-Sánchez R (2009) Chromium uptake, retention and reduction in photosynthetic *Euglena gracilis*. Arch Microbiol 191:431–440

García-García JD, Olin-Sandoval V, Saavedra E, Girard L, Hernández G, Moreno-Sánchez R (2012) Sulfate uptake in photosynthetic *Euglena gracilis*. Mechanisms of regulation and contribution to cysteine homeostasis. Biochim Biophys Acta 1820:1567–1575

García-García JD, Girard L, Hernández G, Saavedra E, Pardo JP, Rodríguez-Zavala JS, Encalada R, Reyes-Prieto A, Mendoza-Cózatl DG, Moreno-Sánchez R (2014) Zn-*bis*-glutathionate is the best co-substrate of the monomeric phytochelatin synthase from the photosynthetic heavy metal-hyperaccumulator *Euglena gracilis*. Metallomics 6:604–616

García-García JD, Sánchez-Thomas R, Moreno-Sánchez R (2016) Bio-recovery of non-essential heavy metals by intra- and extracellular mechanisms in free-living microorganisms. Biotechnol Adv 34:859–873

Garlaschi FM, Garlaschi A, Lombardi A, Forti G (1974) Effect of ethanol on the metabolism of *Euglena gracilis*. Plant Sci Lett 2:29–39

Gekeler W, Grill E, Winnacker EL, Zenk MH (1988) Algae sequester heavy metals via synthesis of phytochelatin complexes. Arch Microbiol 150:197–202

Gillet S, Decottignies P, Chardonnet S, Le Maréchal P (2006) Cadmium response and redoxin targets in *Chlamydomonas reinhardtii*: a proteomic approach. Photosynth Res 89:201–211

Graz M, Jarosz-Wilkołazka A, Pawlikowska-Pawlega B (2009) *Abortiporus biennis* tolerance to insoluble metal oxides: oxalate secretion, oxalate oxidase activity, and mycelial morphology. Biometals 22:401–410

Grill E, Winnacker EL, Zenk MH (1985) Phytochelatins: the principal heavy-metal complexing peptides of higher plants. Science 230:674–676

Grill E, Loffler S, Winnacker EL, Zenk MH (1989) Phytochelatins, the heavy-metal-binding peptides of plants, are synthesized from glutathione by a specific gamma-glutamylcysteine dipeptidyl transpeptidase (phytochelatin synthase). Proc Natl Acad Sci U S A 86:6838–6842

Gutiérrez RL, Rubio-Arias H, Quintana R, Ortega JA, Gutierrez M (2008) Heavy metals in water of the San Pedro River in Chihuahua, Mexico and its potential health risk. Int J Environ Res Public Health 5:91–98

Ha SB, Smith AP, Howden R, Dietrich WM, Bugg S, O'Connell MJ, Goldsbrough PB, Cobbett CS (1999) Phytochelatin synthase genes from *Arabidopsis* and the yeast *Schizosaccharomyces pombe*. Plant Cell 11:1153–1164

Hallick RB, Hong L, Drager RG, Favreau MR, Monfort A, Orsat B, Spielmann A, Stutz E (1993) Complete sequence of *Euglena gracilis* chloroplast DNA. Nucleic Acids Res 21:3537–3544

Halter D, Casiot C, Heipieper HJ, Plewniak F, Marchal M, Simon S, Arsène-Ploetze F, Bertin PN (2012a) Surface properties and intracellular speciation revealed an original adaptive mechanism to arsenic in the acid mine drainage bio-indicator *Euglena mutabilis*. Appl Microbiol Biotechnol 93:1735–1744

Halter D, Goulhen-Chollet F, Gallien S, Casiot C, Hamelin J, Gilard F, Heintz D, Schaeffer C, Carapito C, van Dorsselaer A, Tcherkez G, Arsène-Ploetze F, Bertin PN (2012b) *In situ* proteo-metabolomics reveals metabolite secretion by the acid mine drainage bio-indicator, *Euglena mutabilis*. ISME J 6:1391–1402

Hanna E, Ng KF, MacRae IJ, Bley CJ, Fisher AJ, Segel IH (2004) Kinetic and stability properties of *Penicillium chrysogenum* ATP sulfurylase missing the C-terminal regulatory domain. J Biol Chem 279:4415–4424

Hargreaves JW, Lloyd EJH, Whitton BA (1975) Chemistry and vegetation of highly acidic streams. Freshw Biol 5:563–576

Hashim MA, Mukhopadhyay S, Sahu JN, Sengupta B (2011) Remediation technologies for heavy metal contaminated groundwater. J Environ Manag 92:2355–2388

Hawes CS, Nicholas DJ (1973) Adenosine 5′-Triphosphate sulfurylase from *Saccharomyces cerevisiae*. Biochem J 133:541–550

Hell R, Bergmann L (1990) γ-Glutamylcysteine synthetase in higher plants: catalytic properties and subcellular localization. Planta 180:603–612

Hirata K, Tsujimoto Y, Namba T, Ohta T, Hirayanagi N, Miyasaka H, Zenk MH, Miyamoto K (2001) Strong induction of phytochelatin synthesis by zinc in marine green alga *Dunaliella tertiolecta*. J Biosci Bioeng 92:24–29

Hu G, Bi S, Xu G, Zhang Y, Mei X, Li A (2015) Distribution and assessment of heavy metals off the Changjiang River mouth and adjacent area during the past century and the relationship of the heavy metals with anthropogenic activity. Mar Pollut Bull 96:434–440

Huang J, Nkrumah PN, Anim DO, Mensah E (2014) E-waste disposal effects on the aquatic environment: Accra, Ghana. Rev Environ Contam Toxicol 229:19–34

Inui H, Miyatake K, Nakano Y, Kitaoka S (1985) The physiological role of oxygen-sensitive pyruvate dehydrogenase in mitochondrial fatty acid synthesis in *Euglena gracilis*. Arch Biochem Biophys 237:423–429

Inui H, Ono K, Miyatake K, Nakano Y, Kitaoka S (1987) Purification and characterization of pyruvate:NADP$^+$ oxidoreductase in *Euglena gracilis*. J Biol Chem 262:9130–9135

Inui H, Miyatake K, Nakano Y, Kitaoka S (1990) Pyruvate:NADP$^+$ oxidoreductase from *Euglena gracilis*: mechanism of O2-inactivation of the enzyme and its stability in the aerobe. Arch Biochem Biophys 280:292–298

Ishii N, Uchida S (2006) Removal of technetium from solution by algal flagellate *Euglena gracilis*. J Environ Qual 35:2017–2020

Ivušić F, Šantek B (2015) Optimization of complex medium composition for heterotrophic cultivation of *Euglena gracilis* and paramylon production. Bioprocess Biosyst Eng 38:1103–1112

Jamers A, Blust R, De Coen W, Griffin JL, Jones OA (2013) An omics based assessment of cadmium toxicity in the green alga *Chlamydomonas reinhardtii*. Aquat Toxicol 126:355–364

Jarosz-Wilkołazka A, Graz M, Braha B, Menge S, Schlosser D, Krauss GJ (2006) Species-specific Cd-stress response in the white rot basidiomycetes *Abortiporus biennis* and *Cerrena unicolor*. Biometals 19:39–49

Jasso-Chávez R, Moreno-Sánchez R (2003) Cytosol-mitochondria transfer of reducing equivalents by a lactate shuttle in heterotrophic *Euglena*. Eur J Biochem 270:4942–4951

Jasso-Chávez R, Pacheco-Rosales A, Lira-Silva E, Gallardo-Pérez JC, García N, Moreno-Sánchez R (2010) Toxic effects of Cr(VI) and Cr(III) on energy metabolism of heterotrophic *Euglena gracilis*. Aquat Toxicol 100:329–338

Jensen A, Bro-Rasmunssen F (1992) Environment cadmium in Europe. Rev Environ Contam Toxicol 125:101–181

Kataoka T, Watanabe-Takahashi A, Hayashi N, Ohnishi M, Mimura T, Buchner P, Hawkesford MJ, Yamaya T, Takahashi H (2004) Vacuolar sulfate transporters are essential determinants controlling internal distribution of sulfate in *Arabidopsis*. Plant Cell 16:2693–2704

Keasling JD (1997) Regulation of intracellular toxic metals and other cations by hydrolysis of polyphosphate. Ann N Y Acad Sci 829:242–249

Keasling JD, Hupf GA (1996) Genetic manipulation of polyphosphate metabolism affects cadmium tolerance in *Escherichia coli*. Appl Environ Microbiol 62:743–746

Kobayashi K, Yoshimoto A (1982) Studies on yeast sulfite reductase. IV. Structure and steady-state kinetics. Biochim Biophys Acta 705:348–356

Kondo N, Isobe M, Imai K, Goto T (1983) Structure of cadystin, the unit-peptide of cadmium-binding peptides induced in a fission yeast, *Schizosaccharomyces pombe*. Tetrahedron Lett 24:925–928

Kopriva S (2006) Regulation of sulfate assimilation in *Arabidopsis* and beyond. Ann Bot 97:479–495

Koprivova A, Kopriva S (2014) Molecular mechanisms of reguation of sulfate assimilation: first steps on a long road. Front Plant Sci 5:589

Lancilli C, Giacomini B, Lucchini G, Davidian JC, Cocucci M, Sacchi GA, Nocito FF (2014) Cadmium exposure and sulfate limitation reveal differences in the transcriptional control of three sulfate transport (Sultr1;2) genes in *Brassica juncea*. BMC Plant Biol 14:132

Lappartient AG, Touraine B (1996) Demand-driven control of root ATP sulfurylase activity and SO_4^{2-} uptake in intact canola (the role of phloem-translocated glutathione). Plant Physiol 111:147–157

Lappartient AG, Vidmar JJ, Leustek T, Glass AD, Touraine B (1999) Inter-organism signaling in plants: regulation of ATP sulfurylase and sulfate transporter genes expression in roots mediated by phloem-translocated compound. Plant J 18:89–95

Lee DC, Park CJ, Yang JE, Jeong YH, Rhee HI (2000) Screening of hexavalent chromium biosorbent from marine algae. Appl Microbiol Biotechnol 54:597–600

Lemercier G, Espiau B, Ruiz FA, Vieira M, Luo S, Baltz T, Docampo R, Bakalara N (2004) A pyrophosphatase regulating polyphosphate metabolism in acidocalcisomes is essential for *Trypanosoma brucei* virulence in mice. J Biol Chem 279:3420–3425

León J, Romero LC, Galván F, Vega JM (1987) Purification and physicochemical characterization of O-acetyl-L-serine sulfhydrylase from *Chlamydomonas reinhardtii*. Plant Sci 53:93–99

Levinson SL, Jacobs LH, Krulwich TA, Li HC (1975) Purification and characterization of a polyphosphate kinase from *Arthrobacter atrocyaneus*. J Gen Microbiol 88:65–74

Li JJ, Saidha T, Schiff JA (1991) Purification and properties of two forms of ATP sulfurylase from *Euglena*. Biochim Biophys Acta 1078:68–76

Li Y, Dhankher OP, Carreira L, Lee D, Chen A, Schroeder JI, Balish RS, Meagher RB (2004) Overexpression of phytochelatin synthase in *Arabidopsis* leads to enhanced arsenic tolerance and cadmium hypersensitivity. Plant Cell Physiol 45:1787–1797

Linder SN, Vidaurre D, Willbold S, Schoberth SM, Wendisch VF (2007) NCgl2620 encodes a class II polyphosphate kinase in *Corynebacterium glutamicum*. Appl Environ Microbiol 73:5026–5033

Lira-Silva E, Ramírez-Lima IS, Olín-Sandoval V, García-García JD, García-Contreras R, Moreno-Sánchez R, Jasso-Chávez R (2011) Removal, accumulation and resistance to chromium in heterotrophic *Euglena gracilis*. J Hazard Mater 193:216–224

Lira-Silva E, Santiago-Martínez MG, García-Contreras R, Zepeda-Rodríguez A, Marín-Hernández A, Moreno-Sánchez R, Jasso-Chávez R (2013) Cd^{2+} resistance mechanisms in *Methanosarcina acetivorans* involve the increase in the coenzyme M content and induction of biofilm synthesis. Environ Microbiol Rep 5:799–808

Liu X, Wu FH, Li JX, Chen J, Wang GH, Wang WH, Hu WJ, Gao LJ, Wang ZL, Chen JH, Simon M, Zheng HL (2016) Glutathione homeostasis and Cd tolerance in the *Arabidopsis* sultr1;1-sultr1;2 double mutant with limiting sulfate supply. Plant Cell Rep 35:397–413

Lu SC (2013) Glutathione synthesis. Biochim Biophys Acta 1830:3143–3453

Lueder DV, Phillips MA (1996) Characterization of *Trypanosoma brucei* gamma-glutamylcysteine synthetase, an essential enzyme in the biosynthesis of trypanothione (diglutathionylspermidine). J Biol Chem 271:17485–17490

Luís AT, Teixeira P, Almeida SF, Matos JX, da Silva EF (2011) Environmental impact of mining activities in the Lousal area (Portugal): chemical and diatom characterization of metal-contaminated stream sediments and surface water of Corona stream. Sci Total Environ 409:4312–4325

Ma JF, Ryan PR, Delhaize E (2001) Aluminium tolerance in plants and the complexing role of organic acids. Trends Plant Sci 6:273–278

Marentes E, Rauser WE (2007) Different proportions of cadmium occur as Cd-binding phytochelatin complexes in plants. Physiol Plant 131:291–301

Maruyama-Nakashita A, Watanabe-Takahashi A, Inoue E, Yamaya T, Saito K, Takahashi H (2015) Sulfur-responsive elements in the 3′-nontranscribed intergenic region are essential for the induction of sulfate transporter 2;1 gene expression in *Arabidopsis* roots sulfur deficiency. Plant Cell 27:1279–1296

Mata YN, Blazquez ML, Ballester A, González F, Muñoz JA (2009a) Biosorption of cadmium, lead and copper with calcium alginate xerogels and immobilized *Fucus vesiculosus*. J Hazard Mater 163:555–562

Mata YN, Torres E, Blázquez ML, Ballester A, González F, Muñoz JA (2009b) Gold(III) biosorption and bioreduction with the brown alga *Fucus vesiculosus*. J Hazard Mater 166:612–618

Matamoros MA, Moran JF, Iturbe-Ormaetxe I, Rubio MC, Becana M (1999) Glutathione and homoglutathione synthesis in legume root nodules. Plant Physiol 121:879–888

Matsuda YC, Colman B (1995) Characterization of sulfate transport in the green alga *Chlorella ellipsoidea*. Plant Cell Physiol 36:1291–1296

Matsuda F, Hayashi M, Kondo A (2011) Comparative profiling analysis of central metabolites in *Euglena gracilis* under various cultivation conditions. Biosci Biotechnol Biochem 75:2253–2256

McComb JQ, Han FX, Rogers C, Thomas C, Arslan Z, Ardeshir A, Tchounwou PB (2015) Trace elements and heavy metals in the Gran Bay National Estuarine Reserve in the northern Gulf of Mexico. Mar Pollut Bull 99:61–69

Mehta SK, Gaur JP (2005) Use of algae for removing heavy metal ions from wastewater: progress and prospects. Crit Rev Biotechnol 25:113–152

Mendoza-Cózatl DG, Moreno-Sánchez R (2006) Control of glutathione and phytochelatin synthesis under cadmium stress. Pathway modeling for plants. J Theor Biol 238:919–936

Mendoza-Cózatl D, Devars S, Loza-Tavera H, Moreno-Sánchez R (2002) Cadmium accumulation in the chloroplast of *Euglena gracilis*. Physiol Plant 115:276–283

Mendoza-Cózatl D, Loza-Tavera H, Hernández-Navarro A, Moreno-Sánchez R (2005) Sulfur assimilation and glutathione metabolism under cadmium stress in yeast, protists and plants. FEMS Microbiol Rev 29:653–671

Mendoza-Cózatl DG, Rangel-González E, Moreno-Sánchez R (2006a) Simultaneous Cd^{2+}, Zn^{2+}, and Pb^{2+} uptake and accumulation by photosynthetic *Euglena gracilis*. Arch Environ Contam Toxicol 51:521–528

Mendoza-Cózatl DG, Rodríguez-Zavala JS, Rodríguez-Enríquez S, Mendoza-Hernandez G, Briones-Gallardo R, Moreno-Sánchez R (2006b) Phytochelatin-cadmium-sulfide high-molecular-mass complexes of *Euglena gracilis*. FEBS J 273:5703–5713

Mendoza-Cózatl DG, Zhai Z, Jobe TO, Akmakjian GZ, Song WY, Limbo O, Russell MR, Kozlovskyy VI, Martinoia E, Vatamaniuk OK, Russell P, Schroeder JI (2010) Tonoplast-localized Abc2 transporter mediates phytochelatin accumulation in vacuoles and confers cadmium tolerance. J Biol Chem 285:40416–40426

Mendoza-Cózatl DG, Jobe TO, Hauser F, Schroeder JI (2011) Long-distance transport, vacuolar sequestration, tolerance, and transcriptional responses induced by cadmium and arsenic. Curr Opin Plant Biol 14:554–562

Millard P, Evans LV (1982) Sulphate uptake in the unicellular marine red alga *Rhodella maculata*. Arch Microbiol 131:165–169

Miot J, Morin G, Skouri-Panet F, Férard C, Aubry E, Briand J, Wang Y, Ona-Nguema G, Guyot F, Brown GE (2008) XAS study of arsenic coordination in *Euglena gracilis* exposed to arsenite. Environ Sci Technol 42:5342–5347

Moreno-Sánchez R, Covián R, Jasso-Chávez R, Rodríguez-Enríquez S, Pacheco-Moisés F, Torres-Márquez ME (2000) Oxidative phosphorylation supported by an alternative respiratory pathway in mitochondria from *Euglena*. Biochim Biophys Acta 1457:200–210

Moreno-Sánchez R, Saavedra E, Gallardo-Pérez JC, Rumjanek FD, Rodríguez-Enríquez S (2016) Understanding the cancer cell phenotype beyond the limitations of current omics analyses. FEBS J 283:54–73

Murphy V, Hughes H, McLoughlin P (2008) Comparative study of chromium biosorption by red, green and brown seaweed biomass. Chemosphere 70:1128–1134

Nagalakshmi N, Prasad MN (2001) Responses of glutathione cycle enzymes and glutathione metabolism to copper stress in *Scenedesmus bijugatus*. Plant Sci 160:291–299

Nagata T, Ishikawa C, Kiyono M, Pan-Hou H (2006) Accumulation of mercury in transgenic tobacco expressing bacterial polyphosphate. Biol Pharm Bull 29:2350–2353

Nagata T, Kimura T, Pan-Hou H (2008) Engineering expression of polyphosphate confers cadmium resistance in tobacco. J Toxicol Sci 33:371–373

Nagel K, Adelmeier U, Voigt J (1996) Subcellular distribution of cadmium in the unicellular green alga *Chlamydomonas reinhardtii*. J Plant Physiol 149:86–90

Nakagawa CW, Mutoh N, Hayashi Y (1993) Glutathione synthetase from the fission yeast. Purification and its unique heteromeric subunit structure. Biochem Cell Biol 71:447–453

Nakano Y, Urade Y, Urade R, Kitaoka S (1987) Isolation, purification and characterization of the pellicle of *Euglena gracilis* z. J Biochem 102:1053–1063

Nam SH, Lee WN, Shin YJ, Yoon SJ, Kim SW, Kwak JI, An YJ (2014) Derivation of guideline values for gold (III) ion toxicity limits to protect aquatic ecosystems. Water Res 48:126–136

Nancucheo I, Johnson DB (2012) Acidophilic algae isolated from mine-impacted environments and their roles in sustaining heterotrophic acidophiles. Front Microbiol 3:325

Nefedova Y, Fishman M, Sherman S, Wang X, Beg AA, Gabrilovich DI (2007) Mechanism of all-trans retinoic acid effect on tumor-associated myeloid-derived suppressor cells. Cancer Res 67:11021–11028

Nicolas P, Freyssinet G, Nigon V (1980) Effect of light on glucose utilization by *Euglena gracilis*. Plant Physiol 65:631–634

Nishikawa K, Onodera A, Tominaga N (2006) Phytochelatins do not correlate with the level of Cd accumulation in *Chlamydomonas* spp. Chemosphere 63:1553–1559

Nocito FF, Lancilli C, Crema B, Fourcroy P, Davidian JC, Sacchi GA (2006) Heavy metal stress and sulfate uptake in maize roots. Plant Physiol 141:1138–1148

O'Neill EC, Trick M, Hill L, Rejzek M, Dusi RG, Hamilton CJ, Zimba PV, Henrissat B, Field RA (2015) The transcriptome of *Euglena gracilis* reveals unexpected metabolic capabilities for carbohydrate and natural product biochemistry. Mol Biosyst 11:2808–2820

Olaveson MM, Nalewajko C (2000) Effects of acidity on the growth of two *Euglena* species. Hydrobiologia 433:39–56

Olin-Sandoval V, González-Chávez Z, Berzunza-Cruz M, Martínez I, Jasso-Chávez R, Becker I, Espinoza B, Moreno-Sánchez R, Saavedra E (2012) Drug target validation of the trypanothione pathway enzymes through metabolic modelling. FEBS J 279:1811–1833

Orell A, Navarro CA, Rivero M, Aguilar JS, Jerez CA (2012) Inorganic polyphosphates in extremophiles and their possible functions. Extremophiles 16:573–583

Ortiz DF, Kreppel L, Speiser DM, Scheel G, McDonald G, Ow DW (1992) Heavy metal tolerance in the fission yeast requires an ATP-binding cassette-type vacuolar membrane transporter. EMBO J 11:3491–3499

Ortiz DF, Ruscitti T, McCue KF, Ow DW (1995) Transport of metal-binding peptides by HMT1, a fission yeast ABC-type vacuolar membrane protein. J Biol Chem 270:4721–4728

Osaki Y, Shirabe T, Nakanishi H, Wakagi T, Yoshimura E (2009) Characterization of phytochelatin synthase produced by the primitive red alga *Cyanidioschyzon merolae*. Metallomics 1:353–358

Oven M, Page JE, Zenk MH, Kutchan TM (2002) Molecular characterization of the homo-phytochelatin synthase of soybean *Glycine max*: relation to phytochelatin synthase. J Biol Chem 277:4747–4754

Park H, Bakalinsky AT (2000) SSU1 mediates sulphite efflux in *Saccharomyces cerevisiae*. Yeast 16:881–888

Patron NJ, Durnford DG, Kopriva S (2008) Sulfate assimilation in eukaryotes: fusions, relocations and lateral transfers. BMC Evol Biol 8:39

Paul D, Pandey G, Pandey J, Jain RK (2005) Accessing microbial diversity for bioremediation and environmental restoration. Trends Biotechnol 23:135–142

Pérez-Castiñeira JR, Gómez-García R, López-Marqués RL, Losada M, Serrano A (2001) Enzymatic systems of inorganic pyrophosphate bioenergetics in photosynthetic and heterotrophic protists: remnants or metabolic cornerstones? Int Microbiol 4:135–142

Phartiyal P, Kim WS, Cahoon RE, Jez JM, Krishnan HB (2006) Soybean ATP sulfurylase, a homodimeric enzyme involved in sulfur assimilation, is abundantly expressed in roots and induced by cold treatment. Arch Biochem Biophys 450:20–29

Phartiyal P, Kim WS, Cahoon RE, Jez JM, Krishnan HB (2008) The role of 5′-adenylylsulfate reductase in the sulfur assimilation pathway of soybean: molecular cloning, kinetic characterization, and gene expression. Phytochemistry 69:356–364

Prasanna R, Ratha SK, Rojas C, Bruns MA (2011) Algal diversity in flowing waters at an acidic mine drainage "barrens" in central Pennsylvania, USA. Folia Microbiol (Praha) 56:491–496

Preuss ML, Cameron JC, Berg RH, Jez JM (2014) Immunolocalization of glutathione biosynthesis enzymes in *Arabidopsis thaliana*. Plant Physiol Biochem 75:9–13

Proudfoot M, Kuznetsova E, Brown G, Rao NN, Kitagawa M, Mori H, Savchenko A, Yakunin AF (2004) General enzymatic screens identify three new nucleotidases in *Escherichia coli*. Biochemical characterization of SurE, YfbR, and YjjG. J Biol Chem 279:54687–54694

Ramos J, Clemente MR, Naya L, Loscos J, Pérez-Rontomé C, Sato S, Tabata S, Becana M (2007) Phytochelatin synthases of the model legume *Lotus japonicus*. A small multigene family with differential response to cadmium and alternatively spliced variants. Plant Physiol 143:1110–1118

Ray D, Williams DL (2011) Characterization of the phytochelatin synthase of *Schistosoma mansoni*. PLoS Negl Trop Dis 5:e1168

Richman PG, Meister A (1975) Regulation of gamma-glutamyl-cysteine synthetase by nonallosteric feedback inhibition by glutathione. J Biol Chem 250:1422–1426

Rigouin C, Nylin E, Cogswell AA, Schaumlöffel D, Dobritzsch D, Williams DL (2013) Towards an understanding of the function of the phytochelatin synthase of *Schistosoma mansoni*. PLoS Negl Trop Dis 7:e2037

Robinson BH, Leblanc M, Petit D, Brooks RR, Kirkman JH, Gregg PEH (1998) The potential of *Thlaspi caerulescens* for phytoremediation of contaminated soils. Plant Soil 203:47–56

Rocchetta I, Mazzuca M, Conforti V, Ruiz L, Balzaretti V, Rios de Molina Mdel C (2006) Effect of chromium on the fatty acid composition of two strains of *Euglena gracilis*. Environ Pollut 141:353–358

Rodríguez-Zavala JS, Ortiz-Cruz MA, Moreno-Sánchez R (2006) Characterization of an aldehyde dehydrogenase from *Euglena gracilis*. J Eukaryot Microbiol 53:36–42

Rodríguez-Zavala JS, Ortiz-Cruz MA, Mendoza-Hernández G, Moreno-Sánchez R (2010) Increased synthesis of alpha-tocopherol, paramylon and tyrosine by *Euglena gracilis* under conditions of high biomass production. J Appl Microbiol 109:2160–2172

Romero LC, Aroca MÁ, Laureano-Marin AM, Moreno I, Garcia I, Gotor C (2014) Cysteine and cysteine-related signaling pathways in *Arabidopsis thaliana*. Mol Plant 7:264–276

Roncarati F, Sáez CA, Greco M, Gledhill M, Bitonti MB, Brown MT (2015) Response differences between *Ectocarpus siliculosus* populations to copper stress involve cellular exclusion and induction of the phytochelatin biosynthetic pathway. Aquat Toxicol 159:167–175

Ruelas-Inzunza J, Green-Ruiz C, Zavala-Nevárez M, Soto-Jiménez M (2011) Biomonitoring of Cd, Cr, Hg, and Pb in the Baluarte River basin associated to a mining area (NW Mexico). Sci Total Environ 409:3527–3536

Ruiz FA, Marchesini N, Seufferheld M, Govindjee, Docampo R (2001) The polyphosphate bodies of *Chlamydomonas reinhardtii* possess a proton-pumping pyrophosphatase and are similar to acidocalcisomes. J Biol Chem 276:46196–46203

Ruiz LB, Rocchetta I, Ferreira VDS, Conforti V (2004) Isolation, culture and characterization of a new strain of *Euglena gracilis*. Phycol Res 52:168–173

Saidha T, Stern AI, Lee DH, Schiff JA (1985) Localization of a sulphate-activating system within *Euglena* mitochondria. Biochem J 232:357–365

Saidha T, Na SQ, Li JY, Schiff JA (1988) A sulphate metabolizing centre in *Euglena* mitochondria. Biochem J 253(2):533–539

Sánchez-Thomas R, Moreno-Sánchez R, García-García JD (2016) Accumulation of zinc protects against cadmium stress in photosynthetic *Euglena gracilis*. Environ Exp Bot 131:19–31

Šantek B, Friehs K, Lotz M, Flaschel E (2012) Production of paramylon, a β-1,3-glucan, by heterotrophic growth of *Euglena gracilis* on potato liquor in fed-batch and repeated-batch mode of cultivation. Eng Life Sci 12:89–94

Santiago-Martínez MG, Lira-Silva E, Encalada R, Pineda E, Gallardo-Pérez JC, Zepeda-Rodríguez A, Moreno-Sánchez R, Saavedra E, Jasso-Chávez R (2015) Cadmium removal by *Euglena gracilis* is enhanced under anaerobic growth conditions. J Hazard Mater 288:104–112

Sarmiento AM, DelValls A, Miguel-Nieto J, Salamanca MJ, Caraballo MA (2011) Toxicity and potential risk assessment of a river polluted by acid mine drainage in the Iberian Pyrite Belt (SW Spain). Sci Total Environ 409:4763–4771

Sarry JE, Kuhn L, Ducruix C, Lafaye A, Junot C, Hugouvieux V, Jourdain A, Bastien O, Fievet JB, Vailhen D, Amekraz B, Moulin C, Ezan E, Garin J, Bourguignon J (2006) The early responses of *Arabidopsis thaliana* cells to cadmium exposure explored by protein and metabolite profiling analyses. Proteomics 6:2180–2198

Schäfer HJ, Greiner S, Rausch T, Haag-Kerwer A (1997) In seedlings of the heavy metal accumulator *Brassica juncea* Cu^{2+} differentially affects transcript amounts for gamma-glutamylcysteine synthetase (gamma-ECS) and metallothionein (MT2). FEBS Lett 404:216–220

Schäfer HJ, Haag-Kerwer A, Rausch T (1998) cDNA cloning and expression analysis of genes encoding GSH synthesis in roots of the heavy-metal accumulator *Brassica juncea* L.: evidence for Cd-induction of a putative mitochondrial gamma-glutamylcysteine synthetase isoform. Plant Mol Biol 37:87–97

Schandle VB, Rudolph FB (1981) Isotope exchange at equilibrium studies with rat kidney gamma-glutamylcysteine synthetase. J Biol Chem 256:7590–7594

Scheerer U, Haensch R, Mendel RR, Kopriva S, Rennenberg H, Herschbach C (2010) Sulphur flux through the sulphate assimilation pathway is differently controlled by adenosine 5′-phosphosulphate reductase under stress and in transgenic poplar plants overexpressing gamma-ECS, SO, or APR. J Exp Bot 61:609–622

Schneider T, Betz A (1985) Wax monoester fermentation in *Euglena gracilis* T. Factors favouring the synthesis of odd-numbered fatty acids and alcohols. Planta 166:67–73

Sekine K, Sakakibara Y, Hase T, Sato N (2009) A novel variant of ferredoxin-dependent sulfite reductase having preferred substrate specificity for nitrate in the unicellular red alga *Cyanidioschyzon merolae*. Biochem J 423:91–98

Seufferheld M, Curzi MJ (2010) Recent discoveries on the roles of polyphosphates in plants. Plant Mol Biol Report 28:549–559

Shen H, He LF, Sasaki T, Yamamoto Y, Zheng SJ, Ligaba A, Yan XL, Ahn SJ, Yamaguchi SJ, Sasakawa H, Matsumoto H (2005) Citrate secretion coupled with the modulation of soybean root tip under aluminum stress. Up-regulation of transcription, translation, and threonine-oriented phosphorylation of plasma membrane H^+-ATPase. Plant Physiol 138:287–296

Shum KT, Lui EL, Wong SC, Yeung P, Sam L, Wang Y, Watt RM, Tanner JA (2011) Aptamer-mediated inhibition of *Mycobacterium tuberculosis* polyphosphate kinase 2. Biochemistry 50:3261–3271

Simpson WR (1981) A critical review of cadmium on marine environment. Prog Oceanogr 10:1–70

Sittenfeld A, Mora M, Ortega JM, Albertazzi F, Cordero A, Roncel M, Sánchez E, Vargas M, Fernández M, Weckesser J, Serrano A (2002) Characterization of a photosynthetic *Euglena* strain isolated from an acidic hot mud pool of a volcanic area of Costa Rica. FEMS Microbiol Ecol 42:151–161

Sommer JR, Blum JJ (1965) Cytochemical localization of acid phosphatases in *Euglena gracilis*. J Cell Biol 24:235–251

Sooksa-Nguan T, Yakubov B, Kozlovskyy VI, Barkume CM, Howe KJ, Thannhauser TW, Rutzke MA, Hart JJ, Kochian LV, Rea PA, Vatamaniuk OK (2009) *Drosophila* ABC transporter, DmHMT-1, confers tolerance to cadmium. DmHMT-1 and its yeast homolog, SpHMT-1, are not essential for vacuolar phytochelatin sequestration. J Biol Chem 284:354–362

Sun H, Han J, Li D, Zhang S, Lu X (2010) Chemical weathering inferred from riverine water chemistry in the lower Xijiang basin, South China. Sci Total Environ 408:4749–4760

Suter M, von Ballmoos P, Kopriva S, den Camp RO, Schaller J, Kuhlemeier C, Schurmann P, Brunold C (2000) Adenosine 5′-phosphosulfate sulfotransferase and adenosine 5′-phosphosulfate reductase are identical enzymes. J Biol Chem 275:930–936

Teerawanichpan P, Qiu X (2010) Fatty acyl-CoA reductase and wax synthase from *Euglena gracilis* in the biosynthesis of medium-chain wax esters. Lipids 45:263–273

Trenfield MA, Ng JC, Noller B, Markich SJ, van Dam RA (2012) Dissolved organic carbon reduces uranium toxicity to the unicellular eukaryote *Euglena gracilis*. Ecotoxicology 21:1013–1023

Tsuji N, Hirayanagi N, Iwabe O, Namba T, Tagawa M, Miyamoto S, Miyasaka H, Takagi M, Hirata K, Miyamoto K (2003) Regulation of phytochelatin synthesis by zinc and cadmium in marine green algae, *Dunaliella tertiolecta*. Phytochemistry 62:453–459

Vatamaniuk OK, Mari S, Lu YP, Rea PA (2000) Mechanism of heavy metal ion activation of phytochelatin (PC) synthase: blocked thiols are sufficient for PC synthase-catalyzed transpeptidation of glutathione and related thiol peptides. J Biol Chem 275:31451–31459

Vatamaniuk OK, Bucher EA, Ward JT, Rea PA (2001) A new pathway for heavy metal detoxification in animals. Phytochelatin synthase is required for cadmium tolerance in *Caenorhabditis elegans*. J Biol Chem 276:20817–20820

Vatamaniuk OK, Bucher EA, Sundaram MV, Rea PA (2005) CeHMT-1, a putative phytochelatin transporter, is required for cadmium tolerance in *Caenorhabditis elegans*. J Biol Chem 280:23684–23690

Vauclare P, Kopriva S, Fell D, Suter M, Sticher L, von Ballmoos P, Krähenbühl U, den Camp RO, Brunold C (2002) Flux control of sulphate assimilation in *Arabidopsis thaliana*: adenosine 5′-phosphosulphate reductase is more susceptible than ATP sulphurylase to negative control by thiols. Plant J 31:729–740

Vázquez-Sauceda ML, Pérez-Castañeda R, Sánchez-Martínez JG, Aguirre-Guzmán G (2012) Cadmium and lead levels along the estuarine ecosystem of Tigre River-San Andres Lagoon, Tamaulipas, Mexico. Bull Environ Contam Toxicol 89:782–785

Venkata Mohan S, Rohit MV, Chirajeevi P, Chandra R, Navaneeth B (2015) Heterotrophic microalgae cultivation to synergize biodiesel production with waste remediation: progress and perspectives. Bioresour Technol 184:169–178

Wang S, Wang Y, Zhang R, Wang W, Xu D, Gou J, Li P, Yu K (2015) Historical levels of the heavy metals reconstructed from sedimentary record in the Hejiang River, located in a typical mining region of Southern China. Sci Total Environ 532:645–654

Watanabe K (2001) Microorganisms relevant to bioremediation. Curr Opin Biotechnol 12:237–241

Weber DN, Shaw CF, Petering DH (1987) *Euglena gracilis* cadmium-binding protein-II contains sulfide ion. J Biol Chem 262:6962–6964

Wójcik M, Vangronsveld J, Tukiendorf A (2005) Cadmium tolerance in *Thlaspi caerulescens*: I. Growth parameters, metal accumulation and phytochelatin synthesis in response to cadmium. Environ Exp Bot 53:151–161

Wu JS, Ho TC, Chien HC, Wu YJ, Lin SM, Juang RH (2008) Characterization of the high molecular weight Cd-binding complex in water hyacinth (*Eichhornia crassipes*) when exposed to Cd. J Agric Food Chem 56:5806–5812

Yang JL, Zheng SL, He YF, Matsumoto H (2005) Aluminium resistance requires resistance to acid stress: a case study with spinach that exudes oxalate rapidly when exposed to Al stress. J Exp Bot 56:1197–1203

Yildiz FH, Davies JP, Grossman AR (1994) Characterization of sulfate transport in *Chlamydomonas reinhardtii* during sulfur-limited and sulfur-sufficient growth. Plant Physiol 104:981–987

Yip B, Rudolph FB (1976) The kinetic mechanism of rat kidney gamma-glutamylcysteine synthetase. J Biol Chem 251:3563–3568

Yoshida Y, Tomiyama T, Maruta T, Tomita M, Ishikawa T, Arakawa K (2016) *De novo* assembly and comparative transcriptome analysis of *Euglena gracilis* in response to anaerobic conditions. BMC Genomics 17:182

Yoshimoto A, Sato R (1968) Studies on yeast sulfite reductase. I. Purification and characterization. Biochim Biophys Acta 153:555–575

Zheng C, Chen M, Tao Z, Zhang L, Zhang XF, Wang JY, Liu J (2015) Different expression of sulfur assimilation pathway genes in *Acidithiobacillus ferrooxidans* under Cd^{2+} stress: evidence from transcriptional, enzymatic, and metabolic profiles. Extremophiles 19:429–436

Zhu XF, Zheng C, Hu YT, Jiang T, Liu Y, Dong NY, Yang JL, Zheng SJ (2011) Cadmium-induced oxalate secretion from root apex is associated with cadmium exclusion and resistance in *Lycopersicon esculentum*. Plant Cell Environ 34:1055–1064

Zuber H, Davidian JC, Wirtz M, Hell R, Belghazi M, Thompson R, Gallardo K (2010) Sultr4;1 mutant seeds of *Arabidopsis* have an enhanced sulphate content and modified proteome suggesting metabolic adaptations to altered sulphate compartmentalization. BMC Plant Biol 10:78

Part II

Cell and Molecular Biology

7

Euglena gracilis Genome and Transcriptome: Organelles, Nuclear Genome Assembly Strategies and Initial Features

ThankGod Echezona Ebenezer, Mark Carrington, Michael Lebert, Steven Kelly, and Mark C. Field

Abstract

Euglena gracilis is a major component of the aquatic ecosystem and together with closely related species, is ubiquitous worldwide. Euglenoids are an important group of protists, possessing a secondarily acquired plastid and are relatives to the Kinetoplastidae, which themselves have global impact as disease agents. To understand the biology of E. gracilis, as well as to provide further insight into the evolution and origins of the Kinetoplastidae, we embarked on sequencing the nuclear genome; the plastid and mitochondrial genomes are already in the public domain. Earlier studies suggested an extensive nuclear DNA content, with likely a high degree of repetitive sequence, together with significant extrachromosomal elements. To produce a list of coding sequences we have combined transcriptome data from both published and new sources, as well as embarked on de novo sequencing using a combination of 454, Illumina paired end libraries and long PacBio reads. Preliminary analysis suggests a surprisingly large genome approaching 2 Gbp, with a highly fragmented architecture and extensive repeat composition. Over 80% of the RNAseq reads from E. gracilis maps to the assembled genome sequence, which is comparable with the well assembled genomes of T. brucei and T. cruzi. In order to achieve this level of assembly we employed multiple informatics

T.E. Ebenezer
Department of Biochemistry, University of Cambridge, Cambridge CB2 1QW, UK

School of Life Sciences, University of Dundee, Dundee DD1 5EH, UK

M. Carrington, Ph.D.
Department of Biochemistry, University of Cambridge, Cambridge CB2 1QW, UK

M. Lebert, Ph.D.
Cell Biology Division, Department of Biology, University of Erlangen-Nuremberg, Staudtstraβe 5, Erlangen 91058, Germany

S. Kelly, Ph.D. (✉)
Department of Plant Sciences, University of Oxford, South Parks Road, Oxford OX1 3RB, UK
e-mail: steven.kelly@plants.ox.ac.uk

M.C. Field, D.Phil. (✉)
School of Life Sciences, University of Dundee, Dundee DD1 5EH, UK
e-mail: mfield@mac.com

S.D. Schwartzbach, S. Shigeoka (eds.), *Euglena: Biochemistry, Cell and Molecular Biology*, Advances in Experimental Medicine and Biology 979, DOI 10.1007/978-3-319-54910-1_7

pipelines, which are discussed here. Finally, as a preliminary view of the genome architecture, we discuss the tubulin and calmodulin genes, which highlight potential novel splicing mechanisms.

Keywords
Euglena • Next generation sequencing • Genome assembly • Tubulin • Genome architecture • Splicing • Secondary endosymbiosis

7.1 Introduction

Euglena gracilis is a species of unicellular green flagellate inhabiting aquatic ecosystems (Buetow 1982). These photosynthetic organisms were first discovered by Anton van Leeuwenhoek in 1674 due to their locomotory movement, now known as metaboly (Dobell 1932), and were further described by Ehrenberg in 1830 who established the genus to accommodate those euglenoid organisms that have eyespots. They are photosynthetic, as well as heterotrophic (Buetow 1982). They are freeliving, possess an eyespot, a food vacuole and two flagella—one short and one long, which play both locomotory and sensory functions (Rosati et al. 1991). They also possess a chloroplast which arose as a result of secondary endosymbiosis (Gibbs 1978; McFadden 2001). Euglenoids belong to the supergroup Excavata, and are distantly related to the kinetoplastids, which include *Trypanosoma* and *Leishmania* (see Adl et al. 2012 for a detailed review), important pathogenic protists about which there is considerable understanding.

Whilst the taxonomic position of *E. gracilis* was debated for nearly a century it has recently been resolved (Adl et al. 2005). Euglenids are believed to hold significant importance in the evolutionary history of eukaryotes, particularly due to their position in the eukaryotic tree of life, and their secondary endosymbiotic history, which likely involves both a green and red/brown algae contribution (Weigert et al. 2012). However, the absence of extensive molecular sequence data has made understanding this process difficult. The presence of the secondary endosymbiont suggests that the *E. gracilis* genome is particularly chimeric as contributions from multiple lineages are likely present; at least two algae, a proteobacterium (mitochondrion) and an archaea host. Again, whilst this chimeric aspect may be a contributory factor to their resilience and metabolic flexibility, and specifically their ability to withstand extreme acidic and basic conditions and high concentrations of heavy metals, the absence of a full gene complement precludes the full understanding of the scope of chimericism and the relative contributions of these endosymbiotic-derived genes to this metabolic potential (dos Santos Ferreira et al. 2007). Euglena are also of relevance in biotechnology applications due to their extensive synthesis of a wide range of natural products (O'Neill et al. 2015).

Many species of the genus *Euglena* are known, and these have a broad range of morphologies and ecological niches (Kim et al. 1998). *E. gracilis* is the most widely studied, due to both ubiquity within the biosphere and ease of culture. Over many years, multiple strains have been isolated and include, amongst others, the Z strain and bacillarus (Kim et al. 1998; Gojdics 1953; Zakryś 1986; Zakrys and Walne 1994). The complex and divergent biology makes this unique organism an important model (dos Santos Ferreira et al. 2007), but popularity declined due to the absence of genome data and a means for genetic manipulation. Notwithstanding this, some aspects of the biology of *E. gracilis* continued to gain significant attention as widely reported by a constant stream of publications. The application of *Euglena* to biotechnology remains to be fully explored, since little is known about genetically-encoded metabolic capacity beyond a recent

report (O'Neill et al. 2015). The *E. gracilis* genomic and transcriptomic architecture contains evidence of endosymbiotic origins and the genome is comprised of *Euglena*-specific genes, genes shared with the kinetoplastida, green and red algae-derived genes, and pan-eukaryotic genes, which are inherited from the archaea ancestor of eukaryotes.

7.2 Estimating the Size of the *Euglena* Genome

The DNA of *E. gracilis* is distributed between three compartments, specifically nucleus, chloroplast and mitochondrion (Richards 1967). Early work demonstrated that the composition of DNA associated with these organelles had distinctive base compositions and different buoyant densities in CsCl gradients (Richards 1967). The nuclear DNA comprises ~95% of the cellular DNA in *E. gracilis*, with the chloroplast and mitochondria contributing the remaining 5% (Rawson 1975). The arrangement, size and composition of the *E. gracilis* genome have been rather difficult to estimate (Fig. 7.1). The number of chromosomes in *E. gracilis* has also been somewhat contentious for over half a century, with estimates varying between four (O'Donnell 1965) and 45 (Leedale 1958a, b). Recently, Dooijes et al. 2000 estimated the presence of at least 42 linear chromosomes using light microscopy of mitotic cells, and this value is very close to the number proposed by Leedale (1958a, b). What this may represent in terms of gene expression or genome organisation is unclear; for example chromosome number amongst the related trypanosomatids is highly variable, ranging from 11 in *T. brucei* (Berriman et al. 2005) to 36 in *Leishmania major* (Ivens et al. 2005), and 41 in *T. cruzi* (Souza et al. 2011). Significantly, the arrangement of genes within polycistronic transcription units is strongly conserved between kinetoplastid species (synteny) and this has recently been demonstrated to extend to *Bodo saltans* (Jackson et al. 2016). It will be of interest to determine if *E. gracilis* also retains some level of higher order gene organisation that is similar to that in the kinetoplastids.

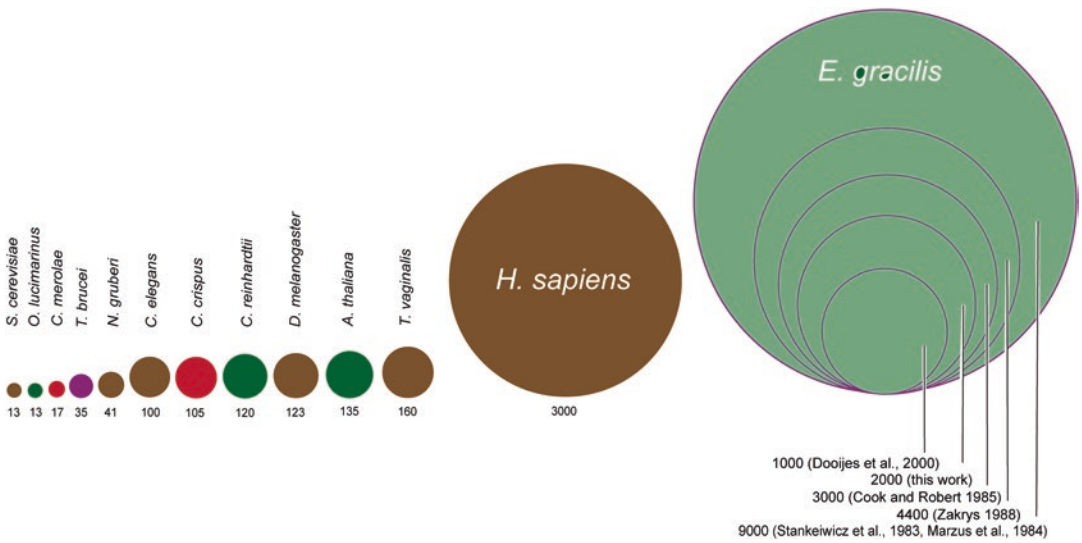

Fig. 7.1 Comparison of genome sizes across selected eukaryotes. The area (×3 magnifications) of the circles represents the sizes of the selected eukaryotic genomes in megabases which are highlighted by numbers corresponding to respective circle. Color codes: *Green* photosynthetic green organisms, *red* photosynthetic red organisms, *purple* kinetoplastids, *grey* other members of the eukaryotic species. Circles embed into each other is *E. gracilis* genome sizes which are calculated/predicted estimates from Zakrys (1988), Cook and Roxby (1985), Dooijes et al. (2000), Mazus et al. (1984) and Stankiewicz et al. (1983), and Ebenezer et al. (2017)

In addition to the uncertainty concerning chromosome number, the size of the nuclear genome remains unknown, with estimates varying by an order of magnitude. For instance, Zakrys (1988), determined the nuclear DNA levels for 71 strains and 10 species of *Euglena*, including *E. viridis*, *E. mutabilis*, and *E. gracilis* using the cytophotometric method. It was estimated that the nuclear DNA of *Euglena* ranges from 3 pg in *E. mutabilis* and *E. pisciformis* to 24 pg in *E. granulata*. In the most widely studied species, *E. gracilis*, estimated DNA levels varied between 3.25 and 4.4 pg. According to Dolezel et al. (2003), since the mass conversion of DNA is 1 Gbp ≈ 1 pg, this suggests that the nuclear genome of *Euglena* ranges from 3 Gbp in *E. mutabilis* and *E. pisciformis* to 24 Gbp in *E. granulata*, and more specifically, up to 4.4 Gbp in *E. gracilis* (Fig. 7.1).

It is also believed that the genomic DNA of *E. gracilis* is highly repetitive. For instance, Cook and Roxby (1985) characterized the small circular extrachromosomal DNA of *E. gracilis* as having a contour length of 11.3 kb, with a consistent restriction map. They found that this makes up 0.5% of the total cellular DNA, i.e. about 0.015 pg/cell, and with a copy number of 1000 per cell. Their experiments also suggest that the cellular DNA of *E. gracilis* is 3 pg, i.e. 3 Gbp, in broad agreement with other estimations. Similarly, other reports are consistent with the DNA values for *E. gracilis* within the ranges: 3.0 and 4.5 pg/cell (Cook 1981), 3 pg (Rawson 1975) and three times calf thymus DNA (Mazus et al. 1984; Stankiewicz et al. 1983), which provides a high end estimate of 9 Gbp (Fig. 7.1). In a study to analyse the DNA of *E. gracilis* for the presence of baseJ and by comparison with the DNA of *T. brucei*, Dooijes et al. (2000), found that *T. brucei* has 30-fold less DNA per nucleus. Since the total size of the *T. brucei* haploid genome is ~35 Mb, the estimated genome size for *E. gracilis* following from these calculations would be ~1 Gbp.

In addition to considerable variation in nuclear genome size between species, exposure to different environments has been shown to lead to changes in genome content within a single species. For example, nutrient starvation reduces the amount of DNA within a cell through changes in ploidy (Hill et al. 1966; Cook 1972; Davis and Epstein 1971; Epstein and Allaway 1967; Leedale 1974; Lefort-Tran et al. 1987). In contrast, DNA content increases as zinc concentrations increase, significantly affecting the biosynthesis and function of all major chromatin components, i.e. RNA polymerases, DNA and histones. The species strain as well as exposure to light has also been associated with an increase in DNA content (Cook 1972).

7.3 The Chloroplast Genome

The *E. gracilis* chloroplast genome has been fully sequenced and is 143 kbp (Hallick et al. 1993). The plastid genome of *E. gracilis* is highly asymmetrical in composition and the circular chromosome is strongly biased as to which strand is coding. The plastid genome encodes 97 proteins and gene loci; 46 of these are protein-coding and 51 are RNA-coding or ribosomal (one 16S, one 23S, and one 5S rRNAs, 27 different tRNA species, 11 ribosomal proteins of the 30S subunit, and 10 ribosomal proteins of the 50S subunit), including group II and III introns, and twintrons (introns within introns) (Hallick et al. 1993; Thompson et al. 1995). The 46 protein-coding genes encode four genes for elongation factor EF-Tu (transcription and translation), 27 photosynthetic proteins (including PSI & II), five ORFs showing similarity to chloroplast genes of other plant and algal species, and ten ORFs with unknown functions (Hallick et al. 1993). The 27 photosynthetic genes encode components of the thylakoid membranes, the chloroplast ATP synthase complex, and large subunit of the CO_2-fixing enzyme, Ribulose-1,5-bisphosphate carboxylase/oxygenase. Of these, five encode photosystem I polypeptides (designated psaA-C, J, M), ten encode photosystem II components (designated psbA-F, H-L), and two encode the cytochrome b_6/f complex (petB, petG) (Hallick et al. 1993). The two strands of the *E. gracilis* chloroplast genome also differ in compositional properties, and codon usage bias (Morton 1999), and it has been proposed that this is due to selection to coordinate transcription and replication (see Morton 1998, 1999; Hallick et al. 1993). The evolutionary transition from an

endosymbiont to the plastid organelle was accompanied by loss of many genes and transfers to the host genome (Martin and Herrmann 1998). *E. gracilis* is not a typical representative photosynthetic euglenoid due to the diversity within the lineage, and is not closely related to the phagotrophic forms believed to have been the host for the endosymbiont, and therefore substantial diversity within the chloroplast genome may exist across the lineage (Wiegert et al. 2012). Consistent with the secondary acquisition of the chloroplast, the plastid of *E. gracilis* is surrounded by three membranes (Bachvaroff et al. 2005; Yoon et al. 2002). However, the cellular mechanisms involved in the evolution of the protein import machineries into these membranes are still unclear since the majority of the plastid proteome, much like the mitochondrion, is encoded by the nuclear genome, and hence remains to be characterised (Bolte et al. 2009).

7.4 The Mitochondrial Genome

Spencer and Gray established the general architecture of the *E. gracilis* mitochondrial genome: a linear fragment of heterogeneous size (modal size 4 kb) bearing terminal repeats and many small, likely nonfunctional, protein and rRNA gene fragments, suggesting extensive ongoing recombination (Spencer and Gray 2011). These authors subsequently suggested, based on electron microscopic observations, that virtually all of the *E. gracilis* mitochondrial genome is in the form of small linear fragments of average length (0.9–1 μm), with estimated sizes of the mtDNA varying from ~15 to 20 kbp to several hundred kbp (Spencer and Gray 2012). The mitochondrial (mt) genomes of the kinetoplastids, euglenids, and other members of the phylum Euglenozoa, exhibit radically different modes of organization and expression, and gene fragmentation is a striking feature of both euglenid and diplonemid mtDNAs (see Flegontov et al. 2011 for an extensive review).

However, the complete mitochondrial genome sequence of *E. gracilis* was recently reported (Dobakova et al. 2015), and has a surprisingly small coding potential, possessing only seven protein-coding genes: three subunits of respiratory complex I (nad1, nad4, and nad5), one subunit of complex III (cob), and three subunits of complex IV (cox1, cox2, and a highly divergent cox3). No genes encoding subunits of succinate:ubiquinone oxidoreductase (complex II) were found, similar to most animal and fungal mitochondrial DNAs (Gray and Doolittle 1982; Tzagoloff and Myers 1986; Attardi and Schatz 1988; Burger et al. 1996). The seven mitochondrial encoded genes are located on six contigs: one gene per contig (Dobakova et al. 2015) except cox2 and cox3 as closely spaced genes on a single contig (Spencer and Gray 2011; Dobakova et al. 2015). The mitochondria DNA size ranges from 5 to 8 kbp and represents one of the smallest mitochondrial genomes known in terms of gene content. Genes encoding subunits of complex V (all atp genes; subunits of ATP synthase), ribosomal proteins and tRNAs are absent from the mitochondria genome, and these are thus likely located in the nuclear genome (Dobakova et al. 2015). Generally, the gene complement is reduced, even when compared with the sister groups Diplonema and Kinetoplasta. The mitochondrion of *E. gracilis* is a facultative anaerobic organelle that produces ATP in the presence and absence of O_2. Unlike the mitochondria of most eukaryotes, which have a pyruvate dehydrogenase multi-enzyme complex, the mitochondrion of *E. gracilis* has an unusual O_2-sensitive enzyme for the oxidative decarboxylation of pyruvate (i.e. pyruvate: NADP1 oxidoreductase) to produce acetyl-CoA (Nakazawa et al. 2000).

7.5 Genome Assembly Strategy; Finding the Right Pathway

Initial efforts towards sequencing *Euglena* rapidly encountered two significant challenges—the physical size of the genome and the high frequency of repetitive sequences. An initial attempt, with now obsolete 454 sequencing, highlighted the large genome size, and whilst this data confirmed the published estimates, it did not provide a realistic size for the genome, beyond a probable size in excess of 1 Gb. Additional sequence data were obtained from extensive long and short read paired

end Illumina next generation sequencing, together with the addition of PacBio long read data. Significantly PacBio was of limited utility due to the high error rate of current technology and the low coverage that was obtained. Below is summarised our approach to a decent draft genome—which required considerable data augmentation as well as a trial and error approach towards assembly. In some instances these pipelines deviated from the standard method of genome assembly. This approach to complex genomes has been highlighted by El-Metwally et al. (2013) as standard pipelines resulted in fragmented, discontiguous assemblies that contained few identifiable genes.

In the discriptions of the assemblies below we used two criteria to evaluate the quality of the assemblies produced. The first was the CEGMA score, i.e. the proportion of core eukaryotic genes (CEGs) that could be detected in the assembled nucleotide sequences. The second was the proportion of the available RNAseq reads from the same species that could be mapped to the genome. Both metrics provide a proxy for the completeness of the gene content of the genome, the first from the perspective of expected highly conserved genes, the latter from the perspective of all genes that are transcribed under cell culture conditions. Together these measures encapsulate the ethos of our assembly strategy, to generate a resource that can be mined for functional and evolutionary studies, both of which require extensive gene catalogs that are as near complete as possible.

The initial draft genome, version 0.7b, used six read libraries with a total per base coverage of 8.2X and a total physical coverage of 18.9X (Table 7.1). Assembling this version of the genome required a multi-step process following the standard process of quality control using the Trimmomatic algorithm (Bolger et al. 2014), *de novo* assembly using ALLPATHS-LG (Gnerre et al. 2011), with additional scaffolding using SSPACE (Boetzer et al. 2011), gapfilling using SGA (Simpson and Durbin 2011) and assembly post processing using Pilon (Walker et al. 2014). This produced an assembly with a scaffold N_{50} of 11144 bp and a total of 257,242 scaffolds. Preliminary genome assessments using contig metrics (Gurevich et al. 2013), proportion of CEGs

Table 7.1 Genome, transcriptome, and protein statistics for *Euglena gracilis*

		Transcriptome	
Parameter	Genome	Transcripts	Proteins
Number of sequences	2,066,288	72,509	36,526
Median sequence length	457	540	254
Mean sequence length	694	869	346
Max. sequence length	166,587	25,763	8406
Min. sequence length	106	202	98
No. sequence > 1 kbp	373,610	19,765	N/A
No. sequence > 10 kbp	1459	25	N/A
No. sequence > 100 kbp	2	0	N/A
No. proteins > 1 kaa	N/A	N/A	1290
No. gaps	0	0	N/A
Bases in gaps	0	0	N/A
N_{50}	955	1242	471
Combined sequence length (bases)	1,435,499,417	63,050,794	N/A

Sequence here refers to either contigs (nucleotides) or proteins (amino acids). Number of sequences is the total number of contigs/proteins in the assembly; no. of sequence > x kbp is total number of contigs of length ≥ x kbp—where x is 1, 10, or 100 kbp; combined sequence length is the total number of bases in the assembly; N50 is the length for which the collection of all contigs/proteins of that length or longer covers at least half an assembly; Gaps is the total number of uncalled bases (N's) in the assembly; Min and Max sequence length are the lengths of the shortest and largest contigs/proteins in the assembly respectively; Mean and Median sequence length are the average length of the sequences and the sequence length separating the minimum and maximum sequence lengths in the assembly respectively. No. of proteins > x aa is total number of proteins of length ≥ x kbp—where x is 1 kaa (Gurevich et al. 2013)

(Parra et al. 2007), and proportion of *de novo* sequenced transcriptome read mapping suggested that this assembly genome was highly fragmented, containing only ~16% of CEGs (when about 80% were expected), and with only 51.9% of the transcriptome reads mapping back to the genome, consistent with the poor CEG score.

To address this, we obtained additional Illumina read libraries (150 bp long 240 bp insert size paired end HiSeq2000 reads, 300 bp long 560 bp insert size MiSeq reads, and 100 bp long 40 kbp insert size illumina mate-pair reads). These additional read libraries were used to generate six further different *de novo* assemblies using a diverse set of assembly and post-assembly processing algorithms summarised in Fig. 7.2. Each assembly started from the same input reads that had been quality trimmed and filtered for adaptor sequences using Trimmomatic (Bolger et al. 2014). The most surprising result was obtained when following the same pipeline as outlined for the initial draft assembly above. Here the addition of substantial extra read data resulted in an assembly with substantially poorer properties, comprising a shorter scaffold N_{50} (6251 bp) and fewer scaffolds (n = 81,015) with only 12.2% of the transcriptome mapping to the genome. Despite significant efforts the precise reason for this reduction in quality was not discovered and thus alternative assembly algorithms were evaluated, these comprised Platanus, DISCOVAR *de novo* and SGA.

The most successful strategy for assembly, as assessed by CEGMA score and the percentage of the RNAseq reads from the transcriptome that mapped to the assembly (Hornett and Wheat 2012; O'Neil and Emrich 2013), utilised the Platanus assembler. Platanus is designed for large, heterozygous polyploid genomes. Assembling the quality controlled error corrected reads with Platanus followed by subsequent rounds of scaffolding with SSPACE and gapfilling using SGA resulted in a *de novo* assembly with a scaffold N_{50} of 1441 bp, comprising 2,595,470 scaffolds. Of note with this assembly was that 87% of the RNAseq reads from the transcriptome could be successfully mapped to this genome assembly. Other assemblies using DISCOVAR *de novo*, ALLPATHS-LG, SGA, or combinations of all four produced assemblies with lower CEGMA scores and fewer mappable RNAseq reads (data not shown).

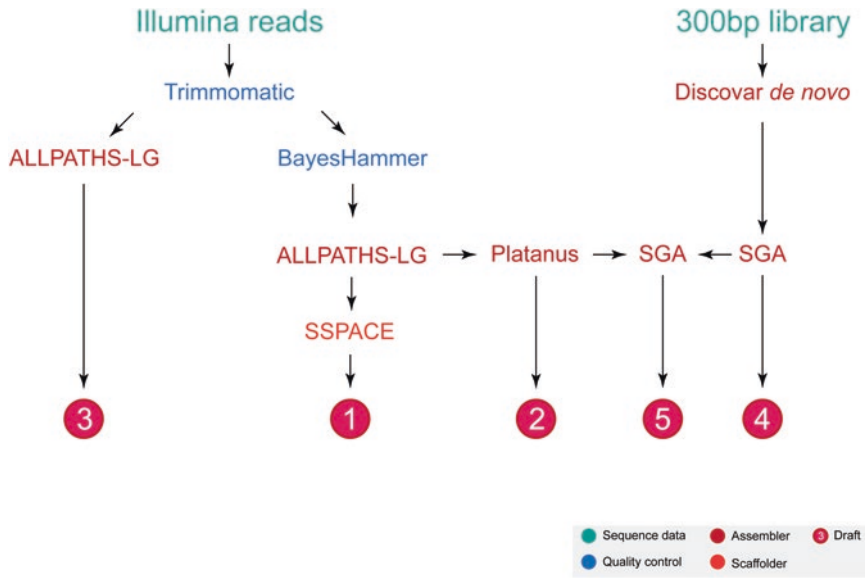

Fig. 7.2 Summary of *E. gracilis* genome assembly pipelines attempted. The numbers (1–5) represents each of the assembly pipeline employed as well as their draft assemblies. *Colors* at the bottom right corner of the figure correspond to sequence data, quality control, assembler, scaffolder, and draft assemblies respectively

Assembly of the genome has been problematic, and the precise reasons remain unclear. The most probable issues are a combination of a high level of repeat sequence, together with the very large size of the genome and polyploidy. This, combined with limited resources for sequencing data result in a significant computational challenge. Our strategy also highlighted difficulties inherent in *de novo* assembly using mainly short read data with a complex genome lacking any close relative suitable as a scaffold. The need for orthogonal quality control monitoring is also highly important and the simple statistics underpinning an assembly are of limited utility as they lack a relevant benchmark. More useful, and of high biological relevance for gene finding purposes, are the ability to map transcripts and RNAseq reads and CEGMA analysis. These latter two were essential in determining the poor quality of several of the earlier assemblies, and this was not apparent from the output of the assemblers and quality control algorithms alone.

7.6 Assembling the Transcriptome

As a complimentary approach to the genome assembly, we also assembled a meta-transcriptome, based on data generously provided by Rob Field (O'Neill et al. 2015) together with additional data generated in house. The transcriptome was considerably less challenging to assemble compared to the genome (Table 7.1), but also involved a multiple-step iterative protocol to achieve good levels of completion and contiguity. Read data from all transcriptome projects were combined prior to *de novo* transcriptome assembly. Raw reads were subject to quality filtering using Trimmomatic and searched for all common Illumina adaptors (the default option) and the settings used for read processing by trimmomatic were LEADING:10 TRAILING:10 SLIDINGWINDOW:5:15 MINLEN:50. The trimmed and quality filtered paired-end reads were then filtered to remove reads coming from ribosomal RNA using SortMeRNA with the default settings, before being subject to read error correction using BayesHammer with the default settings (Nikolenko et al. 2013). Reads were then digitally normalized using khmer with settings –C 20 -k 21 -M 8e9. Following normalization, overlapping paired-end reads were joined together using ALLPATHS-LG and all reads (joined and those that were unable to be joined) were subject to *de novo* assembly using SGA with a minimum overlap size of 80 nucleotides (with no mismatches). The assembled contigs were subject to four additional rounds of assembly using SGA, each round reducing the overlap size by 10 nucleotides such that the last round of assembly was performed with an overlap size of 40 (with no mismatches). The filtered, normalized joined reads were then mapped to this assembly using Bowtie2. Reads that were absent from the assembly were identified and combined to the assembly file. The combined un-assembled reads and assembled contigs were subject to assembly using SGA with an overlap size of 70. This process of identifying unmapped reads and reassembling with SGA was repeated each time, decreasing the overlap size by 10 nucleotides until the final round of assembly was performed with an overlap size of 40 nucleotides. Contigs were then subjected to scaffolding using SSPACE and the full set of non-ribosomal, corrected, normalized paired-end reads using the settings -k 10 -a 0.7 -n 50 -o 20. Scaffolds were gap filled using the SGA gap filling function. Finally, the assembled contigs were subject to base-error correction using Pilon with the default settings. CEGMA (Parra et al. 2007) suggests ~88% completeness.

7.7 A Preliminary Transcriptome and Genome Assembly for *Euglena gracilis*

Our preliminary analysis of the *Euglena* genome suggests an estimated size of ~1.4 giga bases (Table 7.1), with the majority of the sequence noncoding. Analysis of the transcripts, coding sequences and proteins/genes arising from the whole transcriptome suggests a combined sequence length of ~63 Mb, ~38 Mb, and 36,526 proteins respectively (Table 7.1). This is significantly larger

than the genome and predicted proteomes of *T. brucei,* i.e. ~35 Mb arranged in 11 chromosomes and 9 Mb protein-coding sequence respectively (Berriman et al. 2005; Jackson et al. 2010), or *A. thaliana,* with 135 Mb arranged in five chromosomes and 35,386 protein-coding transcripts (Lamesch et al. 2012). Overall, we conclude that the transcriptome assembly is of high quality while the genome is of reasonable quality, but highly fragmented. The fragmentation is, perhaps, due to low read coverage combined with repeats, polyploidy, or near identical sequences which presents some assembling challenge to the algorithms. There is a GC bias between the transcriptome and the genome; with the transcriptome having a richer GC content (~60%), while the genome has a GC content of ~50%, suggesting the presence of significant AT-rich repeats in the genome.

7.8 The Tubulin and Calmodulin Genes

As preliminary candidates for interrogation of the genome and transcriptome we selected the tubulin and calmodulin gene families. Tubulin is a fundamental constituent of eukaryotic cytoskeletons, cell division machinery and motile organelles (Gull 2001), with most eukaryotes expressing multiple tubulin genes in specific regulatory or developmental contexts (Jackson et al. 2006). In general there are seven distinct subfamilies of tubulin that have been defined in eukaryotes, namely: alpha- (α-), beta- (β-), gamma- (ɣ-), epsilon- (ε-), delta- (δ-), zeta- (ζ-), and FtsZ, with an α/β heterodimer being the essential building block for the microtubular cytoskeleton, including kinetoplastids (McKean et al. 2001).

Representatives of all tubulin subfamilies (α-, β-, ɣ-, σ-, δ-, ζ-, and FtsZ-) were identified and classified in the *E. gracilis* transcriptome and genome using phylogenetic inference (FastTree and MrBayes). ɣ and FtsZ tubulin family were not found in the genome assembly, suggesting a lack of completeness (Fig. 7.3). In the *E. gracilis* transcriptome a single copy of all tubulins except σ-tubulin was found, which was unexpected in comparison to the multiple copies reported in many kinetoplastids. Overall, the *E. gracilis* tubulin sequences have good phylogentic support of ≥0.8 (Figs. 7.3 and 7.4) for subfamily assignments and there are no indels in the predicted coding sequences. The tubulin genes however possess multiple intron types and include splice sites (GT/C-AG borders), intermediate splice sites (e.g. AT-AC borders), and nonconventional splice sites (non GT/C-AG or AT-AC borders) (Fig. 7.5) (for details on Euglenoid introns see Milanowski et al. 2014, 2016, and McWaters and Russell, this volume). Overall gene lengths in the transcriptome are similar to those previously reported (Schantz and Schantz 1989; Jackson et al. 2006; Levasseur et al. 1994; Milanowski et al. 2014, 2016; Canaday et al. 2001), but are considerably shorter in the genome owing to truncation and fragmentation.

Overall, 18 introns were identified in the tubulin genes. Five introns (two conventional i.e. GT-AG borders, two intermediate-nonconventional i.e. GG/TA-T/AG borders, and one nonconventional i.e. CC–AA borders) are present in β, five introns (four conventional i.e. GT/C-AG borders and one nonconventional i.e. CC–AA borders) in α, two introns (conventional with GT-AG borders) in σ, four introns (one conventional i.e. GC-AG borders, one intermediate-nonconventional GG-AG borders, and two non conventional CC/GA–C/GG borders) in δ, and two introns (one conventional i.e. GT-AG borders and one intermediate-nonconventional i.e. GT-CG borders) in ζ, suggesting rather complex splice site recognition and likely processing machinery.

The presence of all tubulin subfamilies suggests conserved cytoskeletal function. It is not yet clear why there are single copies of tubulin subfamilies in *E. gracilis,* in contrast to many other kinetoplastids which possess arrays of tandem-duplicated tubulin genes (Jackson et al. 2006). However, *Trypanosome cruzi* is also predicted to have only one β-tubulin gene, and hence this may well represent an assembly artifact. Significantly, on phylogenetic reconstruction the *Euglena* α-, σ-, and FtsZ-tubulin families

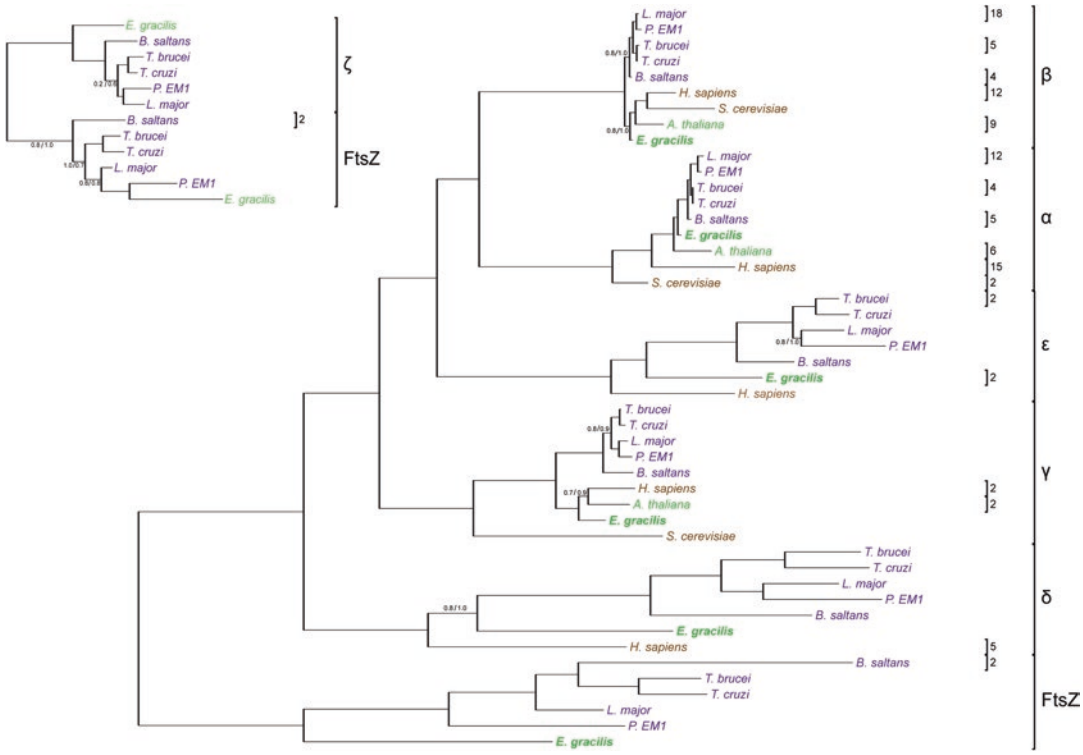

Fig. 7.3 Phylogenetic tree of α-, β-, ɣ-, ε-, δ-, ζ-, and FtsZ tubulin genes in selected eukaryotes. The tree at the top left corner of the diagram depicts ζ-tubulin genes while larger tree depicts α-, β-, ɣ-, ε-, and δ-tubulin genes. In both instances, FtsZ tubulin family was used as the outgroup. Statistical support are in the order FastTree/MrBayes, and generated using Maximum Likelihood based on 1000 bootstrappings and Posterior Probability respectively. Nodes without statistical support implies that this is above the threshold of ≥99/99. The numbers on the right of the tree, corresponding to specific taxa name, represent the copies of the tubulin sub family found in that taxa. Each clade correspond to each tubulin sub family and are classified as either α-, β-, ɣ-, ε-, δ-, ζ-, or FtsZ tubulin. Color codes: *Green* photosynthetic organisms, *purple* kinetoplastids, *orange* other members of the eukaryotes. We decided to show the phylogenetic tree for the transcriptome since all tubulin subfamilies were found in this dataset, and it is a global representatives of the tubulin genes in *E. gracilis*

cluster with kinetoplastids, while the β- and ɣ-tubulins cluster with *A. thaliana*, which may suggest endosymbiotic gene transfer from the green algal endosymbiont but this prediction is very tentative.

Calmodulin (CaM) is an ubiquitous, calcium-binding protein that can bind and regulate a multitude of different protein targets (McDowall 2016). CaM mediates processes such as inflammation, metabolism, apoptosis and muscle contraction in animals. In *E. gracilis,* one calmodulin is located beneath the pellicula may be involved in maintaining cell shape (Lonergan 1985) and responses to external stimuli such as light (phototaxis, see Chap. 11, this volume), oxygen pressure, gravity (gravitaxis, see Chap. 12, this volume) (Porterfield 1997; Streb et al. 2002; Hader et al. 2005a, b; Daiker et al. 2010), and signal transduction (Daiker et al. 2010). Calmodulin and protein kinases are involved in gravitaxis (Streb et al. 2002).Five types of CaM proteins have been discovered in *E. gracilis* and include: CaM.1, CaM.2, CaM.3, CaM.4, and CaM.5, with CaM.2 being implicated in gravitaxis (Toda et al. 1992; Daiker et al. 2010). In general, CaMs consist of ~150 amino acids and the molecule possesses four calcium binding sites (Aykut et al. 2013), each motif consists of a 12-residue loop flanked on either side by a 12-residue α-helix (Kawasaki and Kretsinger 1995).

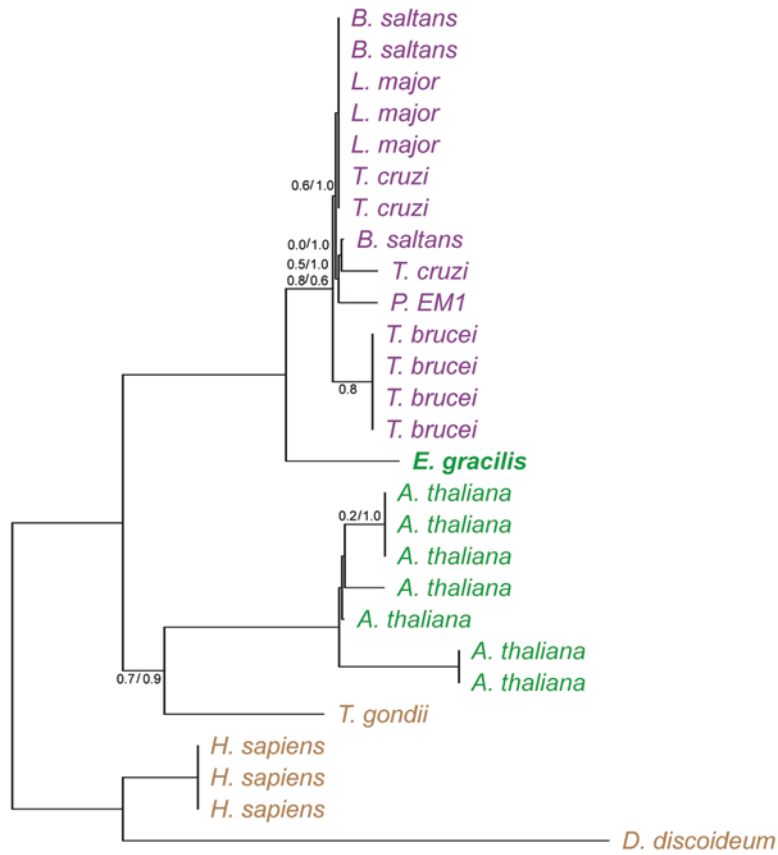

Fig. 7.4 Phylogenetic tree of Calmodulin genes (CaM.1-7) in selected eukaryotes. Statistical support are in the order FastTree/MrBayes, and generated using Maximum Likelihood based on 1000 bootstrappings and Posterior Probability respectively. Nodes without statistical support implies that this is above the threshold of ≥99/99. The numbers on the right of the tree, corresponding to specific taxa name, represent the copies of the tubulin sub family found in that taxa. Only one *E. gracilis* true calmodulin was found. Color codes: *Green* photosynthetic organisms, *purple* kinetoplastids, *orange* other members of the eukaryotes

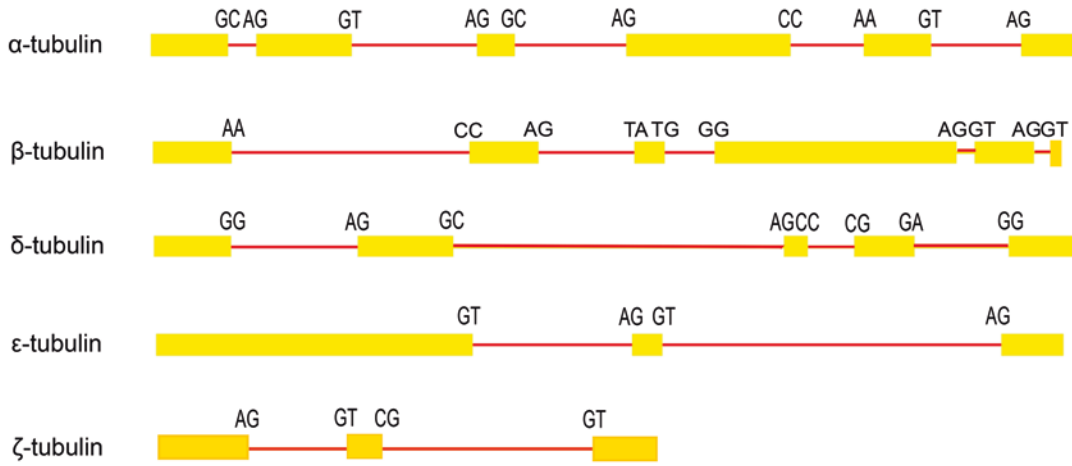

Fig. 7.5 The tubulin gene structure in *E. gracilis*. The *bars* (genes) correspond to α-, β-, ε-, ζ- and δ-tubulins respectively. Splicing is indicated by a combination of two alphabetical letters which correspond to conventional, intermediate, or non conventional splicing types. The *yellow bars* correspond to exons while the *red lines* correspond to introns. The genes are drawn to scale in proportion to the actual gene length

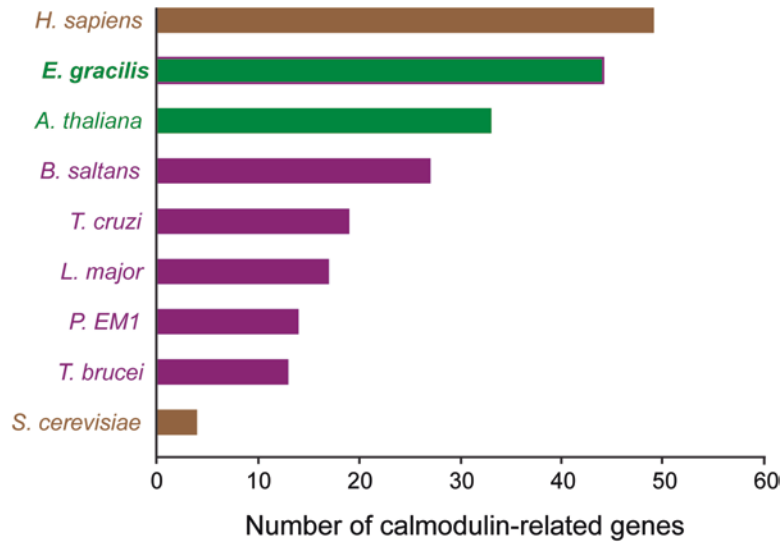

Fig. 7.6 Calmodulin related potential calcium sensors across selected eukaryotes. The x-axis correspond to taxa/species, while the y-axis correspond to the number of proteins found. *Color codes*: *Green* photosynthetic organisms, *purple* kinetoplastids, *orange* other members of the eukaryotes

We analysed the CaM family using the phylogenetic inference method to assign sequences to specific subfamilies. CaM.1-7 were not found in the genome, but one single copy was found in the transcriptome, which could not be classified with reliability. However, analysis does suggest a set of multiple copies of calmodulins as found in kinetoplastids (Fig. 7.6). This is not consistent with Daiker et al. (2010), who found the presence of five calmodulins (CaM.1-5) in *E. gracilis*. The absence of CaM.1-7 from the genome assembly is likely due to incompleteness. Forty-four CaM-related potential calcium sensors (McCormack and Braam 2003) were also found in the *E. gracilis* transcriptome, while only 23 were found in the genome. However, it is significant that *Euglena* possesses a very large predicted cohort of these proteins, which are equalled only by multicellular plants and animals (Fig. 7.6). Overall, these data suggest a highly complex mechanism for the control of signal transduction and that CaM/CaM-related proteins likely have very important roles in the responses of *E. gracilis* to environmental and other cues, and which far exceeds the parasitic kinetoplastids and even the free-living *B. saltans* by a considerable degree.

7.9 Conclusions

A draft genome and transcriptome of *E. gracilis* are now available. Analysis indicates a close relationship to the kinetoplastids, as well as the expected presence of photosynthetic genes that likely were transfered with the secondary endosymbiosis. The genome is very large, confirming earlier estimates of an extremely high level of DNA content, and is highly repetitive, both of which contribute to the difficulty in arriving at a high quality genome. None the less, despite the fragmentary nature of the draft genome, a very high quality transcriptome could be assembled, and which has indicated the presence of large numbers of paralogs within the calmodulin and calmodulin-related gene cohort, as well as additional protein families not discussed here. Furthermore, we found evidence for extensive and divergent splicing within tubulin genes, which suggest complex mechanisms for the control of gene expression and environmental sensing. Whilst size, high frequency of repeats and several other features were all suspected from previous analyses, the availability of genome wide sequence data will allow very rapid progression in mapping the structure of *Euglena* gene families, their

diversity and the origins of cohorts of proteins associated with photosynthesis as well as additional metabolic functions. With the draft genome and transcriptome of *E. gracilis* we anticipate a major step forward for the biology of this fascinating organism and in unravelling its contributions to ecology and exploitation for biotechnology.

Acknowledgements We are greatly indebted to the following for their contributions of data, advice and suggestions: Peter Myler (Seattle), Purificacion Gacia-Lopes and David Moreira (Orsay), Rob Field (Norwich) and Vladimir Hampl (Praha).

References

Adl SM, Simpson AGB, Farmer MA, Andersen RA, Anderson OR, Barta JR, Bowser SS, Brugerolle G, Fensome RA, Fredericq S, James TY, Karpov S, Kugrens P, Krug J, Lane CE, Lewis LA, Lodge J, Lynn DH, Mann DG, Mccourt RM, Mendoz L, Moestrup O, Mozley-Standridge SE, Nerad TA, Shearer CA, Smirnov AV, Spiegel FW, Taylor MFJR (2005) The new higher level classification of eukaryotes with emphasis on the taxonomy of protists. J Eukaryot Microbiol 52:399–451

Adl SM, Simpson AG, Lane CE, Lukeš J, Bass D, Bowser SS, Brown MW, Burki F, Dunthorn M, Hampl V, Heiss A, Hoppenrath M, Lara E, Le Gall L, Lynn DH, McManus H, Mitchell EA, Mozley-Stanridge SE, Parfrey LW, Pawlowski J, Rueckert S, Shadwick RS, Schoch CL, Smirnov A, Spiegel FW (2012) The revised classification of eukaryotes. J Eukaryot Microbiol 59(5):429–493

Attardi G, Schatz G (1988) Biogenesis of mitochondria. Annu Rev Cell Biol 4:289–333

Aykut AO, Atilgan AR, Atilgan C (2013) Designing molecular dynamics simulations to shift populations of the conformational states of calmodulin. PLoS Comput Biol 9(12):e1003366. doi:10.1371/journalpcbi1003366

Bachvaroff TR, Sanchez Puerta MV, Delwiche CF (2005) Chlorophyll c-containing plastid relationships based on analyses of a multigene data set with all four chromalveolate lineages. Mol Biol Evol 22:1772–1782

Berriman M, Ghedin E, Hertz-Fowler C, Blandin G, Renauld H, Bartholomeu DC, Lennard NJ, Caler E, Hamlin NE, Haas B, Böhme U, Hannick L, Aslett MA, Shallom J, Marcello L, Hou L, Wickstead B, Alsmark UC, Arrowsmith C, Atkin RJ, Barron AJ, Bringaud F, Brooks K, Carrington M, Cherevach I, Chillingworth TJ, Churcher C, Clark LN, Corton CH, Cronin A, Davies RM, Doggett J, Djikeng A, Feldblyum T, Field MC, Fraser A, Goodhead I, Hance Z, Harper D, Harris BR, Hauser H, Hostetler J, Ivens A, Jagels K, Johnson D, Johnson J, Jones K, Kerhornou AX, Koo H, Larke N, Landfear S, Larkin C, Leech V, Line A, Lord A, Macleod A, Mooney PJ, Moule S, Martin DM, Morgan GW, Mungall K, Norbertczak H, Ormond D, Pai G, Peacock CS, Peterson J, Quail MA, Rabbinowitsch E, Rajandream MA, Reitter C, Salzberg SL, Sanders M, Schobel S, Sharp S, Simmonds M, Simpson AJ, Tallon L, Turner CM, Tait A, Tivey AR, Van Aken S, Walker D, Wanless D, Wang S, White B, White O, Whitehead S, Woodward J, Wortman J, Adams MD, Embley TM, Gull K, Ullu E, Barry JD, Fairlamb AH, Opperdoes F, Barrell BG, Donelson JE, Hall N, Fraser CM, Melville SE, El-Sayed NM (2005) The genome of the African trypanosome Trypanosoma brucei. Science 309(5733):416–422

Boetzer M, Henkel CV, Jansen HJ, Butler D, Pirovano W (2011) Scaffolding pre-assembled contigs using SSPACE. Bioinformatics 27(4):578–579

Bolger AM, Lohse M, Usade B (2014) Trimmomatic: a flexible trimmer for Illumina sequence data. Bioinformatics 30(15):2114–2120

Bolte K, Bullmann L, Hempel F, Bozarth A, Zauner S, Maier U (2009) Protein targeting into secondary plastids. J Eukaryot Microbiol 56(1):9–15

Buetow DE (1982) The biology of euglena, vol III. Academic, New York

Bumbulis MJ, Balog BM (2013) UV-C exposure induces an apoptosis-like process in Euglena gracilis. ISRN Cell Biol 2013(869216):6 pages

Burger G, Lang BF, Reith M, Gray MW (1996) Genes encoding the same three subunits of respiratory complex II are present in the mitochondrial DNA of two phylogenetically distant eukaryotes. Proc Natl Acad Sci U S A A93:2328–2332

Canaday J, Tessier L, Imbault HP, Paulus F (2001) Analysis of Euglena gracilis alpha-, beta-and gamma tubulin genes: introns and pre-mRNA maturation. Mol Genet Genomics 265:153–160. doi:10.1007/s004380000403

Cook JR (1972) Ultraviolet inactivation of Euglena chloroplasts. I. Effect of light intensity of culture. Biophys J 12:1467–1473

Cook JR (1981) Variation of DNA levels in *Euglena* related to pH of culture medium. J Protozool 28:148–150

Cook JR, Roxby R (1985) Physical properties of a plasmid-like DNA from Euglena gracilis. Biochim Biophys Acta 824(80):83

Daiker V, Lebert M, Richter P, Hader D (2010) Molecular characterization of a calmodulin involved in the signal transduction chain of gravitaxis in Euglena gracilis. Planta 231:1229–1236. doi:10.1007/s00425-010-1126-9

Davis EA, Epstein HT (1971) Some factors controlling step-wise variation of organelle number in Euglena gracilis. Exp Cell Res 65:273–280

Dobakova E, Flegontov P, Skalicky T, Lukes J (2015) Unexpectedly streamlined mitochondrial genome of the Euglenozoan Euglena gracilis. Genome Biol Evol 7(12):3358–3367. doi:10.1093/gbe/evv229

Dobell C (1932) Antony van Leeuwenhoek and his 'little animals': being some account of the father of protozoology and bacteriology and his multifarious discoveries in

these disciplines. Constable, London, UK. Reprinted 1958 Russell and Russell, New York, New York, USA
Dolezel J, Bartos J, Voglmayr H, Greilhuber J (2003) Nuclear DNA and genome size of trout and human. Cytometry 51:127–128
Dooijes D, Chaves I, Kieft R, Dirks-Mulder A, Martin W, Borst P (2000) Base J originally found in Kinetoplastida is also a minor constituent of nuclear DNA of Euglena gracilis. Nucl Acids Res 28(16):3017–3021. doi:10.1093/nar/28163017
Dos Santos Ferreira V, Rocchetta I, Conforti V, Bench S, Feldman R, Levin MJ (2007) Gene expression patterns in Euglena gracilis: insights into the cellular response to environmental stress. Gene 389:136–145
Ebel C, Frantz C, Paulus F, Imbault P (1999) Trans-splicing and cis-splicing in the colourless Euglenoid, Entosiphon sulcatum. Curr Genet 35:542–550
Ebenezer TE, O'Neill E, Zoltner M, Obado S, Hampl V, Ginger M, Jackson A, de Koning H, Lukes J, Dacks J, Lebert M, Carrington M, Kelly S, Field M et al (2017) Gene complement and expression in *Euglena gracilis* (in preparation)
El-Metwally S, Hamza T, Zakaria M, Helmy M (2013) Next-generation sequence assembly: four stages of data processing and computational challenges. PLoS Comput Biol 9(12):1–19
Epstein HT, Allaway E (1967) Properties of selectively starved Euglena. Biochim Biophys Acta 142:195–207
Flegontov P, Gray MW, Burger G, Lukes J (2011) Gene fragmentation: a key to mitochondrial genome evolution in Euglenozoa? Curr Genet 57:225–232. doi:10.1007/s00294-011-0340-8
Gibbs SP (1978) The chloroplasts of Euglena may have evolved from symbiotic green algae. Can J Bot 56:2883–2889
Gnerre S, MacCallum I, Przybylski D, Ribeiro F, Burton J, Walker B, Sharpe T, Hall G, Shea T, Sykes S, Berlin A, Aird D, Costello M, Daza R, Williams L, Nicol R, Gnirke A, Nusbaum C, Lander ES, Jaffe DB (2011) High-quality draft assemblies of mammalian genomes from massively parallel sequence data. Proc Natl Acad Sci USA 108(4):1513–1518
Gojdics M (1953) The Genus Euglena Madison. University of Wisconsin Press, Wisconsin
Goto K, Beneragama CK (2010) Circadian clocks and antiaging: do non-aging microalgae like Euglena reveal anything? Ageing Res Rev 9:91–100
Gray MW, Doolittle WF (1982) Has the endosymbiont hypothesis been proven? Microbiol Rev 46:1–42
Gull K (2001) Protist tubulins: new arrivals, evolutionary relationships and insights to cytoskeletal function. Curr Opin Microbiol 4:427–432
Gurevich A, Saveliev V, Vyahhi N, Tesler G (2013) QUAST: quality assessment tool for genome assemblies. Bioinformatics 29(8):1072–1075. doi:10.1093/bioinformatics/btt086
Hader D-P, Hemmersbach R, Lebert M (2005a) Gravity and the behavior of unicellular organisms. Cambridge University Press, Cambridge
Hader D-P, Hemmersbach R, Lebert M (2005b) Gravity and the behavior of unicellular organisms. Development and cell biology series (no. 40). Cambridge University Press, Cambridge
Hallick RB, Hong L, Drager RG, Favreau MR, Monfort A, Orsat B, Spielmann A, Stutz E (1993) Complete sequence of Euglena gracilis chloroplast DNA. Nucleic Acids Res 21:3537–3544
Hill HZ, Epstein HT, Schiff JA (1966) Studies of chloroplast development in Euglena. XIV. Sequential interactions of ultraviolet light and photoreactivating light in green colony formation. Biophys J 6:135–144
Hornett EA, Wheat CW (2012) Quantitative RNA-Seq analysis in non-model species: assessing transcriptome assemblies as a scaffold and the utility of evolutionary divergent genomic reference species. BMC Genomics 13:361. doi:10.1186/1471-2164-13-361
Ivens AC, Peacock CS, Worthey EA, Murphy L, Aggarwal G, Berriman M, Sisk E, Rajandream MA, Adlem E, Aert R, Anupama A, Apostolou Z, Attipoe P, Bason N, Bauser C, Beck A, Beverley SM, Bianchettin G, Borzym K, Bothe G, Bruschi CV, Collins M, Cadag E, Ciarloni L, Clayton C, Coulson RM, Cronin A, Cruz AK, Davies RM, De Gaudenzi J, Dobson DE, Duesterhoeft A, Fazelina G, Fosker N, Frasch AC, Fraser A, Fuchs M, Gabel C, Goble A, Goffeau A, Harris D, Hertz-Fowler C, Hilbert H, Horn D, Huang Y, Klages S, Knights A, Kube M, Larke N, Litvin L, Lord A, Louie T, Marra M, Masuy D, Matthews K, Michaeli S, Mottram JC, Müller-Auer S, Munden H, Nelson S, Norbertczak H, Oliver K, O'neil S, Pentony M, Pohl TM, Price C, Purnelle B, Quail MA, Rabbinowitsch E, Reinhardt R, Rieger M, Rinta J, Robben J, Robertson L, Ruiz JC, Rutter S, Saunders D, Schäfer M, Schein J, Schwartz DC, Seeger K, Seyler A, Sharp S, Shin H, Sivam D, Squares R, Squares S, Tosato V, Vogt C, Volckaert G, Wambutt R, Warren T, Wedler H, Woodward J, Zhou S, Zimmermann W, Smith DF, Blackwell JM, Stuart KD, Barrell B, Myler PJ (2005) The genome of the kinetoplastid parasite, Leishmania major. Science 309(5733):436–442
Jackson AP, Vaughan S, Gull K (2006) Evolution of tubulin gene arrays in Trypanosomatid parasites: genomic restructuring in Leishmania. BMC Genomics 7:261
Jackson AP, Sanders M, Berry A, McQuillan J, Aslett MA, Quail MA, Chukualim B, Capewell P, MacLeod A, Melville SE, Gibson W, Barry JD, Berriman M, Hertz-Fowler C (2010) The genome sequence of Trypanosoma brucei gambiense, causative agent of chronic human african trypanosomiasis. PLoS Negl Trop Dis 4(4):e658
Jackson AP, Otto TD, Aslett M, Armstrong SD, Bringaud F, Schlacht A, Hartley C, Sanders M, Wastling JM, Dacks JB, Acosta-Serrano A, Field MC, Ginger ML, Berriman M (2016) Kinetoplastid phylogenomics reveals the evolutionary innovations associated with the origins of parasitism. Curr Biol 26:161–172
Kawasaki H, Kretsinger RH (1995) Calcium-binding proteins 1: EF-hands. Protein Profile 2(4):297–490

Kim JT, Boo SM, Zakrys B (1998) Floristic and taxonomic accounts of the genus Euglena (Euglenophyceae) from Korean fresh waters. Algae 13(2):173–197

Lamesch P, Berardini TZ, Li D, Swarbreck D, Wilks C, Sasidharan R, Muller R, Dreher K, Alexander DL, Garcia-Hernandez M, Karthikeyan AS, Lee CH, Nelson WD, Ploetz L, Singh S, Wensel A, Huala E (2012) The Arabidopsis Information Resource (TAIR): improved gene annotation and new tools. Nucleic Acids Res 40:D1202–D1210

Leedale GF (1958a) Mitosis and chromosome numbers in the Euglenineae (Flagellata). Nature 181(4607):502–503

Leedale GF (1958b) Nuclear structure and mitosis in the Euglenineae. Arch Mikrobiol 32:32–64

Leedale GF (1968) The nucleus in Euglena. In: Buetow DE (ed) The Biology of Euglena. Academic, New York, pp 185–272

Leedale GF (1974) Preliminary observations on nuclear cytology and ultrastructure in carbon-starved streptomycin-bleached Euglena gracilis. Colloq Int CNRS 240:285–290

Lefort-Tran M, Bre MH, Pouphile M, Manigault P (1987) DNA flow cytometry of control euglena and cell cycle blockade of vitamin Bl2-starved. Cells Cytometry 8:46–54

Levasseur PJ, Meng Q, Bouck GB (1994) Tubulin genes in the algal protist Euglena gracilis. J Eukaryot Microbiol 41(5):468–477

Linton EW, Karnkowska-Ishikawa A, Kim JI, Shin W, Bennett MS, Kwiatowski J, Zakrys B, Triemer RE (2010a) Reconstructing euglenoid evolutionary relationships using three genes: nuclear SSU and LSU, and chloroplast SSU rDNA sequences and the description of Euglenaria gen nov (Euglenophyta). Protist 161:603–619. doi:10.1016/jprotis201002002

Lonergan TA (1985) Regulation of cell shape in Euglena gracilis. IV. Localization of actin, myosin and calmodulin. J Cell Sci 77:197–208

Martin W, Herrmann RG (1998) Gene transfer from organelles to the nucleus: how much, what happens, and why? Plant Physiol 118:9–17

Mazus B, Falchuk KH, Vallee BL (1984) Histone formation, gene expression, and zinc deficiency in Euglena gracilis. Biochemistry 23:42–47

McCormack E, Braam J (2003) Calmodulins and related potential calcium sensors of Arabidopsis. New Phytol 159:585–598

McDowall J (2016) "Calmodulin" InterPro Protein Archive. Accessed 19 May 2016

McFadden GI (2001) Primary and secondary endosymbiosis and the origin of plastids. J Phycol 37:951–959

McKean PG, Vaughan S, Gull K (2001) The extended tubulin superfamily. J Cell Sci 114:2723–2733

Milanowski R, Gumińska N, Karnkowska A, Ishikawa T, Zakryś B (2016) Intermediate introns in nuclear genes of euglenids—are they a distinct type? BMC Evol Biol 16:49. doi:10.1186/s12862-016-0620-5

Milanowski R, Karnkowska A, Ishikawa T, Zakryś B (2014) Distribution of conventional and nonconventional introns in tubulin (α and β) genes of Euglenids. Mol Biol Evol 31(3):584–593

Morton BR (1998) Selection on the codon bias of chloroplast and cyanelle genes in different plant and algal lineages. J Mol Evol 46:449–459

Morton BR (1999) Strand asymmetry and codon usage bias in the chloroplast genome of *Euglena gracilis*. Proc Natl Acad Sci U S A 96(9):5123–5128

Nakazawa M, Inui H, Yamaji R, Yamamoto T, Takenaka S, Ueda M, Nakano Y, Miyatake K (2000) The origin of pyruvate: NADP1 oxidoreductase in mitochondria of Euglena gracilis. FEBS Lett 479:155–156

Newton AC (2001) Protein kinase C: structural and spatial regulation by phosphorylation, cofactors, and macromolecular interactions. Chem Rev 101:2353–2364

Newton AC (2003) Regulation of the ABC kinases by phosphorylation: protein kinase C as a paradigm. Biochem J 370:361–371

Nikolenko SI, Korobeynikov AI, Alekseyev MA (2013) BayesHammer: Bayesian clustering for error correction in single-cell sequencing. BMC Genomics 14(1):S7

O'Donnell EHJ (1965) Nucleolus and chromosomes in Euglena gracilis. Cytologia 30(2):118–154

O'Neil ST, Emrich SJ (2013) Assessing De Novo transcriptome assembly metrics for consistency and utility. BMC Genomics 14:465

O'Neill EC, Trick M, Hill L, Rejzek M, Dusi RG, Hamilton CJ, Zimba PV, Henrissat B, Field RA (2015) The transcriptome of Euglena gracilis reveals unexpected metabolic capabilities for carbohydrate and natural product biochemistry. Mol BioSyst 11:2808

Parra G, Bradnam K, Korf I (2007) CEGMA: a pipeline to accurately annotate core genes in eukaryotic genomes. Bioinformatics 23:1061–1067

Perez E, Lapaille M, Degand H, Cilibrasi L, Villavicencio-Queijeiro A, Morsomme P, González-Halphen D, Field MC, Remacle C, Baurain D, Cardol P (2014) The mitochondrial respiratory chain of the secondary green alga Euglena gracilis shares many additional subunits with parasitic Trypanosomatidae. Mitochondrion 19(Pt B):338–349. doi:10.1016/jmito201402001

Porterfield DM (1997) Orientation of motile unicellular algae to oxygen: oxytaxis in Euglena. Biol Bull 193:229–230

Rawson JRY (1975) The characterization of Euglena gracilis DNA by its reassociation kinetics. Biochim Biophys Acta 402:171–178

Richards OC (1967) Hybridization of Euglena gracilis chloroplast and nuclear DNA. Biochemistry 57:156–163

Rosati G, Verni F, Barsanti L, Passarelli V, Gualtieri P (1991) Ultrastructure of the apical zone of Euglena gracilis: photoreceptors and motor apparatus. Electron Microsc Rev 4:319–342

Roy J, Faktorovab D, Lukes J, Burger G (2007) Unusual mitochondrial genome structures throughout the Euglenozoa. Protist 158:385–396

Schantz M, Schantz R (1989) Sequence of a cDNA clone encoding β-tubnlin from Euglena gracilis. Nucleic Acids Res 17(16):6727

Schwartzbach SD, Schiff, JA (1983) Control of plastogenesis in Euglena. In: Shropshire W Jr, Mohor H (eds) Encyclopaedia of plant physiology, 6A. New series, Springer, Berlin, pp 312–335

Simpson JT, Durbin R (2011) Efficient de novo assembly of large genomes using compressed data structures. Genome Res 22:549–556

Souza RT, Lima FM, Barros RM, Cortez DR, Santos MF, Cordero EM, Ruiz JC, Goldenberg S, Teixeira MMG, da Silveira JF (2011) Genome size, karyotype polymorphism and chromosomal evolution in Trypanosoma cruzi. PLoS One 6(8):e23042. doi:10.1371/journalpone0023042

Spencer DF, Gray MW (2011) Ribosomal RNA genes in Euglena gracilis mitochondrial DNA: fragmented genes in a seemingly fragmented genome. Mol Gen Genomics 285:19–31

Spencer DF, Gray MW (2012) Ribosomal RNA genes in Euglena gracilis mitochondrial DNA: fragmented genes in a seemingly fragmented genome. Mol Genet Genomics 285:19–31

Stankiewicz AJ, Falchuk KH, Vallee BL (1983) Composition and structure of zinc-deficient Euglena gracilis chromatin. Biochemistry 22:5150–5156

Streb C, Richter P, Ntefidou M, Lebert M, Hader D-P (2002) Sensory transduction of gravitaxis in Euglena gracilis. J Plant Physiol 159:855–862

Thompson MD, Copertino DW, Thompson E, Favreau MR, Hallick RB (1995) Evidence for the late origin of introns in chloroplast genes from an evolutionary analysis of the genus Euglena. Nucleic Acids Res 23(23):4745–4752

Toda H, Yazawa M, Yagi K (1992) Amino acid sequence of calmodulin from Euglena gracilis. Eur J Biochem 205:653–660

Tzagoloff A, Myers AM (1986) Genetics of mitochondrial biogenesis. Annu Rev Biochem 55:249–285

Vallee BL, Falchuk KH (1981) Zinc and gene expression. Philos Trans R Soc Lond B 1(294):185–196

Walker BJ, Abeel T, Shea T, Priest M, Abouelliel A, Sakthikumar S, Cuomo CA, Zeng Q, Wortman J, Young SK, Earl AM (2014) Pilon: an integrated tool for comprehensive microbial variant detection and genome assembly improvement. PLoS One 9(11):e112963

Wiegert KE, Bennett MS, Triemer RE (2012) Evolution of the chloroplast genome in photosynthetic euglenoids: a comparison of Eutreptia viridis and Euglena gracilis (Euglenophyta). Protist 163:832–843

Yoon HS, Hackett JD, Bhattacharya D (2002) A single origin of the peridinin- and fucoxanthin-containing plastids in dinoflagellates through tertiary endosymbiosis. Proc Natl Acad Sci U S A 99:11724–11729

Zakrys B (1988) The nuclear DNA level as a potential taxonomic character in Euglena EHR (Euglenophyceae). Algol Stud 49:483–504

Zakrys B, Walne PL (1994) Floristic, taxonomic and phytogeographic studies of green Euglenophyta from the Southeastern United States, with emphasis on new and rare species. Algol Stud 72:71–114

Zakryś B (1986) Contribution to the monograph of Polish members of the genus *Euglena* Ehrenberg 1830. Nova Hedwig Beih 42:491–540

Zhang T, Zhang X, Hu S, Yu J (2011) An efficient procedure for plant organellar genome assembly, based on whole genome data from the 454 GS FLX sequencing platform. Plant Methods 7:38

Euglena Transcript Processing

8

David C. McWatters and Anthony G. Russell

Abstract

RNA transcript processing is an important stage in the gene expression pathway of all organisms and is subject to various mechanisms of control that influence the final levels of gene products. RNA processing involves events such as nuclease-mediated cleavage, removal of intervening sequences referred to as introns and modifications to RNA structure (nucleoside modification and editing). In *Euglena*, RNA transcript processing was initially examined in chloroplasts because of historical interest in the secondary endosymbiotic origin of this organelle in this organism. More recent efforts to examine mitochondrial genome structure and RNA maturation have been stimulated by the discovery of unusual processing pathways in other Euglenozoans such as kinetoplastids and diplonemids. Eukaryotes containing large genomes are now known to typically contain large collections of introns and regulatory RNAs involved in RNA processing events, and *Euglena gracilis* in particular has a relatively large genome for a protist. Studies examining the structure of nuclear genes and the mechanisms involved in nuclear RNA processing have revealed that indeed *Euglena* contains large numbers of introns in the limited set of genes so far examined and also possesses large numbers of specific classes of regulatory and processing RNAs, such as small nucleolar RNAs (snoRNAs). Most interestingly, these studies have also revealed that *Euglena* possesses novel processing pathways generating highly fragmented cytosolic ribosomal RNAs and subunits and non-conventional intron classes removed by unknown splicing mechanisms. This unexpected

D.C. McWatters • A.G. Russell, Ph.D. (✉)
Department of Biological Sciences, University of Lethbridge, 4401 University Dr W, Lethbridge, AB, Canada, T1K 6T5

Alberta RNA Research and Training Institute, University of Lethbridge, Lethbridge, AB, Canada
e-mail: david.mcwatters@uleth.ca; tony.russell@uleth.ca

S.D. Schwartzbach, S. Shigeoka (eds.), *Euglena: Biochemistry, Cell and Molecular Biology*, Advances in Experimental Medicine and Biology 979, DOI 10.1007/978-3-319-54910-1_8

diversity in RNA processing pathways emphasizes the importance of identifying the components involved in these processing mechanisms and their evolutionary emergence in *Euglena* species.

Keywords
Euglena • RNA processing • Transcript • Small nucleolar RNA • Mitochondrial RNA • Chloroplast RNA • Intron • Gene expression • RNA modification • Spliced leader RNA

Abbreviations

gRNA	Guide RNA
IGS	Intergenic spacer
indel	Insertion/deletion
ITS	Internal transcribed spacer
kbp	Kilo base-pairs
LSU	Large subunit
MITE	Miniature Inverted Repeat Transposable Element
mRNA	Messenger RNA
mtDNA	Mitochondrial DNA
Nm	2′-O-methylation of the ribose sugar
nt	Nucleotide
ORF	Open-reading frame
PCR	Polymerase chain reaction
PRORP	Protein-only ribonuclease P
rDNA	Ribosomal DNA
rprotein	Ribosomal protein
rRNA	Ribosomal RNA
SL RNA	Spliced leader RNA
snoRNA	Small nucleolar RNA
snRNA	Small nuclear RNA
SSU	Small subunit
tRNA	Transfer RNA
Ψ	Pseudouridine modification of RNA

8.1 Nuclear-Encoded Introns

Many nuclear-encoded protein-coding genes in *Euglena* contain introns which possess variable properties resulting in their classification into at least two distinct categories: conventional spliceosomal introns that are predicted to be removed from precursor mRNAs by the characterized *Euglena* spliceosome components and so-called "non-conventional" (non-canonical) introns that are excised by unknown cellular components. From the limited set of *Euglena* genes whose sequences have been determined and compared to their expressed mature mRNA sequences, it appears that having multiple introns and possessing both intron types in an individual gene is relatively common.

The non-conventional introns are defined as containing extensive secondary structural potential via base-pairing of intron 5′ and 3′ end proximal sequences, but little overall intron sequence conservation (Tessier et al. 1991; Canaday et al. 2001; Russell et al. 2005; Milanowski et al. 2014, 2016; Muchhal and Schwartzbach 1992, 1994) (Fig. 8.1b). They also frequently contain direct repeat sequences, of variable length, at the intron termini creating uncertainty in the accurate prediction of splice donor and acceptor sites for some of these introns. The lack of strict conservation of the direct repeats and their sequence variability indicates that they are unlikely to have a role in the splicing mechanism but may instead be remnants of intron sequence insertion and mobility events. Milanowski et al. have noted that these features are reminiscent of MITE-like transposon elements (Milanowski et al. 2014); therefore, if the non-conventional introns have been derived from such elements then perhaps *trans*-acting factors that associate with them may have been co-opted to be involved in the splicing mechanism. While there is no apparent conservation of extended sequence elements in these introns, intron sequence comparisons have revealed a preference for intron 5′ end proximal

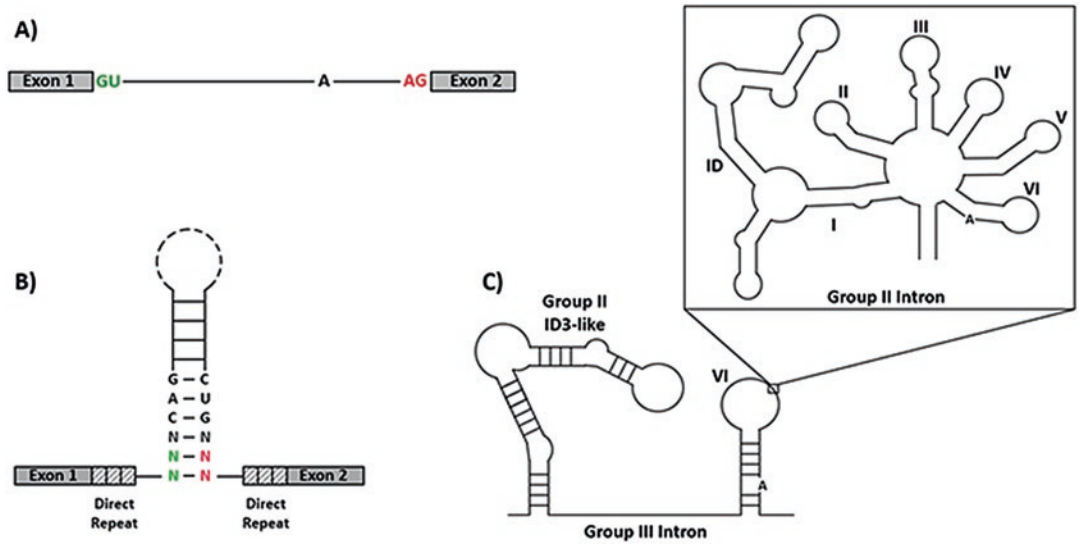

Fig. 8.1 Structural features of the different *E. gracilis* intron classes. (**a**) Canonical structure for a U2-type spliceosomal intron with intronic 5′ splice site boundary nucleotides in green and 3′ nucleotides in red, and the branch point A in black. (**b**) Secondary structure of an *E. gracilis* non-conventional intron. For those introns lacking direct repeats, nucleotides that sometimes show adherence to 5′ and 3′ splice site boundaries of conventional introns are in green and red respectively. Conserved +4 to +6 nucleotides and base paired nucleotides are shown in black. There are variable numbers of nucleotides in the base-paired stems and the dashed line represents the variable length intronic region. (**c**) General secondary structure for a chloroplast twintron arrangement, in this case composed of a group II intron inserted within a group III intron. Conserved structural domains for both introns are labelled. Position of insertion of the group II intron in domain VI of the group III intron is indicated by the small box. Relative positions of branch point A nucleotides for both introns are indicated

nucleotide positions +4 to +6 to be 'CAG' and the complementary sequence (CTG) starting 6 nucleotides from the intron 3′ end (Milanowski et al. 2014, 2016) (Fig. 8.1b). The conservation of these short sequences and their ability to base pair may be required for the splicing mechanism and accurate determination of splice site boundaries.

Some of the *Euglena* non-conventional introns contain intron terminal nucleotides (5′GT or AG3′) identical to those of most conventional spliceosomal introns (Canaday et al. 2001; Milanowski et al. 2014) (Fig. 8.1a). Additionally, some of the predicted spliceosomal introns show extended base-pairing potential in intron locations similar to regions of secondary structure observed in the non-conventional introns. Such observations have raised questions about whether interconversion between intron classes may occur during intron sequence evolution in *Euglena* and whether introns demonstrating mixed features of both classes should be classified as a distinct type called "intermediate" introns (Canaday et al. 2001; Russell et al. 2005). These could potentially be excised using components of both the spliceosome and *trans*-acting non-conventional intron splicing factors.

Milanowski et al. have recently examined the conservation of intron position and class in conserved nuclear genes in different *Euglena* species to shed light on such questions (Milanowski et al. 2014, 2016). These studies have further refined the limited conserved sequence and structural features of non-conventional introns (as described above) and revealed that non-conventional intron gain/loss appears to occur much more frequently than observed for euglenid spliceosomal introns. There is also much greater intron length variation in different species at conserved non-conventional intron positions than is the case for the conserved spliceosomal introns. A preference for a 5′ purine

nucleotide in non-conventional introns has also been observed (Milanowski et al. 2016) that perhaps affects splicing efficiency, thus explaining the frequent observation of non-conventional introns starting with the sequence 5′GT/C (i.e. spliceosomal-like) but also containing all other typical features of non-canonical introns. Such introns had previously been categorized as intermediate type; however, many of these introns have only poor base-pairing potential to the characterized *Euglena* spliceosomal U1 snRNA sequence (Breckenridge et al. 1999) making it unclear whether these introns are in fact in a transition state between intron classes and utilize any spliceosome components.

Identification of many instances of U12-type (minor-type) spliceosomal introns residing in identical gene positions to U2-type (major-type) introns in distantly-related species has provided evidence of evolutionary conversion between spliceosomal intron classes (Burge et al. 1998; Basu et al. 2008). To date, no instance of a conserved intron position being a conventional spliceosomal intron in one *Euglena* species and non-conventional in another species has been identified. Milanowski et al. did however recently discover the first case of a non-conventional intron containing 5′GC and AC3′ intron terminal sequences, the best candidate so far for an intermediate intron since both splice sites match those of conventional spliceosomal introns (Milanowski et al. 2016). They also identified a recently acquired non-conventional intron in the *gapC* gene in *Euglena agilis* that contains significantly longer extended intron boundary direct repeats than had previously been observed, leading them to propose that DNA double-strand break repair processes may be involved in intron emergence/acquisition in *Euglena*.

Only a very limited set of genes and small number of introns have been characterized in detail in *Euglena*. Recent extensive mRNA transcriptome studies under different physiological stress conditions (O'Neill et al. 2015; Yoshida et al. 2016; Ferreira et al. 2007) and future determination of more complete genome sequences from different *Euglena* species should permit a much more extensive analysis of intron evolution in euglenids and the detection of intron class conversion, if it occurs. Also important will be the identification of the cellular factors required for the removal of non-conventional introns, the experimental determination of critical intron structure and sequence requirements for splicing reactions, and the further identification of conventional spliceosomal components in *Euglena.* snRNAs have been identified but no experimental analysis of spliceosomal proteins or snRNP complexes has yet been performed.

8.2 Nuclear-Encoded Cytosolic rRNA

Expression and maturation of cytoplasmic ribosomal RNA in *Euglena gracilis* differs dramatically from what occurs in almost all other examined eukaryotes. The most striking feature is the cytoplasmic large subunit (LSU) rRNA, which in its mature form is fragmented into 14 discrete pieces, including the 5.8S rRNA (also called LSU1) (Schnare and Gray 1990). All 14 LSU fragment species along with the encoding sequence for the intact mature 19S rRNA of the small subunit (SSU) are encoded on an 11,056 base pair extrachromosomal DNA circle that is transcribed as a contiguous large RNA (read-around transcription) by RNA polymerase I (Greenwood et al. 2001; Schnare et al. 1990) . These rDNA circles number between 800 and 4000 copies per cell (Cook and Roxby 1985; Revel-Chapuis et al. 1985; Greenwood et al. 2001) and possess a single origin of DNA replication (Ravel-Chapuis 1988). The 19S, 5.8S (LSU1), and other 13 LSU rRNA fragments are separated by internal transcribed spacer (ITS) sequences ranging in size from 10 to 1188 base pairs in length, while LSU14 and the 19S SSU rRNA sequence are separated by an intergenic spacer (IGS) of 1743 base pairs (Greenwood et al. 2001). The spacer regions are removed post-transcriptionally producing a number of processing intermediates (Schnare et al. 1990; Greenwood and Gray 1998). Despite detection of these intermediate processing steps, very little is known about the mechanisms and components

responsible for processing and maturation of the initial single transcript into each final rRNA species. Even the nearly universally conserved rRNA processing RNase MRP complex still remains uncharacterized (or detected) in *Euglena* (López et al. 2009). Ribosome assembly in *E. gracilis* is almost certainly highly complex and likely requires a number of novel processing components. A better understanding of *E. gracilis* ribosome assembly may shed light on how evolutionary processes have shaped the development of such a fragmented ribosome structure and perhaps even reveal insights about steps in more canonical eukaryotic ribosome assembly pathways. The only RNA species of the cytoplasmic ribosome not found on the rDNA circle is the 5S rRNA (Schnare et al. 1990), which is instead typically genomically-encoded within 600 base pair long tandem repeats with spliced-leader (SL) RNAs, at an estimated copy number of 300 repeated units per haploid genome (Keller et al. 1992). Evidence also suggests single copy 5S and SL genes are present, however these appear to be less conserved.

8.3 *Euglena* snoRNAs and Their Expression

The *E. gracilis* rRNA has the largest number of modified nucleotide positions of any rRNA examined to date. The SSU and LSU rRNA subunits contain 88 and 262 identified modifications respectively (Schnare and Gray 2011). Therefore, there is a significant increase in the density of modifications in the fragmented large subunit (LSU) rRNA species in *E. gracilis* relative to the non-fragmented SSU rRNA suggesting that the additional modifications may have an important structural stabilizing role and/or function in the more complicated ribosome biogenesis pathway in this organism. The majority of these modifications are 2′-O-methylations (Nm) (209) and pseudouridines (Ψ) (119) contradicting the usual trend of multicellular organismal rRNA being more heavily modified than that of simpler organisms. In addition to having conserved modifications at many positions also modified in other eukaryotes, *E. gracilis* also appears to contain a large number of species-specific and euglenozoan-specific modifications (Schnare and Gray 2011; Eliaz et al. 2015).

In eukaryotes, the two most prevalent modifications in rRNA are isomerization of uridine to Ψ and 2′-O-methylation (Li et al. 2016; Sharma and Lafontaine 2015). Most of these modifications are targeted by small guide RNAs called small nucleolar (sno) RNAs. SnoRNAs targeting Nm sites are called C/D box snoRNAs while those that target sites of Ψ formation are called H/ACA box snoRNAs, with both classes defined by conserved sequence and structural features (Bratkovič and Rogelj 2014; Lui and Lowe 2013). Since *E. gracilis* has so many modifications, the initial prediction was that it would also require a large collection of snoRNAs to specify all these modified sites. Identification of *E. gracilis* snoRNAs through biochemical, genomic amplification (PCR) strategies and bioinformatic analysis has revealed that this is indeed the case (Moore and Russell 2012; Russell et al. 2004, 2006). Not only are there a large number of different snoRNA species but also a very large collection of sequence-related isoforms of each species, the full extent of which has yet to be determined.

Elucidation of the organization of snoRNA genes in *E. gracilis* has revealed that these genes are usually tandemly repeated in the genome with genes for the two classes of snoRNAs interspersed (Moore and Russell 2012). This organization pattern is similar to what has been observed in several trypanosome species and various plant species (Barneche et al. 2001; Brown et al. 2003; Liang et al. 2005). The modified sites in *E. gracilis* rRNA are not evenly dispersed along the lengths of the rRNAs, but rather typically clustered and sometimes densely clustered, such as a region in LSU species 6 where in a stretch of 22 nucleotides nearly half are Nm (2′-O-methylated) (Schnare and Gray 2011). This modification pattern is related to the organization of snoRNA genes. We have identified several instances where adjacent or nearby genes encode snoRNA species that target adjacent rRNA modification sites (Moore and Russell 2012). How did such a situation

arise? Many *Euglena* snoRNAs are encoded by tandemly repeated genes and when sequence divergence occurs in a paralogous gene copy that alters the guide region of a snoRNA, new base-pairing potential emerges to target a new modification site; that is, a new snoRNA species has been created. We have documented several cases where small insertion/deletions have occurred in nearby snoRNA gene copies that allows targeting of adjacent rRNA modification sites (Moore and Russell 2012). It seems that the apparent sequence repetitiveness in the *E. gracilis* genome, and the unexplained propensity to create gene copies, has been a driving factor in the creation of the large collection of snoRNA species and modification sites in this organism. However, what is not so clear is why this is selectively affecting modification of the various LSU rRNA species more than the SSU rRNA. Perhaps *E. gracilis* rapidly gains and then loses new snoRNA species through this genomic amplification mechanism but there is stronger selective pressure to retain snoRNAs targeting LSU fragment species as this is more beneficial for ribosome function in this organism. Also intriguing to consider is whether initially the fragmented nature of the *E. gracilis* rRNA necessitated a mechanism to rapidly create new snoRNA isoforms (snoRNAs targeting the same site) and species (those targeting different sites) or vice versa; fragmentation emerged as it could be tolerated in a cellular environment containing an unusually large number of snoRNAs with largely redundant functions.

Most of the *E. gracilis* snoRNA genes are expressed initially as polycistronic precursor transcripts of unknown lengths (we have detected transcripts upwards of 800 nts), containing several individual snoRNA sequences that are then processed into individual snoRNA species (Moore and Russell 2012). They are assembled with conserved core protein binding partners by an undefined processing and assembly mechanism in *Euglena*. Polycistronic transcripts containing both snoRNA classes have been detected. Transcription initiation and termination elements for expression of these genomic snoRNA clusters have yet to be determined; however, some of the spacer regions between mature snoRNA sequences display significant structural potential that may play a role in the expression mechanism (Moore and Russell, unpublished results). Not all *E. gracilis* snoRNAs are expressed polycistronically as the U3 snoRNA, a snoRNA that functions in pre-rRNA processing steps (i.e. specifying rRNA cleavage sites instead of targeting modification sites) appears to be expressed monocistronically (Greenwood et al. 1996; Charette and Gray 2009). Although the U3 snoRNA genes are multi-copy and frequently found associated with either U5 snRNA or tRNA genes, the U3 genes are in the opposite transcriptional orientation to the nearby U5 or tRNA genes (Charette and Gray 2009). Unlike U3, two other predicted *E. gracilis* processing snoRNAs, U14 and the Eg-h1 H/ACA-like RNA, are instead encoded by closely-spaced tandemly repeated genes like the modification-guide snoRNAs and are likely polycistronically expressed (Moore and Russell 2012). Therefore, there is no simple relationship between snoRNA function and expression mode in *E. gracilis*.

Currently, it is not definitively known which RNA polymerases are being used to express different snoRNA species in *E. gracilis.* In trypanosomatids and plants, U3 snoRNA genes are transcribed by RNA polymerase III (Fantoni et al. 1994; Kiss et al. 1991; Marshallsay et al. 1992), and the close linkage of some *E. gracilis* U3 genes with tRNAs suggests that at least these gene copies may be transcribed by this RNA polymerase. However, in trimethylguanosine cap pull-down RNA libraries we have found an abundance of *E. gracilis* U3 sequences consistent with these U3 species being transcribed by RNA polymerase II (Moore and Russell, unpublished results). Since not all *E. gracilis* U3 genes are linked with tRNA genes, it is possible that both RNA polymerases may be involved in U3 snoRNA expression depending on genomic context of individual U3 genes. The frequent expression of *E. gracilis* modification guide snoRNAs as polycistronic transcripts and relative transcript size is more consistent with RNA polymerase II transcriptional properties.

8.4 *Euglena* Chloroplast RNAs and Processing

Most recently, much of what has been deduced about *Euglena* choloroplast genome RNA-coding capacity has been through the determination of complete chloroplast genome structures from a collection of representative species from the Euglenaceae (Hrdá et al. 2012; Wiegert et al. 2012; Dabbagh and Preisfeld 2017; Bennett and Triemer 2015) and comparison to the much earlier determined choloroplast genome structure of *Euglena gracilis* Strain Z (Hallick et al. 1993). An examination of transcription patterns of the 96 genes contained on the *E. gracilis* plastid genome under different physiological states and stress conditions has also been performed (Geimer et al. 2009). Chloroplast RNA processing information has been derived primarily from Richard Hallick's group. They identified and then examined splicing patterns of a large collection of chloroplast introns and investigated expression modes for rRNA and tRNA, and the chloroplast RNA polymerase activities required for their expression. Identification of any other chloroplast non-coding RNAs, and protein or ribonucleoprotein complexes involved in chloroplast RNA maturation will require future biochemical studies and other types of analyses.

8.4.1 Chloroplast rRNA and tRNA

In the two examined strains of *E. gracilis*, chloroplast rRNA is encoded in operons approximately 6000 nt in length. The operon codes for 16S, 23S, and 5S rRNA genes separated by internal transcribed spacers some of which contain tRNA genes or pseudogenes, an overall arrangement similar to many bacterial rRNA operons. The operon structure is tandemly repeated three times, with a fourth partial repeat containing only a complete 16S rRNA sequence and additional open reading frame (ORF) found in Strain Z but was not confirmed in var. bacillaris (Hallick et al. 1993; Bennett and Triemer 2015). These operons make up 13.7% of the length of the genome.

There are a total of 27 tRNAs (not including the pseudogenes) found in Strain Z which are actively expressed (Hallick et al. 1993). An additional 9 pseudo-tRNAs which do not appear to be transcribed are found in regions within the rRNA operon repeats. The bacillaris strain possesses 31 actively transcribed tRNA genes, with only 4 pseudogenes (Bennett and Triemer 2015). trnI-trnA genes are co-transcribed with the rRNA operons and are the only chloroplast tRNAs that are multicopy. Most of the tRNA genes reside in clusters with short spacers, sometimes closely-linked with protein-coding genes.

There are at least two different RNA polymerase activities in *E. gracilis* chloroplasts that can be biochemically separated and are active when used in *in vitro* transcription assays (Greenberg et al. 1984). They display differences in enzymatic properties including salt concentration tolerance, optimum Mg^{2+} concentrations and temperature activity profiles. The RNA polymerase activity that remains tightly associated with chloroplast genomic DNA has been shown to selectively transcribe the rRNA operons (Greenberg et al. 1984). The soluble RNA polymerase activity transcribes most of the chloroplast tRNAs excluding those that are contained within the rRNA operons. Specificity of these RNA polymerase activities for transcribing the various protein-coding genes has not been extensively examined.

Polycistronic transcription and subsequent processing of these extended transcripts appears to be a prevalent mode of gene expression in *E. gracilis* chloroplasts for transcripts produced by either RNA polymerase activity (Christopher and Hallick 1990; Greenberg and Hallick 1986). Greenberg and Hallick were first able to isolate *E. gracilis* soluble chloroplast extracts that were capable of transcribing polycistronic transcripts containing multiple tRNA species that also accurately processed these primary transcripts to generate mature tRNA 5′ and 3′ termini (accurate CCA 3′ end addition was not verified in this study) (Greenberg and Hallick 1986). Either chloroplast DNA or cloned tRNA genes served as appropriate transcription and subsequent processing substrates

for the soluble extracts. Christopher and Hallick then demonstrated that polycistronic transcription also occurs for chloroplast ribosomal protein genes where one transcription unit was characterized that contains 11 rprotein genes, an isoleucine tRNA gene, and an ORF of unknown function (Christopher and Hallick 1990). This transcription unit is also predicted to contain at least 15 introns making it a large polycistronic transcription unit and complex gene expression pathway. It appears that the tRNA is processed and matured from this large transcript, as opposed to alternative individual transcription of the tRNA as a nested transcription unit, since the spacers flanking the mature sequence are short and do not appear to contain obvious promoter or termination elements. The authors noticed that the codon that would be deciphered by this particular isoleucine tRNA isoacceptor is enriched in mRNAs coding for constitutively expressed proteins (such as ribosomal proteins) relative to the codon's frequency in mRNAs for light-induced proteins. They speculate this may be the reason for this tRNA residing in this particular polycistronic unit. Through detection of RNA processing intermediates and products via nucleic acid hybridization experiments, it appears that RNA endonucleases are utilized for liberating individual RNA species from the polycistronic transcript and also for other transcription units containing tRNA species. A prediction would be the key involvement of the tRNA 5′ end maturation endonuclease RNase P in the various polycistronic transcript processing pathways.

8.4.2 Chloroplast Introns

An unusual feature of the *Euglena* chloroplast genome structure is the very large number of introns. Surveys of *Euglenaceae* chloroplast genome sequences have revealed a high degree of variability in intron content (Bennett and Triemer 2015; Pombert et al. 2012). The two sequenced *E. gracilis* chloroplast genomes possess the greatest number of introns in this taxa with the strain Z chloroplast containing 155 introns and var. bacillaris containing 134. This results in 66.7 and 68.3% of protein coding genes containing at least 1 intron in the two strains, respectively (Thompson et al. 1995; Bennett and Triemer 2015; Hallick et al. 1993). Curiously, despite this high intron content, none of the *Euglena* chloroplast tRNA genes contain introns. This differs markedly from what is found in green algae where over 50% of tRNA genes contain introns.

Chloroplast introns in *E. gracilis* include members of both group II (self-splicing) introns and a unique related class designated group III introns (Copertino and Hallick 1993). The *E. gracilis* group II introns contain most of the conserved features of this class of introns including structural domains I-VI (Fig. 8.1c), EBS-IBS pairings, and predicted ε-ε' and γ-γ'interactions (Copertino and Hallick 1993). These introns are however A-U rich (striking scarcity of G-C base-pairs in some cases) and show some structural "looseness" and variability relative to those introns found in more distantly related organisms. The group III introns appear to be degenerate or minimalized group II introns that contain only domain VI (predicted catalytic and branch point 'A' containing) and domain I; although even this later domain can be very minimalized in some predicted group III intron structures (Fig. 8.1c). Since *in vitro* splicing assays have not been performed with any of these *Euglena* introns, it is not known which of them are in fact self-splicing. It seems probable that the group III introns (at least) may have degenerated to the point where they are now completely dependent on *trans-acting* protein and/or RNA splicing factors for either or both of the two transesterification reactions, assuming they use such a splicing pathway.

Euglena chloroplast group II and group III introns can be found individually or as so-called twintrons: introns interrupting introns (Hallick et al. 1993; Bennett and Triemer 2015). Twintrons have been identified containing pairs of group II or group III introns, group II interrupting group III (and vice-versa), and even arrangements containing larger numbers of nested introns than just two. Hong and Hallick (1994) identified a case of a twintron arrangement in the *E. gracilis ycf8* gene where the outer intron can be a group II intron interrupted by two spaced group II introns;

that is, two introns each inserted at different locations within the outer intron or alternatively this outer intron can be classified as a group III intron interrupted by a group II intron. Alternative splicing dictates which combination of introns are removed and if the group II + III intron combination is removed, this pathway prevents removal of the outer group II intron by truncating several key structural regions.

The strict definition of a twintron, as defined for example by Hafez and Hausner (2015), is an embedded arrangement where the inner intron must be removed first to allow formation of the correct structure that catalyzes removal of the outer intron. In many of the *Euglena* twintron arrangements the insertion site of the inner intron is in domain V or VI of a group II intron, insertion positions that would be predicted to disrupt the tertiary structure required for outer intron removal in other well-studied group II introns. However, these *Euglena* group II introns already show some structural differences and flexibility relative to those studied in other organisms and together with the existence of the structurally minimalized group III introns, it may be premature to assume strict adherence to an ordered splicing pathway for all *Euglena* twintron arrangements. The frequency of twintrons in *Euglena* chloroplast genomes and the overall large number of introns suggests that intron mobility and insertion into new genomic sites is a relatively common occurrence in *E. gracilis* and more prevalent than is seen in other euglenids (Thompson et al. 1997; Pombert et al. 2012)—many of these introns appear to be unique to *E. gracilis.* Through recent determination of chloroplast intron structure and location in *Monomorphina aenigmatica*, a species occupying an intermediate branching position in euglenids, Pombert et al. (2012) have provided further evidence that group II/III intron abundance in *Euglena gracilis* appears to have resulted from more "recent" proliferation events, including the establishment of twintron arrangements (Hrdá et al. 2012; Wiegert et al. 2012). They found cases of intermediate stages of intron evolution in which *M. aenigmatica* contains a single group II intron (i.e. no twintron arrangement) inserted at the same gene position as the outer intron of a twintron arrangement in *Euglena gracilis*. The maintenance of twintron arrangements is the strongest argument so far for ordered splicing pathways; that is, insertion into a site that disrupts splicing of the outer intron requires first removing the inner intron to prevent gene function inactivation that would otherwise be the result of the insertion event.

It is curious that both the *E. gracilis* nuclear and chloroplast genomes are so intron-rich and also contain intron classes not known to exist outside of euglenids. We may then speculate about whether there is an evolutionary relationship between the non-conventional nuclear introns and the chloroplast group III introns, both of which maintain few conserved intron structural features for their respective splicing mechanisms. Were the non-canonical introns the end result of a large scale invasion event of the nuclear genome by group III mobility elements derived from an ancestral euglenid chloroplast? A detailed understanding of the splicing mechanisms and components involved for removal of these different intron types, and a large- scale analysis of introns in *E. gracilis* and other euglenids may reveal new insights into intron evolution in eukaryotes and the importance of these various intron classes in regulating gene expression in these organisms.

Perhaps the most surprising feature of gene expression in *E. gracilis* chloroplasts is the fact that there appears to be little differential variation in RNA species level when cells are examined at different stages of development and/or subject to various stress-inducing agents (Geimer et al. 2009) This is somewhat unexpected considering the complexity of processing required to remove the large number of introns in precursor chloroplast transcripts and the unusual adaptability of this organism in general to adjust to a wide range of environmental fluctuations. It was observed however that there can be significant changes to global chloroplast RNA levels under these various tested conditions. Such observations may indicate that if differential changes are occurring at the proteome level in *E. gracilis* chloroplasts, the regulation may be occurring at the translational control level.

8.5 Mitochondrial Genome Structure, Expression, and RNA Editing

RNA processing in Euglenozoan mitochondria has been shown to be both mechanistically unique and amazingly diverse compared to other eukaryotic phyla. The three major groups within Euglenozoa: euglenids, kinetoplastids, and diplonemids show a broad range in mitochondrial chromosome structure, gene expression strategy, and RNA processing mechanisms. Comparatively little is currently known about euglenid mitochondria; in particular, until recently virtually nothing was reported about *E. gracilis* mtDNA structure. It now appears that there are significant differences in *E. gracilis* compared to mitochondria in the other Euglenozoan taxa. An understanding of these other Euglenozoans may then provide evolutionary insight into mitochondrial features in this phylum. Further analysis of mitochondrial DNA and RNA features in *E. gracilis* itself and other euglenids will be indispensable in understanding RNA maturation and genome structure in these species. Here, we put current knowledge of *E. gracilis* mitochondrial chromosome structure, RNA expression and processing, in the broader context of Euglenozoans collectively.

Diplonemid mitochondrial DNA is arranged into two classes of small circular chromosomes of different sizes, Class A (6 kbp) and Class B (7 kbp) (Marande et al. 2005). mRNAs in diplonemid mitochondria are not expressed as single contiguous transcripts but rather as short fragments (known as modules) of several hundred nucleotides (Kiethega et al. 2011; Vlcek et al. 2010; Marande and Burger 2007). Each module is encoded by a different chromosome that carries only that gene. Following expression the module transcripts require processing through endonucleolytic cleavage, polyadenylation of the 3′ module, and *trans*-splicing in order to form mature full length transcripts (Kiethega et al. 2013). The mechanism through which this *trans*-splicing occurs is not yet understood, though it has been proposed that small guide RNAs may help in facilitating this process (Kiethega et al. 2013; Moreira et al. 2016). Additional editing of modules may also occur, including addition of short uridine stretches (1–3 nucleotides) to module ends, as well as both C-to-U and A-to-I editing (Moreira et al. 2016). In the second major Euglenozoan group, the kinetoplastids, mitochondrial DNA (termed kinetoplast or kDNA) is also arranged into two classes of circular chromosomes. In contrast to diplonemids, kinetoplast chromosomes differ quite significantly in size and are classified as either large (maxicircles) or small (minicircles) (Riou and Delain 1969; Kleisen et al. 1976; Steinert and Van Assell 1975). Maxicircle copy number varies between species, from 25 to 50 copies per cell in examined species, while thousands of minicircles can be present. Kinetoplastid maxicircle chromosomes primarily carry the mitochondrial protein-coding and rRNA genes (Eperon et al. 1983; Westenberger et al. 2006; Simpson et al. 1987). Minicircles code for small guide RNAs (gRNA) (Pollard et al. 1990; Corell et al. 1993; Jasmer and Stuart 1986a, b; Deschamps et al. 2011) which form ribonucleoprotein complexes called editosomes that act in a unique form of uridine insertion/deletion (U indel) editing of mRNA. This form of U indel editing has made gene identification difficult as the gene sequence may have little resemblance to the mature edited mRNA, and up to 553 insertion and 89 deletion sites have been characterized for a single transcript (Koslowsky et al. 1990).

The *Euglena gracilis* mitochondrial genome is also atypical but appears to be quite different from those of other Euglenozoans. Rather than circular chromosomes as seen in the diplomenids and kinetoplastids, *E. gracilis* possesses a collection of heterogeneous linear chromosomes ranging in size from a distribution peak at 4 kbp, up to 8 kbp (Spencer and Gray 2011; Dobáková et al. 2015). Only seven protein coding genes (*cox1*, *cox2*, *cox3*, *cob*, *nad1*, *nad4*, and *nad5*) have been identified in the genome (Dobáková et al. 2015; Tessier et al. 1997; Yasuhira and Simpson 1997). This is predicted to be the full complement of protein-coding genes in the mtDNA, with the remaining proteins likely encoded in the nuclear genome. Comparison of the gene

sequence and corresponding mRNA for these genes shows no evidence that editing or splicing is required for the formation of mature transcripts (Dobáková et al. 2015; Spencer and Gray 2011). This is quite surprising as unique and extensive mRNA editing appears to be a core feature of RNA maturation in the mitochondria of many other Euglenozoans. A second surprising feature of *E. gracilis* mtDNA is that in addition to full-length versions of mitochondrial genes, there are also many small mRNA and rRNA gene fragments scattered throughout the genome (Spencer and Gray 2011). These fragments retain high sequence identity to segments of the full length genes, in some cases even being perfect matches, but do not appear to be expressed. These small fragments and the presence of many short direct repeats have been proposed as possible evolutionary predecessors to the minicircle-encoded gRNAs of kinetoplastids, possibly produced through recombination between flanking repeats to produce "guide-like recombination products" (Spencer and Gray 2011). Transcription of the complementary strand of the gene fragments could then result in anti-sense RNAs capable of base-pairing to mRNAs, potentially allowing sequence drift in protein coding regions that could be corrected by RNA editing.

The mitochondrial genomes of two other euglenids, *Peranema trichophorum* and *Petalomonas cantuscygni* have been examined using electron microscopy (Roy et al. 2007). These results show that the *P. trichophorum* genome consists of many linear DNA molecules ranging from 1 to 75 kbp in size. In contrast, *P. cantuscygni* possesses linear 40 kbp molecules, with a small number of circular 40 kbp and much smaller 1–2.5 kbp molecules. More comprehensive examination of mitochondrial genome structure and content in other euglenids will indicate whether linear chromosomes are the predominant form and whether RNA editing is present in euglenids other than kinetoplastids.

The diversity found in structure and transcript processing in Euglenozoan mitochondria raises many questions about the evolutionary history that gave rise to these various states. Flegontov et al. have suggested that the genome of the Euglenozoans last common ancestor (ELCA) was likely circular and that the diversity found in this phylum may have arisen through constructive neutral evolution (Flegontov et al. 2011). It will be important to examine more representatives of all three major groups to determine the extent of possible genome types and novel mechanisms for RNA processing in these organelles.

8.5.1 Mitochondrial Ribosomal RNA

Ribosomal RNA structure and processing in Euglenozoan mitochondria is also highly variable. The mitochondrial SSU and LSU RNAs from *E. gracilis* have been identified and each appears to be expressed as two separate RNAs, termed SSU-R/SSU-L and LSU-R/LSU-L (Spencer and Gray 2011). Both SSU rRNA fragments have been sequenced and found to be chromosomally-unlinked independently transcribed genes, rather than products of cleavage of a single initial contiguous pre-SSU rRNA transcript. Extensive analysis failed to detect any full-length mature SSU RNAs providing strong evidence that these bipartite RNAs represent the mature fragmented functional form of this rRNA, not being further processed through a *trans*-splicing pathway to form a single contiguous SSU RNA. The 3′ end of SSU-R shows little heterogeneity. The SSU-L consists of three variants containing between 1 to 3 terminal A's at its 3′ end. Two LSU fragments have also been identified and found to have discrete 3′ ends; however, full length genomic encoding regions could not be located for either fragment. While it is likely that these represent the functional mitochondrial LSU RNAs, further analysis will have to be done to determine whether, like the SSU, each fragment is encoded individually and contiguously in the genome. Evidence has also been found that both the LSU and SSU contain modified nucleosides, including two tandem N^6,N^6-dimethyladenosines and an N^4-methylcytidine in the SSU and a Ψ in the LSU (Spencer and Gray 2011). Structural modeling has been performed for both the SSU and LSU fragments. The SSU fragments were found to form conserved long range base-pairing interactions

resulting in the formation of a secondary structure with similar features to the eubacterial 16S SSU rRNA. The first several hundred nucleotides of the 5′ end of the SSU show the greatest divergence in structure as a result of a high A + T content. LSU terminal regions also showed great similarity to the eubacterial 23S LSU RNA. In comparison, kinetoplast rRNA secondary structure has been found to be even more divergent from the eubacterial rRNA structure and in fact shows relatively little structural similarity to the *E. gracilis* rRNA.

Fragmented mt-rRNA has also been identified in the diplonemid *Diplonema papillatum*. Like *E. gracilis*, two LSU fragments (534 and 352 nt) are present, encoded on two Class B chromosomes (Valach et al. 2014). These RNAs are *trans*-spliced to produce a single LSU rRNA of approximately 900 nt and appear to go through other additional processing steps. The 3′ fragment contains a poly-A tail that is not present in the mature spliced transcript nor encoded in the gene sequence. The presence of this transient poly-A stretch raises questions about possible extended poly-A tail processing intermediates for the *E. gracilis* SSU-L, considering the observed variable 3′ ends (see above). In *Diplonema papillatum*, a 26 nucleotide poly-U stretch is found separating the 5′ and 3′ portions of the mature spliced LSU that is not encoded in the genes for either LSU fragment indicating that a process related to uridine insertion into mRNA modules can also occur to diplonemid rRNA. A short 366 nt RNA has been proposed as a potential mitochondrial SSU rRNA, but as of yet it is unclear if this represents the entire SSU rRNA or an individual fragment (Moreira et al. 2016). Small rRNAs are not unheard of in Euglenozoans. The kinetoplastid species *Trypanosoma brucei* (Sloof et al. 1985; Eperon et al. 1983), *Leishmania tarentolae* (de la Cruz et al. 1985a, b), and *Crithidia fasciculata* (Sloof et al. 1985) possess the smallest yet identified mitochondrial rRNAs, composed of a 9S SSU (approximately 611–640 nt) and 12S LSU (approximately 1141 and 1230 nt), each expressed as a contiguous transcript from a single gene. It will be important then to examine the SSU in *D. papillatum* and determine if other fragments are required or if the single SSU rRNA represents a potentially minimal rRNA.

In summary, while recent studies have begun to identify key features of the *E. gracilis* mitochondrial genome, our current knowledge about its structure and expression is still lagging somewhat behind what has been elucidated for other Euglenozoans. Continued efforts to characterize *Euglena* RNAs will be required to both further investigate the possibility of unique processing mechanisms and define the full complement of mtDNA encoded genes, including the LSU subunits.

8.6 Spliced-Leader RNA

Spliced-leader *trans*-splicing is a process through which a short RNA sequence (called the spliced-leader exon) is added to form the 5′ end of nuclear pre-mRNAs in a spliceosome-dependent manner. A small non-coding RNA termed the spliced-leader (SL) RNA acts as the donor of the short sequence. It is composed of two regions: the spliced-leader exon at its 5′ end followed by an extended sequence termed the spliced-leader intron (Fig. 8.2a), that is not included in the mature mRNA but is important for forming interactions with the target mRNA. SL RNAs fold into stem-loop secondary structures and contain an internal Sm-protein binding site, similar to what is observed in several of the small nuclear RNAs (snRNAs) of the spliceosome. The 5′ splice site required for the splicing reaction is part of the SL RNA, while the branch point adenosine, polypyrimidine tract and 3′ splice site are located at the 5′ end of the precursor mRNA collectively referred to as the "outron" (Fig. 8.2b, c). Together with the spliceosome components these elements form a substrate competent for splicing.

Spliced-leader *trans*-splicing was described in euglenids (Tessier et al. 1991) following initial discovery in trypanosomatids (Boothroyd and Cross 1982; Sutton and Boothroyd 1986; Milhausen et al. 1984) and nematodes (Krause and Hirsh 1987). Addition of the spliced-leader

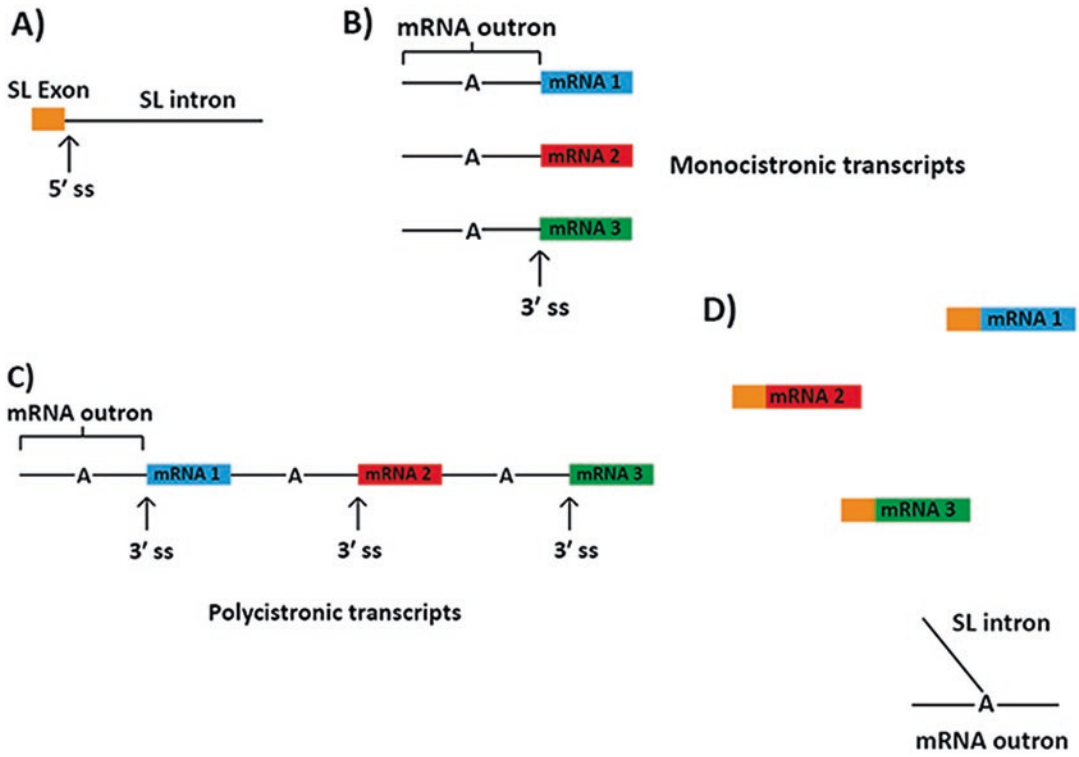

Fig. 8.2 (**a**) General structure of a spliced-leader RNA. Spliced leader *trans*-splicing can add the spliced-leader exon cap structure to (**b**) monocistronic transcripts or (**c**) to liberate individual protein-coding RNAs contained within a precursor polycistronic transcript. Both processing pathways result in (**d**) capped individual transcripts and removed Y shaped introns made up of the spliced-leader intron sequence attached to the mRNA outron. *ss* = splice site

serves a number of purposes in different groups of organisms. In both *C. elegans* (Spieth et al. 1993) and trypanosomes (Muhich and Boothroyd 1988), addition of the spliced-leader exon acts as a mechanism for processing and capping of individual mRNAs contained within long polycistronic precursor transcripts, as well as for capping monocistronic transcripts (Johnson et al. 1987; Zorio et al. 1994) (Fig. 8.2b–d). Analysis of the *E. gracilis* transcriptome has estimated that approximately 56% of pre-mRNA transcripts undergo spliced-leader exon sequence addition (Yoshida et al. 2016). Little is currently known about whether *Euglena* mRNAs are transcribed mono- or polycistronically and therefore the various roles of SL splicing in *Euglena* remains to be determined.

The *E. gracilis* genome encodes at least six variants of a spliced-leader RNA. Each isoform is approximately 101 nucleotides in length, the first 26 nucleotides of which is the SL exon sequence that is added to the pre-mRNA transcript (Tessier et al. 1991). The specific type of cap structure (and extent of modification) of the *Euglena* spliced-leader RNA is unknown. In most organisms in which spliced-leader *trans*-splicing occurs, the SL RNA possess a 2, 2, 7 trimethylguanosine (TMG) cap. Trypanosome SL exons possess a unique type of cap structure termed ‘cap 4’ containing extensive modifications; including 7-methyl guanosine, 2′-O-methylation of the first four nucleotides, additional base methylations at the first and fourth nucleotides, and a Ψ at position 28 (Zamudio et al. 2009). The relatively close phylogenetic relationship between trypanosomes and *E. gracilis* suggests that a number of these modifications may also be present in *Euglena.* Information on *Euglena* SL cap structure may be lacking in part because recent studies indicate that there are an additional two

nucleotides at the 5′ end of the SL RNA exon from what was previously reported (our unpublished results). This is critical as these would be the nucleotides containing most of modified nucleotide positions for these RNAs. These additional nucleotides also prompt further questions about how SL RNA is expressed in *E. gracilis* and whether initial processing of pre-SL RNA may occur prior to capping and splicing. We are learning an increasing amount about SL *trans*-splicing in *E. gracilis* but the exact role and structure of this RNA requires further elucidation.

8.7 RNase P

Efficient and accurate processing of pre-tRNA molecules from both nuclear and organellar genomes is crucial for the production of functional tRNA molecules. RNase P is a key endonucleolytic enzymatic complex responsible for the maturation of the 5′ ends of tRNAs. Found in all three domains of life, RNase P most commonly functions as a ribonucleoprotein complex containing a single RNA (RNase P RNA) which is the catalytic component (Guerrier-Takada et al. 1983; Pannucci et al. 1999; Thomas et al. 2000; Kikovska et al. 2006), and a variable number of proteins depending on the species. A small number of protein-only RNase Ps (PRORP) have also been identified, primarily confined to the organelles of eukaryotes (Holzmann et al. 2008; Gobert et al. 2010). Interestingly however, several members of the phylum Euglenozoa appear to only possess protein-only versions of RNase P. A single predicted PRORP protein has been identified in *Euglena mutabilis* and many trypanosome species possess nuclear (PRORP1) and mitochondrial (PRORP2) protein-only enzymes that have been shown to accurately process 5′ tRNA ends *in vitro* in the absence of any additional protein or RNA factors (Lechner et al. 2015; Taschner et al. 2012). To date, no RNase P has been reported for the plastid or nuclear genomes of *Euglena gracilis* (Lechner et al. 2015). However, when we performed a blastp search using *Trypanosoma brucei* PRORP proteins it revealed a putative PRORP protein in the *E. gracilis* proteome database published by O'Neill et al. (2015) that contains both PRORP and PPR motif repeat domains like those found in other protein- only RNase Ps (our unpublished results). Whether this PRORP-like protein in *E. gracilis* possesses tRNA processing activity and whether or not *E. gracilis* also possesses an RNA dependent RNase P activity will need to be examined. The distribution of the apparent utilization of PRORP enzymes in Euglenozoa suggests that dependence on RNase P RNA may have been lost early in the evolution of this phylum.

8.8 Conclusions and Future Directions

RNA transcript processing in *Euglena* displays remarkable diversity when compared to similar processes in distantly-related eukaryotes but also compared to its most closely-related studied relatives, the kinetoplastids and diplonemids. While some information is now available about processing of select classes of *Euglena* RNA in nuclei, mitochondria and chloroplasts, our knowledge is still limited due to a lack of characterization of RNA processing factors and an incomplete understanding of nuclear and mitochondrial genome structure. These will be key research areas to investigate in the future that should be aided by advances in proteomics and high-throughput nucleic acid sequencing technologies. Also important will be the isolation and characterization of classes of non-coding RNAs through RNA-Seq approaches that will give a more complete picture of the abundance and diversity of non-coding RNA types in different *Euglena* species. So far, key elucidated features are that polycistronic transcription is a common gene expression strategy for several classes of *Euglena* nuclear and chloroplast RNA (unknown for mitochondrial transcripts at this stage), that both cytoplasmic and mitochondrial rRNA is unusually structurally fragmented (extensively so for cytosolic LSU rRNA), that novel introns are prevalent in both organelle and nuclear genes, and that non-coding RNAs and their sequence isoforms are apparently very abundant in *Euglena* which

seems to be related to the repetitiveness of its nuclear genome structure. What roles might these unusual RNA structural features and transcript processing mechanisms have on the environmental adaptability of *Euglena*? Additional surprising features and mechanisms will likely be discovered when we continue our efforts to study this fascinating genus that may provide new insights into the evolution of RNA and protein-RNA complexes in all organisms.

References

Barneche F, Gaspin C, Guyot R, Echeverría M (2001) Identification of 66 box C/D snoRNAs in *Arabidopsis thaliana*: extensive gene duplications generated multiple isoforms predicting new ribosomal RNA 2′-O-methylation sites. J Mol Biol 311:57–73

Basu MK, Rogozin IB, Koonin EV (2008) Primordial spliceosomal introns were probably U2-type. Trends Genet 24:525–528

Bennett MS, Triemer RE (2015) Chloroplast genome evolution in the Euglenaceae. J Eukaryot Microbiol 62:773–785

Boothroyd JC, Cross GAM (1982) Transcripts coding for variant surface glycoproteins of *Trypanosoma brucei* have a short, identical exon at their 5′ end. Gene 20:281–289

Bratkovič T, Rogelj B (2014) The many faces of small nucleolar RNAs. Biochim Biophys Acta 1839: 438–443

Breckenridge DG, Wantanabe Y, Greenwood SJ, Gray MW, Schnare MN (1999) U1 small nuclear RNA and spliceosomal introns in *Euglena gracilis*. Proc Natl Acad Sci 96:852–856

Brown JWS, Echeverria M, Qu L (2003) Plant snoRNAs: functional evolution and new modes of gene expression. Trends Plant Sci 8:42–49

Burge CB, Padgett RA, Sharp PA (1998) Evolutionary fates and origins of U12-type introns. Mol Cell 2:773–785

Canaday J, Tessier LH, Imbault P, Paulus F (2001) Analysis of *Euglena gracilis alpha-, beta-* and *gamma*-tubulin genes: introns and pre-mRNA maturation. Mol Gen Genomics 265:153–160

Charette JM, Gray MW (2009) U3 snoRNA genes are multi-copy and frequently linked to U5 snRNA genes in *Euglena gracilis*. BMC Genomics 10:528–546

Christopher DA, Hallick RB (1990) Complex RNA maturation pathway for a chloroplast ribosomal protein operon with an internal tRNA Cistron. Plant Cell 2:659–671

Cook JR, Roxby R (1985) Physical properties of a plasmid-like DNA from *Euglena gracilis*. Biochim Biophys Acta 824:80–83

Copertino DW, Hallick RB (1993) Group II and group III introns of twintrons: potential relationships with nuclear pre-mRNA introns. Trends Biochem Sci 18:467–471

Corell RA, Feagin JE, Riley GR, Strickland T, Guderian JA, Myler PJ, Stuart K (1993) *Trypanosoma brucei* minicircles enode multiple guide RNAs which can direct editing of extensively overlapping sequences. Nucleic Acids Res 21:4313–4320

Dabbagh N, Preisfeld A (2017) The chloroplast genome of *Euglena mutabilis*—cluster arrangement, intron analysis, and Intrageneric trends. J Eukaryot Microbiol 64(1):31–44

de la Cruz VF, Lake JA, Simpson AM, Simpson L (1985a) A minimal ribosomal RNA: sequence and secondary structure of the 9S kinetoplast ribosomal RNA from *Leishmania tarentolae*. Proc Natl Acad Sci 82: 1401–1405

de la Cruz VF, Simpson AM, Lake JA, Simpson L (1985b) Primary sequence and partial secondary structure of the 12S kinetoplast (mitochondrial) ribosomal RNA from *Leishmania tarentolae*: conservation of peptidyltransferase structural elements. Nucleic Acids Res 13:2337–2356

Deschamps P, Lara E, Marande W, López-García P, Ekelund F, Moreira D (2011) Phylogenomic analysis of kinetoplastids supports that trypanosomatids arose from within Bodonids. Mol Biol Evol 28:53–58

Dobáková E, Flegontov P, Skalický T, Lukeš J (2015) Unexpectedly streamlined mitochondrial genome of the euglenozoan *Euglena gracilis*. Genome Biol Evol 7:3358–3367

Eliaz D, Doniger T, Tkacz ID, Biswas VK, Gupta S, Kolev NG, Unger R, Ullu E, Tschudi C, Michaeli S (2015) Genome-wide analysis of small nucleolar RNAs of Leishmania major reveals a rich repertoire of RNAs involved in modification and processing of rRNA. RNA Biol 12:1222–1255

Eperon IC, Janssen JWG, Hoeijmakers JHJ, Borst P (1983) The major transcripts of the kinetoplast DNA of *Trypanosoma brucei* are very small ribosomal RNAs. Nucleic Acids Res 11:105–125

Fantoni A, Dare AO, Tschudi C (1994) RNA polymerase III-mediated transcription of the trypanosome U2 small nuclear RNA Gene is controlled by both intragenic and Extragenic regulatory elements. Mol Cell Biol 14:2021–2028

Ferreira VS, Rocchetta I, Conforti V, Bench S, Feldman R, Levin MJ (2007) Gene expression patterns in *Euglena gracilis*: insights into the cellular response to environmental stress. Gene 389:136–145

Flegontov P, Gray MW, Burger G, Lukeš J (2011) Gene fragmentations: a key to mitochondrial genome evolution in Euglenozoa? Curr Genet 57:225–232

Geimer S, Belicová A, Legen J, Sláviková S, Herrmann RG, Krajčovič J (2009) Transcriptome analysis of the *Euglena gracilis* plastid chromosome. Curr Genet 55:425–438

Gobert A, Gutmann B, Taschner A, Gößringer M, Holzmann J, Hartmann RK, Rossmanith W, Giegé P

(2010) A single *Arabidopsis* organellar protein has RNase P activity. Nat Struct Mol Biol 17:740–744
Greenberg BM, Hallick RB (1986) Accurate transcription and processing of 19 *Euglena* chloroplast tRNAs in a *Euglena* soluble extract. Plant Mol Biol 6:89–100
Greenberg BM, Narita JO, Deluca-Flaherty C, Gruissem W, Rushlow KA, Hallick RB (1984) Evidence for two RNA polymerase activities in *Euglena gracilis* chloroplasts. J Biol Chem 259:14880–14887
Greenwood SJ, Gray MW (1998) Processing of precursor rRNA in *Euglena gracilis*: identification of intermediates in the pathway to a highly fragmented large subunit rRNA. Biochim Biophys Acta 1443:128–138
Greenwood SJ, Schnare MN, Cook JR, Gray MW (2001) Analysis of intergenic spacer transcripts suggests 'read-around' transcription of the extrachromosomal circular rDNA in *Euglena gracilis*. Nucleic Acids Res 29:2191–2198
Greenwood SJ, Schnare MN, Gray MW (1996) Molecular characterization of U3 small nucleolar RNA from the early diverging protist, *Euglena gracilis*. Curr Genet 30:338–346
Guerrier-Takada C, Gardiner K, Marsh T, Pace N, Altman S (1983) The RNA moiety of Ribonuclease P is the catalytic subunit of the enzyme. Cell 35:849–857
Hafez M, Hausner G (2015) Convergent evolution of twintron-like configurations: one is never enough. RNA Biol 12:1275–1288
Hallick RB, Hong L, Drager RG, Favreau MR, Monfort A, Orsat B, Spielmann A, Stutz E (1993) Complete sequence of *Euglena gracilis* chloroplast DNA. Nucleic Acids Res 21:3537–3544
Holzmann J, Frank P, Löffler E, Bennett KL, Gemer C, Rossmanith W (2008) RNase P without RNA: identification and functional reconstitution of the human mitochondrial tRNA processing enzyme. Cell 135:462–474
Hong L, Hallick RB (1994) A group III intron is formed from domains of two individual group II introns. Genes Dev 8:1589–1599
Hrdá Š, Fousek J, Szabova J, Hampl VV, Vlček Č (2012) The plastid genome of *Eutreptiella* provides a window into the process of secondary endosymbiosis of plastid in euglenids. PLoS One 7:1–10
Jasmer DP, Stuart K (1986a) Conservation of kinetoplastid minicircle characteristics without nucleotide sequence conservation. Mol Biochem Parasitol 18: 257–269
Jasmer DP, Stuart K (1986b) Sequence Organization in African Trypanosome Minicircles is defined by 18 base pair inverted repeats. Mol Biochem Parasitol 18:321–331
Johnson PJ, Kooter JM, Borst P (1987) Inactivation of transcription by UV irradiation of *T. brucei* provides evidence for a multicistronic transcription unit including a VSG Gene. Cell 51:273–381
Keller M, Tessier LH, Chan RL, Weil JH, Imbault P (1992) In *Euglena*, spliced-leader RNA (SL-RNA) and 5S rRNA genes are tandemly repeated. Nucleic Acids Res 20:1711–1715
Kiethega GN, Turcotte M, Burger G (2011) Evolutionarily conserved cox1 trans-splicing without cis-motifs. Mol Biol Evol 28:2425–2428
Kiethega GN, Yan Y, Turcotte M, Burger G (2013) RNA-level unscrambling of fragmented genes in *Diplonema* mitochondria. RNA Biol 10:301–313
Kikovska E, Svärd SG, Kirsebom LA (2006) Eukaryotic RNase P RNA mediates cleavage in the absence of protein. Proc Natl Acad Sci 104:2062–2067
Kiss T, Marshallsay C, Filipowicz W (1991) Alteration of the RNA polymerase specificity of U3 snRNA genes during evolution and in vitro. Cell 65:517–526
Kleisen CM, Weislogel PO, Fonck K, Borst P (1976) The structure of kinetoplast DNA 2. Characterization of a novel component of high complexity present in the kinetoplast DNA network of *Crithidia luciliae*. Eur J Biochem 64:153–160
Koslowsky DJ, Bhat GJ, Perrollaz AL, Feagin JE, Stuart K (1990) The MURF3 Gene of *T. brucei* contains multiple domains of extensive editing and is homologous to a subunit of NADH dehydrogenase. Cell 62:901–911
Krause M, Hirsh D (1987) A trans-spliced leader sequence on actin mRNA in *C. elegans*. Cell 49:753–761
Lechner M, Rossmanith W, Hartmann RK, Thölken C, Gutmann B, Giegé P, Gobert A (2015) Distribution of Ribonucleoprotein and Protein-only RNase P in Eukarya. Mol Biol Evol 32:3189–3193
Li X, Ma S, Yi C (2016) Pseudouridine: the fifth RNA nucleotide with renewed interests. Curr Opin Chem Biol 33:108–116
Liang XH, Uliel S, Hury A, Barth S, Doniger T, Unger R, Michaeli S (2005) A genome-wide analysis of C/D and H/ACA-like small nucleolar RNAs in *Trypanosoma brucei* reveals a trypanosome-specific pattern of rRNA modification. RNA 11:619–645
López MD, Rosenblad MA, Samuelsson T (2009) Conserved and variable domains of RNase MRP RNA. RNA Biol 6:208–221
Lui L, Lowe T (2013) Small nucleolar RNAs and RNA-guided post-transcriptional modification. Essays Biochem 54:53–77
Marande W, Burger G (2007) Mitochondrial DNA as a genomic jigsaw puzzle. Science 318:415
Marande W, Lukeš J, Burger G (2005) Unique mitochondrial genome structure in diplonemids, the sister Group of Kinetoplastids. Eukaryot Cell 4:1137–1146
Marshallsay C, Connelly S, Filipowicz W (1992) Characterization of the U3 and U6 snRNA genes from wheat: U3 snRNA genes in monocot plants are transcribed by RNA polymerase III. Plant Mol Biol 19:973–983
Milanowski R, Gumińska N, Karnkowska A, Ishikawa T, Zakryś B (2016) Intermediate introns in nuclear genes of euglenids—are they a distinct type? BMC Evol Biol 16:1–11
Milanowski R, Karnkowska A, Ishikawa T, Zakryś B (2014) Distribution of conventional and nonconventional introns in tubulin (α and β) genes of euglenids. Mol Biol Evol 31:584–593

Milhausen M, Nelson RG, Sather S, Selkirk M, Agabian N (1984) Identification of a small RNA containing the trypanosome spliced leader: a donor of shared 5′ sequences of Trypanosomatid mRNAs? Cell 38: 721–729

Moore AN, Russell AG (2012) Clustered organization, polycistronic transcription, and evolution of modification-guide snoRNA genes in *Euglena gracilis*. Mol Gen Genomics 287:55–66

Moreira S, Valach M, Aoulad-Aissa M, Otto C, Burger G (2016) Novel modes of RNA editing in mitochondria. Nucleic Acids Res 44:4907–4919

Muchhal US, Schwartzbach SD (1992) Characterization of a *Euglena* gene encoding a polyprotein precursor to the light-harvesting chlorophyll *a/b*-binding protein of photosystem II. Plant Mol Biol 18:287–299

Muchhal US, Schwartzbach SD (1994) Characterization of the unique intron—exon junctions of *Euglena* gene(s) encoding the polyprotein precursor to the light-haresting chlorophyll a/b binding protein of photosystem II. Nucleic Acids Res 22:5737–5744

Muhich ML, Boothroyd JC (1988) Polycistronic transcripts in trypanosomes and their accumulation during heat shock: evidence for a precursor role in mRNA synthesis. Mol Cell Biol 8:3837–3846

O'Neill EC, Trick MH, Lionel RM, Dusi RG, Hamilton CJ, Zimba PV, Henrissat B, Field RA (2015) The transcriptome of *Euglena gracilis* reveals unexpected metabolic capabilities for carbohydrate and natural product biochemistry. Mol BioSyst 11:2808–2820

Pannucci JA, Haas ES, Hall TA, Harris JK, Brown JW (1999) RNase P RNAs from some Archaea are catalytically active. Proc Natl Acad Sci 96:7803–7808

Pollard VW, Rohrer SP, Michelotti EF, Hancock K, Hajduk SL (1990) Organization of Minicircle Genes for guide RNAs in Trypanosoma brucei. Cell 63: 783–790

Pombert J-F, James ER, Janouškovec J, Keeling PJ (2012) Evidence for transitional stages in the evolution of euglenid group II introns and twintrons in the *Monomorphina aenigmatica* plastid genome. PLoS One 7:1–8

Ravel-Chapuis P (1988) Nuclear rDNA in *Euglena gracilis*: paucity of chromosomal units and replication of extrachromosomal units. Nucleic Acids Res 16: 4801–4810

Revel-Chapuis P, Nicolas P, Nigon V, Neyret O, Freyssinet G (1985) Extrachromosomal circular nuclear rDNA in *Euglena gracilis*. Nucleic Acids Res 13:7529–7537

Riou G, Delain E (1969) Electron microscopy of the circular Kinetoplastic DNA from Trypanosoma cruzi: occurrence of catenated forms. Proc Natl Acad Sci 62:210–217

Roy J, Faktorová D, Lukeš J, Burger G (2007) Unusual mitochondrial genome structures throughout the Euglenozoa. Protist 158:385–396

Russell AG, Schnare MN, Gray MW (2004) Pseudouridine-guide RNAs and other Cbf5p-associated RNAs in *Euglena gracilis*. RNA 10:1034–1046

Russell AG, Schnare MN, Gray MW (2006) A large collection of compact box C/D snoRNAs and their isoforms in *Euglena gracilis*: structural functional and evolutionary insights. J Mol Biol 357:1545–1565

Russell AG, Wantanabe Y, Charette JM, Gray MW (2005) Unusual features of fibrillarin cDNA and gene structure in *Euglena gracilis*: evolutionary conservation of core proteins and structural predictions for methylation-guide box C/D snoRNPs throughout the domain Eucarya. Nucleic Acids Res 33:2781–2791

Schnare MN, Cook JR, Gray MW (1990) Fourteen internal transcribed spacers in the circular ribosomal DNA of *Euglena gracilis*. J Mol Biol 215:85–91

Schnare MN, Gray MW (1990) Sixteen discrete RNA components in the cytoplasmic ribosome of *Euglena gracilis*. J Mol Biol 215:73–83

Schnare MN, Gray MW (2011) Complete modification maps for the cytosolic small and large subunit rRNAs of *Euglena gracilis*: functional and evolutionary implications of contrasting patterns between the two rRNA components. J Mol Biol 413:66–83

Sharma S, Lafontaine DLJ (2015) 'View from a bridge': a new perspective on eukaryotic rRNA base modification. Trends Biochem Sci 40:560–575

Simpson L, Neckelmann N, de la Cruz VF, Simpson AM, Feagin JE, Jasmer DP, Stuart K (1987) Comparison of the maxicircle (mitochondrial) genomes of *Leishmania tarentolae* and *Trypanosoma brucei* at the level of nucleotide sequence. J Biol Chem 262:6182–6196

Sloof P, Van den Burg J, Voogd A, Benne R, Agostinelli M, Borst P, Gutell R, Noller H (1985) Further characterization of the extremely small mitochondrial ribosomal RNAs from trypanosomes: a detailed comparison of the 9S and 12S RNAs from *Crithidia fasciculata* and *Trypanosoma brucei* with rRNAs from other organisms. Nucleic Acids Res 13:4171–4190

Spencer DF, Gray MW (2011) Ribosomal RNA genes in *Euglena gracilis* mitochondrial DNA: fragmented genes in a seemingly fragmented genome. Mol Gen Genomics 285:19–31

Spieth J, Brooke G, Kuersten S, Lea K, Blumenthal T (1993) Operons in *C. elegans*: polycistronic mRNA precursors are processed by trans-splicing of SL2 to downstream coding regions. Cell 73:521–532

Steinert M, Van Assell S (1975) Large circular mitochondrial DNA in *Crithidia luciliae*. Exp Cell Res 96: 406–409

Sutton RE, Boothroyd JC (1986) Evidence for trans splicing in trypanosomes. Cell 47:527–535

Taschner A, Weber C, Buzet A, Hartmann RK, Hartig A, Rossmanith W (2012) Nuclear RNase P of *Trypanosoma brucei*: a single protein in place of the multicomponent RNA-protein complex. Cell Rep 2:19–25

Tessier LH, Keller M, Chan RL, Fournier R, Weil JH, Imbault P (1991) Short leader sequences may be transferred from small RNAs to pre-mature mRNAs by trans-splicing in *Euglena*. EMBO J 10:2621–2625

Tessier LH, van der Speck H, Gualberto JM, Grienenberger JM (1997) The cox1 gene from *Euglena gracilis*: a

protist mitochondrial gene without introns and genetic code modifications. Curr Genet 31:208–213

Thomas BC, Chamberlain J, Engelke DR, Gegenheimer P (2000) Evidence for an RNA-based catalytic mechanism in eukaryotic nuclear ribonuclease P. RNA 6:554–562

Thompson MD, Copertino DW, Thompson E, Favreau MR, Hallick RB (1995) Evidence for the late origin of introns in chloroplast genes from an evolutionary analysis of the genus *Euglena*. Nucleic Acids Res 23:4745–4752

Thompson MD, Zhang L, Hong L, Hallick RB (1997) Two new group-II twintrons in the *Euglena gracilis* chloroplast are absent in basally branching *Euglena* species. Curr Genet 31:89–95

Valach M, Moreira S, Kiethega GN, Burger G (2014) Trans-splicing and RNA editing of LSU rRNA in *Diplonema* mitochondria. Nucleic Acids Res 42: 2660–2672

Vlcek C, Marande W, Teijeiro S, Lukeš J, Burger G (2010) Systematically fragmented genes in a multipartite mitochondrial genome. Nucleic Acids Res 39:979–988

Westenberger SJ, Cerqueira GC, El-Sayed NM, Zingales B, Campbell DA, Sturm NR (2006) Trypanosoma cruzi mitochondrial maxicircles display species- and strain-specific variation and a conserved element in the non-coding region. BMC Genomics 7:1–18

Wiegert KE, Bennett MS, Triemer RE (2012) Evolution of the chloroplast genome in photosynthetic Euglenoids: a comparison of *Eutreptia viridis* and *Euglena gracilis* (Euglenophyta). Protist 163: 832–843

Yasuhira S, Simpson L (1997) Phylogenetic affinity of mitochondria of *Euglena gracilis* and kinetoplastids using cytochrome oxidase I and hsp60. J Mol Evol 44:341–347

Yoshida Y, Tomiyama T, Maruta T, Tomita M, Ishikawa T, Arakawa K (2016) *De novo* assembly and comparative transcriptome analysis of *Euglena gracilis* in response to anaerobic conditions. BMC Genomics 17:1–10

Zamudio JR, Mittra B, Chattopadhyay A, Wohlschlegel JA, Sturm NR, Campbell DA (2009) *Trypanosoma brucei* spliced leader RNA maturation by the cap 1 2′-*O*-ribose Methyltransferase and SLA1 H/ACA snoRNA Pseudouridine synthase complex. Mol Cell Biol 29:1202–1211

Zorio DAR, Cheng NN, Blumenthal T, Spieth J (1994) Operons as a common form of chromosomal organization in *C. elegans*. Nature 372:270–272

Photo and Nutritional Regulation of *Euglena* Organelle Development

9

Steven D. Schwartzbach

Abstract

Euglena can use light and CO_2, photosynthesis, as well as a large variety of organic molecules as the sole source of carbon and energy for growth. Light induces the enzymes, in this case an entire organelle, the chloroplast, that is required to use CO_2 as the sole source of carbon and energy for growth. Ethanol, but not malate, inhibits the photoinduction of chloroplast enzymes and induces the synthesis of the glyoxylate cycle enzymes that comprise the unique metabolic pathway leading to two carbon, ethanol and acetate, assimilation. In resting, carbon starved cells, light mobilizes the degradation of the storage carbohydrate paramylum and transiently induces the mitochondrial proteins required for the aerobic metabolism of paramylum to provide the carbon and energy required for chloroplast development. Other mitochondrial proteins are degraded upon light exposure providing the amino acids required for the synthesis of light induced proteins. Changes in protein levels are due to increased and decreased rates of synthesis rather than changes in degradation rates. Changes in protein synthesis rates occur in the absence of a concomitant increase in the levels of mRNAs encoding these proteins indicative of photo and metabolic control at the translational rather than the transcriptional level. The fraction of mRNA encoding a light induced protein such as the light harvesting chlorophyll a/b binding protein of photosystem II, (LHCPII) associated with polysomes in the dark is similar to the fraction associated with polysomes in the light indicative of photoregulation at the level of translational elongation. Ethanol, a carbon source whose assimilation requires carbon source specific enzymes, the glyoxylate cycle enzymes, represses

S.D. Schwartzbach (✉)
Department of Biological Sciences,
University of Memphis, Memphis, TN 38152, USA
e-mail: sdschwrt@memphis.edu

S.D. Schwartzbach, S. Shigeoka (eds.), *Euglena: Biochemistry, Cell and Molecular Biology*,
Advances in Experimental Medicine and Biology 979, DOI 10.1007/978-3-319-54910-1_9

the synthesis of chloroplast enzymes uniquely required to use light and CO_2 as the sole source of carbon and energy for growth. The catabolite sensitivity of chloroplast development provides a mechanism to prioritize carbon source utilization. *Euglena* uses all of its resources to develop the metabolic capacity to utilize carbon sources such as ethanol which are rarely in the environment and delays until the rare carbon source is no longer available forming the chloroplast which is required to utilize the ubiquitous carbon source, light and CO_2.

Keywords

Chloroplast • Catabolite repression • Enzyme induction • *Euglena* • Glyoxylate cycle • Mitochondria • Organelle development • Photoregulation • Translational control

Abbreviations

2-D gel	Two dimensional gel electrophoresis
ALA	δ-Aminolevulinic acid
DCMU	(3-(3,4-Dichlorophenyl)-1,1-dimethylurea)
LHCPI	Light harvesting chlorophyll a/b binding protein of photosystem I
LHCPII	Light harvesting chlorophyll a/b binding protein of photosystem II
PBG	Porphobilinogen
pLHCPII	Precursor to LHCPII
RUBISCO	Ribulose bisphosphate carboxylase-oxygenase

9.1 Introduction

Euglena is a unicellular organism which can utilize a wide variety of organic compounds as the sole source of carbon and energy for growth (Kemper 1982). A common core of metabolic enzymes such as the TCA cycle enzymes and glycolytic enzymes are found in all cells regardless of the organic compound being used. Utilization of other compounds requires enzymes comprising carbon source specific metabolic pathways. Upon switching the carbon source utilized for growth, synthesis of the enzymes required specifically to metabolize the new carbon source are induced; their rate of synthesis and steady- state level is significantly increased when the compound they metabolize is present in the environment. Synthesis of the enzymes required specifically to metabolize the old carbon source are repressed; their rate of synthesis and steady-state level is significantly decreased when the compound they metabolize is not present in the environment.

Light allows CO_2 to be used as the sole source of carbon and energy for growth. The chloroplast is a specific organelle required for growth using light. In the dark, the *Euglena* chloroplast is gratuitous for growth as evidenced by the ease with which bleached mutants which have lost most if not all of their plastid genome are obtained (Heizmann et al. 1976, 1981, 1982; Hussein et al. 1982; Osafune and Schiff 1983; Schiff et al. 1971, 1980). *Euglena* grown on an organic carbon source in the dark has a poorly developed chloroplast, the proplastid, which upon light exposure is converted into a photosynthetically competent chloroplast (Stern et al. 1964a, b). Chloroplast development can thus be viewed as the induction by a carbon source, light which allows CO_2 to be used as the sole source of carbon and energy for growth, of the metabolic pathway, in this case the organelle, required to utilize that carbon source.

Mitochondria are the site of aerobic energy production. In photosynthetic organisms, both mitochondrial and chloroplast metabolism

produce energy during the day, in the light, while mitochondrial metabolism is the sole source of energy production at night in the dark. The light dependent development of the *Euglena* proplastid into a functional chloroplast requires carbon and energy. The initial stages of light induced plastid development are thus entirely dependent upon cellular mitochondrial energy production while mitochondrial metabolism becomes less important once the chloroplast develops to a point where photophosphorylation can make a major contribution to fulfilling cellular energy requirements. Light dependent changes in mitochondrial activity can thus be viewed as responses to changes in the carbon and energy source available to the cell.

The synthesis of the two carbon compound phosphoglycolate appears to be an unavoidable consequence of the competition between CO_2 and O_2 for the active site of ribulose bisphosphate carboxylase-oxygenase (RUBISCO) (Ogren 1984). Photorespiration is the metabolic pathway that converts phosphoglycolate to phosphoglycerate and the glyoxylate cycle is the pathway that is used for assimilation of the two carbon compounds ethanol and acetate. In most organisms, these pathways are found in specialized microbodies, the peroxisome and the glyoxysome. A number of studies suggest that *Euglena* does not contain microbodies and that the photorespiratory and glyoxylate enzymes normally found in microbodies are in mitochondria (see Chap. 3 (Collins and Merrett 1975a; Fayyaz-Chaudhary and Merrett 1984; Ono et al. 2003; Yokota et al. 1985a, b; Yokota and Kitaoka 1981; Yokota et al. 1978) Regardless of whether the enzymes are localized in mitochondria or microbodies, some of the photorespiratory enzymes are only required in the light while some of the glyoxylate cycle enzymes are only required in the presence of acetate or ethanol. The photocontrol of the synthesis of chloroplast and mitochondrial photorespiratory enzymes must be viewed within the context of the synthesis of mitochondrial enzymes required for two carbon metabolism. The purpose of this review is to summarize our understanding of the control of *Euglena* organelle biogenesis in response to the available carbon and energy source.

9.2 Photocontrol of Chloroplast Development

Dark grown *Euglena* contain approximately ten small proplastids lacking internal membranes and containing several prolamellar bodies (Klein et al. 1972; Osafune et al. 1980). The synthesis rate of nuclear and chloroplast encoded plastid proteins is low. The major plastid related metabolic activities are those required for plastid DNA replication and division to ensure the genetic continuity of the plastid. Light grown *Euglena* contain approximately ten chloroplasts with an extensive thylakoid network (Klein et al. 1972). The chloroplasts are photosynthetically competent (Stern et al. 1964b) containing all of the pigments and proteins needed for CO_2 fixation. Chloroplast division is coincident with nuclear division requiring a high level of pigment and protein synthesis to maintain photosynthetic competence in the newly divided chloroplasts.

The synthesis of chloroplast nucleic acids, nucleic acid metabolizing enzymes and components of the chloroplast protein synthetic machinery are light regulated. The amount of chloroplast DNA per cell (Chelm et al. 1977a; Hussein et al. 1982; Rawson and Boerma 1976a; Srinivas and Lyman 1980) increases two to threefold after exposure of dark grown *Euglena* to light. Alkaline DNAse, a nuclear encoded cytoplasmically synthesized enzyme that hydrolyzes both single stranded DNA and RNA (Egan and Carell 1972; Egan et al. 1975; Small and Sturgen 1976) is induced by light. Synthesis ceases upon return to the dark indicating a light dependent process (Egan and Carell 1972; Egan et al. 1975). Photoreactivating enzyme is a nuclear encoded cytoplasmically synthesized enzyme that removes UV induced thymine dimers from chloroplast DNA in a light dependent reaction (Diamond et al. 1975). Photoreactivating enzyme is induced upon light exposure (Diamond et al. 1975) but synthesis continues when cells are returned to the dark indicating that induction is a light triggered process.

Chloroplast encoded proteins are synthesized within the chloroplast using chloroplast ribosomes (Schwartzbach et al. 1974) tRNAs, (Goins et al. 1973; Hallick et al. 1984; Reger et al. 1970;

Schwartzbach et al. 1976a) and tRNA synthetases (Barnett et al. 1976; Hecker et al. 1974; Parthier et al. 1972; Reger et al. 1970). Proplastids in dark grown cells have low levels of chloroplast rRNA (Chelm et al. 1977b, 1978, 1979; Cohen and Schiff 1976; Geimer et al. 2009; Rawson et al. 1981) and tRNA (Goins et al. 1973; Reger et al. 1970; Schwartzbach et al. 1976a). The cellular content of chloroplast rRNA and chloroplast tRNA increases from approximately 5–25% of the cellular rRNA and tRNA content after 72 h of light exposure (Chelm et al. 1977b, 1978, 1979; Cohen and Schiff 1976; Rawson et al. 1981; Schwartzbach et al. 1976a). Transcriptome analysis suggests that the *Euglena* chloroplast genome is constitutively and not differentially expressed in the dark with light exposure increasing the transcription rate of all chloroplast genes proportionately (Geimer et al. 2009).

Electrophoretic analysis has shown a light induced increase in the rate of cytoplasmically and chloroplast synthesized ribosomal proteins (Freyssinet 1977, 1978). Light induced increases in the specific activity of the nuclear encoded chloroplast initiation factors IF1, IF2, IF3, (Gold and Spremulli 1985; Kraus and Spremulli 1986, 1988), the nuclear encoded chloroplast elongation factors EF-Ts, EF-G (Breitenberger et al. 1979; Eberly et al. 1986; Fox et al. 1980) and the chloroplast encoded chloroplast elongation factor EF-Tu (Eberly et al. 1986; Montandon and Stutz 1983; Passavant et al. 1983; Spremulli 1982) have also been reported. The synthesis of the nuclear encoded chloroplast localized aminoacyl-tRNA synthetases (Hecker et al. 1974; Krauspe et al. 1987; McCarthy et al. 1982; Nover 1976; Parthier and Krauspe 1974; Parthier et al. 1972; Reger et al. 1970; Schimpf et al. 1982) is induced by light exposure. The synthesis of chloroplast rRNA (Cohen and Schiff 1976) and chloroplast aminoacyl-tRNA synthetases (McCarthy et al. 1982) continues when cells are returned to the dark indicating that induction is a light triggered process. Increased in-organello rates of chloroplast protein synthesis (Cushman and Price 1986; Miller et al. 1983) are a manifestation of the light induced synthesis of the components of the chloroplast protein synthetic machinery.

The light induced synthesis of chlorophyll, the most easily measured chloroplast constituent, exhibits a 12 h lag period followed by a period of rapid synthesis (Stern et al. 1964b). Exposure of cells to 2 h of light followed by 12 h of darkness, a process termed potentiation (Holowinsky and Schiff 1970) eliminates the lag period. Potentiation is dependent upon protein synthesis on chloroplast ribosomes, and on cytoplasmic ribosomes during both the preillumination period and the subsequent dark period (Schwartzbach et al. 1976b). Metabolism of δ-aminolevulinic acid (ALA), the first committed precursor to chlorophyll, is required during both the light and dark periods of potentiation (Schwartzbach et al. 1976b) suggesting a chlorophyll precursor may be the actual inducer of proteins required for rapid chlorophyll synthesis. Consistent with this idea is the identification of protochlorophyll(ide) which upon light exposure is converted to chlorophyll(ide) as the photoreceptor controlling this process (Egan et al. 1975; Egan and Schiff 1974).

ALA is synthesized in the *Euglena* chloroplast from glutamate by the five carbon pathway which uses glutamyl-tRNA, glutamyl-tRNA synthetase, glutamyl-tRNA reductase, and GSA transaminase (Mayer et al. 1987; Weinstein and Beale 1983). All of the enzymes required for the synthesis of chlorophyll from glutamate are found in the chloroplast (Gomez-Silva and Schiff 1985; Gomez-Silva et al. 1985) and they appear to be synthesized on cytoplasmic ribosomes (Mayer and Beale 1991; Richard and Nigon 1973; Schwartzbach et al. 1976b). ALA dehydratase, the first enzyme required for the conversion of ALA to chlorophyll (Hovenkamp-Obbema et al. 1974), and porphobilinogen (PBG) deaminase (Shashidhara and Smith 1991), an enzyme required for porphyrin synthesis, are also made on cytoplasmic ribosomes. The rate of ALA synthesis increases after a 12 h lag upon light exposure and declines rapidly upon returning cells to the dark (Mayer and Beale 1990, 1991; Ravel-Chapuis and Nigon 1981; Richard and Nigon 1973; Salvador 1978; Salvador et al. 1976). ALA dehydratase (Hovenkamp-Obbema et al. 1974), PBG deaminase (Shashidhara and Smith 1991), the glutamyl-tRNA and all three

enzymes required for ALA synthesis are also light induced (Mayer and Beale 1990, 1991). The increase in PBG deaminase activity represents an increase in enzyme protein (Shashidhara and Smith 1991).

In addition to induction of enzymes required for chlorophyll synthesis, light induces the enzymes needed to fix CO_2. NADP-glyceraldehyde-3-phosphate dehydrogenase (Bovarnick et al. 1974a, b; Egan et al. 1975; Hovenkamp-Obbema and Stegwee 1974; Russell et al. 1978; Schmidt and Lyman 1974), phosphoglycolate phosphatase (Codd and Merrett 1970; James and Schwartzbach 1982), the chloroplast isozyme of fructose-1-6-diphosphate aldolase (Karlan and Russell 1976; Russell et al. 1978; Schmidt and Lyman 1974) and pyruvate kinase (Russell et al. 1978; Schmidt and Lyman 1974) are light induced. RUBISCO composed of a large chloroplast encoded subunit and a small nuclear encoded subunit constitutes approximately 25% of total soluble protein (Freyssinet et al. 1984a; Gingrich and Hallick 1985; Rabinowitz et al. 1975). RUBISCO enzyme activity increases after a 12 h lag period upon light exposure (Bovarnick et al. 1974a, b; Freyssinet et al. 1984a; Hovenkamp-Obbema and Stegwee 1974; Laval-Martin et al. 1981; Neumann and Parthier 1973; Pineau 1982) and the lag period can be eliminated by preillumination (Freyssinet et al. 1984a; Schimpf et al. 1982). The increase in enzyme activity is due to an increase in the amount of the large and the small subunit (Freyssinet et al. 1984a; Keller et al. 1991; Monroy and Schwartzbach 1983; Pineau 1982). Induction is light dependent (Freyssinet et al. 1984a; Pineau 1982). Pulse labeling has shown that the increase in RUBISCO protein levels is due to an increase in the rates of large and small subunit synthesis (Keller et al. 1991; Monroy et al. 1987).

Chlorophyll is bound in the thylakoid membrane to specific chlorophyll binding proteins which are associated with the photosystem I reaction center complex, CP I, the photosystem II reaction center complex, CPa, and the light harvesting complex proteins associated with photosystem I and II (Cunningham and Schiff 1986a, b; Houlne and Schantz 1987, 1988; Ortiz and Stutz 1980; Pineau et al. 1985; Yi et al. 1985). Proteins of the electron transport chain are also in the thylakoid membrane. Assembly of thylakoids requires a large number of proteins, their pigments and prosthetic groups. As found for induction of rapid chlorophyll synthesis, the light induced formation of the photosystem I reaction centers (Yi et al. 1985) exhibit a 12 h lag period while a longer lag period, approximately 18–24 h, is found for induction of photosystem II reaction centers (Dubertret 1981; Yi et al. 1985). The assembly of functional photosystem I reaction centers appears to precede the assembly of photosystem II reaction centers.

The precursors to *Euglena* nuclear encoded light harvesting complex proteins are polyproteins that are processed to the light harvesting chlorophyll a/b binding protein of photosystem I (LHCPI) and the light harvesting chlorophyll a/b complex of photosystem II (LHCPII) within the chloroplast (Enomoto et al. 1997; Houlne and Schantz 1987, 1988; Koziol and Durnford 2008; Muchhal and Schwartzbach 1992; Rikin and Schwartzbach 1988, 1989b). RNAs of 6.6 and 8.3 kb encode the precursors to LHCPII (pLHCPIIs) of 207, 161, 122 and 110 kDa which are transported from the ER, the site of synthesis on membrane bound polysomes, to the golgi apparatus and then to the chloroplast (see Chap. 10) where they are proteolytically processed into the mature 25.6 and 27.2 kDa LHCPIIs of *Euglena* (Cunningham and Schiff 1986b; Enomoto et al. 1997; Kishore et al. 1993; Osafune et al. 1991a, b; Rikin and Schwartzbach 1988; Schiff et al. 1991a; Sulli and Schwartzbach 1995). Pulse labeling with ^{35}S-sulfate and immunoprecipitation showed that pLHCPII is synthesized at a low but detectable rate in the dark (Fig. 9.1; Rikin and Schwartzbach 1989b). The photo induction of LHCPII accumulation exhibited a 12 h lag period as seen for chlorophyll accumulation (Bingham and Schiff 1979b; Bouet et al. 1986; Brandt and Winter 1987; Spano et al. 1987; Weiss et al. 1988; Yi et al. 1985). The maximal rate of pLHCPII synthesis seen 12–24 h after light exposure was 50–100 fold higher than the rate prior to light exposure (Fig. 9.1). The rate of LHCPII synthesis decreased by 80% during the first half hour after

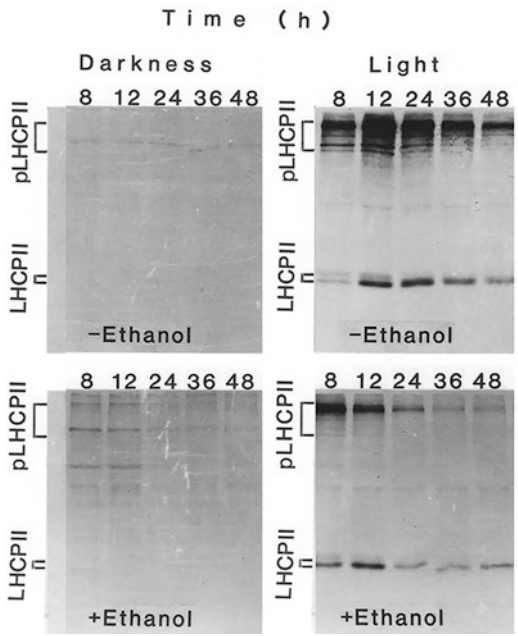

Fig. 9.1 Induction of LHCPII synthesis by light and repression of light induction by ethanol. Dark grown resting *Euglena* were maintained in the dark or exposed to light with or without ethanol addition. At various times, cells were pulse labelled with ^{35}S-sulfate, proteins were immunoprecipitated with an antibody to LHCPII, the immunoprecipitates were analyzed by SDS gel electrophoresis and LHCPII and pLHCPII visualized by fluorography. Cells maintained in the dark with the addition of ethanol showed a small but significant increase in pLHCPII synthesis (increased pLHCPII and processed LHCPII) with a maximum synthesis rate between 8 and 12 h. A large increase in the rate of pLHCPII synthesis is seen in cells exposed to light in the absence of ethanol with the maximum rate 12–24 h after light exposure. Ethanol addition significantly inhibited, at all times, the light induced synthesis of pLHCPII. Modified from (Rikin and Schwartzbach 1989b)

illuminated cells were returned to the dark (Rikin and Schwartzbach 1989b). The half life for conversion of pLHCPII to LHCPII measured by pulse chase experiments was 20 min in the dark or the light (Rikin and Schwartzbach 1988, 1989b). The light dependent accumulation of LHCPII is clearly due to light dependent changes in the rate of LHCPII synthesis.

The photoinduced accumulation of ferredoxin NADP reductase (Spano and Schiff 1987) and cytochrome c-552 (Bovarnick et al. 1974b; Freyssinet et al. 1979), components of the electron transport chain, exhibits a 12 h lag as seen for chlorophyll synthesis. Photoinduction of the CF1-ATPase including the DCCD binding CF_0 subunit occurs without a lag (Timko and Schiff 1983; Yi et al. 1985). Pulse labeling demonstrated that light induced thylakoid proteins are synthesized on both chloroplast and cytoplasmic ribosomes (Bingham and Schiff 1979a, b; Gilbert and Buetow 1982; Gurevitz et al. 1977; Rikin and Schwartzbach 1989b).

A more comprehensive picture of the role of light in *Euglena* organelle development has been obtained using two dimensional gel electrophoresis (2-D gel) to follow changes in the synthesis and accumulation rate of total cellular and organelle proteins upon light exposure. 2-D gels resolve total cellular protein into approximately 640 polypeptides detectable by silver staining (Monroy and Schwartzbach 1983). The relative amounts of 72 polypeptides decreased and 79 increase upon exposure of dark grown *Euglena* to light (Fig. 9.2; Monroy and Schwartzbach 1983). Proteins extracted from purified chloroplasts were resolved into 185 polypeptides and 55 were localized on the whole cell 2-D gels (Monroy et al. 1986). The relative amounts of 49 (90%), of the chloroplast proteins localized to the whole cell map increased, the relative amounts of two decreased and the relative amounts of four were unaltered by light exposure (Fig. 9.2; Monroy et al. 1986; Monroy and Schwartzbach 1983). Analysis by 2-D gels of proteins extracted from cells pulse labeled with ^{35}S-sulfate showed that the relative rate of synthesis of 61 polypeptides increased with the relative rate of synthesis of 18 increasing by more than threefold during the first half hour of light exposure (Monroy et al. 1987). A decreased synthesis rate was seen for 29 polypeptides with the synthesis rate decreasing more than threefold during the first half hour of light exposure. Additional changes in the synthesis rate of specific proteins were initially seen at 1, 4, 14, 24, 48 but not 72 h after light exposure (Monroy et al. 1987). Eighteen chloroplast proteins could be found on both silver stained 2-D gels and fluorograms. The relative rate of synthesis of five chloroplast localized proteins increased during the first half hour of light exposure

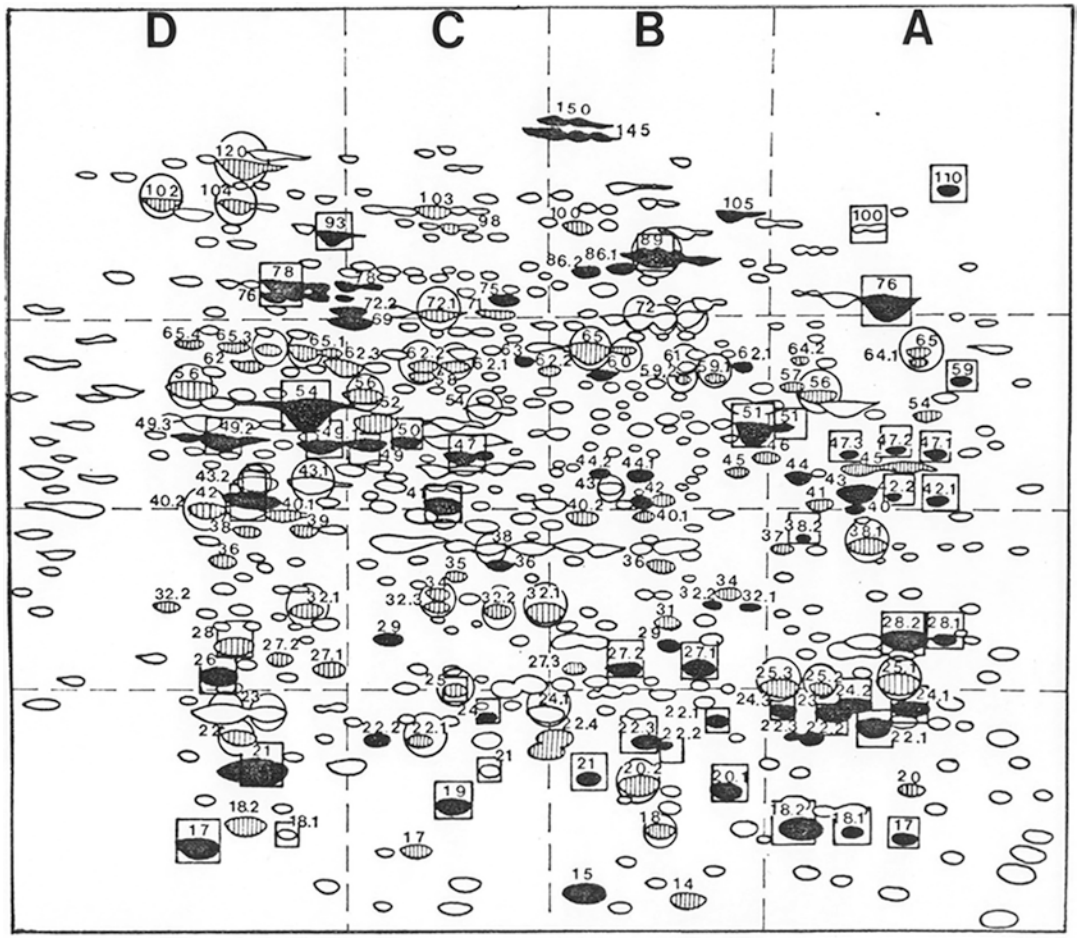

Fig. 9.2 Composite diagram demonstrating the global changes in chloroplast and mitochondrial protein amounts upon exposure of dark grown resting cells of *Euglena* to light. A composite diagram showing the relative positions and shapes of all *Euglena* proteins detectable on silver stained 2-D gels of total cellular protein extracts. Solid and stripped spots represent polypeptides whose relative amounts increased and decreased respectively upon light exposure. *Squares* and *circles* indicate polypeptides found in isolated chloroplasts and mitochondria respectively. The majority of chloroplast localized polypeptides (*solid squares*) increased upon light exposure while the majority of mitochondrial polypeptides (*stripped circles*) decreased. Reproduced from Monroy et al. (1986). "Copyright American Society of Plant Biologists." www.plantphysiol.org

while the highest rate of synthesis for 12 other polypeptides and the large subunit of RUBISCO occurred between 24 and 72 h after light exposure (Monroy et al. 1987). An increase or a decrease in the amount of a polypeptide found on the stained 2-D gel correlated with an increase or decrease in the rate of synthesis of that polypeptide. An analysis of proteins extracted from purified thylakoids found that the synthesis of a majority of the polypeptides was induced during the first 12 h of light exposure (Gilbert and Buetow 1982). Light induced changes in the relative amounts of specific chloroplast and thylakoid proteins are clearly due to stage specific changes in protein synthesis rate.

9.3 Photo and Metabolite Control of Mitochondrial Development

An organic carbon source is used to synthesize cellular constituents and to provide energy through mitochondrial respiration when *Euglena*

is grown in the dark. When grown in the light, photosynthesis allows CO_2 to be used as the sole carbon source for synthesis of cellular constituents and the light reactions of photosynthesis in the chloroplast rather than mitochondrial respiration are the major energy source for cellular growth. Chloroplast development can thus be viewed as the induction by a carbon source, light which allows CO_2 to be used as the sole source of carbon and energy for growth of the enzymes, in this case an entire organelle, required to utilize that carbon source. To separate effects of light on cell division from effects on chloroplast development, a resting cell system was developed (Stern et al. 1964b). Resting cells are carbon starved dark grown cells that upon light exposure develop photosynthetically competent chloroplasts in the absence of an increase in cell number and total cellular protein.

Exposure of dark grown resting cells to light induces the degradation of the storage carbohydrate paramylum ((Dwyer and Smillie 1970, 1971; Dwyer et al. 1970; Freyssinet et al. 1972; Schwartzbach et al. 1975; Sumida et al. 1987), the degradation of cellular lipids (Rosenberg and Pecker 1964) and increases the rate of cellular respiration (Fong and Schiff 1977; Schiff 1963). Chloroplast development is blocked by respiratory inhibitors and uncouplers (Evans 1971; Fong and Schiff 1977; Klein et al. 1972) while inhibitors of photosynthesis have little effect on chlorophyll synthesis in resting cells during the first 24 h of light exposure but are inhibitory after this time (Dwyer and Smillie 1970, 1971; Freyssinet et al. 1984a, b; Horrum and Schwartzbach 1981; Schiff et al. 1967) when the majority of paramylum has been consumed. The inhibition of chlorophyll synthesis by inhibitors of photosynthesis can be overcome by provision of a utilizable carbon source (Freyssinet et al. 1984b; Horrum and Schwartzbach 1981). The amount of chlorophyll synthesized (Freyssinet et al. 1972), the length of the lag period of chlorophyll synthesis (Freyssinet and Schwob 1976), the length of the dark period of potentiation (Freyssinet 1976) and the amount of RUBISCO produced (Freyssinet et al. 1984b) are proportional to the level of paramylum present prior to light exposure. Taken together these results suggest that the aerobic breakdown of cellular reserves provides the carbon and energy required for the early stages of chloroplast development while photosynthesis becomes the major carbon and energy source during the latter stages of plastid development.

Transient changes in the synthesis rate of some mitochondrial proteins are consistent with the importance of respiratory metabolism to the early but not late stages of plastid development. During the first eight to twelve hours after exposure of dark grown resting *Euglena* to light, the specific activity of fumarase (Horrum and Schwartzbach 1980c, 1982), succinate dehydrogenase (Horrum and Schwartzbach 1980c), malate dehydrogenase (Cannons and Merrett 1983) and citrate synthase (Cannons and Merrett 1983, 1984) increases and then declines as the chloroplast becomes photosynthetically competent returning to the levels found prior to light exposure. The transient increase and decrease in fumarase specific activity corresponds to changes in the rate of enzyme synthesis as measured by pulse labeling with ^{35}S-sulfate (Rikin and Schwartzbach 1989a). Transient increases were also seen in the rate of synthesis of a number of mitochondrial localized proteins resolved on 2-D gels (Monroy et al. 1987).

Exposure of dark grown resting *Euglena* to light can be thought of as a nutritional shift up; provision of a utilizable carbon source, light which allows CO_2 to be used as the sole source of carbon and energy for growth, to starving cells. Just as found upon light exposure, the addition of malate or ethanol, utilizable carbon sources, to dark grown resting cells maintained in the dark or the light transiently induced fumarase and succinate dehydrogenase (Horrum and Schwartzbach 1980c, 1982). The ethanol induced rate of fumarase synthesis measured by pulse labeling with ^{35}S-sulfate in the dark was greater than in the light (Rikin and Schwartzbach 1989a). The ethanol induced rate of fumarase synthesis was higher than the malate induced rate which was higher than the light induced rate. Light exposure or ethanol addition to cells in exponential balanced growth had no effect on fumarase levels (Horrum and Schwartzbach 1982) indicating that transient

induction of mitochondrial enzymes by light or organic carbon represents a response of starving cells to a nutritional shift up.

Chloroplast development in resting cells exposed to light occurs in the absence of a net increase in total cellular protein (Bovarnick et al. 1974b; Horrum and Schwartzbach 1980b; Schantz et al. 1975). Amino acid pool sizes remain unchanged during plastid development indicating that breakdown of preexisting proteins provides the amino acids required for synthesis of chloroplast localized proteins (Schantz et al. 1975). Proteolytic activity increases during the period of carbon starvation used to produce dark grown resting cells and light exposure produces additional increases in proteolytic activity (Harris and Kirk 1969; Krauspe et al. 1986; Schantz et al. 1975; Zeldin et al. 1973).

Mitochondrial area (Schantz et al. 1975), levels of mitochondrial lipids (Schantz et al. 1975), cytochromes (Schantz et al. 1975), the mitochondrial enzyme ALA synthetase (Beale et al. 1981; Corriveau and Beale 1986; Foley and Beale 1982; Foley et al. 1982) and mitochondrial elongation factor G (Eberly et al. 1986) decrease upon light exposure. Of 44 mitochondrial proteins localized on the whole cell 2-D gel map, the relative amounts of 31 (70%) decrease after light exposure (Fig. 9.2; Monroy et al. 1986, 1987). Pulse labeling with ^{35}S- sulfate has shown that within the first half hour of light exposure, the rate of synthesis of nine mitochondrial proteins decreases and additional decreases are detected between 1 and 14 h after light exposure (Monroy et al. 1987). The decrease in the levels of specific mitochondrial proteins appears to result from a decrease in their rate of synthesis and their loss through degradation.

Light induced mitochondrial protein loss is selective. Levels of the mitochondrial enzymes serine hydroxymethyltransferase (Horrum and Schwartzbach 1980a), adenosine 5′-phosphosulfate sulfotransferase (Brunold and Schiff 1976), organic thiosulfate reductase ("thiosulfonate reductase") (Brunold and Schiff 1976; Saidha et al. 1985), O-acetyl-L-serine sulfhydrolase (Brunold and Schiff 1976; Saidha et al. 1985) and acetyl CoA carboxylase (Evers and Ernst-Fonberg 1974) are unaltered in dark grown cells exposed to light. The level of phosphoenolpyruvate carboxylase (Laval-Martin et al. 1981; Ponsgen-Schmidt et al. 1988) increases upon light exposure. Studies with 2-D gels found that the rate of synthesis of five mitochondrial polypeptides were unaltered by light exposure while the rate of one increased upon light exposure (Monroy et al. 1987). Selective light induced changes in the rate of synthesis of specific mitochondrial proteins appears to produce differences between the enzyme composition of mitochondria in dark grown *Euglena* and cells containing a photosynthetically competent chloroplast due to light exposure. Since chloroplast development occurs in the absence of a net increase in cellular protein and amino acid pool size (Bovarnick et al. 1974b; Horrum and Schwartzbach 1980b; Schantz et al. 1975), selective decreases in the rate of synthesis of mitochondrial proteins coupled with their loss through degradation suggests that mitochondrial protein degradation is a major source of amino acids for the synthesis of light induced proteins.

Light dependent changes in mitochondrial ALA synthetase and chloroplast enzymes of the 5 carbon ALA synthesizing pathway exemplify the way in which the metabolic role of the mitochondria is redefined by selective protein loss upon light exposure with concomitant induction of chloroplast enzymes performing similar metabolic functions. ALA synthetase appears to be the primary source of ALA for mitochondrial tetrapyrrole biosynthesis (Weinstein and Beale 1983) in dark grown *Euglena*. A detectable decrease in ALA synthetase is observed within 15 min of light exposure and activity increases upon returning cells to the dark (Beale and Foley 1982; Foley et al. 1982). The kinetics of enzyme activity decrease observed upon light exposure are similar to the kinetics observed in cells treated with cycloheximide to inhibit protein synthesis (Foley et al. 1982) suggesting that the light dependent decrease in enzyme activity is due to a light dependent decrease in the rate of ALA synthetase synthesis and subsequent enzyme loss through degradation. The light induction of the chloroplast localized enzymes of the 5 carbon

ALA synthesizing pathway (Mayer and Beale 1990, 1991; Mayer et al. 1987) allows the developing chloroplast to assume the metabolic role of the mitochondria in cellular porphyrin synthesis.

The photorespiratory pathway converting two molecules of phosphoglycolate produced by the oxygenase activity of RUBISCO to 3-phosphoglycerate and CO_2 utilizes enzymes contained in the chloroplast, in the peroxisome, a single membrane bound organelle that is one type of plant microbody, and in mitochondria. Although algal microbodies involved in the photorespiratory pathway use glycolate dehydrogenase rather than glycolate oxidase to convert glycolate to glyoxylate and thus lack peroxidase, they are still referred to as peroxisomes. A second type of microbody, the glyoxysome, contains the enzymes for acetate and ethanol assimilation through the glyoxylate cycle. *Euglena* contains peroxisomal photorespiratory enzymes and glyoxysomal enzymes required for two carbon assimilation by the glyoxylate cycle but these enzymes appear to be localized in mitochondria rather than in microbodies (Collins and Merrett 1975a; Fayyaz-Chaudhary and Merrett 1984; Ono et al. 2003; Yokota et al. 1978, 1985a, b; Yokota and Kitaoka 1979, 1981). Malate synthase and isocitrate lyase are key glyoxylate cycle enzymes. A novel bifunctional enzyme having both malate synthase and isocitrate lyase activity is found in *Euglena* (Nakazawa et al. 2005, 2011). Immunoelectron microscopy of whole cells has localized this enzyme to mitochondria and the cDNA sequence encodes an N-terminal mitochondrial targeting sequence (Nakazawa et al. 2011; Ono et al. 2003). The overwhelming body of evidence clearly shows that in contrast to higher plants and other organisms, *Euglena* mitochondria rather than microbodies are the site of photorespiratory glycolate metabolism and two carbon assimilation by the glyoxylate cycle.

Hydroxypyruvate reductase and glycolate dehydrogenase are required for metabolism of phosphoglycolate. Hydroxypyruvate reductase is organelle localized (Collins and Merrett 1975a) and in addition to being required for phosphoglycolate metabolism during photorespiration it is also required for the synthesis of glycine and serine from phosphoglycerate. Hydroxypyruvate is therefore required regardless of the carbon source used for growth. Light exposure does not effect the synthesis of hydroxypyruvate reductase (Horrum and Schwartzbach 1980a). On the other hand, light induces glycolate dehydrogenase synthesis after a 24 h lag period coinciding with the time required for the cells to develop the capacity for photosynthetic CO_2 fixation (Codd and Merrett 1970; Horrum and Schwartzbach 1980c). Glycolate dehydrogenase levels are higher in cells grown under atmospheric CO_2 concentrations which promote phosophoglycolate synthesis than in cell grown in 5% CO_2 which represses phosphoglycolate synthesis (Codd and Merrett 1971; Lord and Merrett 1971; Yokota et al. 1978). The inhibitor of photosynthetic electron transfer, (3-(3,4dichlorophenyl)-1,1-dimethylurea) (DCMU), inhibits glycolate dehydrogenase photoinduction in resting cells. The photoinduction of most other enzymes is not inhibited by DCMU (Horrum and Schwartzbach 1981; Monroy and Schwartzbach 1985) suggesting that inhibition of glycolate dehydrogenase synthesis by DCMU is not a reflection of a generalized inhibition of cellular protein synthesis due to a lack of photosynthetic energy production. Taken together, the extended lag period for glycolate dehydrogenase photoinduction, the inhibition of glycolate dehydrogenase photoinduction by DCMU and the induction of glycolate dehydrogenase by growth under low CO_2 concentrations suggest that a carbon source produced photosynthetically, presumably glycolate, induces the organelle localized enzymes required to utilize that carbon source. By regulating enzyme synthesis through substrate induction, *Euglena* has evolved a mechanism for adapting mitochondrial metabolism to the constantly changing availability of sources of carbon and energy for growth.

Malate synthase, isocitrate lyase and alcohol dehydrogenase are *Euglena* mitochondrial enzymes required for assimilation of acetate and ethanol by the glyoxylate cycle (Ono et al. 1994, 1995, 2003). In most organisms, malate synthase and isocitrate lyase are distinct enzymes. In *Euglena*, a single bifunctional mitochondrial enzyme catalyzes both reactions (Nakazawa et al.

2005, 2011). Thus when malate synthase or isocitrate lyase induction is discussed, one must keep in mind that we are discussing the induction of a single polypeptide that is responsible for both enzymatic activities even though each activity has been separately measured rather than a single polypeptide catalyzing the measured reaction.

Ethanol and acetate induce alcohol dehydrogenase, malate synthase and isocitrate lyase in the dark or the light (Collins and Merrett 1975b; Cook and Carver 1966; Horrum and Schwartzbach 1981; Ono et al. 1994, 1995; Woodward and Merrett 1975). Increased enzyme levels result from an increase in enzyme protein (Ono et al. 1994). Cells induced in the light accumulate less enzyme than cells induced in the dark (Cook and Carver 1966; Horrum and Schwartzbach 1981) indicating that the induction of malate synthase by ethanol and acetate is partially repressed by light. Photorepression of malate synthase induction occurs in the absence of photosynthetic CO_2 fixation (Horrum and Schwartzbach 1981) indicating that repression is a direct effect of light exposure.

9.4 Photocontrol of Cytosolic Enzyme Synthesis

The cytosol represents the hub of metabolic activity. The cytosolic synthesis and degradation of proteins, amino acids, and nucleotides is required regardless of the carbon source. Other cytosolic activities such as the synthesis and degradation of glucose are essential under organotrophic conditions while these reactions occur at least in part in the chloroplast of photosynthetic cells. A specific metabolite and thus cytosolic metabolic activity may be required under all growth conditions but the level of activity may vary between growing and nongrowing cells or between cells growing on specific organic carbon sources or photosynthetically using CO_2 as the sole source of carbon and energy for growth. Therefore, it should not be surprising to find that the synthesis of some cytosolic enzymes are induced by light, the synthesis of some cytosolic enzymes are repressed by light and the synthesis of some are transiently induced suggesting that their synthesis represents a response to a nutritional shift up.

Cytosolic proteins are defined as those proteins which have not been specifically localized to the chloroplast, mitochondria or microbodies of *Euglena*. It should be noted that a number of these proteins may however be organelle localized. Analysis by 2-D gel electrophoresis of proteins extracted from cells pulse labeled with ^{35}S-sulfate showed that the relative rate of synthesis of 16 out of 54 cytosolic polypeptides localized on a 2-D gel map of total cellular protein decreases after exposure of dark grown resting *Euglena* to light (Monroy et al. 1987). Within the first half hour of light exposure the synthesis rate of six polypeptides decreases. Changes in the rate of polypeptide synthesis are specific as evidenced by the fact that the relative synthesis rate of 17 cytosolic proteins is unaltered by light exposure. A decreased rate of synthesis of a specific polypeptide correlated with a decrease in the amount of that polypeptide indicates that light specifically inhibits the synthesis of some cytosolic proteins and their levels decline through continued degradation (Monroy et al. 1987; Monroy and Schwartzbach 1983). The specific activity of cytosolic aldolase (Dockerty and Merrett 1979; Karlan and Russell 1976), triosephosphate isomerase (Dockerty and Merrett 1979), phosphofructokinase (Dockerty and Merrett 1979), pyruvate kinase (Dockerty and Merrett 1979), phosphoenolpyruvate carboxykinase (Laval-Martin et al. 1981; Miyatake et al. 1984; Ponsgen-Schmidt et al. 1988), NAD-glyceraldehyde-3-phosphate dehydrogenase (Bovarnick et al. 1974a, b; Dockerty and Merrett 1979) and malic enzyme (Karn and Hudock 1973; Peak et al. 1972) decreases after light exposure. Cytosolic enzymes involved in glucose synthesis and utilization appear to be among the polypeptides whose degradation after light exposure provides the amino acids required for the synthesis of chloroplast localized enzymes utilized for glucose synthesis.

The relative rate of synthesis of 21 out of 54 cytosolic polypeptides localized on the whole cell 2-D gel map measured by pulse labeling with

^{35}S-sulfate increases continuously or transiently upon light exposure (Monroy et al. 1987). The specific activity of ornithine decarboxylase (Schuber et al. 1981), the enzyme catalyzing the initial step of polyamine metabolism and NADPH-glutamate dehydrogenase (Fayyaz-Chaudhary et al. 1984, 1985) transiently increased upon light exposure while glutamine synthetase (Fayyaz-Chaudhary et al. 1984) and ascorbate peroxidase (Madhusudhan et al. 2003) exhibited a permanent specific activity increase. The increase in ascorbate peroxidase specific activity was due to an increase in immunologically detectable ascorbate peroxidase protein indicating the synthesis of ascorbate peroxidase is light induced. Since chloroplasts also contain glutamine synthetase (Fayyaz-Chaudhary et al. 1985), it is unclear whether the induced enzyme is the chloroplast isozyme. Associated with the light induced degradation of paramylum is a transient increase in the specific activity of glucan hydrolase, glucan phosphorylase, UDPG pyrophosphorylase and glucose-6-phosphate dehydrogenase (Dwyer and Smillie 1970); enzymes involved in the initial stages of carbohydrate metabolism. Since cycloheximide, an inhibitor of protein synthesis on cytoplasmic ribosomes, induces paramylum breakdown in the dark (Schwartzbach et al. 1975), the light induced transient increase in the specific activity of these enzymes is either due to enzyme activation or the increased levels of these enzymes is not a prerequisite for increased paramylum utilization.

9.5 Catabolite Repression of Chloroplast Development

Euglena can use a wide variety of carbon sources for growth. Some carbon sources such as ethanol and malate can be considered as rarely present in the environment while others such as light and CO_2 utilized for photosynthetic growth can be considered ubiquitous; CO_2 always being present and light being present 12 out of every 24 h. In addition to availability, growth on some carbon sources requires enzymes unique to that carbon source while in other cases, growth is not dependent upon carbon source specific enzymes. For example, assimilation of ethanol and acetate requires the enzymes of the glyoxylate cycle to produce malate while the enzymes required to assimilate malate are not unique; they are required for growth on all carbon sources. To use light and CO_2 as the sole source of carbon and energy for growth requires not simply a few enzymes but rather an entire organelle containing 2000–4000 proteins, the chloroplast. Obviously, significantly more energy is required to develop the capacity for photosynthetic growth by synthesizing a chloroplast than is required to induce the enzymes required to utilize ethanol. On the other hand, light is a ubiquitous carbon source that can always be used while ethanol is not always present. Catabolite repression is the repression by a carbon source of the induction of the enzymes required to utilize an alternative carbon source. It provides a regulatory mechanism that determines which of two carbon sources will be used first thus conserving carbon and energy by not simultaneously synthesizing the enzymes required to utilize both carbon sources. In the case of *Euglena*, chloroplast development is catabolite repressed.

Addition of glucose, ethanol, or acetate to dark grown resting *Euglena* at the time of light exposure inhibits chlorophyll synthesis (App and Jagendorf 1963; Buetow 1967; Garlaschi et al. 1974; Harris and Kirk 1969; Horrum and Schwartzbach 1980b; Schwelitz et al. 1978a, b, c) but malate and succinate are not inhibitory (Garlaschi et al. 1974; Horrum and Schwartzbach 1980b). Ethanol, but not its assimilatory intermediate malate, specifically represses glycolate dehydrogenase (Horrum and Schwartzbach 1981), phosphoglycolate phosphatase (James and Schwartzbach 1982), NADP-glyceraldehyde-3-phosphate dehydrogenase (Horrum and Schwartzbach 1980b), some chloroplast aminoacyl-tRNA synthetases (McCarthy et al. 1982; Schimpf et al. 1982), RUBISCO large subunit (Monroy and Schwartzbach 1984) and LHCPII (Yi et al. 1985) photoinduction. Ethanol but not malate inhibits all of the light dependent changes detectable on silver stained 2-D gels including the induction of chloroplast encoded proteins

(Monroy and Schwartzbach 1984). Pulse labeling with ^{35}S-sulfate indicates that the inhibition of LHCPII accumulation results from an ethanol dependent inhibition of pLHCPII synthesis (Fig. 9.1; Rikin and Schwartzbach 1989b) suggesting that ethanol represses chloroplast development by inhibiting the light dependent increase in the synthesis rate of most chloroplast proteins.

The addition of ethanol to resting cells induces cell division (Horrum and Schwartzbach 1980b). During the first 8 h of light exposure, ethanol had little effect on the induction of LHCPII (Fig. 9.1; Rikin and Schwartzbach 1989b) and chloroplast valyl-tRNA synthetase (McCarthy et al. 1982) even though it was inhibitory after this time. The insensitivity of LHCPII and chloroplast valyl-tRNA synthetase induction during the first eight hours of light exposure probably reflects chloroplast replication required for cell division rather than an insensitivity of enzyme photoinduction to ethanol repression. The catabolite repression of chloroplast development can be viewed as regulatory mechanism that evolved to ensure that energy will be expended to produce the enzymatic machinery required for the metabolism of carbon sources such as acetate, glucose and ethanol that are not always found in the environment prior to expending the significantly greater amount of energy required to produce the enzymes, in this case the organelle, required for growth on light, a carbon source that normally reappears every 12 h.

9.6 Does Light Regulate Chloroplast Gene Expression at the Transcriptional or Translational Level?

A large fraction of the *Euglena* chloroplast genome is transcribed in the dark and continues to be expressed in the light with the abundance of some transcripts increasing five- to tenfold upon light exposure (Chelm et al. 1978, 1979; Chelm and Hallick 1976; Rawson and Boerma 1976a, b; Rawson et al. 1981; Verdier 1979a, b). Some transcripts present in dark grown cells cannot be detected 4 h after light exposure but they are detectable 72 h after light exposure (Chelm et al. 1979; Rawson and Boerma 1979). Other transcripts are not detected in the dark but they are present in the light. Qualitative and quantitative differences were found in the translatable RNAs extracted from plastids isolated from dark adapted *Euglena* and from immature and mature chloroplasts of *Euglena* (Miller et al. 1983). The level of the transcripts coding for a number of light induced proteins, the large subunit of RUBISCO (Hallick et al. 1983), the 32 Kd photosystem II polypeptide, psbA (Hallick et al. 1983; Hollingsworth et al. 1984; Johanningmeier and Hallick 1987; Weiss et al. 1988), and the β subunit of the chloroplast CF_1 coupling factor (Hallick et al. 1983) were reported to increase throughout chloroplast development.

On the other hand, the levels of chloroplast psaA, psaB, psbC and psbD, gene transcripts encoding light induced proteins, increased approximately twofold during the first hour after light exposure remaining constant after this time even though the levels of the proteins encoded by these transcripts increased 10–20 fold upon light exposure (Bouet et al. 1986; Weiss et al. 1988). The steady state level of mRNA for chloroplast EF-Tu remains relatively constant during the first 60 h of chloroplast development (Hallick et al. 1983) even though light induces the synthesis of EF-Tu during this time (Spremulli 1982). A transcriptome analysis using microarrays to quantitate each of the 96 transcribed chloroplast genes isolated from cells in the dark showed that all of the genes in the chloroplast genome were transcribed in the dark, albeit at different rates which are presumably an intrinsic property of the gene, resulting in five RNA abundance classes ranging from a high abundance class, high transcription rate, to a barely detectable low abundance class, low transcription rate (Geimer et al. 2009). Higher levels of all chloroplast transcripts were found in cells grown in the light compared to cells grown in the dark. The relative amount of specific transcripts, ratio of one transcript to another transcript, did not appear to change upon light exposure (Geimer et al. 2009) indicating that the transcription rate of specific genes is not

photoregulated but the transcription rate of all genes is increased to the same extent by light exposure. Chloroplast copy number increases two to threefold after exposure of dark grown *Euglena* to light (Chelm et al. 1977a; Hussein et al. 1982; Rawson and Boerma 1976a; Srinivas and Lyman 1980). If transcript abundance is limited by template availability rather than the transcription machinery, the nonselective light induced increase in transcript abundance of most chloroplast genes could be due to the increased chloroplast copy number. Taken together, these results suggest that light induced chloroplast encoded protein synthesis is controlled at the translational level.

Further complicating an understanding of how light exposure increases the synthesis rate of chloroplast proteins is the fact that some primary chloroplast transcripts are polycistronic, contain numerous introns, and require extensive processing to produce the mature mRNA. For example, the psaA operon encodes a tRNA, psaA and psaB photosystem I genes, and the photosystem II psbE, psbF, psbL and psbJ genes (Stevenson and Hallick 1994). Maturation of the primary transcript requires tRNA processing, splicing of multiple introns and intercistronic cleavages. Intercistronic cleavage of the hexacistronic mRNA produces a psaA and psaB dicistronic mRNA and the mature tetracistronic psbE, psbF, psbJ mRNA. A second intercistronic cleavage produces the mature psaA and psaB mRNA. The hexacistronic mRNA is the most abundant in the dark and the abundance of mRNAs produced by intercistronic processing increase on light exposure indicative of light regulation of pre-mRNA processing (Stevenson and Hallick 1994). It is not known whether the translational efficiency of the processed mRNAs is greater than the unprocessed mRNAs. The increased rate of synthesis of chloroplast encoded proteins upon light exposure in the absence of a corresponding increase in the abundance of chloroplast encoded mRNAs taken together with the regulation of pre-mRNA processing by light exposure strongly suggests that light induced synthesis of chloroplast encoded proteins is controlled at the post-transcriptional level through regulation of primary transcript processing and or translation.

9.7 Does Light Regulate Nuclear Gene Expression at the Transcriptional or Translational Level?

Light exposure increases the synthesis of poly(A)$^+$ RNA (Verdier 1975; Verdier et al. 1973). Polysomes are rapidly formed after exposure of dark grown *Euglena* to light (Heizmann et al. 1972). As early as the first hour of light exposure, newly synthesized poly(A)$^+$ containing RNAs are associated with polysomes. By 24 h after light exposure, the proteins encoded by the polysomal poly(A)$^+$ RNAs differ from the proteins encoded by the polysomal RNAs present prior to light exposure (Verdier 1979b). One explanation of these results is that light acts at the transcriptional level selectively increasing the transcription rate of nuclear genes encoding light induced proteins. The newly transcribed messages associate with ribosomes forming polysomes resulting in an increased rate of synthesis of a subset of proteins encoded by genes whose transcription is light regulated. An alternative explanation of these results is that light acts at the translational level. Light does not selectively alter the mRNAs present in the cell but alters the efficiency with which individual mRNAs are translated resulting in a change in the polysomal mRNA population and thus an increase or decrease in the rate specific proteins are synthesized. The light induced synthesis of poly(A)$^+$ RNA (Verdier 1975; Verdier et al. 1973) occurs in the absence of an increase in the level of total cellular poly(A)$^+$ RNA (Cannons and Merrett 1984) and may, like the light induced synthesis of rRNA (Cohen and Schiff 1976), be a reflection of a light induced nonselective increase in the rate of poly(A)$^+$ RNA synthesis required to replace the poly(A)$^+$ RNA lost through degradation rather than an indication of light induced changes in gene transcription.

By analyzing light induced changes in the levels of individual mRNAs and light induced changes in the synthesis rate of individual proteins, the regulation by light of nuclear gene expression at the transcriptional level can be distinguished from regulation at the translational level. An analysis by 2-D gel electrophoresis

failed to detect light induced quantitative or qualitative changes in abundance of specific transcripts when the cell free translation products programmed by poly(A)$^+$ RNA isolated from dark-grown resting cells and cells exposed to light were compared (Krauspe et al. 1987; McCarthy and Schwartzbach 1984; Monroy et al. 1987). Numerous light induced changes in the synthesis rate of specific proteins were however detected when the pulse labeled *in vivo* translation products were compared (Monroy et al. 1987). An EST microarray analysis of total cellular RNA extracted from cells grown in the dark or in the light found that the relative amounts of the majority of mRNAs were similar (Dos Santos et al. 2007). Changes no greater than twofold were found for a small number of mRNAs. The small light induced changes in the levels of individual mRNAs do not appear to be large enough to account for the large changes in the synthesis rate of individual proteins.

The synthesis rate of nuclear encoded pLHCPII measured by pulse labeling with ^{35}S-sulfate increased 50–100 fold after 12–24 h of light exposure (Fig. 9.1) while the level of pLHCPII mRNA measured by Northern blotting, dot blotting and cell free translation increased approximately two fold (Kishore and Schwartzbach 1992a, b; Rikin and Schwartzbach 1989b; Schiff et al. 1991b; Weiss et al. 1988, 1992). Ethanol addition at the time of light exposure inhibited the light induced increase in pLHCPII synthesis rate (Fig. 9.1) while having no effect on the level of pLHCPII mRNA (Kishore and Schwartzbach 1992a; Rikin and Schwartzbach 1989b; Schiff et al. 1991b). The amount of pLHCPII mRNA associated with polysomes, 68%, in cells maintained in the dark when pLHCPII synthesis rates are low was the same as the amount of pLHCPII mRNA associated with polysomes, 63%, after light exposure (Fig. 9.3) although the rate of pLHPII synthesis increased by 50–100 fold (Fig. 9.1; Kishore and Schwartzbach 1992b; Weiss et al. 1988, 1992). pLHCPII synthesis was undetectable in the bleached mutants, W_3BUL and W_{10}BSmL, which have lost most if not all of their plastid genome even though the level of pLHCPII mRNA was similar to the level in dark grown wild type *Euglena* (Kishore and Schwartzbach 1992a, b; Schiff et al. 1991b; Vesteg et al. 2009). A major fraction of pLHCPII mRNA was associated with polysomes in the bleached mutants, W_3BUL and W_{10}BSmL (Kishore and Schwartzbach 1992b). Taken together, these studies of the catabolite sensitive photoinduction of pLHCPII clearly demonstrate that the expression of this nuclear encoded protein is controlled at the translational rather than the transcriptional level.

The majority of studies indicate that light regulates *Euglena* nuclear gene expression at the translational rather than the transcriptional level. Transient photoinduction of fumarase (Rikin and Schwartzbach 1989a), citrate synthase (Cannons and Merrett 1984, 1985) and NADP-glutamate dehydrogenase (Fayyaz-Chaudhary et al. 1984; Javed and Merrett 1987) occurs in the absence of a change in the steady state level of translatable RNA encoding these proteins. In contrast to the unaltered amount of pLHCPII mRNA associated with polysomes (Fig. 9.3; Kishore and Schwartzbach 1992b; Weiss et al. 1988, 1992), the amount of citrate synthase (Cannons and Merrett 1984) and NADP-glutamate dehydrogenase mRNA (Javed and Merrett 1987) associated with polysomes is increased by light exposure. The photoinduction of the RUBISCO small subunit (Keller et al. 1991), ascorbate peroxidase (Madhusudhan et al. 2003), PBG deaminase (Shashidhara and Smith 1991) and chloroplast translational initiation factor-3 (Lin et al. 1994) also occurs in the absence of an increase in the amount of mRNA encoding these proteins.

Light is just one of a number of inducers of *Euglena* enzymes. The rate of fumarase synthesis was transiently increased by ethanol (Rikin and Schwartzbach 1989a) and NADP-glutamate dehydrogenase synthesis was induced by glutamate (Parker et al. 1985). Increased enzyme synthesis occurred in the absence of an increase in the level of mRNA encoding these proteins (Parker et al. 1985; Rikin and Schwartzbach 1989a). The induction of *Euglena* enzymes by a utilizable nitrogen source and by utilizable carbon sources, organic carbon and light which allows CO_2 to be used as the sole source of carbon

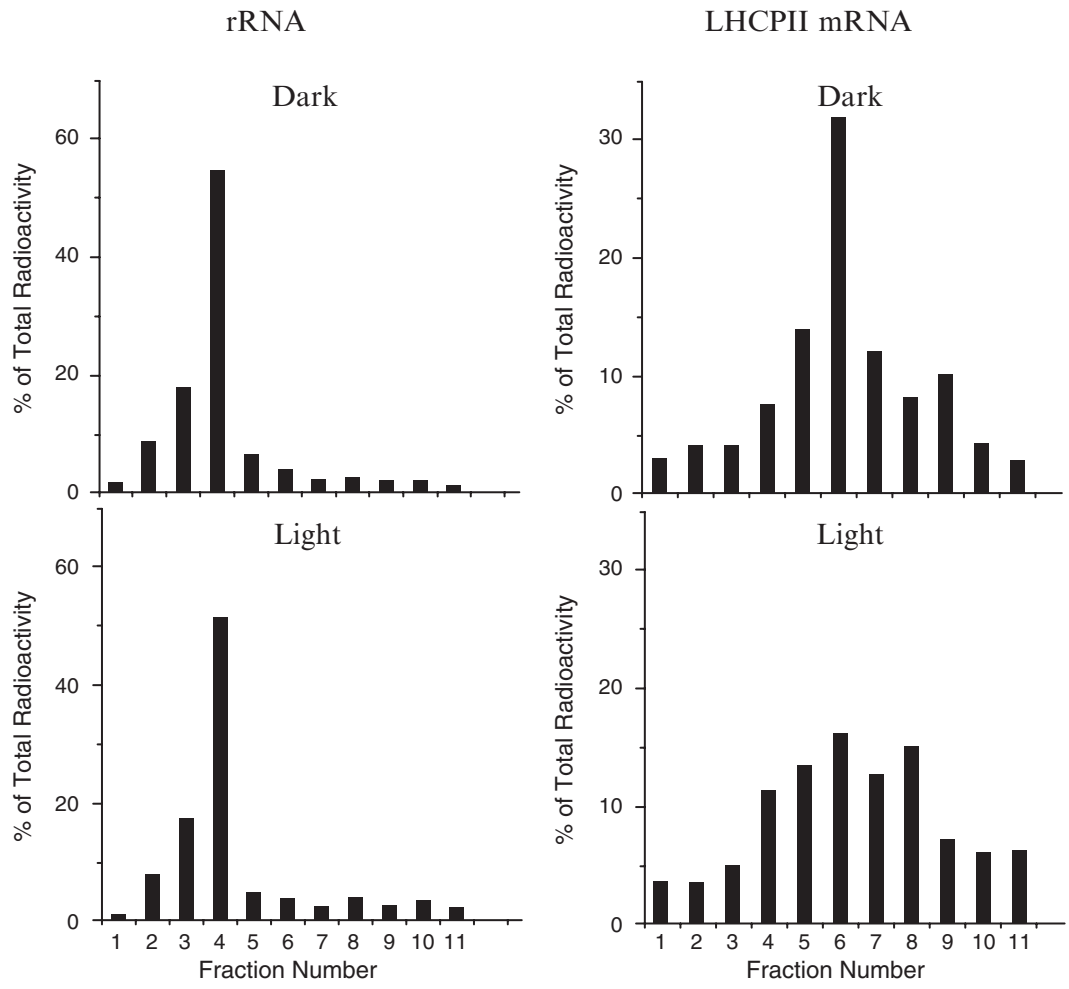

Fig. 9.3 Association of pLHCPII mRNA with polysomes in dark grown resting *Euglena* maintained in the dark or exposed to light for 24 h. Polysomes were extracted from dark grown resting *Euglena* or cells exposed to light for 24 h and size fractionated on sucrose gradients. Gradient fractions were collected from the top, RNA extracted and dot blots prepared. Small subunit rRNA was quantitated by hybridization with a ^{32}P-labelled small subunit ribosomal RNA genomic fragment (rRNA) and pLHCPII mRNA (LHCPII mRNA) was quantitated by hybridization with a ^{32}P-labelled LHCPII genomic fragment. Hybridization was visualized by fluorography and quantitated with a radioanalytical imaging system. The amount of radioactivity in each fraction is plotted as a percentage of the total radioactivity on the gradient. The majority of rRNA is in fraction 4 identifying this as the monosome fraction. The majority of LHCPII mRNA from cells in the dark (68%) and in the light (63%) is in fractions 6–11, the polysome fractions. The association of similar amounts of pLHCPII mRNA with polysomes in the dark when the rate of pLHCPII synthesis is low and in the light when the rate is approximately 100 fold higher indicates that pLHCPII induction is regulated at the translational rather than the transcriptional level. Modified from (Kishore and Schwartzbach 1992b)

and energy for growth, in the absence of increases in the level of mRNA encoding the induced enzymes strongly suggests that *Euglena* nuclear gene expression is controlled predominately at the translational rather than the transcriptional level.

9.8 Conclusions

Euglena is a unicellular organism that can grow on a large variety of organic carbon sources and photosynthetically using light which allows CO_2

to be used as the sole source of carbon and energy for growth. Some carbon sources utilize metabolic pathways that are required regardless of the source of carbon and energy for growth. Other carbon sources utilize metabolic pathways that are unique to a limited number of carbon sources and gratuitous to growth on most carbon sources. *Euglena* has evolved under conditions in which light is available for approximately 12 out of every 24 h and the availability of other carbon sources is highly variable. Days even months can go by until a specific carbon source is available in the environment and availability may be of short duration.

Enzyme synthesis and to a much greater extent, chloroplast biogenesis, utilize large amounts of cellular energy. It is not surprising that regulatory mechanisms evolved to prioritize carbon source utilization by rapidly altering cellular enzyme complement or in the case of light, organelle complement, in response to changes in nutrient availability. The induction of glyoxylate cycle enzymes by ethanol (Collins and Merrett 1975b; Cook and Carver 1966; Horrum and Schwartzbach 1981; Ono et al. 1994, 1995; Woodward and Merrett 1975) is simply the induction by a carbon source of the enzymes required to utilize that carbon source. *Euglena* is unique in that the chloroplast is gratuitous for growth as evidenced by the facile generation of bleached mutants which lack most if not all of their chloroplast genome (Heizmann et al. 1976, 1981, 1982; Hussein et al. 1982; Osafune and Schiff 1983; Schiff et al. 1971, 1980). In the absence of light, formation of a chloroplast is energetically wasteful. Thus, the photoinduction of chloroplast development is also an example of the induction by a carbon source, light which allows CO_2 to be used as the sole source of carbon and energy for growth, of the enzymes, in this case the organelle, required to utilize that carbon source.

The repression of chloroplast development by ethanol represents an example of catabolite repression; the repression by a carbon source of the synthesis of the enzymes, in this case an entire organelle the chloroplast, required to utilize an alternative carbon source, light and CO_2. Catabolite repression establishes a hierarchy of carbon source utilization enabling cellular energy to be expended to synthesize the enzymes required for the metabolism of a carbon source rarely found in the environment prior to expending a much larger amount of energy to produce the enzymes required for metabolism of the ubiquitous carbon source, light, that normally appears every 12 h. Many chloroplast biosynthetic pathways duplicate mitochondrial and cytoplasmic pathways. In carbon starved cells, the light induced repression of the synthesis and resultant degradation of mitochondrial and cytoplasmic proteins mobilizes cellular reserves, especially amino acids, for chloroplast development and can be viewed as a form of catabolite repression by light of mitochondrial biogenesis.

Euglena differs from most prokaryotic and eukaryotic organisms in that chloroplast development is primarily regulated at the translational rather than the transcriptional level. In contrast to most algae, the *Euglena* chloroplast is gratuitous to cell growth. In contrast to higher plants, the synthesis of chloroplast components does not have to be coordinated with cellular differentiation. *Euglena* evolved in an environment where availability of specific carbon sources including light was constantly changing. The major regulatory question facing *Euglena* was what enzyme complement or organelle must be made to utilize the available carbon source before it is no longer present in the environment. By constitutively synthesizing mRNAs for chloroplast constituents and enzymes unique to the metabolism of specific carbon sources such as ethanol while only translating these mRNAs when the encoded proteins are required to utilize the inducing carbon source, *Euglena* maintains the ability to rapidly adapt its metabolic capacity to utilize a constantly changing array of carbon sources including light for growth.

References

App AA, Jagendorf AT (1963) Repression of chloroplast development in *Euglena gracilis*. J Protozool 10:340–343

Barnett WE, Schwartzbach SD, Farrelly JG, Schiff JA, Hecker LI (1976) Comments on the translational and transcriptional origin of Euglena chloroplastic aminoacyl-tRNA synthetases. Arch Microbiol 109(3): 201–203

Beale SI, Foley T (1982) Induction of delta-aminolevulinic-acid synthase activity and inhibition of heme-synthesis in Euglena-gracilis by N-methyl mesoporphyrin-Ix. Plant Physiol 69(6):1331–1333

Beale SI, Foley T, Dzelzkalns V (1981) Delta-aminolevulinic-acid synthase from Euglena-gracilis. Proc Natl Acad Sci U S A 78(3):1666–1669

Bingham S, Schiff JA (1979a) Events surrounding the early development of Euglena chloroplasts. 15. Origin of plastid thylakoid polypeptides in wild-type and mutant cells. Biochim Biophys Acta 547(3):512–530

Bingham S, Schiff JA (1979b) Events surrounding the early development of Euglena chloroplasts. 16. Plastid thylakoid polypeptides during greening. Biochim Biophys Acta 547(3):531–543

Bouet C, Schantz R, Dubertret G, Pineau B, Ledoigt G (1986) Translational regulation of protein synthesis during light-induced chloroplast development in Euglena. Planta 167(4):511–520

Bovarnick JG, Chang SW, Schiff JA, Schwartzbach SD (1974a) Events surrounding the early development of Euglena chloroplasts: experiments with streptomycin in non-dividing cells. J Gen Microbiol 83(0):51–62

Bovarnick JG, Schiff JA, Freedman Z, Egan JM (1974b) Events surrounding early development of Euglena chloroplasts-cellular origins of chloroplast enzymes in Euglena. 4. Cellular origins of chloroplast enzymes in Euglena. J Gen Microbiol 83:63–71

Brandt P, Winter J (1987) The influence of permanent light and of intermittent light on the reconstitution of the light-harvesting system in regreening Euglena-gracilis. Protoplasma 136(1):56–62

Breitenberger CA, Graves MC, Spremulli LL (1979) Evidence for the nuclear location of the gene for chloroplast elongation factor G. Arch Biochem Biophys 194(1):265–270

Brunold C, Schiff JA (1976) Studies of sulfate utilization of algae: 15. Enzymes of assimilatory sulfate reduction in euglena and their cellular localization. Plant Physiol 57(3):430–436

Buetow DE (1967) Acetate repression of chlorophyll synthesis in *Euglena gracilis*. Nature 213(5081): 1127–1128

Cannons A, Merrett MJ (1983) The regulation of synthesis of mitochondrial enzymes in regreening and division-synchronized Euglena cultures. Planta 159(2):125–129

Cannons AC, Merrett MJ (1984) Regulation of synthesis of citrate synthase in regreening Euglena gracilis. Eur J Biochem 142(3):597–602

Cannons A, Merrett MJ (1985) Citrate-synthase mRNA in relation to enzyme synthesis in division-synchronized Euglena cultures. Planta 164(4):529–533

Chelm BK, Hallick RB (1976) Changes in expression of chloroplast genome of Euglena-gracilis during chloroplast development. Biochemistry 15(3):593–599

Chelm BK, Hoben PJ, Hallick RB (1977a) Cellular content of chloroplast DNA and chloroplast ribosomal-RNA genes in Euglena-gracilis during chloroplast development. Biochemistry 16(4):782–786

Chelm BK, Hoben PJ, Hallick RB (1977b) Expression of chloroplast ribosomal-RNA genes of Euglena-gracilis during chloroplast development. Biochemistry 16(4): 776–781

Chelm BK, Gray PW, Hallick RB (1978) Mapping of transcribed regions of Euglena-gracilis chloroplast DNA. Biochemistry 17(20):4239–4244

Chelm BK, Hallick RB, Gray PW (1979) Transcription program of the chloroplast genome of Euglena-gracilis during chloroplast development. Proc Natl Acad Sci U S A 76(5):2258–2262

Codd GA, Merrett MJ (1970) Enzymes of the glycollate pathway in relation to greening in *Euglena gracilis*. Planta 95(2):127–132

Codd GA, Merrett MJ (1971) The regulation of glycolate metabolism in division synchronized cultures of Euglena. Plant Physiol 47(5):640–643

Cohen D, Schiff JA (1976) Events surrounding the early development of Euglena chloroplasts. Photoregulation of the transcription of chloroplastic and cytoplasmic ribosomal RNAs. Arch Biochem Biophys 177(1): 201–216

Collins N, Merrett MJ (1975a) Localization of glycollate-pathway enzymes in Euglena. Biochem J 148(2): 321–328

Collins N, Merrett MJ (1975b) Microbody-marker enzymes during transition from phototrophic to organotrophic growth in Euglena. Plant Physiol 55(6): 1018–1022

Cook JR, Carver M (1966) Partial Photo-repression of glyoxylate by-pass in Euglena. Plant Cell Physiol 7(3):377–383

Corriveau JL, Beale SI (1986) Influence of Gabaculine on growth, chlorophyll synthesis, and delta-aminolevulinic-acid synthase activity in Euglena-gracilis. Plant Sci 45(1):9–17

Cunningham FX, Schiff JA (1986a) Chlorophyll-protein complexes from *Euglena gracilis* and mutants deficient in chlorophyll b: I. Pigment composition. Plant Physiol 80(1):223–230

Cunningham FX, Schiff JA (1986b) Chlorophyll-protein complexes from *Euglena gracilis* and mutants deficient in chlorophyll b: II. Polypeptide composition. Plant Physiol 80(1):231–238

Cushman JC, Price CA (1986) Synthesis and turnover of proteins in proplastids and chloroplasts of *Euglena gracilis*. Plant Physiol 82(4):972–977

Diamond J, Schiff JA, Kelner A (1975) Photoreactivating enzyme from euglena and the control of its intracellular level. Arch Biochem Biophys 167(2):603–614

Dockerty A, Merrett MJ (1979) Isolation and enzymic characterization of euglena proplastids. Plant Physiol 63(3):468–473

Dos Santos FV, Rocchetta I, Conforti V, Bench S, Feldman R, Levin MJ (2007) Gene expression patterns in *Euglena gracilis*: insights into the cellular response to environmental stress. Gene 389(2):136–145

Dubertret G (1981) Functional and structural organization of chlorophyll in the developing photosynthetic membranes of Euglena-gracilis-Z .II. Characteristics of the late formation of active photosystem-II reaction centers during first stages of greening. Plant Physiol 67(1):47–53

Dwyer MR, Smillie RM (1970) A light-induced beta-1,3-glucan breakdown associated with differentiation of chloroplasts in Euglena-Gracilis. Biochim Biophys Acta 216(2):392–401

Dwyer MR, Smillie RM (1971) Beta-1,3-glucan - a source of carbon and energy for chloroplast development in Euglena-gracilis. Aust J Biol Sci 24(1):15–22

Dwyer MR, Smydzuk J, Smillie RM (1970) Synthesis and breakdown of beta-1,3-glucan in Euglena-gracilis during growth and carbon depletion. Aust J Biol Sci 23(5):1005–1013

Eberly SL, Spremulli GH, Spremulli LL (1986) Light induction of the Euglena chloroplast protein synthesis elongation factors: relative effectiveness of different wavelength ranges. Arch Biochem Biophys 245(2): 338–347

Egan JM, Carell EF (1972) Studies on chloroplast development and replication in Euglena: III. A study of the site of synthesis of alkaline deoxyribonuclease induced during chloroplast development in *Euglena gracilis*. Plant Physiol 50(3):391–395

Egan JM, Schiff JA (1974) re-examination of action spectrum for chlorophyll synthesis in Euglena-gracilis. Plant Sci Lett 3(2):101–105

Egan JM, Dorsky D, Schiff JA (1975) Events surrounding the early development of Euglena chloroplasts: VI. Action spectra for the formation of chlorophyll, lag elimination in chlorophyll synthesis, and appearance of TPN-dependent triose phosphate dehydrogenase and alkaline DNase activities. Plant Physiol 56(2): 318–323

Enomoto T, Sulli C, Schwartzbach SD (1997) A soluble chloroplast protease processes the Euglena polyprotein precursor to the light harvesting chlorophyll a/b binding protein of photosystem II. Plant Cell Physiol 38:743–746

Evans WR (1971) The effect of cycloheximide on membrane transport in Euglena. A comparative study with nigericin. J Biol Chem 246(20):6144–6151

Evers A, Ernst-Fonberg ML (1974) Differential responses of two carboxylases from Euglena to state of chloroplast development. FEBS Lett 46(1):233–235

Fayyaz-Chaudhary M, Merrett MJ (1984) Glycollate-pathway enzymes in mitochondria from phototrophic, organotrophic and mixotrophic cells of Euglena. Planta 162(6):518–523

Fayyaz-Chaudhary MF, Cannons AC, Merrett MJ (1984) Photoregulation of nadph-glutamate dehydrogenase in regreening cultures of Euglena-gracilis. Plant Sci Lett 34(1–2):89–94

Fayyaz-Chaudhary M, Javed Q, Merrett MJ (1985) Effect of growth-conditions on nadph-specific glutamate-dehydrogenase activity of Euglena-gracilis. New Phytol 101(3):367–376

Foley T, Beale SI (1982) Delta-aminolevulinic-acid formation from gamma,delta-dioxovaleric acid in extracts of Euglena-gracilis. Plant Physiol 70(5):1495–1502

Foley T, Dzelzkalns V, Beale SI (1982) Delta-aminolevulinic-acid synthase of Euglena-gracilis - regulation of activity. Plant Physiol 70(1):219–226

Fong F, Schiff JA (1977) Mitochondrial respiration and chloroplast development in Euglena-gracilis var bacillaris. Plant Physiol 59(6):92–92

Fox L, Erion J, Tarnowski J, Spremulli L, Brot N, Weissbach H (1980) *Euglena gracilis* chloroplast EF-Ts. Evidence that it is a nuclear-coded gene product. J Biol Chem 255(13):6018–6019

Freyssinet G (1976) Influence of culture conditions on the length of the lag period of chlorophyll synthesis in preilluminated dark-grown Euglena. Plant Physiol 57(5):831–835

Freyssinet G (1977) Protein synthesizing system of euglena - synthesis of ribosomal-proteins invivo and their characterization. Physiol Veg 15(3):519–550

Freyssinet G (1978) Determination of the site of synthesis of some Euglena cytoplasmic and chloroplast ribosomal proteins. Exp Cell Res 115(1):207–219

Freyssinet G, Schwob C (1976) Relation between paramylum content and the length of the lag period of chlorophyll synthesis during greening of dark-grown *Euglena gracilis*. Plant Physiol 57(5):824–830

Freyssinet G, Verdier G, Trabuchet G, Heizmann P, Nigon V (1972) Influence of nutritional conditions on light response in etiolated Euglena cells. Physiol Veg 10(3): 421–442

Freyssinet G, Harris GC, Nasatir M, Schiff JA (1979) Events surrounding the early development of Euglena chloroplasts: 14. Biosynthesis of cytochrome c-552 in wild type and mutant cells. Plant Physiol 63(5): 908–915

Freyssinet G, Eichholz RL, Buetow DE (1984a) Kinetics of accumulation of ribulose-1,5-bisphosphate carboxylase during greening in *Euglena gracilis*: photoregulation. Plant Physiol 75(3):850–857

Freyssinet G, Freyssinet M, Buetow DE (1984b) Kinetics of accumulation of ribulose-1,5-bisphosphate carboxylase during greening in *Euglena gracilis*: nutritional regulation. Plant Physiol 75(3):858–861

Garlaschi FM, Garlaschi AM, Lombardi A, Forti G (1974) Effect of ethanol on metabolism of Euglena-gracilis. Plant Sci Lett 2(1):29–39

Geimer S, Belicova A, Legen J, Slavikova S, Herrmann RG, Krajcovic J (2009) Transcriptome analysis of the *Euglena gracilis* plastid chromosome. Curr Genet 55(4):425–438

Gilbert CW, Buetow DE (1982) Two-dimensional gel analysis of polypeptide appearance in forming thylakoid membranes. Biochem Biophys Res Commun 107(2):649–655

Gingrich JC, Hallick RB (1985) The *Euglena gracilis* chloroplast ribulose-1,5-bisphosphate carboxylase gene. I. Complete DNA sequence and analysis of the nine intervening sequences. J Biol Chem 260(30): 16156–16161

Goins DJ, Reynolds RJ, Schiff JA, Barnett WE (1973) A cytoplasmic regulatory mutant of Euglena: constitutivity for the light-inducible chloroplast transfer RNAs. Proc Natl Acad Sci U S A 70(6):1749–1752

Gold JC, Spremulli LL (1985) *Euglena gracilis* chloroplast initiation factor 2. Identification and initial characterization. J Biol Chem 260(28):14897–14900

Gomez-Silva B, Schiff JA (1985) Synthetic abilities of Euglena chloroplasts in darkness. Biochim Biophys Acta 808(3):448–454

Gomez-Silva B, Timko MP, Schiff JA (1985) Chlorophyll biosynthesis from glutamate or 5-aminolevulinate in intact Euglena chloroplasts. Planta 165(1):12–22

Gurevitz M, Kratz H, Ohad I (1977) Polypeptides of chloroplastic and cytoplastic origin required for development of photosystem-2 activity, and chlorophyll-protein complexes, in Euglena-gracilis Z chloroplast membranes. Biochim Biophys Acta 461(3):475–488

Hallick RB, Greenberg BM, Gruissem W, Hollingsowrth MJ, Karabin GD, Narita JO, Nickoloff JA, Passavant CW, Stiegler GL (1983) Organization and expression of the chloroplast genome of *Euglena gracilis*. Structue and function of plant genomes. Plenum, New York

Hallick RB, Hollingsworth MJ, Nickoloff JA (1984) Transfer RNA genes of *Euglena gracilis* chloroplast DNA: a review. Plant Mol Biol 3(3):169–175

Harris RC, Kirk JT (1969) Control of chloroplast formation in *Euglena gracilis*. Antagonism between carbon and nitrogen sources. Biochem J 113(1):195–205

Hecker LI, Egan J, Reynolds RJ, Nix CE, Schiff JA, Barnett WE (1974) The sites of transcription and translation for Euglena chloroplastic aminoacyl-tRNA synthetases. Proc Natl Acad Sci U S A 71(5): 1910–1914

Heizmann P, Trabuchet G, Verdier G, Freyssinet G, Nigon V (1972) Influence of illumination on polysome formation in dark-grown *Euglena gracilis* cultures. Biochim Biophys Acta 277(1):149–160

Heizmann PH, Salvador GF, Nigon V (1976) Occurrence of plastidial rRNAs and plastidial structures in bleached mutants of *Euglena gracilis*. Exp Cell Res 99(2):253–260

Heizmann P, Doly J, Hussein Y, Nicolas P, Nigon V, Bernardi G (1981) The chloroplast genome of bleached mutants of *Euglena gracilis*. Biochim Biophys Acta 653(3):412–415

Heizmann P, Hussein Y, Nicolas P, Nigon V (1982) Modifications of chloroplast DNA during streptomycin induced mutagenesis in *Euglena gracilis*. Curr Genet 5(1):9–15

Hollingsworth MJ, Johanningmeier U, Karabin GD, Stiegler GL, Hallick RB (1984) Detection of multiple, unspliced precursor mRNA transcripts for the Mr 32,000 thylakoid membrane protein from *Euglena gracilis* chloroplasts. Nucleic Acids Res 12(4):2001–2017

Holowinsky AW, Schiff JA (1970) Events surrounding the early development of Euglena chloroplasts. I. Induction by preillumination. Plant Physiol 45(3): 339–347

Horrum MA, Schwartzbach SD (1980a) Absence of photo and nutritional regulation of 2 glycolate pathway enzymes in Euglena. Plant Sci Lett 20(2):133–139

Horrum MA, Schwartzbach SD (1980b) Nutritional regulation of organelle biogenesis in Euglena - repression of chlorophyll and Nadp-glyceraldehyde-3-phosphate dehydrogenase synthesis. Plant Physiol 65(2):382–386

Horrum MA, Schwartzbach SD (1980c) Nutritional regulation of organelle biogenesis in Euglena: photo- and metabolite induction of mitochondria. Planta 149(4): 376–383

Horrum MA, Schwartzbach SD (1981) Nutritional regulation of organelle biogenesis in Euglena - induction of microbodies. Plant Physiol 68(2):430–434

Horrum MA, Schwartzbach SD (1982) Induction of fumarase in resting Euglena. Biochim Biophys Acta 714(3):407–414

Houlne G, Schantz R (1987) Molecular analysis of the transcripts encoding the light-harvesting chlorophyll a/b protein in *Euglena gracilis*: unusual size of the mRNA. Curr Genet 12(8):611–616

Houlne G, Schantz R (1988) Characterization of cDNA sequences for LHCI apoproteins in *Euglena gracilis*: the mRNA encodes a large precursor containing several consecutive divergent polypeptides. Mol Gen Genet 213(2–3):479–486

Hovenkamp-Obbema R, Stegwee D (1974) Effect of chloramphenicol on development of proplastids in Euglena-gracilis .1. Synthesis of ribulosediphosphate carboxylase, Nadp-linked glyceraldehyde-3-phosphate dehydrogenase and aminolevulinate dehydratase. Z Pflanzenphysiol 73(5):430–438

Hovenkamp-Obbema R, Moorman A, Stegwee D (1974) Aminolevulinate dehydratase in greening cells of Euglena-gracilis. Z Pflanzenphysiol 72(4):277–286

Hussein Y, Heizmann P, Nicolas P, Nigon V (1982) Quantitative estimations of chloroplast DNA in bleached mutants of *Euglena gracilis*. Curr Genet 6(2):111–117

James L, Schwartzbach SD (1982) Differential regulation of phosphoglycolate and phosphoglycerate phosphatases in Euglena. Plant Sci Lett 27(2):223–232

Javed Q, Merrett MJ (1987) Mobilization of Nadph-glutamate dehydrogenase messenger-RNA in regreening cultures of Euglena-gracilis. Plant Sci 49(1): 31–36

Johanningmeier U, Hallick RB (1987) The psbA gene of DCMU-resistant *Euglena gracilis* has an amino acid substitution at serine codon 265. Curr Genet 12(6): 465–470

Karlan AW, Russell GK (1976) Aldolase levels in wild-type and mutant Euglena-gracilis. J Protozool 23(1):176–179

Karn RC, Hudock GA (1973) Photorepressible isoenzyme of malic enzyme in Euglena-gracilis strain-Z. J Protozool 20(2):316–320

Keller M, Chan RL, Tessier LH, Weil JH, Imbault P (1991) Post-transcriptional regulation by light of the biosynthesis of Euglena ribulose-1,5-bisphosphate carboxylase/oxygenase small subunit. Plant Mol Biol 17(1):73–82

Kemper ES (1982) Stimulation and inhibition of the metabolism and growth of *Euglena gracilis*. In: Buetow DE (ed) The biology of Euglena, Physiology, vol 3. Academic Press, New York, pp 197–252

Kishore R, Schwartzbach SD (1992a) Photo and nutritional regulation of the light-harvesting chlorophyll a/b-binding protein of photosystem II mRNA levels in Euglena. Plant Physiol 98(3):808–812

Kishore R, Schwartzbach SD (1992b) Translational control of the synthesis of the Euglena light harvesting chlorophyll a/b binding protein of photosystem II. Plant Sci 85:79–89

Kishore R, Muchhal U, Schwartzbach SD (1993) The presequence of Euglena LHCPII, a cytoplasmically synthesized chloroplast protein, contains a functional endoplasmic reticulum targeting domain. Proc Natl Acad Sci U S A 90:11845–11849

Klein S, Schiff JA, Holowinsky AW (1972) Events surrounding the early development of Euglena chloroplasts. II. Normal development of fine structure and the consequences of preillumination. Dev Biol 28(1): 253–273

Koziol AG, Durnford DG (2008) Euglena light-harvesting complexes are encoded by multifarious polyprotein mRNAs that evolve in concert. Mol Biol Evol 25(1):92–100

Kraus BL, Spremulli LL (1986) Chloroplast initiation factor 3 from *Euglena gracilis*. Identification and initial characterization. J Biol Chem 261(11):4781–4784

Kraus BL, Spremulli LL (1988) Evidence for the nuclear location of the genes for chloroplast IF-2 and IF-3 in Euglena. Plant Physiol 88(4):993–995

Krauspe R, Scheer A, Schaper S, Bohley P (1986) Proteolysis in *Euglena gracilis*: II. Soluble and particle-bound acidic proteinase activities of the cysteine and aspartic types during growth and chloroplast development. Planta 167(4):482–490

Krauspe R, Lerbs S, Parthier B, Wollgiehn R (1987) Light induction of translatable messenger-RNAs for chloroplastic leucyl-transfer-RNA and valyl-transfer-RNA synthetases of Euglena-gracilis. J Plant Physiol 130(4–5):327–342

Laval-Martin D, Farineau J, Pineau B, Calvayrac R (1981) Evolution of enzymes involved in carbon metabolism (phosphoenolpyruvate and ribulose-bisphosphate carboxylases, phosphoenolpyruvate carboxykinase) during the light-induced greening of *Euglena gracilis* strains Z and ZR. Planta 151(2):157–167

Lin Q, Ma L, Burkhart W, Spremulli LL (1994) Isolation and characterization of cDNA clones for chloroplast translational initiation factor-3 from *Euglena gracilis*. J Biol Chem 269(13):9436–9444

Lord JM, Merrett MJ (1971) The intracellular localization of glycollate oxidoreductase in *Euglena gracilis*. Biochem J 124(2):275–281

Madhusudhan R, Ishikawa T, Sawa Y, Shigeoka S, Shibata H (2003) Post-transcriptional regulation of ascorbate peroxidase during light adaptation of *Euglena gracilis*. Plant Sci 165(1):233–238

Mayer SM, Beale SI (1990) Light regulation of delta-aminolevulinic acid biosynthetic enzymes and tRNA in *Euglena gracilis*. Plant Physiol 94(3):1365–1375

Mayer SM, Beale SI (1991) delta-aminolevulinic acid biosynthesis from glutamatein *Euglena gracilis*: photocontrol of enzyme levels in a chlorophyll-free mutant. Plant Physiol 97(3):1094–1102

Mayer SM, Beale SI, Weinstein JD (1987) Enzymatic conversion of glutamate to delta-aminolevulinic acid in soluble extracts of *Euglena gracilis*. J Biol Chem 262(26):12541–12549

McCarthy SA, Schwartzbach SD (1984) Absence of photoregulation of abundant messenger-RNA levels in Euglena. Plant Sci Lett 35(1):61–66

McCarthy SA, James L, Schwartzbach SD (1982) Photo and nutritional regulation of chloroplast valy-transfer RNA-synthetase in Euglena. Arch Microbiol 133(2): 149–154

Miller ME, Jurgenson JE, Reardon EM, Price CA (1983) Plastid translation in organello and in vitro during light-induced development in Euglena. J Biol Chem 258(23):14478–14484

Miyatake K, Ito T, Kitaoka S (1984) Subcellular location and some properties of phosphoenolpyruvate carboxykinase (Pepck) in Euglena-gracilis. Agric Biol Chem Tokyo 48(8):2139–2141

Monroy AF, Schwartzbach SD (1983) Photocontrol of the polypeptide composition of Euglena: analysis by two-dimensional gel electrophoresis. Planta 158(3):249–258

Monroy AF, Schwartzbach SD (1984) Catabolite repression of chloroplast development in Euglena. Proc Natl Acad Sci U S A 81(9):2786–2790

Monroy AF, Schwartzbach SD (1985) Influence of photosynthesis and chlorophyll synthesis on polypeptide accumulation in greening Euglena. Plant Physiol 77(4):811–816

Monroy AF, Gomez-Silva B, Schwartzbach SD, Schiff JA (1986) Photocontrol of chloroplast and mitochondrial polypeptide levels in *Euglena*. Plant Physiol 80: 618–622

Monroy AF, Mccarthy SA, Schwartzbach SD (1987) Evidence for translational regulation of chloroplast and mitochondrial biogenesis in Euglena. Plant Sci 51(1):61–76

Montandon PE, Stutz E (1983) Nucleotide sequence of a *Euglena gracilis* chloroplast genome region coding for the elongation factor Tu; evidence for a spliced mRNA. Nucleic Acids Res 11(17):5877–5892

Muchhal US, Schwartzbach SD (1992) Characterization of a Euglena gene encoding a polyprotein precursor to the light-harvesting chlorophyll a/b-binding protein of photosystem II. Plant Mol Biol 18(2):287–299

Nakazawa M, Minami T, Teramura K, Kumamoto S, Hanato S, Takenaka S, Ueda M, Inui H, Nakano Y, Miyatake K (2005) Molecular characterization of a bifunctional glyoxylate cycle enzyme, malate synthase/isocitrate lyase, in *Euglena gracilis*. Comp Biochem Physiol 141(4):445–452

Nakazawa M, Nishimura M, Inoue K, Ueda M, Inui H, Nakano Y, Miyatake K (2011) Characterization of a bifunctional glyoxylate cycle enzyme, malate synthase/isocitrate lyase, of *Euglena gracilis*. J Eukaryot Microbiol 58(2):128–133

Neumann D, Parthier B (1973) Effects of nalidixic acid, chloramphenicol, cycloheximide, and anisomycin on structure and development of plastids and mitochondria in greening *Euglena gracilis*. Exp Cell Res 81(2):255–268

Nover L (1976) Density labeling of chloroplast-specific leucyl-transfer-RNA synthetase in greening cells of Euglena-gracilis. Plant Sci Lett 7(6):403–407

Ogren WL (1984) Photorespiration - pathways, regulation, and modification. Annu Rev Plant Phys 35: 415–442

Ono K, Miyatake K, Inui H, Kitaoka S, Nakano Y (1994) Induction of glyoxylate cycle-key enzymes, malate synthase, and isocitrate lyase in ethanol-grown *Euglena gracilis*. Biosci Biotech Bioch 58(3): 582–583

Ono K, Kawanaka Y, Izumi Y, Inui H, Miyatake K, Kitaoka S, Nakano Y (1995) Mitochondrial alcohol dehydrogenase from ethanol-grown *Euglena gracilis*. J Biochem 117(6):1178–1182

Ono K, Kondo M, Osafune T, Miyatake K, Inui H, Kitaoka S, Nishimura M, Nakano Y (2003) Presence of glyoxylate cycle enzymes in the mitochondria of *Euglena gracilis*. J Eukaryot Microbiol 50(2):92–96

Ortiz W, Stutz E (1980) Synthesis of polypeptides of the chlorophyll-protein complexes in isolated-chloroplasts of Euglena-gracilis. FEBS Lett 116(2):298–302

Osafune T, Schiff JA (1983) W10BSmL, a mutant of *Euglena gracilis var. bacillaris* lacking plastids. Exp Cell Res 148(2):530–535

Osafune T, Klein S, Schiff JA (1980) Events surrounding the early development of Euglena chloroplasts. Structure of the developing proplastid in the first hours of illumination from serial sections of wild-type cells. J Ultrastruct Res 73(1):77–90

Osafune T, Schiff JA, Hase E (1991a) Stage-dependent localization of LHCP II apoprotein in the Golgi of synchronized cells of *Euglena gracilis* by immunogold electron microscopy. Exp Cell Res 193(2): 320–330

Osafune T, Sumida S, Schiff JA, Hase E (1991b) Immunolocalization of LHCPII apoprotein in the Golgi during light-induced chloroplast development in non-dividing *Euglena* cells. J Electron Microsc 40:41–47

Parker JE, Javed Q, Merrett MJ (1985) Glutamate dehydrogenase (NADP-dependent) mRNA in relation to enzyme synthesis in *Euglena gracilis*. Evidence for post-transcriptional control. Eur J Biochem 153(3): 573–578

Parthier B, Krauspe R (1974) Chloroplast and cytoplasmic transfer RNA of Euglena-gracilis – transfer RNA-Leu of blue-green-algae as a substitute for chloroplast transfer RNA-leu. Biochem Physiol Pfl 165(1–2): 1–17

Parthier B, Krauspe R, Samtleben S (1972) Light-stimulated synthesis of aminoacyl-tRNA synthetases in greening *Euglena gracilis*. Biochim Biophys Acta 277(2):335–341

Passavant CW, Stiegler GL, Hallick RB (1983) Location of the single gene for elongation factor Tu on the *Euglena gracilis* chloroplast chromosome. J Biol Chem 258(2):693–695

Peak MJ, Peak JG, Ting IP (1972) Light-induced reduction in specific activity of malate enzyme in Euglena-gracilis-Z. Biochem Biophys Res Commun 48(5): 1074–1078

Pineau B (1982) Biosynthesis of ribulose-1.5-bisphosphate carboxylase in greening cells of *Euglena gracilis*: the accumulation of ribulose-1.5-bisphosphate carboxylase and of its subunits. Planta 156(2):117–128

Pineau B, Dubertret G, Schantz R (1985) Functional and structural organization of chlorophyll in the developing photosynthetic membranes of Euglena-gracilis Z V-separation and characterization of pigment-protein complexes of the differentiated thylakoids. Photosynth Res 6(2):159–174

Ponsgen-Schmidt E, Schneider T, Hammer U, Betz A (1988) Comparison of phosphoenolpyruvate-carboxykinase from autotrophically and heterotrophically grown Euglena and its role during dark anaerobiosis. Plant Physiol 86(2):457–462

Rabinowitz H, Reisfeld A, Sagher D, Edelman M (1975) Ribulose diphosphate carboxylase from autotrophic *Euglena gracilis*. Plant Physiol 56(3):345–350

Ravel-Chapuis P, Nigon V (1981) Analysis of the production of delta-aminolevulinic-acid and chlorophyll in Euglena-gracilis Z. Plant Sci Lett 21(4):333–343

Rawson JRY, Boerma C (1976a) Influence of growth-conditions upon number of chloroplast DNA-molecules in Euglena-gracilis. Proc Natl Acad Sci U S A 73(7):2401–2404

Rawson JRY, Boerma CL (1976b) Measurement of fraction of chloroplast DNA transcribed during chloroplast development in Euglena-gracilis. Biochemistry 15(3):588–592

Rawson JRY, Boerma CL (1979) Hybridization of EcoRI chloroplast DNA fragments of Euglena to pulse labeled RNA from different stages of chloroplast development. Biochem Biophys Res Commun 89(2): 743–749

Rawson JRY, Boerma CL, Andrews WH, Wilkerson CG (1981) Complexity and abundance of ribonucleic-acid

transcribed from restriction endonuclease fragments of Euglena chloroplast deoxyribonucleic-acid during chloroplast development. Biochemistry 20(9): 2639–2644

Reger BJ, Fairfield SA, Epler JL, Barnett WE (1970) Identification and origin of some chloroplast aminoacyl-tRNA synthetases and tRNAs. Proc Natl Acad Sci U S A 67(3):1207–1213

Richard F, Nigon V (1973) Synthesis of delta-aminolevulinic acid and chlorophyll during illumination of etiolated *Euglena gracilis*. Biochim Biophys Acta 313(1):130–149

Rikin A, Schwartzbach SD (1988) Extremely large and slowly processed precursors to the *Euglena* light harvesting chlorophyll a/b binding proteins of photosystem II. Proc Natl Acad Sci U S A 85:5117–5121

Rikin A, Schwartzbach S (1989a) Translational regulation of the synthesis of *Euglena* fumarase by light and ethanol. Plant Physiol 90:63–69

Rikin A, Schwartzbach SD (1989b) Regulation by light and ethanol of the synthesis of the light harvesting chlorophyll a/b binding protein of photosystem II in Euglena. Planta 178:76–83

Rosenberg A, Pecker M (1964) Lipid alterations in *Euglena gracilis* cells during light-induced greening. Biochemistry 3:254–258

Russell GK, Draffan AG, Schmidt GW, Lyman H (1978) Light-induced enzyme formation in a chlorophyll-less mutant of Euglena-gracilis. Plant Physiol 62(5): 678–682

Saidha T, Stern AI, Lee DH, Schiff JA (1985) Localization of a sulphate-activating system within Euglena mitochondria. Biochem J 232(2):357–365

Salvador GF (1978) Delta-aminolevulinic-acid synthesis from gamma-delta-dioxovaleric acid by acellular preparations of Euglena-gracilis. Plant Sci Lett 13(4): 351–355

Salvador GF, Beney G, Nigon V (1976) Control of delta-aminolevulinic-acid synthesis during greening of dark-grown Euglena-gracilis. Plant Sci Lett 6(3): 197–202

Schantz R, Schantz ML, Duranton H (1975) Changes in amino-acid and peptide composition of Euglena-gracilis cells during chloroplast development. Plant Sci Lett 5(5):313–324

Schiff JA (1963) Oxygen exchange by Euglena cells undergoing chloroplast development. Carnegie Inst Wash Yearbook 62:375–378

Schiff JA, Zeldin MH, Rubman J (1967) Chlorophyll formation and photosynthetic competence in euglena during light-induced chloroplast development in the presence of 3, (3,4-dichlorophenyl) 1,1-dimethyl urea (DCMU). Plant Physiol 42(12):1716–1725

Schiff JA, Lyman H, Russel GK (1971) Isolation of mutants from *Euglena gracilis*. Methods Enzymol 23:143–162

Schiff JA, Lyman H, Russel GK (1980) Isolation of mutants from *Euglena gracilis*: an addendum. Methods Enzymol 69:23–29

Schiff JA, Schwartzbach SD, Osafune T, Hase E (1991a) Photocontrol and processing of Lhcp-II apoprotein in Euglena - possible role of Golgi and other cytoplasmic sites. J Photoch Photobio B Biol 11(2):219–236

Schiff JA, Schwartzbach SD, Osafune T, Hase E (1991b) Photocontrol and processing of LHCPII apoprotein in Euglena: possible role of Golgi and other cytoplasmic sites. J Photchem Photobiol B Biol 11:219–236

Schimpf C, Govindarajan AG, Parthier BP (1982) Influence of preillumination (potentiation) and carbon substrates on plastid aminoacyl-tRNA synthetases in greening Euglena cells. Biochem Physiol Pfl 177(9):777–788

Schmidt GW, Lyman H (1974) Photocontrol of chloroplast enzyme synthesis in mutant and wild type *Euglena gracilis*. In Proceedings of the third international congress. Photosynthesis. Elsevier, Amsterdam, New York

Schuber F, Aleksijevic A, Blee E (1981) Comparative role of polyamines in division and plastid differentiation of Euglena-gracilis. Biochim Biophys Acta 675(2): 178–187

Schwartzbach SD, Frreyssinet G, Schiff JA (1974) The chloroplast and cytoplasmic ribosomes of Euglena .1 stability of chloroplast ribosomes prepared by an improved procedure. Plant Physiol 53:533–542

Schwartzbach SD, Schiff JA, Goldstein NH (1975) Events surrounding the early development of euglena chloroplasts: v. Control of paramylum degradation. Plant Physiol 56(2):313–317

Schwartzbach SD, Hecker LI, Barnett WE (1976a) Transcriptional origin of Euglena chloroplast tRNAs. Proc Natl Acad Sci U S A 73:1984–1988

Schwartzbach SD, Schiff JA, Klein S (1976b) Biosynthetic events required for lag elimination in chlorophyll synthesis in Euglena. Planta 131(1):1–9

Schwelitz FD, Cisneros PL, Jagielo JA (1978a) Effect of glucose on biochemical and ultrastructural characteristics of developing Euglena chloroplasts. J Protozool 25(3):398–403

Schwelitz FD, Cisneros PL, Jagielo JA (1978b) Effect of glucose on developing Euglena plastids. J Cell Biol 79(2):A313–A313

Schwelitz FD, Cisneros PL, Jagielo JA, Comer JL, Butterfied KA (1978c) Relationship of fixed carbon and nitrogen-sources to greening process in Euglena-gracilis strain Z. J Protozool 25(2):257–261

Shashidhara LS, Smith AG (1991) Expression and subcellular location of the tetrapyrrole synthesis enzyme porphobilinogen deaminase in light-grown *Euglena gracilis* and three nonchlorophyllous cell lines. Proc Natl Acad Sci U S A 88(1):63–67

Small GD, Sturgen RS (1976) Purification and properties of a light-inducible nuclease from *Euglena gracilis*. Nucleic Acids Res 3(5):1277–1293

Spano AJ, Schiff JA (1987) Purification, properties, and cellular localization of Euglena ferredoxin-NADP reductase. Biochim Biophys Acta 894(3): 484–498

Spano AJ, Ghaus H, Schiff JA (1987) Chlorophyll-protein complexes and other thylakoid components at the low intensity threshold in Euglena chloroplast development. Plant Cell Physiol 28(6):1101–1108

Spremulli LL (1982) Chloroplast elongation factor Tu: evidence that it is the product of a chloroplast gene in Euglena. Arch Biochem Biophys 214(2):734–741

Srinivas U, Lyman H (1980) Photomorphogenic regulation of chloroplast replication in Euglena - enhanced loss of chloroplast DNA in red-light. Plant Physiol 66(2):295–301

Stern AI, Epstein HT, Schiff JA (1964a) Studies of chloroplast development in Euglena. VI Light intensity as a controlling factor in development. Plant Physiol 39(2):226–231

Stern AI, Schiff JA, Epstein HT (1964b) Studies of chloroplast development in Euglena. V. pigment biosynthesis, photosynthetic oxygen evolution and carbon dioxide fixation during chloroplast development. Plant Physiol 39(2):220–226

Stevenson JK, Hallick RB (1994) The psaA operon pre-mRNA of the *Euglena gracilis* chloroplast is processed into photosystem I and II mRNAs that accumulate differentially depending on the conditions of cell growth. Plant J 5(2):247–260

Sulli C, Schwartzbach SD (1995) The polyprotein precursor to the *Euglena* light harvesting chlorophyll a/b--binding protein is transported to the Golgi apparatus prior to chloroplast import and polyprotein processing. J Biol Chem 270:13084–13090

Sumida S, Ehara T, Osafune T, Hase E (1987) Ammonia-induced and light-induced degradation of paramylum in Euglena-gracilis. Plant Cell Physiol 28(8):1587–1592

Timko MP, Schiff JA (1983) Membrane-bound coupling factor atpase activity during light-induced chloroplast development in Euglena-gracilis. Physiol Plantarum 58(1):41–46

Verdier G (1975) Synthesis and translation site of light-induced mRNAs in etiolated *Euglena gracilis*. Biochim Biophys Acta 407(1):91–98

Verdier G (1979a) Poly(adenylic acid)-containing RNA of *Euglena gracilis* during chloroplast development. 2. Transcriptional origin of the different RNA. Eur J Biochem 93(3):581–586

Verdier G (1979b) Poly(adenylic acid)-containing RNA of *Euglena gracilis* during chloroplast development. I. Analysis of their complexity by hybridization to complementary DNA. Eur J Biochem 93(3):573–580

Verdier G, Trabuchet G, Heizmann P, Nigon V (1973) Effect of illumination on RNA synthesis and poly(adenylic acid) sequences in cultures of etiolated *Euglena gracilis*. Biochim Biophys Acta 312(3):528–539

Vesteg M, Vacula R, Burey S, Loffelhardt W, Drahovska H, Martin W, Krajcovic J (2009) Expression of nucleus-encoded genes for chloroplast proteins in the flagellate *Euglena gracilis*. J Eukaryot Microbiol 56(2):159–166

Weinstein JD, Beale SI (1983) Separate physiological roles and subcellular compartments for two tetrapyrrole biosynthetic pathways in *Euglena gracilis*. J Biol Chem 258(11):6799–6807

Weiss C, Houlne G, Schantz ML, Schantz R (1988) Photoregulation of the synthesis of chloroplast membrane-proteins in Euglena-gracilis. J Plant Physiol 133(5):521–528

Weiss C, Houlne G, Schantz R (1992) Photocontrol of thylakoid protein synthesis in Euglena: differential post-transcriptional regulation depending on nutritional conditions. Planta 188(4):468–477

Woodward J, Merrett MJ (1975) Induction potential for glyoxylate cycle enzymes during the cell cycle of *Euglena gracilis*. Eur J Biochem 55(3):555–559

Yi LSH, Gilbert CW, Buetow DE (1985) Temporal appearance of chlorophyll-protein complexes and the N,N1-dicyclohexylcarbodiimide-binding coupling factoro-subunit-III in forming thylakoid membranes of Euglena-gracilis. J Plant Physiol 118(1):7–21

Yokota A, Kitaoka S (1979) Metabolism of glycolate in Euglena gracilis. 3. Occurrence of glycolate dehydrogenase in mitochondria and microsomes in streptomycin-bleached mutant of Euglena, Gracilis Z. Agric Biol Chem Tokyo 43(4):855–857

Yokota A, Kitaoka S (1981) Metabolism of glycolate in Euglena-gracilis. 5. Occurrence and subcellular-distribution of enzymes involved in the glycolate pathway and their physiological-function in a bleached mutant of Euglena-gracilis Z. Agric Biol Chem Tokyo 45(1):15–22

Yokota A, Nakano Y, Kitaoka S (1978) Different effects of some growing conditions on glycolate dehydrogenase in mitochondria and microbodies in *Euglena gracilis*. Agric Biol Chem 42:115–120

Yokota A, Haga S, Kitaoka S (1985a) Purification and some properties of glyoxylate reductase (NADP+) and its functional location in mitochondria in *Euglena gracilis* z. Biochem J 227(1):211–216

Yokota A, Suehiro S, Kitaoka S (1985b) Purification and some properties of mitochondrial glutamate:glyoxylate aminotransferase and mechanism of its involvement in glycolate pathway in *Euglena gracilis* z. Arch Biochem Biophys 242(2):507–514

Zeldin MH, Skea W, Matteson D (1973) Organelle formation in the presence of a protease inhibitor. Biochem Biophys Res Commun 52(2):544–549

Protein Targeting to the Plastid of *Euglena*

10

Dion G. Durnford and Steven D. Schwartzbach

Abstract

The lateral transfer of photosynthesis between kingdoms through endosymbiosis is among the most spectacular examples of evolutionary innovation. *Euglena*, which acquired a chloroplast indirectly through an endosymbiosis with a green alga, represents such an example. As with other endosymbiont-derived plastids from eukaryotes, there are additional membranes that surround the organelle, of which *Euglena* has three. Thus, photosynthetic genes that were transferred from the endosymbiont to the host nucleus and whose proteins are required in the new plastid, are now faced with targeting and plastid import challenges. Early immunoelectron microscopy data suggested that the light-harvesting complexes, photosynthetic proteins in the thylakoid membrane, are post-translationally targeted to the plastid via the Golgi apparatus, an unexpected discovery at the time. Proteins targeted to the *Euglena* plastid have complex, bipartite presequences that direct them into the endomembrane system, through the Golgi apparatus and ultimately on to the plastid, presumably via transport vesicles. From transcriptome sequencing, dozens of plastid-targeted proteins were identified, leading to the identification of two different presequence structures. Both have an amino terminal signal peptide followed by a transit peptide for plastid import, but only one of the two classes of presequences has a third domain—the stop transfer sequence. This discovery implied two different transport mechanisms; one where the protein was fully inserted into the lumen of the ER and another where the protein remains attached to, but effectively out-

D.G. Durnford, Ph.D.
Department of Biology, University of New Brunswick, 10 Bailey Drive, Fredericton, NB, Canada, E3B 5A3

S.D. Schwartzbach (✉)
Department of Biological Sciences, University of Memphis, Memphis, TN 38152, USA
e-mail: sdschwrt@memphis.edu

S.D. Schwartzbach, S. Shigeoka (eds.), *Euglena: Biochemistry, Cell and Molecular Biology*, Advances in Experimental Medicine and Biology 979, DOI 10.1007/978-3-319-54910-1_10

side, the endomembrane system. In this review, we will discuss the biochemical and bioinformatic evidence for plastid targeting, discuss the evolution of the targeting system, and ultimately provide a working model for the targeting and import of proteins into the plastid of *Euglena*.

Keywords
Chloroplast protein import • Complex plastids • Endosymbiosis • *Euglena* • Plastid evolution • Precursor protein • Signal peptide • Transit peptide

Abbreviations

CER	Chloroplast endoplasmic reticulum
C-terminal	Carboxy terminal
EndoH	Endoglycosidase H
ER	Endoplasmic reticulum
ERAD	ER associated degradation
EST	Expressed sequence tag
LHC	Light-harvesting complex
LHCPII	Light harvesting chlorophyll a/b binding protein of photosystem II
N-linked	Asparagine linked
NSF	N-ethylmaleimide-Sensitive factor
N-terminal	Amino terminal
PCP	Soluble peridinin-chlorophyll a-protein
pLHCPII	Precursor to the light harvesting chlorophyll a/b binding protein of photosystem II
pOEC30	Precursor to the 30-kDa subunit of the oxygen-evolving complex
pRbcS	Precursor to the small subunit of ribulose bisphosphate carboxylase-oxygenase
Rbc	Ribulose bisphosphate carboxylase-oxygenase
RbcS	Small subunit of ribulose bisphosphate carboxylase-oxygenase
SELMA	Symbiont-derived ERAD-like machinery
SNARE	Soluble NSF attachment protein receptor
TIC	Translocon at the inner chloroplast envelope
TOC	Translocon at the outer chloroplast envelope

10.1 Introduction

The challenge of targeting proteins to complex plastids was recognized when microscopy studies found that plastids in a variety of algal groups (Gibbs 1970, 1978, 1981a, b; Lefortran and Pineau 1980) had three or four envelope membranes rather than the two membranes of land plants, red and green algae. The additional membranes clearly pose a challenge for protein import but also act as a living "fossile record" as to the origin of the plastid (Gibbs 1978, 1981b; Whatley and Whatley 1981). The endosymbiotic origin of primary plastids (those with two envelope membranes) from a photosynthetic cyanobacteria-like prokaryote is generally accepted (Gray and Doolittle 1982). But, the discovery of additional membranes around the complex plastids of many eukaryotic algae was crucial evidence supporting the hypothesis that complex plastids evolved secondarily from ancient endosymbioses with photosynthetic eukaryotes (Cavalier-Smith 2003; Keeling 2013).

The complex plastids of *Euglena* and dinoflagellates possess three plastid envelope membranes rather than the two envelope membranes of the simple chloroplasts found in green algae, red algae, glaucophytes and plants (Gibbs 1970, 1978, 1981b; Lefortran and Pineau 1980). The outermost membrane lacks bound ribosomes and it is generally hypothesized to have evolved from the plasma membrane of the host or the phagosomal membrane that surrounded the eukaryotic photosynthetic endosymbiont following uptake by phagocytosis. With the internal endomembrane systems being dynamic, and the difficulties

of purifying distinct membrane systems, it is a challenge to validate the origin of the outer most envelope membrane.

The complex plastids of stramenopiles, cryptomonads, haptophytes, apicoplastida and photosynthetic members of the rhizaria were also acquired via secondary endosymbiosis and have a total of four envelope membranes (Gibbs 1981a; Keeling 2013). Usually, the outermost membrane is studded with ribosomes, implying that this membrane is part of the host's endomembrane system and directly derived from the endoplasmic reticulum (ER), and it has been named the chloroplast ER (CER) (Gibbs 1970, 1981a; Osafune et al. 1991b). Discovery of the CER provided the first clue that nucleus-encoded chloroplast localized proteins are co-translationally imported into complex plastids with four envelope membranes.

Targeting proteins and translocating them into an organelle requires specific targeting information that resides within the protein to be targeted. For many organelles, like the chloroplast, mitochondria and the ER, this information is found in an amino-terminal (N-terminal) presequence that is proteolytically removed within the organelle, yielding the mature protein. Nucleus encoded cytoplasmically synthesized proteins that are post-translationally imported into the simple plastids of red algae, green algae, glaucophytes and plants that evolved directly from a cyanobacterial endosymbiont have N-terminal presequences called transit peptides that are necessary and sufficient for targeting to the organelle (Bruce 2000). The transit peptide is usually removed once the protein enters the plastid by a specific protease.

The ribosome studded CER envelope membrane of complex plastids with four envelope membranes suggests that the requirements for protein import differs fundamentally from the mechanism of import into simple plastids. The sequence of the first nuclear gene encoding a light harvesting complex (LHC) protein localized to the complex plastid of diatoms, which has four membranes, indicated that protein targeting to and import into complex chloroplasts was in fact fundamentally different from import into simple chloroplasts (Bhaya and Grossman 1991; Grossman et al. 1990). To navigate across these four membranes, the LHC has a large N-terminal presequence. The chemical properties of the first portion of this peptide were similar to a classical signal peptide (Grossman et al. 1990) that mediates co-translational import into the ER (von Heijne 1988) leading to the hypothesis that targeting to the plastid was via the endomembrane system. In an *in vitro* ER import system composed of pancreatic canine microsomes, the diatom LHC leader sequence was sufficient to mediate co-translational import of the protein into the microsomes (Bhaya and Grossman 1991). This demonstrated that import of proteins into complex plastids with four envelope membranes is initiated by co-translational transport across the CER. The diatom N-terminal presequence is however bipartite. Signal peptidase cleavage exposes a second presequence domain that functions as a transit peptide that mediates translocation through the remaining three envelope membranes and many details of this process have been elucidated (Maier et al. 2015).

One of the more startling discoveries with respect to *Euglena* biology was the detection by immunoelectron microscopy of the light-harvesting chlorophyll a/b binding protein of photosystem II (LHCPII) in the Golgi apparatus (Osafune et al. 1990, 1991a, b; Schiff et al. 1991). Early sequencing efforts of *Euglena* genes encoding a number of plastid-targeted proteins identified a large bipartite presequence composed of an N-terminal domain having characteristics of a signal peptide that mediates co-translational import into the ER and a second domain having features resembling a transit peptide that mediates import into chloroplasts (Chan et al. 1990; Henze et al. 1995; Houlne and Schantz 1987; Kishore et al. 1993; Lin et al. 1994; Plaumann et al. 1997; Santillan Torres et al. 2003; Sharif et al. 1989; Shigemori et al. 1994; Vacula et al. 1999). Considering the evidence, the absence of ribosomes on the outer plastid envelope membrane, the immunogold localization of LHCPII to the Golgi apparatus and the presence of a N-terminal presequence signal peptide provided compelling evidence for co-translational transport of chloroplast protein precursors into the ER,

vesicular transport from the ER to the Golgi apparatus and then from the Golgi apparatus to the chloroplast for subsequent translocation through the plastid envelope into the plastid.

Although proteins targeted to complex chloroplasts with three and four envelope membranes have similar bipartite presequences, there appears to be fundamental differences in the mechanism of import. The purpose of this review is to discuss the presequence structural features and the *in vivo* and *in vitro* experimental evidence demonstrating vesicular transport of plastid proteins from their site of synthesis in the ER to the *Euglena* plastid. A model for presequence evolution and protein import into *Euglena* complex plastids will also be presented.

10.2 *In Vivo* Elucidation of the Chloroplast Protein Trafficking Pathway.

Immunoelectron microscopy provided the first indication that chloroplast proteins synthesized in the cytoplasm were not directly imported into the triple envelope complex chloroplasts of *Euglena* and dinoflagellates. In light-dark division synchronized *Euglena*, rapid pLHCPII synthesis begins 6–8 h after the start of the light period and synthesis declines during the dark period being undetectable during the last six hours of darkness (Brandt and von Kessel 1983). LHCPII is not immunolocalized to the Golgi apparatus during the latter phase of the dark period and the start of the light period when pLHCPII synthesis is low (Osafune et al. 1991a; Schiff et al. 1991). Coincident with the increased synthesis of pLHCPII during the light period, immunogold labeling of the Golgi apparatus increases. Extensive immunogold labeling of the Golgi apparatus and chloroplast but not the ER is observed in synchronous cells at 10 h of the light period (Fig. 10.1a (Osafune et al. 1991a; Schiff et al. 1991). A three dimensional reconstruction from serial sections of synchronous cells at 10 h of the light period immunogold labeled with LHCPII antibody (Fig. 10.1b yellow dots) localized LHCPII only to the Golgi apparatus (Fig. 10.1b brown) and chloroplast (Fig. 10.1b green (Schwartzbach et al. 1998)). LHCPII was absent from the cytoplasm (Fig. 10.1b black) and the nucleus (Fig. 10.1b blue dots). In light dark synchronized cells of the dinoflagellate *Gonyaulax*, the rate of synthesis of ribulose bisphosphate carboxylase-oxygenase (Rbc,) and the peridinin-chlorophyll a-protein (PCP) is high at the start of the light phase (Nassoury et al. 2003). In *Gonyaulax*, both Rbc, and PCP were immunolocalized to the Golgi apparatus and chloroplast at the time of rapid protein synthesis (Nassoury et al. 2003) suggesting that in both *Euglena* and dinoflagellates, proteins are transported from the Golgi apparatus to the chloroplast.

Exposure of dark grown resting *Euglena* to light slowly increases the rate of pLHCPII synthesis 50–100 fold with the maximum rate being attained 12–24 h after light exposure (Rikin and Schwartzbach 1989; Schiff et al. 1991). LHCPII was immunolocalized to the Golgi apparatus during the early hours of light exposure with little immunogold present in the developing thylakoids (Osafune et al. 1991b; Schiff et al. 1991). Both the Golgi and thylakoids were immunogold labeled with LHCPII antibody in cells exposed to light for 48 h, a time of active pLHCPII synthesis. By 96 h when the rate of pLHCPII synthesis is low, only the thylakoids were immunolabelled (Osafune et al. 1991b; Schiff et al. 1991). Thylakoid formation and LHCPII synthesis are not induced when dark grown *Euglena* are exposed to a low light intensity (Spano et al. 1987). Transfer to high light induces thylakoid formation and pLHCPII synthesis. LHCPII was not detected by immunoelectron microscopy in cells exposed to a low light intensity but was detected in both the Golgi apparatus and developing thylakoids in cells transferred to high light (Osafune et al. 1990; Schiff et al. 1991). Taken together, the immunolocalization of LHCPII to the Golgi apparatus only when cells are actively synthesizing LHCP and prior to thylakoid immunogold labeling suggest that pLHCPII is transported into the Golgi apparatus prior to chloroplast localization.

The *Euglena* LHCs are polyproteins encoded by high molecular weight mRNAs (Houlne and Schantz 1987, 1988; Koziol and Durnford 2008;

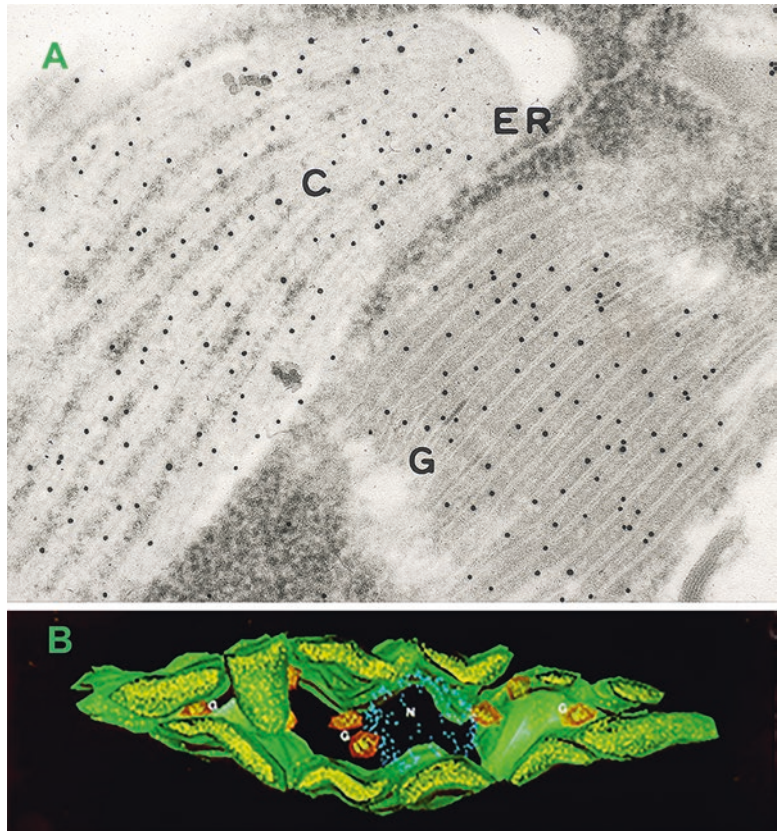

Fig. 10.1 Immunogold localization of LHCPII in synchronously dividing *Euglena*. (**a**) A section of a synchronously dividing cell at 10 h of a 14:10 light dark cycle immunogold labeled with antibody to LHCPII. Immunogold is localized in the chloroplast (C) and Golgi apparatus (G) but not in the endoplasmic reticulum (ER) (modified from (Osafune et al. 1991a). (**b**) A computer generated three dimensional model constructed from serial sections of a synchronously dividing cell at 10 h of a 14:10 light dark cycle immunogold labeled with antibody to LHCPII. Immunogold labeled LHCPII (*yellow dots*) is localized in the chloroplasts (*green*) and Golgi apparatus (*brown*) but not in the nucleus (*blue dots*) or the cytoplasm (*black*) (modified from (Schwartzbach et al. 1998)

Muchhal and Schwartzbach 1992, 1994). Sequence analysis has shown that the pLHC polyproteins are composed of multiple LHC subunits joined by a conserved decapeptide linker. Immunoprecipitation of cell free translation products and total cellular protein from pulse labeled cells with antibody to *Euglena* LHCPII have identified four high molecular weight pLHCPII polyproteins (Rikin and Schwartzbach 1988, 1989; Sulli and Schwartzbach 1995). The protease that cleaves the decapeptide linker releasing individual mature LHCPIIs from the pLHCPII polyprotein is localized in the chloroplast (Enomoto et al. 1997). Pulse chase immunoprecipitation experiments have shown that the half life for conversion of the pLHCPIIs to mature LHCPII is approximately 20 min (Rikin and Schwartzbach 1988). pLHCPII mRNA is associated predominantly with membrane bound polysomes (Kishore and Schwartzbach 1992) suggesting it is translocated into the ER prior to chloroplast localization. It appears that approximately 20 min is required to transport the pLHCPII polyprotein from its site of synthesis on ER associated polysomes to the chloroplast where it is proteolytically processed into mature LHCPIIs.

Pulse chase intracellular localization experiments were performed to determine directly if pLHCPII is transported from its site of synthesis

on ER bound polysomes, to the Golgi apparatus and then to the chloroplast where the polyprotein is proteolytically processed to mature LHCPII. When *Euglena* was exposed to light for 24 h to induce LHCPII synthesis and pulse labeled for 10 min with ^{35}S-sulfate, the high molecular weight pLHCPIIs were the only proteins immunoprecipitated with antibody to LHCPII (Rikin and Schwartzbach 1988, 1989; Sulli and Schwartzbach 1995). The pLHCPIIs were found in the ER and Golgi fractions on sucrose gradients (Sulli and Schwartzbach 1995) but could not be detected in chloroplast fractions. During a 20 and 40 min chase, the fraction of pLHCPII in the ER decreased and the amount in the Golgi increased. Mature LHCPII was never found in the ER and Golgi fractions. Mature LHCPII accumulated in the chloroplast and thylakoid fraction during the 20 and 40 min chase (Sulli and Schwartzbach 1995). The time dependent decrease in ER and Golgi localized pLHCPII coincident with the accumulation of mature LHCPII in the chloroplast and thylakoids indicates that pLHCPII is synthesized in the ER, transported to the Golgi apparatus and then from the Golgi apparatus to the chloroplast.

The precursor to the small subunit of ribulose bisphosphate carboxylase-oxygenase (pRbcS,), a soluble stromal protein, is also a polyprotein composed of 8 RbcS, units covalently joined by a decapeptide linker (Chan et al. 1990). The half life for conversion of pRbcS, to mature RbcS, is 12 min (Keller et al. 1991; Sulli and Schwartzbach 1996) indicating that pRbcS transport from its site of synthesis to the chloroplast, the site of polyprotein processing, is approximately twice as fast as the transport of pLHCPII to the chloroplast. Pulse chase immunoprecipitation studies found that as seen for pLHCPII, pRbcS is found on sucrose gradients first in the ER fractions, then in the Golgi fractions and it is never detected in the chloroplast fractions (Sulli and Schwartzbach 1996). Concomittant with a decrease in Golgi localized pRbcS is an increase in chloroplast localized mature RbcS indicating that as found for pLHCPII, pRbcS is transported from the ER to the Golgi apparatus and then to the chloroplast where it is converted into mature RbcS.

An N-terminal sequence, a signal peptide, initiates co-translational translocation across the ER membrane into the lumen (von Heijne 1988). Hydrophobic domains within the presequence or the mature protein can stop translocation anchoring the protein in the ER membrane. The pLHCPII and pRbcS N-terminal presequences contain a hydrophobic region within the presequence signal peptide domain which is removed upon presequence cleavage by signal peptidase and a second hydrophobic region within the presequence transit peptide domain which is not lost from the presequence upon signal peptidase cleavage (Chan et al. 1990; Durnford and Gray 2006; Kishore et al. 1993; Sulli et al. 1999). Each mature LHCPII contains three additional hydrophobic domains (Muchhal and Schwartzbach 1992). If just one of these hydrophobic domains within the presequence or mature protein functions as a stop transfer membrane anchor sequence, pLHCPII and pRbcS would be co-translationally inserted into the ER membrane and transported to the chloroplast in vesicles as an integral membrane protein rather than in the vesicle lumen as a soluble protein.

Peripheral membrane proteins can be stripped from their associated membranes by washing with potassium acetate leaving behind proteins integrated in the membrane or located in the lumen/stroma of the organelles being washed. Washing with Na_2CO_3 opens the membrane releasing luminal and stromal proteins but not integral membrane proteins. Washing intact chloroplasts, ER or Golgi membranes with potassium acetate did not remove *in vivo* synthesized pLHCPII, LHCPII, pRbcS, or RbcS, from these fractions (Sulli and Schwartzbach 1995, 1996). pLHCPII and pRbcS were not removed from ER or Golgi membranes by Na_2CO_3 indicating they are integral membrane proteins that were co-translationally inserted into the ER membrane. Mature LHPII, an integral thylakoid membrane protein, was not released from the thylakoid by washing chloroplasts with Na_2CO_3 (Sulli and Schwartzbach 1995) while mature RbcS, a soluble stromal protein, was released (Sulli and Schwartzbach 1996). Since the only hydrophobic domain in pRbcS after cleavage of the presequence signal peptide by signal peptide processing protease is the second presequence hydrophobic domain,

these results suggest that this domain must function as a stop transfer sequence anchoring pLHCPII and pRbcS in the ER membrane.

Treatment of an ER, Golgi membrane fraction with a protease that can not penetrate the membrane, a protease protection assay, can provide information regarding the topology of an integral membrane protein. Trypsin digestion of ER and Golgi membranes containing pLHCPII or pRbcS produced multiple protected fragments (Sulli and Schwartzbach 1995, 1996). It appears that both pLHCPII, the precursor of an integral thylakoid membrane protein, and pRbcS, the precursor of a soluble stromal protein, are transported from the ER to the Golgi apparatus to the chloroplast as integral membrane proteins. Upon fusion of the transport vesicle with the chloroplast outer membrane, the precursor would not be within the outermost and middle envelope membrane intermembrane space but would be an integral outer envelope membrane protein with multiple membrane spanning domains. Not only would the precursor need to be translocated through the middle and innermost chloroplast envelope membranes, it would also need to be removed from and translocated through the outermost envelope membrane.

10.3 The *Euglena* Plastid Targeting Presequence Structure; *Two-Classes of Euglena* Plastid Targeting Presequences

Understanding the mechanism of protein import into *Euglena* chloroplasts was limited by the few precursor protein sequences available precluding an assessment of the generality of a proposed targeting mechanism. Completion of an expressed sequence tag (EST) project (Durnford and Gray 2006), however, allowed the identification of over a hundred *Euglena* plastid-targeted proteins and their N-terminal presequences. These bipartite targeting sequences were surprisingly complex (Durnford and Gray 2006) and oddly similar to dinoflagellate plastid-targeting presequences (Nassoury et al. 2003; Patron et al. 2005).

The presequence of proteins imported into the simple chloroplasts of green algae, red algae, glaucophytes and plants contain an N-terminal transit peptide that mediates plastid targeting and import. While there is no sequence conservation in transit peptides, they all share some biochemical similarities (Bruce 2000) such as an elevated content of hydroxylated amino acids (Ser, Thr) and an overall net positive charge due to an under-representation of acidic amino acids. In solution, plant transit peptides are thought to be unstructured, though in a more hydrophobic environment may form regions of amphipathic alpha helices which could be important for receptor recognition (Bruce 2000). Transit peptides are usually removed as they are imported into the chloroplast via a stromal processing peptidase. Plastid proteins targeted to the thylakoid lumen have a bipartite presequence containing additional sequence information that is required to cross the thylakoid membrane. These proteins have an N-terminal transit peptide plus a thylakoid targeting domain similar to the hydrophobic region of a signal peptide. Upon import into the stroma, the transit peptide is cleaved exposing the thylakoid targeting domain which mediates thylakoid import and then is removed upon entry into the thylakoid lumen by a thylakoid protease (Bassham et al. 1991; Smeekens et al. 1986).

Not all chloroplast-localized proteins in plants have a transit peptide. Proteins targeted to the outer membrane often lack a transit peptide and instead have other features such as a N-terminal signal anchor or C-terminal tail-anchor (Lee et al. 2014). These domains are predicted transmembrane regions. They are often followed by a series of positively charged amino acids that are important for proper targeting to the membrane and are recognized by cytosolic factors to facilitate targeting to the organelle (reviewed in (Lee et al. 2014). So while the transit peptide is the canonical mode of targeting to plastids, there are variations depending on target destination.

In *Euglena*, two distinctive presequence classes were identified after examining over 100 different plastid-targeted proteins (Durnford and Gray 2006).

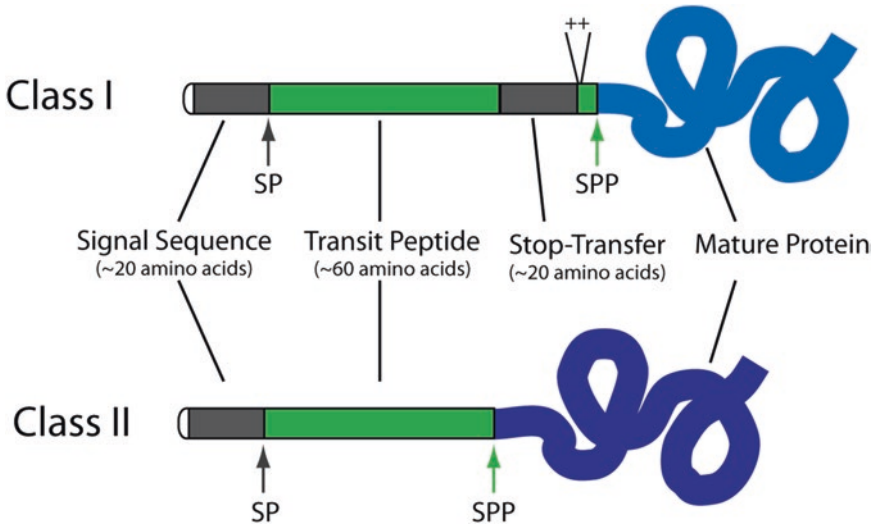

Fig. 10.2 Two classes of plastid-targeting presequences. The plastid-targeting presequences of *Euglena* can be divided into two classes. Class I presequences have a signal sequence with a signal peptidase cleavage site (SP), a transit peptide, a stop-transfer sequence and a stromal processing peptidase site (SPP). A common cluster of two to three positively charged amino acids (+ +), arginine and lysine, is usually found after the stop-transfer sequence. Class II presequences have a signal sequence with a signal peptidase cleavage site (SP), a transit peptide and a stromal processing peptidase site (SPP) but they lack the stop-transfer sequence. The Class I presequences are far more common in the population of plastid-targeted proteins than the class II presequences

The class I presequences were previously identified in a number of *Euglena* chloroplast protein precursors including but not limited to polyprotein precursors (Chan et al. 1990; Henze et al. 1995; Houlne and Schantz 1987; Kishore et al. 1993; Lin et al. 1994; Plaumann et al. 1997; Santillan Torres et al. 2003; Sharif et al. 1989; Shigemori et al. 1994; Vacula et al. 1999). The class I presequence has an N-terminal presequence composed of a predicted signal peptide, for targeting to the ER (Fig. 10.2). Biochemical studies confirmed that this domain functions as a signal peptide responsible for initiating translocation into the ER lumen ((Kishore et al. 1993; Sulli et al. 1999; Sulli and Schwartzbach 1995) see Sect. 10.4). The signal peptide domain is followed by a region approximately 60 ± 8 amino acids long that resembles a chloroplast transit peptide in composition (Fig. 10.2 (Durnford and Gray 2006)). This includes an enrichment of hydroxylated amino acids (Ser/Thr; ca. 20%) but a deficiency in acidic amino acids (Glu/Asp) compared to the mature protein. Unlike classic transit peptides, the *Euglena* transit peptide region contains an elevated proline content, upwards of 20%, but is otherwise similar to transit peptides found in green algae. This region would presumably function in the same fashion as the plant transit peptide, namely interacting with the translocation complex in the chloroplast envelope membranes. Heterologous protein import studies with *Euglena* precursors and plant chloroplasts identified this region as a functional transit peptide (Inagaki et al. 2000; Slavikova et al. 2005) see Sect. 10.4). Within the transit peptide is a second strongly hydrophobic domain (Fig. 10.2) that functions as a membrane anchor stop-transfer sequence preventing the co-translational import of a protein into the ER and anchoring it in the ER membrane (see Sect. 10.4, Sulli et al. (1999)). Immediately following the stop-transfer sequence there are often two or three basic amino acids, a feature commonly seen in stop-transfer sequences in other organisms (Kuroiwa et al. 1991) plus a variable number of additional amino acids N-terminal to the stromal processing peptidase cleavage site (Fig. 10.2).

In addition to the plastid envelope membranes, thylakoid lumen proteins must pass through the thylakoid membrane. A common feature of thylakoid lumen protein presequences is that they are bipartite containing a stromal targeting transit peptide domain which is cleaved upon import into the chloroplast by the stromal processing peptidase followed by a thylakoid lumen-targeting domain (Bassham et al. 1991; Ko and Cashmore 1989; Smeekens et al. 1986). The presequence to *Euglena* thylakoid luminal proteins also possess an additional thylakoid lumen targeting sequence, a hydrophobic domain, about 8–24 amino acids C-terminal to the stop-transfer membrane anchor sequence in class I presequences (Durnford and Gray 2006). As these are a modification of the classic class I presequence structure, they are categorize as a subcategory, class IB (Durnford and Gray 2006).

The second major class of *Euglena* plastid-targeting presequences are the class II presequences. These differ from the class I presequences by the absence of the second stop-transfer hydrophobic domain (Fig. 10.2). The signal peptide and the transit peptide domain of the class II presequences are compositionally identical to the same domains of the class I presequence (Durnford and Gray 2006). The absence of the stop-transfer sequence, however suggests that these proteins are translocated into the ER lumen. In terms of occurrence, the class II targeting sequences are certainly the minority, making up only 14% of the identified plastid targeting presequences. Within the class II group, there is a thylakoid lumen-targeted protein that possesses a second hydrophobic region shortly after the signal peptide domain leaving a very short transit peptide region between them (Durnford and Gray 2006). This presequence was called a class IIB presequence to recognize the distinctive features. Since the separation between the signal peptide and the stop-transfer sequence is highly conserved in class I presequences (60 ± 8 amino acids), the very short spacing in this class IIB sequence is likely required to facilitate appropriate targeting and to prevent it from being recognized by the transport apparatus as a class I presequence.

10.4 *In Vitro* Elucidation of *Euglena* Plastid Targeting Presequence Domain Function

In vitro organelle import experiments have shown that the *Euglena* pLHCPII and pRbcS class I presequences contain a signal peptide domain responsible for initiating co-translational translocation of the precursor into the ER (Kishore et al. 1993; Sulli et al. 1999; Sulli and Schwartzbach 1996). A pLHCPII (Fig. 10.3a top (Kishore et al. 1993; Sulli et al. 1999)) and a pRbcS (Sulli and Schwartzbach 1996) composed of the complete presequence and one mature protein unit were co-translationally imported *in vitro* into canine microsomes and inserted into the microsomal membrane oriented with a portion of the imported protein remaining outside the microsomes. The pLHCPII presequence was cleaved and the change in molecular weight of the imported protein was consistent with cleavage of the N-terminal presequence at the predicted signal peptidase cleavage site (Kishore et al. 1993; Sulli et al. 1999). Although the pRbcS presequence has a signal peptide domain initiating translocation into canine microsomes, the presequence was not cleaved (Sulli and Schwartzbach 1996) suggesting that if it has a signal peptidase cleavage site, it is not recognized by the canine microsomal signal peptidase. Mature LHCPII (Fig. 10.3a bottom), mature RbcS, and pea mature LHCPII (Kishore et al. 1993; Sulli et al. 1999; Sulli and Schwartzbach 1996) were not imported into canine microsomes indicating that the signal peptide is a presequence domain and not a domain within the mature protein.

The Na_2CO_3 resistant association of pLHCPII (Fig. 10.3a top (Kishore et al. 1993; Sulli et al. 1999)) and pRbcS (Sulli and Schwartzbach 1996) with the microsomal membrane indicates that they have been co-translationally inserted into the microsomal membrane; a process requiring a stop transfer membrane anchor sequence. A truncated pLHCPII lacking amino acids 1–43, the presumptive presequence N-terminal signal peptide (Fig. 10.3a middle) based on the criteria of von Heijne (von Heijne 1988), but containing the

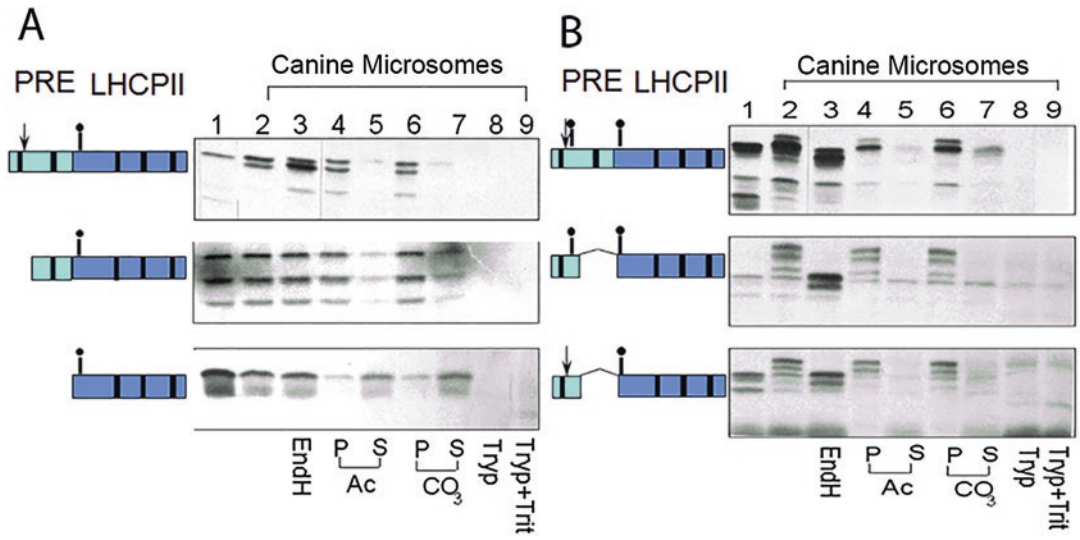

Fig. 10.3 Microsomal import and glycosylation of pLHCPII and pLHCPII presequence deletion glycosylation reporter constructs. (**a** and **b**) Schematic diagrams of the presequence (*light blue*) deletion glycosylation reporter constructs indicating the locations of the predicted signal peptidase cleavage site (*arrow*), hydrophobic domains (*black boxes*) within the presequence and mature protein (*dark blue*), and potential glycosylation sites within the presequence (Asp40) and mature LHCPII (Asp148) (a lollipop shape). mRNA transcribed from the indicated constructs was translated in the absence (*lane 1*) or presence (*lanes 2–9*) of canine microsomes. After terminating translation, microsomal membranes were incubated with endoglycosidase H (EndH), washed with 0.5 M potassium acetate (Ac) or 0.1 M Na_2CO_3, pH 11.5 (CO_3), and separated into a pellet (P) and supernatant (S) fraction or treated with trypsin (Tryp) in the presence and absence of Triton X-100 (Trit). Products were separated by SDS gel electrophoresis and visualized by fluorography (modified from (Sulli et al. 1999)

presequence second hydrophobic domain was also imported *in vitro* into canine microsomes and inserted into the microsomal membrane oriented with a portion of the imported protein remaining outside the microsomes (Sulli et al. 1999). A stop transfer membrane anchor sequence at the N-terminus of a precursor protein can function as a signal peptide initiating translocation of the precursor across the microsomal membrane. The ability of the pLHCPII class I presequence second hydrophobic domain to function as a signal peptide when it is at the precuror's N-terminus suggests that the pLHCPII and by inference the pRbcS class I presequence second hydrophobic domain is in fact the stop transfer membrane anchor domain responsible for co-translational insertion of the precursors into the ER membrane *in vivo* (Sulli and Schwartzbach 1995, 1996).

Protein glycosylation occurs within the ER lumen as proteins are co-translationally translocated across the ER membrane. Glycosylation increases the apparent molecular weight of a protein and digestion with endoglycosidase H (EndoH) removes the glycan decreasing the apparent molecular weight. The changes in apparent molecular weight upon glycosylation and deglycosylation allow glycosylation sites to serve as reporters for regions of a protein translocated across the ER membrane. By studying the import into canine microsomes of pLHCPII presequence deletions and glycosylation reporters, the pLHCPII presequence signal peptide domain, the presequence stop transfer membrane anchor domain and the topology of the imported pLHCPII within the ER membrane were determined (Sulli et al. 1999).

Mature LHCPII contains a potential glycosylation site 8 amino acids from the N-terminus. Upon translocation of pLHCPII across the microsomal membrane, the apparent molecular weight of the protein did not increase and it did not decrease after treatment with EndoH (Fig. 10.3a top (Sulli et al. 1999)) indicating the protein was not glycosylated. Na_2CO_3 did not release the translocated protein from the microsomal mem-

brane indicating that it is an integral membrane protein oriented with the presequence in the microsomal lumen and the N-terminal region of mature LHCPII containing the glycosylation site outside the microsomes (Fig. 10.3a top). A pLHCPII with a glycosylation site inserted into the presequence transit peptide domain at amino acid 40 between the predicted signal peptidase cleavage site and the second presequence hydrophobic domain was imported into canine microsomes and inserted into the membrane (Sulli et al. 1999) as evidenced by the failure of Na_2CO_3 to release the protein from the microsomal membrane (Fig. 10.3b top). The apparent molecular weight of the translocated protein was higher than the molecular weight of the protein synthesized in the absence of microsomes. EndoH digestion decreased the molecular weight of the protein indicating the protein was glycosylated and the molecular weight of the EndoH digested deglycosylated protein was less than that of the protein synthesized in the absence of microsomes (Fig. 10.3b top) indicative of signal peptide cleavage. Since the glycosylation site in the mature protein C-terminal to the second presequence hydrophobic domain was not glycosylated and the glycosylation site at presequence amino acid 40, N-terminal to the second presequence hydrophobic domain was glycosylated, the second presequence hydrophobic domain must function as a stop transfer sequence orienting pLHCPII with the N-terminus formed after signal peptidase cleavage in the ER lumen and the mature protein on the cytoplasmic membrane face (Sulli et al. 1999). The class I presequence stop transfer hydrophobic domain does in fact function to prevent glycosylation of the mature LHCPII; a process which could lead to formation of a nonfuctional protein.

Truncated pLHCPIIs containing only the presequence N-terminal 42 amino acids, the predicted presequence signal peptide domain, containing (Fig. 10.3b middle) or lacking (Fig. 10.3b bottom) a glycosylation site at amino acid 40 were co-translationaly transported into canine microsomes definitively identifying the presequence N-terminal domain as a functional signal peptide (Sulli et al. 1999). Although the presequence lacks the second hydrophobic membrane anchor domain, the protein was not released from the membrane by Na_2CO_3 but it was digested by exogenous protease indicative of the protein N-terminus in the microsomal lumen and the C-terminus outside the microsomal membrane. There are three hydrophobic domains in mature LHCPII (Muchhal and Schwartzbach 1992) and one of these domains probably functioned as the membrane anchor sequence. The apparent molecular weight of both proteins increased upon import but the increase for the protein containing two glycosylation sites was greater than the increase of the protein with a single glycosylation site (Fig. 10.3b middle, bottom). EndoH treatment decreased the apparent molecular weight of both proteins confirming translocation of the asparagine 8 amino acids from the N-terminus of the mature protein into the microsome where it was glycosylated. Glycosylation of the asparagine 8 amino acids from the N-terminus of the mature protein in the absence but not in the presence of the presequence second hydrophobic domain identifies this domain as the membrane anchor sequence responsible for orienting pLHCPII in the ER membrane with the presequence region between the signal peptidase cleavage site and the second hydrophobic domain within the ER lumen and the remainder of the presequence and mature protein in the cytoplasm.

Dinoflagellate presequences are bipartite as found for *Euglena* containing an N-terminal signal peptide domain and a second hydrophobic domain C-terminal to the presumptive signal peptidase cleavage site (Nassoury et al. 2003; Patron et al. 2005). The pPCP N-terminal signal peptide domain directed the co-translational translocation of a dinoflagellate chloroplast protein precursor into canine microsomes (Nassoury et al. 2003). The second PCP hydrophobic domain functioned as a stop transfer sequence orienting the precursor with the N-terminus in the microsomal lumen and the C-terminus outside the microsomal membrane. As found for the bipartite *Euglena* presequence (Sulli et al. 1999), the dinoflagellate pPCP presequence stop transfer sequence functioned as an uncleaved signal

peptide initiating co- translational import of the precursor into canine microsomes (Nassoury et al. 2003). Taken together, the invitro microsomal import studies with *Euglena* and dinofalgellate presequences show that the presequences directing proteins into three envelope complex plastids are both structurally and functionally identical.

Euglena plastid proteins are transported from the Golgi apparatus to the chloroplast in vesicles oriented with the N-terminus in the vesicle lumen and the mature protein on the cytoplasmic membrane face (Kishore et al. 1993; Sulli et al. 1999; Sulli and Schwartzbach 1995, 1996). Upon fusion of the transport vesicles with the outermost of the three chloroplast membranes, the precursor would be anchored in the envelope membrane with the N-terminus in the intermembrane space and the remainder of the protein in the cytoplasm. The molecular mechanism of vesicle budding and target membrane fusion are well characterized reactions requiring numerous proteins to form the budding and fusion complexes (Bonifacino and Glick 2004). N-ethylmaleimide-Sensitive factor (NSF) is an ATPase that functions in the dissociation of the soluble NSF attachment protein receptor (SNARE) mediated membrane fusion complex and it is inactivated by N-ethylmaleimide (Bonifacino and Glick 2004). A number of other proteins binding and hydrolyzing ATP or GTP are also required during the budding and fusion reactions. Multiple GTPases and ATP as a source of energy supplied exogenously or generated internally by photosynthesis is also required for protein import into simple plastids of plants (Paila et al. 2015).

pLHCPII was transferred from purified *Euglena* Golgi membranes to intact purified *Euglena* chloroplasts in a time dependent manner (Slavikova et al. 2005). pLHCPII was processed by the stromal processing protease to mature LHCPII and a protein having a molecular weight consistent with a two unit LHCPII polyprotein indicating the pLHCPII was translocated through all three envelope membranes. Golgi to chloroplast transport and chloroplast import required exogenous ATP, intrachloroplast ATP synthesized photosynthetically in the light and GTP (Slavikova et al. 2005). This differs from import into plant chloroplasts where exogenous or photosynthetically generated ATP supports maximal import rates (Theg et al. 1989). This is however consistent with the requirement for ATP in vesicle fusion reactions and in protein translocation through the intermediate and inner envelope membranes. *Euglena* Golgi to chloroplast transport was not inhibited by N-ethylmaleimide (Slavikova et al. 2005). This suggests that the highly conserved SNARE vesicle fusion apparatus used for all fusions on the endocytic and exocytic pathway (Bonifacino and Glick 2004) is not used for fusion of *Euglena* Golgi derived vesicles with the outer plastid envelope membrane.

The bipartite class I and class II presequences of *Euglena* chloroplast proteins are composed of an N-terminal signal peptide domain and a domain having characteristics of a transit peptide. In plants and green algae, a transit peptide is responsible for post translational import of proteins into chloroplasts. Upon transport into the ER, the signal peptide is cleaved exposing the transit peptide domain. A *Euglena* pRbcS containing the complete N-terminal bipartite presequence linked to a mature RbcS unit and the mature RbcS was not imported into pea chloroplasts (Slavikova et al. 2005). A *Euglena* pRbcS (Slavikova et al. 2005) and the precursor to the 30-kDa subunit of the oxygen-evolving complex (pOEC30) (Inagaki et al. 2000) lacking the signal peptide domain but containing the stop transfer membrane anchor sequence are post translationally imported into pea chloroplasts identifying the second presequence domain as a functional transit peptide. A dinoflagellate pPCP lacking the signal peptide domain but containing the stop transfer membrane anchor sequence was imported *in vivo* into *Solanum chacoense* chloroplasts (Nassoury et al. 2003) demonstrating the functional equivalence of the region of the *Euglena* and dinoflagellate bipartite presequence C-terminal to the signal peptidase cleavage site. A *Euglena* pRbcS class I presequence which lacked the N-terminal signal peptide domain converting it into a class II presequence by deletion of the stop transfer membrane anchor sequence was also post translationally imported into pea

chloroplasts (Slavikova et al. 2005). Import into pea chloroplasts of a *Euglena* pRbcS containing only the presequence region N-terminal to the hydrophobic stop transfer membrane anchor sequence identifies this region as the functional transit peptide domain. The *Euglena* pRbcSs lacking the signal peptide domain which were imported post translationally *in vitro* into pea chloroplasts were not post translationally imported *in vitro* into *Euglena* chloroplasts that were competent to import precursors within Golgi transport vesicles (Slavikova et al. 2005) indicating that vesicular transport from the ER to the Golgi apparatus to the chloroplast is the obligate pathway for protein import into *Euglena* chloroplasts.

10.5 Evolution of the *Euglena* Plastid Targeting and Import System

10.5.1 Evolution of the Chloroplast Envelope Membrane Translocons

The *Euglena* complex plastid evolved through an endosymbiotic association between a eukaryotic host and a eukaryotic green alga most likely related to a prasinophyte (Turmel et al. 2009). The green algal endosymbiont ultimately became enslaved by the host becoming fully integrated into the hosts' metabolic and regulatory pathways. The nature of such events, which include massive gene loss and the transfer of endosymbiont genes to the host nucleus have been discussed extensively (Archibald 2015; Keeling 2013). The question of how proteins were re-targeted back to the plastid through the endomembrane system and the evolution of class I and class II presequences following gene transfer is intriguing.

Of the three membranes surrounding the plastid of *Euglena*, it is generally agreed that the inner two membranes are derived from the chloroplast envelope of the green algal endosymbiont. This being the case, chloroplast proteins encoded in the endosymbiont nucleus would have had a transit peptide for chloroplast targeting and this information was likely retained when the endosymbiotiont's genes were transferred to the host's nucleus. The endosymbiont plastid envelope would also have possessed and likely retained the transit peptide-dependent protein import machinery during evolution of the endosymbiont to a complex plastid. Both class I and class II *Euglena* presequences have a transit peptide domain that initiates translocation of *Euglena* precursors through both envelope membranes of pea chloroplast (Inagaki et al. 2000; Slavikova et al. 2005), providing experimental evidence that the intermediate and inner *Euglena* chloroplast envelope membranes contain translocons and import machinery evolutionarily related to those in plants. This includes the translocon at the outer chloroplast envelope (TOC) and the translocon at the inner chloroplast envelope (TIC) that make up the main apparatus for protein import into plant chloroplasts (Paila et al. 2015).

In the case of the *Euglena* plastid, the more problematic question is the evolution of a protein translocation apparatus for the outermost membrane particularly for those proteins with a class I presequence. Proteins with class I presequences are transported to the plastid as integral membrane proteins and upon fusion of the transport vesicle with the outermost envelope membrane they are integral envelope membrane proteins. These proteins must be extracted from the outer envelope membrane before they can be translocated into the chloroplast. The Sec61 ER complex allows lateral movement of a translocating protein into the ER lipid bilayer (Shao and Hegde 2011) and movement has been proposed to be bidirectional. Sec61 is part of the translocation complex for chloroplast protein translocation through the CER into diatom plastids (Maier et al. 2015). The ER associated degradation (ERAD) system translocates soluble and integral membrane proteins out of the ER into the cytoplasm for degradation (Needham and Brodsky 2013). Protein transport across the second outermost membrane of complex plastids of red algal origin uses a transporter that resembles the ER associated degradation (ERAD) like translocation system known as the symbiont-derived ERAD-like machinery (SELMA) (Agrawal et al. 2009; Felsner et al. 2011; Maier et al. 2015; Stork

et al. 2012). It is thought that the ERAD system evolved into SELMA forming the protein translocon of the second outermost envelope membrane of four envelope membrane complex plastids. It is tempting to speculate that the *Euglena* outermost chloroplast envelope membrane contains a translocation complex that evolved from SELMA or from the Sec61 or ERAD translocation complex in a similar fashion to the evolution of the SELMA translocation complex in the second outermost envelope membrane of complex plastids of red algal origin.

10.5.2 Evolution of the Euglena Plastid Protein Presequence

A probable evolutionary origin of the outermost *Euglena* plastid envelope membrane is the phagosomal membrane that would have surrounded the phagocytosed green algal endosymbiont (Gibbs 1978). While difficult to prove, this is an attractive hypothesis in terms of plastid evolution since a mechanism would have already existed for targeting proteins to phagosomes and related vacuoles providing a starting point for targeting nucleus encoded proteins to the endosymbiont compartment. Phagosome targeted proteins are synthesized by ER bound ribosomes and transported in vesicles from the ER to the Golgi apparatus and then to the phagosome or vacuole. A signal peptide is required for co-translational ER localization (von Heijne 1988). Signals on the proteins interacting with membrane receptors sort proteins into vesicles that contain targeting proteins such as SNAREs ensuring they will dock and fuse with the phagosome or vacuole delivering their cargo to the appropriate cellular location (Bonifacino and Glick 2004; Braulke and Bonifacino 2009; Neuhaus and Rogers 1998). Thus, endosymbiont genes transferred to the host nucleus would have to acquire a presequence with both a signal peptide for targeting to the ER and sorting signals for incorporation into budding vesicles targeted to the phagosome. Upon vesicular fusion with and translocation through the outermost *Euglena* plastid envelope membrane, the transit peptide dependent protein import system used to transport proteins through the endosymbiont's double envelope membrane would provide the basis for the evolution of a mechanism for translocation of precursors through the *Euglena* middle and inner envelope membranes that are derived from the endosymbiont's plastid envelope.

Based on these assumptions, the *Euglena* chloroplast protein presequence is proposed to have evolved through addition of an ER targeting signal peptide to an endosymbiont derived presequence having a chloroplast targeting transit peptide plus any additional structural/sequence information for vesicular cargo sorting and vesicle fusion to ensure delivery to the chloroplast. A clue to how this occurred comes from *in vitro* experimental studies of the functionality of the Euglena class I presequence. When the pLHCPII presequence signal peptide was removed, the pLHCPII containing only the presequence transit peptide domain including the hydrophobic stop transfer sequence was imported into canine microsomes (Fig. 10.3a middle (Sulli et al. 1999)). The presence of the stop-transfer sequence in the presequence transit peptide domain did not prevent the transit peptide domain-dependent import of Euglena pRbcS into pea chloroplasts (Slavikova et al. 2005). Taken together, these experiments demonstrated that the class I presequence transit peptide domain is bifunctional, functioning as a transit peptide and, due to the presence of the hydrophobic stop transfer sequence, a signal peptide.

The first step in the evolution of the class I *Euglena* plastid targeting presequence may not have been the addition of a signal peptide domain to the endosymbiont transit peptide presequence but rather the addition of a hydrophobic stop transfer membrane anchor domain to the existing endosymbiont transit peptide presequence. This would create a bifunctional presequence containing an ER targeting, but uncleaved, signal peptide and a chloroplast targeting transit peptide. Subsequent class I presequence evolution resulted in acquisition of a distinct N-terminal cleaved signal peptide optimizing ER targeting,

an optimized transit peptide for import across the middle and inner plastid envelope membranes and addition to the presequence of vesicular protein sorting sequences for incorporation of chloroplast protein precursors into budding vesicles that will fuse with the outermost plastid envelope membrane. The sorting information remains to be identified but is proposed to be the within transit peptide domain (see Sect. 10.6). In this scenario, evolution of the Class II presequence simply involved the loss of the stop-transfer hydrophobic region within the transit peptide domain, possibly resulting in more efficient plastid protein import due to obviating the need for precursor transport through the outer envelope membrane; a process accomplished with class II presequences upon fusion of Golgi to chloroplast transport vesicles containing plastid proteins within their lumen with the outer plastid envelope membrane. The fact that the entire class II precursors are within the transport vesicle supports the proposal that the transit peptide presequence domain contains the information for precursor sorting into Golgi to chloroplast transport vesicles.

The signal peptide and stop-transfer sequence could have been acquired *de novo* through mutations that extend the reading frame or the insertion of genetic elements from a variety of sources. Alternatively, these could have been acquired from other endomembrane-targeted proteins through events such as unequal crossing over, exon shuffling, or integration of the transferred gene into a gene already possessing an ER-targeting signal peptide. Once effective targeting sequences arose, these could spread to other plastid proteins in a similar fashion. Evidence for the acquisition of chloroplast targeting presequences via crossing over exon shuffling was obtained from the *Euglena* EST project where the sequence similarity of the presequences of several unrelated chloroplast proteins were unusually high, and in one pair, nearly identical (Durnford and Gray 2006). This suggests that the spread of targeting information between genes was common and an effective way to acquire targeting information.

10.5.3 Why Did Multiple Classes of Euglena Plastid Targeting Presequences Evolve?

The presence of *Euglena* chloroplast localized proteins with different N-terminal presequences suggests that there are selective advantages that maintain the two classes of presequences. The presence of the stop-transfer sequence in class I presequence prevents the protein from being inserted into the ER lumen and mediates its insertion in the ER membrane resulting in the precursor being an integral membrane protein (Sulli et al. 1999; Sulli and Schwartzbach 1995, 1996). The lack of a stop-transfer sequence in the class II presequences means that these proteins, barring a substantial hydrophobic domain in the mature protein, would be completely translocated through the ER membrane into the lumen becoming soluble ER luminal proteins. The chloroplast precursor proteins with class I presequences would be transported in vesicles from the ER to the Golgi apparatus and then to the chloroplast as integral membrane proteins while precursors with class II presequences would be soluble vesicle luminal proteins. Upon fusion of the transport vesicle with the chloroplast, the class I presequence precursors would be integral envelope proteins that must be extracted from the outer envelope membrane and translocated through all three envelope membranes. Class II precursors would be in the space between the outer and middle envelope membranes needing only to be translocated through two additional envelope membranes in a process that is probably mechanistically simpler than extraction of the class I precursor from the outermost envelope membrane and similar to transport of proteins from the cytoplasm into plant simple chloroplasts.

An important question is why two different targeting presequences and import mechanisms evolved. There are no obvious differences in protein structure or inter-chloroplast localization that could explain why some proteins have a class I presequences and do not enter the ER, Golgi or transport vesicle lumen and remain on the surface of the Golgi to chloroplast transport vesicle and

others have class II presequences entering the ER, Golgi and transport vesicle lumen. The ER and Golgi apparatus are the site of protein post translational modifications the most common being co-translational asparagine linked (N-linked) glycosylation. N-linked glycosylation of a plastid protein could impair protein function providing a strong selection pressure for incorporation of a stop transfer sequence into a chloroplast protein presequence preventing translocation of the mature protein into the ER and thus its glycosylation. Using the GlycoEP prediction program (http://www.imtech.res.in/raghava/glycoep/) for N-linked glycosylation (Chauhan et al. 2013), 44% of the proteins with a class I presequence had a predicted N-linked glycosylation site while only 7% of the proteins with a class II presequence had a predicted N-linked glycosylation site. While this analysis is flawed by the small sample size and the fact that not all of the proteins in the dataset were full-length (thus missing potential sites), it provides evidence supporting the hypothesis that class I presequences containing a stop transfer membrane anchor sequence evolved to prevent co-translational N-linked glycosylation of plastid proteins. One of the most abundant *Euglena* chloroplast proteins, the thylakoid integral membrane protein LHCPII, contains a potential N-linked glycosylation site 8 amino acids from the N-terminus in front of the first hydrophobic membrane spanning domain (Sulli et al. 1999). Glycosylation of LHCPII would clearly interfere with membrane insertion of LHCPII and thus assembly of the LHC. *In vitro* studies of LHCPII co-translational translocation into canine microsomes (Sulli et al. 1999) have provided direct evidence that this site is co-translationally glycosylated during translocation into the ER and the stop transfer membrane anchor sequence prevents N-linked glycosylation. This finding provides experimental support for the hypothesis that class I presequences evolved to prevent N-linked glycosylation of chloroplast proteins.

Euglena chloroplast proteins with a class II presequence are co-translationally imported into the ER due to the lack of a stop transfer membrane anchor sequence in the presequence. If these proteins contain a N-linked glycosylation site they will be glycosylated. Plant and diatom plastids contain N-linked glycoproteins that are glycosylated in the ER (plants) or CER (diatoms) and glycosylation does not prevent their import into the plastid stroma (Buren et al. 2011; Peschke et al. 2013; Villarejo et al. 2005). The activity of some plant chloroplast proteins is dependent upon N-linked glycosylation (Buren et al. 2011). Euglena proteins possessing a class II presequence may either lack N-linked glycosylation sites and thus they are unaffected by translocation into the ER or their function may be dependent upon glycosylation. In the latter case, this would provide a strong selection pressure for loss of the stop transfer sequence from a typical class I presequence to yield the class II structure.

In addition to N-linked glycosylation, there are other post-translational modifications that can occur in the endomembrane system including proteolytic preprotein processing, disulphide bond formation and O-linked glycosylation. Any of these modification could render a protein nonfunctional providing a positive selection pressure for class I presequences. Alternatively, these modifications could be required for protein function providing a selection pressure for the evolution of class II presequences. The point being that there may not be a single biochemical rational for the existence of class I and class II presequences but rather a variety of explanations that are specific to the transported protein. The role of post translational endomembrane protein modifications in protein function and the consequences of possessing either a class I or class II presequence can not be assessed solely from sequence data but will require biochemical studies of the modified and unmodified protein.

10.5.4 An Unusual Case of Convergent Evolution

Dinoflagellates are a large group of photo- and heterotrophic microalgae within the SAR clade (Burki 2014). Plastid ultrastructure, the plastid-targeting presequences and chloroplast protein localization mechanism of dinoflagellates and *Euglena* are similar. Dinoflagellate plastids have

three envelope membranes and lack bound ribosomes on the outer envelope membrane paralleling the ultrastructure of the *Euglena* plastid. The dinoflagellates have as found in *Euglena* bipartite class I presequences composed of a signal peptide domain and a transit peptide domain containing a hydrophobic stop-transfer membrane anchor sequence and bipartite class II presequences composed of a signal peptide domain and a transit peptide domain lacking the hydrophobic stop-transfer membrane anchor sequence (Nassoury et al. 2003; Patron et al. 2005). Also as observed in *Euglena*, immunogold labelling experiments have demonstrated that dinoflagellate plastid precursors are transported to the plastid via the Golgi apparatus, *in vitro* experiments with canine microsomes have shown they have a functional ER targeting signal peptide with a membrane anchor sequence, and the transit peptide domain is bifunctional mediating both import of the precursor into *Solanum chacoense* simple chloroplasts and translocation of the precursor into canine microsome (Nassoury et al. 2003). Dinoflagellates and *Euglena* are in different eukaryotic supergroups (Burki 2014), so these protein targeting similarities are not related to a common ancestry. This suggests that these mechanisms evolved convergently due to similar selection pressures due to the constraints of having three envelope membranes around the plastid that were not part of the ER (Nassoury et al. 2003).

Despite the similarities between the dinoflagellate and *Euglena* chloroplast protein presequences and plastid ultrastructure, there are features that distinguish them. The dinoflagellate presequence transit peptide domain is, on average, half the size, 26 amino acids, of the *Euglena* presequence transit peptide domain, 60 amino acid (Durnford and Gray 2006; Patron et al. 2005). The N-terminal portion of the dinoflagellate presequence transit peptide domain but not the *Euglena* transit peptide domain often has a phenylalanine followed by three hydrophobic amino acids, the FVAP motif (Patron et al. 2005). This motif which is absent in *Euglena* transit peptides, is a well known requirement for translocation into plastids derived from red algae (Patron and Waller 2007). The dinoflagellate transit peptide with the FVAP motif is however transported into plant chloroplasts (Nassoury et al. 2003). These differences do however reflect the unique origin of the *Euglena* and dinoflagellate plastids from different eukaryotic algae and indicate some variations in the targeting and translocation process.

10.6 A Working Model for Localization of Nuclear Encoded Proteins to *Euglena* Plastids

The results of *in vivo* trafficking studies (see Sect. 10.2), *in vitro* import studies (see Sect. 10.4) and knowledge of the structure of the bipartite chloroplast protein presequence (see Sect. 10.3) has been used to develop a working model (Fig. 10.4) for the mechanism of protein import into the three envelope membrane complex plastids of *Euglena* and by analogy the three envelope membrane complex plastids of dinoflagellates. The N-terminal signal peptide initiates cotranslational transport of the precursor into the ER lumen and the stop transfer membrane anchor sequence in the class I bipartite presequence (Durnford and Gray 2006) stops presequence translocation. The precursor is anchored in the ER membrane with the presequence N-terminus in the ER lumen and the mature protein on the cytoplasmic side of the ER membrane (Kishore et al. 1993; Slavikova et al. 2005; Sulli et al. 1999; Sulli and Schwartzbach 1996). Precursors with the class II presequence that lack the stop transfer sequence will be translocated completely into the ER lumen and become soluble ER luminal proteins. During translocation of proteins with both class I and class II presequences through the ER membrane, signal peptidase cleaves the signal peptide exposing the chloroplast targeting transit peptide . The chloroplast protein precursors are subsequently incorporated into vesicles formed by budding from the ER for transport to the Golgi apparatus. Precursors with class I presequences are integral vesicle membrane proteins while precursors with class II presequences are soluble vesicle luminal proteins (Fig. 10.4).

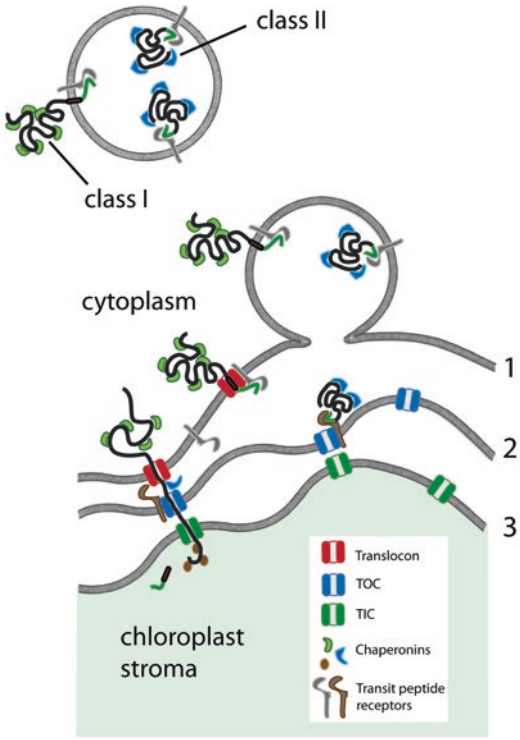

Fig. 10.4 Proposed model for the localization of nuclear encoded proteins to the *Euglena* plastid. Proteins with class I presequences are transported from the Golgi apparatus to the chloroplast envelope in vesicles as integral membrane proteins with approximately 60 presequence transit peptide amino acids (*green*) projecting into the lumen bound to the luminal domain of the transit peptide receptor (*grey*). Proteins with Class II presequences are within the vesicle lumen with the transit peptide bound to the transit peptide receptor. Chaperones in the cytoplasm (*green*) and in the vesicle lumen (*blue*) are bound to the mature proteins. Golgi vesicles fuse with the outer plastid membrane (1). Class I proteins become integral outer envelope membrane proteins while class II proteins are soluble proteins in the intermembrane space between the outer (1) and middle (2) envelope membranes. The class II presequence dissociates from the transit peptide receptor binding first to the TOC like (*blue*) and then TIC like (*green*) complex forming a translocation channel spanning the middle and inner envelope membranes at contact sites. The precursor is translocated through the TOC/TIC channel into the stroma where the presequence is cleaved. Proteins with class I presequences have to be extracted from the outer membrane and translocated into the plastid. The precursor is proposed to migrate laterally out of the outer envelope membrane (1) into the hypothetical translocon (*red*). The luminal presequence transit peptide engages first the TOC like middle envelope membrane and then the TIC like inner envelope membrane complex forming a translocation channel spanning the three membranes at contact sites. The precursor is translocated into the stroma where the presequence is cleaved

To maintain proteins in a transport-competent state, especially for hydrophobic proteins, the model presumes without experimental evidence that cytosolic chaperonins, such as HSP70 and HSP90 (Paila et al. 2015) assist in maintaining proteins in the unfolded state facilitating translocation through the plastid envelop.

Upon vesicle fusion with the Golgi apparatus, the class I precursors are integral Golgi membrane proteins and the class II precursors are soluble Golgi luminal proteins. The chloroplast precursors move by vesicular transport from the cis to the medial to the trans Golgi where they are sorted into vesicles for transport to the chloroplast. The class I precursors are integral trans Golgi membrane proteins with approximately 60 amino acids of the presequence transit peptide in the Golgi lumen and approximately 10–20 presequence amino acids and the mature protein on the cytoplasmic membrane face (Sulli et al. 1999) while the class II presequence transit peptide is soluble in the trans Golgi lumen. The complex chloroplast of *Euglena* is thought to have evolved from a eukaryotic endosymbiont within the ancestral Euglenoid's phagosome. By analogy to trans Golgi protein sorting into vesicles for transport to the vacuole (Lousa and Denecke 2016), it is proposed that the N-terminal transit peptide presequence domain of soluble luminal class II precursors (Durnford and Gray 2006) and the 60 luminal amino acids of the class I presequence transit peptide domain interact directly with membrane bound sorting receptors becoming incorporated into chloroplast targeted transport vesicles budding from the Golgi apparatus (Fig. 10.4). The approximately 60 amino acids of the transit peptide in the lumen mediates protein import into plant chloroplasts (Inagaki et al. 2000; Slavikova et al. 2005) demonstrating that it can interact with the same receptors as the soluble luminal class II transit peptide. As with vacuolar targeting, the cytoplasmic domain of the sorting receptor would contain the information for vesicle targeting to the plastid.

After fusion of Golgi to chloroplast transport vesicles with the outermost of the three *Euglena* chloroplast envelope membranes, the class II

precursors are soluble proteins in the outer envelope middle envelope intermembrane space (Fig. 10.4). Since the *Euglena* presequence transit peptide domain initiates translocation of *Euglena* precursors through both pea chloroplast envelope membranes, (Inagaki et al. 2000; Slavikova et al. 2005), translocation through the intermediate and inner *Euglena* chloroplast envelope membranes is most likely mechanistically similar to translocation into the simple chloroplasts of plants and algae (Paila et al. 2015). It is proposed that the *Euglena* chloroplast intermediate envelope membrane contains a translocation complex, probably evolutionarily related to the TOC translocon of plants, that can interact with the presequence transit peptide domain and that the inner membrane contains a translocon evolutionarily related to the plant TIC complex. In plants, the outer and inner envelope membranes are associated with each other at contact sites which contain the TOC and TIC translocons (Paila et al. 2015) providing a channel for translocation of precursors simultaneously through both membranes. Electron micrographs have shown that in some regions the *Euglena* plastid membranes are tightly appressed reminiscent of the plant TOC TIC containing contact sites while in other regions, three distinct plastid membranes are seen (Fig. 10.5) (Lefort-Tran et al. 1980). Just as the transit peptide of a precursor in the cytoplasm of plants and algae interacts with the TOC complex, the transit peptide of *Euglena* class II presequences which are within the intermembrane space between the outer and middle plastid envelope membranes binds first to the middle membrane TOC like complex and then to the TIC like complex forming a channel spanning the middle and inner envelope membrane at a contact site (Fig. 10.4). The precursor is translocated, assisted by chaperones into the stroma where the presequence is cleaved by stromal processing peptidase and the protein folds into its active conformation assisted by chaperones.

Translocation of proteins with a class I presequence is more problematic as the protein must be extracted from the outer chloroplast envelope membrane prior to translocation into the chloroplast. It is proposed that the outermost *Euglena* envelope membrane contains a translocon that evolved from the Sec61, ERAD or SELMA translocons (Fig. 10.4 red; see Sect. 10.5.1). A characteristic feature of class I transit peptides is that from their N-terminus to the membrane spanning domain they are all 60 ± 8 amino acids long and enriched in proline (Durnford and Gray 2006) promoting a rigid structure. This length is probably long enough to span the outer envelope membrane and intermembrane space allowing the transit peptide to bind the TOC like complex in the middle envelope membrane. The precursor migrates laterally from the outer membrane lipid bilayer into the translocation channel (Fig. 10.4) by a process that is mechanistically similar to the migration of a protein from the ER membrane into the Sec 61 or ERAD translocation channel (Needham and Brodsky 2013; Shao and Hegde 2011). The luminal presequence transit peptide engages first the TOC like middle envelope membrane and then the TIC like inner envelope membrane complex forming a translocation channel spanning the three envelope membranes at a contact site. Assisted by chaperones, the precursor is translocated into the stroma by the same mechanism as precursors with class II presequences, the presequence is cleaved and the mature protein folds assisted by chaperones (Fig. 10.4).

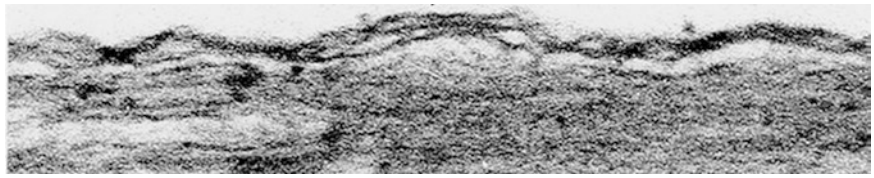

Fig. 10.5 Electron micrograph of the *Euglena* envelope membrane showing contact sites (areas of membrane appression) and areas where the three membranes are not appressed

10.7 Conclusions

The spread of photosynthesis through diverse eukaryotic lineages via endosymbiosis has been a major force in creating novel biological diversity. A massive transfer of genes from the endosymbiont to the host nucleus necessitated evolution of a mechanism to return the encoded proteins to the endosymbiont that evolved into a plastid. This mechanism involved the acquisition by the protein of a targeting presequence and the acquisition by the plastid of protein translocons that recognized the targeting sequence and could translocate the proteins through the plastid envelope membranes. The transit peptide and TOC TIC components of the import system initially evolved during the primary endosymbiotic event between a eukaryotic host and a prokaryotic cyanobacterial ancestor that gave rise to the simple chloroplasts, chloroplasts with two envelope membranes, of green algae, red algae and plants. As eukaryotes continued to evolve, however, eukaryote-eukaryote endosymbiosis arose that gave rise to more complex plastids with additional membranes around the plastid. This provided additional transport challenges as genes were once again transferred from the nucleus of the endosymbiont to the nucleus of the host.

Complex chloroplasts, chloroplasts with three or four envelope membranes appear to have evolved multiple times from a secondary endosymbiotic event between a eukaryotic host and a photosynthetic eukaryotic endosymbiont with a simple chloroplast having two envelope membranes. Once again, massive horizontal gene transfer followed requiring evolution of a mechanism to return the proteins to the endosymbiont evolving into a plastid that now had three or four envelop membranes. The structure of the *Euglena* presequence and the import pathway provide insight into how the pre-existing mechanism of targeting proteins to different cellular locations via the endomembrane system and the mechanism for transporting proteins from the cytoplasm to the chloroplast were repurposed to return proteins to complex plastids.

The outermost of the three *Euglena* membranes likely originated as a component of the endomembrane system, the phagosomal membrane, making the chloroplast, at least functionally, a component of the endomembrane system. The addition of a hydrophobic region to the existing transit peptide converted it into a bifunctional targeting sequence initiating precursor translocation into the ER and across the middle and inner plastid envelope membranes. As the transit peptide lacked a signal peptidase cleavage site, this hydrophobic domain also functioned as a stop transfer membrane anchor sequence preventing translocation into the ER and thus post translational modifications that could inactivate the protein. The addition of a separate N-terminal signal peptide domain to the transit peptide containing presequence and evolution of specific Golgi to chloroplast vesicle targeting information was required to increase the specificity and efficiency of protein localization to the plastid. Modifications of the endosymbiont plastid's TOC and TIC import apparatus that imported soluble cytoplasmic proteins provided a mechanism for a precursor delivered by vesicular transport to transit the middle and inner envelope membranes. As we continue to decipher the mechanism of protein targeting to the *Euglena* plastid and identify the protein components of the translocation complex, our understanding of how endosymbiogenesis unfolded in this unique protist will increase providing insights into the major transitions in the evolution of eukaryotes.

References

Agrawal S, van Dooren GG, Beatty WL, Striepen B (2009) Genetic evidence that an endosymbiont-derived endoplasmic reticulum-associated protein degradation (ERAD) system functions in import of apicoplast proteins. J Biol Chem 284(48):33683–33691

Archibald JM (2015) Genomic perspectives on the birth and spread of plastids. Proc Natl Acad Sci U S A 112(33):10147–10153

Bassham DC, Bartling D, Mould RM, Dunbar B, Weisbeek P, Herrmann RG, Robinson C (1991) Transport of proteins into chloroplasts. Delineation of envelope "transit" and thylakoid "transfer" signals within the pre-sequences of three imported thylakoid lumen proteins. J Biol Chem 266(35):23606–23610

Bhaya D, Grossman AR (1991) Targeting proteins to diatom plastids involves transport through an endoplasmic reticulum. Mol Gen Genet 229:400–404

Bonifacino JS, Glick BS (2004) The mechanisms of vesicle budding and fusion. Cell 116(2):153–166

Brandt P, von Kessel B (1983) Cooperation of cytoplasmic and plastidial translation in formation of the photosynthetic apparatus and its stage-specific efficiency. Plant Physiol 72(3):616–619

Braulke T, Bonifacino JS (2009) Sorting of lysosomal proteins. Biochim Biophys Acta 1793(4):605–614

Bruce BD (2000) Chloroplast transit peptides: structure, function and evolution. Trends Cell Biol 10(10):440–447

Buren S, Ortega-Villasante C, Blanco-Rivero A, Martinez-Bernardini A, Shutova T, Shevela D, Messinger J, Bako L, Villarejo A, Samuelsson G (2011) Importance of post-translational modifications for functionality of a chloroplast-localized carbonic anhydrase (CAH1) in *Arabidopsis thaliana*. PLoS One 6(6)

Burki F (2014) The eukaryotic tree of life from a global phylogenomic perspective. Cold Spring Harb Perspect Biol 6(5):a016147

Cavalier-Smith T (2003) Genomic reduction and evolution of novel genetic membranes and protein-targeting machinery in eukaryote-eukaryote chimaeras (meta-algae). Philos Trans R Soc Lond Ser B Biol Sci 358(1429):109–133

Chan RL, Keller M, Canaday J, Weil JH, Imbault P (1990) Eight small subunits of *Euglena* ribulose 1-5 bisphosphate carboxylase/oxygenase are translated from a large mRNA as a polyprotein. EMBO J 9(2):333–338

Chauhan JS, Rao A, Raghava GP (2013) In silico platform for prediction of N-, O- and C-glycosites in eukaryotic protein sequences. PLoS One 8(6):e67008

Durnford DG, Gray MW (2006) Analysis of *Euglena gracilis* plastid-targeted proteins reveals different classes of transit sequences. Eukaryot Cell 5(12):2079–2091

Enomoto T, Sulli C, Schwartzbach SD (1997) A soluble chloroplast protease processes the Euglena polyprotein precursor to the light harvesting chlorophyll a/b binding protein of photosystem II. Plant Cell Physiol 38:743–746

Felsner G, Sommer MS, Gruenheit N, Hempel F, Moog D, Zauner S, Martin W, Maier UG (2011) ERAD components in organisms with complex red plastids suggest recruitment of a preexisting protein transport pathway for the periplastid membrane. Genome Biol Evol 3:140–150

Gibbs SP (1970) Comparative ultrastructure of algal chloroplast. Ann N Y Acad Sci 175(2):454–473

Gibbs SP (1978) The chloroplasts of *Euglena* may have evolved from symbiotic green algae. Can J Bot 56:2883–2889

Gibbs SP (1981a) The chloroplast endoplasmic reticulum: structure, function and evolutionary significance. Int Rev Cytol 72:49–99

Gibbs SP (1981b) The chloroplasts of some algal groups may have evolved from endosymbiotic eukaryotic algae. Ann N Y Acad Sci 361:193–207

Gray MW, Doolittle WF (1982) Has the endosymbiont hypothesis been proven? Microbiol Rev 46(1):1–42

Grossman A, Manodori A, Snyder D (1990) Light-harvesting proteins of diatoms: their relationship to the chlorophyll a/b binding proteins of higher plants and their mode of transport into plastids. Mol Gen Genet 224(1):91–100

von Heijne G (1988) Transcending the impenetrable: how proteins come to terms with membranes. Biochim Biophys Acta 947:307–333

Henze K, Badr A, Wettern M, Cerff R, Martin W (1995) A nuclear gene of eubacterial origin in *Euglena gracilis* reflects cryptic endosymbioses during protist evolution. Proc Natl Acad Sci U S A 92(20):9122–9126

Houlne G, Schantz R (1987) Molecular analysis of the transcripts encoding the light-harvesting chlorophyll a/b protein in *Euglena gracilis*: unusual size of the mRNA. Curr Genet 12(8):611–616

Houlne G, Schantz R (1988) Characterization of cDNA sequences for LHCI apoproteins in *Euglena gracilis*: the mRNA encodes a large precursor containing several consecutive divergent polypeptides. Mol Gen Genet 213(2–3):479–486

Inagaki J, Fujita Y, Hase T, Yamamoto Y (2000) Protein translocation within chloroplast is similar in Euglena and higher plants. Biochem Biophys Res Commun 277(2):436–442

Keeling PJ (2013) The number, speed, and impact of plastid endosymbioses in eukaryotic evolution. Annu Rev Plant Biol 64:583–607

Keller M, Chan RL, Tessier LH, Weil JH, Imbault P (1991) Post-transcriptional regulation by light of the biosynthesis of Euglena ribulose-1,5-bisphosphate carboxylase/oxygenase small subunit. Plant Mol Biol 17(1):73–82

Kishore R, Schwartzbach SD (1992) Translational control of the synthesis of the Euglena light harvesting chlorophyll a/b binding protein of photosystem II. Plant Sci 85:79–89

Kishore R, Muchhal U, Schwartzbach SD (1993) The presequence of Euglena LHCPII, a cytoplasmically synthesized chloroplast protein, contains a functional endoplasmic reticulum targeting domain. Proc Natl Acad Sci U S A 90:11845–11849

Ko K, Cashmore AR (1989) Targeting of proteins to the thylakoid lumen by the bipartite transit peptide of the 33 kd oxygen-evolving protein. EMBO J 8(11):3187–3194

Koziol AG, Durnford DG (2008) Euglena light-harvesting complexes are encoded by multifarious polyprotein mRNAs that evolve in concert. Mol Biol Evol 25(1):92–100

Kuroiwa T, Sakaguchi M, Mihara K, Omura T (1991) Systematic analysis of stop-transfer sequence for microsomal membrane. J Biol Chem 266(14):9251–9255

Lee J, Kim DH, Hwang I (2014) Specific targeting of proteins to outer envelope membranes of endosymbiotic organelles, chloroplasts, and mitochondria. Front Plant Sci 5:173

Lefortran M, Pineau B (1980) Structure and functional-organization of chloroplastic membranes envelope in Euglena-gracilis. Eur J Cell Biol 22(1):279–279

Lefort-Tran M, Pouphile M, Freyssinet G, Pineau B (1980) Structural and functional significance of the chloro-

plast envelope of Euglena: immunocytological and freeze fracture study. J Ultrastruct Res 73(1):44–63

Lin Q, Ma L, Burkhart W, Spremulli LL (1994) Isolation and characterization of cDNA clones for chloroplast translational initiation factor-3 from *Euglena gracilis*. J Biol Chem 269(13):9436–9444

Lousa CD, Denecke J (2016) Lysosomal and vacuolar sorting: not so different after all! Biochem Soc Trans 44:891–897

Maier UG, Zauner S, Hempel F (2015) Protein import into complex plastids: cellular organization of higher complexity. Eur J Cell Biol 94(7–9):340–348

Muchhal US, Schwartzbach SD (1992) Characterization of a Euglena gene encoding a polyprotein precursor to the light-harvesting chlorophyll a/b-binding protein of photosystem II. Plant Mol Biol 18(2):287–299

Muchhal US, Schwartzbach SD (1994) Characterization of the unique intron-exon junctions of Euglena gene(s) encoding the polyprotein precursor to the light-harvesting chlorophyll a/b binding protein of photosystem II. Nucl Acid Res 22:5737–5744

Nassoury N, Cappadocia M, Morse D (2003) Plastid ultrastructure defines the protein import pathway in dinoflagellates. J Cell Sci 116(Pt 14):2867–2874

Needham PG, Brodsky JL (2013) How early studies on secreted and membrane protein quality control gave rise to the ER associated degradation (ERAD) pathway: the early history of ERAD. Biochim Biophys Acta 1833(11):2447–2457

Neuhaus JM, Rogers JC (1998) Sorting of proteins to vacuoles in plant cells. Plant Mol Biol 38:127–144

Osafune T, Schiff JA, Hase E (1990) Immunogold localization of LHCPII apoprotein in the Golgi of Euglena. Cell Struct Funct 15(2):99–105

Osafune T, Schiff JA, Hase E (1991a) Stage-dependent localization of LHCP II apoprotein in the Golgi of synchronized cells of *Euglena gracilis* by immunogold electron microscopy. Exp Cell Res 193(2):320–330

Osafune T, Sumida S, Schiff JA, Hase E (1991b) Immunolocalization of LHCPII apoprotein in the Golgi during light-induced chloroplast development in non-dividing *Euglena* cells. J Electron Microsc 40:41–47

Paila YD, Richardson LGL, Schnell DJ (2015) New insights into the mechanism of chloroplast protein import and its integration with protein quality control, organelle biogenesis and development. J Mol Biol 427(5):1038–1060

Patron NJ, Waller RF (2007) Transit peptide diversity and divergence: a global analysis of plastid targeting signals. BioEssays 29(10):1048–1058

Patron NJ, Waller RF, Archibald JM, Keeling PJ (2005) Complex protein targeting to dinoflagellate plastids. J Mol Biol 348(4):1015–1024

Peschke M, Moog D, Klingl A, Maier UG, Hempel F (2013) Evidence for glycoprotein transport into complex plastids. Proc Natl Acad Sci U S A 110(26):10860–10865

Plaumann M, Pelzer-Reith B, Martin WF, Schnarrenberger C (1997) Multiple recruitment of class-I aldolase to chloroplasts and eubacterial origin of eukaryotic class-II aldolases revealed by cDNAs from *Euglena gracilis*. Curr Genet 31(5):430–438

Rikin A, Schwartzbach SD (1988) Extremely large and slowly processed precursors to the *Euglena* light harvesting chlorophyll a/b binding proteins of photosystem II. Proc Natl Acad Sci U S A 85:5117–5121

Rikin A, Schwartzbach SD (1989) Regulation by light and ethanol of the synthesis of the light harvesting chlorophyll a/b binding protein of photosystem II in Euglena. Planta 178:76–83

Santillan Torres JL, Atteia A, Claros MG, Gonzalez-Halphen D (2003) Cytochrome f and subunit IV, two essential components of the photosynthetic bf complex typically encoded in the chloroplast genome, are nucleus-encoded in *Euglena gracilis*. Biochim Biophys Acta 1604(3):180–189

Schiff JA, Schwartzbach SD, Osafune T, Hase E (1991) Photocontrol and processing of LHCPII apoprotein in Euglena - possible role of Golgi and other cytoplasmic sites. J Photochem Photobiol B Biol 11(2):219–236

Schwartzbach SD, Osafune T, Löffelhardt W (1998) Protein import into Cyanelles and complex chloroplasts. Plant Mol Biol 38:247–263

Shao S, Hegde RS (2011) Membrane protein insertion at the endoplasmic reticulum. Annu Rev Cell Dev Biol 27:25–56

Sharif AL, Smith AG, Abell C (1989) Isolation and characterisation of a cDNA clone for a chlorophyll synthesis enzyme from *Euglena gracilis*. The chloroplast enzyme hydroxymethylbilane synthase (porphobilinogen deaminase) is synthesised with a very long transit peptide in Euglena. Eur J Biochem 184(2):353–359

Shigemori Y, Inagaki J, Mori H, Nishimura M, Takahashi S, Yamamoto Y (1994) The presequence of the precursor to the nucleus-encoded 30 kDa protein of photosystem II in *Euglena gracilis* Z includes two hydrophobic domains. Plant Mol Biol 24(1):209–215

Slavikova S, Vacula R, Fang Z, Ehara T, Osafune T, Schwartzbach SD (2005) Homologous and heterologous reconstitution of Golgi to chloroplast transport and protein import into the complex chloroplasts of *Euglena*. J Cell Sci 118(Pt 8):1651–1661

Smeekens S, Bauerle C, Hageman J, Keegstra K, Weisbeek P (1986) The role of the transit peptide in the routing of precursors toward different chloroplast compartments. Cell 46(3):365–375

Spano AJ, Ghaus H, Schiff JA (1987) Chlorophyll-protein complexes and other thylakoid components at the low intensity threshold in Euglena chloroplast development. Plant Cell Physiol 28(6):1101–1108

Stork S, Moog D, Przyborski JM, Wilhelmi I, Zauner S, Maier UG (2012) Distribution of the SELMA translocon in secondary plastids of red algal origin and predicted uncoupling of ubiquitin-dependent translocation from degradation. Eukaryot Cell 11(12):1472–1481

Sulli C, Schwartzbach SD (1995) The polyprotein precursor to the *Euglena* light harvesting chlorophyll a/b--binding protein is transported to the Golgi apparatus prior to chloroplast import and polyprotein processing. J Biol Chem 270:13084–13090

Sulli C, Schwartzbach SD (1996) A soluble protein is imported into *Euglena* chloroplasts as a membrane-bound precursor. Plant Cell 8:43–53

Sulli C, Fang ZW, Muchhal U, Schwartzbach SD (1999) Topology of Euglena chloroplast protein precursors within endoplasmic reticulum to Golgi to chloroplast transport vesicles. J Biol Chem 274:457–463

Theg SM, Bauerle C, Olsen LJ, Selman BR, Keegstra K (1989) Internal ATP is the only energy requirement for the translocation of precursor proteins across chloroplastic membranes. J Biol Chem 264(12):6730–6736

Turmel M, Gagnon MC, O'Kelly CJ, Otis C, Lemieux C (2009) The chloroplast genomes of the green algae Pyramimonas, Monomastix, and Pycnococcus shed new light on the evolutionary history of prasinophytes and the origin of the secondary chloroplasts of euglenids. Mol Biol Evol 26(3):631–648

Vacula R, Steiner JM, Krajcovic J, Ebringer L, Loffelhardt W (1999) Nucleus-encoded precursors to thylakoid lumen proteins of *Euglena gracilis* possess tripartite presequences. DNA Res 6(1):45–49

Villarejo A, Buren S, Larsson S, Dejardin A, Monne M, Rudhe C, Karlsson J, Jansson S, Lerouge P, Rolland N, von Heijne G, Grebe M, Bako L, Samuelsson G (2005) Evidence for a protein transported through the secretory pathway en route to the higher plant chloroplast. Nat Cell Biol 7(12):1224–1231

Whatley JM, Whatley FR (1981) Chloroplast evolution. New Phytol 87(2):233–247

Photomovement in *Euglena*

11

Donat-P. Häder and Mineo Iseki

Abstract

Motile microorganisms such as the green *Euglena gracilis* use a number of external stimuli to orient in their environment. They respond to light with photophobic responses, photokinesis and phototaxis, all of which can result in accumulations of the organisms in suitable habitats. The light responses operate synergistically with gravitaxis, aerotaxis and other responses. Originally the microscopically obvious stigma was thought to be the photoreceptor, but later the paraxonemal body (PAB, paraflagellar body) has been identified as the light responsive organelle, located in the trailing flagellum inside the reservoir. The stigma can aid in light direction perception by shading the PAB periodically when the cell rotates helically in lateral light, but stigmaless mutants can also orient with respect to the light direction, and negative phototaxis does not need the presence of the stigma. The PAB is composed of dichroically oriented chromoproteins which is reflected in a pronounced polarotaxis in polarized light. There was a long debate about the potential photoreceptor molecule in *Euglena*, including carotenoids, flavins and rhodopsins. This discussion was terminated by the unambiguous proof that the photoreceptor is a 400 kDa photoactivated adenylyl cyclase (PAC) which consists of two α- and two β-subunits each. Each subunit possesses two BLUF (Blue Light receptor Using FAD) domains binding FAD, which harvest the light energy, and two adenylyl cyclases, which produce cAMP from ATP. The cAMP has been found to activate one of the five protein kinases found in *Euglena*

D.-P. Häder (✉)
Department of Biolology, Friedrich-Alexander Universität, Erlangen-Nürnberg,
Neue Str. 9, 91096, Möhrendorf, Germany
e-mail: donat@dphaeder.de

M. Iseki
Faculty of Pharmaceutical Sciences, Toho University,
Miyama 2-2-1, Funabashi, Chiba 274-8510, Japan

S.D. Schwartzbach, S. Shigeoka (eds.), *Euglena: Biochemistry, Cell and Molecular Biology*,
Advances in Experimental Medicine and Biology 979, DOI 10.1007/978-3-319-54910-1_11

(PK.4). This enzyme in turn is thought to phosphorylate proteins inside the flagellum which result in a change in the flagellar beating pattern and thus a course correction of the cell. The involvements of PAC and protein kinase have been confirmed by RNA interference (RNAi). PAC is responsible for step-up photophobic responses as well as positive and negative phototaxis, but not for the step-down photophobic response, even though the action spectrum of this resembles those for the other two responses. Analysis of several colorless *Euglena* mutants and the closely related *Euglena longa* (formerly *Astasia longa*) confirms the results. Photokinesis shows a completely different action spectrum. Some other *Euglena* species, such as *E. sanguinea* and the gliding *E. mutabilis*, have been investigated, again showing totally different action spectra for phototaxis and photokinesis as well as step-up and step-down photophobic responses.

Keywords

Astasia • *Euglena longa* • *Euglena gracilis* • *Euglena mutabilis* • Flavin • Photoactivated adenylyl cyclase • Photokinesis • Photophobic reactions • Photoreceptor • Phototaxis • Protein kinase • Pterin • Sensory transduction

11.1 Introduction

Many unicellular microorganisms as well as cell colonies are motile and orient themselves with respect to external physical and chemical parameters in their environment such as temperature (Häder et al. 2014), pH, oxygen (Colombetti and Diehn 1978; Porterfield 1997), chemicals and pollutants (Govorunova and Sineshchekov 2005; Ozasa et al. 2013; Azizullah et al. 2014), mechanical stimuli (Mikolajczyk and Diehn 1979; Fenchel 2013), the magnetic field of the Earth (de Araujo et al. 1986; Kavaliers and Ossenkopp 1994) and even electrical currents (Umrath 1959; Votta and Jahn 1972; Kim 2013). Many swimming cells orient themselves in the gravity field of the Earth using a mechanism called gravitaxis (see Chap. 12) (Richter et al. 2002; Nasir 2014).

Photosynthetic organisms such as flagellates require the presence of light for energy harvesting, so that it is not astonishing that they orient with respect to light to guide their migrations (Häder 1979; Häder and Lebert 2009; Peacock and Kudela 2014). But also heterotrophic organisms use phototactic orientation for habitat selection (Hu et al. 2014). Motile flagellates often move toward the light source at low irradiances (positive phototaxis, Fig. 11.1a) (Liu and Häder 1994; Giometto et al. 2015). Since excessive radiation can be detrimental for the cells, many organisms move away from the light source at high irradiances (negative phototaxis, Fig. 11.1b) (Lenci et al. 1984; Josef et al. 2005; Ma et al. 2012). In some cases an orientation at a specific angle to the light direction (e.g. perpendicular to a light beam, Fig. 11.1c) has been found, a behavior called diaphototaxis (Häder and Lipson 1986; Nultsch and Häder 1988; Rhiel et al. 1988). This behavior enables the organisms to swim horizontally at constant optimal light intensity.

In addition, many cells show other light-induced behavioral movement responses. Upon a sudden decrease in light intensity they show a step-down photophobic response which may be a stop, a change in swimming direction or a reversal of movement (Govorunova et al. 2004; Lenci

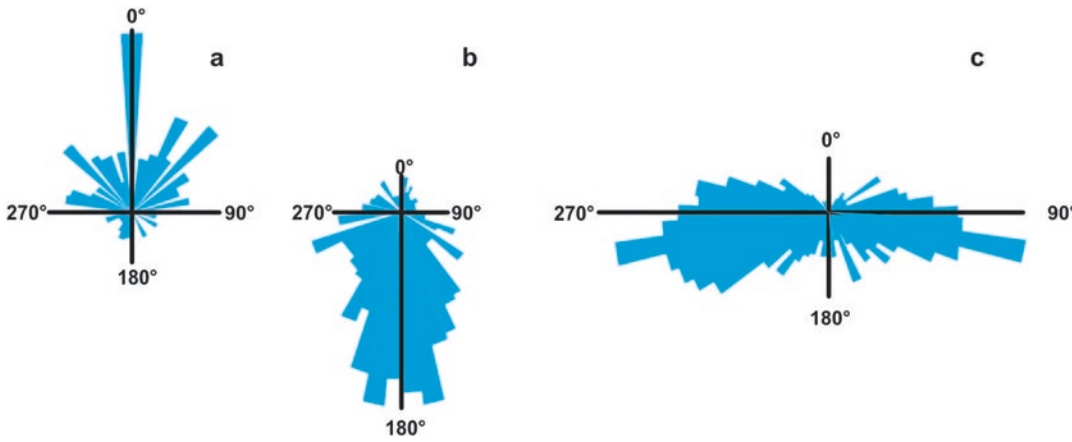

Fig. 11.1 (**a**) Positive phototaxis in *E. gracilis* strain Z swimming in a horizontal cuvette with white light at 10 W m^{-2} impinging from 0°. Tracks of swimming cells were recorded by automatic image analysis and the angles deviating from 0° (direction toward the light source) were binned in 64 sectors. The circular histogram shows the percentage of tracks in each angular sector. (**b**) Negative phototaxis in *E. gracilis* strain Z swimming in a horizontal cuvette with white light at 100 W m^{-2} impinging from 0° (modified from (Lebert and Häder 2000). (**c**) Diaphototaxis in the colorless *E. gracilis* strain FB swimming in a horizontal cuvette with white light at 1000 W m^{-2} impinging from 0° redrawn from (Lebert and Häder 1997)

et al. 2012). Imagine cells swimming in a horizontal container which is covered by a black lid with a square opening in the center irradiated by low intensity light from above. Cells swimming in the shade may enter the irradiated zone without a response, but, if they try to leave it they undergo a step-down photophobic response at the light/dark boundary. This behavior will result in an accumulation of cells in the irradiated area over time. This reaction is exploited in the so-called light trap method used to quantify photophobic responses (Nultsch and Häder 1979). Likewise, a sudden increase in the ambient light intensity may result in a step-up photophobic response which is elicited by a sudden increase in light intensity which would occur when an organism enters a irradiated area from a shaded one (Doughty and Diehn 1984; Ntefidou et al. 2003b; Takeda et al. 2013). This usually occurs at high light intensities. In this case cells trying to cross the border from the shaded area into the brightly lit zone will undergo a step-up photophobic response while they do not react when leaving the light field. This behavior results in a depletion of cells in the lit zone and an accumulation in the dark. Photophobic responses in *Euglena* have also been studied by the observation of individual cells embedded in a small agar chamber (Shimmen 1981).

A dependence of the swimming speed on the ambient irradiance is called photokinesis (Zhenan and Shouyu 1983; Melkonian et al. 1986; Iwatsuki 1992). This phenomenon can also result in accumulations of cells in certain areas (Häder 1987a). Imagine cells swimming fast in light but slow in the shaded area or even stopping (positive photokinesis); these cells will accumulate in the shaded area. This has been observed e.g. in the ciliate *Stentor coeruleus* (Iwatsuki 1992). Also the opposite has been found: cells swimming fast in the dark and slower in light will accumulate in the irradiated field (negative photokinesis). Another mechanism for cell accumulation is phototaxis of cells toward a light field irradiated by a strong light source such as a laser beam as shown for *Euglena* (Itoh and Tamura 2008).

While phototaxis has been studied in many flagellates to some extent only a few were investigated in detail, such as the Chlorophyte *Chlamydomonas reinhardtii* (Sineshchekov et al. 2002; Schmidt et al. 2006; Inaba et al. 2014). *Euglena* has been established as a model system for biochemical and behavioral studies, signal

transduction and molecular biology of the photoreceptor (Iseki et al. 2002; Wolken 2012; Masuda 2013; Ozasa et al. 2014; Giometto et al. 2015).

In the past, the movement and orientation of motile microorganisms was recorded and quantified by manual and video techniques (Colombetti et al. 1982), but are nowadays usually quantified using real-time image analysis and computerized cell tracking (Häder and Lebert 2000; Häder 2003).

11.2 The Organisms

Euglena gracilis is a photosynthetic unicellular flagellate (Buetow 1968a), but it can also live heterotrophically (Sumida et al. 2007). The size ranges between 50 µm and 80 µm length and 8 µm to 12 µm width (Buetow 1968b). Since the cell does not have a rigid cell wall its form is highly flexible ranging from almost spherical to an elongated spindle (Mikolajczyk and Diehn 1976, 1978; Mikolajczyk and Kuznicki 1981; Murray 1981). The cell body is covered with a pellicle which consists of longitudinal interlocked stripes which can slip with respect to one another (Suzaki and Williamson 1986; Leander et al. 2001), and the surface is covered with slime (Diskus 1955). The stripes are composed of the claudin-like, four-trans-membrane protein IP39 which forms linear arrays by a trimeric unit repeat which are similar to tight junctions (Capaldo et al. 2014). At the front end there is a bottle-like 5 µm × 10 µm invagination, called reservoir (Fig. 11.2), which allows pinocytotic uptake of external material (Kivic and Vesk 1974a; Bouck 2012; Omodeo 2013). A system of contractile vacuoles (one main vacuole with several accessory vacuoles) is associated with the reservoir, believed to be involved in osmoregulation (Rosati et al. 1996; Komsic-Buchmann and Becker 2012). At the base of the reservoir two flagella originate in basal bodies, but only one of them extends as a trailing flagellum from the reservoir while the other one reaches up to the paraxonemal body (PAB, also called paraflagellar body) (Tollin 1973; Piccinni and Mammi 1978), located on the long flagellum half way between the bottom and the opening of the invagination, called pharynx (Frey-Wyssling and Mühlethaler 1960; Kisielewska et al. 2015). The PAB is a small organelle (1 µm × 0.7 µm × 0.7 µm) (Wolken 1977; Omodeo 1980; Rosati et al. 1991) (Fig. 11.2). A paraxonemal rod (PAR) inside the flagellum connects the PAB to the cell matrix (Banchetti et al. 1980; Hyams 1982; Verni et al. 1992; Karnkowska et al. 2015). It consists of several proteins like in trypanosomes, the function of which is still unclear (Hyams 1982; Leedale 1982; Ngô and Bouck 1998). The membrane covering the PAB was found to be structurally specialized when observed with the freeze-fracture technique. There are large-sized (10–14 nm) intramembrane particles (Robenek and Melkonian 1983). The side next to the stigma is closely attached to the plasmalemma of the reservoir. Inside the cytoplasm, in close vicinity of the reservoir and next to the PAB it possesses a red structure, the stigma or eyespot which is so obvious that it was detected by early microscopists (Pringsheim 1937; Wolken 1956). This structure gave the flagellate its

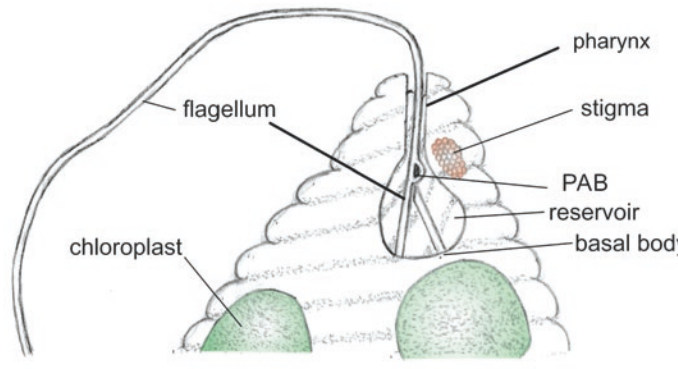

Fig. 11.2 Front end of a *Euglena* cell showing the reservoir and the stigma as well as chloroplasts. Inside the reservoir two flagella originate from basal bodies. One is short and touches the paraxonemal body (PAB) located on the long emerging flagellum (drawn by Dr. Maria Häder)

German name "Augentierchen" (small eye animal) and was considered to be the site of the photoreceptor (Cypionka 2010). The stigma consists of a number of globules (200–300 nm diameter) filled with carotenoids (Strother and Wolken 1960; Sperling et al. 1973; Benedetti et al. 1976; Heelis et al. 1979, 1980; Osafune and Schiff 1980; James et al. 1992). The main carotenoid in *E. gracilis* is antheraxanthin (80%) (Krinsky and Goldsmith 1960). Application of streptomycin to dark-bleached cultures of *Euglena* hampered the carotenoid synthesis, and electron micrographs showed a decrease in the number of stigma vesicles while no effect on the PAB was detected. Phototaxis decreased and finally disappeared after 5 weeks (Ferrara and Banchetti 1976). This does not mean that the photoreceptor is located within the stigma, but that its role as a shading device is compromised. In contrast to other algal groups, such as Chlorophytes, the stigma in *Euglena* is not enclosed within the chloroplast (Kivic and Vesk 1974b; Kronestedt and Walles 1975). Also in contrast to green algae, the globules are not organized in a rigid structure (Walne and Arnott 1967; Dodge 1969; Kivic and Vesk 1972a; b; Kreimer and Melkonian 1990). Therefore it does not function as an interference reflector device which is found in many stigmata of Chlorophytes such as *Chlamydomonas* (Kreimer 1994). Even though the stigma does not harbor the photoreceptor, as suggested by earlier authors (France 1909; Fong and Schiff 1978, 1979), it seems to be involved in photoperception, functioning as a screening device which in lateral light casts a periodic shadow on the photoreceptor (the PAB, see below) as the cell rotates around its long axis when it is propelled by its long flagellum in a forward direction (Barsanti et al. 2012). For comparison, we also shortly discuss several mutant strains of *Euglena gracilis*, some other species in the genus *Euglena* as well as the close relative *E. longa* (formerly *Astasia longa*) (Poniewozik 2014).

11.3 The Paraxonemal Body (PAB)

The PAB shows a paracrystalline structure (Kivic and Vesk 1972a; Forreiter and Wagner 2012). Wolken (1977) proposed a model of packed rods in a helical pattern based on optical diffraction patterns, and Piccinni and Mammi (1978) found monoclinic or slightly hexagonal cell units with the principal axes a = 8.9 nm, b = 7.7 nm, c = 8.3 nm und ß = 110°. This structure can be interpreted as an I-type 3-D crystal (Michel 1990), which is a stacks of 2-D crystal arrays stabilized by hydrophobic interactions between the planes and hydrophilic interactions with the surrounding aqueous environment. More than 100 layers of the 2-D crystals are thought to form the observed structure of the PAB (Gualtieri 1993b). 2-D type crystals have been found e.g. in the purple membrane in *Halobacterium salinarium*, with a very high concentration of bacteriorhodopsin to harvest light energy (Oesterhelt 1998) or in photosynthetic membranes of higher plants (Toporik et al. 2012) and purple bacteria (Sznee et al. 2014).

11.4 Photoresponses

As indicated above *Euglena gracilis* shows three types of photoresponses: both positive and negative phototaxis, step-up and step-down photophobic responses and photokinesis.

11.4.1 Phototaxis

In contrast to photokinesis and photophobic responses phototaxis depends on the direction of the impinging light. Phototaxis in motile microorganisms has been known for more than a century (France 1908, 1909). At low irradiances the flagellates move toward the light source (positive phototaxis) which can be shown both in horizontal or vertical observation chambers. At higher irradiances the cells switch to negative phototaxis and swim away from the light source (Häder et al. 1981). In *Euglena*, the threshold for the change from positive to negative phototaxis is found between 10 and 100 W m^{-2}, but it depends on other external factors (Häder 1987b, 1998) as well as whether the cells swim in a horizontal or vertical cuvette. In the latter case the cells orient simultaneously with respect to light and gravity (see below). At intermediate light intensities

some of the cells show positive others negative phototaxis. As the ecological consequence of this behavior, *Euglena* cells accumulate at a certain depth in the water column at which the impinging sun light has been attenuated to about 30 W m^{-2} (Häder and Griebenow 1988). A similar behavior was found in the freshwater *E. proxima* (Hasle 1950). In comparison, the green flagellate *Chlamydomonas* is much more sensitive than *Euglena* and has a threshold for positive phototaxis at 0.001 W m^{-2} (Feinleib and Curry 1971). This reflects the fact that *Chlamydomonas* is often found much deeper in the water column with less light availability than *Euglena*.

The mechanism of light direction detection was debated for a long time. Some researchers held the notion that oriented movement depends on a series of photophobic responses (Jennings 1906; Mast 1911): When an organism experiences a decrease in irradiance it might make a turn or reverse the direction of movement. When this strategy is repeated over time the organism will move up the light gradient and thus show a positive phototaxis. The same reasoning holds for negative phototaxis being based on consecutive step-up photophobic responses. This hypothesis is based on a two-instant mechanism (Feinleib 1975): The photoreceptor takes readings of the ambient irradiance and compares it to a previous measurement. This orientation mechanism has also been described as "biased random walk" (Hill and Vincent 1993; Hill and Häder 1997), which is also found in chemotaxis of bacteria (Wadhams and Armitage 2004). This theory implies that the photoreceptors for phototaxis and photophobic responses are identical. For *Euglena gracilis* the hypothesis that light direction detection is based on a series of repetitive photophobic responses can be rejected at least for negative phototaxis, since in this flagellate the threshold for negative phototaxis is much lower than that for the step-up photophobic response. We will also see below that the molecular analysis of the photoreceptor showed that the step-down photophobic response in *Euglena* is not mediated by the same photoreceptor which drives phototaxis.

Alternatively, the organism detects the light direction with a more sophisticated sensor than just a light-intensity measuring photoreceptor. This is based on a one-instant mechanism. E.g., some ciliates posses a complicated optical organelle which like a primitive eye, is capable of discerning the direction of the impinging light (Omodeo 1975; Selbach et al. 1999).

Buder devised an ingenious experiment to tackle the question whether phototaxis is controlled by an orientation along a spatial gradient of light or the result of a directional movement with respect to the light direction. He passed light through a biconvex lens so that he produced a converging light beam. The cells swam toward the light source, passed through the focal point and continued to swim toward the light source even though the light intensity decreased with the distance from the focal point (Buder 1919).

In negative phototaxis the rear end of the cell with its chloroplasts casts a shadow on the photoreceptor. Circular histograms of the swimming directions indicate that a course correction is initiated when the cell deviates by more than 25° from the light direction (Häder et al. 1986) indicating that in this position the rear end does no longer shade the photoreceptor.

When exposed to two perpendicular light beams, at low fluence rates which induce positive phototaxis, the cells do not orient on the mathematical resultant of the two vectors but orient themselves with respect to either light beam (Häder 1993). At equal light intensities approximately half of the population swims toward one light source and the remainder toward the other light source. When the intensity of one of the light beams exceeds that of the other by more than 10%, almost all cells move in the direction of the stronger light beam (Lebert and Häder 2000). In contrast, at high fluence rates which induce negative phototaxis the cells orient on the resultant away from the two perpendicularly impinging light beams. When the cells orient with respect to light they are simultaneously exposed to the gravity field of the Earth unless they are under zero-g conditions such as on a satellite or on the International Space Station (ISS). In a vertical

cuvette they show a gravitactic orientation. Shortly after inoculation into new medium the cells swim downward. In contrast, older cells (>10 days) swim upward. When they simultaneously perceive a (horizontal) light beam perpendicular to the gravitational field of the Earth the cells swim on an intermediate track on the resultant; the angular deviation from the vertical depends on the irradiance of the light beam (Kessler et al. 1992). In order to estimate the effect of the simultaneously operating gravitaxis on the precision of phototaxis a space experiment was carried out on a sounding rocket flight inside a TEXUS rocket (Kühnel-Kratz et al. 1993). As expected, under microgravity (μg) conditions the precision of phototaxis was higher than in the 1-g control but the inversion from positive to negative phototaxis was the same for a sample taking shortly after landing of the rocket as in the control cells which had been exposed to 1 g all the time. In addition, phototactic orientation was reached faster at μg than at 1-g conditions (Häder 1997).

The mechanism of changing movement direction is closely linked to the rotation of the cell and the position of the flagellum. While swimming, a cell rotates at about 1 Hz around its long axis describing a cone with a ca. 15° opening angle at the front end. The flagellum is more or less parallel to the long axis. When a low intensity light beam (which induces a positive phototaxis) impinges perpendicular to the long axis, the flagellum swings out at an angle from the long axis, when during rotation the flagellum is oriented away from the light beam. This impulse triggers a small angular turn of the front end toward the light source. This is also seen in the output of a computer simulation (Häder 1993). This course correction is repeated as long as the long axis is not yet aligned with the light direction. When the flagellum is oriented away from the light direction, the stigma intercepts the light path onto the PAB photoreceptor (Häder 1998). Thus it modulates the light intensity seen by the PAB with the frequency of the cell's rotation with a minimum when the flagellum is opposed to the light direction. This was regarded as a proof for the shading hypothesis (Clayton 1964) and seemed to confirm the notion that phototaxis is brought about by a repetitive step-down photophobic response. For negative phototaxis this process has to be just the opposite with the additional shading from the rear end with its chloroplasts.

In order to determine the angle of the course correction a circular cuvette was rotated by an electric motor in a strong lateral light beam (30 klx) which induced negative phototaxis (Häder et al. 1986). The moving cells were recorded from below using a dark red monitoring light (>690 nm) which does not induce a visible movement response. When the cuvette was rotated at a low angular velocity (<20°/s) the cells still showed negative phototaxis but the mean swimming direction was shifted in the direction of the rotation. At higher rotational speeds the precision of orientation decreased and the swimming was more random. This indicates that the cells were capable of course corrections of up to 20°/s. Since the time for one rotation is about 1 s, the cells reorient by about 20° per rotation.

However, some mutants of *E. gracilis* lack a stigma but still show negative phototaxis, but no positive phototaxis (Vavra 1962; Checcucci et al. 1976; Häder 1993). In contrast, mutants which lack both PAB and stigma neither show positive nor negative phototaxis (Pringsheim 1948; Vavra 1962; Lebert and Häder 1997). Though many mutants are known lacking stigma, PAB and/or chloroplasts (Schiff et al. 1971, 1980; Shneyour and Avron 1975; Falke et al. 1997), only a few have been analyzed regarding phototaxis (Lebert and Häder 1997). These mutants have not been induced but occurred spontaneously and were isolated by accident. In one investigation, three of the studied mutants were stable, while one included some revertants which may be due to the fact that *Euglena* is polyploid.

Euglena longa, a close relative of *E. gracilis*, possesses a stigma but no PAB and does not show phototaxis (Suzaki and Williamson 1983; Mikolajczyk 1984a, 1984b) but step-up photophobic responses, while step-down responses were not observed, indicating that separate receptors exist for step-up and step-down photophobic responses. This was later confirmed by the molecular biological identification for the photoreceptor in *Euglena* (Iseki et al. 2002). All these

findings indicate that the PAB is the true photoreceptor in *E. gracilis* and that the stigma only has an accessory role (at least in positive phototaxis). Thus, the classical shading hypothesis had to be discarded.

As indicated above, earlier electron microscopic analyses have revealed a quasicrystalline structure within the PAB (Kivic and Vesk 1972b). Could that mean that the photoreceptor molecules are dichroically oriented in a specific pattern with reference to the long axis and the location of the stigma? In order to answer this question, experiments have been carried out with polarized light impinging from above onto a horizontal swimming chamber with *E. gracilis* (Bound and Tollin 1967; Creutz and Diehn 1976; Häder 1987b). The assumption is that light is only absorbed when the absorption vector is perpendicular to the light direction. When the electric dipole of the polarized light was oriented in a specific direction, the cells swam at an angle of about 30° clockwise from the electric dipole (Fig. 11.3a). This behavior was confirmed and also seen in a computer simulation which assumes the same orientation of the photoreceptor molecules as indicated in the electron micrographs (Häder 1993). Further experiments with polarized light in all three dimensions revealed the orientation of the absorption vectors in 3D with respect to the cell axes (Häder 1987b). Tracing the cells in a vertical cuvette with polarized light impinging from above indicated that the absorption vectors of the photoreceptor pigments are dichroically oriented predominantly 60° counterclockwise from the flagellar plane (when one looks onto the front end of the cell, Fig. 11.3b) (Häder 1987b). These results were confirmed in a mathematical model for the signal received by the dichroic photoreceptor in *E. gracilis* when irradiated by polarized light (Hill and Plumpton 2000). Diehn assumed that *Euglena* has two perpendicularly oriented photoreceptor systems responsible for positive and negative phototaxis, respectively (Diehn 1969c). During the revolution of the cell around its long axis a dichroically oriented photoreceptor has two positions with maximal absorption for light hitting perpendicularly to the swimming direction. This could explain the diaphototactic orientation found in the 1F mutant which does not have a screening

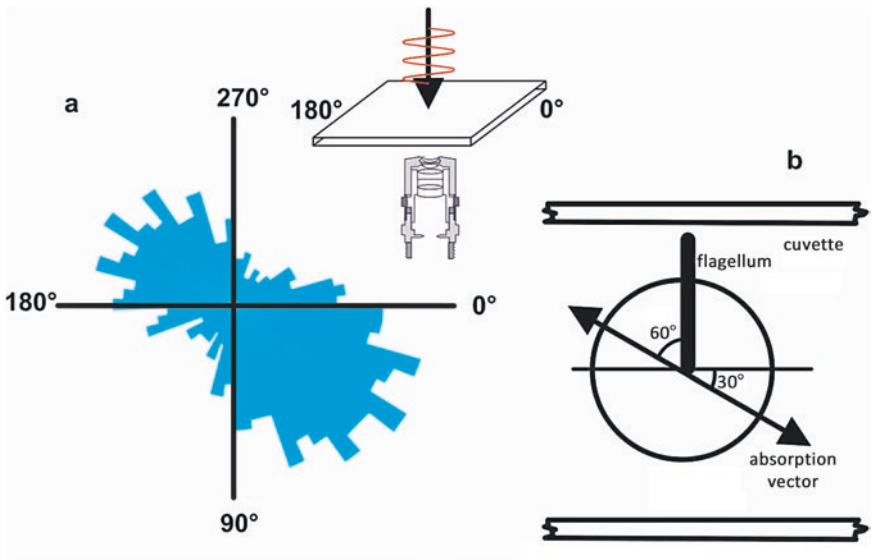

Fig. 11.3 (**a**) *Euglena* cells swimming in a horizontal cuvette orient themselves 30° clockwise from the electric vector of a polarized light beam swinging in a plane 0–180° impinging from above (*inset*), (**b**) absorption vectors of the photoreceptor pigments are dichroically oriented predominantly 60° counterclockwise from the flagellar plane when one looks onto the front end of the cell. Redrawn after (Häder 1987b)

stigma. The 1F mutant lacks chloroplasts, stigma and PAB. It shows only diaphototaxis and neither positive or negative phototaxis. In the wild type cells one of the absorption maxima is excluded by the presence of the stigma, so that the cells orient only in one direction. In negative phototaxis the rear end of the cell assumes the role of a shading device and the presence of the stigma is not required for negative phototaxis.

Euglena shows a strong circadian rhythm which affects orientational responses (Verworn 1889; Bruce and Pittendrigh 1956; Tollin and Robinson 1969; Edmunds 1984; Petersen-Mahrt et al. 1994) as well as other reactions such as cell division and cellular cAMP concentration (Bruce and Pittendrigh 1958; Feldman and Bruce 1972; Bruce 1973; Bünning 1973; Carre et al. 1989; Lebert et al. 1999). This may also be a reason that several authors found different results in their investigations of *Euglena* phototaxis. Also culture conditions and age strongly affect phototactic orientation (Häder et al. 1987).

11.4.2 Photophobic Responses

Photophobic responses (also called phobic reactions or shock responses) were first reported by Engelmann (1883). The older literature has been reviewed (Haupt 1959; Feinleib and Curry 1967; Diehn 1973; Nultsch 1975; Nultsch and Häder 1979). Photophobic responses are elicited by rather sudden changes in irradiance. If the change occurs over a longer time period, the organisms adapt to the new condition without showing a phobic response. The phobic response occurs only when the change in irradiance exceeds a species-specific discrimination threshold (Clayton 1959), which can be as low as a few percent (Nultsch and Häder 1970). In *Euglena* the response is characterized by a stop and tumble which can last a few seconds; after this the cell resumes swimming in a new direction (Doughty 1991). High speed cinemicrography showed that the cells respond with the turning toward the dorsal side when exposed to a sudden increase in light intensity (Diehn et al. 1975). In this organism step-down photophobic responses occur at low irradiances and step-up responses at higher irradiances (Diehn 1969c, 1973). Ecologically this behavior can be interpreted as helping the organism to prevent swimming from a low-irradiance region into an even darker shadow or from a high-irradiance region into excessive light. Very low irradiances may not be sufficient for photosynthesis and very high irradiances may be detrimental for the cells. The action spectra for the step-up and step-down photophobic responses in *Euglena* differ slightly but show a resemblance to a flavin chromophore (Diehn 1969a; Barghigiani et al. 1979b; Walne et al. 1984).

11.4.3 Photokinesis

As described above, photokinesis describes the dependency of the swimming speed on the light intensity. This behavior was first described almost 140 years ago (Strasburger 1878). It can result in an accumulation of organisms in lighted or shaded areas (see above). In *Euglena* a not very pronounced positive photokinesis was described (Wolken and Shin 1958). The increase in velocity saturates at 300 lx white light. However, a 10–15 min adaptation period is needed before the velocity reaches a new steady state (Mast 1911) which might indicate that metabolic processes are involved producing higher energy. The increase in swimming speed seems to be due to an increased flagellar beating frequency (Ascoli 1975). However, also the non-photosynthetic close relative *E. longa* has been found to show positive photokinesis (Mast 1911).

In *Euglena* the action spectrum of this response is still under debate. Some researchers found an effect in red light and proposed the involvement of the photosynthetic pigments such as chlorophyll *b* and β-carotene (Mast 1911; Ascoli 1975). Other researchers claim a strong effect of blue light (Nultsch and Throm 1975). Therefore it is not decided whether photokinesis depends on photosynthesis or is controlled by a blue light receptor (Haupt 1959).

11.5 The Photoreceptor(s)

Before molecular biology tools became available the question for the photoreceptor involved in a light-dependent responses such as phototaxis was tackled using action spectroscopy (Foster 2001). Using narrow band color filters (such as interference line filters) the organism is exposed to a selected wavelength band and the response is quantified at increasing irradiances (Foster 2001). This is repeated for all relevant wavelengths. Next the inverse of the required irradiance for a certain response (e.g. 50%) is plotted versus the wavelength giving an action spectrum or in other words the efficacy of the actinic light in dependence of the wavelength. The form of the action spectrum is compared with the absorption spectrum of a presumed photoreceptor. In reality things can be more complex e.g. by the presence of shading pigments. In order to avoid this complication, the method of threshold action spectra is used which are constructed again by plotting the wavelength-dependent response versus log light intensity (Foster and Smyth 1980). The reciprocals of the threshold intensity at which no reaction occurs, obtained by the linear interpolation of the response-intensity plots, should indicate the properties of the photoreceptor molecule.

11.5.1 Earlier Results and Hypotheses

Most flagellates have sensitivity in the UV/blue-green range (300–550 nm) of the spectrum. But there are exceptions: The action spectrum for phototaxis in *Chlamydomonas reinhardii* extends up to 600 nm (Foster and Smyth 1980; Johnson et al. 1991). In *Ochromonas danica* (Mast 1914) and *Peridinium gatunense* (Häder and Liu 1991) the spectrum even extends into the red region of the spectrum. These diverse spectral sensitivities probably indicate that phototaxis has evolved in multiple parallel events (Kivic and Walne 1983).

Early action spectra for photoaccumulation of green, dark-bleached and streptomycin-treated colorless *Euglena*, all of which possess a PAB, have been published by Checcucci et al. (1976). These spectra indicate the presence of a flavin-type photoreceptor. These measurements have been performed with the "phototaxigraph" (Lindes et al. 1965; Diehn and Tollin 1966; Checcucci et al. 1975). This instrument records the density of cells in a light trap and this is interpreted as a quantification of phototaxis when cells are attracted from the outside of the trap by light scattered from cells already inside the trap. However, as we have seen above, photoaccumulations can be brought about by several photoresponses including phototaxis. Another action spectrum for phototaxis was published by Gössel (1957).

Light microscopic images of the front end of *Euglena gracilis* show the reservoir with the two flagellar bases. Where they join a distinct body which represents the PAB can be seen (Fig. 11.4a). When excited with monochromatic light at 440 nm this spot shows a distinct blue fluorescence with a peak at about 520 nm (Fig. 11.4b). The red background fluorescence is derived from the chlorophyll in the cells. The flagella can be isolated with the PAB still attached (Gualtieri et al. 1986; Brodhun and Häder 1990) after the cells have been osmotically swelled in order to open the reservoir (Fig. 11.4c). Scanning electron micrographs of isolated flagella also show the PAB still attached to the flagellum (Brodhun et al. 1994). In large scale isolation experiments the chromoproteins of the PABs can be separated. SDS gel electrophoresis and isoelectric focusing shows the presence of four major proteins which are lacking in *Euglena longa* (which does not have a PAB) (Brodhun and Häder 1995a; Häder 1998). When excited, all four chromoproteins showed fluorescence emission spectra which were interpreted as representing flavins and pterins (Ghetti et al. 1985; Brodhun and Häder 1990; Häder 1991; Lebert 2001). Three proteins (M_r 27, 27.5. 31.6) contained pterins and the other one a flavin (M_r 33.5) (Lebert and Häder 2000). The excitation spectrum strongly resembled the action spectrum for phototaxis confirming the notion that a flavoprotein might be the photoreceptor for this response in *E. gracilis* (Brodhun and Häder 1990, 1995a). In addition, microspectrofluorometric studies of the PAB confirmed the presence of a flavin chromophore which showed

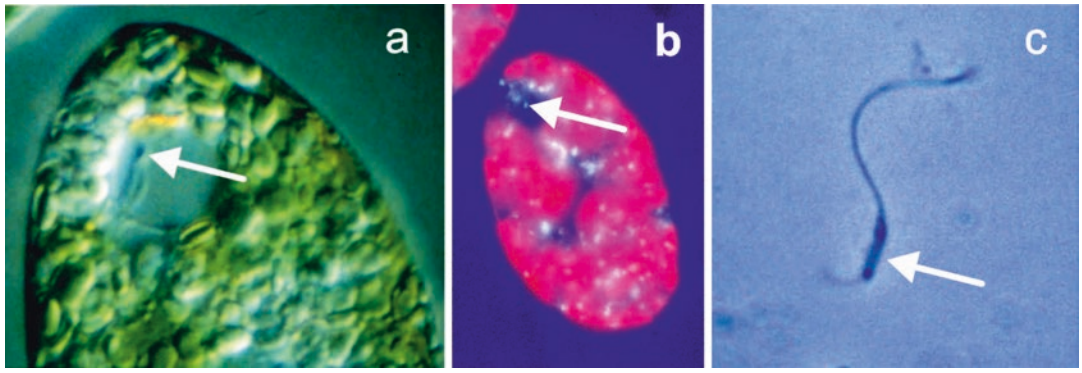

Fig. 11.4 Light microscopic photograph (**a**) and fluorescence microscopic image (**b**) of *Euglena gracilis* with the PAB (*arrows*). The chloroplasts show a red fluorescence and the blue spot in the reservoir indicates the PAB. The two flagellar bases are also seen in (**a**). (**c**) Isolated flagellum with PAB attached

an emission at 520 nm when excited between 400 and 500 nm (Benedetti and Checcucci 1975; Benedetti and Lenci 1977; Schmidt et al. 1990; Sineshchekov et al. 1994b). This interpretation is further strengthened by the fact that the fluorescence emission is strongly polarized, which has to be expected from the paracrystalline structure of the PAB (Sineshchekov et al. 1994b). The PAB fluorescence quantum yield is rather low (0.005 as compared to solubilized riboflavin ~0.25) (Ghetti et al. 1985). This indicates a strong coupling of the photoreceptor molecules to the signal transduction chain. Only when the transduction chain is saturated by excessive light or the coupling of the photoperception to the subsequent steps in the transduction chain is disturbed the fluorescence yield increases. The action spectrum for phototaxis in the green strain Z of *E. gracilis* extends to about 500 nm (Fig. 11.5a). Also when the chloroplasts and chlorophyll are removed by cultivating the cells in an organic medium in the dark, the action spectrum of these colorless strains still has the same shape (Häder and Reinecke 1991) consistent with a flavin chromophore.

Another confirmation for a flavin to be the chromophoric group in the photoreceptor for phototaxis was obtained by feeding *E. gracilis* over several generations with roseoflavin. This molecule is incorporated as a chromophore into the photoreceptor instead of the original flavin. Roseoflavin has an absorption peak at 500 nm and the spectrum extends up to 600 nm (Fig. 11.5a) (Häder 1998; Häder and Lebert 1998). When untreated cells were exposed to actinic light >550 nm produced by a cut-off filter they did not show phototactic orientation since the action spectrum extends only to ~500 nm (Fig. 11.5b). However, the roseoflavin-treated cells showed a clear phototaxis at wavelengths >550 nm (Fig. 11.5c). But it is of interest that the population displayed both positive and negative phototaxis. This can be easily explained by the fact that the carotenoids in the shading stigma do not absorb in this wavelength range, so that the cell cannot distinguish between light coming from the stigma side and the opposite direction.

When exposed to ultraviolet radiation the four proteins isolated by FPLC from the PAB were damaged and their amounts were significantly reduced (Brodhun and Häder 1993, 1995b). Both fluorescence excitation and emission spectra of the isolated PAB proteins decreased upon exposure to ultraviolet radiation (Häder and Brodhun 1991). As a result, exposure to solar or artificial UV-B radiation impaired phototaxis (Häder 1985, 1986; Häder and Häder 1988). However, this inhibition was not specific; chlorophyll content, photosynthetic oxygen production and motility were likewise affected (Gerber and Häder 1995; Richter et al. 2007). A polychromatic action spectrum of the inhibition confirmed that the high-energy UV-B radiation was most effective (Gerber et al. 1996). Filtering out the

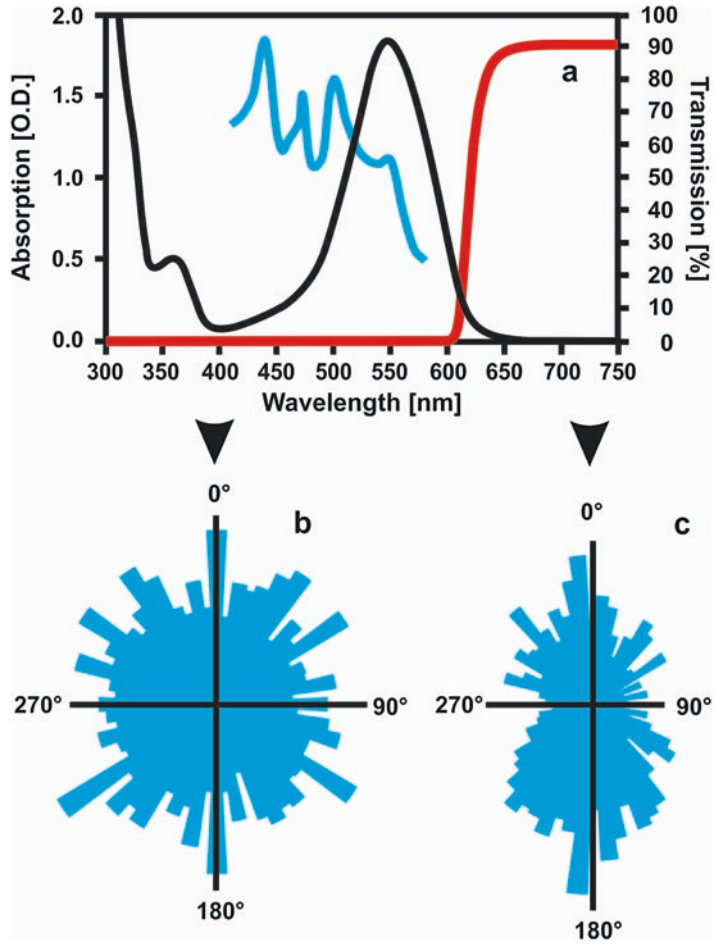

Fig. 11.5 (**a**) Action spectrum for phototaxis in *E. gracilis* (*blue line*), after (Häder and Reinecke 1991), absorption spectrum of roseoflavin (*black line*) and transmission spectrum of the OG 570 cut-off filter (*red line*). Histograms of phototactic orientation in wild type *E. gracilis* grown in medium (**b**) and cells grown in the presence of roseoflavin (**c**) when exposed to actinic light filtered by OG 570 cut-off filter. Redrawn after (Häder and Lebert 1998)

UV-B wavelength band from solar radiation in a field study provided some protection from excessive radiation: bleaching and immobility occurred later than in unfiltered sunlight (Gerber and Häder 1993).

Earlier work using flavin quenchers, such as KI, $MnCl_2$ and NaN_3 which are well known as effective quenchers of the electronically excited state of flavins, were effective in inhibiting the negative phototaxis in the organism (Colombetti et al. 1982; Lenci et al. 1983) but not the step-up photophobic reaction (Mikolajczyk and Diehn 1975). Neither KCN, a general metabolic inhibitor, nor KCl affected phototaxis. Both KI and $MnCl_2$ clearly quenched the fluorescence of 1 mM aqueous solutions of riboflavin.

Galland and coworkers suggested pterins as a possible UV-absorbing chromophore involved in phototactic photoperception of *Euglena gracilis* (Galland and Senger 1988a, b). Using the Okazaki large spectrograph and a computerized video motion analysis, Matsunaga and coworkers found that in addition to UV-A and blue light the action spectrum for photophobic responses of *E. gracilis* extended well into the UV-B with peaks at 270 nm (step-down response) and 280 nm (step-up response), respectively (Matsunaga et al. 1998) which they attributed to the combined action of 6-biopterin and FAD. In addition, fluorescence and emission spectra of the isolated PAB proteins indicated that pterins might also be involved (Galland et al. 1990). The colorless mutant 1F of *Euglena gracilis* does not possess flavins, as indicated by the fluorescence emission spectrum, but it shows the pterin emission band centered around 525 nm (Häder and Lebert

1998). This result indicates that the diaphototaxis found in the 1F and other mutants is not mediated by a flavin but by a pterin.

The separated flavoproteins had an apparent molecular mass of about 33,500 and the pterin-binding protein 27,000 (Brodhun and Häder 1990). Sineshchekov and coworkers suggested that there is an energy transfer from the pterins to the flavins, which can be disrupted by solubilization of the PAB (Sineshchekov et al. 1994a; Lebert and Häder 2000). It is assumed that the pterins are located on the outside of the PAB while the flavins are inside (Häder and Lebert 1998).

In order to confirm that flavins could be involved as chromophoric groups of photoreceptor pigments for phototaxis binding studies with [^{3}H]-labeled riboflavin were carried out (Brodhun et al. 1994). Nebenführ et al. also showed riboflavin-binding sites associated with flagella of *E.gracilis* (Nebenführ et al. 1991). Also Neumann isolated a riboflavin-binding protein from the flagella of *E. gracilis* (Neumann and Hertel 1994).

High and saturable binding was found in *Euglena* flagella with, but also without, attached PABs. In contrast, *Astasia* did not show any binding activity.

To be exhaustive, it should be mentioned that carotenoids have also been discussed as photoreceptors for phototaxis in *Euglena* (Bendix 1960; Wolken 1960, 1977; Batra and Tollin 1964; Bensasson 1975; Gualtieri 1993a; b). In fact carotenoids, especially in the form of rhodopsins (Walne et al. 1998), have been found to be involved in photoorientation in many organisms such as *Chlamydomonas*, *Halobacterium* or *Paramecium* (Nakaoka et al. 1991; Govorunova et al. 2004; Kim et al. 2009). Gualtieri and others, based on theoretical considerations, absorption spectroscopy and gas chromatography-mass spectrometry, proposed that the photoreceptor pigment for *Euglena* phototaxis is a rhodopsin (James et al. 1992; Barsanti et al. 1993a; Gualtieri 2001). This hypothetical rhodopsin was thought to undergo a photocycle which has been analyzed by fluorescence emission spectroscopy (Evangelista et al. 2003). Hydoxylamine reacts with free and opsin-bound retinal. It was found to block the formation of the PAB and impaired photoaccumulation of the cells in the phototaxigraph (Barsanti et al. 1993b). Application of nicotine, an effective inhibitor of carotenoid biosynthesis blocked the biosynthesis of retinal by inhibiting the formation of the cyclohexylidin ring. In *Euglena* it prevented the formation of the PAB and impaired the accumulation of cells in a light field, interpreted as the result of phototaxis (Barsanti et al. 1992). However, when this experiment was repeated by growing *E. gracilis* cells up to 4 months at the highest possible concentration of nicotine (4 mM) the cells survived and neither positive nor negative phototaxis was impaired (Häder and Lebert 1998), indicating that retinal is not likely the chromophoric group of the photoreceptor. It should be mentioned that the accumulation in a light field can be brought about by a number of photoresponses such as phobic reactions or photokinesis (see Sects. 11.4.2 and 11.4.3). In fact, a photoaccumulation of *Euglena* was found in red light fields (Checcucci et al. 1974). This behavior was interpreted as an aerotactic attraction to the photosynthetically produced oxygen by organisms inside the light field. So the underlying mechanism in the experiment by Barsanti et al. might have been inhibited by nicotine, but it was not phototaxis.

11.5.2 Molecular Biology of the Photoreceptor for Phototaxis and the Step-Up Photophobic Response

All the discussions and speculations about the photoreceptor for photomovement in *E. gracilis* have been resolved by the molecular biological identification of the chromoproteins involved (Iseki et al. 2002). Iseki and coworkers succeeded in isolating sufficient quantities of PABs for biochemical analysis by separating the photoreceptors from the flagella followed by subcellular fractionation using a sucrose density gradient centrifugation. They separated a 400-kDa protein that binds flavins from the isolated PAB preparations by liquid chromatography. The protein is

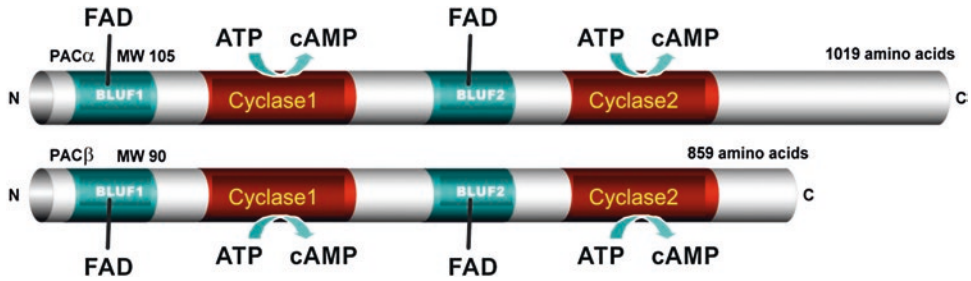

Fig. 11.6 The PACα and PACβ gene products from *E. gracilis* have two FAD binding sites (BLUF1 and BLUF2) and two adenylyl cyclases each

composed of four subunits: two subunits (named PACα) which consist of 1019 amino acids each with a molecular weight of 105 kDa and two more subunits (named PACβ) which consist of 859 amino acids each with a molecular weight of 90 kDa. The α and β subunits are similar to each other. Each of the four subunits has two flavin-binding BLUF (*B*lue *L*ight receptor *U*sing *F*AD) domains and two adenylyl cyclase catalytic domains (Fig. 11.6). The 400-kDa flavoprotein purified from the PAB preparations showed adenylyl cyclase activity that was induced by blue-light irradiation and was accordingly named photoactivated adenylyl cyclase (PAC). The photoactivation of PAC was extensively studied by Yoshikawa et al. (2005). PAC activity was dependent on both the photon fluence rate and the duration of irradiation, between which reciprocity held well within the range of 2–50 μmol m^{-2} s^{-1} (a total fluence of 1200 μmol m^{-2}). Intermittent irradiation also activated PAC in a photon fluence-dependent manner irrespective of the cycle periods, which implies that the increase of PAC activity occurred only during the light period and that elevated PAC activity decreased within 100 ms after the irradiation had stopped (Yoshikawa et al. 2005). Such a sharp switching property of PAC is suitable to be used as a tool to control various cellular processes by light, i.e., optogenetics. In fact, attempts to optogenetically control cAMP levels in *Aplysia* neurons (Nagahama et al. 2007), *Xenopus* oocytes, cultured mammalian cells, *Drosophila* brains (Schröder-Lang et al. 2007), and *Caenorhabditis* neurons (Stierl et al. 2011; Weissenberger et al. 2011) have been reported.

The biological functions of PAC in *Euglena* cells were examined using RNAi knockdown of the genes. When the double stranded RNAs encoding PACα (the 105-kDa subunit) and/or PACβ (the 90-kDa subunit) were introduced into *Euglena* cells, they significantly suppressed the gene expression of PAC, which resulted in the loss of the step-up photophobic response but not the step-down photophobic response (Iseki et al. 2002). Ntefidou et al. (2003b) found that the RNAi knockdown of PAC also effectively suppressed both the positive and negative phototaxis of *Euglena*. Inhibition of either PACα or of PACβ completely blocked negative phototaxis. Knockout of both genes had the same effect. Obviously both genes are required for a functioning phototaxis. From these observations PAC was concluded to act as a sensor for the step-up photophobic response and phototaxis in *Euglena* (Häder et al. 2005; Lüdtke and Häder 2007). However, it is important to emphasize that PAC does not control the step-down photophobic response.

The photoactivation mechanism of PAC still remains to be elucidated mainly due to difficulties in obtaining sufficient amounts of the protein for X-ray crystallography or vibrational spectroscopy. All attempts to express the full-length PAC subunits in *Escherichia coli* have so far failed. Ntefidou et al. (2006) succeeded in expressing PAC in a soluble form in insect cells, but neither crystallization nor spectroscopic analysis using the expressed protein has yet been reported. In contrast, when only the second BLUF domain of PAC (F2) was expressed in *E. coli*, a part of the expressed protein could be collected in a soluble

form that binds flavins (Ito et al. 2005). Although most of the expressed protein collected was insoluble, sufficient amounts of soluble, flavin-binding protein were recovered by refolding the insoluble protein with added flavins after denaturation by guanidine hydrochloride. The recombinant F2 protein showed a photocycle between a dark state and a slightly red-shifted signaling state similar to other bacterial BLUF domains (Ito et al. 2005). The quantum efficiency for the phototransformation of PACαF2 (0.28–0.32) is higher than that of PACβF2 (0.06–0.08), whereas the half-life for the dark relaxation of PACαF2 (34–44 s) is longer than that of PACβF2 (3–6 s) (Ito et al. 2010). Such photocycle features of PACαF2 and PACβF2 indicates different sensitivities for the photoactivation of PACα and PACβ, which may contribute to the wide range of light sensitivity in *Euglena* photobehavioral responses. Iwata et al. (2011) examined the photoreaction of PACαF2 using FTIR spectroscopy and found broad positive peaks in the difference spectrum at the 2900–2400 cm^{-1} region, which were attributed to the O–H stretching vibration of tyrosine, providing direct evidence for the light-induced switching of the hydrogen bond network in the BLUF domain. Single molecule fluorescence spectroscopy was also applied to PACαF2 and native PAC purified from *Euglena* (Fujiyoshi et al. 2011). The fluorescence from a single PACαF2 molecule measured at 1.5 K decreased in one step to background levels, whereas a single PAC molecule bleached in several steps, indicating the involvement of an energy transfer between FADs in the single PAC molecule. Fujiyoshi et al. (2011) also observed reversible spectral jumps of fluorescence from single molecules, which were attributed to a structural change around the hydrogen bonds at the FAD-binding site because the Q514A mutation of PACαF2 suppressed these spectral jumps.

11.6 Mutants and Related Organisms

There are a number of mutants of *E. gracilis* (Lebert and Häder 1997) as well as the close relative *Euglena longa*, formerly known as *Astasia longa* (Krause 2008). All these mutants lack chlorophyll and photosynthesis and consequently live heterotrophically. Table 11.1 summarizes some of the characteristics of these strains. With the exception of *E. longa* all mutants have some form of phototaxis (diaphototaxis and/or negative phototaxis). In addition to the wild type, the FB and 9F mutants have a PAB. The FB mutant is of interest since some cells have a stigma. This mutant may not consist of a uniform population and may contain some revertant cells, which might explain the presence of a stigma in some cells. All mutants are capable of step-up photophobic responses, but only the wild type strain Z shows step-down responses. All mutants and *E. longa* lack positive phototaxis, but all mutants show diaphototaxis at high light intensities and the FB mutant also shows a negative phototaxis component (Lebert and Häder 1997). All strains in this group display both positive and negative gravitaxis.

Even though some of these mutants do not have a PAB, PCR showed the presence of the PACα gene in all mutants but not in *E. longa* (Ntefidou and Häder 2005). However, in the latter organism a largely modified PAC was found, which was dubbed AlPACα (at that time the organisms was still known under the name *Astasia*) (Ntefidou et al. 2003a). The amino acid sequences of the first BLUF domain of PACα and PACβ from the wild type and the mutant strains 9F, FB, 1F and st^- of *E. gracilis* as well as AlPACα and AlPACβ from *E. longa* show a homology of between 43 and 91% (Ntefidou and Häder 2005). The BLUF1 and BLUF2 subunits of the PAC proteins resemble the N-terminal end of the AppA flavoprotein found in the purple bacterium *Rhodobacter sphaeroides*, which also binds FAD (Gomelsky and Kaplan 1995). In this bacterium the photoreceptor regulates the expression of photosynthesis genes (Gomelsky and Kaplan 1998; Masuda and Bauer 2002). The catalytic domain of class III adenylyl cyclases is found in many organisms from bacteria to protists, fungi, trypanosomes, insects and mammals (Koumura et al. 2004). It is interesting to note that the adenylyl cyclase in the *Euglena* PAC genes are more closely related to those found in bacteria than those in eukaryotes including the

Table 11.1 Physiological characteristics of the wild type *E. gracilis* (Eg), the 1F, 9F and FB mutants and the colorless *E. longa* (El, formerly *Astasia longa*). PAB paraxonemal body, dia. Diaphototaxis, pos. and neg. positive and negative phototaxis, PAC photoactivated cyclase, its presence is confirmed by PCR

Strain	Chloroplasts	Stigma	PAB	Phototaxis	Step-up	Step-down	PACα (PCR)
Eg w^+	+	+	+	pos./neg.	+	+	+
Eg 1F	–	–	–	dia.	+	–	+
Eg 9F	–	–	+	dia.	+	–	+
Eg FB	–	(+)	±	dia./neg.	+	–	+
El w^+	–	–	–	–	+	–	AlPACα

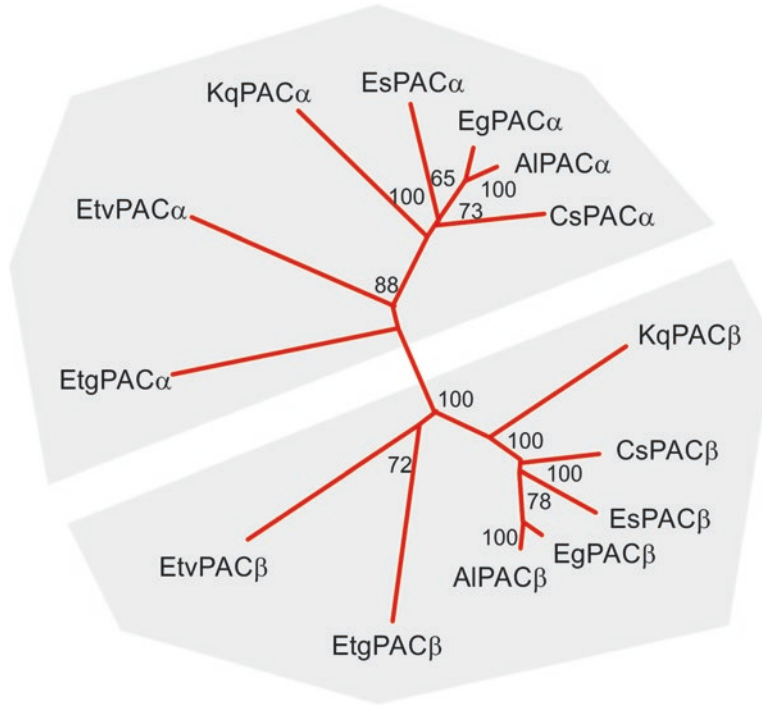

Fig. 11.7 Phylogenetic tree of the PAC proteins in the phototrophic euglenoids *Euglena gracilis* (Eg), *Euglena stellata* (Es), *Colacium sideropus* (Cs), *Eutreptia viridis* (Etv), *Eutreptiella gymnastica* (Etg) as well as the heterotrophic *Khawkinea quartana* (Kq) and *Astasia longa* (Al, new name *Euglena longa*) constructed by the neighbor-joining method using the Clustal X program (Thompson et al. 1997). Redrawn after (Koumura et al. 2004)

trypanosomes. This fact supports the notion that *Euglena* has obtained the gene by secondary endosymbiosis, which is also reflected in the fact that the chloroplasts are covered by a triple membrane. In order to understand the evolution of PAC, protein sequences were compared from several euglenoids by reverse transcriptase-polymerase chain reaction (RT-PCR) including the photosynthetic *Euglena stellata, Colacium sideropus, Eutreptia viridis, Eutreptiella gymnastica* and the heterotrophic *Khawkinea quartana*, but not the phagotrophic *Petalomonas cantuscygni* (Fig. 11.7). Based on these findings the evolutionary tree of PAC starts from a common ancestor. From this the trypanosomes received the trypanosome-type adenylyl cyclases. The other line leads from the common ancestor to phagotrophic euglenoids such as *Petalomonas cantuscygni* (Koumura et al. 2004). The phototrophic euglenoids developed after acquisition of chloroplasts by secondary endosymbiosis which also transferred the PAC genes. The osmotrophic euglenoids such as *Astasia* and *Khawkinea* lost the chloroplasts again but kept the PAC genes.

Confocal immunofluorescence was used to find the localization of PAC proteins in the wild type and mutant strains. It is interesting to note that the flagella of all strains contain PAC gene products even though the fluorescence is much lower than that of the PABs. Furthermore, the

RNAi knockdown of PAC also suppressed the step-up photophobic responses in the wild type and all studied mutant strains as well as in *E. longa* (Ntefidou et al. 2003a). In contrast, only the wild-type strain Z showed step-down photophobic responses which could not be eliminated by RNAi against PAC.

Recently, PAC-like genes were found in genome sequences of a sulfur bacterium *Beggiatoa* sp. (Ryu et al. 2010; Stierl et al. 2011) and a free-living amoeba *Naegleria gruberi* (Fritz-Laylin et al. 2010). Both of them have a BLUF domain and a cyclase domain showing high similarity to the C-terminal half of PACα and PACβ, which implies that they represent an ancestral form of PAC.

11.7 Signal Transduction Chain

The signal transduction chain in photomovement of *Euglena* is still hypothetical. Diehn and Tollin have applied a number of inhibitors and uncouplers of photosynthetic phosphorylation and concluded that the main energy source for phototaxis is photophosphorylation (Diehn and Tollin 1967). However, these experiments were carried out with the so-called phototaxigraph and the observed results probably reflect the reduced motility of the cells due to impaired ATP production since they are in the dark until they enter the light field. In addition, this assumption is ruled out since bleached cells which lack photosynthesis show phototaxis.

Some researchers have speculated about a coupling of the flavin photoreceptor to the signal transduction chain via a cytochrome, but no experimental evidence is available (Fong and Schiff 1978; Gualtieri 1993b). Based on studies with ionophores, inhibitors, on channel blockers, various pH and ion concentrations, Doughty and Diehn proposed a mechanism for the step-down photophobic response (Diehn 1969b; Barghigiani et al. 1979a; Doughty and Diehn 1979, 1982, 1983, 1984) where upon irradiation the PAB is supposed to modulate the activity of a hypothetical NA^+/K^+ exchange pump in the flagellar membrane. This increases the intraflagellar sodium concentration which in turn opens sodium-controlled calcium channels allowing the influx of calcium. The increased calcium concentration finally results in a change in the flagellar beating pattern. However, experiments manipulating the external Ca^{2+} concentration indicated that a Ca^{2+} influx from the medium into the flagellar space is not essential for phototaxis (Meyer and Hildebrand 1988). In a theoretical study, Bovee and Jahn (1972) assumed that the PAB has piezoelectric properties. Upon irradiation it discharges and alters the position or shape of the flagellum and thus the swimming direction. Also Froehlich and Diehn (1974) suggested an electrical type of stimulus transduction by a flavin receptor pigment embedded in a lipid matrix. However, all drugs which impair the photophobic responses did not affect phototaxis: neither the application of ouabain, a specific inhibitor of the Na^+/K^+ exchange pump, nor gallopamin hydrochloride, an organic calcium channel blocker, affected the phototactic orientation in *Euglena* (Häder et al. 1987). In contrast, heavy metal ions (lead, copper, cadmium and mercury) strongly impaired phototactic orientation (Stallwitz 1992; Stallwitz and Häder 1993). The application of triphenylmethyl phosphonium ion ($TPMP^+$) which is a lipophilic membrane-penetrating cation specifically inhibited positive phototaxis and reversed it to negative phototaxis, shifting the transition from positive to negative phototaxis to lower light intensities. These findings indicate that phototaxis might be controlled by a proton or cation gradient across the membrane (Colombetti et al. 1982). Therefore a number of researchers proposed that the membrane potential might be involved (Simons 1981; Harz et al. 1992). In fact, injecting negative electric pulses as well as changing the ionic environment of the cells (Ca^{2+} and Mg^{2+}) changed the flagellar beating pattern (Nichols and Rikmenspoel 1977, 1978, 1980; Nichols et al. 1980; Tamponnet et al. 1988). But exposing swimming cells to an electric field had no effect on phototactic orientation in *Euglena* (Häder et al. 1987). Since *Euglena* shows very sensitive behavioral reactions to heavy metals and other pollutants at very low concentrations it is employed in bioassays based on computerized,

on-line analysis of motility and orientation (Tahedl and Häder 2001; Häder 2004; Ahmed and Häder 2011; Azizullah et al. 2013).

The application of caffeine, an inhibitor of the phosphodiesterase, reversed the negative phototaxis at high irradiances (1000 W m^{-2}) into a positive one (Richter et al. 2006). Ammonium ions specifically enhance step-down photophobic responses, as well as L-methionine-DL-sulfoximine, an inhibitor of ammonium assimilation (Matsunaga et al. 1999). In contrast, cycloheximide, an inhibitor of eukaryotic protein synthesis, impaired the step-down photophobic response and enhanced the step-up reaction, which was interpreted as suggesting that newly synthesized proteins are specific for the photoperception and signal transduction of the step-down photophobic response.

The photoreceptor for the step-up photophobic response and phototaxis has been revealed to be PAC, a light-dependent enzyme that produces cAMP upon blue light irradiation (Iseki et al. 2002; Ntefidou et al. 2003b). Intracellular cAMP levels in *Euglena* remarkably increased within 1 s after the onset of irradiation and then returned to the original level, corresponding well with the kinetics of the step-up photophobic response (Yoshikawa et al. 2005). Two possibilities had been postulated regarding the downstream signaling pathway from cAMP to the photobehavioral responses (Watanabe and Iseki 2005). One is that cAMP opens cyclic nucleotide-gated channels to facilitate an influx of Ca^{2+} that may modulate flagellar motility. The other is that cAMP activates a protein kinase A that may phosphorylate flagellar proteins to change the mode of flagellar beating. The latter seemed more plausible than the former because a catalytic subunit of a protein kinase had been cloned from *Euglena* (Kiriyama et al. 1999). Daiker et al. (2011) found that staurosporine, a protein kinase inhibitor, considerably blocked phototaxis as well as gravitaxis at low concentrations. Using PCR, five different kinases from *Euglena* were cloned. The blockage of only one of the kinases (PK.4) by RNAi suppressed both gravitaxis and phototaxis (Fig. 11.8), which suggested that PK.4 is the downstream component of cAMP signaling in both gravitaxis and phototaxis (Daiker et al. 2011). A hypothetical signaling cascade from PAC to a flagellar apparatus during step-up photophobic response and phototaxis in *Euglena* is summarized in Fig. 11.9. The photoreceptor molecule consisting of two PACα

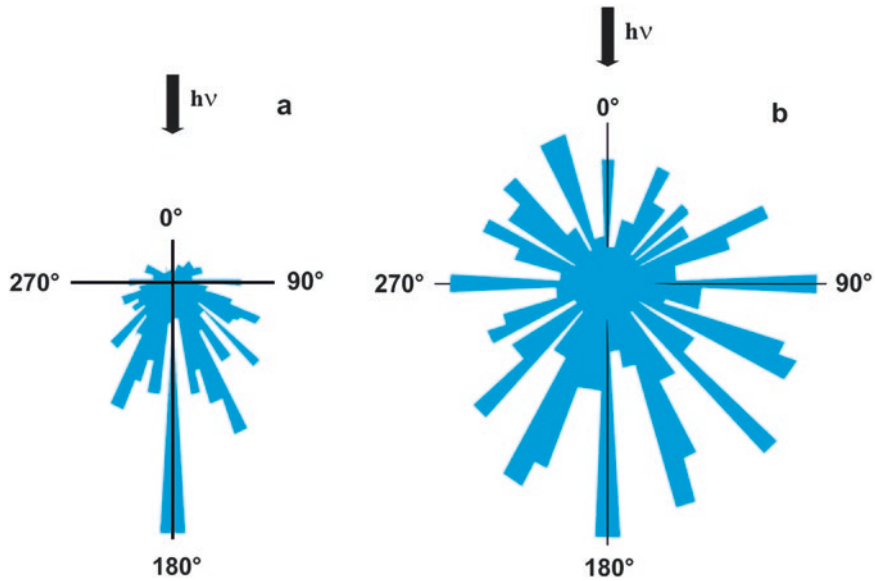

Fig. 11.8 Inhibition of negative phototaxis by RNAi against protein kinase A PK.4 25 days after RNA knockdown (**b**). Control (**a**). Redrawn after (Daiker et al. 2011)

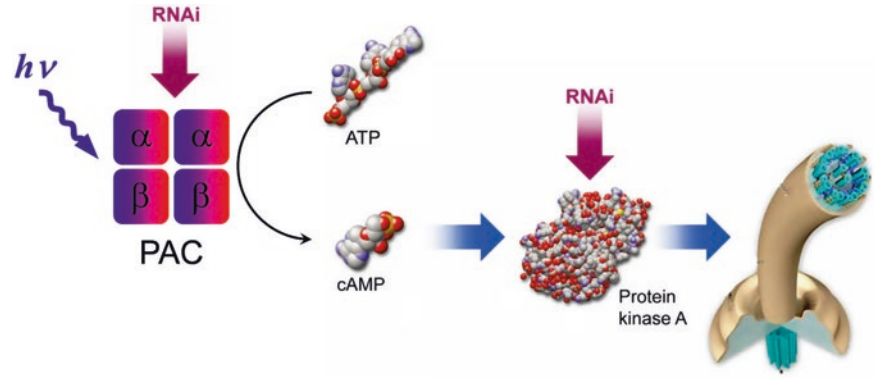

Fig. 11.9 Assumed signal transduction chain for phototaxis and step-down photophobic responses in *E. gracilis*. After light activation of the photoreceptor molecule consisting of two PACα and PACβ subunits, the adenylyl cyclase domain produces cAMP from ATP which is believed to activate a protein kinase A inside the flagellum. The resulting phosphorylation of one or several proteins within the flagellum causes a change in the flagellar activity

and PACβ subunits is activated by light absorbed by FAD bound to the BLUF domains. This activates the adenylyl cyclase domain which produces cAMP from ATP. cAMP in turn is believed to activate a protein kinase A inside the flagellum. The resulting phosphorylation of one or several proteins within the flagellum causes a change in the flagellar activity.

11.8 Other *Euglena* Species

In contrast to *E. gracilis*, the green *Euglena mutabilis* does not possess flagella, but moves in a gliding fashion. The cells contain both a stigma and a PAB, which, however, differ in shape and size from the organelles found in *E. gracilis*. When exposed to lateral light the cells show positive phototaxis (Häder and Melkonian 1983). They swing left and right, as if to scan the light direction, and move in the direction of the light source. The precision of orientation increases with the light intensity up to 100 lx and then decreases again. Negative phototaxis was not observed. The action spectrum is completely different from that in *E. gracilis* as it has a number of peaks in the blue and green range of the spectrum but extends well into the red (Fig. 11.10). It can only be speculated about the nature of the photoreceptor. The peaks in the blue region might be due to the action of a flavin and the long wavelength sensitivity cold be due to the action of photosynthetic pigments as in the case of desmids (Wenderoth and Häder 1979). Since the degree of phototaxis is higher in white light than at any individual wavelength, regardless of the fluence rate, it could be speculated that phototaxis in this organism depends on the interaction of more than one photoreceptor. Since the cells do not rotate during locomotion a periodic shading mechanism can be excluded for the light direction perception.

E. mutabilis also shows step-up and step-down photophobic responses (Melkonian et al. 1986). When a cell moves in the light and enters a shaded area it bends away from the shade. By repeated responses it can maneuver along the dark/light boundary. The same behavior is found when a cell glides in a dark area and suddenly hits a bright area; the sudden increase in light intensity induces a step-up photophobic response and the cell turns away from the bright area.

Photokinesis has also been observed in *E. mutabilis* (Melkonian et al. 1986). In darkness less than 10% of the cell population are motile. The percentage increases when exposed to light at fluence rates >20 W m^{-2} (ca. 4000 lx) white light and reaches about 100% between 50 and 100 W m^{-2} when recorded 10 min after the onset of light. The action spectra for photokinesis as well as step-up and step-down resemble each other and also that of phototaxis.

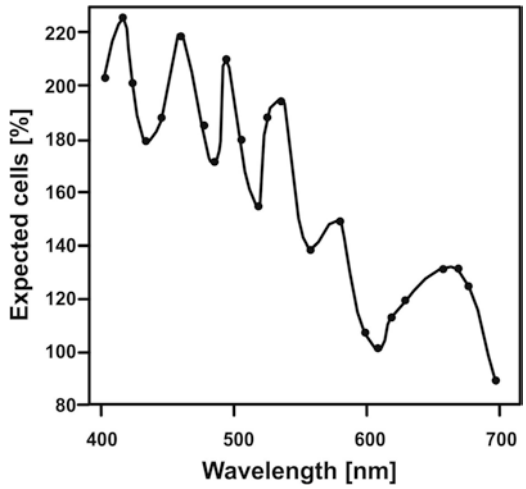

Fig. 11.10 Action spectrum of positive phototaxis in *E. mutabilis* based on fluence-rate response curves. Abscissa, wavelength in nm; ordinate, fraction of cells moving toward the light source within a sector ±30° as percentage of the fraction expected in this sector in a randomly oriented population. Redrawn after (Häder and Melkonian 1983)

The red colored freshwater *Euglena sanguinea* can be occasionally found in the neuston (top layer) of ponds (Gojdics 1939). The color is due to a high concentration of carotenoids such as β-carotene, astaxanthin-diester and diadinoxanthin. The cells possess flagella and orient precisely using positive phototaxis; negative phototaxis has not been observed even at irradiances of 600 klx, which is far in excess of solar radiation (Gerber and Häder 1994). The sensitivity to light is rather low as compared with *E. gracilis* and reaches a plateau at about 10 klx. Further work on this interesting organism was hampered by the fact that nobody has succeeded in cultivating this flagellate.

11.9 Conclusions and Future Directions

The mechanism for photoperception of phototaxis has been revealed by the finding that the photoreceptor is located in the paraxonemal body inside the trailing flagellum inside the reservoir. The PAB has a dichroic structure which is reflected in the polarotaxis in polarized light. The stigma aids in light direction perception by casting a shadow on the PAB when the cell rotates in lateral light during forward locomotion, however it is not indispensable as shown by the fact that stigmaless mutants are capable of a (modified) phototaxis. The long search for the molecular identity of the photoreceptor molecules has been terminated by the molecular biological identification of a photoactivated adenylyl cyclase (PAC) consisting of two α- and β-subunits each. Upon light activation these enzymes produce cAMP from ATP which has been found to activate a specific protein kinase (PK.4). The latter enzyme is thought to phosphorylate proteins inside the flagellum which result in a reorientation and course correction of the swimming path.

While the step-up photophobic response and both positive and negative phototaxis are mediated by PAC, the receptor for the step-down photophobic reaction has not yet been identified but proven not to be PAC. Also the photoreceptor for photokinesis and those for phototaxis in the gliding *E. mutabilis* as well as the red colored *E. sanguinea* still need to be revealed having completely different action spectra extending into the red region of the spectrum. Spectrofluorometric analysis has indicated an additional role for pterins in the photoperception of *E. gracilis*. Their role and location are not yet completely resolved. While the location of PAC inside the PAB (and also in the flagellum outside the reservoir) was confirmed by confocal immunofluorescence, the location of the protein kinase needs to be determined. It is also not clear if further elements are involved in the sensory transduction chain. In addition, the cooperation with the other responses to environmental stimuli has to be elucidated including gravitaxis which uses the same protein kinase (PK.4) but operates with a different adenylyl cyclase. The proteins which control the bending of the trailing flagellum as well as their molecular action have not been characterized.

Acknowledgements The authors thank their long-time coworkers Peter Richter, Maria Ntefidou and Sebastian Strauch, who have critically read this manuscript. The financial support for the underlying work for this review by DFG, DLR, BMBF and JSPS is gratefully acknowledged.

References

Ahmed H, Häder D-P (2011) Monitoring of waste water samples using the ECOTOX biosystem and the flagellate alga *Euglena gracilis*. Water Air Soil Pollut 216(1–4):547–560

de Araujo FFT, Pires MA, Frankel RB, Bicudo CEM (1986) Magnetite and magnetotaxis in algae. Biophys J 50:375–378

Ascoli C (1975) New techniques in photomotion methodology. In: Colombetti G (ed) Biophysics of photoreceptors and photobehaviour of microorganisms. Lito Felici, Pisa, pp 109–120

Azizullah A, Murad W, Adnan M, Ullah W, Häder D-P (2013) Gravitactic orientation of *Euglena gracilis*—a sensitive endpoint for ecotoxicological assessment of water pollutants. Front Environ Sci 1:4

Azizullah A, Jamil M, Richter P, Häder D-P (2014) Fast bioassessment of wastewater and surface water quality using freshwater flagellate *Euglena gracilis*—a case study from Pakistan. J Appl Phycol 26(1):421–431

Banchetti R, Rosati G, Verni F (1980) Cytochemical analysis of the photoreceptor in *Euglena gracilis* Klebs (Flagellata Euglenoidina). Monit Zool Ital (NS) 14:165–171

Barghigiani C, Colombetti G, Lenci F, Banchetti R, Bizzaro MP (1979a) Photosensory transduction in *Euglena gracilis*: effect of some metabolic drugs on the photophobic response. Arch Microbiol 120:239–245

Barghigiani C, Colombetti G, Tranchini B, Lenci F (1979b) Photobehavior of *Euglena gracilis*: action spectrum for the stepdown photophobic response of individual cells. Photochem Photobiol 29:1015–1019

Barsanti L, Passarelli V, Lenzi P, Gualtieri P (1992) Elimination of photoreceptor (paraflagellar swelling) and photoreception in *Euglena gracilis* by means of the carotenoid biosynthesis inhibitor nicotine. J Photochem Photobiol B Biol 13:135–144

Barsanti L, Passarelli V, Lenci P, Walne PL, Dunlap JR, Gualtieri P (1993a) Effects of hydroxylamine, digitonin and triton X-100 on photoreceptor (paraflagellar swelling) and photoreception of *Euglena gracilis*. Vis Res 33:2043–2050

Barsanti L, Evangelista V, Passarelli V, Frassanito AM, Gualtieri P (2012) Fundamental questions and concepts about photoreception and the case of *Euglena gracilis*. Integr Biol 4(1):22–36

Batra PP, Tollin G (1964) Phototaxis in *Euglena*. I. Isolation of the eye-spot granules and identification of the eye-spot pigments. Biochim Biophys Acta 79:371–378

Bendix SW (1960) Pigments in phototaxis. In: Allen MB (ed) Comparative Biochemistry of Photoreactive. Systems Academic Press, New York, pp 107–127

Benedetti PA, Checcucci A (1975) Paraflagellar body (PFB) pigments studied by fluorescence microscopy in *Euglena gracilis*. Plant Sci Lett 4:47–51

Benedetti PA, Lenci F (1977) *In vivo* microspectrofluorometry of photoreceptor pigments in *Euglena gracilis*. Photochem Photobiol 26:315–318

Benedetti PA, Bianchini G, Checcucci A, Ferrara R, Grassi S (1976) Spectroscopic properties and related functions of the stigma measured in living cells of *Euglena gracilis*. Arch Microbiol 111:73–76

Bensasson RW (1975) Spectroscopic and biological properties of carotenoids. In: Colombetti G (ed) Biophysics of Photoreceptors and Photobehaviour of Microorganisms. Lito Felici, Pisa, pp 146–163

Bouck GB (2012) Flagella and the cell surface. Physiology 3:29

Bound KE, Tollin G (1967) Phototactic response of *Euglena gracilis* to polarized light. Nature 216: 1042–1044

Bovee EC, Jahn TL (1972) A theory of piezoelectric activity and ion movements in the relation of flagellar structures and their movements to the phototaxis of *Euglena*. J Theor Biol 35:259–276

Brodhun B, Häder D-P (1990) Photoreceptor proteins and pigments in the paraflagellar body of the flagellate *Euglena gracilis*. Photochem Photobiol 52:865–871

Brodhun B, Häder D-P (1993) UV-induced damage of photoreceptor proteins in the paraflagellar body of *Euglena gracilis*. Photochem Photobiol 58:270–274

Brodhun B, Häder D-P (1995a) A novel procedure to isolate the chromoproteins in the paraflagellar body of the flagellate *Euglena gracilis*. J Photochem Photobiol B Biol 28:39–45

Brodhun B, Häder D-P (1995b) UV-induced damage of photoreceptor pigments and proteins in the paraflagellar body of the flagellate *Euglena gracilis*. Proceedings of the first European symposium on the effects of environmental UV-B radiation on health and ecosystems, EUR, vol 15607, pp 33–332

Brodhun B, Neumann R, Hertel R, Häder D-P (1994) Riboflavin-binding sites in the flagella of *Euglena gracilis* and *Astasia longa*. J Photochem Photobiol B Biol 23:135–139

Bruce VG (1973) The role of the clock in controlling phototactic rhythms. In: Pérez-Miravete A (ed) Behaviour of Microorganisms. Plenum Press, New York, pp 257–266

Bruce VG, Pittendrigh C (1956) Temperature independence in a unicellular clock. Proc Natl Acad Sci U S A 42:676–682

Bruce VG, Pittendrigh CS (1958) Resetting the *Euglena* clock with a single light stimulus. Am Nat 92:295–306

Buder J (1919) Zur Kenntnis der phototaktischen Richtungsbewegungen. Jahrb Wiss Bot 58:105–220

Buetow DE (1968a) The Biology of *Euglena*. Academic Press, New York

Buetow DE (1968b) Morphology and ultrastructure of *Euglena*. In: Buetow DE (ed) The Biology of *Euglena*. Academic Press, New York, pp 109–184

Bünning E (1973) The Physiological Clock, 3rd edn. English Univ. Press, London

Capaldo CT, Farkas AE, Nusrat A (2014) Epithelial adhesive junctions. F1000prime reports 6

Carre IA, Laval-Martin DL, Edmunds LN Jr (1989) Circadian changes in cyclic AMP levels in synchronously dividing and stationary-phase cultures of the

achlorophyllous ZC mutant of *Euglena gracilis*. J Cell Sci 94:267–272
Checcucci A, Colombetti G, del Carratore G, Ferrara R, Lenci F (1974) Red light induced accumulation of *Euglena gracilis*. Photochem Photobiol 19:223–226
Checcucci A, Favati L, Grassi S, Piaggesi T (1975) The measurement of phototactic activity in *Euglena gracilis* Klebs. Monit Zool Ital 9:83–98
Checcucci A, Colombetti G, Ferrara R, Lenci F (1976) Action spectra for photoaccumulation of green and colorless *Euglena*: evidence for identification of receptor pigments. Photochem Photobiol 23:51–54
Clayton R (1959) Phototaxis of purple bacteria. Handbuch der Pflanzenphysiologie 17/1:371–387
Clayton RK (1964) Phototaxis in microorganisms. In: Giese AC (ed) Photophysiology, vol 2. Academic Press, New York, pp 51–77
Colombetti G, Diehn B (1978) Chemosensory responses toward oxygen in *Euglena gracilis*. J Protozool 25:211–217
Colombetti G, Häder D-P, Lenci F, Quaglia M (1982) Phototaxis in *Euglena gracilis*: effect of sodium azide and triphenylmethyl phosphonium ion on the photosensory transduction chain. Curr Microbiol 7:281–284
Creutz C, Diehn B (1976) Motor responses to polarized light and gravity sensing in *Euglena gracilis*. J Protozool 23:552–556
Cypionka H (2010) Eukaryotische Mikroorganismen. Grundlagen der Mikrobiologie 47–60
Daiker V, Häder D-P, R. RP, Lebert M (2011) The involvement of a protein kinase in phototaxis and gravitaxis of *Euglena gracilis*. Planta 233:1055–1062.
Diehn B (1969a) Action spectra of the phototactic responses in *Euglena*. Biochim Biophys Acta 177:136–143
Diehn B (1969b) Phototactic responses of *Euglena* to single and repetitive pulses of actinic light: orientation time and mechanism. Exp Cell Res 56:375–381
Diehn B (1969c) Two perpendicularly oriented pigment systems involved in phototaxis of *Euglena*. Nature 122:366–367
Diehn B (1973) Phototaxis in *Euglena*. 1. Physiological basis of photoreception and tactic orientation. In: Pérez-Miravete A (ed) Behaviour of Microorganisms. Plenum Press, New York, pp 83–90
Diehn B, Tollin G (1966) Phototaxis in *Euglena*. II. Physical factors determining the rate of phototactic response. Photochem Photobiol 5:523–557
Diehn B, Tollin G (1967) Phototaxis in *Euglena*. IV. Effect of inhibitiors of oxidative and photophosphorylation on the rate of phototaxis. Arch Biochem Biophys 121:169–177
Diehn B, Fonseca JR, Jahn TR (1975) High speed cinemicrography of the direct photophobic response of *Euglena* and the mechanism of negative phototaxis. J Protozool 22:492–494
Diskus A (1955) Färbestudien an den Schleimkörperchen und Schleimausscheidungen einiger *Euglenen*. Protoplasma 45:460–477
Dodge JD (1969) A review of the fine structure of algal eyespots. Brit Phycol J 4:199–210
Doughty MJ (1991) A kinetic analysis of the step-up photophobic response of the flagellated alga *Euglena gracilis* in culture medium. J Photochem Photobiol B Biol 9:75–85
Doughty MJ, Diehn B (1979) Photosensory transduction in the flagellated alga, *Euglena gracilis*. I. Action of divalent cations Ca^{2+} antagonists and Ca^{2+} ionophore on motility and photobehavior. Biochim Biophys Acta 588:148–168
Doughty MJ, Diehn B (1982) Photosensory transduction in the flagellated alga, *Euglena gracilis*. III. Induction of Ca^{2+}-dependent responses by monovalent cation ionophores. Biochim Biophys Acta 682:32–43
Doughty MJ, Diehn B (1983) Photosensory transduction in the flagellated alga, *Euglena gracilis*. IV. Long term effects of ions and pH on the expression of step-down photobehaviour. Arch Microbiol 134:204–207
Doughty MJ, Diehn B (1984) Anion sensitivity of motility and step-down photophobic responses of *Euglena gracilis*. Arch Microbiol 138:329–332
Edmunds LN Jr (1984) Physiology of circadian rhythms in microorganisms. In: Rose AH, Tempest DW (eds) Advances in Microbial Physiology, vol 25. Academic Press, London, pp 61–148
Engelmann TW (1883) *Bakterium photometricum*. Ein Beitrag zur vergleichenden Physiologie des Licht- und Farbensinnes. Pflugers Arch 30:95–124
Evangelista V, Passarelli V, Barsanti L, Gualtieri P (2003) Fluorescence behavior of *Euglena* photoreceptor. Photochem Photobiol 78(1):93–97
Falke JJ, Bass RB, Butler SL, Chervitz SA, Danielson MA (1997) The two-component signaling pathway of bacterial chemotaxis: a molecular view of signal transduction by receptors, kinases, and adaptation enzymes. Annu Rev Cell Dev Biol 13:457–512
Feinleib ME (1975) Phototactic response of *Chlamydomonas* to flashes of light. I. Response of cell population. Photochem Photobiol 21:351–354
Feinleib ME, Curry GM (1967) Methods for measuring phototaxis of cell populations and individual cells. Physiol Plant 20:1083–1095
Feinleib MEH, Curry GM (1971) The relationship between stimulus intensity and oriented phototactic response (topotaxis) in *Chlamydomonas*. Physiol Plant 25:346–352
Feldman JF, Bruce VG (1972) Circadian rhythm changes in autotrophic *Euglena* induced by organic carbon sources. J Protozool 19:370–373
Fenchel T (2013) Ecology of Protozoa: The Biology of Free-living Phagotropic Protists. Springer-Verlag, Berlin
Ferrara R, Banchetti R (1976) Effect of streptomycin on the structure and function of the photoreceptor apparatus of *Euglena gracilis*. J Exp Zool 198:393–402
Fong F, Schiff JA (1978) Blue-light absorbance changes and phototaxis in *Euglena*. Plant Physiol 61(Suppl):74
Fong F, Schiff JA (1979) Blue-light-inducted absorbance changes associated with carotenoids in *Euglena*. Planta 146:119–127

Forreiter C, Wagner G (2012) Photomovement versus photoadaptation. Progr Bot Genet Physiol System Ecol 64:258

Foster KW (2001) Action spectroscopy of photomovement. In: Häder D-P, Lebert M (eds) Photomovement, vol 1. Elsevier, Amsterdam, pp 51–115

Foster KW, Smyth RD (1980) Light antennas in phototactic algae. Microbiol Rev 44:572–630

France RH (1908) Experimentelle Untersuchungen über Reizbewegungen und Lichtsinnesorgane der Algen. Ztschrift Ausbau Entwicklungslehre 2:29–43

France RH (1909) Untersuchungen über die Sinnesorganfunktion der Augenflecke bei Algen. Arch Hydrobiol 4:37–48

Frey-Wyssling A, Mühlethaler K (1960) Über den Feinbau der *Euglena*-Zelle. Schweiz Z Hydrol 22:122–130

Fritz-Laylin LK, Prochnik SE, Ginger ML, Dacks JB, Carpenter ML, Field MC, Kuo A, Paredez A, Chapman J, Pham J (2010) The genome of *Naegleria gruberi* illuminates early eukaryotic versatility. Cell 140(5):631–642

Froehlich O, Diehn B (1974) Photoeffects in a flavin-containing lipid bilayer membrane and implications for algal phototaxis. Nature 248:802–804

Fujiyoshi S, Hirano M, Matsushita M, Iseki M, Watanabe M (2011) Structural change of a cofactor binding site of flavoprotein detected by single-protein fluorescence spectroscopy at 1.5 K. Phys Rev Lett 106(7):078101

Galland P, Senger H (1988a) The role of flavins as photoreceptors. J Photochem Photobiol B Biol 1:277–294

Galland P, Senger H (1988b) The role of pterins in the photoreception and metabolism of plants. Photochem Photobiol 48:811–820

Galland P, Keiner P, Dörnemann D, Senger H, Brodhun B, Häder D-P (1990) Pterin- and flavin-like fluorescence associated with isolated flagella of *Euglena gracilis*. Photochem Photobiol 51:675–680

Gerber S, Häder D-P (1993) Effects of solar irradiation on motility and pigmentation of three species of phytoplankton. Environ Exp Bot 33:515–521

Gerber S, Häder D-P (1994) Effects of enhanced UV-B irradiation on the red coloured freshwater flagellate *Euglena sanguinea*. FEMS Microbiol Ecol 13:177–184

Gerber S, Häder D-P (1995) Effects of artificial UV-B and simulated solar radiation on the flagellate *Euglena gracilis*: physiological, spectroscopical and biochemical investigations. Acta Protozool 34:13–20

Gerber S, Biggs A, Häder D-P (1996) A polychromatic action spectrum for the inhibition of motility in the flagellate *Euglena gracilis*. Acta Protozool 35:161–165

Ghetti F, Colombetti G, Lenci F, Campani E, Polacco E, Quaglia M (1985) Fluorescence of *Euglena gracilis* photoreceptor pigment: an *in vitro* microspectrofluorometric study. Photochem Photobiol 42:29–33

Giometto A, Altermatt F, Maritan A, Stocker R, Rinaldo A (2015) Generalized receptor law governs phototaxis in the phytoplankton *Euglena gracilis*. Proc Natl Acad Sci U S A 112(22):7045–7050

Gojdics M (1939) Some observations on *Euglena sanguinea* Ehrbg. Trans Am Microsc Soc 58:241–248

Gomelsky M, Kaplan S (1995) *appA*, a novel gene encoding a *trans*-acting factor involved in the regulation of photosynthesis gene expression in *Rhodobacter sphaeroides* 2.4.1. J Bacteriol 177:4609–4618

Gomelsky M, Kaplan S (1998) AppA, a redox regulator of photosystem formation in *Rhodobacter sphaeroides* 2.4.1, is a flavoprotein. Identification of a novel FAD binding domain. J Biol Chem 273:35319–35325

Gössel I (1957) Über das Aktionsspektrum der Phototaxis chlorophyllfreier Euglenen und über die Absorption des Augenflecks. Arch Microbiol 27:288–305

Govorunova EG, Sineshchekov OA (2005) Chemotaxis in the green flagellate alga *Chlamydomonas*. Biochemistry (Mosc) 70(7):717–725

Govorunova EG, Jung KH, Sineshchekov OA, Spudich JL (2004) *Chlamydomonas* sensory rhodopsins A and B: cellular content and role in photophobic responses. Biophys J 86(4):2342–2349

Gualtieri P (1993a) A biological point of view on photoreception (no-imaging vision) in algae. J Photochem Photobiol B Biol 18:95–100

Gualtieri P (1993b) *Euglena gracilis*: is the photoreception enigma solved? J Photochem Photobiol B Biol 19:3–14

Gualtieri P (2001) Rhodopsin-like-proteins: light detection pigments in *Leptolyngbya, Euglena, Ochromonas, Pelvetia*. In: Häder D-P, Lebert M (eds) Photomovement, vol 1. Elsevier, Amsterdam, pp 281–295

Gualtieri P, Barsanti L, Rosati G (1986) Isolation of the photoreceptor (paraflgellar body) of the phototactic flagellate *Euglena gracilis*. Arch Microbiol 145:303–305

Häder D-P (1979) Photomovement. In: Haupt W, Feinleib ME (eds) Encyclopedia of Plant Physiology, New Series, vol 7. Springer, Berlin, Heidelberg, pp 268–309

Häder D-P (1985) Effect of UV-B on motility and photobehavior in the green flagellate, *Euglena gracilis*. Arch Microbiol 141:159–163

Häder D-P (1986) Effects of solar and artificial UV irradiation on motility and phototaxis in the flagellate *Euglena gracilis*. Photochem Photobiol 44:651–656

Häder D-P (1987a) Photomovement in eukaryotic microorganisms. Photobiochem Photobiophys, Suppl: 203–214

Häder D-P (1987b) Polarotaxis, gravitaxis and vertical phototaxis in the green flagellate, *Euglena gracilis*. Arch Microbiol 147:179–183

Häder D-P (1991) Phototaxis and gravitaxis in *Euglena gracilis*. In: Lenci F, Ghetti F, Colombetti G, Häder D-P, Song P-S (eds) Biophysics of Photoreceptors and Photomovements in Microorganisms. Plenum Press, New York, pp 203–221

Häder D-P (1993) Simulation of phototaxis in the flagellate *Euglena gracilis*. J Biol Phys 19:95–108

Häder D-P (1997) Gravitaxis and phototaxis in the flagellate *Euglena* studied on TEXUS missions. In: Cogoli A, Friedrich U, Mesland D, Demets R (eds) Life Science Experiments Performed on Sounding Rockets

(1985–1994). ESTEC, ESA Publications Division, Noordwijk, pp 77–79
Häder D-P (1998) Orientierung im Licht: Phototaxis bei *Euglena gracilis*. Mikrokosmos 87:3–11
Häder D-P (2003) UV-B impact on the life of aquatic plants. In: Ambasht RS, Ambasht NK (eds) Modern Trends in Applied Aquatic Ecology. Kluwer Acad./ Plenum Publ, New York, pp 149–172
Häder D-P (2004) Photoecology and environmental photobiology. In: Horspool W, Lenci F (eds) CRC Handbook of Organic Photochemistry and Photobiology, vol 2. CRC Press, Boca Raton, pp 1161–1167
Häder D-P, Brodhun B (1991) Effects of ultraviolet radiation on the photoreceptor proteins and pigments in the paraflagellar body of the flagellate, *Euglena gracilis*. J Plant Physiol 137:641–646
Häder D-P, Griebenow K (1988) Orientation of the green flagellate, *Euglena gracilis*, in a vertical column of water. FEMS Microbiol Ecol 53:159–167
Häder D-P, Häder MA (1988) Inhibition of motility and phototaxis in the green flagellate, *Euglena gracilis*, by UV-B radiation. Arch Microbiol 150:20–25
Häder D-P, Lebert M (1998) The photoreceptor for phototaxis in the photosynthetic flagellate *Euglena gracilis*. Photochem Photobiol 68:260–265
Häder D-P, Lebert M (2000) Real-time tracking of microorganisms. In: Häder D-P (ed) Image Analysis: Methods and Applications. CRC Press, Boca Raton, pp 393–422
Häder D-P, Lebert M 2009 Photoorientation in photosynthetic flagellates. In: Jin T, Hereld D, editors. Methods in Molecular Biology. Totowa: Humana Press. 571. p. 51–65.
Häder D-P, Lipson ED (1986) Fourier analysis of angular distributions for motile microorganisms. Photochem Photobiol 44:657–663
Häder D-P, Liu SM (1991) Biochemical isolation and spectroscopic characterization of possible photoreceptor pigments for phototaxis in a freshwater *Peridinium*. Photochem Photobiol 54:143–146
Häder D-P, Melkonian M (1983) Phototaxis in the gliding flagellate, *Euglena mutabilis*. Arch Microbiol 135:25–29
Häder D-P, Reinecke E (1991) Phototactic and polarotactic responses of the photosynthetic flagellate, *Euglena gracilis*. Acta Protozool 30:13–18
Häder D-P, Colombetti G, Lenci F, Quaglia M (1981) Phototaxis in the flagellates, *Euglena gracilis* and *Ochromonas danica*. Arch Microbiol 130:78–82
Häder D-P, Lebert M, Di Lena MR (1986) New evidence for the mechanism of phototactic orientation of *Euglena gracilis*. Curr Microbiol 14:157–163
Häder D-P, Lebert M, DiLena MR (1987) Effects of culture age and drugs on phototaxis in the green flagellate, *Euglena gracilis*. Plant Physiol 6:169–174
Häder D-P, Ntefidou M, Iseki M, Watanabe M (2005) Phototaxis photoreceptor in *Euglena gracilis*. In: Wada M, Shimazaki K, Iino M (eds) Light Sensing in Plants. Springer, Tokyo, pp 223–229
Häder D-P, Richter P, Villafañe VE, Helbling EW (2014) Influence of light history on the photosynthetic and motility responses of *Gymnodinium chlorophorum* exposed to UVR and different temperatures. J Photochem Photobiol B Biol 138:273–281
Harz H, Nonnengässer C, Hegemann P (1992) The photoreceptor current of the green alga *Chlamydomonas*. Philos Trans R Soc London B 338:39–52
Hasle RG (1950) Phototactic vertical migration in marine dinoflagellates. Oikos 2:162–175
Haupt W (1959) Die Phototaxis der Algen. Handbuch der Pflanzenphysiologie 17(1):318–370
Heelis DV, Kernick W, Philips GO, Davies K (1979) Separation and identification of the carotenoid pigments of stigmata isolated from light-grown cells of *Euglena gracilis* strain Z. Arch Microbiol 121: 207–211
Heelis DV, Heelis PF, Kernick WA, Phillips GO (1980) The stigma of *Euglena gracilis* strain Z: an investigation into the possible occurance of carotenoproteins and nuleic acids. Cytobios 29:135–143
Hill NA, Häder D-P (1997) A biased random walk for the trajectories of swimming micro-organisms. J Theor Biol 186:503–526
Hill N, Plumpton L (2000) Control strategies for the polarotactic orientation of the microorganism *Euglena gracilis*. J Theor Biol 203(4):357–365
Hill NA, Vincent RV (1993) A simple model and strategies for orientation in phototactic microorganisms. J Theor Biol 163:223–235
Hu C, Wang S, Guo L, Xie P (2014) Effects of the proximal factors on the diel vertical migration of zooplankton in a plateau meso-eutrophic Lake Erhai, China. J Limnol 73(2):375–386
Hyams JS (1982) The *Euglena* paraflagellar rod: structure, relationship to other flagellar components and preliminary biochemical characterization. J Cell Sci 55:199–210
Inaba K, Mizuno K, Shiba K (2014) Structure, function, and phylogenetic consideration of calaxin. In: Sexual Reproduction in Animals and Plants. Springer, Tokyo, pp 49–57
Iseki M, Matsunaga S, Murakami A, Ohno K, Shiga K, Yoshida C, Sugai M, Takahashi T, Hori T, Watanabe M (2002) A blue-light-activated adenylyl cyclase mediates photoavoidance in *Euglena gracilis*. Nature 415:1047–1051
Ito S, Murakami A, Sato K, Nishina Y, Shiga K, Takahashi T, Higashi S, Iseki M, Watanabe M (2005) Photocycle features of heterologously expressed and assembled eukaryotic flavin-binding BLUF domains of photoactivated adenylyl cyclase (PAC), a blue light receptor in *Euglena gracilis*. Photochem Photobiol Sci 4:762–769
Ito S, Murakami A, Iseki M, Takahashi T, Higashi S, Watanabe M (2010) Differentiation of photocycle characteristics of flavin-binding BLUF domains of α-and β-subunits of photoactivated adenylyl cyclase of *Euglena gracilis*. Photochem Photobiol Sci 9(10): 1327–1335

Itoh A, Tamura W (2008) Object manipulation by a formation-controlled *Euglena* group. In: Bio-mechanisms of Swimming and Flying. Springer, Tokyo, pp 41–52

Iwata T, Watanabe A, Iseki M, Watanabe M, Kandori H (2011) Strong donation of the hydrogen bond of tyrosine during photoactivation of the BLUF domain. J Phys Chem Lett 2(9):1015–1019

Iwatsuki K (1992) *Stentor coeruleus* shows positive photokinesis. Photochem Photobiol 55:469–471

James TW, Crescitelli F, Loew ER, McFarland WN (1992) The eyespot of *Euglena gracilis*: a microspectrophotometric study. Vis Res 32:1583–1591

Jennings HS (1906) Behavior of the Lower Organisms. Columbia University Press, New York

Johnson CH, Kondo T, Hastings JW (1991) Action spectrum for resetting the circadian phototaxis rhythm in the CW15 strain of *Chlamydomonas*. Plant Physiol 97:1122–1129

Josef K, Saranak J, Foster KW (2005) Ciliary behavior of a negatively phototactic *Chlamydomonas reinhardtii*. Cell Motil Cytoskeleton 61:97–111

Karnkowska A, Bennett MS, Watza D, Kim JI, Zakryś B, Triemer RE (2015) Phylogenetic relationships and morphological character evolution of photosynthetic Euglenids (Excavata) inferred from taxon-rich analyses of five genes. J Eukaryot Microbiol 62(3):362–373

Kavaliers M, Ossenkopp K-P (1994) Effects of magnetic and electric fields in invertebrates and lower vertebrates. In: Carpenter DO, Ayrapetyan S (eds) Biological Effects of Electric and Magnetic Fields. Sources and Mechanisms, vol 1. Academic Press Inc., San Diego, pp 205–240

Kessler JO, Hill NA, Häder D-P (1992) Orientation of swimming flagellates by simultaneously acting external factors. J Phycol 28:816–822

Kim D (2013) Control of *Tetrahymena pyriformis* as a microrobot. PhD thesis, Drexel University

Kim YJ, Chizhov I, Engelhard M (2009) Functional expression of the signaling complex sensory rhodopsin II/transducer II from *Halobacterium salinarum* in *Escherichia coli*. Photochem Photobiol 85(2):521–528

Kiriyama H, Nanmori T, Hari K, Matsuoka D, Fukami Y, Kikkawa U, Yasuda T (1999) Identification of the catalytic subunit of cAMP-dependent protein kinase from the photosynthetic flagellate, *Euglena gracilis* Z. FEBS Lett 450(1):95–100

Kisielewska G, Kolicka M, Zawierucha K (2015) Prey or parasite? The first observations of live Euglenida in the intestine of Gastrotricha. Eur J Protistol 51(2):138–141

Kivic PA, Vesk M (1972a) Structure and function in the euglenoid eyespot apparatus: The fine structure, and response to environmental changes. Planta 105:1–14

Kivic PA, Vesk M (1972b) Structure and function of the euglenoid eyespot. The probable location of the phototaxis photoreceptor. J Exp Bot 23:1070–1075

Kivic PA, Vesk M (1974a) Pinocytotic uptake of protein from the reservoir in *Euglena*. Arch Microbiol 96:155–159

Kivic PA, Vesk M (1974b) The structure of the eyespot apparatus in bleached strains of *Euglena gracilis*. Cytobiologie 10:88–101

Kivic PA, Walne PL (1983) Algal photosensory apparatus probably represent multiple parallel evolutions. Biosystems 16:31–38

Komsic-Buchmann K, Becker B (2012) Contractile Vacuoles in Green Algae–Structure and Function. Advances in Algal Cell Biology. Walter de Gruyter, Berlin, pp 123–141

Koumura Y, Suzuki T, Yoshikawa S, Watanabe M, Iseki M (2004) The origin of photoactivated adenylyl cyclase (PAC), the *Euglena* blue-light receptor: phylogenetic analysis of orthologues of PAC subunits from several euglenoids and trypanosome-type adenylyl cyclases from *Euglena gracilis*. Photochem Photobiol Sci 3(6):580–586

Krause K (2008) From chloroplasts to "cryptic" plastids: evolution of plastid genomes in parasitic plants. Curr Genet 54(3):111–121

Kreimer G (1994) Cell biology of phototaxis in flagellate algae. Int Rev Cytol 148:229–309

Kreimer G, Melkonian M (1990) Reflection confocal laser scanning microscopy of eyespots in flagellated green algae. Eur J Cell Biol 53:101–111

Krinsky NI, Goldsmith TH (1960) The carotenoids of the flagellated alga, *Euglena gracilis*. Arch Biochem Biophys 91(2):271–279

Kronestedt E, Walles B (1975) On the presence of plastids and the eyespot apparatus in a porfiromycin-bleached strain of *Euglena gracilis*. Protoplasma 84:75–82

Kühnel-Kratz C, Schäfer J, Häder D-P (1993) Phototaxis in the flagellate, *Euglena gracilis*, under the effect of microgravity. Microgravity Sci Technol 6:188–193

Leander BS, Witek RP, Farmer MA (2001) Trends in the evolution of the euglenid pellicle. Evolution 55:2215–2235

Lebert M (2001) Phototaxis of *Euglena gracilis* - flavins and pterins. In: Häder D-P, Lebert M (eds) Photomovement, vol 1. Elsevier, Amsterdam, pp 297–341

Lebert M, Häder D-P (1997) Behavioral mutants of *Euglena gracilis*: functional and spectroscopic characterization. J Plant Physiol 151:188–195

Lebert M, Häder D-P (2000) Photoperception and phototaxis in flagellated algae. Res Adv Photochem Photobiol 1:201–226

Lebert M, Porst M, Häder D-P (1999) Circadian rhythm of gravitaxis in *Euglena gracilis*. J Plant Physiol 155:344–349

Leedale GF (1982) Ultrastructure. In: Buetow DE (ed) The Biology of *Euglena*. Physiology, vol 3. Academic Press, New York, pp 1–27

Lenci F, Colombetti G, Häder D-P (1983) Role of flavin quenchers and inhibitors in the sensory transduction of the negative phototaxis in the flagellate, *Euglena gracilis*. Curr Microbiol 9:285–290

Lenci F, Häder D-P, Colombetti G (1984) Photosensory responses in freely motile microorganisms. In: Colombetti G, Lenci F (eds) Membranes and Sensory Transduction. Plenum Press, New York, pp 199–229

Lenci F, Ghetti F, Colombetti G, Häder D, Song P-S (2012) Biophysics of photoreceptors and photomovements in microorganisms. Springer Science & Business Media

Lindes DA, Diehn B, Tollin G (1965) Phototaxigraph: recording instrument for determination of rate of response of phototactic microorganisms to light of controlled intensity and wavelength. Rev Sci Instrum 36:1721–1725

Liu SM, Häder D-P (1994) Isolation and characterization of proteins from the putative photoreceptor for positive phototaxis in the dinoflagellate, *Peridinium gatunense* Nygaard. Photochem Photobiol 59:86–90

Lüdtke T, Häder D-P (2007) Molecular genetics of the novel photoreceptor PAC in euglenophytes and bacteria. In: Thangadurai D, Tang W, Pullaiah T (eds) Genes, Genomes & Genomics, vol 2. Vedams eBooks Ltd., New Delhi, pp 189–200

Ma Z, Helbling EW, Li W, Villafañe VE, Gao K (2012) Motility and photosynthetic responses of the green microalga *Tetraselmis subcordiformis* to visible and UV light levels. J Appl Phycol 24(6):1613–1621

Mast SO (1911) Light and Behavior of Organisms. Chapman & Hall ltd., London

Mast SO (1914) Orientation in *Euglena* with some remarks on tropisms. Biol Zent Bl 34:641–664

Masuda S (2013) Light detection and signal transduction in the BLUF photoreceptors. Plant Cell Physiol 54(2):171–179

Masuda S, Bauer CE (2002) AppA is a blue light photoreceptor that antirepresses photosynthesis gene expression in *Rhodobacter sphaeroides*. Cell 110:613–623

Matsunaga S, Hori T, Takahashi T, Kubota M, Watanabe M, Okamoto K, Masuda K, Sugai M (1998) Discovery of signaling effect of UV-B/C light in the extended UV-A/blue-type action spectra for step-down and step-up photophobic responses in the unicellular flagellate alga *Euglena gracilis*. Protoplasma 201:45–52

Matsunaga S, Takahashi T, Watanabe M, Sugai M, Hori T (1999) Control by ammonium ion of the change from step-up to step-down photophobically responding cells in the flagellate alga *Euglena gracilis*. Plant Cell Physiol 40:213–221

Melkonian M, Meinicke-Liebelt M, Häder D-P (1986) Photokinesis and photophobic responses in the gliding flagellate, *Euglena mutabilis*. Plant Cell Physiol 27:505–513

Meyer R, Hildebrand E (1988) Phototaxis of *Euglena gracilis* at low external calcium concentration. J Photochem Photobiol B Biol 2(4):443–453

Michel H (1990) General and practical aspects of membrane protein crystallization. In: Michel H (ed) Crystallization of Membrane Proteins. CRC Press, Boca Raton, FL, pp 73–89

Mikolajczyk E (1984a) Photophobic responses in *Euglenina*. 1. Effects of excitation wavelength and external medium on the step-up response of light- and dark-grown *Euglena gracilis*. Acta Protozool 23:1–10

Mikolajczyk E (1984b) Photophobic responses in *Euglenina*: 2. Sensitivity to light of the colorless flagellate *Astasia longa* in low and high viscosity medium. Acta Protozool 23:85–92

Mikolajczyk E, Diehn B (1975) The effect of potassium iodide on photophobic responses in *Euglena*: evidence for two photoreceptor pigments. Photochem Photobiol 22:269–271

Mikolajczyk E, Diehn B (1976) Light-induced body movement of *Euglena gracilis* coupled to flagellar photophobic responses by mechanical stimulation. J Protozool 23:144–147

Mikolajczyk E, Diehn B (1978) Morphological alteration in *Euglena gracilis* induced by treatment with CTAB (Cetyltrimethylammonium bromide) and Triton X-100: correlations with effects on photophobic behavioral responses. J Protozool 25:461–470

Mikolajczyk E, Diehn B (1979) Mechanosensory responses and mechanoreception in *Euglena gracilis*. Acta Protozool 18:591–602

Mikolajczyk E, Kuznicki L (1981) Body contraction and ultrastructure of *Euglena*. Acta Protozool 20:1–24

Murray JM (1981) Control of cell shape by calcium in the Euglenophyceae. J Cell Sci 49:99–117

Nagahama T, Suzuki T, Yoshikawa S, Iseki M (2007) Functional transplant of photoactivated adenylyl cyclase (PAC) into *Aplysia* sensory neurons. Neurosci Res 59(1):81–88

Nakaoka Y, Tokioka R, Shinozawa T, Fujita J, Usukura J (1991) Photoreception of *Paramecium* cilia: localization of photosensitivity and binding with anti-frog-rhodopsin IgG. J Cell Sci 99:67–72

Nasir A (2014) Analysis of the gravitaxis signal transduction chain in *Euglena gracilis*. 40th COSPAR Scientific Assembly. Held 2–10 August 2014, in Moscow, Russia, Abstract F1. 1–18-14. p 2234

Nebenführ A, Schäfer A, Galland P, Senger H, Hertel R (1991) Riboflavin-binding sites associated with flagella of *Euglena*: a candidate for blue-light photoreceptor? Planta 185:65–71

Neumann R, Hertel R (1994) Purification and characterization of a riboflavin-binding protein from flagella of *Euglena gracilis*. Photochem Photobiol 60:76–83

Ngô HM, Bouck GB (1998) Heterogeneity and a coiled coil prediction of trypanosomatid-like flagellar rod proteins in *Euglena*. J Eukaryot Microbiol 45:323–333

Nichols KM, Rikmenspoel R (1977) Mg^{2+}-dependent electrical control of flagellar activity in *Euglena*. J Cell Sci 23:211–225

Nichols KM, Rikmenspoel R (1978) Control of flagellar motion in *Chlamydomonas* and *Euglena* by mechanical microinjection of Mg^{2+} and Ca^{2+} and by electric current injection. J Cell Sci 29:233–247

Nichols KM, Rikmenspoel R (1980) Flagellar waveform reversal in *Euglena*. Exp Cell Res 129:377–381

Nichols KM, Jacklet A, Rikmenspoel R (1980) Effects of Mg^{2+} and Ca^{2+} on photoinduced *Euglena* flagellar responses. J Cell Biol 84:355–363

Ntefidou M, Häder D-P (2005) Photoactivated adenylyl cyclase (PAC) genes in the flagellate *Euglena gracilis* mutant strains. Photochem Photobiol Sci 4:732–739

Ntefidou M, Iseki M, Richter P, Streb C, Lebert M, Watanabe M, Häder D-P (2003a) RNA interference of genes involved in photomovement in *Astasia longa* and *Euglena gracilis* mutants. Rec Res Dev Biochem 4:925–930

Ntefidou M, Iseki M, Watanabe M, Lebert M, Häder D-P (2003b) Photoactivated adenylyl cyclase controls phototaxis in the flagellate *Euglena gracilis*. Plant Physiol 133(4):1517–1521

Ntefidou M, Lüdtke T, Ahmad M, Häder D-P (2006) Heterologous expression of photoactivated adenylyl cyclase (PAC) genes from the flagellate *Euglena gracilis* in insect cells. Photochem Photobiol 82:1601–1605

Nultsch W (1975) Phototaxis and photokinesis. In: Carlile MJ (ed) Primitive Sensory and Communication Systems. Academic Press, New York, pp 29–90

Nultsch W, Häder D-P (1970) Bestimmungen der photophobotaktischen Unterschiedsschwelle bei *Phormidium uncinatum*. Ber Dtsch Bot Ges 83:185–192

Nultsch W, Häder D-P (1979) Photomovement of motile microorganisms. Photochem Photobiol 29:423–437

Nultsch W, Häder D-P (1988) Photomovement in motile microorganisms—II. Photochem Photobiol 47:837–869

Nultsch W, Throm G (1975) Effect of external factors on phototaxis of *Chlamydomonas reinhardtii*. I. Light. Arch Microbiol 103:175–179

Oesterhelt D (1998) The structure and mechanism of the family of retinal proteins from halophilic archaea. Curr Opin Struct Biol 8:489–500

Omodeo P (1975) Phototactic system morphology: Florenz

Omodeo P (1980) The photoreceptive apparatus of flagellated algal cells: Comparative morphology and some hypothesis on functioning. In: Lenci F, Colombetti G (eds) Photoreception and Sensory Transduction in Aneural Organisms. Plenum Press, New York, pp 127–154

Omodeo P (2013) Istituto di Biologia Animale de11'Università di Padova 35100 Padova, Italy. Photoreception and Sensory Transduction in Aneural Organisms 33: 127

Osafune T, Schiff JA (1980) Stigma and flagellar swelling in relation to light and carotenoids in *Euglena gracilis var. bacillaris*. J Ultrastruct Res 73:336–349

Ozasa K, Lee J, Song S, Hara M, Maeda M (2013) Gas/liquid sensing via chemotaxis of *Euglena* cells confined in an isolated micro-aquarium. Lab Chip 13(20):4033–4039

Ozasa K, Lee J, Song S, Maeda M (2014) Transient freezing behavior in photophobic responses of *Euglena gracilis* investigated in a microfluidic device. Plant Cell Physiol 55(10):1704–1712

Peacock MB, Kudela RM (2014) Evidence for active vertical migration by two dinoflagellates experiencing iron, nitrogen, and phosphorus limitation. Limnol Oceanogr 59(3):660–673

Petersen-Mahrt SK, Ekelund NGA, Widell S (1994) Influence of UV-B radiation and nitrogen starvation on daily rhythms in phototaxis and cell shape of *Euglena gracilis*. Physiol Plant 92:501–505

Piccinni E, Mammi M (1978) Motor apparatus of *Euglena gracilis*: ultrastructure of the basal portion of the flagellum and the paraflagellar body. Bollettino di Zoologia 45:405–414

Poniewozik M (2014) The euglenoid genera *Astasia* and *Menoidium* (Euglenozoa) from eastern Poland. Nova Hedwigia 99(1–2):193–212

Porterfield DM (1997) Orientation of motile unicellular algae to oxygen: Oxytaxis in *Euglena*. Biol Bull 193:229–230

Pringsheim EG (1937) Über das Stigma bei farblosen Flagellaten. Cytologia 1:234–255

Pringsheim EG (1948) The loss of chromatophores in *Euglena gracilis*. New Phytol 47:52–87

Rhiel E, Häder D-P, Wehrmeyer W (1988) Diaphototaxis and gravitaxis in a freshwater *Cryptomonas*. Plant Cell Physiol 29:755–760

Richter P, Ntefidou M, Streb C, Lebert M, Häder D-P (2002) Cellular perception and transduction mechanisms of gravity in unicellular organisms. Curr Top Plant Biol 3:143–154

Richter PR, Streb C, Häder D-P (2006) Sign change of phototaxis in *Euglena gracilis*. Trends Photochem Photobiol 11:57–61

Richter P, Helbling W, Streb C, Häder D-P (2007) PAR and UV effects on vertical migration and photosynthesis in *Euglena gracilis*. Photochem Photobiol 83:818–823

Robenek H, Melkonian M (1983) Structural specialization of the paraflagellar membrane of *Euglena*. Protoplasma 117:154–157

Rosati GF, Verni L, Barsanti V, Passarelli V, Gualtieri P (1991) Ultrastructure of the apical zone of *Euglena gracilis*: photoreceptors and motor apparatus. Electron Microsc Rev 4:319–342

Rosati G, Barsanti L, Passarelli V, Giambelluca A, Gualtieri P (1996) Ultrastructure of a novel non-photosynthetic *Euglena* mutant. Micron 27:367–373

Ryu MH, Moskvin OV, Siltberg-Liberles J, Gomelsky M (2010) Natural and engineered photoactivated nucleotidyl cyclases for optogenetic applications. J Biol Chem 285:41501–41508

Schiff JA, Lyman H, Russel GK (1971) Isolation of mutants from *Euglena gracilis*. In: San Pietro A (ed) Methods in Enzymology: Photosynthesis. Part A, vol 23. Academic Press, New York, pp 143–162

Schiff JA, Lyman H, Russel GK (1980) Isolation in *Euglena gracilis*: An addendum. In: San Pietro A (ed) Methods in Enzymology: Photosynthesis and Nitrogen Fixation. Part C, vol 69. Academic Press, New York, pp 23–29

Schmidt W, Galland P, Senger H, Furuya M (1990) Microspectrophotometry of *Euglena gracilis*. Planta 182:375–381

Schmidt M, Geßner G, Luff M, Heiland I, Wagner V, Kaminski M, Geimer S, Eitzinger N, Reissenweber T, Voytsekh O, Fiedler M, Mittag M, Kreimer G (2006) Proteomic analysis of the eyespot of *Chlamydomonas reinhardtii* provides novel insights into its components and tactic movements. Plant Cell 18(8):1908–1930

Schröder-Lang S, Schwärzel M, Seifert R, Strünker T, Kateriya S, Looser J, Watanabe M, Hegemann P, Nagel G (2007) Fast manipulation of cellular cAMP level by light *in vivo*. Nat Methods 4(1):39–42

Selbach M, Häder D-P, Kuhlmann HW (1999) Phototaxis in *Chlamydodon mnemosyne*: determination of illuminance-response curve and the action spectrum. J Photochem Photobiol B Biol 49:35–40

Shimmen T (1981) Quantitative studies on step-down photophobic response of *Euglena* in an individual cell. Protoplasma 106:37–48

Shneyour A, Avron M (1975) Properties of photosynthetic mutants isolated from *Euglena gracilis*. Plant Physiol 55:137–141

Simons PJ (1981) The role of electricity in plant movements. New Phytol 87:11–37

Sineshchekov V, Geiß D, Sineshchekov O, Galland P, Senger H (1994a) Fluorometric characterization of pigments associated with isolated flagella of *Euglena gracilis*: evidence for energy migration. J Photochem Photobiol B Biol 23(2):225–237

Sineshchekov OA, Jung KH, Spudich JL (2002) Two rhodopsins mediate phototaxis to low- and high-intensity light in *Chlamydomonas reinhardtii*. Proc Natl Acad Sci U S A 99:8689–8694

Sperling PG, Walne PL, Schwarz OJ, Triplett LL (1973) Studies on characterization of pigments from isolated eyespots of Euglenoid flagellates. J Phycol Suppl 9:20

Stallwitz E (1992) Einfluß von Schwermetallionen auf Motilität, Orientierung, Wachstum und Pigmentierung des Flagellaten *Euglena gracilis*. Diplom, Friedrich-Alexander University Erlangen-Nürnberg, Germany

Stallwitz E, Häder D-P (1993) Motility and phototactic orientation of the flagellate *Euglena gracilis* impaired by heavy metal ions. J Photochem Photobiol B Biol 18:67–74

Stierl M, Stumpf P, Udwari D, Gueta R, Hagedorn R, Losi A, Gärtner W, Petereit L, Efetova M, Schwarzel M, Oertner TG, Nagel G, Hegemann P (2011) Light modulation of cellular cAMP by a small bacterial photoactivated adenylyl cyclase, bPAC, of the soil bacterium *Beggiatoa*. J Biol Chem 286:1181–1188

Strasburger E (1878) Wirkung des Lichtes und der Wärme auf Schwärmsporen. G. Fischer Verlag, Jena

Strother GK, Wolken JJ (1960) Microspectrophotometry of *Euglena*. Chloroplast and eyespot. Nature 188:601–602

Sumida S, Lyman H, Nobuhiko K, Osafune T (2007) Mechanism of conversion from heterotrophy to autotrophy in *Euglena gracilis*. Cytologia 72:447–457

Suzaki T, Williamson RE (1983) Photoresponse of a colorless euglenoid flagellate, *Astasia longa*. Plant Sci Lett 32:101–107

Suzaki T, Williamson RE (1986) Ultrastructure and sliding of pellicular structures during euglenoid movement in *Astasia longa* Pringsheim (Sarcomastigophora, Euglenoida). J Protozool 33:179–184

Sznee K, Crouch LI, Jones MR, Dekker JP, Frese RN (2014) Variation in supramolecular organisation of the photosynthetic membrane of *Rhodobacter sphaeroides* induced by alteration of PufX. Photosynth Res 119(1–2):243–256

Tahedl H, Häder D-P (2001) The use of image analysis in ecotoxicology. In: Häder D-P (ed) Image Analysis: Methods and Applications. CRC Press, Boca Raton, pp 447–458

Takeda J, Nakashima M, Ueno H, Mori T, Iseki M, Watanabe M (2013) Search for pterin-binding protein from *Euglena*. J Biol Macromol 13(1):13–20

Tamponnet C, Rona JP, Barbotin JN, Calvayrac R (1988) Effects of high external calcium concentrations on etiolated *Euglena gracilis* Z cells and evidence of an internal membrane potential. Biochim Biophys Acta 943:87–94

Thompson JD, Gibson TJ, Plewniak F, Jeanmougin F, Higgins DG (1997) The CLUSTAL_X windows interface: flexible strategies for multiple sequence alignment aided by quality analysis tools. Nucleic Acids Res 25(24):4876–4882

Tollin G (1973) Phototaxis in *Euglena*. II. Biochemical aspects. In: Pérez-Miravete A (ed) Behaviour of Microorganisms. Plenum Press, New York, pp 91–105

Tollin G, Robinson MJ (1969) Phototaxis in *Euglena*. V. Photosupression of phototactic activity by blue light. Photochem Photobiol 9:411–416

Toporik H, Carmeli I, Volotsenko I, Molotskii M, Rosenwaks Y, Carmeli C, Nelson N (2012) Large photovoltages generated by plant photosystem I crystals. Adv Mater 24(22):2988–2991

Umrath K (1959) Galvanotaxis. Handbuch der Pflanzenphysiologie 17(1):164–167

Vavra J (1962) Instability of the stigma in apochlorotic *Euglena gracilis var. bacillaris*. J Protozool 9 Suppl:28–29

Verni F, Rosati G, Lenzi P, Barsanti L, Passarelli V, Gualtieri P (1992) Morphological relationship between paraflagellar swelling and paraxial rod in *Euglena gracilis*. Micron Microsc Acta 23:37–44

Verworn M (1889) Psychophysiologische Protistenstudien. Gustav Fischer Verlag, Jena, pp 25–130

Votta JJ, Jahn TL (1972) Galvanotaxis of *Euglena gracilis*. J Protozool 19(Suppl):43

Wadhams GH, Armitage JP (2004) Making sense of it all: bacterial chemotaxis. Nat Rev Mol Cell Biol 5(12):1024–1037

Walne PL, Arnott HJ (1967) The comparative ultrastructure and possible function of eyespots: *Euglena granulata* and *Chlamydomonas eugemetos*. Planta 77:325–353

Walne PL, Lenci F, Mikolajczyk E, Colombetti G (1984) Effect of pronase treatment on step-down and step-up photophobic responses in *Euglena gracilis*. Cell Biol Int Rep 8:1017–1027

Walne PL, Pasarelli V, Barsanti L, Gualtieri P (1998) Rhodopsin: A photopigment for phototaxis in *Euglena gracilis*. Crit Rev Plant Sci 17:559–574

Watanabe M, Iseki M (2005) Discovery and characterization of photoactivated adenylyl cyclase (PAC), a novel blue-

light receptor flavoprotein, from *Euglena gracilis*. In: Briggs WR, Spudich JL (eds) Handbook of Photosensory Receptors. Wiley-VCH, Weinheim, pp 447–460

Weissenberger S, Schultheis C, Liewald JF, Erbguth K, Nagel G, Gottschalk A (2011) PACα–an optogenetic tool for in vivo manipulation of cellular cAMP levels, neurotransmitter release, and behavior in *Caenorhabditis elegans*. J Neurochem 116(4):616–625

Wenderoth K, Häder D-P (1979) Wavelength dependence of photomovement in desmids. Planta 145:1–5

Wolken JJ (1956) A molecular morphology of *Euglena gracilis var. bacillaris*. J Protozool 3(4):211–221

Wolken J (1960) Photoreceptors: Comparative studies. In: Allen MB (ed) Comparative Biochemistry of Photoreactive Systems. Academic Press, New York, pp 145–167

Wolken JJ (1977) *Euglena*: the photoreceptor system for phototaxis. J Protozool 24:518–522

Wolken JJ (2012) Euglena: an Experimental Organism for Biochemical and Biophysical Studies. Springer

Wolken JJ, Shin E (1958) Photomotion in *Euglena gracilis*. I. Photokinesis. II. Phototaxis. J Protozool 5:39–46

Yoshikawa S, Suzuki T, Watanabe M, Iseki M (2005) Kinetic analysis of the activation of photoactivated adenylyl clclase (PAC), a blue-light receptor for photomovements of *Euglena*. Photochem Photobiol Sci 4:727–731

Zhenan M, Shouyu R (1983) The effect of red light on photokinesis of Euglena gracilis. In: Tseng CK (ed) Proceedings of the joint China-U.S. phycology symposium. Science in China Press, Beijing, pp 311–321

Gravitaxis in *Euglena*

12

Donat-P. Häder and Ruth Hemmersbach

Abstract

Motile microorganisms utilize a number of responses to external stimuli including light, temperature, chemicals as well as magnetic and electric fields. Gravity is a major clue to select a niche in their environment. Positive gravitaxis leads an organism down into the water column and negative gravitaxis brings it to the surface. In *Euglena* the precision of gravitaxis is regulated by an internal rhythm entrained by the daily light/dark cycle. This and the cooperation with phototaxis bring the cells into an optimal position in the water column. In the past a passive orientation based on a buoy mechanism has been proposed for *Euglena gracilis*, but now it has been proven that this flagellate possesses a physiological gravireceptor and an active orientation. Numerous experiments in space using satellites, rockets and shuttles as well as in parabolic flights have been conducted as well as in functional weightlessness (simulated microgravity) on ground-based facilities such as clinostats to characterize the gravitaxis of *Euglena*. The threshold for gravity perception was determined and physiological, biochemical and molecular components of the signal transduction chain have been identified. In contrast to higher plants, some algae and ciliates, *Euglena* does not possess sedimenting statoliths to detect the direction of the gravity vector of the Earth. The gravireceptors were found to be mechano-sensitive Ca^{2+}-conducting ion channels thought to be located at the front end of the cell underneath the trailing flagellum. When activated by gravity-induced pressure due to sedimentation of the whole cell body, they allow a passive influx of calcium along a previously established ion gradient. The entering calcium binds to a specific calmodulin (CaM.2) which in turn activates an adenylyl cyclase producing cAMP

D.-P. Häder (✉)
Department of Biology, Friedrich-Alexander Universität, Erlangen-Nürnberg,
Neue Str. 9, 91096 Möhrendorf, Germany
e-mail: donat@dphaeder.de

R. Hemmersbach
Gravitational Biology, Institute of Aerospace Medicine, German Aerospace Center (DLR),
Linder Höhe, 51147 Cologne, Germany
e-mail: Ruth.Hemmersbach@DLR.DE

S.D. Schwartzbach, S. Shigeoka (eds.), *Euglena: Biochemistry, Cell and Molecular Biology*,
Advances in Experimental Medicine and Biology 979, DOI 10.1007/978-3-319-54910-1_12

from ATP. This cAMP is believed to activate a specific protein kinase A (PK.4), which is postulated to phosphorylate proteins inside the flagellum resulting in a bending and thus a course correction and reorientation with respect to the direction of the gravity vector. The elements of the signal transduction chain have been characterized by inhibitors and by RNAi to prove their involvement in gravitaxis.

Keywords
Adenylyl cyclase • Calmodulin • cAMP • *Euglena* • Gravitaxis • Gravireceptor • Microgravity • Hypergravity • Protein kinase • Sensory transduction • Space flight

Abbreviations

DCFA-DAL	2′,7′ dichlorodihydrofluorescein diacetate
ATP	Adenosine triphosphate
BLAST	Basic local alignment search tool
CaM	Calmodulin
cAMP	Cyclic adenosine monophosphate
dsRNA	Double-stranded RNA
EGTA	Ethylene glycol-bis (β-aminoethyl ether)-N,N,N′,N′-tetraacetic acid
IBM-X	3-Isobutyl-1-methylxanthin
ISS	International Space Station
LED	Light emitting diode
mRNA	Messenger RNA
NiZeMi	Slow rotating centrifuge microscope
PAC	Photoactivated adenylyl cyclase
PCR	Polymerase chain reaction
PK	Protein kinase
RNA	Ribonucleic acid
RNAi	RNA interference
ROS	Reactive oxygen species
RPM	Random Positioning Machine
rpm	Revolutions per minute
TEXUS	Technical experiments under microgravity
$TPMP^+$	Triphenylmethyl phosphonium ion
TRP	Transient receptor potential
UV	Ultraviolet radiation
W7	N-(6-Aminohexyl)-5-chlor-1-naphthalinsulfonamid

12.1 Introduction

Living organisms are exposed to a large number of environmental stimuli which are physical or chemical factors. Motile organisms such as bacteria, phytoplankton or animals respond to light (phototaxis) (Fraenkel and Gunn 1961; Häder 1991; Fiedler et al. 2005), chemicals (chemotaxis) (Clegg et al. 2003; Wadhams and Armitage 2004), the magnetic fields of the Earth (magnetotaxis) (Lohmann et al. 2004; Simmons et al. 2004), electrical fields or currents (galvanotaxis) (Votta and Jahn 1972) and temperature (thermotaxis) (Steidinger and Tangen 1996; Maree et al. 1999). All organisms on this planet are exposed to gravity. Most of them, including humans, have developed sensors to detect the direction of the gravitational field of the Earth and mechanisms to respond to the gravity vector (Hemmersbach et al. 1999a; Hock and Häder 2006; Ullrich and Häder 2006; Ullrich and Thiel 2012). The discipline of gravitational biology started in the nineteenth century when Julius Sachs (1882), Charles Darwin (1859) and Wilhelm Pfeffer (1904) studied the effects of gravity on plants (Hemmersbach et al. 2011) and demonstrated the role of the root cap in downward growing plants roots (positive gravitropism). They constructed machines (centrifuges and clinostats) in order to change the influence of gravity and observed the resulting gravity-related responses.

Viruses and bacteria are considered to be too small to react to the gravitational field; their swimming paths are mainly affected by Brownian

motion (Buttinoni et al. 2012). In contrast, unicellular phytoplankton and colonies clearly respond to gravity and use their responses for vertical migrations in order to optimize their spatial position in the water column (Richter et al. 2007). This has been studied in many motile microorganisms including *Tetraselmis*, *Dunaliella*, *Prorocentrum*, *Cryptomonas* and *Gymnodinium* (Rhiel et al. 1988; Eggersdorfer and Häder 1991a; Richter et al. 2007). The vertical migrations result in pronounced distributions of phytoplankton in the water column, the depth and density of which is affected by solar irradiance and the action of wind and waves (Piazena and Häder 1995; Häder 1997b; Raymont 2014). Vertical migrations of *Euglena deses* have been found also in the sand layer of the intertidal zone on the beaches in Sierra Leone (Taylor 1967). Their abundance is so high that they stain the sand green. This phenomenon is governed by diurnal migrations to the surface. Graviorientation and vertical migrations are also the basis for pattern formation in microbial populations (Bean 1984).

The phenomenon of gravitaxis has been studied for more than 100 years when cells were swimming in a vertical open or closed tube to the top (Platt 1899; Köhler 1921). The original term "geotaxis" was replaced by "gravitaxis" since this behavior is not solely induced by the Earth (greek gaia), but also by any heavy celestial body (e.g. Moon, Mars) and even by artificial accelerations such as on a centrifuge. The earlier investigations were basically descriptive observations by e.g. Jennings (1906) and Davenport (1908) which later on resulted in various interpretations and models how gravity is perceived. These earlier hypotheses have been reviewed by e.g. (Haupt 1962; Kuznicki 1968; Dryl 1974; Machemer and Bräucker 1992; Hemmersbach et al. 1999b). The interpretations were rather controversial. Stahl concluded from his observations that neither *Euglena* nor *Chlamydomonas* orient with respect to gravity (Stahl 1880). In contrast, Schwarz noted that *Euglena* swims upwards by an oriented movement and is not passively carried by currents (Schwarz 1884). He also concluded that this orientational movement is not induced by a higher oxygen concentration at the surface since the gravitational force of the Earth could be replaced by a centrifugal force. *Euglena* was capable of swimming against acceleration forces of up to 8.5 g. In contrast, Aderhold made an attraction to the higher oxygen tension at the surface responsible for upward movement in this organism (aerotaxis) (Aderhold 1888). A number of motile protists are especially useful as model systems including *Paramecium*, *Loxodes* and *Euglena* (Hemmersbach-Krause and Häder 1990; Hemmersbach-Krause et al. 1991b, 1994; Neugebauer et al. 1998; Streb et al. 2001) to study gravity-signal transduction chains within a single cell.

Also gliding organisms such as the desmid *Closterium* were found to show negative gravitaxis: when the cells were free to move on the surface of a glass plate within a water filled tube they were found to accumulate at the surface over night (Gerhardt 1913). Their meandering paths could be visualized by dying their slime trails. It was also noted rather early that light and gravity are competing stimuli in *Euglena*: in strong irradiances gravitaxis was weak while in the absence of light, gravity is the sole driver for upward movement (Wager 1911).

Movement in the direction of the center of the Earth guides the organisms into deeper layers of the water column; this is called positive gravitaxis (Fig. 12.1a). Moving away from the center is called negative gravitaxis and guides the organisms to the surface (Fig. 12.1b). Graviperception has probably been developed several times during evolution in different classes of organisms (Barlow 1995).

The precision of gravitactic orientation can be quantified using the r-value which runs between 0 (random orientation) and 1 (all cells swim in the same direction).

$$r = \frac{\sqrt{\left(\sum \sin\alpha\right)^2 + \left(\sum \cos\alpha\right)^2}}{n} \qquad (12.1)$$

where α is the deviation from the stimulus direction (here the gravity vector of the Earth) and n the number of recorded cell tracks (Batschelet 1981; Häder et al. 2005a). However, this value does not indicate in which direction the organisms swim. The mean swimming direction θ can be calculated as

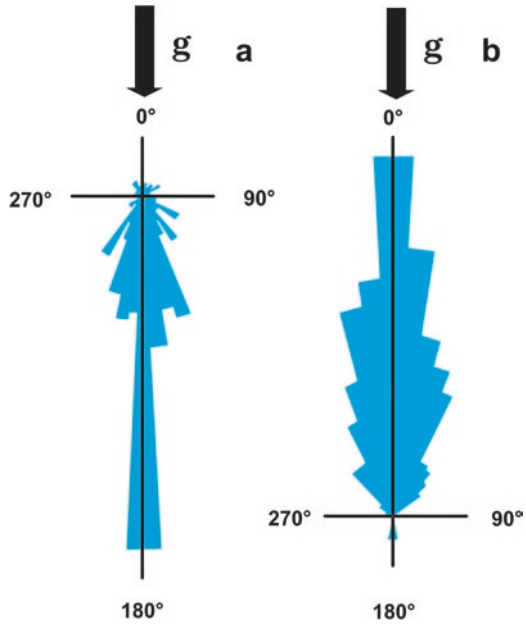

Fig. 12.1 (**a**) Positive gravitaxis in the ciliate *Loxodes striatus*. Tracks of swimming cells were recorded by automatic image analysis and the angle deviating from 0° (top of the swimming flask) were binned in 64 sectors. The circular histogram shows the percentage of tracks in each angular sector. Redrawn after (Hemmersbach and Häder 1999). (**b**) Negative gravitaxis in *E. gracilis* swimming in a vertical cuvette. Redrawn after (Häder and Vogel 1960)

$$\theta = \arctan\left(\frac{\Sigma \sin \alpha}{\Sigma \cos \alpha}\right) \qquad (12.2)$$

The direction of movement seems to be species-specific as in the case of ciliates (Massart 1891) and may depend on other environmental factors such as temperature as in the case of the flagellate *Chromulina*. Also in the ciliate *Paramecium,* the direction and precision of gravitaxis depends on temperature and the feeding status (Moore 1903) as well as the oxygen concentration in the medium (Hemmersbach-Krause et al. 1990, 1991a).

There have been many speculations on the mechanism of gravitactic orientation (Roberts 1970; Bean 1984; Barlow 1995). Some assume a pure passive phenomena, e.g. by buoyancy: when a cell is tail-heavy the tip points upwards which dictates the direction of movement (Fukui and Asai 1985; Grolig et al. 2004, 2006). In contrast to assuming that passive alignment in the water column results in vertical movements is the notion of an active gravireceptor driving a signal transduction chain which results in controlled steering movements orienting the cell parallel to the gravitational field of the Earth (Dennison and Shropshire 1984; Häder et al. 1995).

Since most cells are heavier than water their swimming velocity should be different whether they move upward or downward due to their sedimentation (Hemmersbach-Krause et al. 1993). Besides a pure vectorial addition or subtraction some species can even actively accelerate during upward swimming and decelerate during downward swimming, thereby at least partially compensate passive sedimentation (Häder et al. 2005a), a phenomenon which is called gravikinesis (Machemer et al. 1991; Machemer and Machemer-Röhnisch 1996; Gebauer et al. 1999; Häder 1999; Bhaskaran et al. 2009) and is found in many ciliates such as *Paramecium*, *Loxodes*, *Didinium* and *Stylonychia* (Krause et al. 2010) and is controversially discussed in *Euglena* (Machemer-Röhnisch et al. 1999; Häder et al. 2005a).

12.2 Ecological Consequences

Negative gravitaxis guides swimming organisms to the surface of the water column (Hemmersbach-Krause and Häder 1990). This is supported by positive phototaxis (Hopkins 1965; Häder 1988; Häder and Lebert 2001a, 2009). This behavior warrants that e.g. photosynthetic organisms accumulate close to the surface in order to harvest solar energy (Hopkins 1965). Often this movement pattern is modulated by a circadian rhythm; some flagellates start moving upward before dawn which results in their being near the surface when the sun rises (Ohata et al. 1997; Lebert et al. 1999a). However, since excessive irradiation can be detrimental these cells can reverse the direction of movement using positive gravitaxis which brings them to a lower level in the water column (Häder et al. 1999). This behavior can also be supported by negative phototaxis (Josef et al. 2005). In the presence of both light and gravity stimuli the cells respond to the resulting vector which depends on the incidence angle and irradiance of the actinic light (Kessler et al.

1992). Over the day the change from positive to negative gravitaxis and back results in vertical migrations within the water column (Eggersdorfer and Häder 1991b; Richter et al. 2007; Hu et al. 2014; Peacock and Kudela 2014). Dinoflagellates have been found to migrate up to 30 m (Yentsch et al. 1964; Taylor et al. 1966). When exposed to excessive solar radiation–especially high-energetic, short-wavelength ultraviolet radiation, some flagellates stop swimming actively and sediment passively (Häder and Liu 1990a; Häder et al. 1990a). Also in *Prorocentrum* exposure to solar or artificial ultraviolet radiation was found to impair graviorientation and velocity (Sebastian et al. 1994). In *E. gracilis* motility and gravitactic orientation are impaired by artificial and solar UV-B radiation (Häder and Liu 1990b).

Gravitaxis is also useful for non-photosynthetic organisms such as gametes and spores. Gametes have a higher chance of meeting their sexual partners when both use negative gravitaxis to reach the surface which enhances the gamete density. Zoospores usually swim around in their medium for a while which warrants their distribution in the habitat. After that they move to the bottom in order to anchor themselves and grow into a multicellular plant such as an algal thallus (Callow et al. 1997).

Some ciliates, such as *Paramecium* show negative gravitaxis (Hemmersbach-Krause and Häder 1990; Machemer and Bräucker 1992; Hemmersbach and Donath 1995). This behavior is modulated by the oxygen concentration in the water: at low oxygen tensions negative gravitaxis is less pronounced than at higher (Hemmersbach-Krause et al. 1991a) as shown in an experimental set-up without an oxygen gradient. In contrast, the ciliate *Loxodes* displays a strong positive gravitaxis at high oxygen concentrations, but is less well oriented at low oxygen concentrations. This behavior guides these microaerophilic ciliates into the sediment where they find their ecological niche (Fenchel and Finlay 1984, 1990; Finlay et al. 1993). This behavior demonstrates that under non-optimal conditions motile microorganisms swim upwards or downwards depending on their oxygen demands. After reaching an optimal area, swimming velocity is reduced and random swimming sets in.

Even not actively swimming microorganisms show vertical migrations in the water column. Cyanobacteria produce gas vacuoles to increase their buoyancy which brings them closer to the surface (Walsby 1987) where e.g. *Nodularia* ssp. are found to form large blooms (Sivonen et al. 1989). When exposed to excessive solar radiation they absorb the gas vacuoles and consequently sink out of the dangerous zone (Sinha et al. 2003). Diatoms produce oil droplets to alter their buoyancy which is also used to move up and down in the water column (Talbot and Bate 1987). However, using these examples of vertical migration may stress the term "gravitaxis".

12.3 Gravireceptors

12.3.1 Plants and Animals

Graviresponses have been observed in many motile and sessile organisms. Vertebrates possess otoliths in the inner ear, which have been found to press on the underlying cilia signaling the position of the animal with respect to the gravity vector (Rahmann et al. 1996; Anken 2006). Higher plants grow with respect to the gravity field of the Earth: primary roots grow downward (positive gravitropism) and stems upward (negative gravitropism). Thus, trees grow vertically up and not perpendicular to a slope of an ascending hill (Häder 2000). Lateral roots and branches often grow at a specific angle to the gravity vector (dia-or transversal gravitropism) (Willemoes et al. 1987; Kelly and Leopold 1992). The graviresponsive cells in the roots of higher plants are localized in a specific tissue in the root tip called statenchym located in the columella (Hou et al. 2004). However the growth response, guiding the root tip in the direction of the center of the Earth is located a few mm above the root tip which requires a signal transduction pathway between receptor and effector based on the transport of the plant hormone auxin guided by PIN proteins (Löfke 2011). The sedimentation of amyloplasts onto the endosplasmatic reticulum located in the lower part of the cell has been assumed to be responsible for the graviperception mechanism (Hensel and Sievers 1981). However, corn

mutants which lack amyloplasts in the root statenchym also show a (less precise) gravitropism; therefore the statolith hypothesis needs to be modified (Švegždienė et al. 2011). Mosses also seem to use sedimenting statoliths to sense the gravity vector (Salmi et al. 2011). However, it could also be possible that the contact between the amyloplasts and the membrane constitutes the stimulus and no force is necessary.

The freshwater alga *Chara* grows in shallow ponds where it is rooted in the sediment with rhizoids (Blancaflor 2013). In the tip of this unicellular structure there is an array of barium sulfate crystals which operate as statoliths (Sarafis 2013). When the rhizoid is turned into a horizontal position the statoliths are seen to sediment onto the lower surface and the rhizoid tip starts growing at the opposite side so that it bends until it is again in a vertical position (Braun and Limbach 2006).

In the unicellular ciliate *Loxodes* statoliths of barium sulfate have been identified within the so-called Müller organelles. A Müller organelle consists of a heavy body of barium sulfate fixed to a modified ciliary complex. Their function as mechanoreceptors (statocyst-like organelles) has been proposed and studied by Penard (1917), Fenchel and Finlay (1986), Hemmersbach et al. (1996, 1998) and Neugebauer et al. (1998). The specific density of the barium sulfate particles has been determined to be 4.4 g/mL (Hemmersbach et al. 1998). Severing the statoliths from their supporting cilia by laser beams abolishes gravitaxis in this organism. Electrophysiological studies indicated that this ciliate uses, in addition to the intracellular statocyst-like organelle, the mechanism of sensing its own cell mass via mechano-(gravi-) sensitive ion channels in the cell membrane to modify the membrane potential and thus ciliary activity to control the reorientation mechanism in the same way as in *Paramecium* (Nagel 1993).

12.3.2 Graviperception in *Euglena*

Earlier explanations for the orientation in the water column were based on a gravity-buoyancy model: If a cell is tail-heavy it would be oriented by buoyancy with the front end pointing upward (Richter et al. 2002a). Consequently, the trailing flagellum would propel the cell upwards. In a stable position the center of buoyancy is located above the center of gravity (Fukui and Asai 1985; Häder et al. 2005a). However, this hypothesis does not explain positive gravitaxis in young cultures. Microscopic analysis also does not show any heavy organelles, such as nucleus, chloroplast or mitochondria accumulated in the rear end of the cells. Kessler assumes that motile cells are passively reoriented by the torque generated by the swimming organism (Kessler and Hill 1997; Kessler 2007). If the gravity-buoyancy model would apply to the gravitactic orientation of *Euglena* one would expect that the cells smoothly reorient with respect to the gravity vector from a horizontal position. In fact, this behavior could be demonstrated by analysis of the reorientation maneuvers at high spatial and temporal resolution (Häder et al. 1997). The most pronounced directional change was found when the cells were oriented perpendicular to the gravivector of the Earth and is related to the calculated signal strength which follows the sine function of the angular deviation. In order to determine whether the cells are actually tail-heavy we compared dead (immobilized by injecting a cell suspension into liquid nitrogen) with living motile cells (Häder et al. 2005c). While the living cells showed negative gravitaxis with their front ends pointing upwards, the long axes of the immobilized cells pointed in random directions indicating that the cells were not tail-heavy; thus gravitaxis in *E. gracilis* cannot be described by a simple buoyancy model (Lebert and Häder 1999b).

Most of the analyses in this review on the graviorientation of *Euglena* and some other organisms were performed with a real time, computer-based cell tracking systems which we had developed in several iterations (Häder and Lebert 1985; Häder 1990; Vogel and Häder 1990; Häder and Vogel 1991; Häder 1992; Kühnel-Kratz and Häder 1993; Häder 1994b; Häder and Lebert 2000). A video camera with a microscope objective records the swimming tracks of numerous cells in parallel in a vertical cuvette in an infrared monitoring light, which does not affect

motility or photoorientation (Vogel and Häder 1990). The software calculates the size, form parameters, direction of movement and swimming velocity of the cells.

An alternative model for graviperception in cells with no obvious sedimenting statoliths was proposed by Roberts (1970) known as drag-gravity model. The gravity-buoyancy model is based on the assumption that one Reynolds number is sufficient to describe the sedimentation. The Reynolds number describes the ratio of inertial forces to viscous forces and it is dimensionless. Roberts introduced a second Reynolds number: one for the front and one for the rear end of a non-spherical asymmetrical body such as *Paramecium* or *Euglena,* which can be viewed as an assembly of two (or more) coupled spheres. Stokes's law predicts that a bigger (e.g. rear) end will sediment faster than the smaller front even when the specific density in the two parts is identical.

$$v = \frac{2(\rho_b - \rho_m) g r^2}{9\eta} \qquad (12.3)$$

where v = velocity, ρ_b = specific density of the body, ρ_m = specific density of the medium, g = acceleration (9.81 m s^{-2}), r = radius, η = viscosity of the medium [cP]. Experiments with immobilized *Paramecium* cells indicated that indeed the cells turned at a speed of 0.5–3°/s. The swimming speed of the cells should not have any effect on the rotational rate, however measurements in *Paramecium* showed such a dependence invalidating both the buoyancy-gravity and the drag-gravity model (Taneda and Miyata 1995). The same applies to *Euglena* where a change in the helical parameters was found during forward locomotion (Kamphuis 1999).

Another model for gravitactic orientation is the propulsion-gravity model which takes into account the helical path during forward locomotion (Winet and Jahn 1974). This results in the fact that the front end rotates with a larger radius that the rear end. This is due to the distance between the center of effort (the vectorial sum of all vertical forces) exerted by the flagella or cilia and the geometric center of the cell. Since the center of effort is closer to the front end of the cell than the geometric center, a torque occurs that moves the front end up and down in a horizontally swimming cell. However, this is not fully symmetrical since gravity applies an additional force. The sedimentation is countered by the viscosity of the medium especially at low Reynolds numbers and lifts the front end upwards. The vertical force of the flagellum (or cilia) is proportional to the sine function of the angular deviation of the cell from the vertical. During the upward part of the rotation it supports the sedimentation resistance. In the opposite position it counteracts the sedimentation resistance which finally results in an upward turning helical axis and finally a vertical reorientation of the cell. This model should work better in *Euglena* with a single flagellum at the front end than in *Paramecium* with cilia covering the whole cell body. However, a high-resolution analysis of the swimming paths did not show a strong correlation between the upswing of the helical movement and reorientation in *Euglena* (Kamphuis 1999).

So the basic question persists: What is the mechanism for gravitactic orientation in unicellular motile organisms such as *Euglena*? In this flagellate no obvious sedimenting particle(s) have been found. A possible alternative explanation could be that the whole cytoplasm with its organelles is heavier than water so that the cell content presses onto the lower cell envelope where it exerts a signal which could be used to control orientation movements (Sack 1997; Schnabl 2002). In fact, Wager had calculated the specific weight of a *Euglena* cell to be 1.016 g/mL (Wager 1911). In order to explore this possibility a simple experiment can help to distinguish between the action of an internal statolith and a heavy cell content (Fig. 12.2). In order to precisely calculate the intracellular specific weight *Euglena* cells were exposed to isopygnic centrifugation using layers with increasing Ficoll concentrations. The cells sedimented to the border between the layers with specific densities of 1.045 and 1.05 g/mL (Lebert et al. 1999b). The specific density of the cells depends on the culture age and conditions and varied between 1.046 and 1.054 g/mL (Lebert et al. 1999b). Freshly inoculated cultures showed

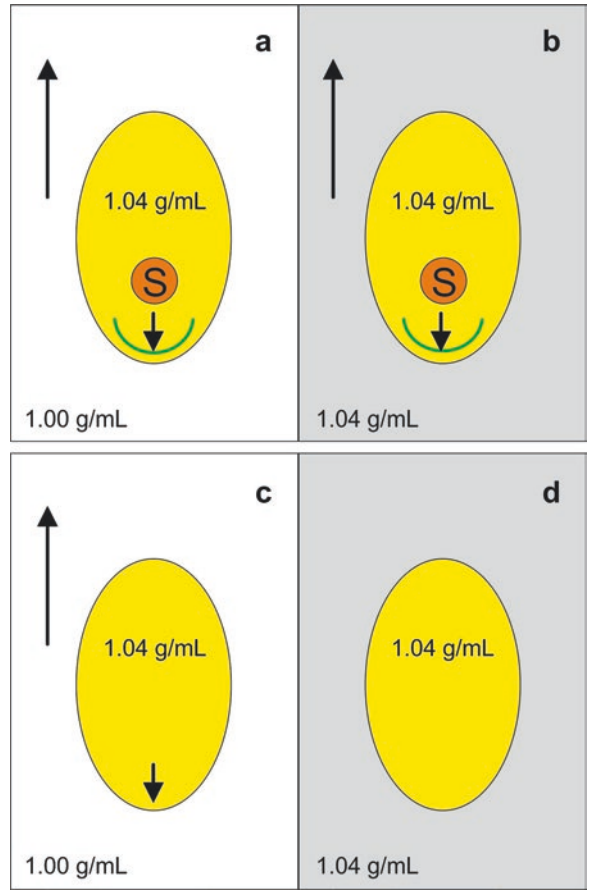

Fig. 12.2 Models for gravisensing. If an internal statolith plays the role of a gravireceptors the cell would be capable of orienting in a medium of a density of 1.00 g/cm^3 (**a**). It would also orient in a medium with a higher density (1.04 g/cm^3) (**b**), since it still presses on a receptive structure. If in contrast the cell content with an assumed specific density of 1.04 g/cm^3 presses onto a receptive structure, the cell would be able to orient in an outer medium of 1.00 g/cm^3 (**c**), but not in an adjusted medium with a specific density of 1.04 g/cm^3 (**d**), since the inner and outer medium are in an equilibrium

two bands during isopygnic centrifugation, indicating that the older cells were heavier than the young ones. One *Euglena* culture was kept for over 600 days completely enclosed. At the end of the experiment these cells had a specific density of 1.011 g/mL and did not show any gravitaxis (Häder et al. 2005a). In comparison, the cell bodies of the ciliates *Bursaria truncatella* and *Paramecium caudatum* have a specific density of 1.04 g mL (Krause 1999; Machemer-Röhnisch et al. 1999). In contrast, the barium sulfate statolith (Müller vesicle) has a specific density of 4.4 g mL (Hemmersbach et al. 1998).

The consequence of the hypothesis that the internal heavier cytoplasm presses onto the lower membrane to stimulate a gravitational signal transduction chain is that gravitaxis is abolished when the external and intracellular medium have the same specific weight and that the direction of movement should be reversed when the specific weight of the extracellular medium is higher than that of the intracellular space. This was in fact found by analyzing the swimming direction in Ficoll suspensions of increasing density (Fig. 12.3a–e) (Lebert and Häder 1996; Lebert et al. 1997).

A mathematical model for photo- and gravitactic orientation in *Euglena* by Hill and Häder describes a biased random walk (Hill and Häder 1997). It is based on the assumption that the cells initially swim in random directions, but when they deviate from the light direction or with respect to the gravivector they undergo a course correction. A similar strategy was found for e.g. chemotaxis of bacteria (Sourjik and Wingreen 2012).

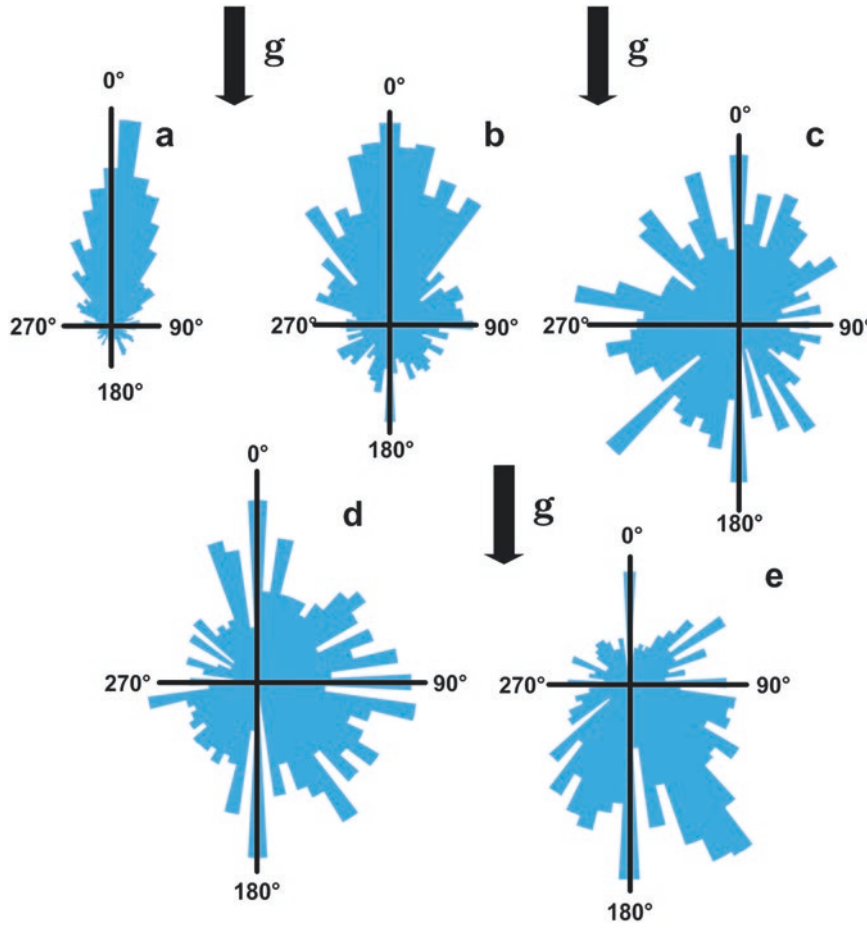

Fig. 12.3 Circular histograms of gravitactic orientation of *E. gracilis* in different Ficoll concentrations of 0% (**a**), 2.5% (**b**), 5% (**c**), 7.5% (**d**) and 10% (**e**). 0° indicates upwards; redrawn after (Lebert and Häder 1996)

12.4 Cell Behavior in Artificial Gravity: Simulated Microgravity and Hypergravity

In order to identify the mechanism by which an organism perceives an external clue resulting in an intensity-dependent response, the stimulus has to be modified and the impact on the response studied. In the case of gravity, representing a unique omnipresent stimulus, experimenters have to apply some tricks to alter its influence. Besides experiments in real microgravity which are rare to perform, different ground-based approaches have been developed based on various physical principles to simulate microgravity conditions on ground (for review see (Herranz et al. 2013; Brungs et al. 2016). Rotation of an object is applied in such a way that the influence of gravity is randomized. This approach is based on the assumption that biological systems need to be exposed to the gravity vector for a minimal presentation time in order to perceive it. It is postulated that under constant changes of the influence of gravity the object will lose its sense of direction and thus will show a behavior similar to the one seen under real microgravity conditions. So-called clinostats have either one single horizontal axis of rotation (2D clinostat) or two axes mounted perpendicular to each other (3D clinostat). The question arises how fast a

device has to be rotated to prevent an omnilateral gravistimulation but to achieve an optimal simulation of microgravity conditions for the exposed systems. Furthermore, the effective radius has to be taken into account, reducing on the one hand centrifugal forces which increase with distance from the center of rotation, but on the other hand providing enough space for e.g. undisturbed swimming of an organism such as *Euglena*. The effective centrifugal accelerations can be calculated by

$$a = \omega^2 r \qquad (12.4)$$

with r = radius, ω = angular velocity and a = acceleration. Based on studies such as the sedimentation behavior of immobilized cells, the speed of rotation was determined in the range of 50–100 revolutions per minute (rpm, fast-rotating clinostat) (Briegleb 1992; Herranz et al. 2013). In an experimental set-up for observation of *Euglena* or *Paramecium* in a clinostat equipped with a microscope the maximal centrifugal force of 3.5×10^{-3} g is calculated for the border of an observation field (radius 1 mm) and 4.5×10^{-2} g at the border of the observation chamber (radius 15 mm) during clinorotation at 50 rpm (Hemmersbach-Krause et al. 1993; Vogel et al. 1993).

Another approach to achieve simulated microgravity is to operate clinostats with two rotation axes, called 3-D clinostats, at a randomly changing speed and direction mode controlled by a dedicated algorithm. This device is called a Random Positioning Machine (RPM). Magnetic levitation is based on the principle that the gravitational force is counterbalanced by a magnetic force. A superconducting magnet with a high magnetic force field can levitate diamagnetic materials. It is assumed that a biological system experiences microgravity under this condition. *Euglena* has been exposed to the above mentioned simulation devices. All of them were equipped with in situ observation capabilities to study the impact on gravitaxis. Under two-dimensional fast clinorotation (60 rpm) the cells lost their gravitactic orientation and showed a random distribution comparable to the swimming pattern in real microgravity (Vogel et al. 1993).

Exposure on the RPM, however, indicated a completely different behavior. The random speed and random direction mode on the RPM induced numerous course corrections and even passive drifting of the *Euglena* cells, which demonstrates that *Euglena* experienced positive and negative acceleration forces (Herranz et al. 2013).

Exposure to high-gradient magnetic fields with different magnetic field strengths up to 30 T induced a perpendicular orientation of swimming *Euglena* with respect to the applied field, while *Paramecium* cells were aligned along the magnetic field lines in the same experimental set-up. This behavior clearly demonstrates that the magnetic field determines the orientation, preventing the organisms from random swimming known in real microgravity and furthermore demonstrated species-specific differences. *Euglena longa* (formerly *Astasia longa*) as well as the chloroplast-free *E. gracilis* mutant 1F showed no orientation perpendicular to the magnetic field lines. These results indicate that the chloroplasts in green *Euglena* operate as anisotropic structures which determine the orientation in the magnetic field. Thus, magnetic fields are not suitable to simulate microgravity for gravitactic unicellular organisms (Hemmersbach et al. 2014). Likewise, a centrifuge can be used to expose the swimming organisms to a higher acceleration (hypergravity) (Miller and Keller 2006). When this is combined with a video microscope the effect of hypergravity on the movement patterns of swimming cells can be studied (Friedrich et al. 1996; Häder 1996).

12.5 Real Microgravity in Space Experiments

Zero-g conditions are never completely reached on rockets, in a Shuttle or during parabolic airplane flights; the term microgravity is used to indicate low acceleration forces. During parabolic flights 10^{-2} g can be reached, on the International Space Station (ISS) 10^{-3} g and in drop towers 10^{-5} g (Schmidt 2004). The first real proof that upward orientation in an older *Euglena* culture is due to the detection of the gravity field of the Earth—and not to the magnetic field lines of the Earth or a

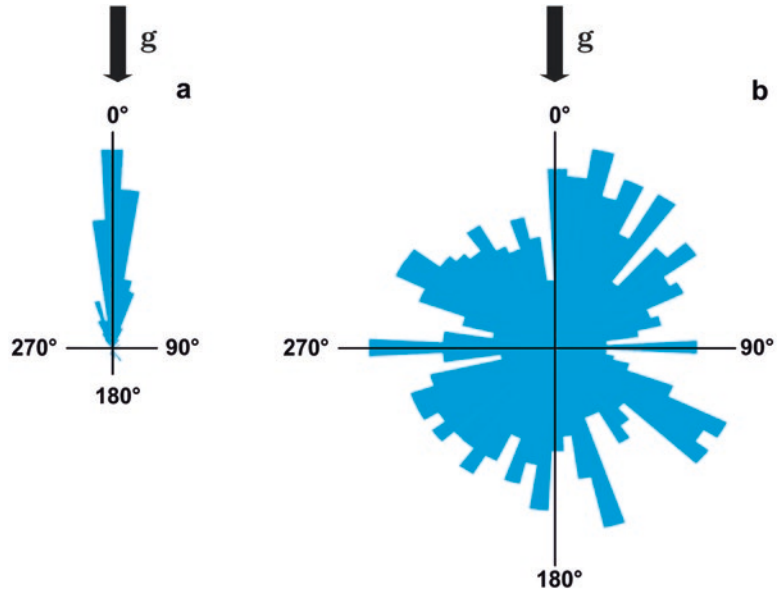

Fig. 12.4 On Earth at 1 g *Euglena* cells in their late logarithmic phase show a pronounced negative gravitaxis (**a**). In microgravity during a space flight on a TEXUS rocket they moved in random directions (**b**); redrawn after (Vogel et al. 1993)

chemical gradient such as oxygen—was provided by space experiments (Häder et al. 1990b). Cell cultures were flown on a TEXUS (technical experiments under microgravity) rocket launched in Kiruna (Sweden) on a parabolic path which provides microgravity for about 6 min (Häder et al. 2010). The swimming cells were observed online in space by means of a video downlink. Before launch the cells showed a precise negative gravitaxis (Fig. 12.4) and during the flight they moved in random directions (Vogel et al. 1993). Since the residual acceleration during the space flight is in the range of 10^{-3}–10^{-4} g the threshold for gravitaxis in *Euglena* must be higher.

Since the cells are heavier than the surrounding medium they sediment at the same time as they are swimming. This sedimentation velocity adds vectorially to the swimming velocity. Therefore the cells show a higher swimming speed in microgravity than at 1 g (negative gravitaxis) and an even higher speed during positive gravitaxis (Vogel et al. 1993)).

So what is the threshold for gravitaxis in this flagellate? The answer to this question was difficult to obtain since it required observing the cells in space (under microgravity) on a centrifuge with adjustable accelerations. This came true by the development of the NiZeMi (slow rotating centrifuge microscope) (Joop et al. 1989; Friedrich et al. 1996). This instrument was installed in the Space Shuttle Columbia for the second International Microgravity mission (IML-2) (Cogoli 1996; Häder 1996; Manieri et al. 1996). While in orbit under microgravity conditions, the cells were transferred into the NiZeMi and exposed to increasing accelerations in the range of 0–1.5 g and the swimming patterns were recorded for different accelerations. The results indicate that the threshold is found at ≤0.16 g, and that the precision of gravitaxis of *Euglena* was found to saturate at around 0.64 g (Fig. 12.5) (Häder et al. 1996). The dose-response curve shows a typical sigmoidal shape indicating the involvement of an active physiological receptor rather than a passive orientation in the water column, which would have been represented by a linear relationship (Häder 1997a). No adaptation to microgravity with respect to behavioral responses of *Euglena* was observed during the prolonged space mission as normal gravitactic behavior was found in populations returned to Earth. Analyzing the velocity distribution at different accelerations on the centrifuge indicated that this closely follows Stokes' law for sedimentation (Häder; 1994a; Häder et al. 1996). Thus *Euglena* does not show an adaptation in

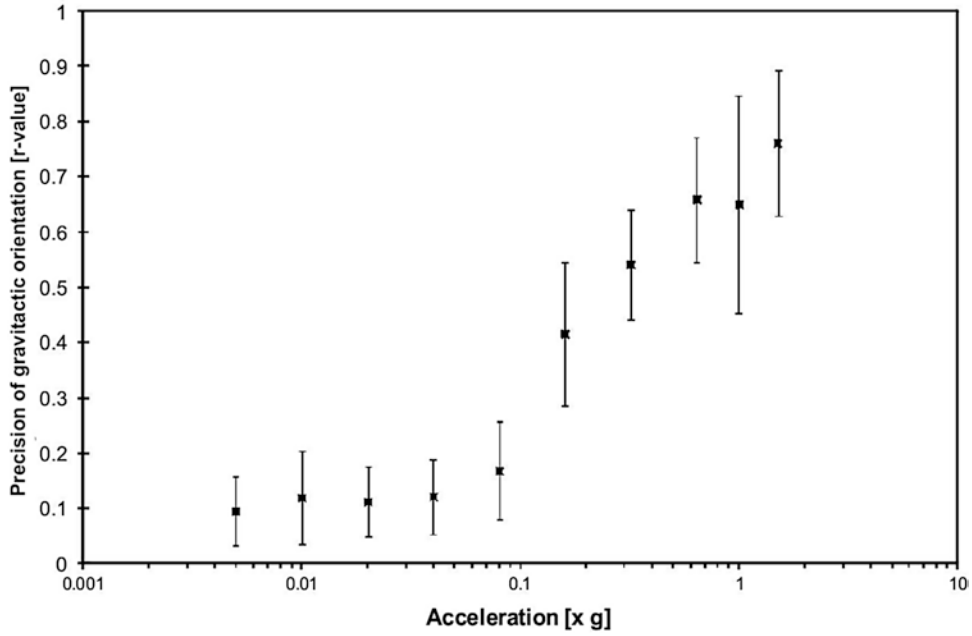

Fig. 12.5 Precision of orientation of *E. gracilis* exposed to increasing accelerations on the slow rotating centrifuge microscope on board the American Shuttle Columbia during the IML-2 mission. The threshold for gravitaxis has been calculated to be about 0.16 g from the pooled data from all four experimental runs; redrawn after (Häder et al. 1996)

swimming velocity (gravikinesis) which is in contrast to the ciliates *Paramecium* and *Loxodes* (Machemer et al. 1997; Machemer-Röhnisch et al. 1998). The gravitactic threshold could be further determined with more precision during a sounding rocket flight on a TEXUS rocket and was found to be below 0.12 g (Häder et al. 1997). Thus, the threshold for gravitaxis in *Euglena* would be sufficient for an orientation on Mars or the Moon (Kiss 2014). The threshold for graviperception in *Paramecium* was found between 0.16 and 0.3 g (Hemmersbach et al. 1996).

The next question is: what happens at higher accelerations (hypergravity)? In order to elucidate this problem the ground model of the centrifuge microscope NiZeMi was employed (Häder et al. 1991b). When the centrifuge is at rest the cells show a precise negative gravitaxis. At a total acceleration of 2 g (1 g Earth gravity plus 1 g from the acceleration perpendicular to the Earth gravitation field) the cells move along the resultant of the two forces. With increasing accelerations the cells orient more and more with respect to the centrifugal force up to 9 g. At higher accelerations (10 g) most of the cells were centrifuged down and could not swim against this force. Also *Paramecium* was found to be capable of swimming against an acceleration force of 8 g (Hemmersbach-Krause et al. 1992), while *Peridinium* could swim only against 3.8 g (Häder et al. 1991a).

As discussed above, the swimming speed results from the vectorial addition of the swimming velocity and the sedimentation velocity. The mean velocity decreased linearly with increasing accelerations of the centrifuge up to 9 g. In comparison, the sedimentation velocity of dead cells (killed with 0.1% glutaraldehyde) indicates a linear relationship of the sedimentation velocity with the acceleration force (Häder et al. 1991b).

12.6 Physiology of Gravitaxis in *Euglena*

12.6.1 Circadian Rhythm

In *E. gracilis* a pronounced circadian rhythm has been detected which governs many biochemical, physiological and behavioral parameters (Wolff and Künne 2000; Mittag 2001; Kiyota et al.

2006; Bolige and Goto 2007). Also the precision of gravitactic orientation follows a very distinct rhythm (Lebert et al. 1999a). When the cultures are kept in constant light the individual cells are in different phases of their rhythm so that no circadian changes in behavior are detected (Nasir et al. 2014). But when the cultures are exposed to a light/dark rhythm the gravitactic orientation follows a very distinct pattern with a minimum in the dark phase, an increase before the onset of light and a peak in the precision of orientation in the early afternoon (Häder and Lebert 2001b). This change in the expression of gravitaxis is not induced by the light or dark phase since the increase in precision of orientation occurs even before the light is switched on. It is rather an internal rhythm which is entrained by the light/dark cycle. This rhythm even persists when cells, which had been previously entrained, are transferred into constant light (Lebert et al. 1999a; Häder and Lebert 2001b). In parallel to the precision of gravitactic orientation, the form factor changes with cells being more elongated during daytime and more rounded at night. Also the swimming velocity increases in synchrony with the precision of gravitactic orientation. In addition, the concentration of intracellular cyclic adenosine monophosphate (cAMP) increases in parallel with the increase in gravitactic orientation (for the involvement of cAMP in the gravitactic signal transduction chain see below). In a follow-up publication the effect of shorter rhythms was investigated (1:1 h, 2:2 h, 4:4 h, 6:6 h and 8:16 h) (Richter et al. 2014). It was amazing that gravitactic orientation even followed the shortest rhythm. However, in this study graviorientation decreased after the light was switched on and increased after the beginning of the dark phase. The number of motile cells increased during the dark phase while the swimming speed was higher in the light phase. In contrast, during the light period the precision of gravitaxis increased while motility and velocity decreased after some hours of irradiation.

In *Chlamydomonas* the addition of a red background light strongly increases gravitaxis which is further augmented by the absence of calcium ions in the medium (Sineshchekov et al. 2000). In contrast, a blue light flash strongly decreased the precision of gravitactic orientation and could even reverse the direction of negative into positive gravitaxis. The spectral dependence of this response suggests the involvement of the photoreceptor for phototaxis, which is assumed to be a chlamy-rhodopsin (Kianianmomeni and Hallmann 2014).

12.6.2 Change in Gravitactic Orientation

Older cultures of *Euglena* (in stationary growth phase) show a pronounced negative gravitaxis and swim upward. In contrast, young cultures (shortly after inoculation, logarithmic growth phase) show a positive gravitaxis. The ecological reason for this differential behavior has not yet been revealed, but it could be speculated that in older cultures the concentration of nutrients is lower or the concentration of paramylon is different. However, it came as a surprise to find that the precise positive gravitaxis in young cultures was completely reversed by the application of heavy metals such as copper, mercury, cadmium or lead (Fig. 12.6) (Stallwitz and Häder 1994). Later on it could be shown that exposure to high UV and visible irradiances reverses the negative gravitaxis in older cells into a clear positive one (Ntefidou et al. 2002b; Richter et al. 2002c). The responsible wavelength band is in the UV

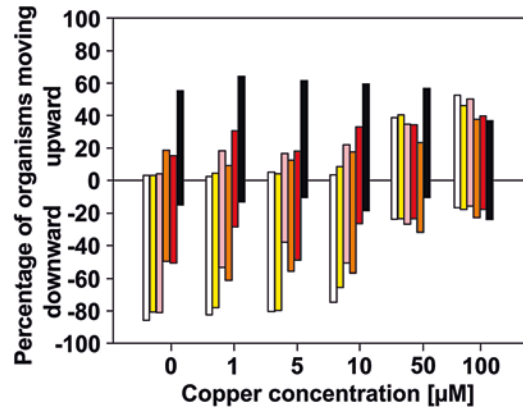

Fig. 12.6 Reversal of gravitactic orientation in young cells from downward (positive) to upward (negative) after the application of copper. The bars indicate (from *left* to *right*) a culture age of 4, 5, 6, 7, 8 and 11 days. Redrawn after (Stallwitz and Häder 1994)

and blue region of the spectrum. The sign change of gravitaxis is not brought about by an influence of the photoreceptor or the photosynthetic apparatus, because colorless and blind mutants (which do not possess a photoreceptor for phototaxis) as well as the colorless and non-phototactic *E. longa* also showed this reversal in movement direction. Rather it is mediated by reactive oxygen species (ROS) as shown by the fluorescence of the probe 2′,7′-dichlorodihydrofluorescein diacetate (DCFA-DAL). Removing the oxygen by flushing the cells with nitrogen largely blocked this effect (Ntefidou et al. 2002a). Also the application of reduced dithionite suppressed the sign change (Richter et al. 2003b, 2003d). Likewise, the addition of Trolox, potassium cyanide or ascorbic acid, known scavengers of ROS, largely inhibited the sign reversal (Richter et al. 2003d). Cyanide blocks the cytochrome-c-oxidase which could hint to a possible role of hydrogen peroxide. In contrast, application of hydrogen peroxide induced a gravitactic sign change even in the absence of external stressors. It was concluded that the change in the sign of gravitaxis is induced by ROS, most likely hydrogen peroxide, which is known to be produced e.g. by the mitochondrial cytochrome-c-oxidase. Longer exposure to solar radiation reduced the precision of gravitactic orientation (Häder and Liu 1990b; Richter et al. 2002c).

The response of gravitaxis to stress factors such as heavy metals, but also herbicides, organic pollutants etc. is very sensitive (Ekelund and Aronsson 2004; Pettersson and Ekelund 2006; Streb et al. 2006; Azizullah 2011; Azizullah et al. 2011a, 2011b, 2011c). Therefore organisms such as *Euglena* are being used in bioassays based on image analysis of tracked cells. In addition to motility, swimming velocity and cellular form, the gravitactic orientation is used as an endpoint to monitor pollution and toxicity in drinking water, waste water and natural ecosystems (Ahmed 2010; Ahmed and Häder 2011; Azizullah et al. 2013).

E. gracilis is a freshwater organism, but tolerates moderate salinity. When exposed to increased salt concentrations (5–19 g/L) the percentage of motile organisms in a population, the swimming velocity and the precision of gravitactic orientation decreased (Richter et al. 2003a). At a concentration of 15 g/L those cells which were still motile switched from negative to positive gravitaxis. This positive gravitaxis persisted for several hours or days even when the cultures were returned to zero salinity. At very high salt concentrations (20 g/L) the cells entered the so-called palmella stage characterized by immobilized cells surrounded by a mucus layer (Karnkowska-Ishikawa et al. 2012). At this time the cells lost most of their carotenoids. When they recovered from this stage after being transferred into a salt-free medium the cells became motile again and positive gravitaxis persisted (Richter et al. 2003a).

Exposure of swimming *E. gracilis* to high-energy carbon irradiation or ^{60}Co gamma-rays (1–200 Gy) resulted in a decrease of the precision of negative gravitaxis (Sakashita et al. 2002c, 2002b). Motility was not affected, but the swimming velocity decreased during exposure to ionizing radiation. A calculation of the effective doses indicated that ionizing radiation in low Earth orbits would not affect gravitaxis in *Euglena*, but during solar flares there would be an inhibition of the orientation in low Earth orbits. It is interesting to note that the inhibition of negative gravitaxis by exposure to gamma-ray irradiation could be partially prevented by the application of 100 µM Trolox C as in the case of high salt stress (see above) indicating that the inhibition by gamma-rays may be brought about by the formation of free radicals (Sakashita et al. 2002a).

12.7 Gravireceptor in *Euglena* and Sensory Transduction Chain

Let us assume the hypothesis is correct that the intracellular content of the *Euglena* cell presses onto the lower membrane and activates a gravireceptor (Häder et al. 2005b); then the next logical question is: what is the gravireceptor? Many organisms–from bacteria to vertebrates–posses mechano-sensitive ion channels (Balleza and Gómez-Lagunas 2009; Jarman and Groves 2013). These pore proteins can be opened by minute

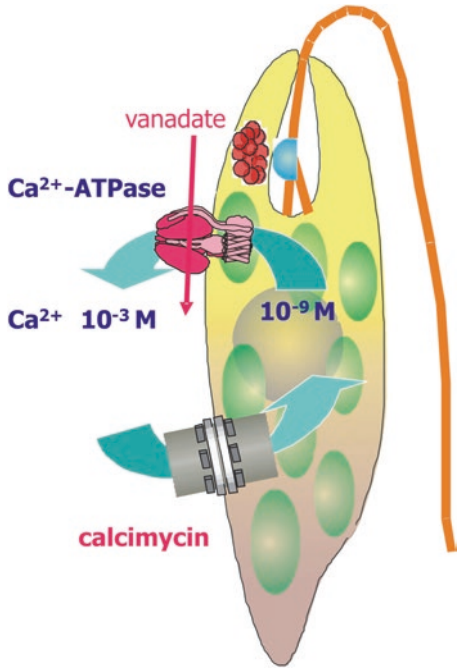

Fig. 12.7 Model of a *Euglena* cell showing the ATPase which pumps Ca^{2+} out of the cell. This pump can be blocked by vanadate. In the lower part the insertion of the ionophores A23187 is indicated which allows the passive leakage of Ca^{2+} from the outside

mechanical forces and allow the influx of ions. This passive influx follows an ion gradient across the membrane which had been previously established by active, energy-consuming ion pumps. *Euglena* uses a number of different ion pumps such as a calcium-specific ATPase which pumps Ca^{2+} out of the cell so that a resting internal concentration of about 10^{-9} M is established which is about six orders of magnitude lower than in the surrounding pond water (Weisenseel and Meyer 1997). This Ca^{2+} pump can be blocked by vanadate (Fig. 12.7). As a consequence the Ca^{2+} ion gradient across the membrane decreases and less Ca^{2+} flows in when the mechano-sensitive ion channels open upon gravistimulation and as a result the precision of gravitactic orientation decreases with increasing vanadate concentrations (Fig. 12.8a) (Lebert and Häder 1996; Lebert et al. 1997; Häder et al. 1999). Alternatively, an artificial ionophore (calcimycin, A23187) can be incorporated into the membrane which allows a passive leakage of Ca^{2+} ions into the cell which also reduces the Ca^{2+} gradient across the membrane. As a result the insertion of the ionophores decreases the precision of gravitactic orientation (Fig. 12.8b) (Lebert et al. 1996, 1997). Finally the mechano-sensitive channel itself, which allows the Ca^{2+} influx during gravistimulation, can be blocked by the application of gadolinium, which has a similar size as the Ca^{2+} ion and is thought to hinder the Ca^{2+} influx; also this measure impairs the gravitactic orientation (Häder and Hemmersbach 1997). Furthermore, addition of potassium or cadmium nitrate to the medium strongly impaired gravitaxis in *Euglena* (Fig. 12.8c) (Lebert et al. 1996, 1997). Also in *Chlamydomonas* mechano-sensitive channels have been found (Yoshimura 2011). A mutant which lacks these channels was found not to be capable of gravitaxis (Häder et al. 2006).

Due to the small size and low difference in the specific densities between the outer medium and the cellular content the force pressing onto the assumed mechano-sensitive ion channels is minute. Using a measured cell density of 1.05 g/mL the force can be calculated according to eq. (4) (Björkman 1992)

$$F = V \times g_n \times \Delta\rho \qquad (12.5)$$

where F = force [N], V = volume [L], g_n = acceleration [m s^{-2}] and $\Delta\rho$ = specific density difference between cell body and medium [kg/L]. Applying the values of *Euglena* to this equation the resulting force on the lower membrane is between 0.57 and 1.13 pN depending on the cell volume and the specific density (Lebert et al. 1999b).

If the hypothesis is true that the first step in the gravitactic signal transduction chain is a passive influx of Ca^{2+} along a previously established ion gradient by gating a mechano-sensitive ion channel it should be possible to visualize the increase in internal Ca^{2+} inside the cell. This can be done by loading a fluorescent chromophore such as Calcium Crimson into the cells which emits a fluorescence when binding to Ca^{2+} ions (McLachlan et al. 2012). In order to avoid the intensive chlorophyll fluorescence of green *Euglena*, *E. longa* was chosen, which also shows a pronounced negative gravitaxis. The fluorescence indicator was loaded

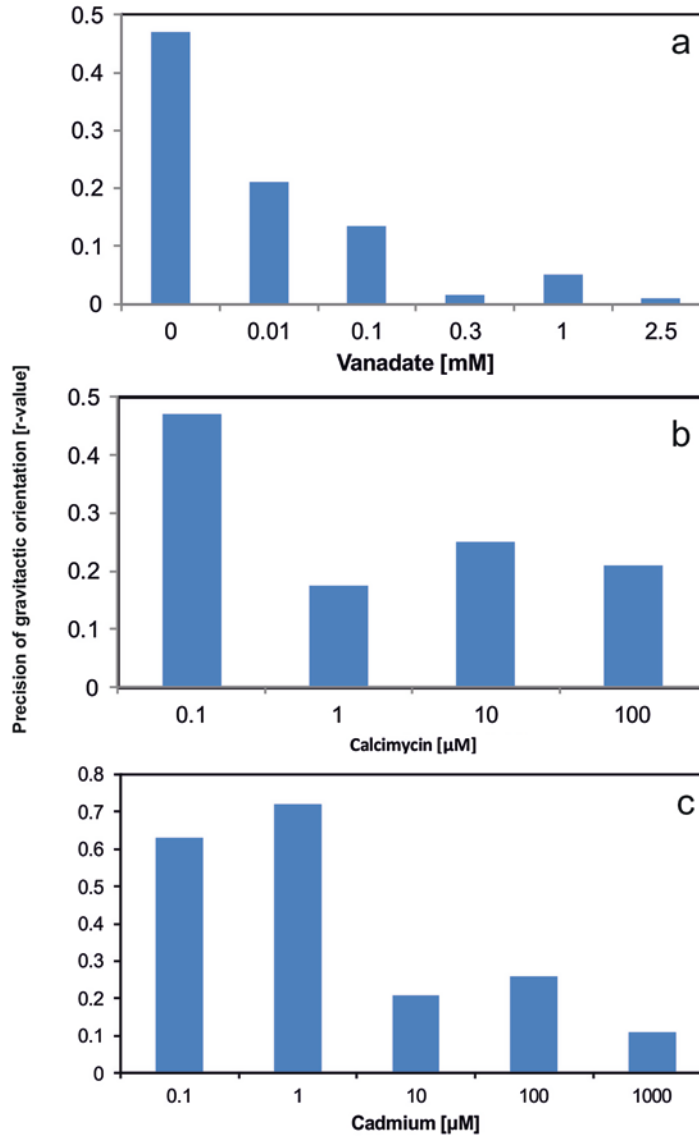

Fig. 12.8 (**a**) Precision of gravitactic orientation (r-value) in dependence of the vanadate concentration in the medium. (**b**) Effect of the ionophore calcimycin (A23187) on the precision of gravitactic orientation in *Euglena*. Redrawn after (Lebert et al. 1996). (**c**) Inhibition of gravitaxis by cadmium; redrawn after (Stallwitz and Häder 1994)

into the cells by electroporation, and the cells were allowed to orient themselves in a vertical cuvette. Then the cuvette was turned upside down so that the cells had to reorient; this was controlled by cell tracking. During reorientation a strong calcium signal was observed at the tip of the cell near the reservoir. This result was verified with the gravitactic competent, but colorless *Euglena gracilis* mutants 1F, 9F and FB (Häder and Lebert 2001b).

Using a spectrofluorometer, the fluorescence intensity could be quantified in *E. longa* cells loaded with Calcium Crimson after gravitactic stimulation (mixing the cells with a suction pipette after they had become precisely oriented (Richter et al. 2001b). The excitation beam was set to 580 nm and the fluorescence emission was monitored in the wavelength band 610–650 nm. During reorientation the fluorescence intensity rose with a short delay which corresponds with the delay found for the reorientation kinetics. Changes in Calcium Crimson fluorescence were also recorded during the microgravity and hypergravity phases produced by parabolic

airplane maneuvers (see below) (Richter et al. 2002d). In order to further prove the calcium-influx hypothesis we measured the Ca^{2+} fluorescence signal after gravitactic stimulation in the presence of gadolinium which blocks the inward Ca^{2+} current through the mechano-sensitive ion channels; indeed, the Calcium Crimson fluorescence was much lower than in the uninhibited control. Gadolinium has been found to inhibit stretch-activated ion channels (Sachs and Morris 1998). In contrast, addition of caffeine (10 mmol/L), which increases the cAMP concentration in *E. gracilis* (Porst 1998; Tahedl et al. 1998), reproducibly increases the calcium fluorescence in *E. longa* (Richter et al. 2003c) and in the 1F mutant of *E. gracilis* (Richter et al. 2001b). These results were confirmed on a parabolic flight using a sounding rocket (MAXUS 3). For this purpose a module was designed consisting of two identical epifluorescence microscopes with observation chambers filled with *E. longa* suspensions mounted on a centrifuge inside the payload (Häder and Lebert 1998). During launch the microscopes were rotated at 2 Hz to avoid cell sedimentation out of the field of view caused by the high acceleration forces during takeoff. During the parabolic flight the cells could be observed by an on-line video downlink. Focusing and lateral movement of the observation chamber could be realized by telecommands. During the flight three defined centrifugal acceleration steps (0.1, 0.2 and 0.3 g) were applied during the total time of 840 s in microgravity (Häder and Lebert 1998). After onset of microgravity the cells showed an intermediate Ca fluorescence signal. After acceleration by the centrifuge the calcium signal increased steeply and decreased again to the initial level about 10 s after the centrifuges had stopped.

In addition to missions on the American Shuttle, the ISS, satellites and rockets, parabolic flights on airplanes provide valuable opportunities to study the behavior of organisms under microgravity (Volkmann et al. 1991; Richter et al. 2002d; Krause et al. 2006; Bock et al. 2007; Strauch et al. 2010; Studer et al. 2011; Grosse et al. 2012). During the flight maneuver phases of 1 g are followed by an increase in acceleration to 1.8 g when the pilot pulls the airplane up. Afterwards the airplane enters a free-fall phase and the cells are exposed to microgravity for 20–25 s, followed again by a 1.8 g period. During the 1.8 g acceleration periods the Ca^{2+} fluorescence increases as compared to the 1 g phase, and during the microgravity phases it decreases.

The hypothetical mechano-sensitive calcium ion channels triggered by gravity cannot be located all around the cell but must be localized in a specific region in order to be fired when the cell is in the correct position for a course correction (Häder et al. 1997). When the cell is swimming upward during negative gravitaxis the channels should not be activated, thus, we would expect them to be located in the front end of the cell. Furthermore, during horizontal swimming these channels should be triggered when the flagellum points downward so that, when it swings out, it can initiate an upward turn of the front end. In that case the cell content should exert pressure on the channels. Thus, the location has to be at the front end underneath the trailing flagellum (Häder et al. 2005a). By repetitive reorientation maneuvers the cell steers into a vertical swimming direction.

The assumed Ca^{2+} influx into the cell during reorientation should result in a change in the electrical potential difference between inside and outside of the cell. Measuring the intracellular potential of *Euglena* cells using microelectrodes has failed up to now (Häder 2003). An alternative possibility to determine the membrane potential is measuring the electrochromic absorbance bandshift of natural components of the cell such as carotenoids (Armitage and Evans 1981). Another option is to load the cells with an artificial dye, such as Oxonol VI, which changes its distribution between the cytoplasm and the membrane accompanied with an absorption change between 590 and 610 nm when the membrane potential changes (Haugland 1997). We constructed a photometer with two sets of LEDs with maximal emission at 590 and 610 nm, respectively. After passing the beams through the *Euglena* suspension loaded with Oxonol VI, the absorption was measured alternatively at the two wavelengths by an array of four phototransistors as sensors and the ratio was calculated which

serves as a proxy for the membrane potential (Richter et al. 2001a). In parallel the gravitactic orientation was measured by cell tracking (Lebert and Häder 1999a). At the beginning of the experiment the cells were disturbed by gentle mixing and then allowed to reorient. During the cellular reorientation the membrane potential transiently increased (became more positive) which can be explained by the influx of Ca^{2+} ions through the membrane-sensitive ion channels. Sequestering calcium ions in the outer medium by the application of EGTA affected gravitactic orientation and abolished the membrane potential change measured with oxonol VI as shown during a parabolic flight campaign (Richter et al. 2006).

If indeed gravitactic orientation is coupled with a change in the membrane potential, it should be possible to interfere with the signal transduction mechanism by experimentally manipulating the membrane potential. This can be achieved by using a lipophilic cation such as triphenylmethyl phosphonium ($TPMP^+$) which penetrates the membrane and thus reduces the internal negative potential (Finichiu et al. 2013). Application of $TPMP^+$ at micromolar concentrations effectively reduces the precision of orientation in *E. gracilis* (Lebert et al. 1996).

12.8 Molecular Biology to Disentangle the Gravitactic Signal Transduction Chain

The existence of mechano-sensitive channels in *Euglena* was confirmed by molecular biological methods. In *Saccharomyces* a gene for a mechano-sensitive channel has been sequenced. When we employed several primers against conserved regions of this gene during PCR on the cDNA extracted from *Euglena*, four sequences of different lengths were detected corresponding to the homologue sequence in *Saccharomyces* (Häder et al. 2003). More than 1500 PCR products from many potential mechano-sensitive channel families were isolated, cloned in plasmids and sequenced (Häder et al. 2009). These proteins belong to the families of MID1 (*S. cerevisiae*), MEC (*C. elegans*), MSCL (*E. coli*), BNC1/BNAC (*H. sapiens*) and TRP (*D. melanogaster*, *H. sapiens* and others). However, most of these sequences coded for proteins were involved in other functions; but one sequence resembled the gene for a TRP channel. The TRP protein family is involved in many different physiological functions in the cell such as photoperception, nociception (pain sensation), thermosensation, tactile sensation, mechanosensing, taste, osmolar sensation and fluid flow sensation (Nilius and Owsianik 2011; Nilius et al. 2012). The assumed structure of the mechano-sensitive ion channel TRPC7 consists of six membrane spanning helices and the TRP pore (Häder et al. 2009).

One way of determining whether a specific gene product is involved in the signal transduction chain of gravitaxis is the application of RNA interference (RNAi) (Tuschl et al. 2014). In this process double-stranded RNA (dsRNA) induces a sequence-specific post-transcriptional gene silencing. Short RNA fragments (19–23 nucleotides) are introduced into the cells by electroporation. The injected RNA combines with the mRNA of the related protein in an antisense fashion and by this interferes with the function of the mRNA, effectively blocking translation and thus the synthesis of the corresponding protein. Using degenerated primers designed according to the pore region of the mechano-sensitive channel four PCR transcripts were isolated from *E. gracilis*. These products were cloned, sequenced and analyzed with BLAST. Three of the products did not resemble TRP channels while the fourth had a low similarity to the C-terminal end of TRP channels (Häder et al. 2009). Applying RNAi to the first three PCR products did not affect gravitactic orientation, but the forth effectively inhibited gravitaxis. This effect lasted for up to 30 days.

After characterization of the primary gravireceptor to be a transient receptor potential-like (TRP) channel protein, the next logical question was: What do the Ca^{2+} ions do inside the cell during gravitactic reorientation? Ca^{2+} ions are universal messengers in many organisms from bacteria to vertebrates and bind to proteins called calmodulins (Panina et al. 2012; Adler 2013) which usually consist of about 150 amino acids

and normally have four binding sites for calcium ions (Means 2013). Each calcium binding motif consists of a 12 amino acids loop flanked on both sides by a 12-residue α-helix which undergoes a conformational change upon calcium binding. Following the hypothesis that Ca^{2+} ions bind to a calmodulin during gravitactic orientation in *Euglena* we searched for a calmodulin gene in this organism. To our surprise we did not find one gene but at least five calmodulin genes (Daiker et al. 2010). The amino acid sequence coded by one of these genes (CaM.1) was already known from *Euglena* (Toda et al. 1992). We sequenced the genes of all five calmodulins (CaM.1–CaM.5) isolated from *E. gracilis*. All five calmodulin gene sequences differ from each other, but the EF motif, typical for calmodulins, is conserved in all five genes (Daiker et al. 2010).

Using the RNA inhibition method described above we blocked the protein synthesis of each calmodulin separately by electroporating the dsRNA of each calmodulin gene in separate *Euglena* populations by electroporation. RNAi against CaM.1 resulted in severe abnormalities of the cell form (Daiker et al. 2010). Even though the flagellum was visible the cells did not swim but showed only euglenoid (crawling) movement (Häder et al. 2009). Cell division was impaired and the cells showed abnormal outgrowths. By means of RT-PCR it could be confirmed that no mRNA of the blocked calmodulin was expressed (Daiker et al. 2010).

Application of RNAi against CaM.2 also resulted in euglenoid movement and cell abnormalities but only transiently for several days (Daiker et al. 2010). After about 1 week the cells recovered and swam normally, but they did not show any gravitactic orientation. RNAi against the remaining calmodulins (CaM.3–CaM.5) had no visible effect on the cell form, swimming behavior or gravitaxis. These surprising results indicate that only one of the identified calmodulins (CaM.2) is involved in the signal transduction chain of gravitaxis. In *Chlamydomonas* a calmodulin was detected in the flagella (Gitelman and Witman 1980). In *Euglena* the previously known calmodulin (CaM.1) was found underneath the pellicula (Toda et al. 1992) where it may be responsible for the cell form and the euglenoid movements which might explain the effects of RNAi of CaM.1 on motility and cell form abnormalities.

What is the next step in the gravitactic signal transduction chain? Masakatsu Watanabe and Mineo Iseki had shown that the light signal for photophobic responses is absorbed by a novel PAC photoreceptor molecule, a light-activated adenylyl cyclase, which produces cyclic AMP (cAMP) from ATP when activated by light (Iseki et al. 2002) (cf. chapter on photomovement in *Euglena*, this volume). Could it be possible that cAMP is also involved in the signal transduction chain of gravitaxis?

Preliminary experiments had shown that during the circadian rhythm in *E. gracilis* the intracellular concentration of cAMP increases in parallel with the precision of gravitactic orientation during the day (see above) (Lebert et al. 1999a). In order to prove the involvement of cAMP in the gravitactic signal transduction chain a very complex space experiment was devised for a flight on a sounding rocket (TEXUS 36) (Tahedl et al. 1998). Aliquots of 1 mL cell suspension were filled into 2-mL syringes which were connected by a tube with a second 2-mL syringe containing 1 mL ethanol, but separated by a rubber ball. A total of 112 of these assemblies were housed in frames and the fixative could be injected explosively into the cell suspension by hydraulic pistons at predetermined times during the sounding rocket flight. The frames were oriented radially on a centrifuge to provide three different radii to allow different accelerations at the same centrifugal speed. In addition to the controls, some of the experiments contained 1 mM gadolinium chloride which is an inhibitor of mechano-sensitive channels (Yang and Sachs 1989; Lebert and Häder 1996) or 10 mM caffeine, an inhibitor of phosphodiesterases (Lebert et al. 1997; Spoto et al. 1997; Häder and Lebert 2002). During the flight, individual groups of experiments (8–12 syringes in parallel) were activated so that the cells were fixed at different times and accelerations. The cAMP concentration inside the cells after a given exposure time to a given acceleration was quantified using a

radioimmunoassay and a scintillation counter. During microgravity the cAMP content of the cells was low and did not increase significantly at an acceleration of 0.08 g, which previous experiments had shown to be below the threshold for gravitaxis in *Euglena*. However, when accelerations of 0.12 g or 0.16 g were applied the cellular cAMP concentrations increased considerably (Tahedl et al. 1997). Gadolinium-treated cells showed a significantly lower increase in cAMP upon gravitactic stimulation (Tahedl et al. 1998). In caffeine-treated cells no increase in cAMP could be observed during stimulation, but caffeine-treated cells had about three times higher concentrations of cAMP in microgravity. Probably no further increase could be produced by the adenylyl cyclase. It is interesting to note that also in a motile slime mold an activated adenylyl cyclase has been found to be responsible for the control of movement and development (Renart et al. 1981; Sultana et al. 2012). Also the ciliate *Paramecium* has been found to involve cAMP in its gravitactic sensory transduction chain (Bräucker et al. 2001; Hemmersbach and Braun 2006).

In order to confirm the hypothesis of involvement of calmodulin and an adenylyl cyclase in the gravitactic sensory transduction chain a number of inhibitor studies were carried out. Trifluoperazine and fluphenazin as well as W7 are specific calmodulin inhibitors (Naccache 1985; Russo et al. 2014; Son et al. 2014) and were found to inhibit gravitaxis in *E. gracilis* (Häder et al. 2006). Likewise, indomethacine impairs the adenylyl cyclase (Wang et al. 2012) and decreases the precision of gravitactic orientation in *E. gracilis* (Richter et al. 2002b; Häder et al. 2006), while forskolin activates the adenylyl cyclase (Schwer et al. 2013) and augments gravitaxis in *Euglena* (Häder et al. 2006). Phosphodiesterase quenches the cAMP signal (Cai et al. 2015). When this enzyme is inhibited by caffeine, theophylline or IBM-X the cellular cAMP concentration increases (Cameron and Baillie 2012; Steck et al. 2014) which explains why e.g. application of caffeine or IBM-X enhances the gravitactic orientation (Streb et al. 2002). 8-Bromo-cAMP is an analog of cAMP which is not degraded by the phosphodiesterase but seems to have a similar function. Addition of this drug consequently augmented the precision of gravitactic orientation in *Euglena* (Lebert et al. 1997).

The final piece in the puzzle of the sensory transduction chain is how cAMP controls the flagellar activity which finally results in a course correction of the cell. cAMP has been found to activate a protein kinase A (Favaro et al. 2012) which could be responsible for the change in flagellar activity. Staurosporine is an effective inhibitor of protein kinases (Chang and Kaufman 2000). When applied to swimming *Euglena* the cells lost their ability of gravitactic orientation with increasing exposure time (Häder et al. 2010). 225 min after application a positive gravitaxis was observed (Daiker et al. 2011). This result reminds us of the fact that negative gravitaxis can be reversed into a positive one by several stress factors (see above). But the full meaning of this finding is not yet fully understood. Also, negative phototaxis was blocked by staurosporine with increasing exposure time (see chapter on photomovement in *Euglena*, this volume). This indicates that gravitaxis and phototaxis share the same last step in their sensory transduction chain. While the initial parts are different, in the end the production of cAMP activates a phosphokinase A which controls the flagellar reorientation.

Euglena possesses at least five isoforms of the protein kinase A (PK.1–PK.5) as has been found by using degenerate primers. RACE-PCR was used to reveal the full range of the RNA sequences and sequence the genes. Since these five genes differ in certain sequences it was possible to produce specific ds-RNA against the individual genes. These were inserted into different *Euglena* populations by electroporation for RNA interference. The resulting populations were tested for gravitaxis. RNAi of PK.1–PK.3 and PK.5 did not affect gravitactic orientation, indicating that these protein kinases were not involved in the gravitactic signal transduction chain (Daiker et al. 2011). In contrast, application of RNAi on PK.4 strongly affected the precision of gravitaxis up to several weeks. After about 22 days a positive gravitaxis was observed which reminds us of the fact that also staurosporine

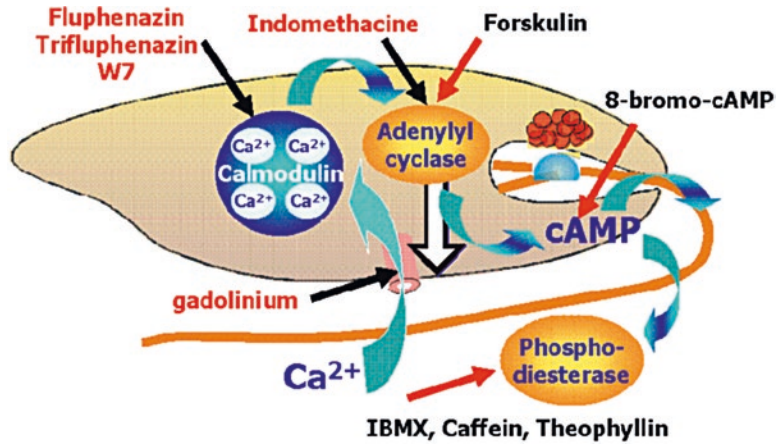

Fig. 12.9 The model shows the proposed signal transduction chain for gravitactic stimuli with the components involved as well as the inhibitors and enhancers

inverted the negative into a positive gravitaxis after prolonged application (see above). Furthermore, RNAi on PK.4 impaired phototaxis (see chapter on photomovement in *Euglena*, this volume). This again confirms that gravitaxis and phototaxis share the same last step—the activation of a protein kinase A by cAMP—in their sensory transduction chain.

Combining all these results we can construct a signal transduction chain for gravitactic orientation in *Euglena* (Fig. 12.9) (Häder 2010). The cell interior has a higher specific density than the surrounding medium. During horizontal swimming it exerts a pressure onto the lower membrane with the mechano-sensitive TRP channel whenever the flagellum points downwards during its helical path. The gating of the channel can be blocked by gadolinium. The inflowing Ca^{2+} binds to a specific calmodulin (CaM.2) which can be blocked by fluphenazin, trifluphenazin or W7. The activated calmodulin in turn activates an adenylyl cyclase. This can be inhibited by applying indomethacine, while forskolin augments its action. The adenylyl cyclase uses ATP to produce cAMP which in turn is broken down by a phosphodiesterase. 8-bromo-cAMP can substitute the cAMP function but is not broken down by the phosphodiesterase. IBMX, caffeine or theophylline inhibit the phosphodiesterase, so that the intracellular cAMP concentration is enhanced. All inhibitory or stimulatory actions are mirrored in impaired or augmented gravitactic orientation of *Euglena*.

Figure 12.10 shows the key players in the sensory transduction chain for gravitaxis and phototaxis which share the final element (protein kinase A) which is believed to control the reorientation of the flagellum. Whether or not calmodulin itself could activate the protein kinase A has not yet been revealed. The sensory transduction chain of the photoorientation starts with the activation of the PAC photoreceptor by light which results in the production of cAMP by the light-activated adenylyl cyclase which in turn is thought to activate the same protein kinase A, involved in graviperception. The components which have been blocked by RNAi to prove their involvement in the respective transduction pathways are indicated.

12.9 Conclusions and Outlook

Euglena gracilis uses a physiological gravireceptor for an active orientation with respect to the gravity vector of the Earth. The basic elements of the sensory transduction chain such as the mechano-sensitive transient receptor potential Ca^{2+}-conducting ion channel, the specific calmodulin (CaM.2) (Häder et al. 2009), the adenylyl cyclase and protein kinase (PK.4) (Daiker et al. 2011) have been identified. The number and localization of the TRP channels still need to be confirmed e.g. by immunofluorescence using polyclonal antibodies. Likewise, the location of the specific CaM.2, thought to be located inside

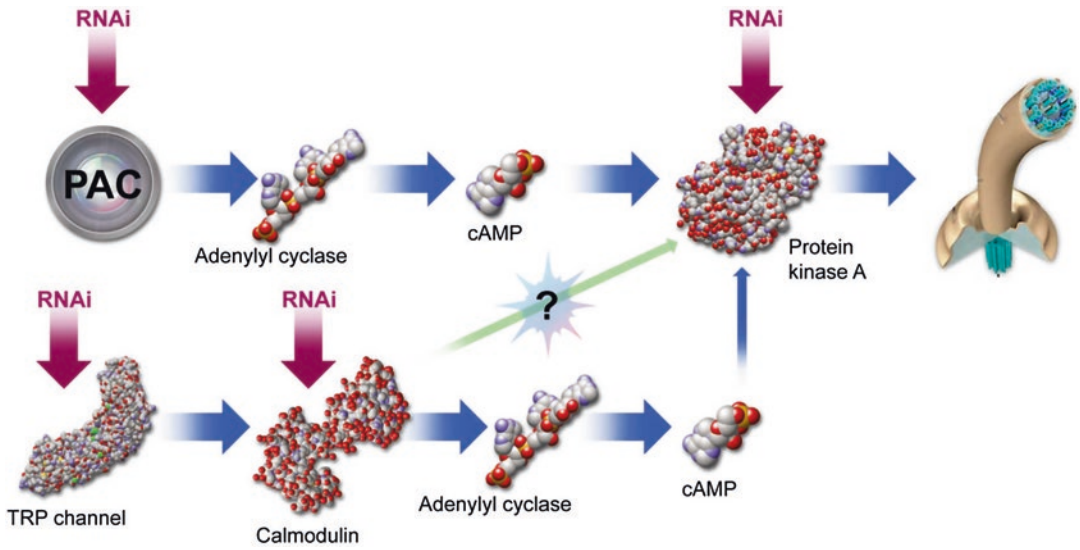

Fig. 12.10 Assumed sensory transduction chain of gravitaxis in the flagellate *E. gracilis*. When the pressure of the cell content activates a mechano-sensitive channel during horizontal swimming, calcium ions enter the cell passively along a previously established Ca^{2+} gradient and activate a specific calmodulin (CaM.2) which in turn induces an adenylyl cyclase to produce cAMP from ATP. This messenger activates a protein kinase A (PK.4) which is thought to provoke the change in the flagellar bending resulting in a reorientation response of the cell. The phototactic sensory transduction chain is included in this model showing the PAC photoreceptor which is a light-activated adenylyl cyclase. The produced cAMP is thought to activate the same protein kinase which is involved in gravitaxis. The molecular structures resemble typical members of the respective protein families. The structures of the specific proteins in *Euglena* are still unknown. Redrawn after (Häder 2010)

the flagellar membrane needs to be confirmed. Also the cellular positions of the adenylyl cyclase and phosphokinase (PK.4) need to be identified. Another open question is the nature of the adenylyl cyclase which is probably not identical with the adenylyl cyclase involved in phototaxis since this is part of the photoreceptor located in the paraxonemal body (Iseki et al. 2002). The protein kinase is hypothesized to phosphorylate proteins inside the trailing flagella. These proteins need to be identified to understand the molecular mechanism of flagellar reorientation. The potential involvement of the second flagellum, which does not extent out of the reservoir, as well as the axonemal rod (Bouck 2012), a specific element found in Euglenoid cells, need to be revealed.

Another open question concerns the control of the direction of gravitaxis. The existing results indicate that ROS are involved in changing the direction of gravitaxis (Richter et al. 2003d). However, how ROS operates on the molecular signal transduction chain to reverse the direction of movement still remains to be resolved.

Acknowledgements The authors thank their coworkers P. Richter, M. Ntefidou and S. Strauch for critically reading the manuscript. Funding of the underlying research by DFG, DLR, ESA, NASA and BMBF is gratefully acknowledged.

References

Aderhold R (1888) Beiträge zur Kenntnis richtender Kräfte bei der Bewegung niederer Organismen. Jena Ztsch Med Naturwiss 22:311–342

Adler EM (2013) Bacteria under pressure, calcium channel internalization, and why cockroaches avoid glucose-baited traps. J Gen Physiol 142(1):1–2

Ahmed H (2010) Biomonitoring of aquatic ecosystems. Ph.D. thesis, Friedrich-Alexander-Universität, Erlangen-Nürnberg

Ahmed H, Häder D-P (2011) Monitoring of waste water samples using the ECOTOX biosystem and the flagellate alga *Euglena gracilis*. Water Air Soil Pollut 216(1–4):547–560

Anken RH (2006) On the role of the central nervous system in regulating the mineralisation of inner-ear otoliths of fish. Protoplasma 229(2):205–208

Armitage JP, Evans CW (1981) Comparison of the carotenoid bandshift and oxonol dyes to measure membrane potential changes during chemotactic

stimulation of *Rhodopseudomonas sphaeroides* and *Escherichia coli*. FEBS Lett 126:98–102
Azizullah A (2011) Ecotoxicological assessment of anthropogenically produced common pollutants of aquatic environments. Ph.D. thesis, Friedrich-Alexander University, Erlangen, Germany
Azizullah A, Nasir A, Richter P, Lebert M, Häder D-P (2011a) Evaluation of the adverse effects of two commonly used fertilizers, DAP and urea, on motility and orientation of the green flagellate *Euglena gracilis*. Environ Exp Bot 74:140–150
Azizullah A, Richter P, Häder D-P (2011b) Ecotoxicological evaluation of wastewater samples from Gadoon Amazai Industrial Estate (GAIE), Swabi, Pakistan. Int J Environ Sci 1(5):959–976
Azizullah A, Richter P, Häder D-P (2011c) Toxicity assessment of a common laundry detergent using the freshwater flagellate *Euglena gracilis*. Chemosphere 84(10):1392–1400
Azizullah A, Murad W, Adnan M, Ullah W, Häder D-P (2013) Gravitactic orientation of *Euglena gracilis*—a sensitive endpoint for ecotoxicological assessment of water pollutants. Front Environ Sci 1:4
Balleza D, Gómez-Lagunas F (2009) Conserved motifs in mechanosensitive channels MscL and MscS. Eur Biophys J 38(7):1013–1027
Barlow PW (1995) Gravity perception in plants: a multiplicity of systems derived by evolution? Plant Cell Environ 18:951–962
Batschelet E (1981) Circular Statistics in Biology. Academic Press, London, New York
Bean B (1984) Microbial geotaxis. In: Colombetti G, Lenci F (eds) Membranes and sensory transduction. Plenum Press, London, pp 163–198
Bhaskaran S, Jagtap SS, Vidyasagar PB (2009) Life and gravity. Biophys Rev Lett 4(04):299–318
Björkman T (1992) Perception of gravity by plants. Adv Space Res 12:195–201
Blancaflor EB (2013) Regulation of plant gravity sensing and signaling by the actin cytoskeleton. Am J Bot 100(1):143–152
Bock O, Girgenrath M, Carnahan H (2007) Grasping of virtual objects is affected by near-weightlessness of parabolic flight. J Gravit Physiol 13:1–6
Bolige A, Goto K (2007) High irradiance responses involving photoreversible multiple photoreceptors as related to photoperiodic induction of cell division in *Euglena*. J Photochem Photobiol B Biol 86:109–120
Bouck GB (2012) Flagella and the cell surface. Physiol 3:29
Bräucker R, Cogoli A, Hemmersbach R (2001) Graviperception and graviresponse at the cellular level. In: Baumstark-Khan C, Horneck G (eds) Astrobiology: the Quest for the Conditions of Life. Springer, Berlin, pp 284–297
Braun M, Limbach C (2006) Rhizoids and protonemata of characean algae: model cells for research on polarized growth and plant gravity sensing. Protoplasma 229(2):133–142
Briegleb W (1992) Some qualitative and quantitative aspects of the fast-rotating clinostat as a research tool. ASGSB Bull 5:23–30
Brungs S, Egli M, Wuest SL, Christianen PCM, van Loon JWA, Ngo Anh TJ, Hemmersbach R (2016) Facilities for simulation of microgravity in the ESA ground-based facility programme. Micrograv Sci Techn 28(3):191–203
Buttinoni I, Volpe G, Kümmel F, Volpe G, Bechinger C (2012) Active Brownian motion tunable by light. J Phys Condens Matter 24(28):284129
Cai Y, Nagel DJ, Zhou Q, Cygnar KD, Zhao H, Li F, Pi X, Knight PA, Yan C (2015) Role of cAMP-phosphodiesterase 1C signaling in regulating growth factor receptor stability, vascular smooth muscle cell growth, migration, and neointimal hyperplasia. Circ Res 116(7):1120–1132
Callow ME, Callow JA, Pickett-Heaps JD, Wetherbee R (1997) Primary adhesion of *Enteromorpha* (Chlorophyta, Ulvales) propagules: quantitative settlement studies and video microscopy. J Phycol 33(6):938–947
Cameron R, Baillie GS (2012) cAMP-specific phosphodiesterases: modulation, inhibition, and activation. In: Botana LM, Loza M (eds) Therapeutic Targets: Modulation, Inhibition, and Activation. Wiley, Hoboken, NJ, p 1
Chang SC, Kaufman PB (2000) Effects of staurosporine, okadaic acid and sodium fluoride on protein phophorylation in graviresponding oat shoot pulvini. Plant Physiol Biochem 38:315–323
Clegg MR, Maberly SC, Jones RI (2003) Chemosensory behavioural response of freshwater phytoplanktonic flagellates. Plant Cell Environ 27(1):123–135
Cogoli A (1996) Biology under microgravity conditions in Spacelab International Microgravity Laboratory 2 (IML-2). J Biotechnol 47(2–3):67–70
Daiker V, Häder D-P, Lebert M (2010) Molecular characterization of calmodulins involved in the signal transduction chain of gravitaxis in *Euglena*. Planta 231(5):1229–1236
Daiker V, Häder D-P, Richter RP, Lebert M (2011) The involvement of a protein kinase in phototaxis and gravitaxis of *Euglena gracilis*. Planta 233:1055–1062
Darwin C (1859) On the origin of species by means of natural selection, or the preservation of favoured races in the struggle for life. London: John Murray
Davenport CB (1908) Experimental Morphology. Macmillan Publishing, New York
Dennison DS, Shropshire W Jr (1984) The gravireceptor of *Phycomyces*. Its development following gravity exposure. J Gen Physiol 84:845–859
Dryl S (1974) Behavior and motor response of *Paramecium*. In: van Wagtendonk WJ (ed) *Paramecium*: a Current Survey. Elsevier Scientific, Amsterdam, pp 165–218
Eggersdorfer B, Häder D-P (1991a) Phototaxis, gravitaxis and vertical migrations in the marine dinoflagellate *Prorocentrum micans*. FEMS Microbiol Ecol 85:319–326
Eggersdorfer B, Häder D-P (1991b) Phototaxis, gravitaxis and vertical migrations in the marine dinoflagellates,

Peridinium faeroense and *Amphidinium caterea*. Acta Protozool 30:63–71

Ekelund NGA, Aronsson KA (2004) Assessing *Euglena gracilis* motility using the automatic biotest ECOTOX application to evaluate water toxicity (cadmium). Vatten 60:77–83

Favaro E, Granata R, Miceli I, Baragli A, Settanni F, Perin PC, Ghigo E, Camussi G, Zanone M (2012) The ghrelin gene products and exendin-4 promote survival of human pancreatic islet endothelial cells in hyperglycaemic conditions, through phosphoinositide 3-kinase/Akt, extracellular signal-related kinase (ERK) 1/2 and cAMP/protein kinase A (PKA) signalling pathways. Diabetologia 55(4):1058–1070

Fenchel T, Finlay BJ (1984) Geotaxis in the ciliated protozoon *Loxodes*. J Exp Biol 110:17–33

Fenchel T, Finlay BJ (1986) The structure and function of Müller vesicles in loxodid ciliates. J Protozool 33:69–76

Fenchel T, Finlay BJ (1990) Anaerobic free-living protozoa: growth efficiencies and the structure of anaerobic communities. FEMS Microbiol Ecol 74:269–276

Fiedler B, Börner T, Wilde A (2005) Phototaxis in the cyanobacterium *Synechocystis* sp. PCC 6803: role of different photoreceptors. Photochem Photobiol 81(6):1481–1488

Finichiu PG, James AM, Larsen L, Smith RA, Murphy MP (2013) Mitochondrial accumulation of a lipophilic cation conjugated to an ionisable group depends on membrane potential, pH gradient and pK a: implications for the design of mitochondrial probes and therapies. J Bioenerg Biomembr 45(1–2): 165–173

Finlay BJ, Tellez C, Esteban G (1993) Diversity of free-living ciliates in the sandy sediment of a Spanish stream in winter. J Gen Microbiol 139:2855–2863

Fraenkel GS, Gunn DL (1961) The Orientation of Animals (Kineses, Taxes and Compass Reactions). Dover Publications, New York

Friedrich ULD, Joop O, Pütz C, Willich G (1996) The slow rotating centrifuge microscope NIZEMI—a versatile instrument for terrestrial hypergravity and space microgravity research in biology and materials science. J Biotechnol 47:225–238

Fukui K, Asai H (1985) Negative geotactic behavior of *Paramecium caudatum* is completely described by the mechanism of buoyancy-oriented upward swimming. Biophys J 47:479–482

Gebauer M, Watzke D, Machemer H (1999) The gravikinetic response of *Paramecium* is based on orientation-dependent mechanotransduction. Naturwissenschaften 86:352–356

Gerhardt K (1913) Beitrag zur Physiologie von *Closterium*. Dissertation, Friedrich-Schiller-Universität Jena

Gitelman SE, Witman GB (1980) Purification of calmodulin from *Chlamydomonas*: calmodulin occurs in cell bodies and flagella. J Cell Biol 98:764–770

Grolig F, Herkenrath H, Pumm T, Gross A, Galland P (2004) Gravity susception by buoyancy: floating lipid globules in sporangiophores of *Phycomyces*. Planta 218:658–667

Grolig F, Döring M, Galland P (2006) Gravisusception by buoyancy: a mechanism ubiquitous among fungi? Protoplasma 229(2):117–123

Grosse J, Wehland M, Pietsch J, Ma X, Ulbrich C, Schulz H, Saar K, Hübner N, Hauslage J, Hemmersbach R (2012) Short-term weightlessness produced by parabolic flight maneuvers altered gene expression patterns in human endothelial cells. FASEB J 26(2):639–655

Häder D-P (1988) Ecological consequences of photomovement in microorganisms. J Photochem Photobiol B Biol 1:385–414

Häder D-P (1990) Tracking of flagellates by image analysis. In: Alt W, Hoffmann G (eds) Biological Motion, Proceedings Königswinter 1989. Springer, Berlin, pp 343–360

Häder D-P (1991) Strategy of orientation in flagellates. In: Riklis E (ed) Photobiology. The Science and its Applications. Plenum Press, New York, pp 497–510

Häder D-P (1992) Real-time tracking of microorganisms. In: Häder D-P (ed) Image Analysis in Biology. CRC Press, Boca Raton, pp 289–313

Häder D-P (1994a) Gravitaxis in the flagellate *Euglena gracilis*—results from Nizemi, clinostat and sounding rocket flights. J Gravit Physiol 1:P82–P84

Häder D-P (1994b) Real-time tracking of microorganisms. Binary 6:81–86

Häder D-P (1996) NIZEMI-Experiments on the slow rotating centrifuge microscope during the IML-2 mission. J Biotechnol 47:223–224

Häder D-P (1997a) Gravitaxis in flagellates. Biol Bull 192:131–133

Häder D-P (1997b) Vertical migration and distribution of primary producers in aquatic ecosystems—the effects of enhanced solar UVB. Photochem Photobiol 65(2):263–264

Häder D-P (1999) Gravitaxis in unicellular microorganisms. Adv Space Res 24:843–850

Häder D-P (2000) Graviperzeption in Pflanzen und Mikroorganismen. In: Keller MH, Sahm PR (eds) Bilanzsymposium Forschung unter Weltraumbedingungen, 21–23 September 1998. Wissenschaftliche Projektführung, Norderney, pp 633–641

Häder D-P (2003) Wie unterscheiden Einzeller oben und unten—Beispiele für biologische Experimente im Weltraumlabor. In: Nordmeier V (ed) Didaktik der Physik-Beiträge der Frühjahrstagung der DPG-Augsburg 2003. Lehmanns Media, Berlin, pp 1–5

Häder D-P (2010) Rock 'n' Roll—Wie Mikroorganismen die Schwerkraft spüren. In: Spektrum der Wissenschaft Extra, Schwerelos Europa forscht im Weltall, pp 114–120

Häder D-P, Hemmersbach R (1997) Graviperception and graviorientation in flagellates. Planta 203:7–10

Häder D-P, Lebert M (1985) Real time computer-controlled tracking of motile microorganisms. Photochem Photobiol 42:509–514

Häder D-P, Lebert M (1998) Mechanism of gravitactic signal perception and signal transduction of *Euglena gracilis*. Microgravity News 11:14

Häder D-P, Lebert M (2000) Real-time tracking of microorganisms. In: Häder D-P (ed) Image Analysis:

Methods and Applications. CRC Press, Boca Raton, pp 393–422
Häder D-P, Lebert M (2001a) Einzeller als Modelle für das Verständnis der Wirkung der Gravitation auf biologische Systeme. In: Rahmann H, Hirsch KA (eds) Mensch–Leben–Schwerkraft–Kosmos. Verlag Günter Heimbach, Stuttgart, pp 150–161
Häder D-P, Lebert M (2001b) Graviperception and gravitaxis in algae. Adv Space Res 27:861–870
Häder D-P, Lebert M (2002) Graviorientation in flagellates. In: Proceedings 2nd China-Germany Workshop on Microgravity Sciences, 1–3 September 2002. National Microgravity Laboratory, Chinese Academy of Sciences, Dunhuang, China, pp 189–194
Häder D-P, Lebert M (2009) Photoorientation in photosynthetic flagellates. In: Jin T, Hereld D (eds) Methods in Molecular Biology, vol 571. Humana Press, New York, pp 51–65
Häder D-P, Liu SM (1990a) Effects of artificial and solar UV-B radiation on the gravitactic orientation of the dinoflagellate, *Peridinium gatunense*. FEMS Microbiol Ecol 73:331–338
Häder D-P, Liu SM (1990b) Motility and gravitactic orientation of the flagellate, *Euglena gracilis*, impaired by artificial and solar UV-B radiation. Curr Microbiol 21:161–168
Häder D-P, Vogel K (1960) Graviorientation in photosynthetic flagellates. In: Proceedings of the Fourth European Symposium on Life Science Research in Space (ESA SP-307), pp 521–526
Häder D-P, Vogel K (1991) Simultaneous tracking of flagellates in real time by image analysis. J Math Biol 30:63–72
Häder D-P, Liu SM, Häder M, Ullrich W (1990a) Photoorientation, motility and pigmentation in a freshwater *Peridinium* affected by ultraviolet radiation. Gen Physiol Biophys 9:361–371
Häder D-P, Vogel K, Schäfer J (1990b) Responses of the photosynthetic flagellate, *Euglena gracilis*, to microgravity. Appl Micrograv Techn 3:110–116
Häder D-P, Liu SM, Kreuzberg K (1991a) Orientation of the photosynthetic flagellate, *Peridinium gatunense*, in hypergravity. Curr Microbiol 22:165–172
Häder D-P, Reinecke E, Vogel K, Kreuzberg K (1991b) Responses of the photosynthetic flagellate, *Euglena gracilis*, to hypergravity. Eur Biophys J 20:101–107
Häder D-P, Rosum A, Schäfer J, Hemmersbach R (1995) Gravitaxis in the flagellate *Euglena gracilis* is controlled by an active gravireceptor. J Plant Physiol 146:474–480
Häder D-P, Rosum A, Schäfer J, Hemmersbach R (1996) Graviperception in the flagellate *Euglena gracilis* during a shuttle space flight. J Biotechnol 47:261–269
Häder D-P, Porst M, Tahedl H, Richter P, Lebert M (1997) Gravitactic orientation in the flagellate *Euglena gracilis*. Microgravity Sci Technol 10:53–57
Häder D-P, Lebert M, Richter P (1999) Gravitaxis and graviperception in flagellates and ciliates. In: Proceedings 14th ESA Symposium on European Rocket and Balloon Programmes and Related Research (ESA SP-437), Potsdam, Germany, pp 479–486
Häder D-P, Lebert M, Richter P, Ntefidou M (2003) Gravitaxis and graviperception in flagellates. Adv Space Res 31(10):2181–2186
Häder D-P, Hemmersbach R, Lebert M (2005a) Gravity and the Behavior of Unicellular Organisms. Cambridge University Press, Cambridge
Häder D-P, Richter P, Daiker V, Lebert M (2005b) Molecular transduction chain for graviorientation in flagellates. ELGRA News 24:74
Häder D-P, Richter P, Ntefidou M, Lebert M (2005c) Gravitational sensory transduction chain in flagellates. Adv Space Res 36:1182–1188
Häder D-P, Richter P, Lebert M (2006) Signal transduction in gravisensing of flagellates. Signal Transduct 6:422–431
Häder D-P, Richter P, Schuster M, Daiker V, Lebert M (2009) Molecular analysis of the graviperception signal transduction in the flagellate *Euglena gracilis*: involvement of a transient receptor potential-like channel and a calmodulin. Adv Space Res 43(8):1179–1184
Häder D-P, Faddoul J, Lebert M, Richter P, Schuster M, Richter R, Strauch SM, Daiker V, Sinha R, Sharma N (2010) Investigation of gravitaxis and phototaxis in *Euglena gracilis*. In: Sinha R, Sharma NK, Rai AK (eds) Advances in Life Sciences. IK International Publishing House, New Delhi, pp 117–131
Haugland RP (1997) Handbook of Fluorescent Probes and Research Chemicals. Molecular Probes, Eugene, Oregon
Haupt W (1962) Geotaxis. In: Ruhland W (ed) Handbuch der Pflanzenphysiologie, vol 17/2. Springer, Berlin, pp 390–395
Hemmersbach R, Braun M (2006) Gravity-sensing and gravity-related signaling pathways in unicellular model systems of protists and plants. Signal Transduct 6:432–442
Hemmersbach R, Donath R (1995) Gravitaxis of *Loxodes* and *Paramecium*. Eur J Protistol 31:433
Hemmersbach R, Häder D-P (1999) Graviresponses of certain ciliates and flagellates. FASEB J 13:S69–S75
Hemmersbach R, Voormanns R, Briegleb W, Rieder N, Häder D-P (1996) Influence of accelerations on the spatial orientation of *Loxodes* and *Paramecium*. J Biotechnol 47:271–278
Hemmersbach R, Voormanns R, Bromeis B, Schmidt N, Rabien H, Ivanova K (1998) Comparative studies of the graviresponses of *Paramecium* and *Loxodes*. Adv Space Res 21:1285–1289
Hemmersbach R, Volkmann D, Häder D-P (1999a) Graviorientation in protists and plants. J Plant Physiol 154:1–15
Hemmersbach R, Voormanns R, Häder D-P (1999b) Graviresponses in *Paramecium biaurelia* under different accelerations: studies on the ground and in space. J Exp Biol 390:2199–2205
Hemmersbach R, Anken RH, Lebert M (2011) Gravitational biology. In: Encyclopedia of Astrobiology. Springer, Berlin, pp 688–692
Hemmersbach R, Simon A, Waßer K, Hauslage J, Christianen PC, Albers PW, Lebert M, Richter P, Alt

W, Anken R (2014) Impact of a high magnetic field on the orientation of gravitactic unicellular organisms—a critical consideration about the application of magnetic fields to mimic functional weightlessness. Astrobiology 14(3):205–215

Hemmersbach-Krause R, Häder D-P (1990) Negative gravitaxis (geotaxis) of *Paramecium*—demonstrated by image analysis. Appl Micrograv Techn 4:221–223

Hemmersbach-Krause R, Häder D-P, Köhler M, Perdigao J, Briegleb W (1990) Cellular functions of *Paramecium* under different gravity conditions. In: Proceedings of the 4th European Symposium on Life Sciences Research in Space, ESA SP-307, Trieste, Italy, pp 285–290

Hemmersbach-Krause R, Briegleb W, Häder D-P (1991a) Dependence of gravitaxis in *Paramecium* on oxygen. Eur J Protistol 27:278–282

Hemmersbach-Krause R, Briegleb W, Häder D-P, Plattner H (1991b) Gravity effects on *Paramecium* cells: an analysis of a possible sensory function of trichocysts and of simulated weightlessness of trichocyst exocytosis. Eur J Protistol 27:85–92

Hemmersbach-Krause R, Briegleb W, Häder D-P (1992) Swimming behavior of *Paramecium*—first results with the low-speed centrifuge microscope (NIZEMI). Adv Space Res 12:113–116

Hemmersbach-Krause R, Briegleb W, Vogel K, Häder D-P (1993) Swimming velocity of *Paramecium* under the conditions of weightlessness. Acta Protozool 32:229–236

Hemmersbach-Krause R, Briegleb W, Häder D-P, Vogel K, Klein S, Mulisch M (1994) Protozoa as model systems for the study of cellular responses to altered gravity conditions. Adv Space Res 14:49–60

Hensel W, Sievers A (1981) Induction of gravity-dependent plasmatic responses in root statocytes by short time contact between amyloplasts and the distal endoplasmic reticulum complex. Planta 153:303–307

Herranz R, Anken R, Boonstra J, Braun M, Christianen PC, de Geest M, Hauslage J, Hilbig R, Hill RJ, Lebert M (2013) Ground-based facilities for simulation of microgravity: organism-specific recommendations for their use, and recommended terminology. Astrobiology 13(1):1–17

Hill NA, Häder D-P (1997) A biased random walk for the trajectories of swimming micro-organisms. J Theor Biol 186:503–526

Hock B, Häder D-P (2006) Graviresponses in fungi and slime molds. Signal Transduct 6:443–448

Hopkins JT (1965) Some light-induced changes in behaviour and cytology of an estuarine mud-flat diatom. In: Bainbridge R (ed) Light as an Ecological Factor. Blackwell Scientific Publishing, Oxford, pp 335–358

Hou G, Kramer VL, Wang YS, Chen R, Perbal G, Gilroy S, Blancaflor EB (2004) The promotion of gravitropism in *Arabidopsis* roots upon actin disruption is coupled with the extended alkalinization of the columella cytoplasm and a persistent lateral auxin gradient. Plant J 39(1):113–125

Hu C, Wang S, Guo L, Xie P (2014) Effects of the proximal factors on the diel vertical migration of zooplankton in a plateau meso-eutrophic Lake Erhai, China. J Limnol 73(2):375–386

Iseki M, Matsunaga S, Murakami A, Ohno K, Shiga K, Yoshida C, Sugai M, Takahashi T, Hori T, Watanabe M (2002) A blue-light-activated adenylyl cyclase mediates photoavoidance in *Euglena gracilis*. Nature 415:1047–1051

Jarman AP, Groves AK (2013) The role of Atonal transcription factors in the development of mechanosensitive cells. Semin Cell Dev Biol 24(5):438–447

Jennings HS (1906) Behavior of the Lower Organisms. Columbia University Press, New York

Joop O, Kreuzberg K, Treichel R (1989) The slow-rotating centrifuge microscope (NIZEMI). ASGSB Bull 3:55

Josef K, Saranak J, Foster KW (2005) Ciliary behavior of a negatively phototactic *Chlamydomonas reinhardtii*. Cell Motil Cytoskeleton 61:97–111

Kamphuis A (1999) Digitale Pfadanalyse am Beispiel der Schwerkraftausrichtung von *Euglena gracilis* in Flachküvetten (in German). Dissertation, Rheinische-Friedrich-Wilhelms-Universität Bonn

Karnkowska-Ishikawa A, Milanowski R, Triemer RE, Zakryś B (2012) Taxonomic revisions of morphologically similar species from two euglenoid genera: *Euglena* (*E. granulata* and e. velata) and *Euglenaria* (*Eu. anabaena*, *Eu. caudata*, and *Eu. clavata*). J Phycol 48(3):729–739

Kelly MO, Leopold AC (1992) Springback and diagravitropism in merit corn roots. Plant Physiol 99: 632–634

Kessler JO (2007) The dynamics of unicellular swimming organisms. Gravitat Space Res 4(2)

Kessler JO, Hill NA (1997) Complementarity of physics, biology and geometry in the dynamics of swimming micro-organisms. In: Flyvbjerg H, Hertz J, Jensen MH, Mouritsen OG, Sneppen K (eds) Physics of Biological Systems, vol 480. Springer, Berlin, pp 325–340

Kessler JO, Hill NA, Häder D-P (1992) Orientation of swimming flagellates by simultaneously acting external factors. J Phycol 28:816–822

Kianianmomeni A, Hallmann A (2014) Algal photoreceptors: in vivo functions and potential applications. Planta 239(1):1–26

Kiss J (2014) Plant biology in reduced gravity on the moon and Mars. Plant Biol 16(s1):12–17

Kiyota M, Numayama N, Goto K (2006) Circadian rhythms of the *L*-ascorbic acid level in *Euglena* and spinach. J Photochem Photobiol B 84(3):197–203

Köhler O (1921) Über die Geotaxis von *Paramecium*. Verhandl Dtsche Zool Ges 26:69–71

Krause M (1999) Elektrophysiologie, Mechanosensitivität und Schwerkraftbeantwortung von *Bursaria truncatella*. Diploma thesis, Fakultät für Biologie der Ruhr-Universität Bochum

Krause M, Bräucker R, Hemmersbach R (2006) Graviresponses of *Paramecium biaurelia* during parabolic flights. Protoplasma 229(2):109–116

Krause M, Bräucker R, Hemmersbach R (2010) Gravikinesis in *Stylonychia mytilus* is based on membrane potential changes. J Exp Biol 213(1):161–171

Kühnel-Kratz C, Häder D-P (1993) Real time three-dimensional tracking of ciliates. J Photochem Photobiol B Biol 19:193–200

Kuznicki L (1968) Behavior of *Paramecium* in gravity fields. I. Sinking of immobilized specimens. Acta Protozool 6:109–117

Lebert M, Häder D-P (1996) How *Euglena* tells up from down. Nature 379:590

Lebert M, Häder D-P (1999a) Image analysis: a versatile tool for numerous applications. GIT Imag Microsc 1:5–6

Lebert M, Häder D-P (1999b) Negative gravitactic behavior of *Euglena gracilis* can not be described by the mechanism of buoyancy-oriented upward swimming. Adv Space Res 24:851–860

Lebert M, Richter P, Porst M, Häder D-P (1996) Mechanism of gravitaxis in the flagellate *Euglena gracilis*. In: Proceedings of the 12th C.E.B.A.S.Workshops. Annual Issue 1996, Ruhr-University of Bochum, Bochum, Germany, pp 225–234

Lebert M, Richter P, Häder D-P (1997) Signal perception and transduction of gravitaxis in the flagellate *Euglena gracilis*. J Plant Physiol 150:685–690

Lebert M, Porst M, Häder D-P (1999a) Circadian rhythm of gravitaxis in *Euglena gracilis*. J Plant Physiol 155:344–349

Lebert M, Porst M, Richter P, Häder D-P (1999b) Physical characterization of gravitaxis in *Euglena gracilis*. J Plant Physiol 155:338–343

Löfke C (2011) Einfluss von Gibberellin auf den Gravitropismus der Wurzel durch Regulation der PIN-Stabilität. Dissertation, Georg-August Universität, Göttingen

Lohmann KJ, Lohmann CMF, Ehrhart LM, Bagley DA, Swing T (2004) Geomagnetic map used in sea-turtle navigation. These migratory animals have their own equivalent of a global positioning system. Nature 428(6986):909–910

Machemer H, Bräucker R (1992) Gravireception and graviresponses in ciliates. Acta Protozool 31:185–214

Machemer H, Machemer-Röhnisch S (1996) Is gravikinesis in *Paramecium* affected by swimming velocity? Eur J Protistol 32:90–93

Machemer H, Machemer-Röhnisch S, Bräucker R, Takahashi K (1991) Gravikinesis in *Paramecium*: theory and isolation of a physiological response to the natural gravity vector. J Comp Physiol A 168:1–12

Machemer H, Nagel U, Bräucker R (1997) Assessment of *g*-dependent cellular gravitaxis: determination of cell orientation from locomotion track. J Theor Biol 185:201–211

Machemer-Röhnisch S, Bräucker R, Machemer H (1998) Graviresponses of gliding and swimming *Loxodes* using step transition to weightlessness. J Eukaryot Microbiol 45:411–418

Machemer-Röhnisch S, Nagel U, Machemer H (1999) A gravity-induced regulation of swimming speed in *Euglena gracilis*. J Comp Physiol A 185:517–527

Manieri P, Brinckmann E, Brillouet C (1996) The BIORACK facility and its performance during the IML-2 Spacelab mission. J Biotechnol 47:71–82

Maree AFM, Panfilov AV, Hogeweg P (1999) Migration and thermotaxis of *Dictyostelium discoideum* slugs, a model study. J Theor Biol 199:297–309

Massart J (1891) Recherches sur les organismes inférieurs (1). Academie Royale des Sciences, des Lettres et des Beaux-Arts de Belgique 22:148–167

McLachlan DH, Underwood GJ, Taylor AR, Brownlee C (2012) Calcium release from intracellular stores is necessary for the photophobic response in the benthic diatom *Navicula perminuta* (Bacillariophyceae). J Phycol 48(3):675–681

Means AR (2013) Molecular mechanisms of action of calmodulin. In: Proceedings of the 1987 Laurentian Hormone Conference. Recent Progress in Hormone Research. Academic Press, p 223

Miller MS, Keller TS (2006) *Drosophila melanogaster* (fruit fly) locomotion during the microgravity and hypergravity portions of parabolic flight. J Gravit Physiol 13:35–48

Mittag M (2001) Circadian rhythms in microalgae. Int Rev Cytol 206:213–247

Moore A (1903) Some facts concerning geotropic gatherings of paramecia. Am J Phys 9:238–244

Naccache PH (1985) Neutrophil activation and calmodulin antagonists. In: Hidaka H, Hartshorne DJ (eds) Calmodulin Antagonists and Cellular Physiology. Academic Press, Orlando, pp 149–160

Nagel U (1993) Elektrische Eigenschaften und elektromotorische Kopplung im Verhalten von *Loxodes striatus*. Diploma thesis, Faculty of Biology, Ruhr-University Bochum

Nasir A, Strauch S, Becker I, Sperling A, Schuster M, Richter P, Weißkopf M, Ntefidou M, Daiker V, An Y (2014) The influence of microgravity on *Euglena gracilis* as studied on Shenzhou 8. Plant Biol (Stuttg) 16(s1):113–119

Neugebauer DC, Machemer-Röhnisch S, Nagel U, Bräucker R, Machemer H (1998) Evidence of central and peripheral gravireception in the ciliate *Loxodes striatus*. J Comp Physiol A 183:303–311

Nilius B, Owsianik G (2011) The transient receptor potential family of ion channels. Genome Biol 12(3):218

Nilius B, Appendino G, Owsianik G (2012) The transient receptor potential channel TRPA1: from gene to pathophysiology. Pflügers Arch—Eur J Physiol 464(5):425–458

Ntefidou M, Richter P, Streb C, Lebert M, Häder D-P (2002a) High light exposure leads to a sign change in gravitaxis of the flagellate *Euglena gracilis*. J Gravit Physiol 9(1):277–278

Ntefidou M, Richter P, Streb C, Lebert M, Häder D-P (2002b) High light exposure leads to a sign change in gravitaxis of the flagellate *Euglena gracilis*. In: ESA SP-501: 8th European Symposium on Life Sciences Research in Space: Life in Space for Life on Earth. 23rd Annual International Gravitational Physiology Meeting. Karolinska Institutet, Stockholm, Sweden, pp 301–302

Ohata K, Murakami T, Miwa I (1997) Circadian rhythmicity of negative gravitaxis in *Paramecium bursaria*. Zool Sci 14(Suppl):58

Panina S, Stephan A, la Cour JM, Jacobsen K, Kallerup LK, Bumbuleviciute R, Knudsen KV, Sánchez-González P, Villalobo A, Olesen UH (2012) Significance of calcium binding, tyrosine phosphorylation, and lysine trimethylation for the essential function of calmodulin in vertebrate cells analyzed in a novel gene replacement system. J Biol Chem 287(22): 18173–18181

Peacock MB, Kudela RM (2014) Evidence for active vertical migration by two dinoflagellates experiencing iron, nitrogen, and phosphorus limitation. Limnol Oceanogr 59(3):660–673

Penard E (1917) Le genre *Loxodes*. Rev Suisse Zool 25:453–489

Pettersson M, Ekelund NGA (2006) Effects of the herbicides roundup and Avans on *Euglena gracilis*. Arch Environ Contam Toxicol 50:175–181

Pfeffer W (1904) Pflanzenphysiologie Bd. 2. In: Ein Handbuch der Lehre vom Stoffwechsel und Kraftwechsel in der Pflanze. Leipzig

Piazena H, Häder D-P (1995) Vertical distribution of phytoplankton in coastal waters and its detection by backscattering measurements. Photochem Photobiol 62:1027–1034

Platt JB (1899) On the specific gravity of *Spirostomum, Paramecium* and the tadpole in relation to the problem of geotaxis. Am Nat 33:31

Porst M (1998) *Euglena gracilis*: Langzeitversuche in artifiziellen Ökosystemen und Untersuchungen zur Gravitaxis. Dissertation, Friedrich-Alexander-University, Erlangen-Nürnberg

Rahmann H, Hilbig R, Flemming J, Slenzka K (1996) Influence of long-term altered gravity on the swimming performance of developing cichlid fish: including results from the 2nd German spacelab mission D-2. Adv Space Res 17:121–124

Raymont JE (2014) Plankton & Productivity in the Oceans, vol 1. Phytoplankton, Elsevier

Renart MF, Sebastian J, Mato JM (1981) Adenylate cyclase activity in permeabilized cells from *Dictyostelium discoideum*. Cell Biol Int Rep 5:1045–1054

Rhiel E, Häder D-P, Wehrmeyer W (1988) Diaphototaxis and gravitaxis in a freshwater *Cryptomonas*. Plant Cell Physiol 29:755–760

Richter P, Lebert M, Korn R, Häder D-P (2001a) Possible involvement of the membrane potential in the gravitactic orientation of *Euglena gracilis*. J Plant Physiol 158:35–39

Richter P, Lebert M, Tahedl H, Häder D-P (2001b) Calcium is involved in the gravitactic orientation in colorless flagellates. J Plant Physiol 158:689–697

Richter P, Ntefidou M, Streb C, Lebert M, Häder D-P (2002a) Cellular perception and transduction mechanisms of gravity in unicellular organisms. Curr Topics Plant Biol 3:143–154

Richter P, Ntefidou M, Streb C, Lebert M, Häder D-P (2002b) Physiological characterization of gravitaxis in *Euglena gracilis*. J Gravit Physiol 9:279–280

Richter PR, Ntefidou M, Streb C, Faddoul J, Lebert M, Häder D-P (2002c) High light exposure leads to a sign change of gravitaxis in the flagellate *Euglena gracilis*. Acta Protozool 41:343–351

Richter PR, Schuster M, Wagner H, Lebert M, Häder D-P (2002d) Physiological parameters of gravitaxis in the flagellate *Euglena gracilis* obtained during a parabolic flight campaign. J Plant Physiol 159:181–190

Richter P, Börnig A, Streb C, Ntefidou M, Lebert M, Häder D-P (2003a) Effects of increased salinity on gravitaxis in *Euglena gracilis*. J Plant Physiol 160:651–656

Richter P, Ntefidou M, Streb C, Lebert M, Häder D-P (2003b) The role of reactive oxygen species (ROS) in signaling of light stress. Recent Res Develop Biochem 4:957–970

Richter PR, Schuster M, Lebert M, Häder D-P (2003c) Gravitactic signal transduction elements in *Astasia longa* investigated during parabolic flights. Microgravity Sci Technol 14(3):17–24

Richter PR, Streb C, Ntefidou M, Lebert M, Häder D-P (2003d) High light-induced sign change of gravitaxis in the flagellate *Euglena gracilis* is mediated by reactive oxygen species. Acta Protozool 42:197–204

Richter PR, Schuster M, Meyer I, Lebert M, Häder D-P (2006) Indications for acceleration-dependent changes of membrane potential in the flagellate *Euglena gracilis*. Protoplasma 229:101–108

Richter PR, Häder D-P, Gonçalves RJ, Marcoval MA, Villafañe VE, Helbling EW (2007) Vertical migration and motility responses in three marine phytoplankton species exposed to solar radiation. Photochem Photobiol 83(4):810–817

Richter PR, Strauch SM, Ntefidou M, Schuster M, Daiker V, Nasir A, Haag FWM, Lebert M (2014) Influence of different light-dark cycles on motility and photosynthesis of *Euglena gracilis* in closed bioreactors. Astrobiology 14(10):848–858

Roberts AM (1970) Geotaxis in motile micro-organisms. J Exp Biol 53:687–699

Russo E, Salzano M, De Falco V, Mian C, Barollo S, Secondo A, Bifulco M, Vitale M (2014) Calcium/calmodulin-dependent protein kinase II and its endogenous inhibitor α in medullary thyroid cancer. Clin Cancer Res 20(6):1513–1520

Sachs F, Morris CE (1998) Mechanosensitive ion channels in nonspecialized cells. In: Blaustein MP, Greger R, Grunicke H, Jahn R, Mendell LM, Miyajima A, Pette D, Schultz G, Schweiger M (eds) Reviews of Physiology and Biochemistry and Pharmacology, vol 132. Springer, Berlin, pp 1–78

Sachs J (1882) Über Ausschließung der geotropischen und heliotropischen Krümmungen während des Wachsens. Arbeiten des Botanischen Instituts Würzburg Bd. 2:209–225

Sack FD (1997) Plastids and gravitropic sensing. Planta 203:63–68

Sakashita T, Doi M, Yasuda H, Fuma S, Häder D-P (2002a) Protection of negative gravitaxis in *Euglena gracilis* Z against gamma-ray irradiation by Trolox C. J Radiat Res 43(Suppl):S257–S259

Sakashita T, Doi M, Yasuda H, Takeda H, Fuma S, Nakamura Y, Häder D-P (2002b) Comparative study

of gamma-ray and high-energy carbon ion irradiation on negative gravitaxis in *Euglena gracilis* Z. J Plant Physiol 159:1355–1360

Sakashita T, Doi M, Yasuda H, Takeda H, Fuma S, Nakamura Y, Häder D-P (2002c) High-energy carbon ion irradiation and the inhibition of negative gravitaxis in *Euglena gracilis* Z. Int J Radiat Biol 78:1055–1060

Salmi ML, Bushart TJ, Roux SJ (2011) Autonomous gravity perception and responses of single plant cells. Gravitat Space Res 25(1):6–13

Sarafis V (2013) 31. X-ray microscopy as a possible tool for the investigation. In: X-ray microscopy: Proceedings of the International Symposium, 14–16 September 1983, Göttingen, Federal Republic of Germany. Springer, p 294

Schmidt W (2004) Quickly changing acceleration forces (QCAFs) vibration analysis on the A300 ZERO-G. Microgravity Sci Technol 15(1):42–48

Schnabl H (2002) Gravistimulated effects in plants. Springer, Berlin

Schwarz F (1884) Der Einfluß der Schwerkraft auf die Bewegungsrichtung von *Chlamydomonas* und *Euglena*. Ber Dtsch Bot Ges 2:51–72

Schwer CI, Lehane C, Guelzow T, Zenker S, Strosing KM, Spassov S, Erxleben A, Heimrich B, Buerkle H, Humar M (2013) Thiopental inhibits global protein synthesis by repression of eukaryotic elongation factor 2 and protects from hypoxic neuronal cell death. PLoS One 8(10):e77258

Sebastian C, Scheuerlein R, Häder D-P (1994) Graviperception and motility of three *Prorocentrum* strains impaired by solar and artificial ultraviolet radiation. Mar Biol 120:1–7

Simmons SL, Sievert SM, Frankel RB, Bazylinski DA, Edwards KJ (2004) Spatiotemporal distribution of marine magnetotactic bacteria in a seasonally stratified coastal salt pond. Appl Environ Microbiol 70(10):6230–6239

Sineshchekov O, Lebert M, Häder D-P (2000) Effects of light on gravitaxis and velocity in *Chlamydomonas reinhardtii*. J Plant Physiol 157:247–254

Sinha RP, Ambasht NK, Sinha JP, Klisch M, Häder D-P (2003) UV-B-induced synthesis of mycosporine-like amino acids in three strains of *Nodularia* (cyanobacteria). J Photochem Photobiol B Biol 71:51–58

Sivonen K, Kononen K, Carmichael W, Dahlem A, Rinehart K, Kiviranta J, Niemela S (1989) Occurrence of the hepatotoxic cyanobacterium *Nodularia spumigena* in the Baltic Sea and structure of the toxin. Appl Environ Microbiol 55(8):1990–1995

Son YK, Li H, Jung ID, Park Y-M, Jung W-K, Kim HS, Choi I-W, Park WS (2014) The calmodulin inhibitor and antipsychotic drug trifluoperazine inhibits voltage-dependent K^+ channels in rabbit coronary arterial smooth muscle cells. Biochem Biophys Res Commun 443(1):321–325

Sourjik V, Wingreen NS (2012) Responding to chemical gradients: bacterial chemotaxis. Curr Opin Cell Biol 24(2):262–268

Spoto G, Papponetti M, Barbacane RC, Repola D, Beradi S (1997) Caffein, theophilline, and bamifylline are similar as competive inhibitors of 3',5'-cyclic AMP phosphodiesterase in vitro. Int J Immunopathol Pharmacol 10:153

Stahl E (1880) Über den Einfluß von Richtung und Stärke der Beleuchtung auf einige Bewegungserscheinungen im Pflanzenreich. Bot Zeitung 38:297–413

Stallwitz E, Häder D-P (1994) Effects of heavy metals on motility and gravitactic orientation of the flagellate, *Euglena gracilis*. Eur J Protistol 30:18–24

Steck R, Hill S, Robison RA, O'Neill KL (2014) Pharmacological reversal of caffeine-mediated phagocytic suppression. Cancer Res 74(19 Supplement):4861

Steidinger KA, Tangen K (1996) Dinoflagellates. In: Tomas CR, Hasle GR, Syvertsen EE (eds) Identifying Marine Diatoms and Dinoflagellates. Academic Press, London, pp 387–585

Strauch S, Richter P, Schuster M, Häder D-P (2010) The beating pattern of the flagellum of *Euglena gracilis* under altered gravity during parabolic flights. J Plant Physiol 167(1):41–46

Streb C, Richter P, Lebert M, Häder D-P (2001) Gravisensing microorganisms as model systems for gravity sensing in eukaryotes. In: Proceeding of the First European Workshop on Exo−/Astro-biology, Frascati, pp 251–254

Streb C, Richter P, Ntefidou M, Lebert M, Häder D-P (2002) Sensory transduction of gravitaxis in *Euglena gracilis*. J Plant Physiol 159:855–862

Streb C, Richter P, Häder D-P (2006) ECOTOX—a biomonitoring system for UV-effects and toxic substances. In: Ghetti F, Checcucci G, Bornman JF (eds) Environmental UV Radiation: Impact on Ecosystems and Human Health and Predictive Models. Springer, The Netherlands, p 288

Studer M, Bradacs G, Hilliger A, Hürlimann E, Engeli S, Thiel CS, Zeitner P, Denier B, Binggeli M, Syburra T (2011) Parabolic maneuvers of the Swiss Air Force fighter jet F-5E as a research platform for cell culture experiments in microgravity. Acta Astronaut 68(11):1729–1741

Sultana H, Neelakanta G, Rivero F, Blau-Wasser R, Schleicher M, Noegel AA (2012) Ectopic expression of cyclase associated protein CAP restores the streaming and aggregation defects of adenylyl cyclase a deficient *Dictyostelium discoideum* cells. BMC Dev Biol 12(1):3

Švegždienė D, Koryznienė D, Raklevičienė D (2011) Comparison study of gravity-dependent displacement of amyloplasts in statocytes of cress roots and hypocotyls. Microgravity Sci Technol 23(2):235–241

Tahedl H, Richter P, Lebert M, Häder D-P (1997) cAMP is involved in gravitxis signal transduction of *Euglena gracilis*. Microgravity Sci Technol 10:53–57

Tahedl H, Richter P, Lebert M, Häder D-P (1998) cAMP is involved in gravitaxis signal transduction of *Euglena gracilis*. Microgravity Sci Technol 11:173–178

Talbot M, Bate G (1987) Rip current charactersitics and their role in the exchange of water and surf diatoms

between the surf zone and nearshore. Estuar Coast Shelf Sci 25(6):707–720

Taneda K, Miyata S (1995) Analysis of motile tracks of *Paramecium* under gravity field. Comp Biochem Physiol 111A:673–680

Taylor F (1967) The occurrence of *Euglena deses* on the sands of the Sierra Leone peninsula. J Ecol 55:345–359

Taylor WR, Seliger HH, Fastie WG, McElroy WD (1966) Biological and physical observations on a phosphorescent bay in Falmouth Harbor, Jamaica, W.I. J Mar Res 24:28–43

Toda H, Yazawa M, Yagi K (1992) Amino acid sequence of calmodulin from *Euglena gracilis*. Eur J Biochem 205:653–660

Tuschl T, Elbashir SM, Lendeckel W (2014) RNA interference mediating small RNA molecules: Google Patents

Ullrich O, Häder D-P (2006) Editorial. Signal transduction in gravity perception: from microorganisms to mammals. Signal Transduct 6:377–379

Ullrich O, Thiel CS (2012) Gravitational Force: triggered stress in cells of the immune system. In: Stress Challenges and Immunity in Space. Springer, Berlin, pp 187–202

Vogel K, Häder D-P (1990) Simultaneuos tracking of flagellates in real time by image analysis. In: Proceedings of the Fourth European Symposium on Life Science Research in Space (ESA SP-307). pp 541–545

Vogel K, Hemmersbach-Krause R, Kühnel C, Häder D-P (1993) Swimming behavior of the unicellular flagellate, *Euglena gracilis*, in simulated and real microgravity. Microgravity Sci Technol 4:232–237

Volkmann D, Bucher B, Hejnowicz Z, Tewinkel M, Sievers A (1991) Oriented movement of statoliths studied in a reduced gravitational field during parabolic flights of rockets. Planta 185:153–161

Votta JJ, Jahn TL (1972) Galvanotaxis of *Chilomonas paramecium* and *Trachelomonas volvocina*. J Protozool 19(Suppl):43

Wadhams GH, Armitage JP (2004) Making sense of it all: bacterial chemotaxis. Nat Rev Mol Cell Biol 5(12):1024–1037

Wager H (1911) On the effect of gravity upon the movements and aggregation of *Euglena viridis*, Ehrb., and other micro-organisms. Philosoph Trans Roy Soc London B 201:333–390

Walsby AE (1987) Mechanisms of buoyancy regulation by planktonic cyanobacteria with gas vesicles. In: Fay P, Van Baalen C (eds) The Cyanobacteria. Elsevier Science, Amsterdam, The Netherlands, pp 385–392

Wang J, Sun Y, Tomura H, Okajima F (2012) Ovarian cancer G-protein-coupled receptor 1 induces the expression of the pain mediator prostaglandin E2 in response to an acidic extracellular environment in human osteoblast-like cells. Int J Biochem Cell Biol 44(11): 1937–1941

Weisenseel M, Meyer AJ (1997) Bioelectricity, gravity and plants. Planta 203:98–106

Willemoes JG, Beltrano J, Montaldi ER (1987) Diagravitropism in bermudagrass (*Cynodon dactylon* (L.) Pers.) as determined by a gravitropic and a geoepinastic phenomenon. Plant Sci 51:187–191

Winet H, Jahn TL (1974) Geotaxis in protozoa: I. A propulsion-gravity model for *Tetrahymena* (Ciliata). J Theor Biol 46:449–465

Wolff D, Künne A (2000) Light-regulated, circadian respiration activity of *Euglena gracilis* mutants that lack chloroplasts. J Plant Physiol 156:52–59

Yang XC, Sachs F (1989) Block of stretch-activated ion channels in *Xenopus* oocytes by gadolinium and calcium ions. Science 243:1068–1071

Yentsch CS, Backus RH, Wing A (1964) Factors affecting the vertical distribution of bioluminescence in the euphotic zone. Limnol Oceanogr 9:519–524

Yoshimura K (2011) Stimulus perception and membrane excitation in unicellular alga *Chlamydomonas*. In: Coding and Decoding of Calcium Signals in Plants. Springer, pp 79–91

Part III

Biotechnology

Wax Ester Fermentation and Its Application for Biofuel Production

13

Hiroshi Inui, Takahiro Ishikawa, and Masahiro Tamoi

Abstract

In *Euglena* cells under anaerobic conditions, paramylon, the storage polysaccharide, is promptly degraded and converted to wax esters. The wax esters synthesized are composed of saturated fatty acids and alcohols with chain lengths of 10–18, and the major constituents are myristic acid and myristyl alcohol. Since the anaerobic cells gain ATP through the conversion of paramylon to wax esters, the phenomenon is named "wax ester fermentation". The wax ester fermentation is quite unique in that the end products, i.e. wax esters, have relatively high molecular weights, are insoluble in water, and accumulate in the cells, in contrast to the common fermentation end products such as lactic acid and ethanol.

A unique metabolic pathway involved in the wax ester fermentation is the mitochondrial fatty acid synthetic system. In this system, fatty acid are synthesized by the reversal of β-oxidation with an exception that *trans*-2-enoyl-CoA reductase functions instead of acyl-CoA dehydrogenase. Therefore, acetyl-CoA is directly used as a C_2 donor in this fatty acid synthesis, and the conversion of acetyl-CoA to malonyl-CoA, which requires

H. Inui, Ph.D. (✉)
Department of Nutrition, Osaka Prefecture University,
30-7-3 Habikino, Habikino, Osaka 583-8555, Japan
e-mail: inui@biochem.osakafu-u.ac.jp

T. Ishikawa
Faculty of Life and Environmental Science,
Department of Life Science and Biotechnology,
Shimane University,
1060 Nishikawatsu, Matsue, Shimane 690-8504, Japan
e-mail: ishikawa@life.shimane-u.ac.jp

M. Tamoi
Faculty of Agriculture, Kindai University,
3327-204 Nakamachi, Nara 631-8505, Japan
e-mail: tamoi@nara.kindai.ac.jp

S.D. Schwartzbach, S. Shigeoka (eds.), *Euglena: Biochemistry, Cell and Molecular Biology*,
Advances in Experimental Medicine and Biology 979, DOI 10.1007/978-3-319-54910-1_13

ATP, is not necessary. Consequently, the mitochondrial fatty acid synthetic system makes possible the net gain of ATP through the synthesis of wax esters from paramylon. In addition, acetyl-CoA is provided in the anaerobic cells from pyruvate by the action of a unique enzyme, oxygen sensitive pyruvate:$NADP^+$ oxidoreductase, instead of the common pyruvate dehydrogenase multienzyme complex.

Wax esters produced by anaerobic *Euglena* are promising biofuels because myristic acid ($C_{14:0}$) in contrast to other algal produced fatty acids, such as palmitic acid ($C_{16:0}$) and stearic acid ($C_{18:0}$), has a low freezing point making it suitable as a drop-in jet fuel. To improve wax ester production, the molecular mechanisms by which wax ester fermentation is regulated in response to aerobic and anaerobic conditions have been gradually elucidated by identifying individual genes related to the wax ester fermentation metabolic pathway and by comprehensive gene/protein expression analysis. In addition, expression of the cyanobacterial Calvin cycle fructose-1,6-bisphosphatase/sedohepturose-1,7-bisphosphatase, in *Euglena* provided photosynthesis resulting in increased paramylon accumulation enhancing wax ester production. This chapter will discuss the biochemistry of the wax ester fermentation, recent advances in our understanding of the regulation of the wax ester fermentation and genetic engineering approaches to increase production of wax esters for biofuels.

Keywords

Wax esters • Fermentation • Anaerobic energy metabolism • Mitochondrial fatty acid synthetic system • Pyruvate:$NADP^+$ oxidoreductase • Biofuel production • Genetic engineering

Abbreviations

ATP-PFK	ATP-dependent phosphofructokinase
F26BP	Fructose 2,6-bisphosphate
FBPase	Fructose-1,6-bisphosphatase
PEP	Phosphoenolpyruvate
PEPCK	Phosphoenolpyruvate carboxykinase
Pi	Orthophsphate
PNO	Pyruvate:$NADP^+$ oxidoreductase
PPi	Pyrophosphate
PPi-PFK	Pyrophosphate-dependent phosphofructokinase
SBPase	Sedoheptulose-1,7-bisphosphatase
TER	*trans*-2-enoyl-CoA reductase
TPP	Thiamine pyrophosphate
WSD	Wax ester synthase/acyl-CoA:diacylglycerol acyltransferase

13.1 Introduction

13.1.1 Anaerobic Energy Generating System in Eukaryotes

Life in low O_2 environments (hypoxia), or in environments totally devoid of O_2 (anoxia) are not uncommon on our planet. To sustain viability in either aerobic or anaerobic conditions, cells must produce energy (mostly ATP) and maintain the redox balance. Under aerobic conditions, most eukaryotes synthesize ATP effectively through oxidative phosphorylation in mitochondria with O_2 serving as the terminal electron acceptor of the respiratory electron transport chain. In contrast, when eukaryotes experience anoxic conditions, there are two processes for maintaining redox balance and conserving

energy: (1) fermentation, which usually entails substrate-level phosphorylation, and (2) anaerobic respiration, which involves a terminal electron acceptor other than O_2 (such as NO_3^- and fumarate (Atteia et al. 2013; Catalanotti et al. 2013; Tielens et al. 2002).

The cytosolic glycolytic pathway is the backbone of carbon and energy metabolism in eukaryotes. In the glycolytic pathway, glucose is catabolized to pyruvate, yielding a net gain of 2 ATP from substrate-level phosphorylation and 2 NADH per molecule of metabolized glucose. In order to regenerate NAD^+ necessary to sustain the metabolic flux through glycolysis, cytosolic NADH can be oxidized to regenerate NAD^+ through a variety of routes involving either cytosolic fermentation or the shuttling of NADH into the electron transport chain in mitochondria. The most common cytosolic fermentation processes to regenerate NAD^+ from pyruvate, are the ethanol fermentation *via* pyruvate decarboxylase and alcohol dehydrogenase (typical of yeasts, plants, certain animals and fungi) or lactic acid fermentation *via* lactate dehydrogenase (typical of many eukaryotic cells involving mammalian muscle) (Atteia et al. 2013). Anaerobic fermentation provides cells with energy, generating ~2–3 molecules of ATP per glucose metabolized compared to the over 30 molecules of ATP generated by oxidative metabolism of glucose.

Among eukaryotes, anaerobic pyruvate metabolism is typically more diversified than aerobic pyruvate metabolism including multiple anaerobic pathways and enzymes, which often localize to mitochondria or hydrogenosomes, anaerobic mitochondria that lack cytochromes and produce ATP fermentatively (Müller et al. 2012). In the case of green algae such as *Chlamydomonas* and *Chlorella*, starch is fermented to a variety of end products such as acetate, formate, H_2 and CO_2 (Atteia et al. 2013; Catalanotti et al. 2013; Müller et al. 2012). Chloroplasts, in addition to mitochondria, play a pivotal role in the fermentation metabolism. In these organisms, pyruvate is converted to acetyl-CoA by the action of pyruvate-formate lyase or pyruvate:ferredoxin oxidoreductase (Ginger et al. 2010). Pyruvate-formate lyase produces formate in addition to acetyl-CoA. CO_2 and reduced ferredoxin are formed in addition to acetyl-CoA by pyruvate:ferredoxin oxidoreductase. The reduced ferredoxin then serves as the electron donor for H_2 production catalyzed by hydrogenase. The acetyl-CoA formed by either enzyme is then converted to acetate by the sequential reactions of phosphoacetyltransferase and acetate kinase. The phosphoacetyltransferase-acetate kinase pathway generates one ATP per molecule of pyruvate, but does not convert NADH to NAD^+. To regenerate NAD^+, acetyl-CoA is metabolized to ethanol with the oxidation of 2 molecules of NADH to NAD^+ by the action of the bifunctional acetaldehyde/alcohol dehydrogenase.

As an alternative to fermentation, ATP can be also produced by anaerobic respiration in mitochondria, in which NADH is oxidized by transferring electrons to the mitochondrial electron transport chain developing a proton gradient for ATP synthesis and using a terminal electron acceptor other than O_2 (Ginger et al. 2010). In some marine invertebrates and helminthes, fumarate is used as the terminal electron acceptor for anaerobic respiration. Since fumarate provides an electron sink of endogenous origin, the production of succinate by the reduction of fumarate could be viewed as a type of fermentation, but the fumarate reductase reaction is coupled to proton-pumping across the inner-mitochondrial membrane and ATP synthesis (Tielens et al. 2002).

13.1.2 Biofuel Production by Algae

The world is faced with an energy crisis due to the depletion of fossil fuels caused by growth of the global economy and population. The current human societies are highly dependent on fossil fuels for energy. Furthermore, the use of fossil fuels increases CO_2 levels in the atmosphere. There is a great need for renewable energy supplies that do not cause significant environmental harm and do not compete with the food supply. Biomass is a clean, renewable energy source and can be converted directly into liquid fuels, called biofuels, to help meet transportation fuel needs.

During photosynthesis, algae and other photosynthetic organisms capture sunlight, produce oxygen and convert carbon dioxide into biomass. Recently, competing demands between foods and other biofuel sources and a world food crisis have ignited interest in algaculture (farming algae) for making biofuels including biodiesel (Li et al. 2008; Schenk et al. 2008).

Microalgae have a strong potential as vectors for biofuels, because in some species their oil content may exceed 70% of dry weight, compared with 5% for the best agricultural oil crops (Malcata 2011). Furthermore, microalgae are considered to be more advantageous than terrestrial crops that are currently utilized as energy feed stocks due to their faster growth rates, higher lipid productivity, and cultivation on non-arable land areas avoiding competition with food production. The per-unit area yield of oil from algae is estimated to be from 4.6 to 18.4 L per square meter (5000 and 20,000 gallons per acre) per year. This yield is up to 30 times greater than the yield from the next best crop (Yeang 2008).

To realize the promise of microalgae as an economically viable biofuel feedstock, problems associated with consistently producing biomass on a large scale in highly variable outdoor cultures must be overcome (Alam et al. 2012; Bull and Collins 2012; Yeang 2008). One problem is that algal strains with high oil content are generally less hardy or have a slower growth rate than algal strains with a low oil content which grow more easily in the harsher conditions of an open system. Thus, the efficient production of algal biofuels requires finding an algal strain with a high oil content and fast growth rate. Another obstacle has been the type of equipment and substructure needed to enable mass algae growth. Efforts to improve microalgal biofuel production are therefore focused on selection of species with many desirable biofuel traits, the optimization of microalgal cultivation systems, and the genetic manipulation of lipid biosynthesis are considered to be important.

Triacylglycerols with long-chain fatty acids, such as palmitic acid ($C_{16:0}$) and stearic acid ($C_{18:0}$), are the major component of oils produced by many algae (Hu et al. 2008). On the other hand, wax esters produced by *Euglena* are the esters coupled with middle-chain fatty acids and alcohols, mainly myristic acid ($C_{14:0}$) and myristyl alcohol ($C_{14:0}$). Kerosene used as a jet fuel consists mainly of hydrocarbons with carbon numbers of 9 through 15 (Maurice et al. 2001). Myristic acid and myristyl alcohol in *Euglena* wax esters are more suitable as a drop-in jet fuel than the long-chain fatty acids found in the oils produced by most algae. *Euglena* can grow under photoautotrophic, heterotrophic and photoheterotrophic conditions. The doubling time of *Euglena* (approx. 12 h) is faster than that of many algae. Furthermore, *Euglena* can grow under an extremely high concentration of CO_2, even up to 40%, and at low pH conditions (approx. pH 3.0). As such, based on these factors, *Euglena* is one of the most attractive and ideal resources for biofuel production.

13.2 Discovery of Wax Ester Fermentation

It had been known that *Euglena* cells synthesize wax esters (Kolattukudy 1970; Rosenberg 1967), and that synthesis is enhanced when cells are cultured without shaking (under semi-anaerobic conditions) (Nagai et al. 1971). Inui et al. (1982) found that wax esters were synthesized and accumulated with the concomitant degradation of the reserve polysaccharide, paramylon (β-1,3-glucan), in *E. gracilis* cells under strictly anaerobic conditions by bubbling N_2 gas into the culture media (around 10^{-8} M of O_2). The amount of wax esters accumulated and paramylon degraded after 24 h of anaerobic incubation were 39 and 105 μg/10^6 cells, respectively. These values correspond to 1.287 and 1.296 μmol/10^6 cells, respectively, of acetyl-CoA, indicating that all of the carbon in the wax esters was supplied by paramylon degradation.

Wax esters produced by anaerobic *E. gracilis* are composed of saturated fatty acids and alcohols with carbon chain-lengths of 10 through 18 (Inui et al. 1983). The major constituents are

myristic acid ($C_{14:0}$) and myristyl alcohol ($C_{14:0}$); these accounted for 44.4% and 46.8% of the fatty acid and alcohol moieties of the wax esters, respectively. The average chain-lengths of the constituent fatty acids and alcohols were 13.9 and 14.4, respectively, indicating that the fatty alcohol moiety is slightly longer than the fatty acid moiety. Interestingly, substantial amounts (around 35%) of odd-numbered (11, 13, 15 and 17) fatty acids and alcohols were found in the constituents of the anaerobically produced wax esters. The percentages of odd-numbered fatty acids and alcohols increased in response to a decrease in the availability of O_2 in *Euglena* cells (Schneider and Betz 1985).

Transfer of aerobically grown *E. gracilis* cells to anaerobic conditions caused a prompt fall in the cellular ATP level, but after 2 min, when the synthesis of wax esters became evident, the ATP level started to gradually increase reaching the pre transfer aerobic level after 13 min, and this level was maintained during anaerobiosis (Inui et al. 1982). These results show that the synthesis of wax esters from paramylon is coupled with the generation of ATP in *Euglena* cells; hence, this phenomenon is called "wax ester fermentation".

The wax ester fermentation is quite unique in that the end products have a relatively high molecular weight and are insoluble in water. Wax esters are present within the cytosol as a suspended solid, and apparently do not interfere with other metabolic reactions. Ordinary fermentation products, such as ethanol and lactic acid, are water-soluble and may be harmful when accumulated in cells so that they must be excreted from the cells with the loss of carbon. In contrast, wax esters produced during anaerobiosis are retained in *Euglena* with little a loss of carbon and they are rapidly converted back to paramylon when aerobic conditions were restored (Inui et al. 1982, 1992). The phenomenon resembles, in a sense, lactic acid formation in anaerobic mammalian muscle and gluconeogenesis from lactic acid in aerobic liver, except in unicellular *Euglena* the interconversion between glucan and wax esters takes place in the same cells.

13.3 Metabolic Pathways and Enzymes Involved in the Wax Ester Fermentation

13.3.1 Degradation of Paramylon

Euglena cells accumulate a storage polysaccharide, paramylon, that is a liner glucan consisting of only β-1,3-glycosidic linkages (Barras and Stone 1968; Barsanti et al. 2001), in contrast to green algae and higher plants in which the storage polysaccharide is starch consisting of α-1,4-, and in some cases α-1,6-glycosidic linkages. Paramylon is a granule in the cells, it contains no more than 700 polymerized glucose molecules, and its content often exceeds 50% of the dry weight of the cell (Kiss et al. 1988; Kuda et al. 2009). Paramylon is synthesized by membrane-bound paramylon synthases (UDP-glucose:β-1,3-glucan β-glucosyltransferase), that preferentially uses UDP-glucose (but not ADP-glucose) as the glucose donor (Marechal and Goldemberg 1964; Tomos and Northcote 1978). A recent comprehensive gene expression analysis of *Euglena* identified two probable paramylon synthases, which have 14 and 19 membrane spanning domains (Yoshida et al. 2016).

In the wax ester fermentation, paramylon would be degraded to glucose units by the cooperation of endo- and exo-β-1,3-glucanases. Endo-β-1,3-glucanases hydrolyze internal β-1,3-glycosidic bonds at random sites to generate oligosaccharides, and exo-β-1,3-glucanases release glucose from the generated oligosaccharides. In *Euglena*, both endo- and exo-β-1,3-glucanase activities were found and separated by gel filtration chromatography (Barras and Stone 1969a, b). In purified exo-β-1,3-glucanase, K_m values for laminaripentose and insoluble laminarin were 0.11 mM and 0.008%, respectively, and pH optimum was 4.7–5.2. Recently, it was reported that *E. gracilis* expressed at least three isozymes of endo-β-1,3-glucanases (Takeda et al. 2015). One of them was produced heterogeneously in *Aspergillus oryzae* and studied in detail. The enzyme was able to hydrolyze native paramylon, but the activity was significantly lower

than the activity with alkaline-treated paramylon or laminarin as a substrate. The K_m value for laminarin was 0.21 mg/mL.

β-1,3-Oligoglucan phosphorylase, which catalyzes the reversible phosphorolysis of low molecular weight β-1,3-glucans, would also participate in the degradation of paramylon in the wax ester fermentation. Laminaribiose phosphorylase was differentiated from β-1,3-oligoglucan phosphorylase by calcium phosphate gel chromatography (Marechal 1967a). The two enzymes catalyze the same reaction but with different quantitative specificities: The β-1,3-oligoglucan phosphorylase showed higher activity against laminaritriose and higher homologues compared with laminaribiose while the opposite result was observed with laminaribiose phosphorylase (Marechal 1967b). Three laminaribiose phosphorylase isozymes with very similar properties except for their isoelectric points were found in *Euglena* (Kitaoka et al. 1993).

13.3.2 The Glycolytic Pathway and Its Regulation

Glucose or glucose 1-phosphate produced from paramylon by the cooperation of β-1,3-glucanases and β-1,3-oligoglucan phosphorylases would be catabolized to pyruvate through the glycolytic pathway yielding a net gain of ATP from substrate-level phosphorylation. In mammalian cells, ATP-dependent phosphofructokinase (ATP-PFK) catalyzes the conversion of fructose 6-phsophate to fructose 1,6-bisphosphate, which is the rate-limiting step of glycolysis. In *E. gracilis*, as in plant cells, a pyrophosphate-dependent phosphofructokinase (PPi-PFK), which catalyzes a reversible conversion from fructose 6-phsophate and pyrophosphate (PPi) to fructose 1,6-bisphosphate and orthophosphate (Pi), was found in the cytosol in addition to ATP-PFK (Miyatake et al. 1984a). The activity of PPi-PFK was 10–30 times higher than that of ATP-PFK throughout cell growth. *Euglena* PPi-PFK activity was highly regulated by fructose 2,6-bisphosphate (F26BP) which is known to be a potent activator of mammalian ATP-PFK and plant PPi-PFK (Enomoto et al. 1988; Miyatake et al. 1986). In the forward reaction, the saturation curve for fructose 6-phosphate was sigmoidal and the apparent $K_{0.5}$ value was 2.5 mM. The saturation curve for PPi was hyperbolic with a K_m value of 100 μM. When F26BP was present, the affinity of *Euglena* PPi-PFK for fructose 6-phosphate was increased greatly and the saturation curve became hyperbolic with K_m value of 0.3 mM. The K_a value for F26BP was as low as 38 μM. In the reverse reaction, the saturation curve for both fructose and Pi were hyperbolic, and the affinity for Pi was decreased when F26BP was present.

When the concentration of O_2 in medium was reduced, the level of F26BP in *Euglena* cells initially decreased until the O_2 concentration became less than 1 μM when it began to increase reaching a level threefold higher than the original level (Enomoto et al. 1990). Synthesis of wax esters from paramylon started in the cells when the level of F26BP began to increase. In addition, the activated form of PPi-PFK that binds F26BP increased greatly in response to the increased level of F26BP during acclimation of the aerobic *Euglena* cells to anaerobiosis (Enomoto et al. 1991). These results indicate that F26BP exerts a stimulatory effect on glycolysis through activation of PPi-PFK enabling wax ester fermentation in anaerobic *Euglena* cells.

6-Phosphofructo-2-kinase and fructose-2,6-bisphosphatase catalyze the synthesis and degradation of F26BP. As reported in mammalian cells, these reactions are catalyzed in *Euglena* by a cytosolic bifunctional enzyme composed of a single polypeptide chain with two distinct active catalytic sites (Enomoto et al. 1989). Pyruvate kinase catalyzes the conversion of phosphoenolpyruvate to pyruvate with the concomitant formation of ATP from ADP and it is one of the regulatory enzyme of glycolysis. In addition to PPi-PFK, pyruvate kinase was also strongly activated by F26BP in *Euglena* (Miyatake et al. 1986).

13.3.3 Pyruvate:NADP+ Oxidoreductase

In *Euglena*, as well as in most eukaryotes, the pyruvate dehydrogenase multienzyme complex

occurs in mitochondria and is thought to be responsible for the oxidative decarboxylation of pyruvate supplying acetyl-CoA for the TCA cycle under aerobic conditions (Hoffmeister et al. 2004). This multienzyme complex is a large aggregate with a molecular weight of 3–7 million and consists of three component enzymes (pyruvate dehydrogenase, dihydrolipoyl transacetylase and dihydrolipoyl dehydrogenase). The reducing power of the substrate is transferred to NAD^+ in the multienzyme complex. Under the anaerobic conditions in which the *Euglena* wax ester fermentation takes place, pyruvate:$NADP^+$ oxidoreductase (PNO), catalyzes the oxidative decarboxylation of pyruvate with $NADP^+$ as the electron acceptor, supplying acetyl-CoA for mitochondrial fatty acid synthesis (Inui et al. 1984a, 1985, 1987). PNO is a homodimeric protein with a subunit molecular weight of about 195,000 and contains two functional domains that are easily separated by limited proteolysis with trypsin (Inui et al. 1991; Nakazawa et al. 2000) (Fig. 13.1). One of the two domains, the iron-sulfur domain, located in the N-terminal portion of the protein had a molecular weight of about 130,000 and still retained a homodimeric structure even after limited proteolysis. This domain, which contained one thiamine pyrophosphate (TPP) and three [4Fe-4S] clusters as prosthetic groups, catalyzed the oxidative decarboxylation of pyruvate to form acetyl-CoA when artificial electron acceptors such as methyl viologen instead of $NADP^+$ were present. The other domain, the flavodomain, was monomeric with a molecular weight of about 65,000, contained FAD and FMN, and was capable of catalyzing an electron-transfer reaction from NADPH to artificial electron acceptors. The amino acid sequence of the iron-sulfur domain closely resembled the sequences of the homodimeric type of pyruvate:ferredoxin oxidoreductase found in amitochondriate eukaryotes and in eubacteria. In contrast, the flavodomain showed structural similarity to mammalian NADPH-cytochrome P450 reductase and to bacterial NADPH-sulfite reductase α subunit. It was proposed that PNO evolved by gene fusion linking a homodimeric pyruvate:ferredoxin oxidoreductase with a flavoprotein containing both FAD and FMN. However, this enzyme was inactive when ferredoxin replaced $NADP^+$ as the electron accep-

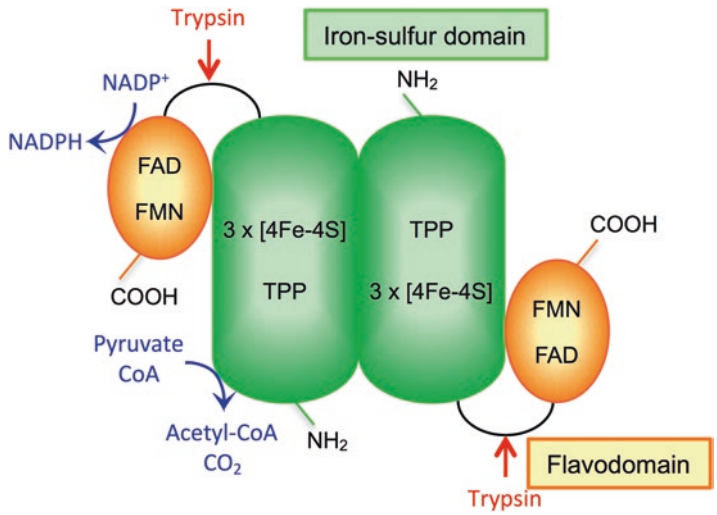

Fig. 13.1 Domain structure and proposed reaction mechanism of Pyruvate:$NADP^+$ Oxidoreuctase (PNO) (Nakazawa et al. 2000). PNO, a homodimeric protein, consists of the iron-sulfur domain and flavodomain, and these are easily separated at the sites indicated by the *red arrows* by limited proteolysis with trypsin. The iron-sulfur domain that contains thiamin pyrophosphate (TPP) as a prosthetic group catalyzes the oxidative decarboxylation of pyruvate with the concomitant acylation of CoA to form acetyl-CoA and CO_2. Two electrons produced by the oxidative decarboxylation of pyruvate are accepted by the [4Fe-4S] clusters in the iron-sulfur domain, and then transferred to the flavodomain containing FMN and FAD. Finally, $NADP^+$ is reduced to NADPH on the surface of the flavodomain

tor (Inui et al. 1987). PNO was oxygen-labile *in vitro* so that the enzyme reaction did not proceed at a liner rate in the presence of O_2 (Inui et al. 1984a, 1987). The O_2-inactivated enzyme was reactivated partially by incubating with Fe^{2+} and reducing reagents such as dithiothreitol in the absence of O_2 suggesting that the O_2-inactivation of the enzyme might be triggered by a release of Fe from the iron-sulfur cluster due to oxidation with O_2 (Inui et al. 1990). In contrast, PNO was stable in cells and in isolated intact mitochondria even under aerobic conditions (in air), but the enzyme was inactivated in air when intact mitochondria were incubated with detergents such as Triton X-100.

13.3.4 Mitochondrial Fatty Acid Synthetic System

Two types of *de novo* fatty acid synthetic systems have been reported in *Euglena*. One is the cytoplasmic FAS I, which is a mammalian type fatty acid synthase multienzyme complex found in both dark and light grown cells. The second, a chloroplast-localized FAS II, is an ACP-dependent plant type fatty acid synthetic system induced when cells are illuminated (Delo et al. 1971; Ernst-Fonberg and Bloch 1971; Hendren and Bloch 1980). In the wax ester fermentation, neither FAS I nor FAS II can explain the net synthesis of ATP, because more ATP is consumed in fatty acid synthesis than generated in glycolysis. The malonyl-CoA which is needed as a C_2 donor for fatty acid elongation by FAS I and FAS II, is synthesized by the ATP-dependent acetyl-CoA carboxylase. In addition, ATP is also required to transport an acetyl unit out of the mitochondria.

Inui et al. (1984b) discovered a novel malonyl-CoA-independent *de novo* fatty acid synthetic system in *Euglena* mitochondria, which is used for fatty acid synthesis in anaerobic *Euglena* cells during the wax ester fermentation. In the *Euglena* mitochondrial system, fatty acids are synthesized with acetyl-CoA as both primer and C_2 donor using NADH as an electron donor by the reverse of the β-oxidation reaction except that *trans*-2-enoyl-CoA reductase (TER) is used instead of acyl-CoA dehydrogenase (Fig. 13.2). This system resembles the malonyl-CoA-independent chain elongation system found in mammalian mitochondria (Hinsch et al. 1976) but is novel in that it functions for the *de novo* synthesis of fatty acids from only acetyl-CoA. Myristic acid ($C_{14:0}$) is the major product of the mitochondrial fatty acid synthetic system (Inui et al. 1984b) in contrast to FAS I and FAS II in which palmitic acid ($C_{16:0}$) and stearic acid ($C_{18:0}$), respectively, were the main products (Delo et al. 1971; Goldberg and Bloch 1972). In addition, fatty acid synthesis in the *Euglena* mitochondrial system was greatly accelerated when a high ratio of acetyl-CoA *versus* CoA was maintained in the presence of an acetyl-CoA-regenerating system (Inui et al. 1984b). Under the physiological conditions in which the wax ester fermentation takes place, PNO would act as an

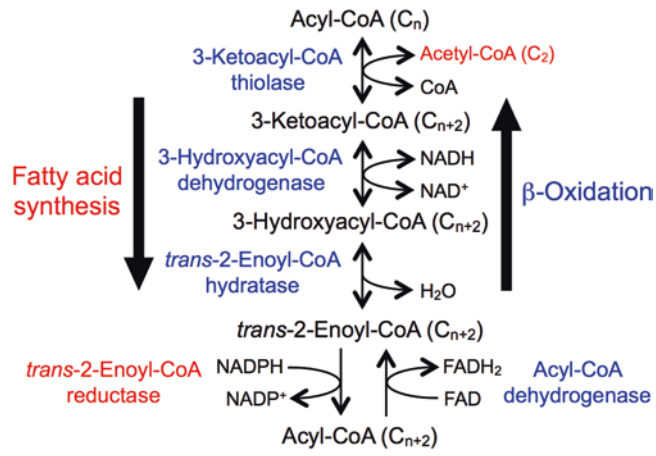

Fig. 13.2 Mitochondrial fatty acid synthetic system. Fatty acids are synthesized in a reaction sequence going from the top to the bottom by the fundamentally reverse reaction of β-oxidation. In this fatty acid synthesis, *trans*-2-enoyl-CoA reductase functions instead of acyl-CoA dehydrogenase, which catalyzes the irreversible step of the β-oxidation

acetyl-CoA regenerating system to facilitate the mitochondrial fatty acid synthesis (Inui et al. 1985). Three TER isozymes with different substrate specificities were found in *Euglena* mitochondria (Inui et al. 1984b). One of the three isozymes catalyzing the reduction of short chain length *trans*-2-enoyl-CoAs, especially crotonyl-CoA (C_4), with NADH as an electron donor was purified and characterized (Inui et al. 1986). A second TER isozyme was purified from *Euglena* and its cDNA sequence was determined (Hoffmeister et al. 2005). This isozyme was highly active with both crotonyl-CoA and *trans*-2-hexenoyl-CoA (C_6), and both NADH and NADPH were suitable electron donors. In addition to TER, 3-ketoacyl-CoA thiolase isozymes that catalyze the condensation reaction of acyl-CoA and acetyl-CoA in the mitochondrial fatty acid synthesis, have been studied in *Euglena* (Nakazawa et al. 2015) (for details, see Sect. 13.4.3).

13.3.5 Wax Ester Synthesis

Wax esters are synthesized in two consecutive steps; the reduction of fatty acyl-CoA to fatty alcohol catalyzed by acyl-CoA reductase and the subsequent esterification of fatty acyl-CoA and fatty alcohol by wax ester synthase. These enzyme activities were found in *E. gracilis* microsomes (Khan and Kolattukudy 1973). cDNAs encoding the putative *Euglena* acyl-CoA reductase and wax ester synthase were obtained by a homology search of the *Euglena* EST database using jojoba enzymes as query sequences and by 5′- and 3′-RACE (Teerawanichpan and Qiu 2010). When expressed in yeast, *Euglena* acyl-CoA reductase converted myristic acid and palmitic acid to the corresponding fatty alcohols with myristic acid as the preferred substrate. The *Euglena* enzyme, as well as those found in higher plants (Pollard et al. 1979; Vioque and Kolattukudy 1997), was able to reduce fatty acyl-CoAs to fatty alcohols directly, without the participation of aldehyde reductase. *Euglena* wax ester synthase could utilize a broad range of fatty acyl-CoAs and fatty alcohols as substrates with a preference towards myristic acid and palmitoleyl alcohol. Recently, a comprehensive gene analysis of *Euglena* indicates that there are different types of wax ester synthesizing enzymes that are classified as wax ester synthase/acyl-CoA:diacylglycerol acyltransferase (WSD), which were first identified and characterized from *Acinetobacter calcoaceticus* (Kalscheuer and Steinbüchel 2003). Gene silencing experiments for WSD and experiments with a yeast recombinant WSD expression system showed that WSD functions as a dominant enzyme for wax ester synthesis in *Euglena* (Tomiyama et al. in preparation).

13.3.6 Formation of Propionyl-CoA as a Primer for Odd-Numbered Fatty Acid Synthesis

Substantial amounts of odd-numbered (mainly 13 and 15) fatty acids and alcohols are found in wax esters produced by anaerobic *Euglena* cells (Inui et al. 1983). Propionyl-CoA instead of acetyl-CoA would be used as a primer for odd-numbered fatty acid synthesis (Nagai et al. 1971; Schneider and Betz 1985). It is thought that propionyl-CoA is synthesized from phosphoenolpyruvate (PEP) through oxaloacetate, succinate and methylmalonyl-CoA (Tucci et al. 2010). Indeed, radioactivity was incorporated preferentially into the odd-numbered fatty acids and alcohols of wax esters when *Euglena* cells were incubated with [3-^{14}C]propionate, [1,4-^{14}C]succinate or $H^{14}CO_3^-$ under anaerobic conditions, whereas even-numbered rather than odd-numbered fatty acids and alcohols were labeled when cells were incubated with [2-^{14}C]pyruvate (Schneider and Betz 1985). The synthesis of propionyl-CoA is thought to be important to maintain redox balance under anaerobic conditions because two molecules of NADH are consumed during propionyl-CoA synthesis.

In the first step of the propionyl-CoA synthesis, PEP carboxykinase (PEPCK) catalyzes the carboxylation of PEP to form oxaloacetate with the concomitant phosphorylation of GDP. *Euglena* PEPCK was purified and shown to have a relatively high affinity for HCO_3^- suggesting

that the carboxylation of PEP is the preferred reaction direction for the *Euglena* enzyme in contrast to the chicken liver enzyme which participates in gluconeogenesis (Pönsgen-Schmidt et al. 1988). PEPCK was localized to the cytosol in *E. gracilis* (Miyatake et al. 1984b). Oxaloacetate produced by PEPCK is reduced to malate using NADH by malate dehydrogenase and transferred to the mitochondria. Then, malate is dehydrated to form fumarate by the action of fumarase.

The next step is the reduction of fumarate to form succinate. This reaction seems to be the reversal of the succinate dehydrogenase (mitochondrial complex II) reaction in the TCA cycle. However, the reduction of fumarate is generally carried out by a different enzyme, fumarate reductase, found in the inner mitochondrial membrane of eukaryotes (Ginger et al. 2010; Tielens et al. 2002). In addition, fumarate reduction uses rhodoquinone which has a lower standard redox potential than ubiquinone which is used by succinate dehydrogenase for electron transfers. When *Euglena* cells were cultured under low oxygen conditions, the fumarate reductase activity increased whereas the succinate dehydrogenase activity decreased together with a reduction of the ubiquinone content (Castro-Guerrero et al. 2005; Hoffmeister et al. 2004). For the fumarate reductase reaction, rhodoquinone would be reduced with NADH. If mitochondrial complex I functions for the reduction of rhodoquinone, in *Euglena*, as has been reported in other eukaryotes such as helminths, the establishment of proton motive force across the inner mitochondrial membrane could conceivably be coupled to ATP synthesis by mitochondrial complex V (Ginger et al. 2010; Müller et al. 2012).

Succinyl-CoA is formed from succinate by succinyl-CoA synthetase, and then converted to L-methylmalonyl-CoA by the action of an adenosylcobalamin-dependentL-methylmalonyl-CoA mutase. *Euglena* L-methylmalonyl-CoA mutase was purified and its cDNA sequence was determined (Miyamoto et al. 2010). This enzyme, a homodimeric protein with a molecular mass of 78 kDa, contained one adenosylcobalamin per subunit, and sequence similarity betwee n *Euglena* and mammalian enzymes was over 65%. Finally, L-methylmalonyl-CoA is converted to propionyl-CoA through D-methylmalonyl-CoA by the sequential reactions of methylmalonyl-CoA epimerase and propionyl-CoA carboxylase. Unfortunately, these two enzymes have not yet been studied in *Euglena*.

13.4 Production of Wax Esters as a Biofuel

13.4.1 Optimization of Culture Conditions for Enhanced Wax Ester Production

It has been reported that not only the C/N ratio but also the types of carbon and nitrogen sources in the media have a great impact on lipid content and fatty acid distribution in algae. It has also been reported that the amount of specific fatty acids was related to the growth phase in various algal strains (Bigogno et al. 2002; Mansour et al. 2003; Tonon et al. 2002).

Schwarzhans et al. (2015) analyzed the amounts of 22 fatty acids in *Euglena* grown under heterotrophic and photoheterotrophic conditions in media containing various concentration of glucose and proteose peptone in aerobiosis. Under either the heterotrophic or photoheterotrophic conditions, the most abundant fatty acids were myristic acid ($C_{14:0}$) and palmitic acid ($C_{16:0}$), accounting for about 50% of the total fatty acids. Interestingly, the content of palmitic acid dropped from early to late cultivation stage while myristic acid increased at the same time. They suggested that this behavior indicated a change in the composition of the cell membrane when cells shift from the exponential growth phase to the stationary phase.

Mahapatra et al. (2013) showed that *Euglena* cultivated in wastewater had a high lipid content, 24.6% of dry weight, with a biomass density of 1.24 g dry weight/L. The lipids contained 13 different types of fatty acids and approximately 50% were unsaturated fatty acids. Among the fatty acids produced, 46% was palmitic acid ($C_{16:0}$), 23% was α-linolenic acid ($C_{18:3}$), and 22% was lin-

oleic acid ($C_{18:2}$) while a very low amount, 3.3% of myristic acid ($C_{14:0}$) was produced. These results suggest that high biofuel production by *Euglena* using low-cost materials will be feasible.

Tucci et al. (2010) reported that various strains of *E. gracilis* accumulated wax esters in concentration between 0.3–8.9% of dry weight under ambient aerobic conditions. Under strictly anaerobic conditions, several of the tested cultures died, but those strains that survived anaerobiosis accumulated about tenfold more wax esters than in the presence of oxygen; in one of those strains the wax ester concentration reached over 31% of the dry weight of the cells. In addition, under anaerobic conditions, compared with aerobic conditions, the proportion of even-numbered constituents was reduced and fatty acid and alcohol patterns were shifted toward shorter and odd-numbered chains.

These studied demonstrate that *Euglena* possesses the potential to be used as a biorefinery to produce high value biofuel and biomass by selective optimization of the culture conditions.

13.4.2 Enhanced Biomass Production Through Improvement of Photosynthetic CO_2 Fixation

Bioprocess and metabolic engineering involving the introduction of the appropriate genes appears to be a useful approach for enhanced biomass production. Paramylon is the source of carbon for wax ester synthesis in anaerobic *E. gracilis* cells (Inui et al. 1982). Accordingly, the metabolic engineering of photosynthetic CO_2 fixation is a promising approach to create *Euglena* strains capable of industrial scale production of biodiesel. The rate-limiting enzymes involved in the Calvin cycle, fructose-1,6-bisphosphatase (FBPase) and sedoheptulose-1,7-bisphosphatase (SBPase) are potential targets for the optimization of photosynthetic reactions (Miyagawa et al. 2001; Woodrow and Mott 1993). Indeed, transgenic tobacco and lettuce plants overexpressing the cyanobacterial FBPase/SBPase gene, which encodes a bifunctional enzyme having both FBPase and SBPase activities, in chloroplasts showed an enhanced CO_2 assimilation rate and increased biomass production (Miyagawa et al. 2001; Yabuta et al. 2008). In order to enhance photosynthesis and biomass production in *E. gracilis*, Ogawa et al. (2015) have introduced the cyanobacterial FBPase/SBPase gene into *Euglena* cells to generate transformed cell lines, *EpFS4* and *EpFS11*. The *EpFS4* cells had a larger cell volume and enhanced photosynthetic activity compared to wild-type cells (Fig. 13.3a, b). Specifically, paramylon content was significantly higher in either the *EpFS4* or *EpFS11* cell line than in wild-type cells, when cultured under high light (350 μmol photons/m^2/s) and high CO_2 (0.3%) (Fig. 13.3c). Furthermore, the amount of wax esters produced after 24-h of static culture (semi-anaerobic conditions) in the dark was substantially greater in the both *EpFS* cell lines (Fig. 13.3d).

13.4.3 Genetic Engineering of the Metabolic Pathways from Paramylon to Wax Esters

To promote the efficiency of the wax ester fermentation in *Euglena*, the metabolic pathway converting paramylon to wax esters (paramylon degradation, glycolysis, and fatty acid and wax ester biosynthesis) must be improved. As described above, when aerobically grown *Euglena* is transferred to anaerobic conditions, 105 μg/10^6 cells of paramylon was degraded after 24 h of anaerobic incubation (Inui et al. 1982), indicating that the calculated degradation rate of paramylon was approx. 4.4 μg/10^6 cells/h. It has been reported that 150 μg/10^6 cells of paramylon was immediately degraded and excreted as glycolate when cells grown with 5% CO_2 were incubated under highly photorespiratory conditions (100% O_2 at 20,000 lux) for 8 h (Yokota and Kitaoka 1982), indicating that the calculated degradation rate of paramylon was approx. 18.8 μg/10^6 cells/h. This rate was much faster than the rate under anaerobic conditions. The reduced rate of paramylon degradation under anaerobic conditions might be due to an insufficient supply of NAD^+ because paramylon degradation

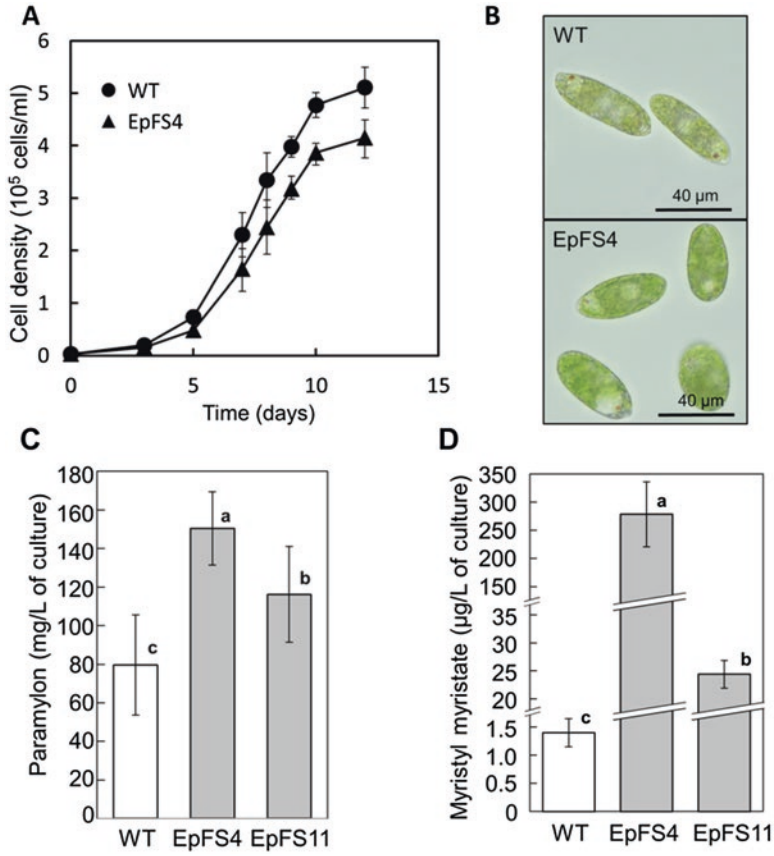

Fig. 13.3 Characterization of wild-type and transgenic *Euglena* cells (Ogawa et al. 2015). (Panel **a**, **b**) Growth curve (**a**) and phenotypes (**b**) of wild-type and transgenic (*EpFS4*) cells grown under high-light (350 μmol photon/m^2/s). The average cell volumes of the wild-type and *EpFS4* cells were 2980 ± 414 and 3357 ± 194 fl/cell, respectively. (Panel **c**) Paramylon content of wild-type and transgenic (*EpFS4* and *EpFS11*) cells grown under high-light and high-CO_2 for 8 days. (Panel **d**) Wax ester (C_{28}) content in wild-type and transgenic (*EpFS4* and *EpFS11*) cells after 24-h anaerobic incubation. Different letters indicate statistically significant differences ($p < 0.05$)

during glycolate excretion does not go through 1,3-bisphosphoglycerate. The activity of *trans*-2-enoyl-CoA reductase (TER) is extremely low compared to the activity of the other enzymes involved in the mitochondrial fatty acid synthesis (i.e. 3-ketoacyl-CoA thiolase, 3-hydroxyacyl-CoA dehydrogenase and *trans*-2-enoyl-CoA hydratase) (Hoffmeister et al. 2005; Inui et al. 1984b; Winkler et al. 2003). Therefore, it is considered that TER is the rate-limiting step in fatty acid biosynthesis and even limits the glycolytic pathway due to the low amount of NAD^+ produced. A likely strategic point for increased production of wax esters in *Euglena* is thus elevating the TER activity by genetic engineering.

Nakazawa et al. (2015) reported that at least three isozymes of 3-ketoacyl-CoA thiolase (EgKAT1–3) participated in mitochondrial fatty acid synthesis in the wax ester fermentation. It was also shown that silencing of EgKAT3 led to a decreased wax ester content while silencing of EgKAT1 and EgKAT2 led to a significant shift to shorter carbon chain lengths in the wax esters. These data suggest that EgKAT3 is specific for short-chain length substrates, whereas EgKAT1 and EgKAT2 are medium- or long-chain length-specific isozymes. This is the first report demonstrating that genetic manipulation of the enzymes involved in wax ester biosynthesis is a good strategy for improving the quality and quantity of wax esters in *Euglena*.

A metabolome analysis of *E. gracilis* (Matsuda et al. 2011) showed dynamic shifts in metabolic states in response to changes in culture conditions and provides important information on strategies to improve wax ester fermentation by genetic engineering. To that end, further optimization of genetic tools, such as expression vectors, strong promoters and transformation methods, for *E. gracilis* are required.

References

Alam F, Date A, Rasjidin R, Mobin S, Moria H, Baqui A (2012) Biofuel from algae—is it a viable alternative? Procedia Eng 49:221–227

Atteia A, van Lis R, Tielens AGM, Martin FM (2013) Anaerobic energy metabolism in unicellular photosynthetic eukaryotes. Biochim Biophys Acta 1827:210–223

Barras DR, Stone BA (1968) In: Buetow DE (ed) Biology of *Euglena*, vol II. Academic Press, New York, p. 141–191

Barras DR, Stone BA (1969a) β-1,3-glucan hydrolases from *Euglena gracilis*. I. The nature of the hydrolases. Biochim Biophys Acta 191:329–341

Barras DR, Stone BA (1969b) β-1,3-glucan hydrolases from *Euglena gracilis*. II. Purification and properties of the β-1,3-glucan exo-hydrolase. Biochim Biophys Acta 191:342–353

Barsanti L, Vismara R, Passarelli V, Gualtieri P (2001) Paramylon (β-1,3-glucan) content in wild type and WZSL mutant of *Euglena gracilis*. Effects of growth conditions. J Appl Phycol 13:59–65

Bigogno C, Khozin-Goldberg I, Boussiba S, Vonshak A, Cohen Z (2002) Lipid and fatty acid composition of the green oleaginous algae *Parietochloris incisa*, the richest plant source of arachidonic acid. Phytochemistry 60:487–503

Bull JJ, Collins S (2012) Algae for biofuel: will the evolution of weeds limit the enterprise? Evolution 66:2983–2987

Castro-Guerrero NA, Jasso-Chávez R, Moreno-Sánchez R (2005) Physiological role of rhodoquinone in *Euglena gracilis* mitochondria. Biochim Biophys Acta 1710:113–121

Catalanotti C, Yang W, Posewitz MC, Grossman AR (2013) Fermentation metabolism and its evolution in algae. Front Plant Sci 4:150

Delo J, Ernst-Fonberg ML, Bloch K (1971) Fatty acid synthetases from *Euglena gracilis*. Arch Biochem Biophys 143:384–391

Enomoto T, Miyatake K, Kitaoka S (1988) Purification and immunological properties of fructose 2,6-bisphosphate-sensitive pyrophosphate:D-fructose 6-phosphate 1-phosphotransferase from the protist *Euglena gracilis*. Comp Biochem Physiol 90B:897–902

Enomoto T, Kakihara K, Miyatake K, Kitaoka S (1989) Occurrence and characterization of fructose 6-phosphate, 2-kinase and fructose 2,6-bisphosphatase in *Euglena gracilis*. Comp Biochem Physiol 92B:477–480

Enomoto T, Ohyama H, Inui H, Miyatake K, Nakano Y, Kitaoka S (1990) Roles of pyrophosphate:D-frucotse-6-phosphate 1-phosphotransferase and fructose-2,6-bisphosphate in the regulation of glycolysis during acclimation of aerobic *Euglena gracilis* to anaerobiosis. Plant Sci 67:161–167

Enomoto T, Ohyama H, Inui H, Miyatake K, Nakano Y, Kitaoka S (1991) Regulation mechanism of the pyrophosphate:d-frucotse 6-phosphate 1-phosphotransferase activity by fructose 2,6-bisphosphate in *Euglena gracilis*. Plant Sci 73:11–18

Ernst-Fonberg ML, Bloch K (1971) A chloroplast-associated fatty acid synthetase system in *Euglena*. Arch Biochem Biophys 143:392–400

Ginger ML, Fritz-Laylin LK, Fulton C, Cande WZ, Dawson SC (2010) Intermediary metabolism in protist: a sequence-based view of facultative anaerobic metabolism in evolutionarily diverse eukaryotes. Protist 161:642–671

Goldberg I, Bloch K (1972) Fatty acid synthetases in *Euglena gracilis*. J Biol Chem 247:7349–7357

Hendren RW, Bloch K (1980) Fatty acid synthetases from *Euglena gracilis*. Separetion of component activities of the ACP-dependent fatty acid synthetase and partial purification of the β-ketoacyl-ACP synthetase. J Biol Chem 255:1504–1508

Hinsch W, Klages C, Seubert W (1976) On the mechanism of malonyl-CoA-independent fatty-acid synthesis. Different properties of mitochondrial chain elongation and enoyl-CoA reductase in various tissues. Eur J Biochem 64:45–56

Hoffmeister M, van der Klei A, Rotte C, van Grinsven KWA, van Hellemond JJ, Henze K, AGM T, Martin W (2004) *Euglena gracilis* rhodoquinone:ubiquinone ratio and mitochondrial proteome differ under aerobic and anaerobic conditions. J Biol Chem 279:22422–22429

Hoffmeister M, Piotrowski M, Nowitzki U, Martin W (2005) Mitochondrial *trans*-2-enoyl-CoA reductase of wax ester fermentation from *Euglena gracilis* defines a new family of enzymes involved in lipid synthesis. J Biol Chem 280:4329–4338

Hu Q, Sommerfeld M, Jarvis E, Ghirardi M, Posewitz M, Seibert M, Darzins A (2008) Microalgal triacylglycerols as feedstocks for biofuel production: perspectives and advances. Plant J 54:621–639

Inui H, Miyatake K, Nakano Y, Kitaoka S (1982) Wax ester fermentation in *Euglena gracilis*. FEBS Lett 150:89–93

Inui H, Miyatake K, Nakano Y, Kitaoka S (1983) Production and composition of wax esters by fermentation of *Euglena gracilis*. Agric Biol Chem 47:2669–2671

Inui H, Miyatake K, Nakano Y, Kitaoka S (1984a) Occurrence of oxygen-sensitive, $NADP^+$-dependent pyruvate dehydrogenase in mitochondria of *Euglena gracilis*. J Biochem 96:931–934

Inui H, Miyatake K, Nakano Y, Kitaoka S (1984b) Fatty acid synthesis in mitochondria of *Euglena gracilis*. Eur J Biochem 142:121–126

Inui H, Miyatake K, Nakano Y, Kitaoka S (1985) The physiological role of oxygen-sensitive pyruvate dehydrogenase in mitochondrial fatty acid synthesis in *Euglena gracilis*. Arch Biochem Biophys 237:423–439

Inui H, Miyatake K, Nakano Y, Kitaoka S (1986) Purification and some properties of short chain-length specific *trans*-2-enzylo-CoA reductase in mitochondria of *Euglena gracilis*. J Biochem 100:995–1000

Inui H, Ono K, Miyatake K, Nakano Y, Kitaoka S (1987) Purification and characterization of pyruvate:NADP$^+$ oxidoreductase in *Euglena gracilis*. J Biol Chem 262:9130–9135

Inui H, Miyatake K, Nakano Y, Kitaoka S (1990) Pyruvate:NADP$^+$ oxidoreductase from *Euglena gracilis*: mechanism of O_2-inactivation of the enzyme and its stability in the aerobe. Arch Biochem Biophys 280:292–298

Inui H, Yamaji R, Saidoh H, Miyatake K, Nakano Y, Kitaoka S (1991) Pyurvate:NADP$^+$ oxidoreductase from *Euglena gracilis*: limited proteolysis of the enzyme with trypsin. Arch Biochem Biophys 286:270–276

Inui H, Miyatake K, Nakano Y, Kitaoka S (1992) Synthesis of reserved polysaccharide from wax esters accumulated as the result of anaerobic energy generation in *Euglena gracilis* returned from anaerobic to aerobic conditions. Int J Biochem 24:799–803

Kalscheuer R, Steinbüchel A (2003) A novel bifunctional wax ester synthase/acyl-CoA:diacylglycerol acyltransferase mediates wax ester and triacylglycerol biosynthesis in Acinetobacter calcoaceticus ADP1. J Biol Chem 278:8075–8082

Khan AA, Kolattukudy PE (1973) A microsomal fatty acid synthetase coupled to acyl-CoA reductase in *Euglena gracilis*. Arch Biochem Biophys 158:411–420

Kiss JZ, Roberts EM, Brown RM, Triemer RE (1988) X-ray and dissolution studies of paramylon storage granules from *Euglena*. Protoplasma 146:150–156

Kitaoka M, Sasaki T, Taniguchi H (1993) Purification and properties of laminaribiose phosphorylase (EC 2.4.1.31) from *Euglena gracilis* Z. Arch Biochem Biophys 304:508–514

Kolattukudy PE (1970) Reduction of fatty acids to alcohols by cell-free preparations of *Euglena gracilis*. Biochemistry 9:1095–1102

Kuda T, Enomoto T, Yano T (2009) Effects of two storage β-1,3-glucans, laminaran from *Eicenia bicyclis* and paramylon from *Euglena gracilis*, on cecal environment and plasma lipid levels in rats. J Funct Foods 1:399–404

Li Y, Horsman M, Wu N, Lan Q, Dubolis-Calero N (2008) Biofuels from microalgae. Biotechnol Prog 24:815–820

Mahapatra DM, Chanakya NH, Ramachandra TV (2013) *Euglena* so. As a suitable source of lipids for potential use as biofuel and sustainable wastewater treatment. J Appl Phycol 25:855–865

Malcata FX (2011) Microalgae and biofuels: a promising partnership. Trends Biotechnol 29:542–549

Mansour MP, Volkman JK, Blackburn SI (2003) The effect of growth phase on the lipid class, fatty acid and sterol composition in the marine dinoflagellate, *Gymnodinium* sp. in batch culture. Phytochemistry 63:145–153

Marechal LR (1967a) β-1,3-oligoglucan:orthophosphate glucosyltransferases from *Euglena gracilis*. I. Isolation and some properties of a β-1,3-oligoglucan phosphorylase. Biochim Biophys Acta 146:417–430

Marechal LR (1967b) β-1,3-oligoglucan:orthophosphate glucosyltransferases from *Euglena gracilis*. II. Comparative studies between laminaribiose- and β-1,3-oligoglucan phosphorylase. Biochim Biophys Acta 146:431–442

Marechal LR, Goldemberg SH (1964) Uridine diphosphate glucose-β-1,3-glucan β-3-glucosyltransferase from *Euglena gracilis*. J Biol Chem 239:3163–3167

Matsuda F, Hayashi M, Kondo A (2011) Comparative profiling analysis of central metabolites in *Euglena gracilis* under various cultivation conditions. Biosci Biotechnol Biochem 75:2253–2256

Maurice LQ, Lander H, Edwards T, Harrison WE III (2001) Advanced aviation fuels: a look ahead via a historical perspective. Fuel 80:747–756

Miyagawa Y, Tamoi M, Shigeoka S (2001) Overexpression of a cyanobacterial fructose-1,6−/sedoheptulose-1,7-bisphosphatase in tobacco enhances photosynthesis and growth. Nat Biotechnol 19:965–969

Miyamoto E, Tanioka Y, Nishizawa-Yokoi A, Yabuta Y, Ohnishi K, Misono H, Shigeoka S, Nakano Y, Watanabe F (2010) Characterization of methylmalonyl-CoA mutase involved in the propionate photoassimilation of *Euglena gracilis* Z. Arch Microbiol 192:437–446

Miyatake K, Enomoto T, Kitaoka S (1984a) Detection and subcellular distribution of pyrophosphate:D-fructose 6-phosphate phosphotransferase (PFP) in *Euglena gracilis*. Agric Biol Chem 48:2857–2859

Miyatake K, Ito T, Kitaoka S (1984b) Subcellular location and some properties of phosphoenolpyruvate carboxykinase (PEPCK) in *Euglena gracilis*. Agric Biol Chem 48:2139–2141

Miyatake K, Enomoto T, Kitaoka S (1986) Fructose-2,6-bisphosphate activates pyrophosphate:D-fructose 6-phosphate 1-phosphotransferase from *Euglena gracilis*. Agric Biol Chem 50:2417–2418

Müller M, Mentel M, van Hellemond JJ, Henze K, Woehle C, Gould SB, Yu R-Y, van der Giezen M, Tielens AGM, Martin WF (2012) Biochemistry and evolution of anaerobic energy metabolism in eukaryotes. Microbiol Mol Biol Rev 76:444–495

Nagai J, Ohta T, Saito E (1971) Incorporation of propionate into wax esters by etiolated *Euglena*. Biochem Biophys Res Commun 42:523–529

Nakazawa M, Inui H, Yamaji R, Yamamoto T, Takenaka S, Ueda M, Nakano Y, Miyatake K (2000) The origin of pyruvate:NADP$^+$ oxidoreductase in mitochondria of *Euglena gracilis*. FEBS Lett 479:155–157

Nakazawa M, Andoh H, Koyama K, Watanabe Y, Nakai T, Ueda M, Sakamoto T, Inui H, Nakano Y, Miyatake K (2015) Alteration of wax ester content and composition in *Euglena* with gene silencing of 3-ketoacyl-CoA thiolase isozymes. Lipids 50:483–492

Ogawa T, Tamoi M, Kimura A, Mine A, Sakuyama H, Yoshida E, Maruta T, Suzuki K, Ishikawa T, Shigeoka S (2015) Enhancement of photosynthetic capacity in *Euglena gracilis* by expression of cyanobacterial fructose-1,6−/sedoheptulose-1,7-bisphosphatase leads to increases in biomass and wax ester production. Biotechnol Biofuels 8:80

Pollard MR, McKeon T, Gupta LM, Stumpf PK (1979) Studies on biosynthesis of wax esters by developing jojoba seed. II. The demonstration of wax biosynthesis by cell-free homogenates. Lipids 14:651–662

Pönsgen-Schmidt E, Schneider T, Hammer U, Betz A (1988) Comparison of phosphoenolpyruvate-carboxykinase from autotrophically and heterotrophically grown *Euglena* and its role during dark anaerobiosis. Plant Physiol 86:457–462

Rosenberg A (1967) *Euglena gracilis*: a novel lipid energy reserve and arachidonic acid enrichment during fasting. Science 157:1189–1191

Schenk P, Thomas-Hall SR, Stephans E, Marx UC, Mussgnug JH, Posten C, Kruse O, Hankamer B (2008) Second generation biofuels: high-efficiency microalgae for biodiesel production. Bioenergy Res 1:20–43

Schneider T, Betz A (1985) Waxmonoester fermentation in *Euglena gracilis* T. Factors favouring the synthesis of odd-numbered fatty acids and alcohols. Planta 166:67–73

Schwarzhans J-P, Cholewa D, Grimm P, Beshay U, Risse J-M, Friehs K, Flaschel E (2015) Dependency of the fatty acid composition of *Euglena gracilis* on growth phase and culture conditions. J Appl Phycol 27:1389–1399

Takeda T, Nakano Y, Takahashi M, Konno N, Sakamoto Y, Arashida R, Murakawa Y, Yoshida E, Ishikawa T, Suzuki K (2015) Identification and enzymatic characterization of an endo-1,3-β-glucanse from *Euglena gracilis*. Phytochemistry 116:21–27

Teerawanichpan P, Qiu X (2010) Fatty acyl-CoA reductase and wax synthase from *Euglena gracilis* in the biosynthesis of medium-chain wax esters. Lipids 45:263–273

Tielens AGM, Rotte C, van Hellemond JJ, Martin W (2002) Mitochondria as we don't know them. Trends Biochem Sci 27:564–572

Tomos AD, Northcote DH (1978) A protein-glucan intermediate during paramylon synthesis. Biochem J 174:283–290

Tonon T, Larson TR, Graham IA (2002) Long chain polyunsaturated fatty acid production and partitioning to triacylglycerols in four microalgae. Phytochemistry 61:15–24

Tucci S, Vacula R, Krajcovic J, Proksch P, Martin W (2010) Variability of wax ester ferementation in natural and bleached *Euglena gracilis* strain in response to oxygen and the elongase inhibitor flufenacet. J Eukaryot Microbiol 57:63–69

Vioque J, Kolattukudy PE (1997) Resolution and purification of an aldehyde-generating and an alcohol-generating fatty acyl-CoA reductase from pea leaves (*Pisum sativum* L.) Arch Biochem Biophys 340:64–72

Winkler U, Säftel W, Stabenau H (2003) A new type of a multifunctional β-oxidation enzyme in *Euglena*. Plant Physiol 131:753–762

Woodrow IE, Mott KA (1993) Modeling C_3 photosynthesis: a sensitivity analysis of the photosynthetic carbon-reduction cycle. Planta 191:421–432

Yabuta Y, Tamoi M, Yamamoto K, Tomizawa K, Yokota A, Shigeoka S (2008) Molecular designing of photosynthesis-elevated chloroplasts for mass accumulation of a foreign protein. Plant Cell Physiol 49:375–385

Yeang K (2008) Biofuel from algae. Archit Design 78:118–119

Yokota A, Kitaoka S (1982) Synthesis, excretion, and metabolism of glycolate under highly photorespiratory conditions in *Euglena gracilis* Z. Plant Physiol 70:760–764

Yoshida Y, Tomiyama T, Maruta T, Tomita M, Ishikawa T, Arakawa K (2016) *De novo* assembly and comparative transcriptome analysis of *Euglena gracilis* in response to anaerobic conditions. BMC Genomics 17:182

Large-Scale Cultivation of *Euglena*

14

Kengo Suzuki

Abstract

From the middle of the twentieth century, microalgae have been exploited as a candidate biomass source of food and other products. One such candidate source is the fast-proliferating microalga *Euglena gracilis*. The commercial cultivation of *E. gracilis* began in 2007, after the success of its outdoor mass cultivation and improvement of the harvesting and drying methods suitable for *Euglena* cells. The commercialization of *Euglena* production is based on the strategy of "5Fs of Biomass," which refers to the development and production of commercial products including food, fiber, feed, fertilizer, and fuel from biomass." Although room for improvement remains in the productivity of *Euglena* biomass, the product with the highest value—food—is already profitable. By enhancing the productivity of its biomass, other *Euglena* products, including fiber, feed, fertilizer, and fuel, can be commercialized. Breeding and recombinant DNA technology studies are being conducted to accomplish more extensive application of *Euglena*. In addition, the search for a better place for outdoor mass cultivation of *Euglena* is ongoing.

Keywords

Large-scale cultivation • Commercial application • Business • Breeding

Abbreviations

EPA	Environmental Protection Agency
euglena Co.	euglena Co. Ltd
FACS	Fluorescence activated cell sorting
GM	Genetically modified
TERA	TSCA (Toxic Substances Control Act) Environmental Release Application

K. Suzuki, Ph.D. (✉)
Department of Research and Development, euglena Co., Ltd., 5-33-1 Shiba, Minato-ku, Tokyo 108-0014, Japan
e-mail: suzuki@euglena.jp

S.D. Schwartzbach, S. Shigeoka (eds.), *Euglena: Biochemistry, Cell and Molecular Biology*, Advances in Experimental Medicine and Biology 979, DOI 10.1007/978-3-319-54910-1_14

14.1 Introduction

Microalgae proliferate more efficiently than higher plants, and can be used as a resource to obtain large amounts of biomass when provided with a proliferative environment (Chisti 2007). Algae can be cultivated at sites that are not used for agriculture, thus ensuring that they do not compete with existing agricultural resources. Hence, the use of various microalgal species such as *Chlorella* and *Spirulina* has been investigated. Specifically, the use of microbial protein-based food and feed has been anticipated globally since around the 1940s in preparation for a possible future food crisis, and several studies have reported the feasibility of the use of mass-cultivated microalgae as a food source (Spolaore et al. 2006).

Spirulina is indigenous to the areas in the vicinity of Lake Chad in Africa, and have been used as a protein food source for a considerable time by the local inhabitants. Consequently, the use of *Spirulina* as food has been actively investigated. Large-scale *Spirulina* production was achieved in the early 1970s. *Chlorella* is presently used in many food products, and investigations pertaining to its use began at the same time as those for *Spirulina*. The manufacture of actual food products through large-scale outdoor cultivation of *Chlorella* has been achieved in the 1960s (Borowitzka 1999).

Microalgae have various distinctive metabolic systems; therefore, by selecting one that produces a particular substance, substances that are difficult to produce from the higher plants can be efficiently produced. For example, while *Spirulina* is commonly used in food products as a protein and vitamin source, it is also used as a pigment source for blue food coloring (Eriksen 2008). Additionally, *Haematococcus* is exploited to produce a particularly useful substance, astaxanthin, which is a well-known antioxidant used as an ingredient of feed and cosmetics (Pulz and Gross 2004).

Some researchers focus on the commercial application of microalgae of the genus *Euglena*. Serious investigations into the nutritional value of *Euglena gracilis* began in the 1970s with reports of its protein content and amino acid scores. It was established as a highly valuable source of protein with high methionine content, which is a characteristic of animal proteins (Kott and Wachs 1964; Hosotani and Kitaoka 1977; Kitaoka and Hosotani 1977). *E. gracilis* also contains all essential vitamins and nutritionally important polyunsaturated fatty acids, docosahexaenoic acid, and eicosapentaenoic acid in the cells (Stern et al. 1960; Baker et al. 1981) (euglena Co., Ltd., unpublished). In addition, recent studies have demonstrated the functionality of the *Euglena*-specific reserve polysaccharide, paramylon (Sugiyama et al. 2009, 2010; Watanabe et al. 2013), suggesting the commercial potential of *E. gracilis*.

In 2005, euglena Co., Ltd. (hereafter referred to as euglena Co.) was established with the aim of producing and supplying *Euglena*, and in the same year, it succeeded in accomplishing the world's first outdoor large-scale cultivation of *Euglena* as a food source. Initially, the amount of production was quite limited; however, it was gradually scaled up, and the first *Euglena*-containing food products entered the market in 2007 (Fig. 14.1). Recently, non-food commercial *Euglena*-containing products, such as cosmetics, have also been launched. In this chapter, a review of the current large-scale cultivation of *Euglena* will be presented.

14.2 The Current State of Large-Scale Cultivation and Associated Challenges

In order to cultivate microalgae in an open system, it is necessary to either provide an environment difficult for other microbes to proliferate in, or to use microalgae that proliferate more rapidly and outcompete other microbes. Successful cases of the former strategy include *Spirulina* and *Dunaliella*, which can be cultivated in media with high pH and high salinity, respectively; thus, the proliferation of other microorganisms is inhibited in the media, thereby making the high-purity microalgal cultivation possible. The latter strategy includes the fast-proliferating microalgae, *Chlorella*. It is possible to cultivate and harvest large amounts of *Chlorella* before the other microorganisms have proliferated.

Fig. 14.1 Major *Euglena*-containing products. The product shown on the left is a nutritional drink, Midorijiru, provided as a powder to be dissolved in water. The products shown on the right are the cosmetics containing *Euglena* extracts

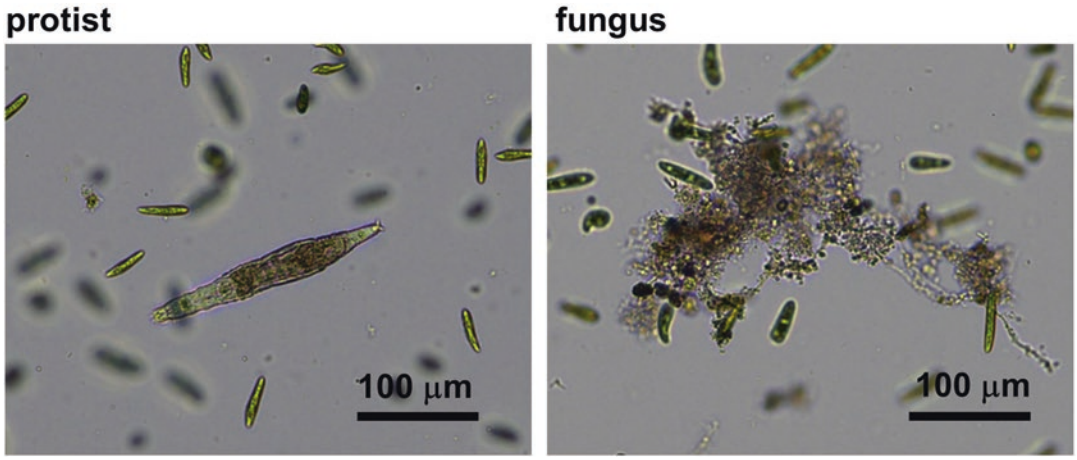

Fig. 14.2 Examples of contaminant organisms. *Left panel* shows an unidentified protist that preys on *E. gracilis*. *Right panel* shows a filamentous fungus that inhibits the growth of *E. gracilis*. Scale bars indicate 100 μm

Euglena gracilis has long been used as a model species in fundamental research, and is known to proliferate markedly faster than other members of the *Euglena* genus. Hence, the use of this microalga in large-scale outdoor cultivation was attempted. Initial attempts at the outdoor cultivation of *E. gracilis* were hampered by factors such as predation by other protists, fungi, and bacteria (Fig. 14.2). However, the ability of *E. gracilis* to proliferate at low pH (~3.5) could be leveraged to prevent contamination by other organisms during its cultivation. euglena Co. performs the large-scale outdoor cultivation of *E. gracilis* in a repaired cultivation pool that was previously used for the growth of *Chlorella* on Ishigaki Island, Japan (Fig. 14.3).

E. gracilis can also proliferate heterotrophically. Although the proliferation rate of heterotrophic cultures is considerably higher than that of the autotrophic cultures, the former are more vulnerable to contaminants even at low pH, and require more sterile conditions. This implies that the heterotrophic growth cannot be conducted in the outdoor open culture ponds, but requires expensive closed culture tanks, thereby resulting in an increased cost of production. In addition, the large-scale heterotrophic cultures often yield white *Euglena* cells lacking well-developed chloroplasts.

Fig. 14.3 Cultivation facilities at Ishigaki Island (as of 2010). The round-shaped pools are approximately 30 m in diameter

The white-cells have relatively low food value not only owing to the loss of their positive image as a fresh vegetable, but also on account of their having altered nutritional content.

Various techniques, other than growth at low pH, have been implemented by euglena Co. to increase and stabilize the production of *Euglena* in large-scale outdoor ponds; however, these are proprietary and therefore cannot be disclosed. The culture ponds used for cultivating *E. gracilis* are 30 m in diameter, 20 cm in depth, and are aerated by stirring with rotating apparatuses. The theoretical upper limit of the productivity of *E. gracilis* in autotrophic culture was estimated to be 48 g/m^{2}d under defined conditions, as reported in materials (NEDO 2014a) published by the New Energy and Industrial Technology Development Organization (NEDO) in Japan.

In the report, the ideal rate of carbon fixation and increase in dry weight were estimated by determining the carbon composition of the dried *E. gracilis* cells. As in other photosynthetic plants, the photosynthetic reduction of CO_2 molecules in *E. gracilis* requires eight photons of light. Photosynthesis utilizes only the visible light spectrum ranging from 400 to 700 nm, which constitutes approximately 45% of solar radiation. As carbon comprises approximately 49.7% of the dry weight of *E. gracilis* cells in the log growth phase, the optimum carbon dioxide fixation rate of *E. gracilis* was calculated to be 6.2 g/m^{2}d for 1 MJ/m^{2}d (equivalent to 4.57 μmol photons/m^{2}d) of sunlight. On Ishigaki Island, where euglena Co. produces *E. gracilis*, the reference intensity of the solar radiation is approximately 18 MJ/m^{2}d. With reference to the studies using higher plants, if the decrement due to light scattering and photorespiration is taken to be approximately 57%, the theoretical biomass yield was calculated to be 48 g/m^{2}d. This ideal production value does not depend on the depth of the pond, because most of the light is absorbed at the surface of the pond at sufficient *E. gracilis* cell density. The absorption coefficient (ε) of the *E. gracilis* cells was estimated to be 139 m^2/kg using the Lambert-Beer's equation, indicating the decrement of light with increasing depth. For example, only 0.25% of the light was estimated to reach a depth of 4 cm in a pond with a cell density of 0.55 g/L.

In an experiment on *Euglena* cultivation using an indoor 10-m^2 raceway-type cultivation tank exposed to 18 MJ/m^{2}d of light, a proliferation rate of 40.4 g/m^{2}d was obtained, which was close to the theoretical maximum value of 48 g/m^{2}d. However, outdoor cultivation at Ishigaki Island

using apparatus similar to those used for indoor cultivation resulted in the maximum proliferation rate of ~25 g/m^{2}d. This shows that various unidentified environmental burdens affect outdoor cultivation, and the identification and elimination of these factors is important for increasing productivity.

Besides cultivation, the mass production of algae requires the development of various harvesting and processing methods. The commonly used techniques for harvesting microalgae include centrifugation, filtration, flotation, and sedimentation. It is important to evaluate the technical advantages and disadvantages while selecting a harvesting method. For example, sedimentation takes time for collecting microalgal cells, but it can decrease the energy consumption compared to filtration and centrifugation, which need power-driven machines.

The method used for harvesting and drying *E. gracilis* grown in outdoor ponds used by euglena Co. for a medium-scale (50–1000 L) cultivation is described below. The lipid and/or carbohydrate is extracted according to the demand.

1. The *E. gracilis* cells are condensed to 50 times in concentration using ultrafiltration (PELLICON, Merck Millipore Corp., Darmstadt, Germany). The concentrated culture liquid is centrifuged at 3500 g for 5 min to recover the cells. Subsequently, the pelleted cells are resuspended in de-ionized water to achieve a concentration of 15–20% solids. This procedure is required to eliminate the components of the culture medium from the harvested *E. gracilis* cells.
2. The concentrated *E. gracilis* suspension is converted to a dried powder using a spray dryer (SD-1000, EYELA, Tokyo, Japan) with a constant inlet air temperature of 155 °C and outlet temperature of 95 °C. The dried powder is used directly in many *Euglena* powder products.
3. Lipids are obtained by subjecting the dried *E. gracilis* powder to extraction with organic solvents. n-hexane is typically used as the solvent for neutral lipid extraction (Ayers and Dooley 1948).
4. Paramylon and other carbohydrates are obtained by washing the grinded cells with acetone. Then, the collected precipitation is boiled with sodium dodecyl sulfate solution. The resulted precipitation is recovered as pure paramylon (Inui et al. 1982).

14.3 Strategies for Business Development Using *Euglena*

The "5Fs of Biomass" refers to the five uses of biomass, which are, in the order of their price per unit weight (highest value first): food, fiber, feed, fertilizer, and fuel (Fig. 14.4). Using biomass as the source of the most valuable product is the basic strategy for the commercialization of biomass. For example, although the rice plant is cultivated to produce rice (food), the rice straw can be used as the material of straw sandal (fiber), fodder for cattle (feed), and compost pile (fertilizer). In addition, the excess amount of rice straw can be burned (fuel). euglena Co. is aiming to begin production of the commercially valuable *Euglena* biomass products based on the "5Fs of Biomass" strategy.

The main product of euglena Co. is the nutritional foods made by directly blending *E. gracilis* dried powder in various foods and drinks to enhance their nutritive value. The *Euglena*-containing products sold primarily in Japan so far include cookies, cereal bars, and nutritional drinks. In addition, various kinds of supplements and cosmetics containing the extracts of *E. gracilis* are also marketed. Paramylon, the carbohydrate extracted from the *Euglena* cells, can be converted into plastic, which can be used as fiber (Shibakami et al. 2014), and its residues can be used as animal feed or fertilizer. The wax produced during its anaerobic fermentation holds promise for use as a fuel. In contrast to the cultivation of *E. gracilis* for its use as a food source, cultivation for paramylon extraction and production of oil needs to be performed in nitrogen-limited and anaerobic culture conditions, respectively. By investing the income obtained from the more profitable uses of *Euglena* biomass into the development of more efficient cultivation methods,

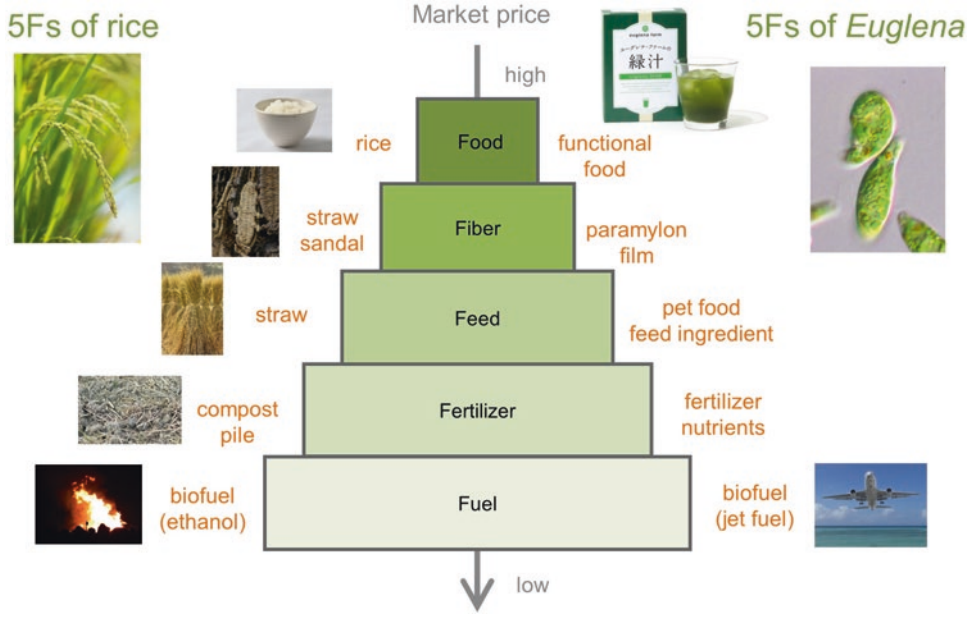

Fig. 14.4 "5Fs" cascading use of biomass The "5Fs" indicate the five uses of biomass: food, fiber, feed, fertilizer, and fuel. At the top of the 5F pyramid, the food is located as the highest value. The most popular food product is "Midorijiru," a nutritional supplement drink. Paramylon can be used as a fiber in cosmetic products. *Euglena* can also be added to pet foods as a supplement, indicating the use of *Euglena* as animal feed. The application of *Euglena* biomass as fertilizer and biofuel is currently under investigation

the overall production costs can be reduced, leading to a virtuous cycle. Additionally, the identification of the uses of *Euglena* byproducts leads to more efficient utilization of the produced biomass with an overall reduction in production costs. At present, capitalizing on the fact that *Euglena* contains a diverse range of nutrients, the commercial production of its highest-value product—food—has been achieved. In future, further reduction in its production costs might expand its application in various areas.

14.4 Breeding Potential of *Euglena*

In order to broaden the industrial utility of *Euglena*, efficient techniques are required for its cost-effective, stable, and large-scale production. To achieve this as well as to improve the cultivation equipment and methodology, techniques are required to develop cultivars with improved characteristics, such as adaptation to the cultivation environment and the acquisition of resistance to unfavorable conditions. Reports suggest that *E. gracilis* exhibits polyploidy (Schiff and Epstein 1965; Hill et al. 1966), which might be responsible for the observed difficulty in obtaining the nuclear genome mutants of *E. gracilis* (Schiff et al. 1980). Although it is difficult to breed mutated *E. gracilis*, in the recent years, the use of heavy ion beams for inducing mutations has resulted in the appearance of mutants that exhibit previously unknown phenotypes such as tolerance to high temperature (Yamada et al. 2016a) and higher lipid content (Yamada et al. 2016b). Mutants generated by heavy ion irradiation are recognized as natural mutants. Therefore, they might be advantageous for the outdoor mass cultivation as they are not subject to legislation regarding the use of recombinant organisms.

For efficient selective breeding of *E. gracilis*, the application of cell sorters for isolating cells with desirable traits was investigated (Yamada et al. 2016b). Fluorescence activated cell sorting (FACS) is an established technology and brings

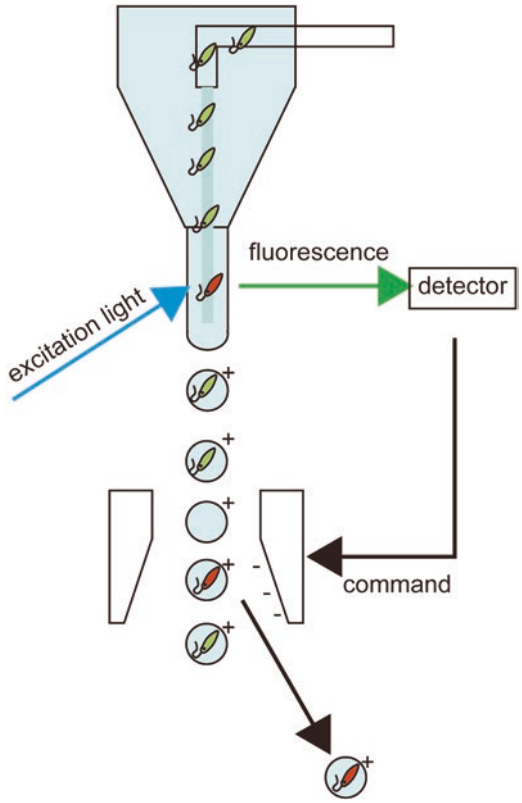

Fig. 14.5 Outline of FACS (fluorescence-activated cell sorting). The cells are aligned in the stream and their features monitored using scattered light and fluorescence. The cells of interest are isolated by applying an electric field to the positively charged droplets in which the cells are embedded

about meaningful outcomes in various research and clinical fields. The scattered light and fluorescence derived from the cells in fluids are detected as signals, enabling their morphology and cellular physiology to be recognized (Fig. 14.5). The cells are confined to a droplet, which can be deflected from the stream by an electric field. By monitoring the selected parameters, the desirable cells can be isolated from the heterogeneous cell suspensions. The live cell sorting of *Euglena* cells is more difficult than that of the other microalgae in that the shear forces make it difficult to obtain viable cells; however, *Euglena* cells were found to be able to survive FACS with the use of wider nozzles (Yamada et al. 2016b).

The successful isolation of *Euglena* mutants with relatively higher lipid content was based on staining the cells with BODIPY$^{505/515}$, which is a fluorescent dye known to stain neutral lipids, followed by the isolation of cells having higher lipid content by FACS (Yamada et al. 2016b). To obtain *E. gracilis* mutants with relatively high lipid content, a population with random mutations was produced by heavy-ion beam irradiation. The cells were stained with BODIPY, and FACS was used to isolate the cells with the highest BODIPY fluorescence, and thus the highest lipid content. After three rounds of selecting the cells with the highest BODIPY fluorescence, the candidate high lipid-producing mutant cells were individually isolated. Among the isolated strains, a mutant strain producing 40% more lipid than the wild-type strain was isolated.

Recombinant DNA technology has recently succeeded in producing transgenic *E. gracilis* strains with enhanced photosynthetic potential (Ogawa et al. 2015). The successful production of a population of random mutants by heavy-ion beam irradiation and the use of recombinant DNA technology to produce transgenic *Euglena* coupled with appropriate screening techniques will enable the breeding of *E. gracilis* with desirable traits suitable for specific commercial applications. Moreover, while the current large-scale production is limited to *E. gracilis*, it is highly possible that various other species of *Euglena* with diverse morphological and desirable properties can be used for industrial application. Indeed, a species, *Euglena (Euglenaria) anabaena* var. *minor*, has been found to proliferate relatively faster than the other *Euglena* species, and has the preferable characteristic of rapid sinking, which will facilitate its harvesting process (Suzuki et al. 2015).

14.5 Feasibility of Large-Scale Cultivation of Genetically Modified (GM) *Euglena*

The development of the methods for the stable and efficient transformation of *Euglena* (Ogawa et al. 2015), will enable the production of diverse GM *Euglena*. Some possible uses of the GM *Euglena* include the production of useful recombinant proteins that are difficult to express in other

host organisms. In addition, the high wax ester-producing GM *Euglena* will be useful for biofuel production. In most countries, the commercial cultivation of the GM algae outdoors is strongly restricted; thus, even if permission is obtained, it is likely that the cultivation of GM algae will be limited to the enclosed cultivation systems.

In the United States, a TSCA (Toxic Substances Control Act) Environmental Release Application (TERA) to the Environmental Protection Agency (EPA) is required for the outdoor cultivation of GM organisms. Based on this approval, GM *Scenedesmus* is being cultivated outdoors in San Diego (California, USA), indicating the feasibility of the commercial large-scale outdoor cultivation of GM microalgae in the future. With respect to the GM *Euglena*, only studies on semi-outdoor cultivation have been performed to date. The outdoor cultivation of the GM *Euglena* is not currently being performed due to the hold-ups with the TERA application (euglena Co. IR materials).

14.6 Optimum Land Candidates for Large-Scale Global Cultivation

Currently, commercial large-scale cultivation of *Euglena* is performed on the Ishigaki Island in Okinawa prefecture, Japan; however, further studies are required in order to identify places where even larger-scale cultivations of *Euglena* can be performed in the future. The global screening of such land candidates was performed on the basis of the usable land area (at least 3000 ha), climate (3 h of average sunlight per day; average annual rainfall of no less than 500 mm; and tropical, dry or temperate climate under the Köppen climate classification system), and country risk (low level of crime and terrorism). The countries that have been reported to be suitable for the deployment of the large-scale algae cultivation as a business include Malaysia, Brazil, the United States of America, Vietnam, Thailand, and Australia (NEDO 2014b). Other candidate countries not listed might have potential as the suitable sites having some, but not all of the desirable features. For example, Oman in the Middle East was excluded from the list of suitable candidate sites because it has an annual precipitation of 500 mm or less, and therefore, does not have the water resources necessary for cultivation. However, large amount of water, which can be used for the algal cultivation, is produced when drilling for oil in Oman. This has ameliorated the problem associated with low precipitation and, therefore, the outdoor cultivation of *Euglena* has been attempted there (unpublished). Future studies investigating the use of wastewater or seawater for algal cultivation and the development of new strains suitable for the environments currently deemed unsuitable for algal cultivation will broaden the range of areas suited for the large-scale algal cultivation. Research progress in these areas is expected to contribute to the successful commercial cultivation of *Euglena* and other microalgae.

14.7 Outlook

It has been about 10 years since the start of the large-scale commercial cultivation of *Euglena*. Throughout this period, a variety of foods, cookies, cereal bars, drinks, and supplements containing *Euglena* have been developed based on the concept of the "5Fs of Biomass." Meanwhile, the development of cosmetics has also begun to take advantage of the *Euglena* crude extracts. In the next 10 years, further technical innovations in the large-scale cultivation will enable the application of *Euglena* in the fields of fiber, feed, fertilizer, and fuel, making other products available in the lower layers of the "5Fs of Biomass." Among these applications, the development and utilization of *Euglena* as feed and fuel are highly feasible. In particular, the "defatted *Euglena*," which is what remains after the extraction of oil from the *Euglena* biomass produced for fuel use, might be used as an alternative to defatted soybean and/or fishmeal. The crude protein is approximately 50% in the defatted residue that was treated with hexane or supercritical CO_2 to remove the fat. On the other hand, by adjusting the cultivation method, the production of "feed *Euglena*" which includes

the relatively higher amounts of the unsaturated fatty acid will be in high demand. The price of fishmeal has remained high (at approximately $2.00/kg in 2015), thus making *Euglena* the perfect substitute for fishmeal, and is expected to be of great assistance to the feed industry.

In conclusion, the large-scale cultivation of *Euglena* itself is not a goal, but could be a first step to solve the problems including malnutrition and fuel depletion by providing alternative biomass. In addition to following the "5Fs of biomass," continuous improvements are required to large-scale algal cultivation methods as a fundamental technique to achieve advances in the commercialization of *Euglena* production.

References

Ayers AL, Dooley JJ (1948) Laboratory extraction of cottonseed with various petroleum hydrocarbons. J Am Oil Chem Soc 25:372–379

Baker ER, McLaughlin JJA, Hutner SH et al (1981) Water-soluble vitamins in cells and spent culture supernatants of Poteriochromonas stipitata, *Euglena gracilis*, and Tetrahymena thermophila. Arch Microbiol 129:310–313. doi:10.1007/BF00414703

Borowitzka MA (1999) Commercial production of microalgae: ponds, tanks, and fermenters. Prog Ind Microbiol 35:313–321. doi:10.1016/S0079-6352(99)80123-4

Chisti Y (2007) Biodiesel from microalgae. Biotechnol Adv 25:294–306. doi:10.1016/j.biotechadv.2007.02.001

Eriksen NT (2008) Production of phycocyanin—a pigment with applications in biology, biotechnology, foods and medicine. Appl Microbiol Biotechnol 80:1–14

Hill HZ, Schiff JA, Epstein HT (1966) Studies of chloroplast development in Euglena XIII. Variation of ultraviolet sensitivity with extent of chloroplast development. Biophys J 6(2):125–133

Hosotani K, Kitaoka S (1977) Determination of the nutritive value of *Euglena gracilis* protein by in vitro digestion experiments and rat feeding tests. J Agric Chem Soc Jpn 51:483–488

Inui H, Miyatake K, Nakano Y, Kitaoka S (1982) Wax ester fermentation in *Euglena gracilis*. FEBS Lett 150:89–93. doi:10.1016/0014-5793(82)81310-0

Kitaoka S, Hosotani K (1977) Studies on culture conditions for the determination of the nutritive value of *Euglena gracilis* protein and the general and amino acid compositions of the cells. J Agric Chem Soc Jpn 51(8):477–482

Kott Y, Wachs AM (1964) Amino acid composition of bulk protein of Euglena grown in waste water. Appl Microbiol 12:292–294

NEDO (2014a) Development of elemental technology concerning bio-jet fuel manufacturing of microalgae origin. (FY2010-FY2013) Final report (2014-1)

NEDO (2014b) Study of candidate place concerning feasibility of demonstration study of biofuel production from microalgae. (FY2013) Final report (2014-2)

Ogawa T, Tamoi M, Kimura A et al (2015) Enhancement of photosynthetic capacity in *Euglena gracilis* by expression of cyanobacterial fructose-1,6-/sedoheptulose-1,7-bisphosphatase leads to increases in biomass and wax ester production. Biotechnol Biofuels 8:80. doi:10.1186/s13068-015-0264-5

Pulz O, Gross W (2004) Valuable products from biotechnology of microalgae. Appl Microbiol Biotechnol 65:635–648. doi:10.1007/s00253-004-1647-x

Schiff JA, Epstein HT (1965) The continuity of the chloroplast in Euglena. In: Locke M (ed) Reproduction: molecular, subcellular, and cellular. Academic Press, New York, pp 131–189

Schiff JA, Lyman H, Russell GK (1980) Isolation of mutants of *Euglena gracilis*: An addenum. Methods Enzymol 69:23–29

Shibakami M, Tsubouchi G, Hayashi M (2014) Thermoplasticization of euglenoid β-1, 3-glucans by mixed esterification. Carbohydr Polym 105:90–96

Spolaore P, Joannis-Cassan C, Duran E, Isambert A (2006) Commercial applications of microalgae. J Biosci Bioeng 101:87–96. doi:10.1263/jbb.101.87

Stern AI, Schiff JA, Klein HP (1960) Isolation of ergosterol from *Euglena gracilis*; Distribution among mutant strains. J Protozool 7:52–55. doi:10.1111/j.1550-7408.1960.tb00707.x

Sugiyama A, Suzuki K, Mitra S et al (2009) Hepatoprotective effects of paramylon, a beta-1, 3-D-glucan isolated from *Euglena gracilis* Z, on acute liver injury induced by carbon tetrachloride in rats. J Vet Med Sci 71:885–890. doi:10.1292/jvms.71.885

Sugiyama A, Hata S, Suzuki K et al (2010) Oral administration of paramylon, a beta-1,3-D-glucan isolated from *Euglena gracilis* Z inhibits development of atopic dermatitis-like skin lesions in NC/Nga mice. J Vet Med Sci 72:755–763. doi:10.1292/jvms.09-0526

Suzuki K, Mitra S, Iwata O et al (2015) Selection and characterization of Euglena anabaena var. minor as a new candidate Euglena species for industrial application. Biosci Biotechnol Biochem 79:1730–1736. doi:10.1080/09168451.2015.1045828

Watanabe T, Shimada R, Matsuyama A et al (2013) Antitumor activity of the β-glucan paramylon from Euglena against preneoplastic colonic aberrant crypt foci in mice. Food Funct 4:1685–1690. doi:10.1039/c3fo60256g

Yamada K, Kazama Y, Mitra S et al (2016a) Production of a thermal stress resistant mutant *Euglena gracilis* strain using Fe-ion beam irradiation. Biosci Biotechnol Biochem 80:1650–1656. doi:10.1080/09168451.2016.1171702

Yamada K, Suzuki H, Takeuchi T et al (2016b) Efficient selective breeding of live oil-rich *Euglena gracilis* with fluorescence-activated cell sorting. Sci Rep 6:26327. doi:10.1038/srep26327

Index

S.D. Schwartzbach, S. Shigeoka (eds.), *Euglena: Biochemistry, Cell and Molecular Biology*,
Advances in Experimental Medicine and Biology 979, DOI 10.1007/978-3-319-54910-1